Revision of the *Halitherium*-species complex (Mammalia, Sirenia) from the late Eocene to early Miocene of Central Europe and North America

D i s s e r t a t i o n

zur Erlangung des akademischen Grades

d o c t o r r e r u m n a t u r a l i u m
(Dr. rer. nat.)

im Fach Biologie

eingereicht an der

Mathematisch-Naturwissenschaftlichen Fakultät I
der Humboldt-Universität zu Berlin

von

Dipl.-Geol. Manja Voß

Präsident der Humboldt-Universität zu Berlin
Prof. Dr. Jan-Hendrik Olbertz

Dekan der Mathematisch-Naturwissenschaftlichen Fakultät I
Prof. Stefan Hecht PhD

Gutachter:
1. PD Dr. Oliver Hampe
2. Prof. Dr. Johannes Müller
3. Prof. Annalisa Berta, Ph.D.

Tag der mündlichen Prüfung: 06.11.2013

To Robert

Hiermit versichere ich, dass ich die vorliegende Arbeit ohne Hilfe Dritter und ohne Verwendung anderer als der angeführten Hilfsmittel und Quellen angefertigt habe, und dass die Arbeit in gleicher oder ähnlicher Form noch keiner anderen Prüfungsbehörde vorgelegen hat. Alle Ausführungen der Arbeit die wörtlich oder sinngemäß übernommen wurden, sind entsprechend gekennzeichnet.

Ort, Datum Dipl.-Geol. Manja Voß

Taxonomic Disclaimer

This doctoral thesis is produced only for the purpose of a public examination. Following the recommendations 8A and 8E of the International Code of Zoological Nomenclature (IKZN, 2000), new scientific names are not proposed herein in order to avoid unintentional publication. New nomenclatural acts introduced in this thesis, like any changes of the classification concept provided above, will not become available until they are formally published within the meaning of the ICZN (Articles 8.1. and 8.3.; IKZN, 2000).

CONTENT

ZUSAMMENFASSUNG

Die vorliegende Doktorarbeit ist das Ergebnis der systematischen und taxonomischen Revision einer Gruppe ausschließlich ausgestorbener Seekühe (Sirenia), die unter dem Gattungsnamen *Halitherium* Kaup, 1838 bekannt ist. Neben der Typusart *H. schinzii* Kaup, 1838 (Unteroligozän, Zentraleuropa) werden zwei weitere Taxa innerhalb des europäischen Paläogens anerkannt, *H. cristolii* Fitzinger, 1842 (Oberoligozän, Österreich) und *H. taulannense* Sagne, 2001a (Obereozän, Frankreich). Obwohl erst kürzlich die Aufstellung einer neuen Art innerhalb dieser Gattung impliziert, dass *Halitherium* als monophyletisch angesehen wird, weisen jedoch alle bisherigen phylogenetischen Analysen auf eine Paraphylie dieser Gruppe hin. So ist die auf *H. schinzii* basierende, nur fossil bekannte Unterfamilie Halitheriinae paraphyletisch und umfasst nahezu ausnahmslos Gattungen, die ebenfalls paraphyletisch sind. Das Klassifikationskonzept der Sirenia unterlag in der Vergangenheit nur wenig Veränderung. Die Aufrechterhaltung der Unterfamilie „Halitheriinae“ ist somit einer der wesentlichen Gründe für eine Paraphyla-basierte Systematik der gesamten Ordnung. Viele Taxa innerhalb der Sirenia, insbesondere auf Gattungsebene, sind daher nur unzureichend definiert. Dies erschwert einerseits die zuverlässige taxonomische und systematische Einordnung neuer Fossilfunde, und andererseits eine zweckmäßige Erfassung der einstigen Diversität dieser Ordnung.

Die im Rahmen dieser Arbeit durchgeführten detaillierten Studien von Skelettresten führen nicht nur zu einer kritischen Überprüfung und Revision der Monophylie der Gattung *Halitherium*, sondern auch zum Test der Hypothese über das Vorkommen zweier verschiedener Morphospezies im Unteroligozän Zentraleuropas. Weitere Schwerpunkte dieser Arbeit bilden die Analyse der Verwandtschaftsverhältnisse der dieser Gattung traditionell zugeordneten Arten und die Ermittlung ihrer phylogenetischen Stellung innerhalb der Ordnung Sirenia. Der wesentliche Fokus der morphologischen Analyse liegt auf der Typusart *H. schinzii*. Außerdem werden die oligozänen zentral- und nordamerikanischen Arten *H. alleni* Simpson, 1932a und *H. antillense* Matthew, 1916, deren Status und Verwandtschaftsverhältnisse bislang ungeklärt waren, zum ersten Mal in einer morphologisch-systematischen Studie berücksichtigt. Die phylogenetische Position der vermutlich miozänen Art *H. bellunense* De Zigno, 1875 wird ebenfalls geprüft.

Über morphologische Vergleiche im Rahmen dieser Doktorarbeit wird der Holotyp von *H. schinzii*, ein Premolar, als undiagnostisch definiert. Infolgedessen wird dieser Artname als *nomen dubium* eingestuft und sämtliches *„H. schinzii“* zugeordnete Skelettmaterial morphologisch neu- oder erstbearbeitet. Für die phylogenetische Analyse der Sirenia werden einerseits strenge kladistische Prinzipien berücksichtigt, die das Ordnen und Gewichten von Merkmalen ausschließen. Andererseits wird eine revidierte, ergänzte und erweiterte Merkmals-Taxon-Matrix erarbeitet, die den bisher größten Datensatz über Sirenia auf morphologischer Basis darstellt. Dabei wird auch Wert auf postkraniale Merkmale gelegt, die in vorangegangenen Studien weitgehend vernachlässigt wurden.

Molekulare Daten finden in dieser Arbeit keine Berücksichtigung, da diese nur für die vier heute noch lebenden Sirenenarten zur Verfügung stehen.

Sechs verschiedene kladistische Analysen wurden durchgeführt. Diese zeigen, dass die Vertreter des früheren *„Halitherium“*-Spezies Komplexes keine monophyletische Gruppe bilden, sondern über die Stamm- und Kronengruppe der Sirenia verteilt sind. Aufgrund der Ergebnisse der systematisch-taxonomischen Revision im Rahmen dieser Studie sind die Gattung *„Halitherium“* und die darauf basierende Unterfamilie „Halitheriinae“ ebenfalls *nomina dubia*. Infolgedessen werden vier neue Gattungen aufgestellt. Eine dieser Gattungen behinhaltet die Art *alleni* und eine Schwestergruppe, welche Individuen umfasst, die ursprünglich *„H. schinzii“* zugeordnet wurden. In Folge der Hinfälligkeit der Typusart *„H. schinzii“*, wird für eine der beiden Schwestertaxa ein neuer Artname eingeführt. Gleichzeitig wird der Artname *bronni*, der ursprünglich als Synonym zu *„H. schinzii“* geführt wurde, als valide erklärt. Die Hypothese, dass zwei sympatrische Morphospezies im Unteroligozän Zentraleuropas vorkamen (insbesondere in Deutschland und Belgien), wird hiermit bestätigt. Beide Schwestertaxa können unter anderem eindeutig aufgrund der Morphologie des Supraoccipitale und der permanenten Zahnformel unterschieden werden.

Ein weiteres bedeutendes Resultat dieser Studie und gleichzeitig ein Indikator für den Einfluss der Revision des *„Halitherium“*-Spezies Komplexes auf die Systematik der Sirenia, besteht in der phylogenetischen Stellung der Trichechidae (Manatees im weitesten Sinne). Diese werden auf der Basis von postkranialen Merkmalen als nächste Verwandte jener Gruppe hypothetisiert, welche die ausgerottete Art *Hydrodamalis gigas* (Stellersche Seekuh) beinhaltet. Somit kann für die Trichechidae erstmals ein jüngerer Ursprung als bislang angenommen postuliert werden. Die Ergebnisse dieser Studie spiegeln sich in einer neuen Klassifikation der Ordnung Sirenia wider. Allen voran wird eine konsequente Unterscheidung in Stamm- und Kronengruppensirenen vorgenommen. Dabei wird die Kronengruppe im Wesentlichen in zwei neue Unterordnungen weiter unterteilt.

Diese Doktorarbeit forciert einen neuen taxonomischen und systematischen Ansatz und stellt neue Daten über die Morphologie, Diversität und Biogeographie von Seekühen im Allgemeinen zur Verfügung. Die herausragendsten Ergebnisse dieser Studie bestehen einerseits in der Revision einer der umstrittensten Gruppen innerhalb der Sirenia, die „Halitheriinae“ basierend auf *„Halitherium“*. Andererseits wird für den Ursprung der Kronengruppensirenen, einschließlich der vier rezenten Arten, ein eher unteroligozäner statt eozäner Zeitpunkt bekräftigt.

SUMMARY

The present doctoral thesis is the result of the systematic and taxonomic revision of a group of exclusively extinct sea cows (Sirenia) generally known under the genus *Halitherium* Kaup, 1838. Beside the type species *H. schinzii* Kaup, 1838 (lower Oligocene of Central Europe), two further taxa *H. cristolii* Fitzinger, 1842 (late Oligocene of Upper Austria) and *H. taulannense* Sagne, 2001a (late Eocene of France) are considered valid within the European Palaeogene until now. Although the latest introduction of a new species assigned to this genus indicates that *Halitherium* is assumed to be monophyletic, all previous phylogenetic analyses confirm this group as a paraphyletic assemblage. As such, the exclusively extinct subfamily Halitheriinae established on the basis of *H. schinzii* is also paraphyletic, comprising a number of genera that are invariably paraphyletic as well. There have been very few changes made to the classification concept of Sirenia in the past. Accordingly, the maintenance of the subfamily “Halitheriinae” is still on of the major causes for a paraphyla-based systematic of the entire order. Therefore, many sirenian taxa are only inadequately defined, especially on the genus level. On the one hand, this hampers a reliable taxonomic and systematic assignment of new fossil sirenian finds, and on the other hand, a proper handling of the past diversity of this order.

The detailed morphological investigation of skeletal remains carried out through this study resulted not only in the critical evaluation and revision of the monophyly of the genus *Halitherium*, but also in the test of the hypothesis of the presence of two different morphospecies in the lower Oligocene of Central Europe. Further focal areas of this work are the analysis of the interrelationships of the species traditionally assigned to that genus, and the identification of their phylogenetic position within the order Sirenia. The major focus lies on the type species *H. schinzii* and the morphological basis for its establishment. Additionally, the Oligocene Central and North American species *H. alleni* Simpson, 1932a and *H. antillense* Matthew, 1916 that hitherto remained unconsidered for cladistic treatment and are of uncertain status and affinities, are incorporated in this study for the first time. The phylogenetic position of the supposedly Miocene species *H. bellunense* De Zigno, 1875 from Italy is also tested.

Morphological comparisons performed in this study, reveal the premolar holotype of *H. schinzii* to be non-diagnostic. This resulted in the recognition of this taxon name as a *nomen dubium* and the re-investigation or initial examination of abundant skeletal material originally assigned to this species. For the phylogenetic analysis of the Sirenia robust cladistic principles are applied that refrain from weighting and ordering of characters. For this purpose, a revised, supplemented and extended character-taxon matrix is compiled resulting in the largest data set on Sirenia on a morphological basis so far. Attention is also given to postcranial characters that were usually neglected in previous studies. Molecular data remain unconsidered, because they are only available for the four sirenian species still living today.

Six varied cladistic analyses were performed showing that the representatives of the former *“Halitherium”*-species complex do not form a monophyletic group, but instead are distributed over the stem group and the crown group of the order Sirenia. According to the results of the systematic and taxonomic revision in the course of this study, the genus *“Halitherium”* and the thereon based subfamily “Halitheriinae” are likewise *nomina dubia* hence invalid terms. As a consequence, four new genera are introduced. One of these genera comprises the species *alleni* and a sister group including specimens that were formerly designated as *“H. schinzii”*. Due to the fact that the type species *“H. schinzii”* is a *nomen dubium*, a new species name is erected for one of the sister taxa. At the same time, the species name *bronni* that was synonymous with *“H. schinzii”* is shown to be valid confirming the hypothesis of the presence of two sympatric morphospecies in the lower Oligocene of Central Europe, especially from Germany and Belgium. Both sister taxa are amongst others conspicuously distinguishable on the basis of the supraoccipital morphology and the permanent dental formula.

Another important result of this study and likewise an indicator for the impact of the revision of the *“Halitherium”*-species complex on sirenian systematics refers to the phylogenetic position of the Trichechidae (manatees in the broader sense). On the basis of postcranial characters, trichechids are identified to be closely related to the group commencing the exterminated species *Hydrodamalis gigas* (Steller’s sea cow). Hence, for the first time a more recent origin than previously hypothesised can be postulated for the Trichechidae. The results of the present study are reflected in a new systematic framework introduced for Sirenia. Primarily, a consequent distinction between stem group and crown group sirenians is performed and, essentially, two new suborders are established for the crown group.

This thesis accelerates a novel taxonomic and systematic approach providing new data on the morphology, diversity and biogeography of sirenians in general. The most important results of this study are that one of the most disputed sirenian groups, the “Halitheriinae” based on *“Halitherium”*, is revised, and that the divergence time of crown group sirenians, including the four extant taxa, is estimated as early Oligocene rather than Eocene.

INTRODUCTION

Main features and specialisations of sea cows (Sirenia)

Sirenia, or sea cows, are a group of mammals, which are secondarily adapted to fully aquatic life-styles (Fig. 1). They are commonly present in near-shore shallow-water environments and mainly distributed in the tropical and subtropical Atlantic and Indo-Pacific oceans today. Convergent to derived cetaceans, sirenians possess large, stout but streamlined bodies with a short neck and rounded flipper-like forelimbs, completely reduced hindlegs, a highly reduced pelvis without bony connection to the vertebrae, and a powerful horizontal tail fluke for propulsion (Domning, 2001a; Gheerbrandt *et al*., 2005a; Berta *et al*., 2006).

Sirenia are unique among living marine mammals in being strictly herbivorous, specialised on marine angiosperms, i.e. seagrass (De Iongh *et al*., 1995; Domning, 1981, 2001a; Phillips & Meñez, 1988) or a variety of freshwater macrophytes (Domning, 1980, 1982). They are distinguished from all other mammals by several morphological features such as retracted and enlarged external nares and five premolars in early sirenians. However, the interpretation of the latter is still unresolved (Domning, 1994).

The presence of pachyostosis and osteosclerosis (Domning & Buffrénil, 1991; Domning, 1994), also known as pachyosteosclerosis (Gheerbrandt *et al*., 2005a; Buffrénil *et al*.,

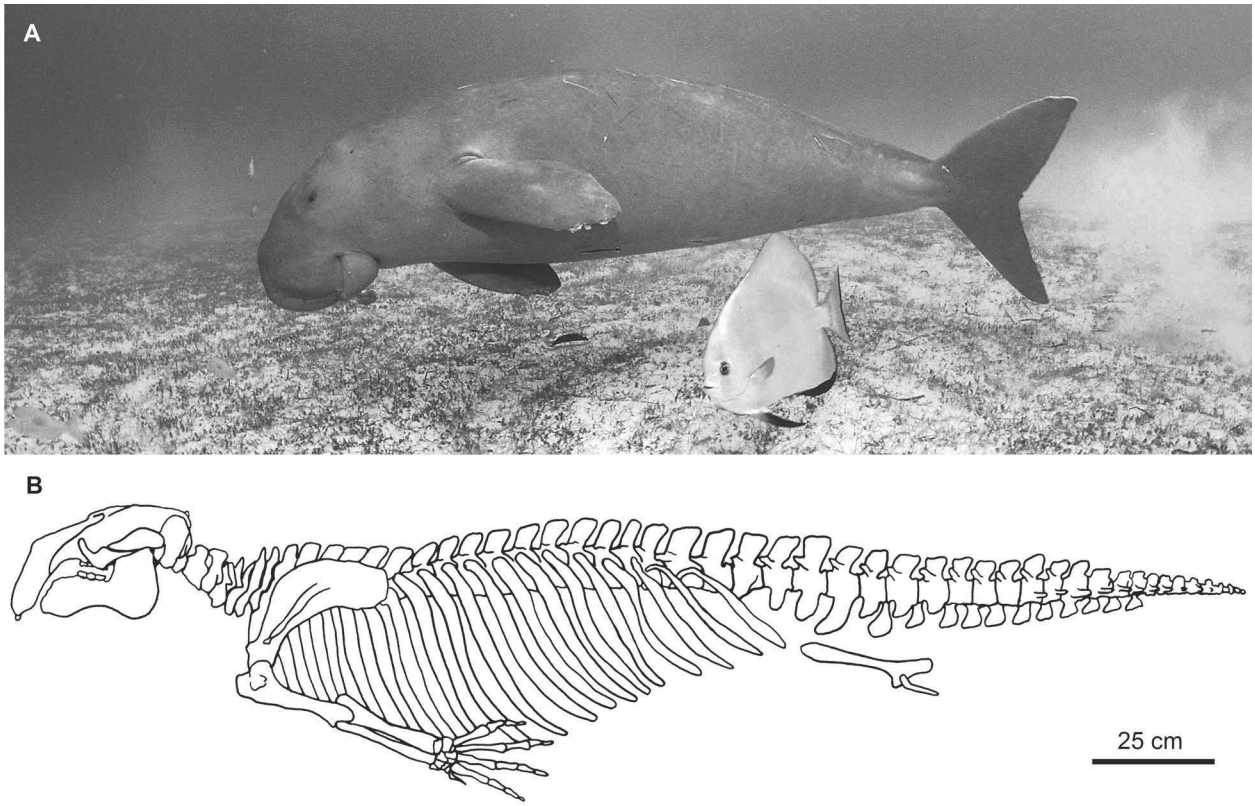

Figure 1. A, a dugong cruising over a seagrass bed (© Jurgen Freund). **B**, life-size reconstruction of a sea cow skeleton from the lower Oligocene of Germany (modified after Voss, 2012).

2010), in the skeleton of sirenians additionally supports this clade (Domning, 1994). These modifications refer to thickened, voluminous bones, like the commonly fossilised ribs, and an increased density of individual bones due to the partial or complete loss of cancellous bony tissue. As a result ballast is provided to neutralise the buoyancy of the lungs in connection with the achievement of equilibrium in the aqueous medium (Kaiser, 1974; Kleinschmidt, 1982; Domning & Buffrénil, 1991; Domning, 2001a; Buffrénil *et al*., 2010).

Sirenian affinities

Sirenians form a monophyletic group with proboscideans (which include elephants); the latter considered being their closest living relatives (Thewissen & Domning, 1992). Together with the extinct desmostylians both taxa make up the universally accepted clade Tethytheria (McKenna, 1975; McKenna & Bell, 1997). The Tethytheria hypothesis favours an Old World origin of sirenians and their relatives that putatively radiated in the former east-west seaway Tethys (Domning, 2001a). Tethytheria are well supported by morphological (Domning *et al*., 1986; Novacek & Wyss, 1986; Tassy & Shoshani, 1988) as well as molecular genetic data (Lavergne *et al*., 1996; Murphy *et al*., 2001a). Some molecular analyses also indicate a sister grouping of either [Sirenia + Hyracoidea] or [Proboscidea + Hyracoidea] (Amrine & Springer, 1999; Madsen *et al*., 2001; Murphy *et al*., 2001b; Kuntner *et al*., 2010). Either way, these studies provide strong support for the clade Paenungulata, comprising sirenians, proboscideans and hyracoids (hyraxes) (Gheerbrant *et al*., 2005a). Recent investigations based on molecular data from mitochondrial and nuclear genes or a combination of these reveal a consistent sister clade of Tethytheria + Hyracoidea (Lavergne *et al*., 1996; Stanhope *et al*., 1998; Murphy *et al*., 2001a). Several studies (e.g., Novacek & Wyss, 1986; Novacek *et al*., 1988; Shoshani & McKenna, 1998) provide morphological support for the depicted relationships within Paenungulata. Asher *et al.* (2003) demonstrated the impact of fossils and morphological features combined with DNA sequence data inferring not only the Paenungulata hypothesis, but also a sirenian-proboscidean clade. This study recognises another supraordinal clade, the Afrotheria, including elephant shrews, tenrecs, golden moles and aardvarks in addition to Paenungulata, which is strongly supported by other combined analyses (e.g., Asher, 2007) and molecular studies (Murphy *et al*., 2001a, b; Murata *et al*., 2003; Kuntner *et al*., 2010).

Sirenian evolution, fossil record and major groups

According to Domning (2001a), Sirenia have a long and rich fossil record and reflect the evolutionary transition between terrestrial and aquatic life-styles as one of the best documented examples in vertebrate evolution. Their morphological evolution related to adapting to a life in water involve modifications in locomotion and feeding and can be reconstructed over some 50 Ma back into the early Eocene. Sirenians are well known

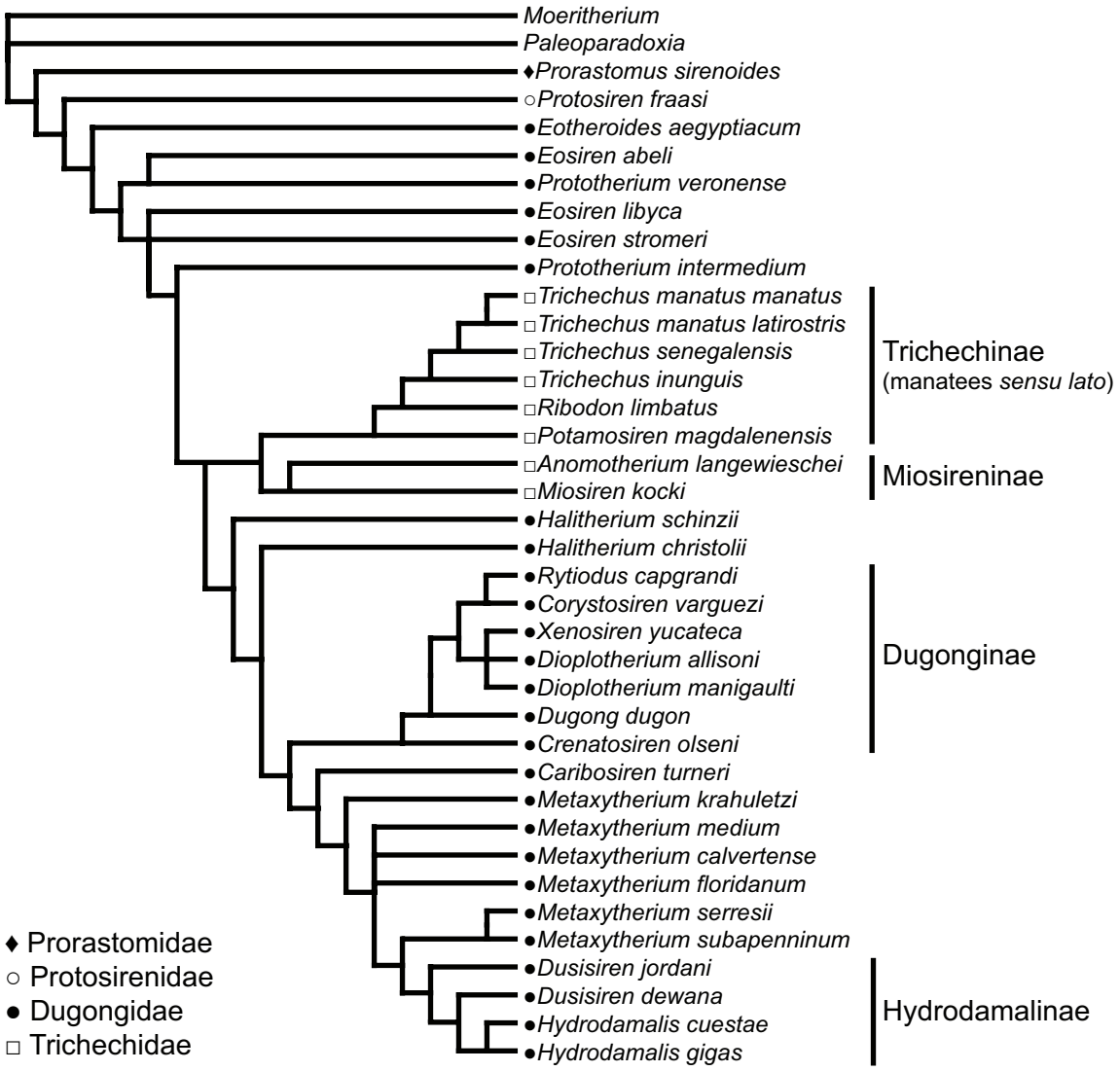

Figure 2. Nelson consensus tree of the Sirenia including 36 species and subspecies, and 62 informative cranial and dental characters (modified after Domning, 1994). TL = 162, CI = 0.76, RI = 0.91.

from Africa, North America and Europe and were most diverse during the Oligocene and Miocene, often characterised by short sympatric offshoots of particular taxa (Domning, 2001b). Their taxonomic diversity distinctly declines in the late Miocene due to rapid climate cooling and oceanographic changes during the latter half of the Cenozoic and their impacts on available dietary resources (Clementz *et al*., 2009).

Phylogenetic analyses reveal deeper insights into the systematic relationships of different groups of sirenians (Savage, 1976; Domning, 1994). The hitherto most comprehensive cladistic analysis was provided by Domning (1994) encompassing all better known taxa (Fig. 2). His suprageneric classification of the Sirenia (Domning, 1994, 1996) maintains the traditional taxonomic concept of Simpson (1945). Four families are accordingly distinguished: the Prorastomidae Cope, 1889 and Protosirenidae Sickenberg, 1934a are extinct and restricted to the Eocene, whereas the Dugongidae Gray, 1821 (including the three subfamilies Halitheriinae, Hydrodamalinae and Dugonginae)

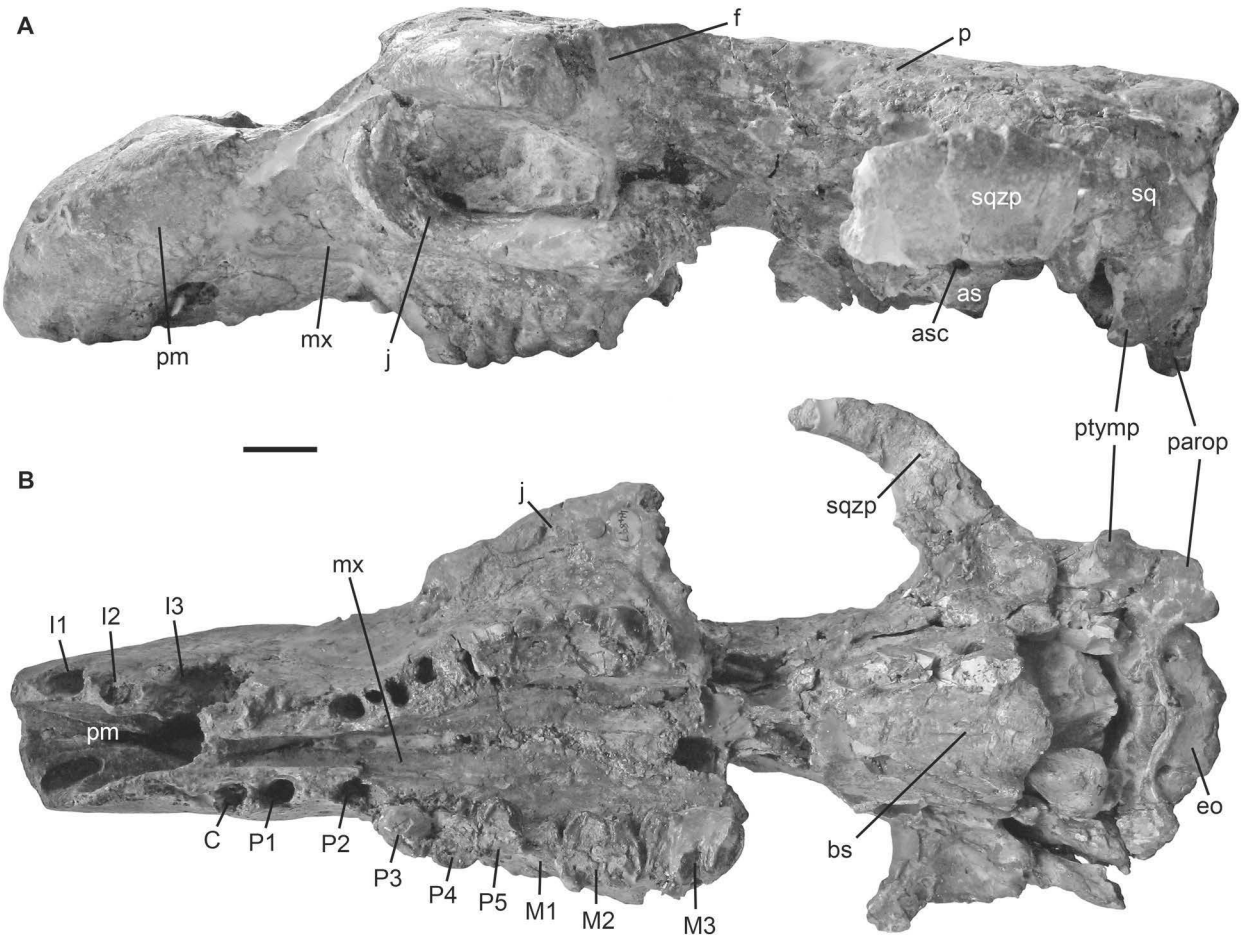

Figure 3. Holotype skull of *Prorastomus sirenoides* (NHMUK PV M44897). **A**, in lateral view. **B**, in ventral view. Scale bar equals 2 cm.

and Trichechidae Gill, 1872 (1821) (including the two subfamilies Miosireninae and Trichechinae) have extant representatives.

The Prorastomidae are considered to be paraphyletic (Domning, 1994; Fig. 2), comprising two monospecific genera, with *Prorastomus sirenoides* Owen, 1855 representing the oldest known sirenian so far. This species was found in late early Eocene sediments of Jamaica indicating a rapid dispersal of sirenians from their generally accepted Old World origin. This taxon is about the size of a pig and still has a morphologically plesiomorphic skull which, however, is already pachyostotic. Exceptional is the occurrence of a fifth premolar (3.1.5.3), which is generally lost in all other post-Cretaceous Eutheria (Fig. 3B). The rostrum is nearly undeflected and bulbous forming a prow-like or forceps-like snout (Fig. 3A) suggesting a selective browsing habit on diverse submerged and emergent plants (Savage, 1976; Savage *et al*., 1994).

Pezosiren portelli from the early middle Eocene of Jamaica is considered a close relative of *P. sirenoides* and was therefore placed into the Prorastomidae by Domning (2001c). The discovery of an almost complete skeleton of *P. portelli* reveals evidence documenting the transition between terrestrial and aquatic life (Domning, 2001c). This animal was fully capable of dwelling on land with four well developed legs, hip and knee

Figure 4. Life-size skeletal reconstruction (**A**) and life-sketch (**B**) of *Pezosiren portelli* (A: http://commons.wikimedia.org/wiki/User:Thesupermat/gallery; B: © Calvert Marine Museum, 2002).

joints (Fig. 4A). A multivertebral sacrum and strong sacroiliac articulation supported the body weight out of water as in land mammals. Adaptations to a life-style in water, like the pachyostotic bones counterbalancing the buoyancy of air-filled lungs as is typical for sea-cows, show that *P. portelli* probably lived predominantly in the water. This also is supported by the distribution of fossils in lagoonal deposits. Morphological, ecological and taphonomic data support the interpretation of prorastomids being fluviatile or estuarine semiaquatic herbivores (Savage *et al*., 1994; Fig. 4B), which probably swam by spinal extension with simultaneous pelvic paddling, similar to contemporary cetaceans (Domning, 2001a, c; Berta *et al*., 2006).

Protosiren from the middle Eocene of Egypt (Abel, 1907; Sickenberg, 1934a) and Pakistan (Gingerich *et al*., 1995; Zalmout *et al*., 2003) is the hitherto only known genus of the Protosirenidae (Domning, 1994, 1996; Fig. 2). *Protosiren* has a slightly downturned rostrum and a broadened mandibular symphysis that may indicate less selective grazing (Domning & Gingerich, 1994; Domning, 2001b; Fig. 5A). The postcranial skeleton of *Protosiren* shows many aquatic features like the incipient reduction of the hindlimbs (Fig. 5B). However, these still were well developed and probably usable on land, revealing

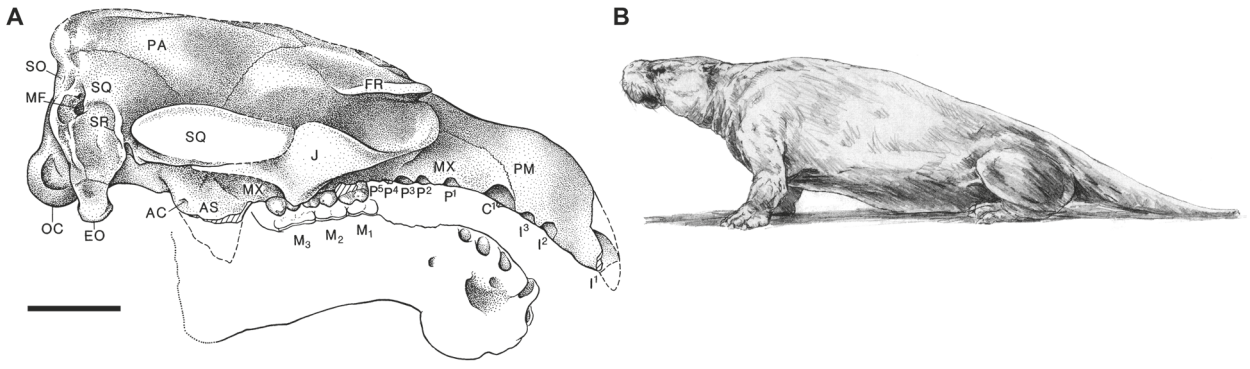

Figure 5. A, lateral view of newly reconstructed holotype skull of *Protosiren fraasi* (modified after Gingerich *et al.,* 1994). Scale bar equals 5 cm. **B**, life-sketch of *Protosiren* (© Calvert Marine Museum, 2002). Not to scale. *Anatomical abbreviations for Figure 5A*: **AC**, alisphenoid canal; **AS**, alisphenoid; **C^1**, upper canine; **EO**, exoccipital; **FR**, frontal; **$I^{1–3}$**, upper incisor 1–3; **J**, jugal; **$M_{1–3}$**, lower molar 1–3; **MF**, mastoid foramen; **MX**, maxilla; **OC**, occipital condyle; **$P^{1–5}$**, upper premolar 1–5; **PA**, parietal; **PM**, premaxilla; **SO**, supraoccipital; **SQ**, squamosal; **SR**, sigmoid ridge.

protosirenids as amphibious quadrupeds (Abel, 1907; Domning & Gingerich, 1994; Gingerich *et al*., 1995). CT scans of *Protosiren fraasi* (Gingerich *et al*., 1994) present small olfactory bulbs and optic tracts, which are consistent with the diminished importance of olfaction and vision in an aquatic environment.

The Dugongidae are by far the most diverse and successful sirenian group (Domning, 1994). They were either associated with, or eventually replaced, the prorastomids and protosirenids and became widely distributed by the early Oligocene (Domning, 2001a). According to Domning's (1994) definition, the Dugongidae are conspicuously paraphyletic (Fig. 2) as is the extinct subfamily Halitheriinae that in turn comprises almost exclusively paraphyletic genera.

Halitheriine dugongids, which form the focus of this study, first appeared in the middle and late Eocene of the Mediterranean region with taxa like *Eotheroides* and *Eosiren* from Egypt (Abel, 1913; Sickenberg, 1934a; Gingerich, 1992; Zalmout & Gingerich, 2012) and *Prototherium* from Italy (De Zigno, 1875; Bizzotto, 2005). These early forms were fully aquatic as indicated by the complete loss of their functional hindlimbs and capable of swimming by dorsoventral undulations of their enlarged tail (Berta *et al*., 2006).

The oldest representative of *Halitherium*, *H. taulannense*, occurs in the late Eocene of France (Sagne, 2001a), and is regarded to be the sister taxon of all other derived Dugongidae (Domning & Aguilera, 2008). *Halitherium* is represented by several taxa from Central Europe as well as the West Atlantic (Domning, 1996). In particular, the early Oligocene *H. schinzii* is known by numerous skeletal material from various German localities (Fischer & Krumbiegel, 1982; Voss, 2008), especially the Mainz Basin (Lepsius, 1882; Heizmann, 1992), but also from Belgium (Sickenberg, 1934a), France (Bizzarini & Reggiani, 2010) and Hungary (pers. obs.). *Halitherium cristolii* from Upper Austria (Spillmann, 1959) and probably *H. alleni* from North America (Simpson, 1932a) are restricted to the late Oligocene as is *H. antillense* from Puerto Rico (Matthew, 1916) that is supposed to represent an additional but different *Halitherium*-species.

Among halitheriines, a close relationship between the late Oligocene *Caribosiren* from Puerto Rico (Reinhart, 1959) and the cosmopolitan genus *Metaxytherium* is supported by the cladistic analysis of Domning (1994; Fig. 2). The diverse *Metaxytherium*-species complex is known since the early Miocene and represented by European taxa like *M. krahuletzi* from the lower Miocene of Austria (Domning & Pervesler, 2001) and *M. serresii* from the Pliocene of France (Domning & Thomas, 1987; Carone & Domning, 2007). North American forms are known from the middle Miocene by *M. arctodites*, *M. crataegense* (= *M. calvertense*) (Kellogg 1966; Aranda-Manteca *et al*., 1994) and *M. floridanum* (Domning, 1988). Sea cows like *Metaxytherium* and *Halitherium* have strongly down-turned snouts with small upper incisor tusks and were most likely generalised bottom-feeders that probably consumed rhizomes of small to moderate sized seagrasses and seagrass leaves (Berta *et al*., 2006).

The oldest representative of the Dugonginae (Fig. 2), including the only extant species *Dugong dugon*, is known from the late Oligocene (Domning, 1994, 1996). Fossil members of this group have been found worldwide as indicated by taxa like *Rytiodus* from the early Miocene of France (Lartet, 1866) or the diverse Oligo-Miocene sirenian fauna from India (Fig. 6) with *Bharatisiren* (Bajpai & Domning, 1997; Bajpai *et al*., 2006), *Kutchisiren* (Bajpai *et al*., 2010) and *Domningia* (Thewissen & Bajpai, 2009). The Dugonginae apparently have their origin in the West Atlantic and Caribbean region, indicated by their most plesiomorphic member *Crenatosiren olseni* (Domning, 1994, 1997) from the late Oligocene of Florida (Fig. 2). Dugongines reached their highest diversity in this region from the late Oligocene until the early Pliocene (Fig. 6), documented by taxa like *Dioplotherium* (Domning, 1978, 1989a; Toledo & Domning, 1989), *Xenosiren* (Domning, 1989b), *Nanosiren* (Domning & Aguilera, 2008) and *Corystosiren* (Domning, 1990). These animals show the tendency to evolve large, blade-like and self-sharpening tusks, in contrast to the smaller, sub-conical tusks of Oligocene and Miocene halitheriines like *Halitherium* and *Metaxytherium,* and may have used them to dig up rhizomes of more robust seagrasses (Domning & Beatty, 2007).

In contrast, the exclusively marine living dugong is characterised by cheek teeth reduced to open-rooted, ever-growing pegs, whose vestigial enamel crowns soon wear off (Lanyon & Sanson, 2006). This species now prefers smaller seagrasses in the Indo-Pacific region and has apparently abandoned a diet of robust rhizomes due to its inability to chew these adequately. Fossil representatives of *Dugong* are only scarcely known (Fitzgerald, 2005) and therefore its origin still remains unclear (Domning, 1994; Fig. 2).

In the Miocene the dugongid subfamily Hydrodamalinae occurred in the fossil record and its monophyly is well supported (Domning, 1994; Fig. 2). The hitherto oldest known record of this group is represented by the genus *Dusisiren* from the Miocene of North and Central America and Japan (Domning, 1978; Takahashi *et al*., 1986; Kobayashi *et al*., 1995). The hydrodamalines are characterised by a new adaptive trend involving an increasing body size with a maximum of up to nine meters in the recently exterminated *Hydrodamalis* (Domning, 2001a). Hydrodamalinae show only a moderate snout deflection

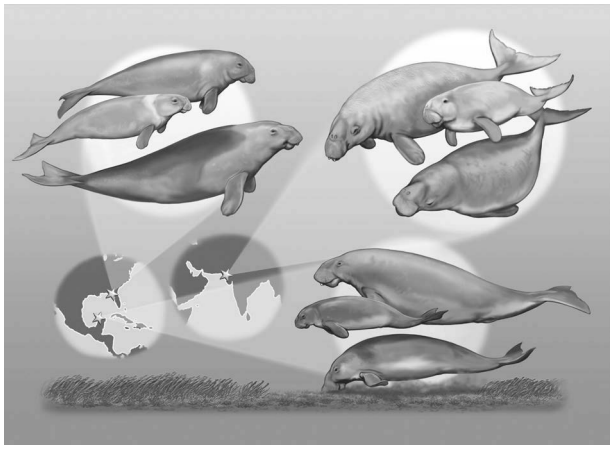

Figure 6. Illustration showing reconstructions of fossil dugongid assemblages from Florida (*Crenatosiren olseni*, *Metaxytherium* sp., and *Dioplotherium manigaulti*), India (*Bharatisiren kachchhensis*, *Kutchisiren cylindrica*, and *Domningia sodhae*) and Mexico (*Corystosiren varguezi*, *Nanosiren* cf. *N. garciae*, and *Dioplotherium* sp.) during the past ~26 million years (Velez-Juarbe *et al.,* 2012).

and lost their tusks gradually. They became adapted to temperate and even cold climates in the North Pacific region and departed from bottom-feeding to consuming kelp growing higher within the water column than seagrasses. This is consistent to a general cooling of the North Pacific climate and the respectively widespread replacement of seagrasses by kelps (Domning, 1978, 1989c; Domning & Furusawa, 1994).

The evolution of the Trichechidae was named a “speculative history” by Domning (1982: 599) and is still unresolved. They either derived from late Eocene or early Oligocene dugongids as assumed by Domning (1994; Fig. 2) or from middle Eocene protosirenids as hypothesised by Savage (1976), Domning (1982) and Sagne (2001b).

The extant genus *Trichechus* known since the Pliocene is represented by three living species inhabiting the coastal rivers and estuaries on both sides of the Atlantic. Whereas the West Indian manatee (*Trichechus manatus*) and the West African manatee (*Trichechus senegalensis*) occur in both marine and freshwater environments, the smallest of all Sirenia, the Amazon manatee (*Trichechus inunguis*), is restricted to the freshwater systems of the Amazonian basin (Domning & Hayek, 1986).

Within the Trichechidae, the manatees belong to the subfamily Trichechinae (Fig. 2), the earliest member of which possibly is *Potamosiren* from the middle Miocene of Colombia indicating a probable evolution of this clade in South America (Domning, 1982). *Potamosiren* still has three molars (Reinhart, 1951) lacking the continuous horizontal tooth replacement characteristic for later trichechines and suggesting that siliceous aquatic plants belonging to true grasses and constituting the principal diet of trichechines had not yet become an important part in its diet (Domning, 1982).

The evolution of unlimited numbers of supernumerary molars that are horizontally replaced throughout life appears first in *Ribodon* from the Mio-Pliocene of Argentina (Ameghino, 1883). In sirenians, this type of tooth wear is considered an adaptation to the newly abundant, but silicate-rich and therefore abrasive food source in South American rivers caused by the late Miocene uplift of the Andean orogeny (Domning, 1982). It is presumed that climatic changes in the West-Atlantic and Caribbean region caused the decrease of available seagrass and hence the extinction of the dugongines, whereas this process might have stimulated the evolution of trichechines in being more adapted to floating or emergent and submerged aquatic macrophytes (Domning, 1982, 2001b).

As a result of Domning’s (1994) cladistic analysis of the Sirenia, the subfamily Miosireninae is member of the trichechid clade (Fig. 2). The Miosireninae include the aberrant forms *Anomotherium* from the late Oligocene of Westphalia, Germany (Siegfried, 1965), and *Miosiren* from the early Miocene of Belgium (Sickenberg, 1934a). They are regarded as specialists in their diet compared to all other Sirenia in possessing reinforced palates possibly related to a durophagous life-style (Sickenberg, 1934a; Domning, 2001a). Their diet would be consistent with their comparatively high-latitude occurrence

in north-western Europe where they might have compensated seasonal deficiencies of nutrients in the available seagrass (Domning, 2001a).

The problematic *Halitherium*-species complex

Domning (1994) stated that his cladistic analysis (Fig. 2) should be regarded as a preliminary work pending further systematic revisions of the sirenian groups treated above. This is indicated by the most controversial parts, which are in urgent need of revision and that refer to the Eocene dugongids (and Eocene Sirenia in general), the incompletely resolved clade of the dugongines and the inter- and intrageneric relationships of *Metaxytherium*. Having a closer look at the paraphyletic Dugongidae, it turns out that the Halitheriinae constitute one of the most questionable sirenian groups. The type genus of this subfamily, *Halitherium* (Domning, 1996), is the main focus of this work.

Since the introduction of the genus *Halitherium* via the description of *H. schinzii* (Kaup, 1838), sirenian remains from the early Oligocene of Germany are generally assigned to this taxon, because it usually is assumed that it constitutes the only sea cow species that had evolved in that region to that time. Based on personal morphological studies of early Oligocene sirenians from Germany, however, an additional species recently has been postulated (Voss, 2012).

According to Domning (1994), the genus *Halitherium*, comprising *H. schinzii* and *H. cristolii*, is paraphyletic. Despite the tentativeness of Domning's (1994) cladistic analysis, the resulting classification forms a hitherto largely accepted systematic framework of Sirenia. For example, an additional taxon regarded as belonging to *Halitherium*, *H. taulannense* Sagne, 2001a, was subsequently included in a slightly modified version of Domning's (1994) analysis revealing this taxonomic grouping as still being paraphyletic, because *H. taulannense* occupies a position basal to *H. schinzii* and *H. cristolii* and all later dugongids (Domning & Aguillera, 2008). Additionally, the recent establishment of *H. taulannense* (Sagne, 2001a) indicates that the genus *Halitherium* is nevertheless considered monophyletic. The resulting lack of genus defining characters caused a very unsatisfying taxonomy of the specimens supposed by Voss (2012) to belong to a new species, and necessitates a closer examination of *Halitherium*.

INITIAL QUESTIONS AND OBJECTIVES OF THE STUDY

The present study predominantly addresses the monophyly of the genus *Halitherium* and how this taxon is defined. Additionally, the presence of two different sirenian species especially in the German and Belgian Oligocene is hypothesised (Voss, 2012) focussing on a revision of the type species *H. schinzii.* Therefore, the crucial questions of the project "Revision of the *Halitherium*-species complex" are:

1. Is *Halitherium* monophyletic?
2. Can the presence of different sirenian species be revealed in the early Oligocene of Central Europe?
3. What are the morphological similarities and differences between the species grouped in the genus *Halitherium*?

Resolving these questions includes the following key objectives:

1. to clarify the definition and origin of the genus *Halitherium*.
2. to re-examine the *Halitherium* morphology.
3. to review the systematics and taxonomy of *Halitherium*.
4. to clarify the phylogenetic position of the *Halitherium*-species complex within Sirenia.
5. to fathom the influence of the *Halitherium*-species complex on the phylogeny of the crown group sirenians.

To verify genus and species defining characters, three hitherto unconsidered taxa of the paraphyletic *Halitherium*-species complex (Domning, 1996) are incorporated in this study: *H. antillense*, *H. alleni* and *"Halitherium" bellunense*. The dugongine status of the latter species initially anticipated by Domning (1996) was recently supported by Sorbi (2007) and is again tested here. However, the status and systematic affinities of the other two species are still dubious and require further revision.

Further essential parts of this study are the re-examination of all taxa traditionally assigned to *Halitherium* and their morphological and systematic re-description. For example, many sirenian finds presently assigned to *H. schinzii* have not been investigated since e.g., Lepsius (1882) and Sickenberg (1934a). Additionally, new and as yet undescribed cranial and skeletal specimens are included in this thesis.

This work is complemented by investigations of skeletons of both extant genera (*Dugong* and *Trichechus*) considering intraspecific variability, ontogenetic changes and sexual dimorphism to evaluate these matters in the fossil sirenians in question.

The final and crucial aim of this study is the implementation of a phylogenetic analysis investigating as many sirenian taxa as possible and employing strict cladistic principles in order to clarify the intrageneric relationships of *Halitherium* and its systematic position within the Sirenia. Thereby, testing the already existing character-matrices based on Domning (1994), complement and amendment of these by personal observations form an initial basis for the revision of the *Halitherium*-species complex.

MATERIAL AND METHODS

Material examined

The morphological and systematic investigations for this doctoral thesis are based on three sources: a) the fossil species complex of the genus *Halitherium* being the focus of this project, b) the fossil taxa for comparison, which were considered as complete as possible, and c) the extant taxa for comparative studies, *Dugong* and *Trichechus*, comprising the recently exterminated *Hydrodamalis*.

For all taxa the available literature was recognised, however most species were personally examined following a thorough morphological approach. While it was aspired to review as many available specimens referred to any taxon as possible, the focus was especially placed on the investigation of holotypes.

With respect to *Halitherium* skeletal and dental material, accessible in museums and universities all over Europe, North America and Australia, was investigated and analysed, especially the German and Belgian sirenians obligatorily assigned to *H. schinzii*. Additionally, isolated elements, such as teeth and individual bones were considered. The *Halitherium* material available in the different collections refers not only to specimens already described, but also to undescribed individuals and sometimes hitherto unknown finds.

Conservation lagerstätten yielding *Halitherium* remains are the upper Eocene of Taulanne (Alpes-de-Haute-Provence, France), the lower Oligocene of the Mainz Basin and the Lower Rhine area (western Germany), the Bay of Leipzig (eastern Germany), the Antwerp and East Flanders Provinces in North Belgium, the upper Oligocene of the Linz sand quarries (Austria), probably the Ashley River phosphate deposits near Charleston (South Carolina, USA), the West Bank of Rio Jacaguas (Puerto Rico), and the lower Miocene of the glauconitic sands near Belluno (Italy).

The fossil and extant sirenian materials cited were derived from the collections listed in the Appendices 1 and 2.

General methodology

The material studied in person was described, measured and photographed. The macroscopic descriptions consider the cranial and postcranial osteology making up the basis for the evaluation of morphological characters used in the subsequent cladistic analyses. The sequence of morphological descriptions is provided as follows considering the respective state of preservation of the available material: skull, lower jaw, dentition, vertebrae, ribs, sternum, scapula, bones of the forelimb, pelvis and, if present, bones of the hindlimb. Measurements were carried out with either a digital calliper of standard size (max. 150 mm) or a large scale calliper (up to 200 cm). All measurements are quoted in

millimetres, unless otherwise stated, and listed in the Appendix 3.

The images were taken with a digital camera in all relevant views mostly using the macro-function under normal light or a special photo-desk with camera-stand and lights. Preparing line drawings of important skeletal elements or complete skulls in different views, respectively, complement the documentation of the fossil Sirenia.

Casts of the skull, lower jaw and the cervical series of a well preserved *Halitherium* individual were produced to allow direct comparative investigations. With respect to hitherto unknown *Halitherium* specimens stored in certain collections, the preparation of a cranium from the Forschungsinstitut und Naturmuseum Senckenberg, Frankfurt a. M. (FIS) was arranged and implemented by the Museum für Naturkunde Berlin (MB) to improve the acquisition of morphological data. Another, nearly complete skeleton was prepared in the Hessisches Landesmuseum Darmstadt (HLMD).

For the documentation and evaluation of intraspecific and intrageneric variations the morphometric data sets from Spain & Heinsohn (1974), Spain *et al.* (1976) and Domning & Hayek (1986) on the extant *Dugong* and the three living *Trichechus* species, respectively, were studied concentrating on the size allometry of the skulls and the lower jaws. Ontogenetic changes and morphological differences due to sexual dimorphism were seized on the basis of specimens of known age and known sex in order to enhance comparative analyses within the *Halitherium*-species complex.

The layout and formatting of this thesis follows the instructions for authors of the *Zoological Journal of the Linnean Society*.

Phylogenetic methodology

In this study, the members of the clade Sirenia are defined by using the total group concept from Jefferies (1979) distinguishing between a crown group and a stem group. The crown group is monophyletic and consists of all extant sirenians, their last common ancestor and all of its descendents. Its paraphyletic complement of extinct taxa is called the stem group. Consequently, stem group sirenians are all taxa that precede the major cladogenesis event forming the crown group, but are more closely related to crown group sirenians than to any other extant clade.

Taxon sampling

The phylogenetic interrelationships of the Sirenia, especially of the taxa originally referred to the genus *Halitherium*, were explored by applying cladistic principles (Wiley *et al*., 1991). For the cladistic analyses implemented in this thesis, the phylogeny of the order Sirenia provided by Domning (1994) is especially considered. The subsequent studies for several subsets of the order from Bajpai & Domning (1997), Sagne (2001b), Furusawa (2004), Domning & Aguilera (2008) and Sorbi (2007) are taken partially into account. Additionally,

the cladistic analyses are supposed to be performed under the most objective criteria. Accordingly, the set of taxa of the previous studies was adopted, but reassessed and extended by the incorporation of recently discovered sirenians and entirely unconsidered species up to now.

The proboscideans *Phosphaterium escuilliei* and *Numidotherium koholense* were chosen for outgroup comparison following the hypothesis of a sister grouping between Proboscidea and Sirenia (e.g., Asher *et al*., 2003). Both taxa are combined to form a single, artificial outgroup-complex on the basis of their great morphological consistency and complementarity, and the inability of the used software to consider more than a single outgroup.

The recently described and earliest known proboscidean *Eritherium azzouzorum* Gheerbrant, 2009 is excluded from the outgroup due to its inadequate preservation. *Phosphaterium escuilliei* from the lower Eocene Ouled Abdoun phosphatic basin of Morocco occupies a similarly basal position one rank higher than *Eritherium* (Gheerbrandt & Tassy, 2009; Gheerbrandt, 2009). This species is represented by abundant cranial and dental material, comprising partial skulls and mandibles, making it to one of the best known fossil representatives of that order (Gheerbrant *et al*., 2005b).

Numidotherium comprises two species that also are close to the base of Proboscidea (Court, 1995). From both taxa, the late lower or early middle Eocene *N. koholense* makes up a considerable faunistic part of its type locality El Kohol in southern Algeria (Mahboubi *et al*., 1984, 1986; Court, 1995), and is anatomically one of the best documented proboscideans. This species is known, on the one hand, by complete skulls and, on the other, by postcranial material (Court, 1994a), which complement and enhance the available dataset and, therefore, renders this taxon of particular importance for the cladistic treatment of the outgroup.

The ingroup comprises 56 taxa including three invalid *Halitherium* species, *H. bronni* (SMNS 1539), *H. pergense* (LI 1899/11) and *H. abeli* (LI 1939/257). These species are currently regarded as synonymous to *H. schinzii* (*H. bronni*) and *H. cristolii* (*H. pergense* and *H. abeli*) and were included separately in the new dataset to test their status and affinities. The taxon *H. schinzii*, or those specimens commonly assigned to this species, is incorporated on the basis of individuals first and represented by ten articulated specimens or partial skeletons, respectively. There is indeed much more skeletal material known that is assigned to *H. schinzii*, but the majority consists of only isolated elements. Therefore, this study focusses on a representative set of *H. schinzii* individuals that are preferable the most complete and well preserved available. This method is applied in order to prove the hypothesis of two different morpho-species in the lower Oligocene of Central Europe. The Central and North American species *H. alleni* Simpson, 1932a and *H. antillense* Matthew, 1916 are added into a cladistic analysis for the first time. An overview on the *Halitherium* specimens investigated in this study is given in the Appendix 1 showing their

original taxonomic assignment, locality and age. A list of all analysed sirenian taxa and outgroups is provided in the Appendix 2 including references, distribution and age.

Unlike Domning (1994), some fossil skeletal elements are not taken into account for the morphological investigations and scoring of the ingroup taxa due to their unclear taxonomic position. For example, a tusk and ribs of specimens from Jamaica referred to *Prorastomus sirenoides* (Savage *et al*., 1994) are excluded in favour of an objective evaluation of this taxon. These individual elements are neither from the taxon's type locality nor are they present in the holotype specimen and, therefore, not directly comparable. The same applies to maxillary fragments assigned to *Potamosiren* and *Ribodon*. Domning (1994, 1996) synonymised *Metaxytherium ortegense* represented by a left maxillary fragment including M1–M3 with *Potamosiren magdalenensis*, whose type and hitherto only specimen is however a left mandible. Additionally, both taxa are from Colombia, but not from the same locality. Furthermore, a right maxillary fragment from North Carolina referred to *Ribodon* sp. (Domning, 1982) is included in the scoring of *Ribodon limbatus* (Domning, 1994). However, the latter is only known by two left mandibles and isolated maxillary teeth from Argentina.

Some taxa are excluded *á priori* from cladistic treatment, because their scarce fossil record is considered here to hamper a robust cladistic analysis and/or there are reasonable doubts on their validity. This mainly refers to three species of *Protosiren* from the middle Eocene (Lutetian), *P. minima* from France (see Domning, 1996), and *P. eothene* (Zalmout *et al*., 2003) and *P. sattaensis* (Gingerich *et al*., 1995) from Pakistan. *Protosiren minima* relates to three isolated molars only (Sickenberg, 1934a: fig. 36). The two Pakistan forms are merely known by postcranial elements comprising vertebrae, ribs and, with respect to *P. sattaensis*, the pelvic bones, which, however, are considered diagnostic to a minor degree (Domning & Ray, 1986; Domning, 1994).

Another taxon, *Eosiren abeli* Sickenberg, 1934a from the middle Eocene of Cairo (Egypt), is excluded, because it is most likely synonymous with *Eotheroides aegyptiacum* Abel, 1913. Even Sickenberg (1934a) himself noted that the association of the holotype, an isolated molar, with several other elements (vertebrae, skull and mandible) is questionable. Putting aside the fact that the holotype together with the referred skull and mandible cannot be re-evaluated anymore due to their destruction in World War II (Domning, 1996), their original assignment to the taxon *Eotheroides aegyptiacum* by Abel (1913) seems to be more likely based on their apparently similar locality, stratigraphy and age.

The species *Metaxytherium subapenninum* is excluded *á posteriori* from the phylogenetic analyses, because it revealed a disturbing impact on the stability of the phylogenies. Clarifying the cause of this problem is beyond the focus of this study and will be left open until later treatment. However, to enhance transparency, *M. subapenninum* is included in the data matrix showing the character states according to the morphological review by Sorbi (2007) and Sorbi *et al.* (2012) considering discrepancies between the

descriptions and scoring of characters. Here, it is worth noting that some other taxa and specimens, known only by very incomplete material, are likewise subsequently excluded *á posteriori* from the cladistic analyses, as detailed in the chapter “Phylogenetic analyses”. Their reduced value for a cladistic analysis is indicated, amongst other things, by the high degree of question marks in the character matrix shown in the Appendix 4.

Additionally, subspecies like *Trichechus manatus bakerorum* Domning, 2005 are not incorporated into the present study considering the species level as the basic and smallest unit in biological classification. With the exception of *Halitherium bellunense* and *Dusisiren reinharti*, only known from a juvenile, and *Hydrodamalis cuestae*, *Nanosiren sanchezi* and a few specimens of the representative set of *H. schinzii* that are of subadult age, the cladistic treatment of all taxa is preferably focussed on adults.

By meeting the criteria of completeness as close as possible, the following taxa are newly added to the cladistic analyses implemented in this study: *Pezosiren portelli, Ashokia antiqua, Eotheroides lambondrano, Eotheroides babiae, Halitherium alleni* and *Halitherium antillense*.

In this study, the classification provided below is based on Domning (1996), the PBDB (http://www.paleodb.org/) and personal completions taken from recent publications. The smallest unit given in this classification is the genus level referring to the Appendix 2 for indication of species.

Order **Sirenia** Illiger, 1811
- Family **Prorastomidae** Cope, 1889
  - Genus ***Pezosiren*** Domning, 2001c
  - Genus ***Prorastomus*** Owen, 1855
- Family **Protosirenidae** Sickenberg, 1934a
  - Genus ***Ashokia*** Bajpai, Thewissen, Kapur, Tiwari & Sahni, 2009
  - Genus ***Protosiren*** Abel, 1907
- Family **Dugongidae** Gray, 1821
  - Subfamily **Halitheriinae** (Carus, 1868) Abel, 1913
    - Genus ***Caribosiren*** Reinhart, 1959
    - Genus ***Eosiren*** Andrews, 1902
    - Genus ***Eotheroides*** Palmer, 1899
    - Genus ***Halitherium*** Kaup, 1838
    - Genus ***Metaxytherium*** De Christol, 1840
    - Genus ***Prototherium*** De Zigno, 1887
  - Subfamily **Dugonginae** (Gray, 1821) Simpson, 1932a
    - Genus ***Bharatisiren*** Bajpai & Domning, 1997
    - Genus ***Corystosiren*** Domning, 1990
    - Genus ***Crenatosiren*** Domning, 1991a

Genus ***Dioplotherium*** Cope, 1883
Genus ***Domningia*** Thewissen & Bajpai, 2009
Genus ***Dugong*** Lacépède, 1799
Genus ***Kutchisiren*** Bajpai, Domning, Das, Vélez-Juarbe & Mishra, 2010
Genus ***Nanosiren*** Domning & Aguilera, 2008
Genus ***Rytiodus*** Lartet, 1866
Genus ***Xenosiren*** Domning, 1989b
Subfamily **Hydrodamalinae** (Palmer, 1895 [1833]) Simpson, 1932a
Genus ***Dusisiren*** Domning, 1978
Genus ***Hydrodamalis*** Retzius, 1794
Dugongidae *incertae sedis*
Genus ***Sirenavus*** Kretzoi, 1941
Family **Trichechidae** Gill, 1872 (1821)
Subfamily **Miosireninae** Abel, 1919
Genus ***Anomotherium*** Siegfried, 1965
Genus ***Miosiren*** Dollo, 1889
Subfamily **Trichechinae** (Gill, 1872 [1821]) Domning, 1994
Genus ***Potamosiren*** Reinhart, 1951
Genus ***Ribodon*** Ameghino, 1883
Genus ***Trichechus*** Linnaeus, 1758

Character coding

The cladistic analyses in this study were carried out on the basis of 202 morphological characters referring to the skull, mandible, dentition and the postcranium. Almost all characters from previous studies, especially those applied by Domning (1994) are incorporated into the cladistic analyses presented here. After verifying and revising all of them, most have to be changed, emended and simplified. Complexes of anatomical characteristics recorded in multi-state characters are re-assessed and transformed into binary characters. The method of splitting multi-state characters is justified here in several ways. One of the most important arguments refers to the prevention of contradictions and duplications or overlapping of character states. Additionally, the single states of multi-state characters given by Domning (1994) sometimes contain a high complexity making them ambiguous and call in question their conclusiveness. Such characters with a less ideal fitting refer, for example, to numbers 36 and 43 or numbers 136 and 142 from Domning (1994). According to personal observations, some character states are considered either non-existent or unsubstantiated mostly due to the insufficient state of preservation of the fossil material. This refers for example to character 125[0] from Domning (1994). Finally, multi-state characters are split to facilitate the coding of taxa according to exclusion criteria, i.e. the preserved material of certain taxa permit unam-

biguous statements for one of the given character states while missing information for the others.

The polarity of character states was indirectly determined by outgroup comparison (Maddison *et al*., 1984) setting all available character information for the outgroup to [0]. Consequently, character state [0] designates the plesiomorphic condition, [1] stands for the derived state and [?] indicates uncertain or missing information in the data matrix (Appendix 4). Some features of *Numidotherium koholense* are more derived than those of *Phosphaterium escuilliei* (Gheerbrant & Tassy, 2009). This is indicated in the present data matrix of the outgroup by seven characters that are scored as polymorphisms. In that case, i.e. if the character states of both outgroup taxa are incongruent, state 0 refers to the more ancestral *Phosphaterium*.

A few non-accessible characters of the exclusively extinct outgroup members were not deleted from the matrix, but coded as [?]. Due to the fact that the majority of these non-accessible characters are not available in the oldest known fossil sirenian, *Prorastomus*, the *á priori* model of ingroup commonality is favoured in this study against the stratigraphic criterion (Bryant, 2001). By ingroup comparison, the character state that occurs in the largest number of taxa within the ingroup is set to [0]. In contrast to the methodical approaches by Domning (1994) to score polymorphisms unambiguously according to the majority of present states, entering polymorphism into the character matrix in order to keep objective criteria here seizes intraspecific variation.

The quantitative phylogenetic settings are summarised as follows: Two outgroups, 56 ingroup species in addition to ten sirenian specimens are included in the present dataset and applied to 202 binary characters in total. The character set is divided into 156 cranial, 26 dental and 20 postcranial characters, 43 thereof are added here for the first time. All character states were treated as unweighted, unordered and non-additive. The cladistic analyses using parsimony were performed with NONA 2.0 (Goloboff, 1999) implemented by WinClada software version 1.0000 for PC of Nixon (1999–2002). Cladograms were produced by means of heuristic search with tree-bisection-reconnection (TBR) branch-swapping under the conditions of 1,000 replicates and 10 trees to keep per replicate. A bootstrap analysis (Felsenstein, 1985) was exercised to test the statistical robustness of the final tree topology using heuristic search with random step-wise addition and 10 repetitions for 1,000 search procedures. The data matrix with all taxa and characters analysed is shown in the Appendix 4.

Anatomical abbreviations

a, acromion; **ac**, anterior *cingulum*; **acc**, accessory cuspules; **act**, *acetabulum*; **amef**, accessory mental foramen; **amr**, ascending mandibular ramus; **an**, auditory (VIII) nerve; **ang**, angle; **as**, alisphenoid; **asc**, alisphenoid canal; **bf**, bony *falx cerebri*; **bigr**, bicipital

groove; **bl**, break line; **bo**, basioccipital; **bs**, basisphenoid; **C/c**, upper/lower canine or alveolus; **C1–7**, cervical vertebra 1–7; **Ca1–26**, caudal vertebra 1–26; **cap**, *caput*; **capi**, *capitulum*; **cnf**, coronoid foramen; **cnfos**, coronoid fossa; **cnp**, coronoid process; **col**, *collum*; **colsc**, *collum scapulae*; **corp**, coracoid process; **decr**, deltoid crest; **depecr**, deltopectoral crest; **der**, distal epiphysis of radius; **detu**, deltoid tuberosity; **dex**, distal extremity; **dh**, diaphysis of humerus; **dorma**, dorsal margin; **DP1–5/dp1–5**, upper/lower deciduous premolar or alveolus 1–5; **dr**, diaphysis of radius; **du**, diaphysis of ulna; **e**, ethmoid; **eam**, external auditory meatus; **elf**, endolymphatic foramen; **eo**, exoccipital; **exocr**, external occipital crest; **exopr**, external occipital protuberance; **f**, frontal; **finc**, *foramen incisivum*; **fl**, *foramen lacerum*; **fm**, *foramen magnum*; **fn**, facial (VII) nerve; **fo**, *fenestra ovalis*; **fob**, *foramen obturatum*; **fproc**, frontal process; **fpsut**, frontoparietal suture; **fs**, fracture surface; **gcav**, glenoid cavity; **gt**, greater tubercle; **hgf**, hypoglossal foramen; **hmr**, horizontal mandibular ramus; **hy**, hypocone; **hy-mcl**, hypocone-metaconule; **I1**, first upper incisor; **ifsut**, interfrontal suture; **il**, ilium; **indsq**, indentation of sqaumosal; **iof**, infraorbital foramen; **iosp**, interosseus space; **isch**, ischium; **ispf**, infraspinous fossa; **j**, jugal; **jzp**, zygomatic process of jugal; **l**, lacrimal; **latec**, lateral epicondyle; **lfor**, lacrimal foramen; **lP1–5**, left upper premolar 1–5; **lt**, lower tubercle; **m**, malleus; **M1–3/m1–3**, upper/lower molar or alveolus 1–3; **ma**, mandibular angle; **mas**, masticating surface; **mc**, mandibular condyle; **mcan**, mandibular canal; **mcaud**, *margo caudalis*; **mcl**, metaconule; **mcran**, *margo cranialis*; **mdf**, mandibular foramen; **mdor**, *margo dorsalis*; **me**, metacone; **medec**, medial epicondyle; **mef**, mental foramen; **mf**, mastoid foramen; **mfos**, mandibular fossa; **ml**, metaloph; **mpmsut**, maxillopremaxillary suture; **mrf**, mesorostral fossa (= external nares); **msym**, mandibular symphysis; **mx**, maxilla; **n**, nasal; **ncr**, nuchal crest; **nproc**; nasal process; **occ**, occipital condyle; **ol**, olecranon; **olf**, olecranon fossa; **os**, orbitosphenoid; **osp**, occipital spine; **otcr**, orbito-temporal crest; **p**, parietal; **P1–5/p1–5**, upper/lower premolar 1–5; **pa**, paracone; **pal**, palatine; **parop**, paroccipital process; **pb**, posterior basin; **pc**, posterior *cingulum*; **per**, periotic; **pet**, petrosal; **pft**, *processus fonticulus*; **pgp**, postglenoid process; **pl**, proto-loph; **plf**, perilymphatic foramen; **pm**, premaxilla; **pmsym**, premaxillary symphysis; **pop**, postorbital process; **pr**, protocone; **prl**, protoconule (= paraconule according to Thenius, 1998); **prop**, preorbital process; **prtm**, promontorium; **prv**, *processus retroversus*; **ps**, presphenoid; **pt**, pterygoid; **ptp**, pterygoid process; **ptymp**, posttympanic process; **pub**, pubis; **pyr**, pyramid; **r**, radius; **R1–19**, rib 1–19; **rart**, articulation for rib; **scf**, supracondylar fossa; **scsp**, scapular spine; **sfc**, suprafacial commissure; **sln**, semilunar notch; **so**, supraoccipital; **soe**, sphenooccipital eminence; **sop**, supraorbital process; **sq**, squamosal; **sqzp**, zygomatic process of squamosal; **sr**, sigmoid ridge; **sspf**, supraspinous fossa; **suted**, suture between epiphysis and diaphysis; **t**, tympanic; **T1–19**, thoracic vertebra 1–19; **tcr**, temporal crest; **tf**, fragment of tympanic; **to**, *tentorium osseum*; **tproc**, tentoric process; **trsul**, transverse sulcus; **tt**, *tegmen tympani*; **tu**, tuberosity; **tub**, *tuberculum*; **tv**,

transverse valley; **u**, ulna; **v**, vomer; **vprt**, ventral protuberance; **zobr**, zygomatic-orbital bridge; **?**, unknown element.

Institutional abbreviations

AGM, Geologisch Museum Artis, Amsterdam (Netherlands); **ALMD**, Aquazoo Löbbecke-Museum Düsseldorf (Germany); **AMNH**, American Museum of Natural History New York (USA); **BSPG**, Bayerische Staatssammlung für Paläontologie und Geologie München (Germany); **CDGG**, private collection Dieter Grüll, Gernsheim (Germany); **CGM**, Cairo Geological Museum (Egypt); **DM**, Doberg-Museum Bünde, Westfalen (Germany); **FCM**, Facultad de Ciencias Marinas, Universidad Autónoma de Baja California, Ensenada, Baja California (Mexico); **FIS**, Forschungsinstitut und Naturmuseum Senckenberg, Frankfurt a. M. (Germany); **FMD**, Fossilienmuseum Dotternhausen (Germany); **GIPT**, Paläontologische Sammlung der Eberhard Karls Universität Tübingen (Germany); **GPL**, Geologisch-Paläontologische Sammlung der Universität Leipzig (Germany); **GPMH**, Geologisch-Paläontologisches Museum der Universität Heidelberg (Germany); **GSI, Palaeontology Division-I**, Geological Survey of India, Kolkata (India); **GU**, Garyounis University, Department of Geology, Benghazi (Libya); **HLMD**, Hessisches Landesmuseum Darmstadt (Germany); **HMH**, Höbart-Museum, Horn (Austria); **IGM**, Instituto de Geologia, Universidad Nacional Autonoma de Mexico, Mexico City; **IITR-SB**, Indian Institute of Technology, Roorkee, Department of Geosciences, Uttaranchel (India); **IRSNB**, Institut Royal des Sciences Naturelles de Belgique, Bruxelles (Belgium); **JCU,** James Cook University, Townsville, Queensland (Australia); **KME**, Krahuletz-Museum, Eggenburg (Austria); **KÜH**, specimens in KME collection; **LI**, Oberösterreichisches Landesmuseum Linz (Austria); **LS RLP**, Landessammlung Rheinland-Pfalz (Germany); **LUVP/MP**, Vertebrate Paleontology Collection, Geology Department, Lucknow University, Lucknow (India); **MB**, Museum für Naturkunde Berlin (Germany); **MCZ**, Museum of Comparative Zoology, Harvard University, Cambridge, MA (USA); **MGPD**, Museo dell'Istituto di Geologia e Paleontologia, Padova (Italy); **MNHM**, Mainzer Naturhistorisches Museum (Germany); **MNHN**, Muséum National d'Histoire Naturelle (et Grande Galerie de l'Évolution) Paris (France); **MPEG**, Museu Paraense Emilio Goeldi, Belém (Brazil); **MSNVE**, Museo di Storia Naturale di Venezia; **MTQ**, Museum of Tropical Queensland, Townsville, Queensland (Australia); **MTTM**, Magyar Természettudományi Múzeum, Budapest (Hungary); **MWNH**, Museum Wiesbaden, Naturhistorische Landessammlung (Germany); **NHMB**, Naturhistorisches Museum Basel (Switzerland); **NHMUK**, National History Museum London (UK); **NL**, Naturkundemuseum Leipzig (Germany); **NMDU**, Naturwissenschaftliches Museum Duisburg (Germany); **NMV**, National Museum Victoria, Melbourne (Australia); **NRM**, Naturhistoriska Riksmuseet Stockholm (Sweden); **PMN**, Paläontologisches Museum Nierstein (Germany); **QB**, Quadrat Bottrop, Museum für Ur-und Ortsgeschichte

(Germany); **RGHP**, Réserve Géologique de Haute-Provence, Digne (France); **SAM**, South Australian Museum Adelaide (Australia); **SC**, South Carolina State Museum, Columbia (USA); **SDSM**, South Dakota School of Mines, Rapid City (USA); **SMNS**, Staatliches Museum für Naturkunde Stuttgart (Germany); **SZ**, Steinmetzhaus Zogelsdorf in Zogelsdorf (Austria); **TA**, Takasato Archive, Yama County, Fukushima (Japan); **UA**, Université d'Antananarivo, Antananarivo (Madagaskar); **UCMP**, University of California Museum of Paleontology, Berkeley, California (USA); **UF**, Florida Museum of Natural History, University of Florida, Gainesville (USA); **UF/FGS**, Florida Geological Survey now housed in the UF; **UNEFM**, Universidad Nacional Experimental Francisco de Miranda, Coro (Venezuela); **UO**, University of Oran (Algeria); **USNM**, Department of Paleobiology, U.S. National Museum of Natural History, Smithonian Institution, Washington, D.C. (USA); **YPM**, Yale Peabody Museum, New Haven, Connecticut (USA).

HISTORICAL REVIEW OF *HALITHERIUM*

The early Oligocene sea cow *Halitherium schinzii* Kaup, 1838 (Europe, mainly Germany and Belgium) forms together with *H. cristolii* Fitzinger, 1842 (late Oligocene of Upper Austria) and *H. taulannense* Sagne, 2001a (late Eocene of France) the *Halitherium*-species complex presently regarded as valid in the European Palaeogene. According to the currently used systematic framework, *H. schinzii* is the type species of the genus *Halitherium*, which is subsequently the type genus of the extinct subfamily Halitheriinae (Abel, 1913; Domning, 1996).

Kaup & Scholl (1834) were the first, who mentioned a not otherwise specified tooth from the early Oligocene of Germany near Flonheim (Mainz Basin) as *Pugmeodon schinzii*. However, both the genus and species names are *nomina nuda* according to Domning (1996), because these authors neither provided a description nor a figure of the respective tooth. A description and figure of a premolar (HLMD-WT Az 48) under the same species name was given by Kaup (1838), who subsequently transferred it to the genus *Halitherium*, which seemingly is the correct taxon name as indicated by later studies (e.g., Kaup, 1855; Lepsius, 1882; Sickenberg, 1934a).

Therefore, Domning (1987) opened the nomenclatural case 2569 to apply for a proper designation of the holotype of *Pugmeodon schinzii*. By Opinion 1535 of the Bulletin of Zoological Nomenclature Volume 46 (ICZN, 1989), all previous designations of type species for the nominal genus *Halitherium* Kaup, 1838 are set aside and *Pugmeodon schinzii* Kaup, 1838 is designated as type species under the plenary powers. Furthermore, the names *"Halitherium"* and *"schinzii"* are ruled to be placed on the Official lists and indexes of names and works in Zoology by the International Commission on Zoological Nomenclature (2001).

The preservation and nature of the holotype of *H. schinzii* pose major problems when dealing with *Halitherium*. Voss (2010) already postulated that no significant taxonomic definition can be deduced from the premolar HLMD-WT Az 48 and, consequently, a diagnosis for this species and genus currently is unavailable. A diagnosis limited to premolar characters is impossible, because the premolar can be identified only insufficiently due to its high degree of wear. For example, it remains uncertain whether the premolar comes from the upper or lower, or the right or left jaw. The exact position within the tooth arcade is also not identifiable. This is mainly due to the fact that complete and unworn tooth series of *H. schinzii* and other fossil sirenian taxa are unknown, often only revealing the root alveoli in the bone (e.g., Spillmann, 1959). Mostly, preserved premolars are isolated and their degree of abrasion is often very variable. Thus the diagnostic value of the holotype of *H. schinzii* and its assignment to a certain taxon remains ambiguous as discussed by Voss (2010) and later in this thesis.

Controversies concerning the species content and identification of species within the genus also exist. Considerable intra- and interspecific morphological variations have

been postulated for both, *H. schinzii* and *H. cristolii* since the middle of the 19th century (e.g., Kaup, 1855; Lepsius, 1882; Abel, 1904; Sickenberg, 1934a; Spillmann, 1959; Fischer & Krumbiegel, 1982). Attempted revisions of *H. schinzii* consequently resulted in the description of numerous specimens forming the basis of new species, as are the skull roofs of *H. kaupi* and *H. bronni* (Krauss, 1858), respectively. However, those are considered to be not valid and synonymous with *H. schinzii* by Domning (1996). Hartlaub (1886) erected another species, *Manatherium delheidi*, based on cranial remains from the lower Oligocene of Antwerp (North Belgium) in comparison with *H. schinzii* from the Mainz Basin (Germany). However, Sickenberg (1934a) revised Hartlaub's (1886) species, focussing on aspects of juvenile stages and intraspecific variability. Sickenberg (1934a), who already mentioned that a revision of *Halitherium* and *H. schinzii* was necessary, provided a comprehensive and critical review of the Belgian material, but without considering a separation on species level. According to his investigations, all known Belgian records belong exclusively to smaller animals. Therefore, Sickenberg (1934a: 271) defined separate morphological groups, *"forma typica"* for the German and *"forma delheidi"* for the Belgian one, and assigned both to *H. schinzii* (see also Domning, 1996). The most recent new combination for *H. schinzii* refers to skeletal material from the lower Oligocene of France known as *H. schinzii lareolensis* (Pilleri, 1987; Domning, 1996).

The taxonomic history of *H. cristolii* is similar to that of *H. schinzii* although to a lesser extent. For example, Toula (1899) erected the species *H. pergense* on the basis of a fragmentary skull roof from the late Oligocene of Perg (Upper Austria). Conversely, Abel (1904) assigned all finds from northern Austria to a single species, *H. cristolii*, and attributed skeletal differences to intraspecific variability or ontogeny. Spillmann (1959), however, proposed a new species, *H. abeli*, based on a lower jaw from Linz (Upper Austria), and simultaneously confirmed the validity of *H. pergense*. In the meantime, both species are considered to be synonyms of *H. cristolii* according to Domning (1996).

As mentioned above, the *Halitherium*-species complex is considered a paraphyletic assemblage (Domning, 1994) and has to be complemented with three additional taxa following the index of the Sirenia proposed by Domning (1996).

Halitherium antillense Matthew, 1916 is based on a fragment of a left mandible from the late Oligocene of Puerto Rico. Its status and affinities remain uncertain according to Domning (1996).

Simpson (1932a) revised *H. antiquus* Allen, 1926, which is based on a single upper molar considered to be undiagnostic. Consequently, Simpson (1932a) transferred all specimens to *H. alleni* and proposed a parietal-supraoccipital skullcap as its type. The holotype specimen and several other referred skullcaps and postcranial elements are from the Ashley River phosphate deposits near Charleston, South Carolina (USA), and probably of late Oligocene age (Simson, 1932a; Domning, 1996). These skeletal remains were subsequently assigned to *Felsinotherium alleni* by Kellogg (1996) due to

the dimensional correspondence of the cranial roof with *F. serresii*. Fondi & Pacini (1974) established the taxon *Metaxytherium alleni* in the course of the revision of the genus *Felsinotherium*. However, Domning (1996) also synonymised these taxa in favour of *H. alleni,* but stated its status and affinities to be uncertain.

"Halitherium" bellunense De Zigno, 1875 from Italy considered to be early Miocene in age (De Zigno, 1875) is regarded as being part of the *Halitherium*-species complex here. Even though Domning (1996) already postulated dugongine affinities for this taxon that recently were verified by Sorbi (2007), its status is unchanged until today.

This review of the genus *Halitherium* documents that the attempts of different authors to identify morphological distinctions on species level remain ambiguous until today. Domning (1996) claimed several synonyms, which, however, are lacking any justification for the invalidity of the new combinations that were carried out over the past decades. Therefore, these synonyms have to be regarded as subjective.

The debate on splitting and lumping of species currently referred to *H. schinzii* was revived by Voss (2009a, b, 2010, 2012), who stated that morphological variations within German and Belgian Oligocene Sirenia might be related to the species level. The presence of two morpho-species within the European lower Oligocene is hypothesised as a target for a revision of the genus *Halitherium*.

SYSTEMATIC PALAEONTOLOGY

Class Mammalia Linneaus, 1758
Superorder Afrotheria Stanhope *et al*., 1998
Mirorder Tethytheria McKenna, 1975

Order Sirenia Illiger, 1811

Remarks: In this study, Sirenia are composed of a stem group and a crown group based on a phylogenetic analysis of all sirenians (see chapter “Phylogenetic analyses”). The stem group representatives (*Prorastomus, Pezosiren, Protosiren, Ashokia, Sirenavus, Eotheroides, Prototherium,* and *Eosiren*) also include most of the taxa that were originally referred to the genus *Halitherium* (gen. nov. 1 *taulannense*, gen. nov. 2 spec. nov. 1, gen. nov. 2 *bronni*, gen. nov. 2 *alleni* and gen. nov. 3 *cristolii*). The crown group is subdivided in two suborders. One suborder is composed of 11 genera including *Crenatosiren, Nanosiren, Dugong, Rytiodus, Corystosiren, Bharatisiren, Domningia, Kutchisiren, Dioplotherium, Xenosiren,* and gen. nov. 4 *bellunense*, which was also previously referred to the genus *Halitherium*. The second suborder comprises the genera *Metaxytherium* and *Caribosiren* at the base of the sister group relationship between Trichechidae (*Anomotherium, Miosiren, Potamosiren, Ribodon,* and *Trichechus*) and the clade commencing the genera *Dusisiren* and *Hydrodamalis* (including the recently exterminated Steller’s sea cow).

Genus nov. 1

Type species: Halitherium taulannense (Sagne, 2001a).

Included species: Gen. nov. 1 *taulannense*.

Generic diagnosis: Premaxillary symphysis enlarged relative to the condylobasal length of the skull and strongly downturned. Lacrimal and premaxilla in contact. Nasals large, length of internasal suture greater than half the length of interfrontal suture exposed dorsally. Temporal crests prominent on frontal and parietal and reach nuchal crest. Intertemporal constriction strong with its maximum at the centre of the skull roof. Infraorbital foramen small and rounded. Palatines extend anteriorly beyond posterior edge of zygomatic-orbital bridge. Orbitotemporal crest present and prominent. Parietal longer than frontal in midline. Ventral extremity of jugal posterior to orbit. *Processus retroversus* moderately inflected. Mastoid foramen defined by exclusion of supraoccipital. Nuchal crest narrow and sharp-edged. External occipital protuberance indistinct and external occipital crest broad and undefined. Bony *falx cerebri* prominent, not flattening out anterad, but maintaining height along length of parietal. Mandibular symphysis broad. Ventral border of horizontal ramus moderately concave, sharply downturned anteriorly and not tangent to angle. Anterior

border of coronoid process extends slightly anterad. *Processus angularis* indistinct. One pair of upper incisors (I1) present with alveoli extending up to about half the length of the symphysis. Canines present. Permanent fifth premolar absent. Pelvis reduced with *acetabulum* forming a distinct concavity and a small *foramen obturatum* present.

Character states: 4[1]; 12[1]; 74[1]; 39[0]; 56[1]; 57[0]; 88[0]; 54[0]; 55[1]; 25[0]; 30[1]; 33[0]; 58[0]; 59[0]; 65[0]; 80[0]; 101[1]; 111[1]; 113[0]; 116[0]; 118[1]; 68[1]; 69[1]; 137[1]; 144[1]; 147[1]; 151[1]; 149[1]; 158[1]; 166[0]; 171[0]; 198[0]; 199[1].

Differential diagnosis: Differs from all other stem group representatives, except *Eosiren imenti* and gen. nov. 2, in possessing a nasal incisure, which is, additionally, small. The temporal crests are not weak in contrast to *Eosiren imenti*. Differs from gen. nov. 2 in showing concave sphenooccipital eminences and a mastoid foramen that is defined by the exoccipital and squamosal only. Differs from all crown group taxa in having external nares that are retracted and enlarged, but do not reach beyond the anterior margin of the orbit (except for *Anomotherium* and *Miosiren*, which share this character, and gen. nov. 4 *bellunense*, in which this character is not preserved). Differs from *Anomotherium*, *Miosiren*, and gen. nov. 4 *bellunense* in lacking a weak intertemporal constriction.

Gen. nov. 1 *taulannense* (Sagne, 2001a)

Halitherium taulannense; Sagne, 2001a: 471, figs. A–E.

Holotype: Complete cranium of an adult specimen (RGHP D040).

Paratype: Isolated cranial and postcranial material comprising: cranium RGHP D349 of an adult, mandible RGHP C001 of a subadult, mandible RGHP E.7.096a of an adult, scapula RGHP D350, humerus RGHP C035, radius and ulna RGHP C006, autopod RGHP D024 and innominate RGHP C050.

Referred material: RGHP: D345, D057, D349, D055, D275, C009, E.5.031, C054, D273, E.9.001; AGM: 13, 26. Sagne (2001b) considered a total of 16 skulls and cranial elements as well as nine mandibles and mandibular fragments. In this study, only those specimens are listed (Appendix 1) that were either personally investigated and/or described on the basis of Sagne (2001b).

Type horizon and locality: Found in Priabonian (late Eocene) marine calcareous sediments approximately 1 km northwest of the village Taulanne, near Castellanne, Alpes-de-Haute-Provence, France.

Range and distribution: Known only from type locality.

Emended diagnosis: As for the genus.

Description

Figures 7–16; Appendix 3

This species was recently established with its main morphological features summarised by Sagne (2001a). Therefore, the following description of the skeletal material is only briefly treated focussing on the holotype and paratypes, and aiming at the systematically important features for this study.

Premaxilla: The external nares are retracted and enlarged up to the level of the anterior margin of the orbit (2[1]) and show no indentations anteriorly by the nasal processes of the premaxilla (11[1]; Fig. 7). The latter are thin and tapering posteriorly by having lengthy overlap with the frontals and nasals (17[0]; 20[1]). The rostrum is enlarged relative to the condylobasal skull length (4[1]) and longer than half the total length of the premaxilla (5[1]). In lateral view (Fig. 8B), the premaxillary symphysis is strongly downturned with an angle of about 57° in the holotype specimen (12[1]) and shows a middorsal ridge along

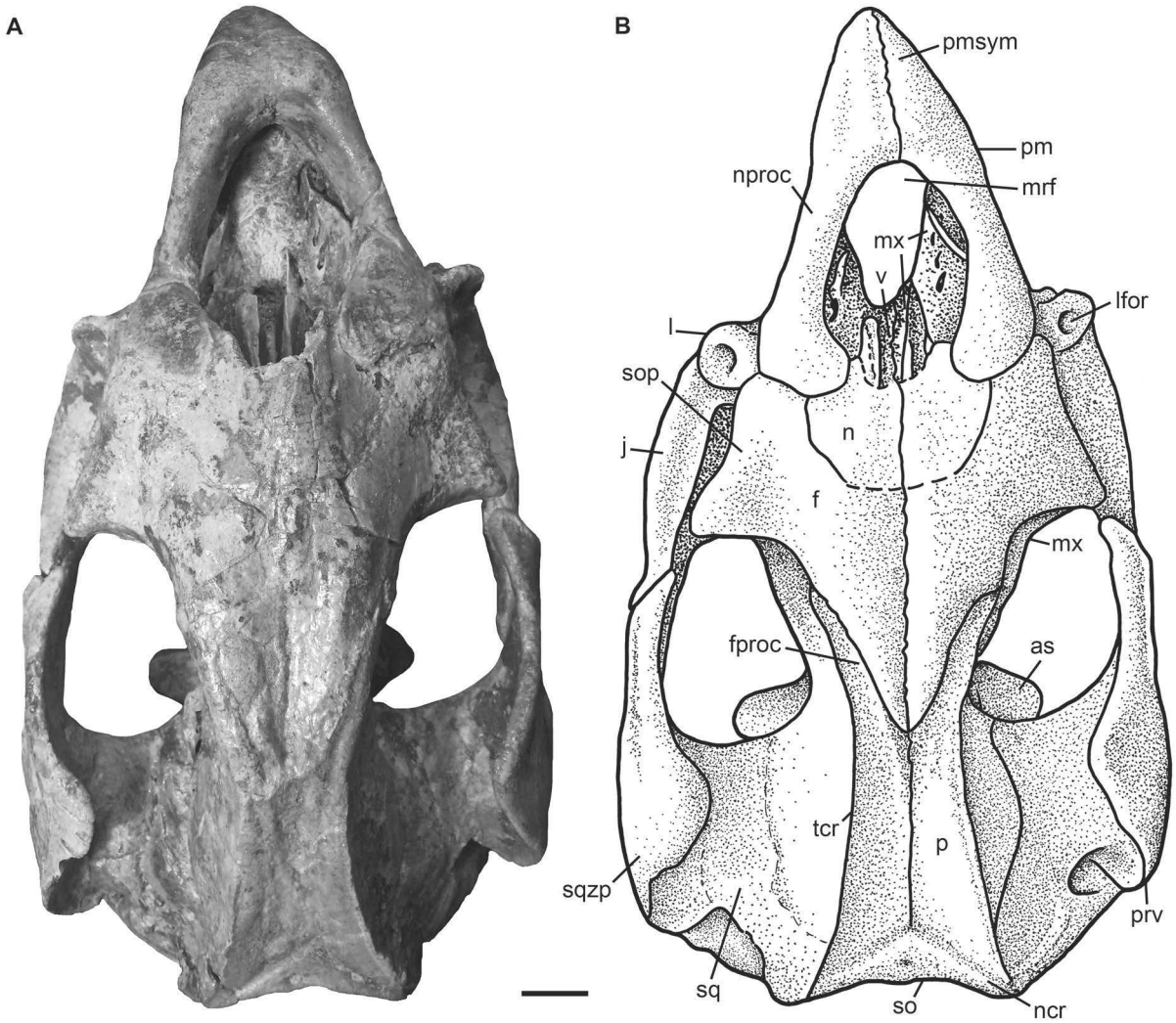

Figure 7. Cranium of gen. nov. 1 *taulannense* (RGHP D040, holotype) in dorsal view. **A**, photography. **B**, drawing (redrawn from Sagne, 2001b). Dashed lines indicate broken parts. Scale bar equals 2 cm.

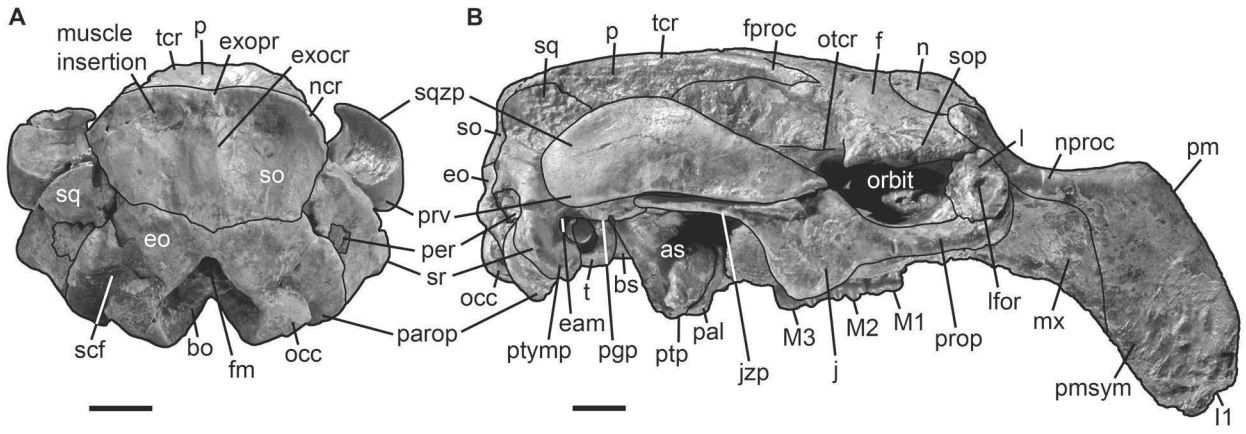

Figure 8. Cranium of gen. nov. 1 *taulannense* (RGHP D040, holotype). **A**, in caudal view. **B**, in right lateral view (© MNHN and RGHP). Scale bars equal 2 cm.

its length that is upraised to form a boss posteriorly (9[1]; 10[1]). The anteroventral most maxillopremaxillary suture lies in the rear of the posterior end of the symphysis, below the mesorostral fossa (6[0]). In ventral view (Fig. 9), the anterior palatal roof in front of the infraorbital foramina is very narrow compared with the posterior palate 13[0]). The rostral masticating surface has a lanceolate shape (14[1]), bearing a *foramen incisivum* that is not sharply demarcated anteriorly (15[0]). Instead of a dentiform process, two alveoli for the incisor tusks are present (16[0]).

Nasal: The anterior ends of the nasals are broken medially, but still reveal these elements to be well developed with a dorsally exposed internasal suture (about 40 mm long) exceeding half the length of the interfrontal suture (39[0], 40[0]; Fig. 7). A small nasal incisure is present at the posterior end of the mesorostral fossa (42[1]).

Ethmoidal region: Not preserved in any specimen.

Vomer: The vomer is partially exposed as a mediolaterally narrow ridge in the holotype specimen and only visible in dorsal view (Fig. 7). It extends in a longitudinal trough on the dorsal surface of the maxilla slightly forward into the mesorostral fossa. In specimen RGHP D345, the vomer is partially visible through the broken palatine as the cranial extension of the median crest coming from the presphenoid.

Lacrimal: The lacrimal is well developed filling a considerable space between the jugal and frontal (Fig. 8B). It forms a rounded bone pierced by a distinct nasolacrimal canal (75[0]) and contacts the premaxilla (73[0]); 74[1]). The right element measures 20 mm in anteroposterior length and about 29 mm in dorsoventral height. The lacrimal foramen is 4 mm in maximum diameter.

Frontal: The supraorbital processes are dorsoventrally flattened (44[0]) having a dorsal surface inclined gently ventrolaterad (45[0]). Laterally (Fig. 8B), each process shows a

smooth margin (46[0]) ending in a prominent posterolateral corner that is not projecting posteriorly (47[1]; 48[0]; 49[1]). The frontal roof is more or less flat (52[0]) and characterised by a strong intertemporal constriction with its maximum at the centre of the skull roof (54[0]; 55[1]; Fig. 7). The temporal crests are as prominent on the frontal as on the parietal (56[1]), forming distinct keels (57[0]) that are lacking a knoblike boss medially (53[0]).

Anteriorly, the frontonasal area is broken in most specimens, but preserved in the holotype showing only slight crushes superficially. The frontonasal suture is laterally and posteriorly concave indicating the absence of an internasal process. However, a short internasal process is developed in the juvenile RGHP D345 (see also Sagne, 2001b: fig. 21). Considering the advanced age of the holotype, which preserves the frontonasal area as the only adult, and the fact that the frontonasal suture is still discernable (Fig. 7), this character is scored as the plesiomorphic condition (43[0]).

In lateral view (Fig. 8B), a prominent orbitotemporal crest is present on both sides of the skull (58[0]; 59[1]). The *lamina orbitalis*, forming the anterior part of the medial wall of the temporal fossa, is not thickened (60[0]).

Parietal: The parietal roof is more or less flat between the temporal crests lacking a sagittal crest (61[1]; 62[1]; Fig. 7). The proportions of the cranial roof slightly exceed the ratio l_{FP}/w_{SO} that is about 2.03 in the holotype (64[0]). In comparison with the frontal, the parietal is distinctly longer in midline (65[0]). The frontal processes of the parietal are long exceeding half the length of the frontal roof (63[1]). Internally, the bony *falx cerebri* is distinct keeping its height along the length of the parietal up to the frontoparietal suture (68[1]). An internal occipital spine is present between the parietal and supraoccipital (70[1]) as well as a prominent tentoric process and a *tentorium osseum* (71[0]; 72[1]).

Supraoccipital: The supraoccipital is enlarged transversally, according to the ratio width to height, which exceeds 1.5 (112[1]; Fig. 8A). Its dorsal margin is convex, forming a narrow and sharp-edged nuchal crest that extends up to one third of the lateral margin of the supraoccipital (113[0]); 114[0]). In the median plane, the nuchal crest lacks a notch (115[0]), but shows a weak external occipital protuberance that remains below the level of the parietal roof (116[0]). The external occipital crest is differentiated from the protuberance by its broad and laterally undefined shape (118[1]). It enters the ventral tip of the supraoccipital that forms an angle of about 145° in the holotype (119[0]). Aside from rounded muscle insertions for the semispinal muscle (117[0]), the external lamina is characterised by a smooth surface.

The internal lamina of the supraoccipital reveals a deep transverse sulcus (120[0]) indicating the parietooccipital suture that slopes under the median occipital spine and the pointed lateral ends of the parietal. The remaining portion of the internal lamina remains flat.

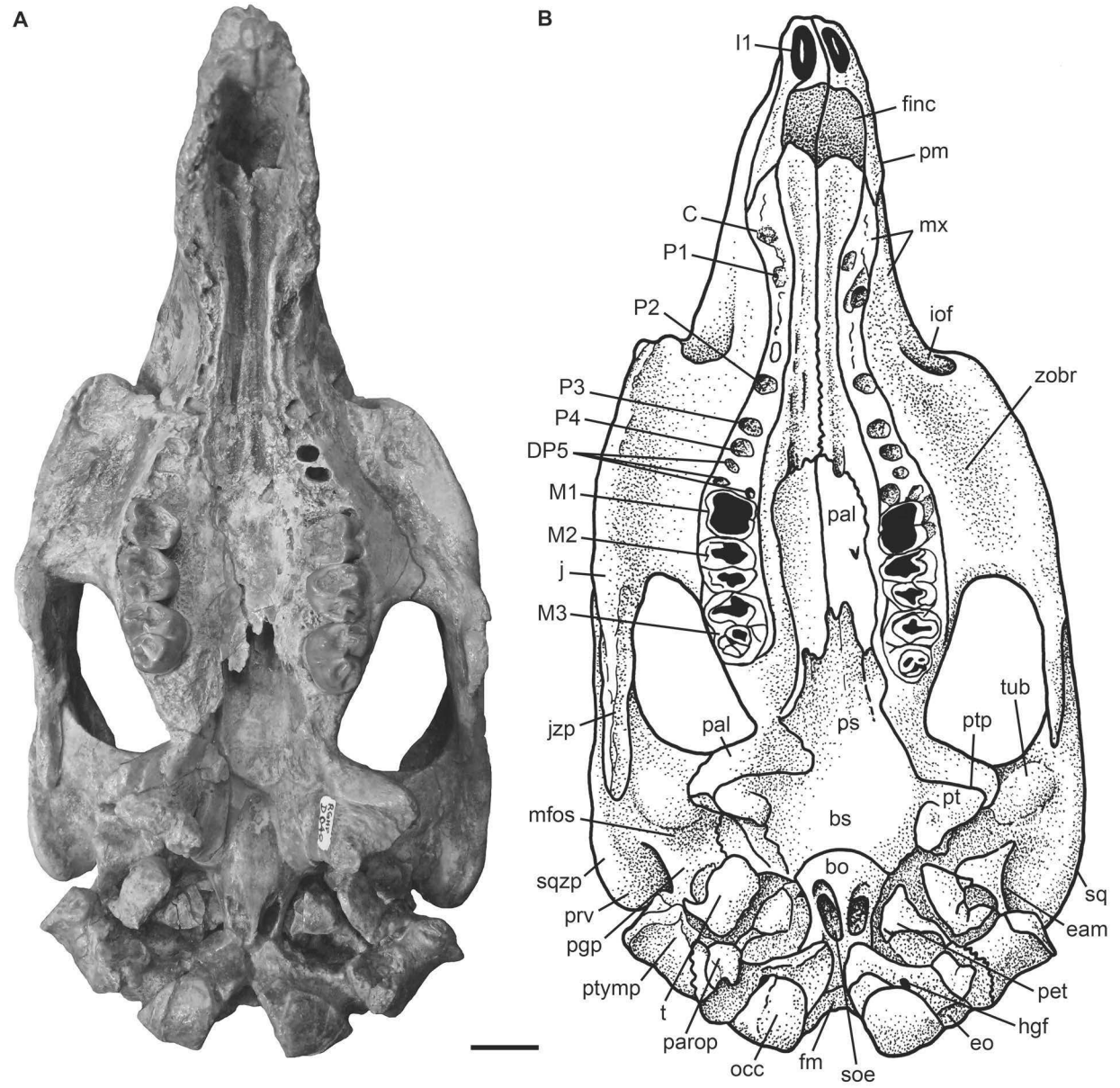

Figure 9. Cranium of gen. nov. 1 *taulannense* (RGHP D040, holotype) in ventral view. **A**, photography. **B**, drawing (redrawn from Sagne, 2001b). Scale bar equals 2 cm.

Exoccipital: The exoccipitals meet in a suture of 10 mm in length dorsal to the *foramen magnum* (121[0]; Fig. 8A). The *foramen magnum* is triangular in shape having its dorsal peak above the level of the occipital condyles (129[1]; (130[1]). Dorsolaterally, the exoccipitals are rounded, more or less smooth and not flange-like (124[0]). The supracondylar fossae are deep and extend across the entire width of the condyles (123[1]). Ventrolateral to the condyles (Fig. 9) a hypoglossal foramen is present forming an opening completely surrounded by bone (127[0]). The paroccipital processes are long and reach as far ventrally as the occipital condyles (131[0]; Fig. 8).

Basioccipital: The basioccipital is firmly fused with the exoccipitals and basisphenoid indicating adulthood in the holotype specimen (Fig. 9). Its anterior basicranial half is short

and columnar with deeply concave and oval shaped sphenooccipital eminences on its ventral surface (128[0]). These insertions for the *longus capitis* muscles are separated by a prominent median ridge.

Basisphenoid, presphenoid, orbitosphenoid: The main part of the basisphenoid contributes to the basicranium and is fused with the presphenoid and orbitosphenoid anteriorly, the alisphenoid dorsally, the basioccipital posteriorly, and the pterygoid posterolaterally (Fig. 9). Anterolaterally, it contacts the palatine via sutures that are still discernable. The basisphenoid and presphenoid are flat ventrally with their posterior ends being higher than their fronts. The median crest of the presphenoid is indicated in the holotype at about the level of the posterior end of the alveolar margin of the maxilla. In RGHP D345, this crest represents a prominent ridge joining the vomer anterodorsally.

Alisphenoid: The alisphenoid is well visible in lateral view of the holotype specimen forming the posterolateral wall of the pterygoid process (Fig. 8B). Its lateral surface is irregularly shaped, roughly concave dorsally and convex and rugose ventrally. It contacts the squamosal, parietal and frontal dorsally, the palatine anteriorly, and the pterygoid medially. An alisphenoid canal is absent (132[1]) and the *foramen ovale* is opened to form a notch or incisure (133[1]).

Pterygoid: The pterygoid is fused with the surrounding bones and forms the posteromedial part of the pterygoid process (Fig. 9). Each pterygoid process has a narrow, hook-like ventromedial projection at its end forming a hamuli process (135[1]). The pterygoid fossa extends posteriorly above the level of the roof of the internal nares (134[0]).

Palatine: The palatine forms the anteromedial component and ventral tip of each pterygoid process (Fig. 9). It contacts the pterygoid posteromedially, the alisphenoid posterolaterally and the maxilla anteroventrally. Both palatines also curve anteromediad to contact the presphenoid and orbitosphenoid dorsally contributing to a posterior wall between the internal nares and the temporal fossa. All sutures of the palatine remain evident in adults, only those at the intersection between the alveolar portion of the maxilla and the anteromedial part of the pterygoid process are sometimes difficult to detect. Both elements meet in midline and extend forward between the maxillae beyond the posterior edge of the zygomatic-orbital bridge (33[0]). The posterior border of the palatine is incised or deeply indented (35[1]).

Maxilla: The zygomatic-orbital bridge of the maxilla (Fig. 9) is anteroposteriorly elongated (22[0]) and nearly on the same level as the palate (21[1]). It does not form a transverse vertical wall, but is posteriorly thickened compared to the thin anterior margin (23[0]; 24[1]). The infraorbital foramina to both sides of the skull (Fig. 9) do not exceed 200 mm² (25[0]), each measuring approximately 150 mm², and are about as wide as high (30[1]). The

infraorbital canal is not obstructed (31[0]). In ventral view (Fig. 9), the palate is thin at the level of the penultimate cheek tooth being distinctly below 10 mm in height (32[0]).

Squamosal: The cranial part of the squamosal extends to the temporal crests (87[1]), which are not separated from, but merging with the nuchal crest of the supraoccipital (88[0]; Fig. 7). On the lateral side of the skull (Fig. 8B), the sigmoid ridge extends as a prominent structure up to the ventral margin of the supraoccipital and is well visible in posterior view (99[1]; 100[1]; Fig. 8A). The mastoid foramen is present posterolaterally (110[1]) and defined dorsally by the exclusion of the supraoccipital (111[1]). This is best observable on the right side of the holotype skull (Fig. 8), where the squamosal surrounds the periotic that fills the mastoid foramen by connecting with the exoccipital.

Lateral to the skull (Figs. 7, 8B), the zygomatic process projects as triangular, anteriorly tapering element (89[1]) from the zygomatic root that is characterised by a distinct notch posteriorly (92[1]). The medial and lateral sides of the process are flat to concave (90[0]), the dorsal margin is distinctly inclined inward and sigmoidal in shape (91[1]; Fig. 7). Posterodorsally, the zygomatic process is straight to concave (98[0]) before entering its posterior end, the *processus retroversus* (Fig. 8B). The latter is moderately inclined inwards (101[1]). In ventral view (Fig. 9), the zygomatic process reveals a distinct relief composed of transversely elongated elements for the articulation with the mandible (93[0]). The mandibular fossa is deep between a prominent *tuberculum* anteriorly and a distinct, and knob-like postglenoid process posteriorly (94[1]; 95[1]); 96[0]; 97[1]).

The posttympanic process is not club-like, but forms a ventral extremity of the squamosal with a rostrad projecting tip for the attachment of the sternomastoid muscle (108[0]; 109[0]; Fig. 8B). Together with the postglenoid process, it defines the external auditory meatus that is short mediolaterally (104[0]) and about as wide anteroposteriorly as high (106[1]).

Jugal: The jugal (Figs. 7, 8B) has a thin preorbital process (76[1]; 77[0]) that is in contact with the lacrimal (79[1]), but not reaching the premaxilla (78[0]). The ventral rim of the orbit is not overhanging (86[0]). Dorsal to the central body of the jugal, a prominent postorbital process rises in front of the anterior tip of the zygomatic process of the squamosal (84[1]). A frontojugal (postorbital) bar is not developed (85[0]). The ventralmost extremity of the jugal lies posterior to the orbit (80[0]) and the posterior (zygomatic) process exceeds the orbital diameter (83[0]).

Ear region: Sagne (2001b) describes a well preserved periotic from a juvenile specimen (RGHP D057), which was not investigated in person. However, the holotype RGHP D040 reveals all information of systematic relevance in this study and is the focus of the following description (Fig. 10). The terminology of the external morphology of the ear region is essentially based on Robineau's (1969) comprehensive work on extant sirenians and complemented by the studies of Court (1990, 1994b).

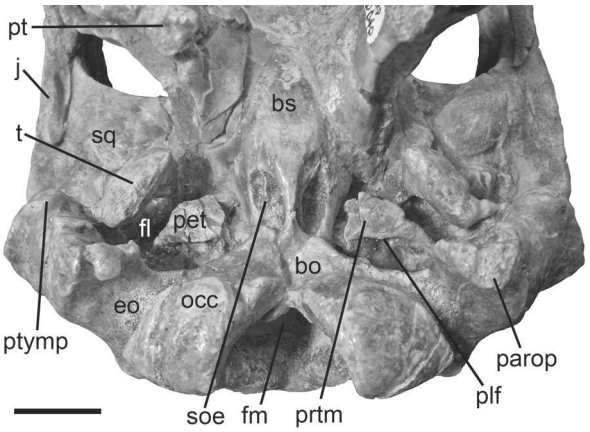

Figure 10. Close-up of cranium of gen. nov. 1 *taulannense* (RGHP D040, holotype) in posteroventral view exhibiting the ear region. Scale bar equals 2 cm.

In the holotype, the periotic is visible in ventral (Figs. 9, 10) and partially posterior views (Fig. 8) comprising the petrosal (*pars petrosa*), the mastoid (*pars mastoidea*), and the *tegmen tympani* (*pars temporalis*). On the ventral side of the skull (Fig. 10), the periotic is visible through the large *foramen lacerum*, set in a closely fitting socket in the squamosal and not fused with any other skull bone (136[1]). The petrosal projects mediad into the *foramen lacerum* and bears ventrally a subconical promontorium (*pars cochlearis*). The promontorium tapers posterolaterad forming a prominent, but steadily declining ridge and terminates at the junction between the paroccipital process of the exoccipital and the posttympanic process of the squamosal. The oval window (*fenestra ovalis* or *fenestra vestibuli*) opens anterolateral to the promontorium while a perilymphatic foramen is present on its posteromedial side. This conspicuous opening dominating the posterior wall of the *pars cochlearis* is not the true round window (*fenestra rotundum* or *fenestra cochleae*), but rather a secondarily undivided perilymphatic foramen (Fischer, 1990; Court, 1994b). Between the promontorium and the posterior articulation surface of the tympanic, the petrosal has a deep furrow that serves as insertion area for the muscle supporting the stapes.

The mastoid is partially exposed by the oval *processus fonticulus*, which fits into the mastoid foramen on the posterolateral surface of the skull (Fig. 8). According to Sagne (2001b), the mastoid is slightly larger than the *tegmen tympani*. The latter is not visible in the holotype, because the anterolateral part of the periotic is still enclosed by matrix remaining in the skull. None of the auditory ossicles is known.

The tympanic is preserved *in situ* on both sides in the holotype and arranged in an anteromedial-posterolateral axis (Fig. 10). Its ventral extremity is more or less triangular in shape and asymmetric with its anteromedial side shorter than its posterolateral side. The anterior process of the tympanic is adjacent to the *tegmen tympani* while the posterior one occupies a position between the paroccipital and posttympanic processes attached to the anterior side of the latter.

Mandible: In lateral view (Fig. 11A), the mandibular symphysis is higher than long (142[1]) and houses the mental foramen (141[0]) that is accompanied by several accessory mental foramina dorsoposteriorly and ventrally (140[0]). The overall shape of the horizontal mandibular ramus is slender (156[0]). Its ventral border is moderately concave, sharply downturned anteriorly (144[1]), and not tangent to the angle posteriorly (147[1]). The

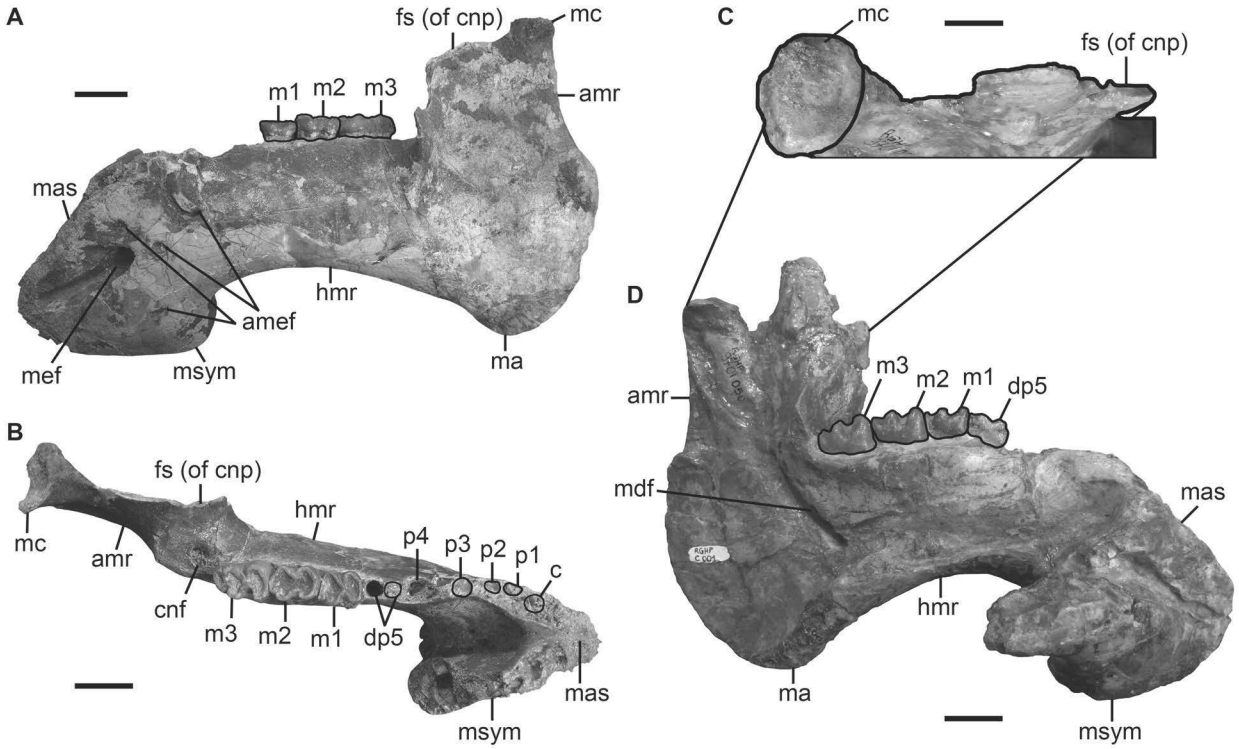

Figure 11. Mandibles of gen. nov. 1 *taulannense*. **A**, RGHP E.7.096a (paratype) in left lateral view. **B**, RGHP E.7.096a (paratype) in occlusal view. **C**, Close-up of condyle of RGHP C001 (paratype) in occlusal view. **D**, RGHP C001 (paratype) in medial view. Scale bars equal 2 cm in A, B and D. Scale bar equals 1 cm in C.

posterior border of the mandible bears no distinct *processus angularis superior*, but has a broadly convex outline beginning well below the condyle (149[1]). Anteriorly, the ascending mandibular ramus bears the coronoid process that has a slight slope in anterior direction (151[1]). At the basis of the coronoid process, an enlarged coronoid foramen is present having about 7 mm in diameter in the adult RGHP E.7.096a (153[1]; Fig. 11B). In ventral view, the symphysis is broad transversally (137[1]). The masticating surface is narrow, scarcely wider than the two rows of tooth alveoli it bears, and shows no median furrow (138[0]; 139[0]; Fig. 11B). The condyle is characterised by an evenly elliptical articulation surface that is as broad medially as laterally (148[0]; Fig. 11C). The mandibular foramen (Fig. 11D) is undivided (154[0]) and reveals the dental capsule of the m3 to be exposed posteroventrally (155[1]).

Dentition: The dentition was already extensively outlined by Sagne (2001b). Hence the following description focusses on the dental characteristics that have proven informative for the cladistic analyses in this study. The lifetime dental formula is here determined to be I1, C1, P1–4, DP5, M1–3 in the upper jaw, and most likely i0, c1, p1–4, dp5, m1–3 in the lower jaw (164[1]; 166[0]; 167[0]; 168[0]; 169[0]; 170[0]; 180[0]; 181[0]).

Upper dentition: One pair of alveoli for the incisor tusks (I1) is preserved in the holotype specimen (Fig. 9). The alveolus for I1 extends about half the total length of the

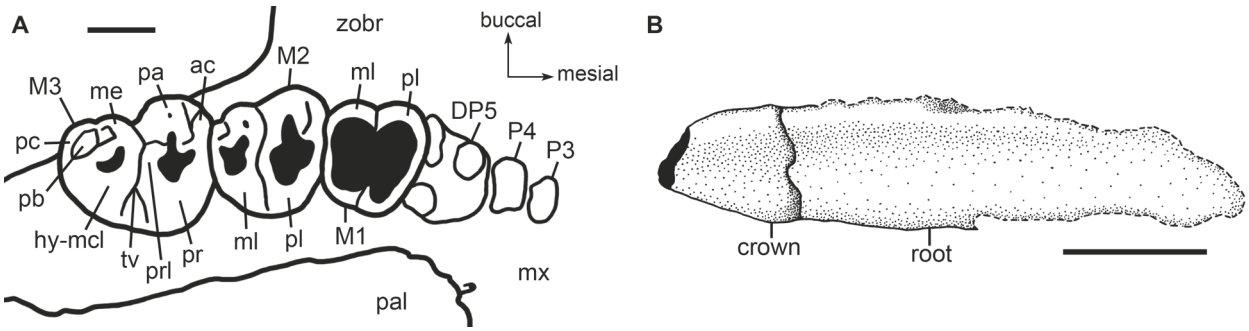

Figure 12. Dentition of gen. nov. 1 *taulannense*. **A**, outline drawing of the right upper cheek teeth of cranium RGHP D040 (holotype) showing the alveoli for P3–DP5 and the crowns of M1–M3 in occlusal view. **B**, drawing of the right incisor tusk (I1) of E.5.031 in posterior view (redrawn from Sagne, 2001b). Scale bars equal 1 cm.

premaxillary symphysis (158[1]), which is indicated by the longitudinal swelling of the symphysis laterally (Fig. 8B). Several isolated first incisor teeth (Fig. 12A) that were not observable at MNHN are also described and illustrated by Sagne (2001b). The tallest of which, specimen AGM 13, measures 60 mm in preserved length and has a slightly worn crown about 12 mm long. The crown of I1 is conical in shape and consists of enamel on all sides (160[0]). It is suboval or subelliptical in cross section (161[0]) and distinctly separated from its root (165[0]). I2 and I3 are absent.

A few millimetres just behind the maxillopremaxillary suture, the alveoli of the single-rooted canines occur (Fig. 9). The teeth themselves are not preserved.

All permanent premolars, P1–P4, are single-rooted (173[1]) and mainly represented by their alveoli in the maxillary bone (Fig. 9) except for (DP) or P1 and P2–P3 from the right side in the juvenile specimen RGHP D055 and the left P4 in the adult specimen RGHP D349 (Sagne, 2001b). The teeth of RGHP D055 are still unerupted, but already reflect their arrangement in the dental arcade similar to adult specimens. According to Sagne (2001b), the successional premolars in RGHP D055 and in RGHP D349 are positioned labially in the maxilla, which is the opposite observation to Luckett (1993), who states that successional teeth develop only lingual to its deciduous predecessor in a wide range of therians. Sirenia that are not included in Luckett's (1993) ontogenetic assessment of dental development might, therefore, represent an exception at least in the developmental pattern of its maxillary dentition.

In the adult type specimen (Fig. 9), the alveolus of P1 is rounded, having a maximum diameter of 6 mm, and close to the canine at an interval of about 13 mm. A diastema of about 21 mm separates P1 and P2. The P2 alveolus is slightly larger than the preceding premolar and measures 7 mm in maximum diameter. About 8 mm behind P2, the alveolus of P3 occurs closely followed by that of P4. Both alveoli are about as large as the P2 locus.

Maxilla RGHP D055 reveals information on the cusp pattern of (DP) or P1 and P2–P3, which is simple in showing a high central cusp surrounded by lower accessory

cuspules (Sagne, 2001b). On (DP) or P1 a single accessory cuspule is present distally, on P2 and P3 a second cuspule occurs mesially. According to Sagne's (2001b) observations, P2 and P3 have lingually a *cingulum* that is prominent and extends mesiad and distad on P3. The P4 in RGHP D349 shows a cusp pattern similar to that of P2 and P3 except for the *cingulum* that surrounds the complete crown.

The tooth at the fifth premolar locus is known by its partially broken crown in the juvenile specimens RGHP D345 and in RGHP D275 (Sagne, 2001b). In the holotype specimen (Figs. 9, 12A), the alveoli in front of M1 are resorbed and show only traces of the original three alveoli indicating that no replacement occurs at this locus (171[0]). The persisting DP5 is molariform and similar to the anterior molars according to Sagne (2001b). It differs in aspects referring to the *precingulum* that is short and not attached to the protocone. Additionally, the metaconule and hypocone are connected with each other, and the *postcingulum* encloses a deep posterior basin.

The molars are three-rooted, bunolophodont teeth and not reduced in size relative to the skull (182[0]; Figs. 9, 12A). Their crowns are covered by smooth enamel of about 2 mm thickness in average. The molars increase in size distad within the tooth row, while their degree of wear decreases. The worn surfaces of the molars are oblique, higher labially (or buccally) than lingually. All molars are morphologically characterised by a roughly heart-shaped outline, the presence of two transverse lophs separated by a deep transverse valley, and a distinct *pre*- and *postcingulum* (Fig. 12A).

M1 is best preserved and nearly unworn in specimen RGHP D345. The *precingulum* forms a straight, transverse ridge that is separated from the protoloph by a distinct furrow, which is labially open and lingually closed. Proto- and metaloph show the characteristic threefold division and transversal arrangement of their single cusps. Thereby, the protocone forms the highest cusp on M1 resulting in a pronounced lingual side of the protoloph. On the protoloph, each cusp is clearly separated from each other by a deep furrow that is crossing the whole loph mesiodistally. Both, paracone and protoconule are slightly inclined lingually. The transverse valley forms a deep, undistorted furrow separating the protoloph from the metaloph. On the metaloph, the metaconule is slightly shifted anterad and closer to the hypocone than to the metacone. However, the hypocone and metaconule are separated by a distinct furrow though not as deep as the one separating the metaconule from the metacone. The metaloph is defined distally by a *postcingulum* that is attached to the hypocone and open labially enclosing a small posterior basin.

The holotype specimen preserves M2, whose crown, however, is too much worn in order to reveal more details aside from the general molar morphology (Fig. 12A). Only one addition can be made in so far that the basis of the protoconule is slightly shifted distad so that the transverse valley appears to be slightly obstructed. The metaloph does not deviate from the transverse arrangement of its cusps (178[0]).

The crown of M3 is best preserved in the holotype specimen showing a moderate degree of tooth wear (Fig. 12A). This tooth differs in some aspects from the preceding molars. Its heart-shaped outline is slightly elongated mesiodistally with the lingual tip at the level of the protocone. The protoconule is shifted distad to some extent, but without obstructing the transverse valley significantly. The latter reaches its deepest level on the labial side, where it opens widely. On the metaloph, the hypocone and metaconule are closely associated, but without the trace of a distinct furrow separating both cups (177[0]). In contrast to the *precingulum* that surrounds a narrow anterior basin, the *postcingulum* is connected to the hypocone-metaconule and encloses a large and deep posterior basin (175[1]).

Lower dentition: Several mandibles or mandibular fragments of different age stages are reported by Sagne (2001b), three of which were examined in person. The subadult paratype RGHP C001 preserves the complete tooth arcade of the left side revealing insights into the cusp pattern of the molars and even the permanent premolars and therefore provides the main reference for the following description of the tooth morphology.

The mandibular symphysis bears two closely spaced rows of alveoli that are interpreted by Sagne (2001b) to correspond to three lower incisors and one canine. The alveoli for the incisors, however, represent quite shallow concavities that are large and oval in oblique dorsoventral direction. The same is indicated in the paratype mandible RGHP E.7.096a of a very old specimen, but to a much greater degree (Fig. 11B). There, the i1 alveolus is nearly flat, and those for i2 and i3 show spongy bone tissue, where deep and clearly bordered grooves that might have housed single-rooted teeth are missing. These observations correspond to Luckett's (1993) identification of vestigial deciduous teeth that are amongst others characterised by their relatively superficial position and lack of typical roots. Therefore, the absence of permanent lower incisors is postulated for this taxon in this study, which might be supported also by the fact, that of all teeth the incisors are entirely unknown in the paratypes and the referred specimens, except for the first upper incisor tusks.

The presence of a single-rooted canine is, however, well documented in RGHP E.7.096a by remains of its root on the right side and a deep alveolus, very clear in shape, on the left side at the respective position of c (Fig. 11B).

The permanent premolars are single-rooted (173[1]). On the one hand, this is indicated by the alveoli for the respective teeth in mandible RGHP E.7.096a (Fig. 11B), and on the other hand, by remnants of the roots for p1–4 from the left and p4 from the right side in mandible RGHP C001. As a special feature of specimen RGHP C001, two further alveoli are present superficially between the left p2 and p3 with the anterior one shifted labially and the posterior one positioned along the longitudinal axis of the tooth arcade. These alveoli are interpreted by Sagne (2001b) to represent vestigial remnants of deciduous teeth not yet resorbed, which is supported in this study. Luckett (1993) provided a comprehensive account on dental homologies in therians based on ontoge-

netic analyses of the dentition. He concluded that a deciduous tooth becomes secondarily displaced buccally while its successor develops lingually. This buccal displacement of a deciduous tooth or alveolus is clearly observable behind the left p2 in RGHP C001. Luckett (1993) also stated that in some eutherians the developing lingual successional tooth might extend anterior or posterior to its deciduous predecessor. For example, this observation is made in a chiropterian juvenile skull of *Pteropus*, which still shows an empty alveolus of dp4 between the erupted p4 and m1 in an anterior-posterior sequence (Luckett, 1993). The observations in RGHP C001 would well fit to this situation if the alveoli behind p2 and in front of p3 are interpreted to belong to dp2 and dp3 respectively. Sagne (2001b) identified dp2 and dp3 to be bi-rooted in this species and it could be argued that the two alveoli in between of the functional p2 and p3 represent the remnants of a single deciduous teeth. This situation is, however, regarded unlikely due to the displacement of both alveoli within the tooth arcade. Therefore, Sagne's (2001b) interpretation is favoured here in so far that the anterior single alveolus corresponds most likely to the distal root of dp2 while the posterior one represents the mesial root of dp3.

The crowns of the permanent premolars are preserved in isolated form and most likely correspond to the left p1–4 and the right p4 in RGHP C001. The crowns show a simple morphology comprising a high central cusp that is surrounded by lower cusps mesially and distally on p1 and from p2 onwards also lingually. The mesial cusp on p1 and the lingual ones on p2 and p4 range between the size of the central cusp and the accessory cuspules to the very base of the crown. On p3, two medium sized cusps are present lingually. The number of the accessory cuspules increases up to five on p4. Accordingly, the premolar crowns increase slightly in size from anterior to posterior within the tooth arcade. The labial side of the central cusp remains smooth and is convex.

A two-rooted dp5 is preserved in mandible RGHP C001 (Fig. 11D). Its crown is broken, but still reveals a molariform morphology comprising two main lophs separated by a transverse valley and a posterior *cingulum*. In mandible RGHP E.7.096a, only a single alveolus is present in front of m1 and separated from p4 by a rough-surfaced diastema (Fig. 11B). This observation provides different hypotheses on the presence and absence of a permanent fifth premolar, which is discussed below. In this study, the absence of a p5 is postulated for this species in general. Additionally, the alveolus in front of m1 in RGHP E.7.096a is interpreted to correspond to the yet unresorbed distal root of dp5. The "diastema" between dp5 and p4, accordingly, represents the already resorbed mesial root of dp5.

The molars are best preserved in the paratype RGHP C001 (Fig. 11D) with m1 showing moderate tooth wear while m2 is only slightly and m3 not yet worn. The wear surfaces of the lower molars are oblique, higher lingually than labially, which is the opposite direction compared to the upper molars. Each molar is characterised by paired roots and mesiodistally elongated crowns that increase in size from anterior to posterior within

the tooth row. The morphology of their crowns is similar and, therefore, the following description generalised (compare also Fig. 11B). Each crown bears two transverse lophs that are more or less perpendicular to the longitudinal axis of the tooth arcade. On m1, the proto- and hypolophid are about equal in size, while m2 and m3 taper in distal direction and show a slightly narrower hypolophid. Proto- and hypolophid are separated by a deep transverse valley, which is obstructed by a *crista obliqua* that extends lingually between the protoconid and hypoconid. In mandibles RGHP C001 and C009, a small *precingulum* is present on the labial side of m1 and m2. The m3 of RGHP C001 is missing such a *cingulum* or it is not yet developed considering the subadult age of this specimen and the observations in the adult E.7.096a, where a weak mesial *cingulum* is present on m3. A *postcingulum*, the hypoconulid, is always developed in the lower molars and includes a varying number of cuspules between the molars of the same specimen and the molars of corresponding positions within the tooth arcade. In the paratype for example, both m2 have four cuspules while the left and right m3 differ in showing two and three cuspules. The hypoconulid encloses a distinct posterior basin that increases in size from m1 to m3.

Hyoid apparatus: Not preserved in any specimen.

Postcranium – general remarks: In this study, relevant postcranial elements are evaluated on the basis of Sagne's (2001b) data source, because they were not investigated personally. Hence, the postcranial characteristics of this species are only briefly treated in the following. Additionally, a considerable number of vertebrae and ribs are mentioned in Sagne (2001b), for which no descriptions or illustrations are provided, except for the first rib. This is mainly why these elements do not contribute to the systematic treatment of this species implemented by Sagne (2001b), which is also the case in the present study.

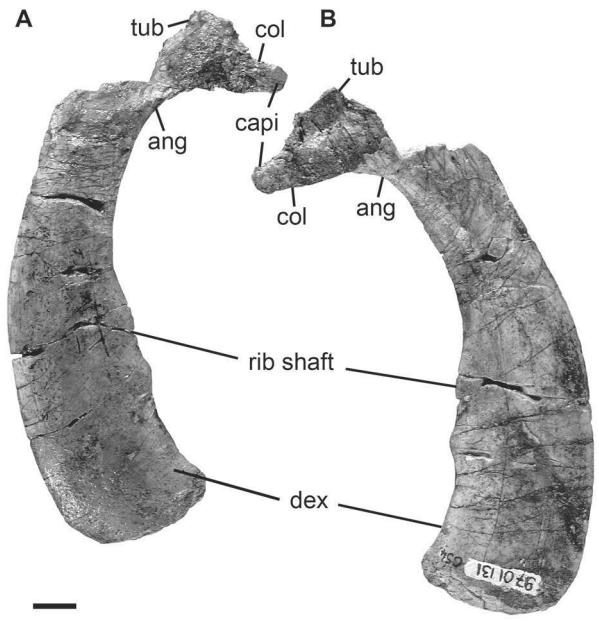

Figure 13. Right first rib of gen. nov. 1 *taulannense* (RGHP C054; © MNHN and RGHP). **A**, in anterior view. **B**, in posterior view. Scale bar equals 1 cm.

Vertebral column: A detailed description of the vertebrae is deferred until a later stage, because these are not relevant for this study and were not investigated in person.

Ribs: Sagne's (2001b) description is laid on two anteriormost ribs, which she regards to be systematically important. One of these ribs belongs to an adult specimen (RGHP C054; Fig. 13) that is characterised by a strong extension of its distal extremity (196[1]). A protuberance ventral to the *capitulum* is not developed (195[0]).

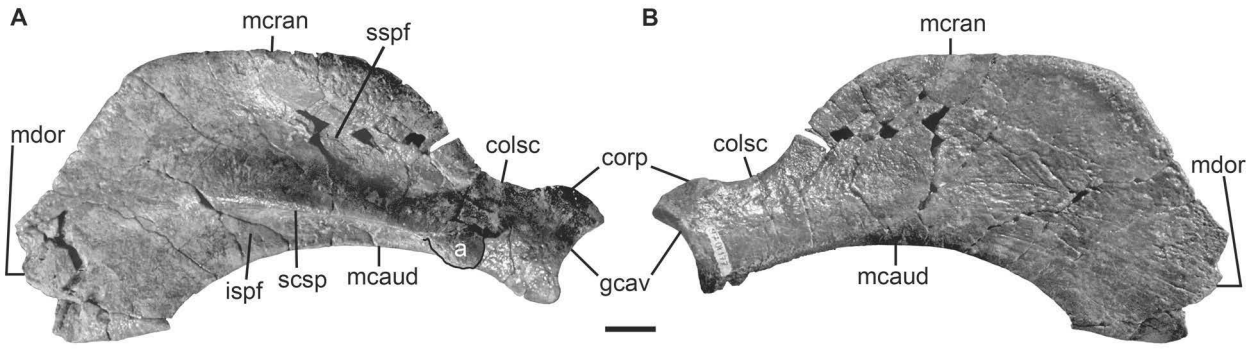

Figure 14. Right scapula of gen. nov. 1 *taulannense* (RGHP D350; © MNHN and RGHP). **A**, in lateral view. **B**, in medial view. Scale bar equals 2 cm.

Sternum: Not preserved in any specimen.

Scapula: The nearly complete scapula of an adult (RGHP D350; Fig. 14) is described and illustrated by Sagne (2001b: fig. 43A). This element is relatively slender and sickle-shaped (187[0]). The scapular spine forms a more or less straight ridge lacking a proximal rugosity (183[1]). It is shortened and diffusely tapering off about half the length of the scapular blade (184[1]). On its distal end, the spine forms the acromion, which inhabits a position at the level of the scapular neck (188[0]). The outer surface of the scapular blade is characterised by a supraspinous fossa that is distinctly larger than the infraspinous fossa (186[1]). Distally, a moderately developed coracoid process defines the glenoid fossa anterodorsally (185[0]). The process is slightly inclined medially and not disjoint from the anterior apex of the articular glenoid.

Humerus: The right humerus of an adult specimen (RGHP C035; Fig. 15A, B) is described and illustrated by Sagne (2001b: fig. 45). It represents a compact element with distinctly developed epiphyses (189[1]). In anterior view (Fig. 15A), the humerus shaft has a prominent, recurved deltoid crest, which is characterised by a deltoid tuberosity on its upper half before it is continued by the deltopectoral crest distally. The greater tubercle is distinctly elevated above the level of the rounded caput (190[1]). Medially, a well developed bicipital groove separates the greater tubercle from the lesser tubercle, the latter which occupies a position well below the upper caput level. Distally, the trochlea is canted obliquely at an angle of about 70° relative to the axis of the humerus shaft (191[1]). The trochlear articular surface is almost symmetrical in shape. Both, the coronoid fossa anteriorly (Fig. 15A) and the olecranon fossa posteriorly (Fig. 15B) are well defined and deep.

Radius and ulna: The left radius and ulna (RGHP C006; Fig. 15C–D) of a mature animal are described and illustrated by Sagne (2001b: fig. 46). Both elements are proximally fused below their articulation surfaces for the humerus. The diaphyses of radius and ulna

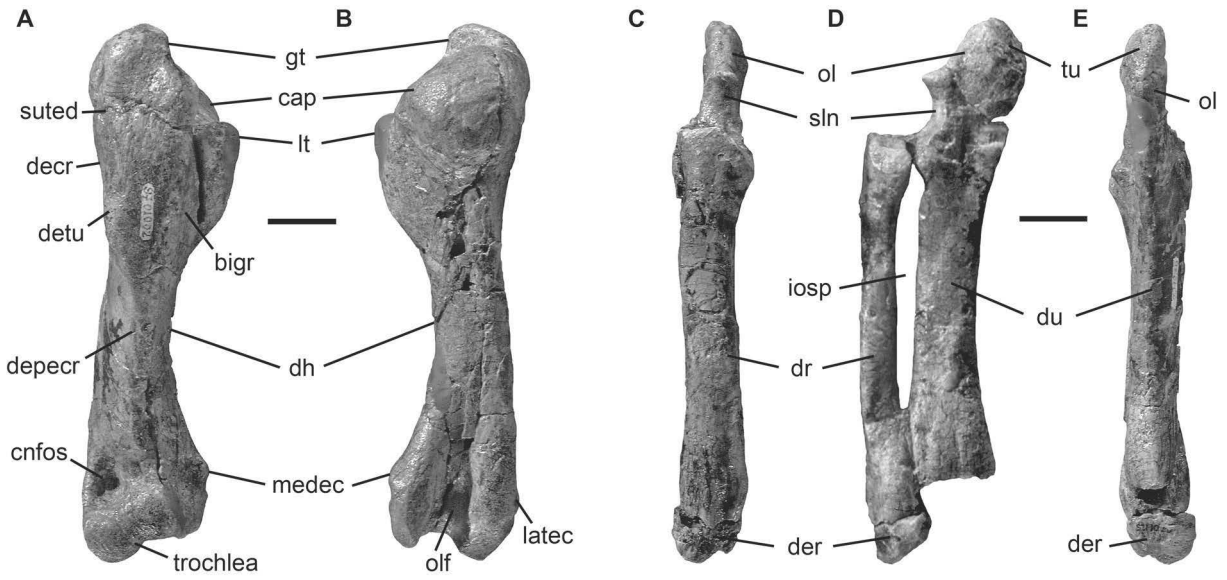

Figure 15. Stylopod and zeugopod of gen. nov. 1 *taulannense* (© MNHN and RGHP). **A–B**, right humerus RGHP C035 in anterior (A) and posterior (B) views. **C–E**, left radius and ulna RGHP C066 in anterior (C), lateral (D) and posterior (E) views. Scale bars equal 2 cm.

are straight (194[0]). Distally, only the epiphysis of the radius is preserved measuring 10 mm in maximum length. The anterior side of the olecranon is tilted back at an angle of about 50° relative to the axis of the ulna shaft (Fig. 15D). The summit of the olecranon is thickened and bears a tuberosity. In medial and lateral (Fig. 15D) views, the ulnar shaft shows a great anteroposterior thickness that is by far exceeding that of the radius (192[0]). In anterior and posterior views (Fig. 15C, E), the diaphyses of radius and ulna reach a similar transversal length (193[1]).

Manus: Specimen RGHP D024 preserves ten elements of the right autopod, five carpals, four metacarpals and one phalange, which are extensively described and illustrated by Sagne (2001b: 82–95, figs. 49–51). There is nothing more to add, because these elements were not investigated for this study. Hence, reference is given to the thesis of Sagne (2001b) for informative purposes.

Innominate: Two specimens from the left side, assigned to the right side by mistake, are described and illustrated by Sagne (2001b: fig. 54A, C; Fig. 16). The ilium is a long, slender bone with a rounded cross section and a thickened anterior end. The ischium is transversally flattened, only slightly expanded dorsoventrally, and shorter than the ilium. Ventrally, the pubis forms a short bone of more or less triangular shape. A rounded and

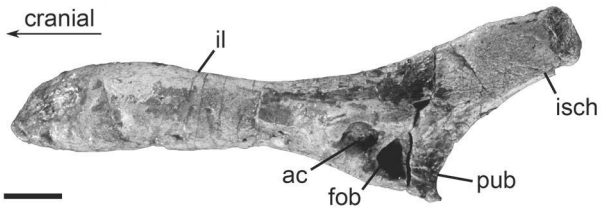

Figure 16. Left innominate of gen. nov. 1 *taulannense* (RGHP C050) in right lateral view (© MNHN and RGHP). Scale bar equals 2 cm.

distinct *acetabulum* is present at the junction of the three pelvic elements (198[0]) and was articulated with a rudimental femur in the animal's lifetime. Ventral to the *acetabulum* in the upper part of the pubis, a small *foramen obturatum* is present (199[0]) measuring 6 mm x 8 mm (RGHP C050; Fig. 16) and 2 mm x 3 mm (AGM 26) in diameter.

Femur: Sagne (2001b: fig. 54B, pl. 18) illustrated and described two femura of 107 mm (RGHP D273) and 117 mm (RGHP E.9.001) lenght. Both elements are overall slender with proximal epiphyses each bearing a well developed femur head. A distal articulation facet is not present on the diaphysis indicating the absence of the zeugopod and autopod.

Remarks

Taxon gen. nov. 1 *taulannense* from the site of Taulanne in southeastern France (Fig. 17) was established and first described as *Halitherium taulannense* by Sagne (2001a) on the basis of numerous skeletal material well established to represent a single species. Sagne (2001a), however, also acknowledged that the taxonomic concept of Sirenia requires careful revision, especially in the subfamily Halitheriinae.

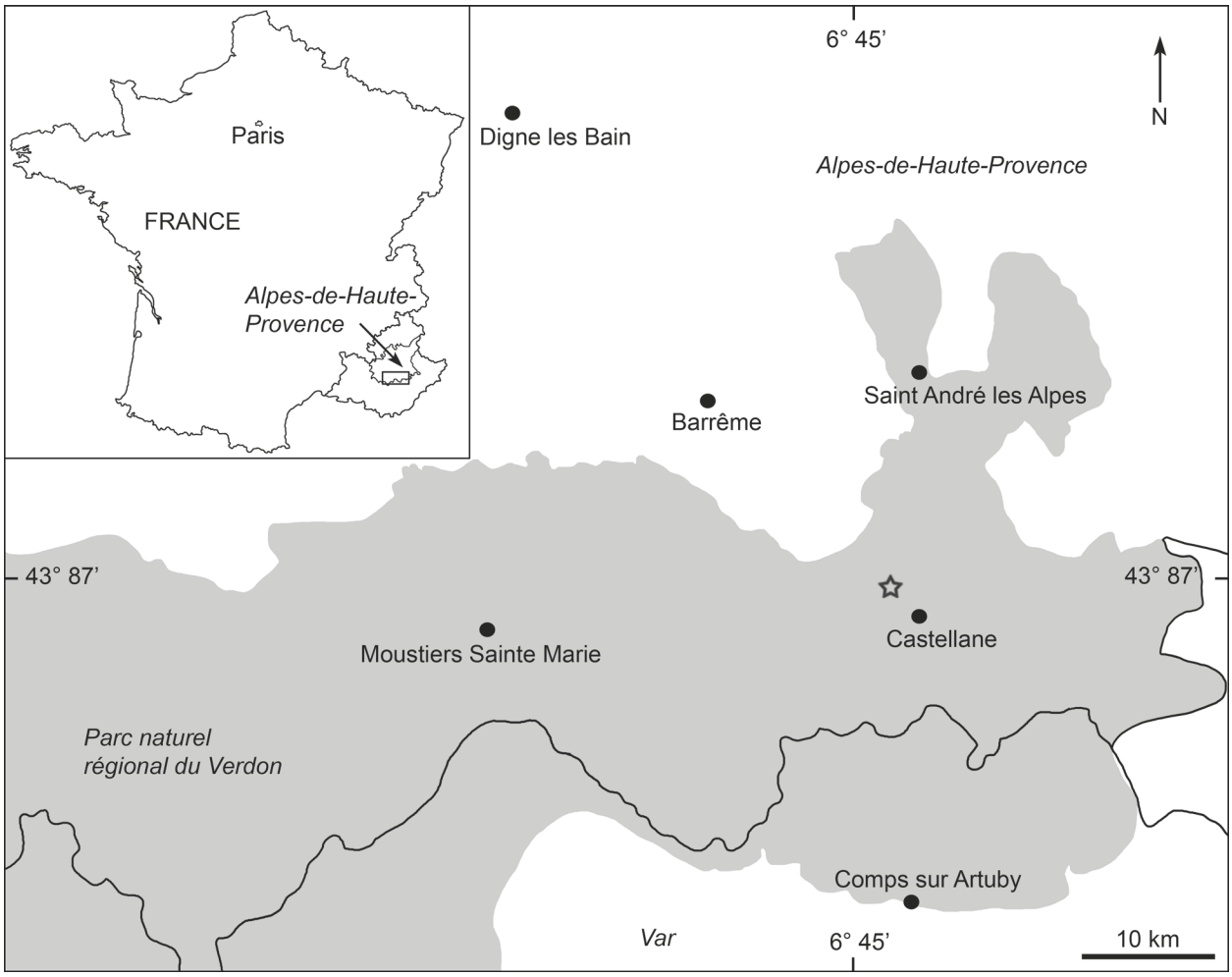

Figure 17. Geographic setting and sketch map of Taulanne, near Castellanne, Alpes-de-Haute-Provence, France. Asterisk indicates estimated locality of species gen. nov. 1 *taulannense*.

In comparison to Sagne's (2001a, b) morphological observations, a particular difference in this study refers to the interpretation of the dental formula of gen. nov. 1 *taulannense*. While Sagne (2001a, b) postulated the presence of three permanent incisors in the mandibular symphysis, the lower lifetime dental formula is amended to i0, c1, p1–4, dp5, m1–3. This is based on the dimensions and bone structure of the incisor alveoli indicating the presence of vestigial deciduous incisors as described above.

Additionally, the conditions given in mandible RGHP E.7.096a, raise the question whether a successional fifth premolar is variably developed in this taxon. Sagne (2001b) hypothesised that the single alveolus in front of the left m1 might indicate a retarded replacement of dp5 and consequently the presence of a permanent fifth premolar in this specific specimen. However, the holotype and all other known specimens show no replacement at the DP/dp5 locus. Sagne (2001b) also concluded that no resorption occurs in one of the two alveoli of dp5. However, personal examinations of specimen RGHP E.7.096a reveal that this is most probably not the case. The "diastema" mentioned by Sagne (2001b) separating the alveolus of the putative p5 from that of p4 is characterised by a roughened, spongy surface and supports the hypothesis of bone resorption. Hence, in this study the single alveolus in front of m1 is interpreted to correspond to the yet unresorbed distal root of dp5. The "diastema" is considered to represent the already resorbed mesial root of dp5. This interpretation is supported by the dimensions of the distal alveolus and the "diastema". The distal alveolus is slightly mesiodistally longer than transversely broad measuring 7 mm x 6.5 mm in maximum diameters. Interestingly, a rounded outline of the "diastema" is roughly detectable, whose dimensions equal those of the distal alveolus. Consequently, it could have also housed an equally sized mesial root of dp5 at an earlier stage of the individual's life. Similar observations have been made in the maxilla of *Dioplotherium manigaulti* (Domning, 1989a), in which the antemolar area is characterised by bone-filled, degenerated alveoli indicating the former presence of deciduous premolars. According to Domning (1989a), the only distinct socket remaining in this roughened area is for the lingual root of the originally three-rooted DP5. The hypothesis of a resorbed mesial dp5 root in RGHP E.7.096a would also be in accordance with Luckett's (1993) observations in mammals, where the process of resorption can take place to different degrees. In conclusion, the absence of a permanent fifth premolar is postulated for gen. nov. 1 *taulannense* in this study suggesting irregular resorption of DP/dp5 in specimens of advanced age.

Genus nov. 2

Type species: Gen. nov. 2 spec. nov. 1 (see remarks below).

Included species: Gen. nov. 2 spec. nov. 1; gen. nov. 2 *bronni*; gen. nov. 2 *alleni*.

Generic diagnosis: Nasals small, length of internasal suture less than half the length of

interfrontal suture. Internasal process of frontal present. Ventral extremity of jugal lies approximately under posterior edge of orbit. *Processus retroversus* moderately inflected. Supraoccipital with thickened nuchal crest and indistinct muscle insertions. Transverse sulcus present on endocranial surface of supraoccipital. I1 alveolus extends about half the length of premaxillary symphysis. Canines and P1/p1 absent. Permanent fifth premolar absent. First rib with protuberance ventral to *capitulum*. Absence of anterior process of manubrium. Pelvis reduced.

Character states: 39[1]; 43[1]; 81[1]; 101[1]; 113[1]; 117[1]; 128[1]; 158[1]; 166[1]; 167[1]; 171[0]; 195[1]; 201[1].

Differential diagnosis: Differs from all other stem group representatives, in that the ventral extremity of the jugal lies not posterior to the orbit (except for *Pezosiren portelli*, *Eosiren stromeri*, and gen. nov. 3 *cristolii*, in which this character is not preserved). A nasal incisure at the posterior end of the mesorostral fossa is present, but not deep in contrast to all other stem group representatives, except for *Eosiren imenti* and gen. nov. 1 *taulannense*. Differs from all crown group taxa in having permanent premolars except for *Anomotherium* and *Miosiren.* Differs from *Anomotherium* and *Miosiren* in lacking a thickened *lamina orbitalis* of the frontal.

Remarks: "Halitherium schinzii" is the type species of the genus *"Halitherium"*, which, however, is only based on a non-diagnostic premolar as the holotype and therefore must be regarded as a *nomen dubium*. Consequently, a new genus, gen. nov. 2, is erected based on a new type species, gen. nov. 2 spec. nov. 1, which comprises the material of the former taxon *"H. schinzii"*, but not of the species *bronni* and not the non-diagnostic premolar. The name *"H. schinzii"* is preoccupied and only applicable to the premolar. This decision is justified by the fact that the second species *bronni*, which was formerly treated synonymous with *"H. schinzii"*, is validated in this study. The species *bronni* is based on a skullcap (SMNS 1539) showing a diagnostic supraoccipital morphology. Gen. nov. 2 spec. nov. 1 is chosen as type species, because its holotype comprises a nearly complete skull associated with a partial skeleton in contrast to the type specimen of gen. nov. 2 *bronni* and, therefore, provides a broader basis to define the new genus.

Gen. nov. 2 spec. nov. 1

Halitherium schinzi; Kaup [partim], *sensu* Kaup, 1855: 11, pl. 2: fig. 1.
Halitherium kaupi; Krauss, 1858: 528.
Halitherium schinzi (Kaup); Krauss, 1862: 385, pls. 6, 7.
Halitherium schinzi; Kaup [partim], *sensu* Lepsius 1882: 1, pl. 5: fig. 52, pl. 10: figs. 96, 97.
Halitherium schinzi (Kaup); Schmidtgen, 1912: 457, pl. 29: figs. 4, 5.
Halitherium schinzi Kaup *forma delheidi*; Sickenberg, 1934a: 271, fig. 2a, pl. 9: fig. 1.

Halitherium schinzi (Kaup); Bizzarini, 1995: 163, fig. 1, pl. 1.
Halitherium schinzii (Kaup); Voss, 2008: 257, figs. 2–7.
Halitherium (Kaup); Voss, 2008: 263, figs. 9, 10.
Halitherium schinzi (Kaup); Bizzarini & Reggiani, 2010: 131, figs. 1–4.

Holotype: A partially preserved associated skeleton of an adult specimen (BSPG 1956 I 540) including the skull, the mandible, the nearly complete vertebral column, the full rib series of the left side and the left innominate.

Referred material: For detailed listing of the preserved skeletal parts see Appendix 1.

Type horizon and locality: Alzey Formation of the Selztal Group (lower Oligocene) from Eckelsheim in the Mainz Basin, Germany.

Range and distribution: Known only from lower Oligocene deposits of the Mainz Basin, Germany (Alzey Formation and Hochberg Subformation (Bodenheim Formation)); the Lower Rhine, western Germany (upper Ratingen Member); the Antwerp and East Flanders Provinces, North Belgium (Boom Clay Formation); and the Paris Basin (Sables de Fontainebleau). Most likely also known from the early Oligocene of the Bay of Leipzig (East Germany), Hungary and Switzerland.

Diagnosis: Represents a species of gen. nov. 2 that is characterised by the combination of the following features: infraorbital foramen oval, distinctly higher than wide; temporal crests as prominent on frontal as on parietal and distinctly converge at centre of skull roof; supraorbital process of frontal dorsoventrally flattened with its dorsal surface gently inclined ventrolaterad; frontal processes of parietal short, do not exceed half the length of frontal roof; cranial roof elongated relative to supraoccipital width; contact between lacrimal and premaxilla; supraoccipital enlarged transversely; external occipital protuberance and external occipital crest prominent; exoccipitals meet in a suture dorsal to *foramen magnum*; supracondylar fossa of exoccipital deep and extending across entire width of occipital condyle; ventral border of horizontal mandibular ramus moderately concave and sharply downturned anteriorly; and pelvis reduced with *acetabulum* still well developed.

Character states: 28[1]; 56[1]; 57[0]; 54[0]; 55[1]; 43[1]; 44[0]; 45[0]; 63[0]; 64 [0]; 74[1]; 112[1]; 116[1]; 118[0]; 121[0]; 123[1]; 144[1]; 198[0]; 199[1].

Differential diagnosis: Differs from gen. nov. 2 *bronni* in that the infraorbital foramen is not rounded; the frontal processes of parietal are not elongated; the cranial roof is not shortened relative to transversal extension of supraoccipital; the maxilla does not extend between lacrimal and premaxilla; the nuchal crest is not notched in median plane; the external occipital protuberance is not reduced; and the P2/p2 are present.

Differs from gen. nov. 2 *alleni* in that the parietosquamosal indentations are less deep; and the supraoccipital shows a small occipital spine of the bony *falx cerebelli* on its endocranial surface.

Description

Figures 18–31; Appendix 3

The following description is mainly based on the holotype material and the partial skeleton NHMUK PV M9415.

Premaxilla: In dorsal view (Fig. 18), the rostrum is laterally compressed forming a mid-dorsal ridge anterodorsally (9[1]). The summit of the premaxillary symphysis is upraised to form a bulbous boss (10[1]) that is separated in midline by the interpremaxillary suture. The mesorostral fossa is not indented anteriorly (11[1]), but retracted and enlarged, reaching to the level of the anterior margin of the orbit (2[1]). The nasal process is thin and tapers at its posterior end (17[0]). It contacts the anteromedial margin of the supraorbital process of the frontal (20[1]), the nasal anteriorly and the lacrimal laterally (74[1]).

In lateral view (Fig. 19A), the premaxillary symphysis is enlarged relative to the condylobasal skull length (4[1]) and strongly downturned anteroventrally by forming an angle between 55° and 60° with the horizontal plane (12[1]). The rostrum exceeds half the total anteroposterior extension of the premaxilla (5[1]). The anteroventralmost maxillo-premaxillary suture lies perpendicular to the posterior end of the symphysis (7[1]).

In ventral view (Fig. 20), the alveoli for the first incisor tusks are preserved while those for I2 and I3 are absent. A dentiform process is not developed (16[0]). The masticating surface of the premaxilla is lanceolate in shape (14[1]) reaching its maximum transversal dimension at the level of the posterior end of the *foramen incisivum*. The latter opens anteriorly in the premaxillary symphysis without distinct demarcation (15[0]). The anterior palatal roof in front of the infraorbital foramina is distinctly narrower than the posterior palate (13[0]).

Nasal: The nasals (Figs. 18, 21A) are relatively small with the internasal suture being shorter than half the length of the interfrontal suture (39[1]). The internasal area is thin and hence often broken. However, its full extent is best observable in the specimens LS RLP PW 2005/5042-LS and PMN SSN12WD14, in which both nasals are completely preserved. Anterolaterally, the nasals reach the level of the anterior margin of the supraorbital process, then slope backwards and taper to form a median tip that remains somewhat behind the level of their anterolateral ends. Both nasals meet in midline (40[0]), but not posteriorly, where they are separated by a nasal process from the frontal (43[1]). A nasal incisure is present at the posterior end of the mesorostral fossa, but it is small not extending posterior to the supraorbital processes of the frontal (42[1]).

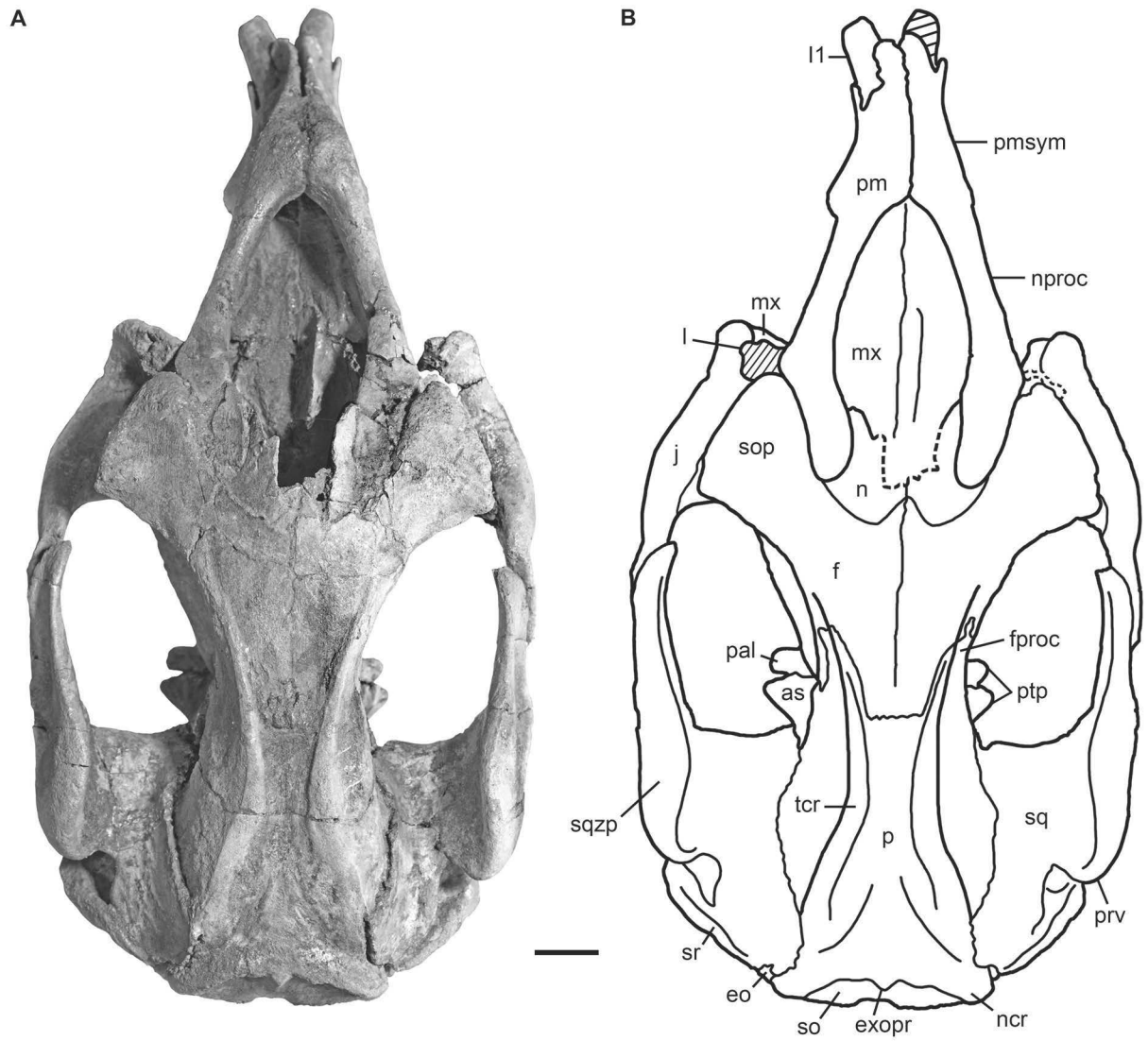

Figure 18. Cranium of gen. nov. 2 spec. nov. 1 (BSPG 1956 I 540, holotype) in dorsal view. **A**, photography. **B**, outline drawing. Shaded areas indicate missing or reconstructed parts. Dashed lines indicate broken parts. Scale bar equals 2 cm.

Ethmoidal region: Where preserved, the mesethmoid forms a distinct perpendicular plate of 15 mm in maximum width in the olfactory chamber. It becomes narrower and is constricted dorsally and ventrally. By becoming narrower also posteriorly, this vertical wall extends below the nasals and along the narial passages to fuse with the presphenoid. Both bones contribute to the *crista galli*, which projects upward from a relatively broad base to the roof of the cranial cavity. The *crista galli* is triangular in cross section as it becomes thinner dorsad. On either side of the *crista galli*, the cribiform plates of the exethmoids are deeply grooved and perforated for the passage of the olfactory nerves. These plates are often not well preserved in the available specimens or only hardly detectable. Usually, a large, vertically directed ethmoturbinal (*concha maxima ethmoidalis* according to Kaiser, 1974) is visible below the nasals and medial to the frontal. Lateral to this ethmoturbinal, a thin *lamina papyracea* is sometimes preserved that, however, is

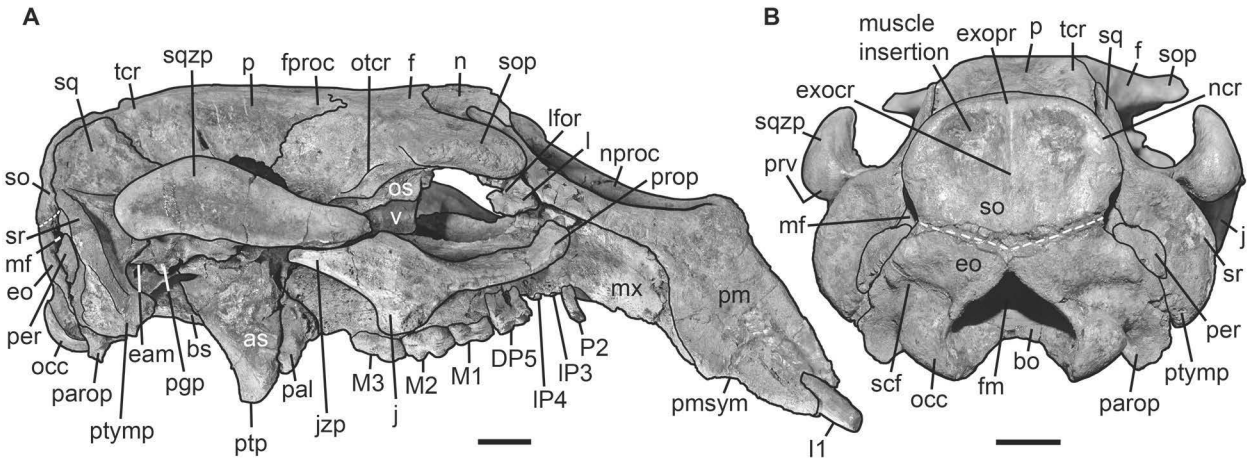

Figure 19. Cranium of gen. nov. 2 spec. nov. 1 (BSPG 1956 I 540, holotype). **A**, in right lateral view. **B**, in caudal view. White dashed lines indicate the supposed course of the suture between the supraoccipital and exoccipital. Scale bars equal 2 cm.

broken on the ventromedial side of the supraorbital process of the frontal in all available specimens. Other ethmoturbinals are either not developed or not preserved.

Vomer: The vomer is, respectively, not completely preserved or visible in any specimen. It is exposed on the ventral side of the holotype skull forming the anterodorsal extension of the median crest of the presphenoid with which it is fused (Fig. 20). The Vomer passes trough most of the internal narial passage and contacts the maxilla and palatine before it runs out anterad in a longitudinal groove on the dorsal side of the maxilla. Only the right lateral border of this maxillary groove is visible through the mesorostral fossa in the holotype (Fig. 18). The vomer itself is not preserved there. Instead, it is visible in right lateral view through the damaged anterior medial wall of the temporal fossa reaching with its broken end up to the level of the posterolateral corner of the supraorbital process of the frontal (Fig. 19A).

Lacrimal: The lacrimal is not completely preserved in any specimen, but its extent can be judged from the imprints in the adjacent jugal and maxilla. It is arranged in an oblique dorsoventral axis and fills a considerable space between the jugal and frontal of about 20 mm in height (73[0]). The contact between the lacrimal and premaxilla is present anterodorsally (74[1]) and a nasolacrimal canal is well discernable in specimen BSPG 1956 I 540 (75[0]; Fig. 19A).

Frontal: The frontal roof (Fig. 18) is flat (52[0]) and delimited by the temporal crests, which form distinct keels (57[0]) that are as prominent on the frontal as on the parietal (56[1]). A knoblike boss is not developed posteromedial to the temporal crests (53[0]). The intertemporal constriction is distinct, reaching its maximum at about the centre of the skull roof (54[0]; 55[1]). The anterior margin of the frontal bears an internasal process

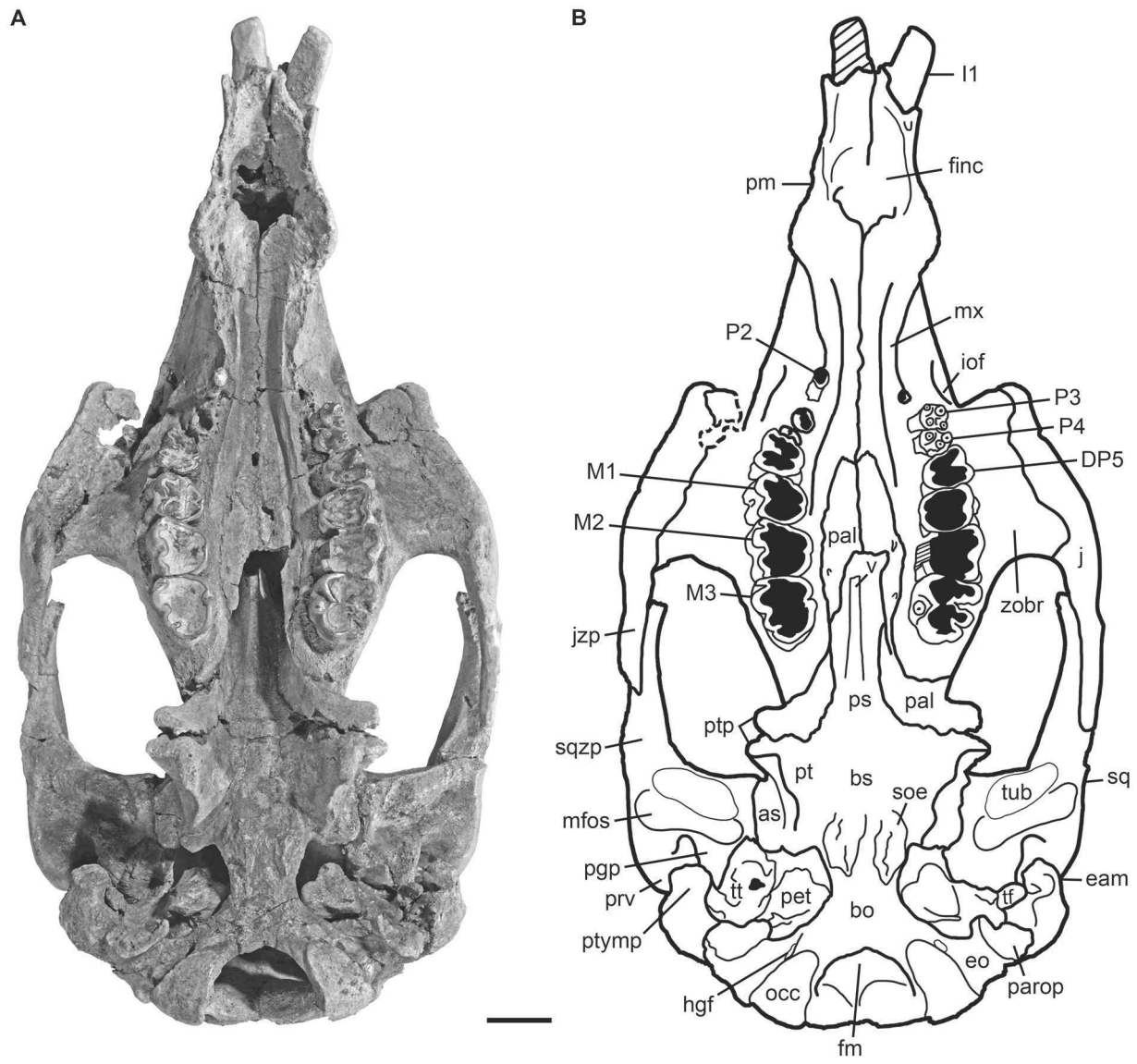

Figure 20. Cranium of gen. nov. 2 spec. nov. 1 (BSPG 1956 I 540, holotype) in ventral view. **A**, photography. **B**, outline drawing. Shaded areas indicate missing or reconstructed parts. Dashed lines indicate broken parts. Scale bar equals 2 cm.

(43[1]). This process can be differently developed, but it is generally short and does not exceed half the length of the internasal suture (Figs. 18, 21A).

In lateral view (Fig. 19A), the supraorbital process is dorsoventrally flattened (44[0]) with a dorsal surface that is gently inclined ventrolaterad (45[0]). Its lateral margin is smooth (46[0]) and arranged diagonally in an anteromedial-posterolateral axis ending in a prominent posterolateral corner (47[1]; 48[0]; 49[1]). The lateral wall of the frontal bears a slight ridge, the orbitotemporal crest (58[0]; 59[1]). The *lamina orbitalis* is clearly discernible by its falciform anterior edge, which is thin forming in part the medial wall of the temporal fossa (60[0]).

Parietal: The parietals are firmly fused with the upper third of the anterior surface of

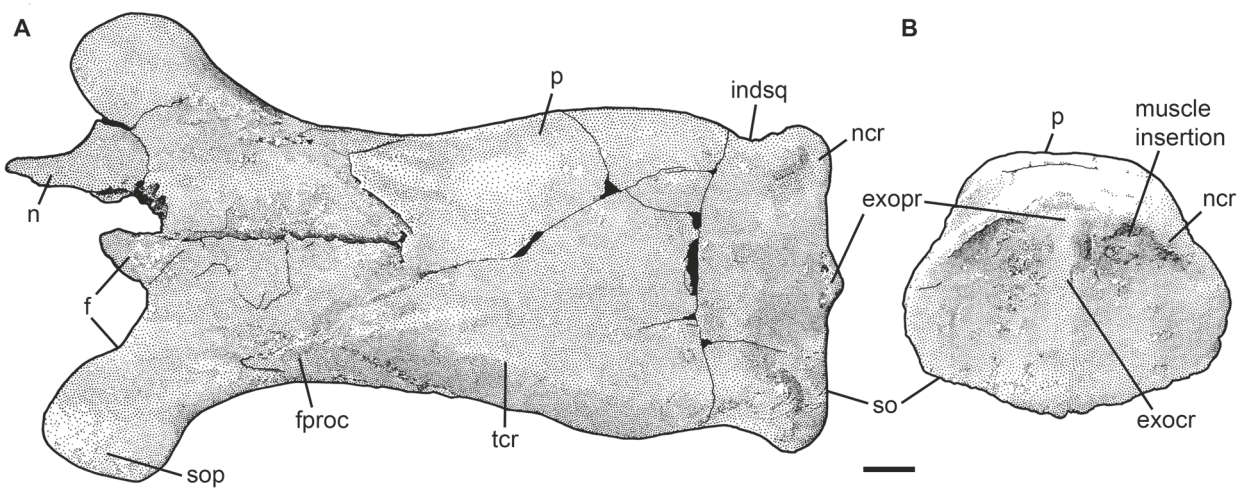

Figure 21. Drawings of supraoccipital-parietal skullcap of juvenile FMD SRK Eck 124 (gen. nov. 2 spec. nov. 1). **A**, in dorsal view. **B**, in caudal view. Black areas indicate broken parts. Scale bar equals 1 cm.

the supraoccipital posterodorsally and with the frontals anteriorly, forming a v-shaped frontoparietal suture (Fig. 18). In dorsal view, the parietal roof is flat and separated from the temporal plane by prominent and lyriform temporal crests (61[1]; 62[1]). In adults of advanced age (FIS M8002), the temporal crests can rise highly above the parietal roof that, in consequence, becomes slightly concave. The temporal crests converge in anterior direction, come closest to the midline in front of the frontoparietal suture and diverge again to join the frontal processes sent off rostrad by the parietals. The frontal processes overlie the frontal roof posterolaterally, but do not exceed half of the interfrontal length (63[0]).

In sagittal plane, the parietal of all studied specimens is longer than the frontal (65[0]). The cranial roof tends to be elongated relative to the transversal extension of the supraoccipital (64[0]). The ratio l_{FP}/w_{SO} varies between 2.07 in BSPG 1956 I 540 and 2.6 in FIS M8002. Due to the distinct intertemporal constriction, the parietals bulge laterally.

In endocranial view (Fig. 22), the parietooccipital suture is usually determinable as a slight furrow or at least as deep dorsolateral pits (transverse sulcus). The suture is overhung ventrally by the double-curved posterior margin of the parietal, which forms an internal occipital spine in the median plane (70[1]). A well-developed *tentorium osseum* extends transversally between the parietal and supraoccipital (72[1]). Medially, the tentoric process is prominent (71[0]) releasing rostrad a strong ridge, the bony *falx cerebri*, which gradually flattens out before reaching the frontoparietal suture (69[0]). The internal parietal surface is characterised by wide grooves and traces of vessels on both sides to the bony *falx* reflecting the relief of the inner surface of the braincase.

Supraoccipital: In dorsocaudal view, the supraoccipital occupies the upper posterior wall of the skull and is intercalated between the parietals following the angle of the lambdoid suture (Figs. 18, 19B). Both, parietal and supraoccipital articulate in an angle that varies

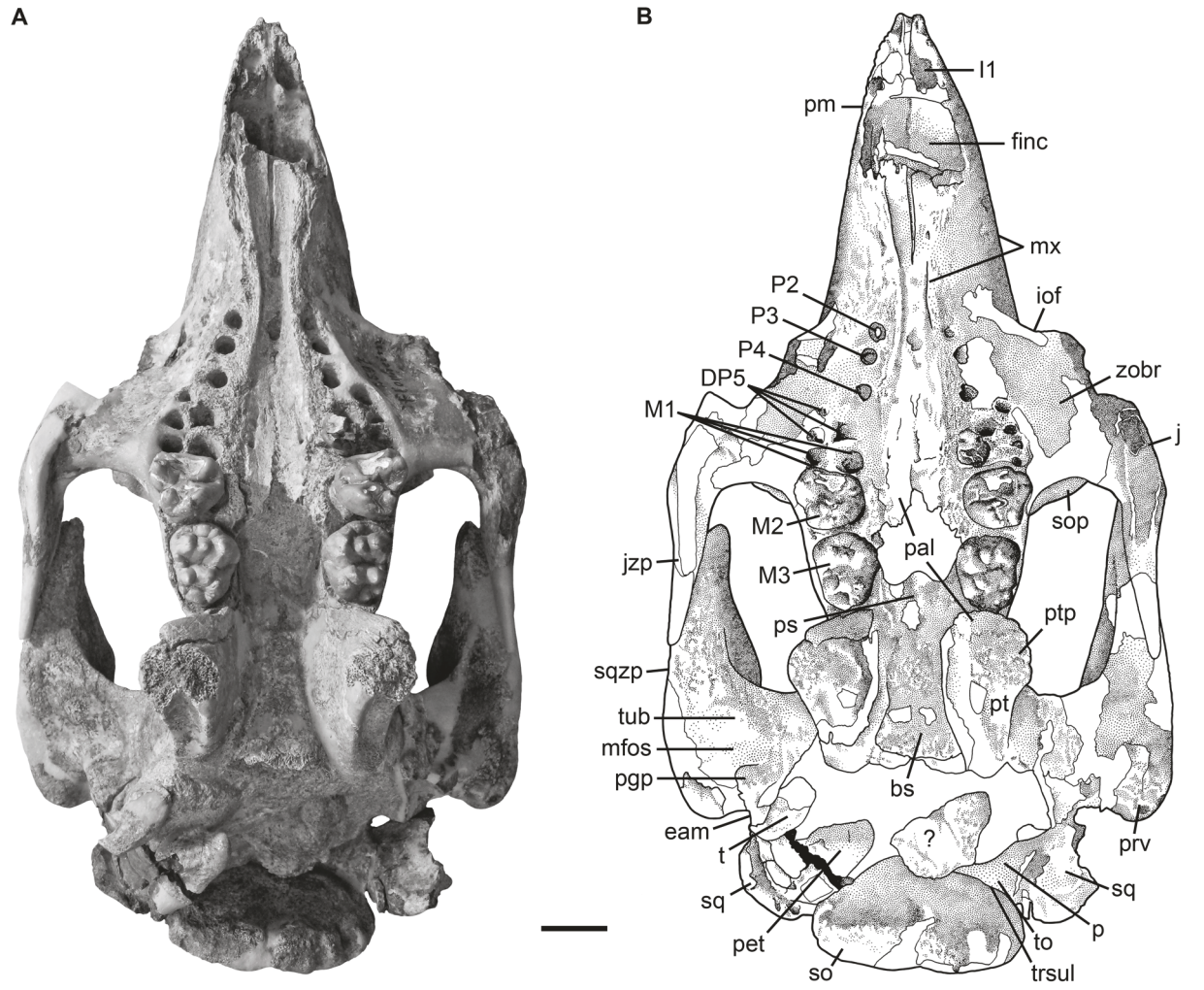

Figure 22. Cranium of gen. nov. 2 spec. nov. 1 (FIS M2597) in ventral view. **A**, photography. **B**, drawing. White areas indicate either missing or reconstructed parts. Scale bar equals 2 cm.

between 120° (e.g., BSPG 1956 I 540 (Fig. 19A), ALMD-JBH A92) and 140° (e.g, FIS M2597, MNHM PW 1991/66-LS). The supraoccipital is relatively low dorsoventrally and wide transversely (Figs. 19B, 21B), according to the ratio width to height that exceeds 1.5 (112[1]). A pronounced nuchal crest forms the broadly convex dorsal margin of the outer surface and extends downwards to about half the height of the supraoccipital (113[1]; 114[0]). In the median plane, the nuchal crest bears a caudally prominent external occipital protuberance in all specimens that have been investigated, even in the juvenile FMD SRK Eck 124 (115[0]); 116[1]; Fig. 21).

The external occipital protuberance either remains approximately at the level of the parietal roof (e.g., NHMUK PV M9415 (Fig. 23A), NMDU-Geo 0001 (Fig. 23C), BSPG 1956 I 540 (Fig. 19B)) or is slightly rising above it (e.g., IRSNB unnumbered (Fig. 23B), HLMD-WT Az 174 and 177, MCZ 8830). Ventral to the protuberance, the external occipital crest projects as a distinct median ridge that exceeds half the height of the supraoccipital (118[0]; 119[0]) and sometimes even enters into its ventral margin (ALMD-JBH A92, see

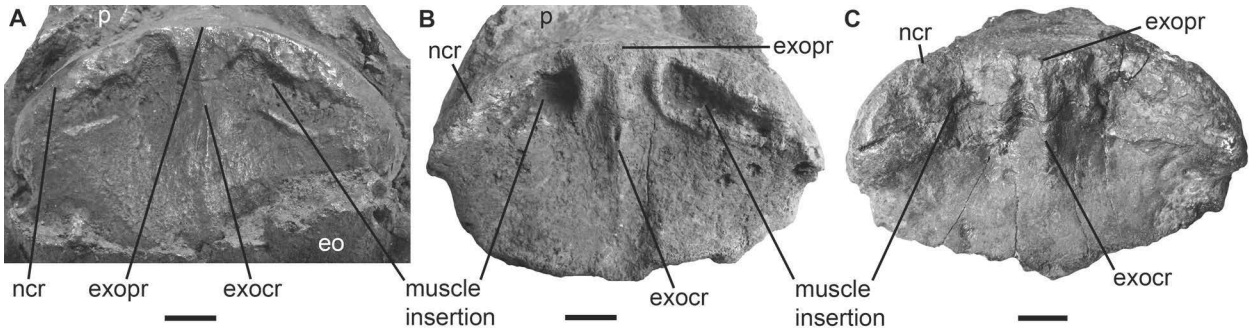

Figure 23. Selection of supraoccipitals of gen. nov. 2 spec. nov. 1 in caudal views. **A**, NHMUK PV M9415. **B**, IRSNB unnumbered. **C**, NMDU-Geo 0001. Scale bars equal 1 cm.

also Voss, 2008: fig. 9). In some specimens like FIS M2715 or an unnumbered supraoccipital in IRSNB (Fig. 23B) a vessel passage separates the upper part of the external occipital crest. Two shorter ridges, which correspond to the medial edges of the muscle insertions, are present lateral to the external occipital crest. These edges are usually distinctly developed and cause a crown-shaped appearance of the external occipital protuberance. This feature is observable to a less distinct degree in BSPG 1956 I 540 (Fig. 19B) and the juvenile specimen FMD SRK Eck 124 (Fig. 21B). Either way, the protuberance is prominent posteriorly and does not remain behind the level of the vertical ridges lateral to it, but rather exceeds that level. The insertions for the semispinal muscle form rugose and irregularly shaped depressions (117[1]). These are also defined ventrally by more or less prominent ridges that meet the nuchal crest laterally causing a roughly triangular form.

In endocranial view (Fig. 22), the upper third of the supraoccipital is firmly fused with the parietals. A transverse sulcus indicates the parietooccipital suture (120[0]) that is most distinctly developed dorsolaterally, forming deep pits. The remaining relief of the internal lamina is characterised by a more or less pronounced median furrow (FIS M2597) that can accompany a median ridge in some specimens (NMDU-Geo 0001). Other specimens (ALMD-JBH A92) show a foramen located at the base of this furrow indicating the presence of a vessel passage. Dorsolateral to this furrow, paired bulges are present that either can be ovoid or terete in shape. The attachment surface for the exoccipitals has an irregular relief and is pointed medially by forming an angle that varies between 140° (BSPG 1956 I 540 (Fig. 19B), NMDU-Geo 0001 (Fig. 23C), ALMD-JBH A92) and 150° (IRSNB unnumbered; Fig. 23B).

Exoccipital: In caudal view (Fig. 19B), the exoccipitals meet in a suture of 10 mm dorsal to the *foramen magnum* (121[0]). Dorsolaterally, these elements are rounded, more or less smooth and not flange-like (124[0]). Each of the exocciptals terminates ventrolaterally in a long paroccipital process, which reaches as far ventrally as the occipital condyles (131[0]). The *foramen magnum* has a triangular outline with its dorsal peak ex-

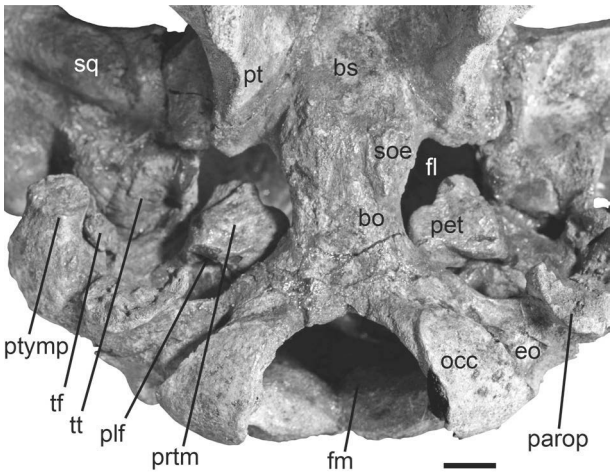

Figure 24. Close-up of cranium of gen. nov. 2 spec. nov. 1 (BSPG 1956 I 540, holotype) in posteroventral view exhibiting the ear region. Scale bar equals 1 cm.

ceeding the level of the occipital condyles (129[1]; 130[1]). The supracondylar fossae are deep and extend across the entire width of the condyles (123[1]). In ventral view (Fig. 20), a hypoglossal (condyloid) foramen completely surrounded by bone is present (127[0]).

Basioccipital: In adults (Figs. 20, 24), the basiocciptal is firmly fused with the basisphenoid, so that the suture is obliterated between both elements. The sphenooccipital eminences for the *longus capitis* muscles form bilateral rugosities that are convex and separated by a slight furrow (128[1]).

Basisphenoid, presphenoid, orbitosphenoid: The sphenoidal region is well preserved in the holotype (Fig. 20). Despite a breakline between the basi- and presphenoid, both bones are identified to be firmly fused with each other as well as with the surrounding elements, the orbitosphenoid, alisphenoid and pterygoid. The sutures to the palatines are still visible. The basi- and presphenoid have a flat ventral surface with a slight anterodorsad slope. At about the level of the posterior end of the maxillary alveolar margin, the presphenoid forms a median crest that projects out cranially to join the vomer. The orbitosphenoid is not completely preserved in the holotype, but partially exposed on the right lateral side of the skull (Fig. 19A). It abuts against the frontal dorsally, the alisphenoid posterodorsally and the palatine ventrolaterally and contributes to the anterior medial wall of the temporal fossa.

Alisphenoid: Wing-shaped pterygoid processes originate ventrolateral to the basisphenoid, whose posterolateral sides are each formed by the alisphenoid (Fig. 19A). The outer surface of the alisphenoid is flat to slightly uneven. In lateral view, the alisphenoid canal is no more discernable (132[1]) and the *foramen ovale* forms a distinct incisure (133[1]). This is excellently visible laterally and also ventrally in the holotype (Figs. 19A, 24), where the *foramen ovale* opens into the *foramen lacerum*.

Pterygoid: The pterygoid processes are posteromedially formed by the pterygoid, whose sutures to the surrounding bones are no more traceable (Fig. 20). Posteriorly, the pterygoid fossa extends above the level of the roof of the internal nares (134[0]). Its ventromedial border contributes to the distal end of each pterygoid process by forming a hook-shaped hamuli process (135[1]).

Palatine: In ventral view of the skull (Fig. 20), the anterior parts of the palatines are dorsoventrally flattened and anteroposteriorly elongated between the maxillae. Both bones extend anteriorly beyond the posterior edge of the zygomatic-orbital bridge of the maxilla (33[0]) up to the anterior margin of DP5 in subadults (FIS M2597; Fig. 22) or even to the level of P4 in adult specimens (BSPG 1956 I 540; Fig. 20). If preserved, the posterior border of the palatine shows an incisure (35[1]) that does not exceed the level of M2 even though the palatines are broken posteriorly in some specimens. For the remaining horizontal distance both elements meet in midline. Laterally on the horizontal portion of the palatines, a small pair of foramina is present, which can occupy a position more or less medial to M3 (BSPG 1956 I 540; Fig. 20) or to M1 (FIS M2597; Fig. 22). In BSPG 1956 I 540, another, larger foramen is also present medial to the left M2. The posterior parts of the palatines form the anteromedial margins of the pterygoid processes by having sutural contact with the pterygoid posteromedially, the alisphenoid posterolaterally and the maxilla anteriorly. Both palatines also form a posterior wall between the internal nares and the temporal fossa by curving anteromediad up to the presphenoid and orbitosphenoid.

Maxilla: Anteroventrally (Fig. 20), the maxilla surrounds a small infraorbital foramen that does not exceed 200 mm² (25[0]) and is oval in cross section, distinctly higher than wide (28[1]). The infraorbital canal is not obstructed (31[0]). The posterior opening of the maxillopremaxillary canal can be detected through the orbit in lateral view of the skull. The zygomatic-orbital bridge extends laterally and is nearly level with the palate ranging between 10 mm and 15 mm above the alveolar margin (21[1]).

In ventral view (Fig. 20), the zygomatic-orbital bridge is elongated anteroposteriorly (22[0]) and concave with a smooth surface. Its anterior margin is very thin measuring 2 mm in average while the posterior margin is always thickened in a range between 10 mm to 20 mm (23[0]; 24[1]). The maxillary tooth arcades are lyriform, broadly convex between the molars, tapering at the level of the premolars and widening again towards the *foramen incisivum*. The palate is thin at the level of the penultimate cheek tooth (32[0]).

Squamosal: On the lateral side of the skull (Fig. 19A), the squamosal extends to the temporal crests (87[1]) and forms conspicuous indentations in the posterior corners of the parietal roof causing the separation of the temporal crests from the nuchal crest (88[1]; Fig. 18). Posterolaterally (Fig. 19), the squamosal defines the mastoid foramen anteriorly together with the exoccipital posteriorly and the supraoccipital dorsally (110[1]), 111[0]). The posttympanic process bears a prominent sigmoid ridge extending to the level of the ventral margin of the supraoccipital (99[1]; 100[1]). Ventrally, the sigmoid ridge inserts into the rostrad projecting ventral tip of the posttympanic process (Fig. 19A), which is roughened and serves as attachment area for the sternomastoid muscle (108[0]; 109[0]). The external auditory meatus is short mediolaterally (104[0]) and about as wide anteroposteriorly as high (106[1]).

The zygomatic process projecting lateral to the skull is strongly developed, triangular in lateral view with a rounded posterior and a tapering anterior end (89[1]; Fig. 19A). Its anterior end terminates often into a slightly dorsad rising tip. Posterodorsally, the zygomatic process is straight to concave (98[0]) while its anterodorsal and ventral margins are nearly straight. The lateral surface is generally smooth. On its anterior half, a slight horizontal concavity flattens out dorsad and posterad. The medial side of the zygomatic process is flat to concave (90[0]) and defined dorsally by a sigmoid ridge (91[1]; Fig. 18). Posteriorly, the zygomatic root shows a distinct notch (92[1]).

In ventral view (Fig. 20), the *processus retroversus* is moderately inflected (101[1]) forming the posterior end of the zygomatic process. The uneven ventral surface houses a deep mandibular fossa and a broad, prominent *tuberculum* (94[1]; 95[1]), which are both transversely directed for the articulation with the mandible (93[0]). Posteriorly, the mandibular fossa is defined by a prominent, knob-like postglenoid process (96[0]; 97[1]).

Jugal: In lateral view (Fig. 19A), the jugal defines the orbit anteroventrally and contacts the lacrimal (79[1]) anterodorsally and the squamosal posterodorsally. Its thin preorbital process (76[1]; 77[0]) does not reach the premaxilla (78[0]). The ventral rim of the orbit is not overhanging (86[0]). The ventral extremity of the jugal lies approximately under the posterior edge of the orbit (81[1]). A postorbital process is present dorsally (84[1]), but distant to the supraorbital process of the frontal (85[0]). Unless broken, the zygomatic process of the jugal extends posteriorly on the ventral side of the zygomatic process of the squamosal to the anterior margin of the *tuberculum*. Its length exceeds the diameter of the orbit (83[0]).

Ear region: The ear region is best observable in specimens NHMUK PV M9415, MNHM PW 1991/66-LS, BSPG 1956 I 540 (Fig. 24) and CDGG S3. They all preserve the periotic completely or in parts, comprising the mastoid, petrosal and *tegmen tympani*. The periotic is set in a closely fitting cavity of the squamosal, not fused with the alisphenoid or any other skull bone (136[1]), and visible through the *foramen lacerum* in ventral view of the skull. In many specimens, the periotic is medially broken lacking the petrosal and revealing the dense histology of this bone.

The mastoid makes up the dorsoposterior part of the periotic and is fused anteriorly with the petrosal and the *tegmen tympani*. The transition from the mastoid to the *tegmen tympani* is smooth and continuous. Posterolaterally, the mastoid bears a *processus fonticulus*, which forms an oval and roughened protuberance that fits into the mastoid foramen (Fig. 19). The *tegmen tympani* is convex, kidney-like shaped and attached to the lateral side of the cranium forming the roof of the tympanic chamber. It tapers anteromedially into a blunt end, where it faces the alisphenoid. Posteroventrally, the *tegmen tympani* is in contact with the posttympanic process of the squamosal. Both, the *tegmen tympani* and the mastoid are of similar size.

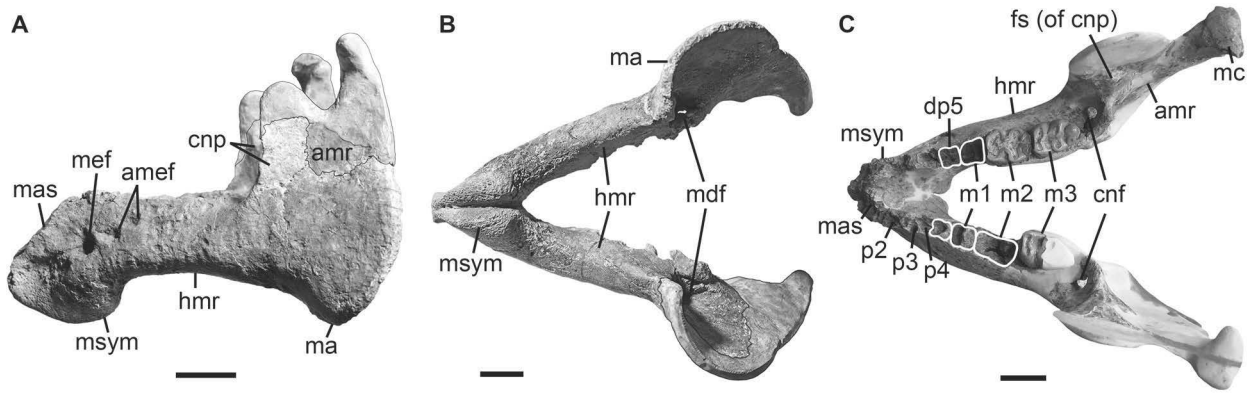

Figure 25. Mandibles of gen. nov. 2 spec. nov 1. **A–B**, BSPG 1956 I 540 (holotype) in left lateral (A) and ventral (B) views. **C**, CDGG S3 in occlusal view. Both, framed and white areas, indicate missing or reconstructed parts. Scale bars equal 3 cm.

In transversal plane (Fig. 24), the petrosal extends far into the *foramen lacerum* ending in a roughly convex medial margin. The petrosal is nearly spherical in cross section and characteristically bears a smooth-surfaced, mediocentrally knoblike promontorium on its ventral side. The promontorial ridge extends posterolaterad and terminates at about the level of the squamosoexoccipital suture. Anterolateral to the promontorium, the oval window (*fenestra ovalis* or *fenestra vestibuli*) opens, which is, unless its name suggests, round reflecting the shape of the stapedial foot plate. An oval and large perilymphatic foramen opens posteromedial to the promontorium. Medial to the posterior attachment surface of the tympanic, a distinct, mediolaterally elongated concavity for the insertion of the *musculus stapedius* is present. In endocranial view, the endolymphatic foramen forms a narrow and slit-like opening.

The tympanic forms an asymmetrical and bulbous element with a smooth outer surface. Its distal border is v-shaped bearing a blunt medioventrally directed tip. The anterior branch of the tympanic is shorter than the posterior one and attached to the *tegmen tympani*. The posterior branch is expanded into a rounded and flat plate that faces the anteromedial side of the posttympanic process (Fig. 24). The lumen of the tympanic arch is filled by the malleus, which is present *in situ* in HLMD-WT 420 on the left side as the only preserved auditory ossicle. The malleus is a massive and stout element characterised by a sharp horizontal ridge on its lateral side.

Mandible: In lateral view (Fig. 25A), the symphysis is distinctly higher than long (142[1]) and exhibits the mental foramen (141[0]). Dorsoposterior to the latter, several accessory mental foramina are present (140[0]). The horizontal mandibular ramus is slender (156[0]), moderately concave ventrally and sharply downturned anteriorly at the level of the symphysis (144[1]). Posteriorly, the horizontal ramus is not tangent to the angle (147[1]). The mandible has a broadly convex outline well below the condyle (149[1]) lacking a *processus angularis superior*. Although broken or replaced by plaster in most specimens,

the ascending ramus can be determined to have a coronoid process with a slight anterior slope (151[1]). The condyle occupies a position below the level of the coronoid process, which however, is erroneously reconstructed in the holotype (Fig. 25A). In ventral view (Fig. 25B), the mandibular symphysis is broad and bulging laterally (137[1]). Ventromedial to the anterior border of the ascending ramus, the undivided mandibular foramen exposes the dental capsule of m3 posteroventrally (154[0]; 155[1]). In occlusal view (Fig. 25C), the masticating surface is narrow and roughened without a furrow in the median plane (138[0]; 139[0]). The condyle is elliptical in shape, as broad medially as laterally (148[0]) and the coronoid foramen at the base of the coronoid process is enlarged with 7 mm in average diameter (153[1]).

Dentition: Though often heavily worn, the complete cheek tooth series including the persistent fifth premolar is preserved in the upper and/or lower jaws of some specimens (BSPG 1956 I 540, NHMUK PV M9415, MNHM PW 1949/157). The complete tooth series is only known from BSPG 1956 I 540 and the dental formula mostly has to be judged from the preserved alveoli. The lifetime dental formula is interpreted here to be I1, C0, P2–4, DP5, M1–3 in the upper jaw, and i0, c0, p2–4, dp5, m1–3 in the lower jaw (164[1]; 166[1]; 167[1]; 168[1]; 169[0]; 170[0]; 180[0]; 181[0]).

Upper dentition: Incisor tusks of good preservation and associated with a partial skeleton are known from specimens LS RLP PW 2005/5042-LS and PMN SSN12EC55 (Fig. 26B). The tusks are slightly curved along their longitudinal axis and extend about half the length of the premaxillary symphysis (158[1]). Both, the crown and root are clearly separated from each other (165[0]). The crown is composed of enamel on all sides (160[0]) and suboval or subelliptical in cross section (161[0]). Its ventral tip is often slightly worn. The tusks protruded about 2.0 cm from the premaxillae.

The permanent premolars are single-rooted (173[1]) and comprise P2–4 mostly known from specimens like FIS M2597 that preserve the corresponding alveoli (Fig. 22). Of all specimens, BSPG 1956 I 540 also preserves the left P3-4 and the right P2 (Fig. 20). The crown of P2 shows an advanced state of tooth wear in having a flat to concave occlusal surface, which causes a pencil-shaped appearance of that tooth.

The moderately worn P3–4 still reveal the characteristic cusp pattern already described for gen. nov. 1 *taulannense*. A high central cusp is surrounded mesially, lingually and distally by accessory cuspules, whose number apparently increases in distal direction within the tooth arcade. The crowns of the left P3–4 of specimen PMN SSN12WD14 are nearly unworn and preserved *in situ* in the maxilla. However, PMN SSN12WD14 is on display in find situation and therefore the teeth were not fully accessible and only visible from their smooth and convex labial side.

If preserved, the DP5 crown is heavily worn preventing any detailed description of its cusp pattern (Fig. 20). However, it can be clearly identified as a three-rooted molariform premolar indicating that no replacement occurs at this locus (171[0]). The persisting

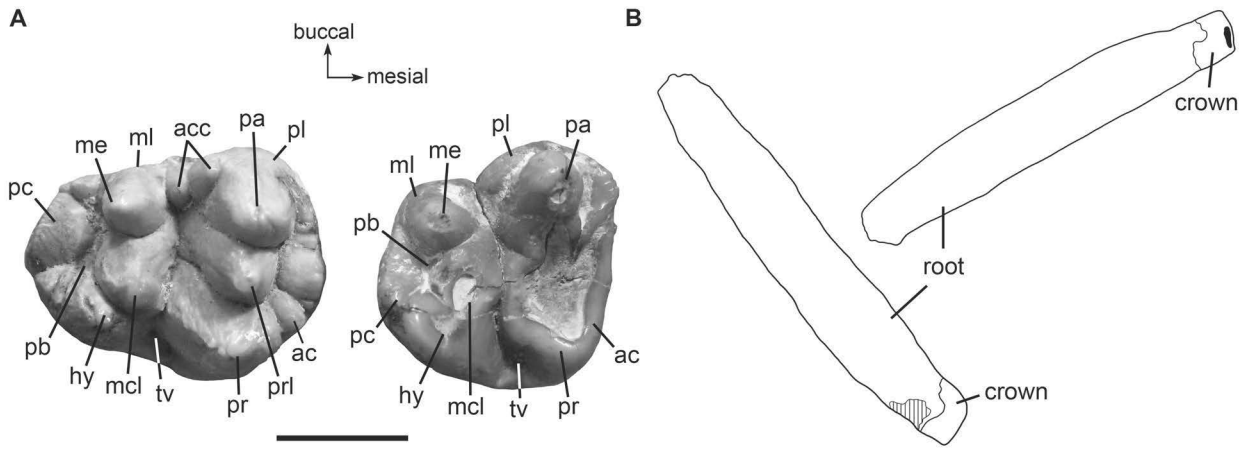

Figure 26. Dentition of gen. nov. 2 spec. nov. 1. **A**, photography of the right upper molars M3–M2 (from left to right) of specimen FIS M2597 in occlusal views. Scale bar equals 1 cm. **B**, outline drawings of the left and right incisor tusks (I1) of specimen PMN SSN12EC55. Shaded area indicates broken part. The exact scale and anatomical provenance of the originals was not determinable, because the respective skeleton is on display.

DP5 is heart-shaped in outline as are the subsequent molars, but smaller than M1. The presence of the proto- and metaloph as well as an anterior *cingulum* is observable in specimen PMN SSN12WD14.

The molars are usually characterised by intense tooth wear showing the highest degree on M1 and the lowest degree on M3. Only in very old individuals like BSPG 1956 I 540 the occlusal surfaces of M1–3 are uniformly flattened and concave (Fig. 20). The size of the molars is not reduced relative o the skull (182[0]), but increases in distal direction within the tooth arcade revealing M3 to be the largest molar. Although M1 is strongly worn in all specimens observed, all molars are morphologically similar. They comprise the transversally arranged protoloph and metaloph, both separated by a transverse valley, and a *precingulum* and *postcingulum* each enclosing an anterior and posterior basin, respectively. Their crowns are roughly heart-shaped and their roots always consist of three parts, a mesiolabial, a distolabial and a lingual root. The enamel of the molars is smooth and about 2 mm thick.

Specimens FIS M2597 (Fig. 26A) and NHMUK PV M9415 preserve the left and right M2 in a moderate state of tooth wear revealing the cusp pattern. Paracone, protoconule and protocone are arranged in a transverse row forming the protoloph. On the metaloph, the metacone and hypocone are at the same level. The metaconule in between, however, is shifted towards the protoloph with about one third of its cusp by obstructing the transverse valley centrally (178[1], 179[1]). Otherwise, the transverse valley is deep and opens v-shaped into the lingual and labial sides separating the two main transverse lophs. Sometimes, the lingual and labial terminations of the transverse valley have an accessory cuspule, as in the left M2 of FIS M2597. The *pre-* and *postcingula* form strong ridges that

are attached lingually to the proto- and metaloph. Both *cingula* decrease in height and open to the labial (or buccal) side. The *postcingulum* is usually bicuspid. The anterior and posterior basins are about equal in size and do not exceed the maximum mesiodistal dimensions of the transverse valley. The overall form of M2 is heart-shaped with the median tip facing the lingual side, and the protoloph is slightly larger than the metaloph.

This proportional difference of the crown is developed to a marked degree on M3, where the metaloph is distinctly shorter transversally than the protoloph causing an elongated form of the tooth. Specimens FIS M2597 (Fig. 26A) and NHMUK PV M9415 preserve nearly unworn crowns of M3, which are not yet fully erupted indicating the subadult age of both individuals. The proto- and metaloph are characterised by the three main cusps, which are aligned transversally only on the protoloph. Distolabial to the paracone, one or two accessory cuspules can be present, which then close the transverse valley labially (Fig. 26A). Mesial to the protoloph, a cuspid *precingulum*, which is attached to the paracone and open lingually, encloses a narrow and deep anterior basin.

The metaloph of M3 reveals the same situation as on M2 with the metaconule obstructing the transverse valley centrally. In FIS M2597 (Fig. 26A), the metaconule is not a small cusp between the usually slightly larger metacone and hypocone, but it is at least as large as the adjacent cusps. The apex of the metaconule slopes lingually towards the hypocone while its broad basis contacts the metacone, protocone and protoconule. Both, hypocone and metaconule are clearly separated by a distinct furrow (177[1]). Additionally, the hypocone is somewhat set back within the metaloph and not on the same level with the metacone causing a convex arrangement of the hypoloph in mesial direction. The posterior basin is larger than the anterior one and generally enclosed by two to three cingular cusps (175[1]). The *postcingulum* is attached to the hypocone and opens labially.

Lower dentition: The mandibles associated with NHMUK PV M9415 and CDGG S3 (Fig. 25C) provide the most comprehensive information on the lower dentition. If the teeth are preserved at all, their crowns represent an advanced stage of tooth wear limiting their potential information.

The masticating surface of the mandibular symphysis is characterised by four closely spaced and shallowly concave pairs of alveoli filled with spongy bone tissue. Permanent lower incisors and canines are, accordingly, not developed in this taxon, but most likely four pairs of vestigial teeth, three incisors and one canine on each side.

The presence of permanent lower premolars is indicated by the single alveoli for p2–4, which are broken out in some specimens and, therefore, not always clearly determinable. Although collections like the HLMD and the MNHM house numerous isolated premolars from the lower Oligocene of Germany, such teeth associated with any of the investigated mandibular specimens are not known up to date.

Specimen NHMUK PV M9415 preserves dp5 to m3 from the left and right sides. The teeth commencing dp5 to m2 are worn and therefore their description is generalised

and summarised in the following. All teeth are two-rooted and characterised by mesiodistally elongated crowns indicating dp5 to have a molariform morphology. The teeth slightly increase in size distad within the tooth arcade. Their crowns typically consist of the mesial protolophid and the distal hypolophid, both separated by a deep transverse valley. Both lophs are about equal in transversal length and approximately perpendicular to the mesiodistal axis of the tooth arcade. The wear surfaces of the proto- and hypolophid fuse roughly in the centre of the transverse valley with progressive tooth wear and, finally, lead to an almost flattened occlusal surface as it can be most distinctly noticed in dp5. The lingual sides of the teeth are always higher than the labial ones, so that the occlusal surfaces slope in labial direction.

In comparison with dp5 and m1, the m2 is only moderately worn and still reveals the metaconid of the protolophid and the presence of an accessory cuspule connected mesiolingually to the hypoconid of the hypolophid. This cuspule projects mesiad obstructing the transverse valley more or less in the middle of m2. Anterolabially, a slight *precingulum* is detectable at least on m1 and m2. A *postcingulum* is always present and encloses a distinct talonid basin that increases in size from dp5 to m2. The still unworn hypoconulid lophule of m2 enclosing the talonid basin is bicuspid.

The m3 is best observable in NHMUK PV M9415, showing an erupting tooth, and in CDGG S3 (Fig. 25C), where it is completely preserved in a moderate state of wear on the right side. This tooth has an elongated oval shape tapering distad with the protolophid being slightly larger than the hypolophid and the hypoconulid forming the narrow distal end. All cusps are entirely unworn on the m3 of NHMUK PV M9415 revealing the proto- and metaconid subequal in size and shape forming a transverse row perpendicular to the longitudinal axis of the tooth. An indistinct anterior *cingulum* is present anterolabially on m3 of CDGG S3. The transverse valley forms a deep furrow separating the protolophid from the hypolophid. Its obstruction by a hypoconid accessory cuspule is already indicated in NHMUK PV M9415. This condition is more distinctly developed in CDGG S3 and resembles the cusp pattern observable in the preceding molars. Otherwise, the hypo- and entoconid are similar in size and form the transverse hypolophid parallel to the protolophid. The hypoconulid is nearly unerupted in NHMUK PV M9415 showing only one large cusp distolingual to the hypoconid. In addition to this cusp, a smaller lingual cusp is present behind the entoconid of CDGG S3 (Fig. 25C). The hypoconulid is clearly separated from the hypolophid by a talonid basin of variable width.

Hyoid apparatus: Not known from any available specimen assignable to gen. nov. 2 spec. nov. 1.

Vertebral column: The morphology of the thoracic, lumbar and caudal segments of the vertebral column including 14 vertebrae is already published for specimen NMDU-Geo 0001 (Voss, 2008), which is now assigned to gen. nov. 2 spec. nov. 1. Therefore, the

following description is kept generalised and mainly complemented by data received from complete or nearly complete skeletons like NHMUK PV M9415 and BSPG 1956 I 540.

In specimen NHMUK PV M9415, a most likely complete vertebral column is preserved. The atlas is broken and attached to the posterior side of the skull. The remaining column is isolated from the skull, but present in two parts separated between thoracics T17 and T18. Each part represents a series of articulated vertebrae, which are in most cases completely preserved. Only the anterior part of the column up to the level of T8 is compressed and partially broken. The vertebral column of specimen NHMUK PV M9415 includes 55 vertebrae, thereof seven cervicals, 19 thoracics, two lumbars, a single sacral and 26 caudals.

Cervicals: The atlas is completely preserved in BSPG 1956 I 540 and characterised by kidney-shaped cranial and caudal articular facets. These facets form distinct concavities with dorsolaterad flaring edges slightly directed to the vertebral canal. The transverse processes are aliform and slope posterodorsad bearing the atlantal fossa on their ventral sides. The *foramen transversarium* opens ventrally at the base of the transverse processes. On the ventrointernal side of the lower arch, the articular surface for the odontoid process of the axis is distinct forming an oval concavity and a caudad extending process. The upper arch is broadly convex and bears a slight median keel. Posterodorsally, the upper arch shows a slight indentation for the articulation with the neural spine of the axis.

The axis has a prominent odontoid process with a flattened and rounded ventral articulation surface for the atlas and a roughened rostral tip. Hook-shaped transverse processes originate on the ventrolateral sides of the centrum and surround an oval *foramen transversarium*. The longitudinal axis of the latter extends in transversal plane. The anterior articular facets are suboval, dorsoventrally higher than transversely broad, and flat to slightly convex. The lateral parts of the neural arch are flattened in oblique mediolateral view and diverge posteriorly. Posterodorsal to the vertebral foramen, the flattended ventral sides of the postzygapophyses face posterolaterad and ventrad. The summit of the neural arch is formed by a rounded and massive neural spine. It has a median keel anteriorly that terminates into a pointed rostral tip with an articular facet for the atlas. Its posterior side has a median cleft. In specimen BSPG 1956 I 540 the axis and C3 are fused in their dorsal half as a peculiar characteristic. Both vertebrae are visible to be separated only in lateral view.

Cervicals 3–7 are characterised by anteroposteriorly flattened centra, slender neural arches pointed dorsally to a median keel, and large vertebral foramina. The transverse processes are short and hook-shaped often with small and irregular protuberances on their ventral sides. They enclose the *foramen transversarium* except in C7, where it is opened to form an incisure lacking a dorsolateral bony bar. The articular facets of the prezygapophyses are directed dorsad and anteromediad while those of the postzygapo-

physes show ventrad and posterolaterad. Both, pre- and postzygapophyses are at the same level.

Thoracics: The thoracic vertebrae are clearly identifiable by the articular facets for the *capitulum* and *tuberculum* of the corresponding rib on the lateral sides of the centrum and the lateroventral ends of the transverse processes. The transverse processes are knob-like and characteristically attach dorsally on the lateral side of the vertebral body, close to the root of the neural arch. The centra are always wider than high, but their length and width slightly increase in caudal direction. On the ventral side, the centra have more or less pronounced longitudinal keels. Dorsally, a shallow and flat longitudinal depression is present giving the centra a roughly heart-shaped outline. The cranial and caudal surfaces of the centra are flat. Nutrient foramina are often present in the longitudinal depression on the dorsal surface of the centra and/or below the base of the transverse processes.

The neural arch surrounds a keyhole-shaped vertebral foramen in the majority of thoracics. On T1–3, however, the vertebral foramen is distinctly larger resembling that of the preceding cervicals. Additionally, the neural spines of T1–3 are narrower craniocaudally than in the following thoracics, strongly elongated dorsoventrally and pointed. A distinct caudad inclination of the neural spines starts from T6. The neural spines reach their maximum craniocaudal extension commencing on T15, where they also slightly decrease in caudad slope. All neural spines are keeled anteriorly and concave posteriorly, sometimes with a thin median crest. The summits of the neural spines are roughened forming a more or less triangular tuberosity. Dorsolateral to the vertebral foramen, the prezygapophyses form dorsally flat articular facets extending in horizontal plane. They are delimited laterally by short, but distinct mamillary processes. The postzygapophyses form backward-pointed processes with a flat ventral side.

Lumbars: The lumbar vertebrae are characterised by mediolaterally long transverse processes that attach with craniocaudally broad bases lateral to the centra. The transverse processes are often convex anteriorly and slightly concave posteriorly sloping in caudoventral direction to terminate in bluntly tapered ends. Like the thoracics, the centra of the lumbars are always wider than high while their length slightly increase craniocaudally within the column. The outline of the centra is either broadly oval or heart-shaped. A dorsal longitudinal depression is always present and, in the heart-shaped forms, also a pronounced ventral crest. Otherwise, the ventral keel is developed to a lesser degree or absent. The lateral sides of the centra are concave with the edges of the cranial and caudal surfaces projecting laterad. Both, the cranial and caudal epiphyses are slightly concave centrally. The neural arches morphologically agree with the posterior thoracics except for the mamillary processes that are absent and the neural canals, which are suboval, wider than high. The neural spines are keeled not only anteriorly, but also posteriorly.

Sacral: The sacral vertebra does not differ from the preceding lumbars. However, its transverse processes are roughened ventrally ending in a thickened, bluntly pointed

distal tip for the attachment of the pelvic tendons.

Caudals: The caudal vertebrae exhibit ventrally the characteristic more or less prominent, anterior and posterior demifacets for the paired chevron bones. The demifacets are often pointed towards the centre of the ventral surface and sometimes result in a longitudinal ridge defining a flat furrow. Several oval or stretched pairs of various sized foramina occur in the middle of this furrow at different intervals of some millimetres. Length, width and height of the centra gradually decrease caudad within the column. The cranial and caudal epiphyses are flat, equal in size and often possess a central cavity. In the more anterior caudals, a broad longitudinal depression extends dorsally and the ventral side is keeled causing a slight heart-shaped outline. The more posterior caudals are either elliptical or hexagonal. The dorsal depression bears several nutrient foramina of varying sizes, often adjoined in a horizontal row, as does the posterior side of the transverse processes.

The transverse processes originate laterally from about the centre of the vertebral body, but, starting with Ca9, they arise from the upper third of the centrum. Caudals 1–4 still have transverse processes similar to the lumbars and sacral vertebra with respect to their transversal length and more or less horizontal lateral extension. From Ca5 onwards, the transverse processes progressively sweep back extending up to or exceed the level of the caudal epiphysis of the centrum. They become approximately parallel to the centrum length between Ca9 and Ca13, straighten again at Ca14 and are perpendicular to the horizontal body axis commencing Ca16 to Ca23. On Ca24–26, the transverse processes form merely slight lateral extensions of the vertebral body. A rhomboid tuberosity is often present on the rear side of their distal ends. In anterior view, the transverse processes often have a sharp edge.

The transversely oval vertebral foramen is surrounded by a low neural arch, from which a moderately high neural spine extends. The lateral flanges of the neural spine taper anteriorly to form a mid-cranial keel. Posteriorly, the neural spine is, if at all, only slightly cleaved in the more anterior caudals. Otherwise, the spine slopes straight downward or forms a mid-caudal keel. A distinct inclination of the neural spine begins with Ca4 and increases continuously in caudal direction. Caudals 20–26 lack a bony cover on the dorsal side and, accordingly, a real vertebral canal. Dorsal to the vertebral foramen on both sides of the neural arch, the prezygapophyses form distinct cranial articular processes, which are directed slightly dorsad and laterad. Caudals 1–2 still bear short and pointed postzygapophyses, which are not developed on the remaining ones.

Chevrons: The complete series of chevron bones is not preserved in any specimen. A number of these elements are known from HLMD-WT 420 comprising four isolated halves and one pair of chevrons. They are roughly y-shaped or u-shaped, broadened ventrally and narrower dorsally. The dorsal and ventral edges are thickened and rugose. The four pieces of chevrons may have been articulated, but not fused with their counterparts.

Ribs: The following description is kept short and generalised referring to NMDU-Geo 0001 published in Voss (2008). The complete rib series of the left side is preserved in specimens NHMUK PV M9415 and BSPG 1956 I 540 including 19 ribs and most of their right complements. All ribs are elliptical in cross section (197[0]) and show a dense and pachyostotic bone histology. Their overall shape either can be slender (e.g., NHMUK PV M9415) or compact (e.g., BSPG 1956 I 540, NMDU-Geo 0001). Only the cranial- and caudalmost ribs differ from the otherwise uniform rib morphology from the middle part of the thorax.

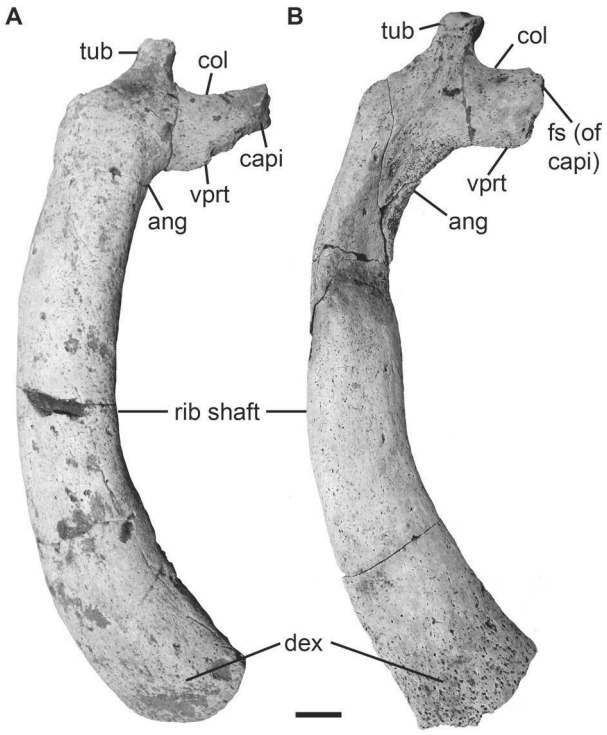

Figure 27. First ribs of gen. nov. 2 spec. nov. 1 (MNHM PW 1991/66-LS). **A**, right R1 in anterior view. **B**, left R1 in posterior view. Scale bar equals 1 cm.

The first rib (Fig. 27) articulates with vertebrae C7 and T1. It bears a prominent protuberance below the *capitulum* for the insertion of the *musculus longus capitis* (195[1]). The distal end of R1 is extended mediolaterally (196[1]), in some specimens (BSPG 1956 I 540) to a remarkable extent, and has a rugose concavity for cartilage attachment to the sternum. R2 and R3 are medium sized in comparison with the following ribs and characterised by truncated distal ends with a rugose concavity. R1–3 probably represent the only true ribs as they were connected to the sternum in the animal's lifetime. From R4 onwards, the ribs are convex and more or less smooth distally and most likely had no sternal connection. On R1–6, *capitulum* and *tuberculum* are distant to each other reflecting the significant length of the *collum*, i.e. the neck of the rib. R1–6 also are characterised by a distinct angle, whose curvature is kept in R4–6 through the total length of the ribs so that their shafts are strongly bent inward.

On R7–18 the *capitulum* and *tuberculum* come progressively closer together, the angle is less distinctly developed and the shaft mediolaterally compressed about mid-length of each rib. The ribs reach their maximum craniocaudal width and mediolateral thickness in their distal third before they taper gradually into smoothly convex ends. R19 is the shortest of all ribs. Its *capitulum* and *tuberculum* are virtually fused.

Sternum: Known sternal elements of this species comprise only the manubrium, which is preserved in LS RLP PW 2005/5042-LS (Fig. 28) and the juvenile specimen FMD SRK Eck 124. The manubrium is elongated anteroposteriorly and flattened to slightly concave dorsally. The ventral side is slightly convex and sometimes has a knoblike convexity

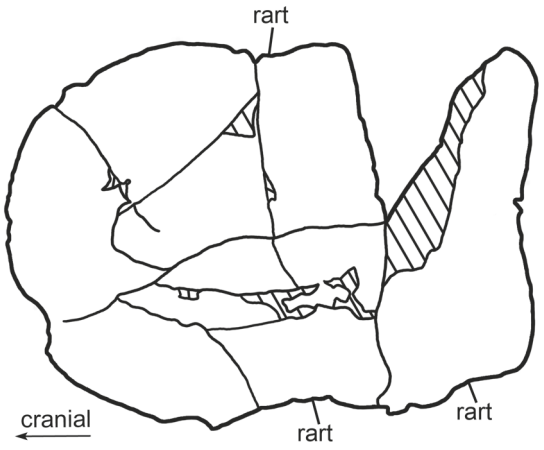

Figure 28. Outline drawing of manubrium of gen. nov. 2 spec. nov. 1 (LS RLP PW 2005/5042-LS) in ventral view. Shaded areas indicate broken parts. The exact scale of the original was not determinable, because the respective skeleton is on display.

anterocentrally as present in LS RLP PW 2005/5042-LS. However, a real median sternal keel is not developed (202[0]). Lepsius (1882: pl. 6, fig. 63) figures a manubrium (HLMD-WT Az12) that was found in the same deposits like gen. nov. 2 spec. nov. 1 and shows ventrally a distinct median keel. This manubrium looks distorted, but more importantly, represents an isolated find and, therefore, is not considered in this study.

The cranial half of the manubrium is slightly narrower than the caudal half ending in a bluntly rounded and straight anterior margin in the juvenile specimen FMD SRK Eck 124. However, the manubrium of LS RLP PW 2005/5042-LS keeps a more or less constant mediolateral width anteroposteriorly and has a smoothly convex cranial end (Fig. 28). In either case, the manubrium lacks an anterior process (201[1]). Laterocentrally, the articulation facets for the first ribs are present. There, the bone also reaches its greatest mediolateral width. This is best developed in LS RLP PW 2005/5042-LS, where the large and rugose rib articulation is formed by a slight, laterally raised concavity. More posteriorly, a further articulation for the second rib is developed on the right side. The caudal margin of the manubrium is straight to concave and thickened for the cartilaginous attachment to the supposed corpus. According to this observation, the sternum of gen. nov. 2 spec. nov. 1 is definitively composed of more than one element (200[0]). Most likely, it resembles that of gen. nov. 2 *bronni* comprising a compact corpus and an elongated, posterad tapering xiphisternum in addition to the manubrium.

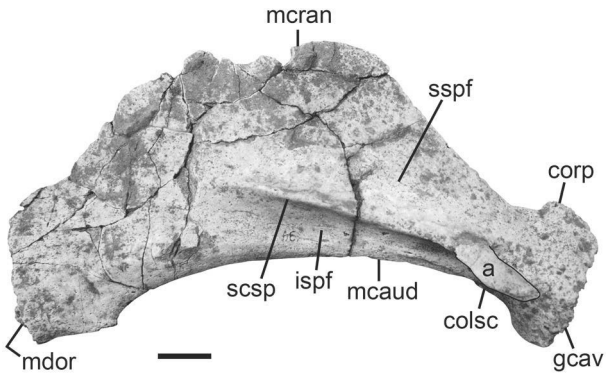

Figure 29. Right scapula of gen. nov. 2 spec. nov. 1 (MNHM PW 1991/66-LS) in lateral view. Scale bar equals 2 cm.

Scapula: The scapula (Fig. 29) forms a slender and sickle-shaped bone (187[0]). Its lateral surface is smooth and divided by a short (184[1]), straight ridge, the scapular spine. Instead of a proximal rugosity that is not developed there (183[1]), the scapular spine forms a slightly caudad inflected flange that runs diffusely out about half the length of the scapular blade. The flange either is low and smoothly rounded rising from a broad base (NHMUK PV M9415) or it is more elevated above the outer surface

and somewhat sharpened (MNHM PW 1991/66-LS; Fig. 29). In most individuals, the acromion is missing, but preserved in MNHM PW 1991/66-LS, where it is broken, but still attached to the distal end of the scapular spine. The acromion lies at the level of the neck (188[0]), i.e the *collum scapulae*, and ends in a smoothly convex tip. Furthermore, the scapular spine separates a smoothly concave and wide supraspinous fossa from a narrower infraspinous fossa (186[1]). Distad, the scapular blade tapers gradually into a narrow neck that bears anterodistally a moderately sized and blunt coracoid process (185[0]). The coracoid process is inflected mediad and not disjoint from the anterior apex of the articular glenoid. The glenoid cavity is large, moderately concave and oval in shape. In medial view, the side of the scapular facing the ribs forms a flat to smoothly concave plane.

Humerus: Humeri associated with a nearly complete skeleton are preserved in NHMUK PV M9415 (Fig. 30A–D), HLMD-WT 420 and MNHM PW 1991/66-LS, for example. The humerus is a compact element with distinctly developed epiphyses (189[1]). The greater tubercle is elevated above the level of the caput (190[1]) and continues distad into the deltoid crest (Fig. 30A, B). In anterior view (Fig. 30C), the deltoid crest overhangs laterally, forming a marked deltoid tuberosity, and tapers into a narrow deltopectoral crest at about

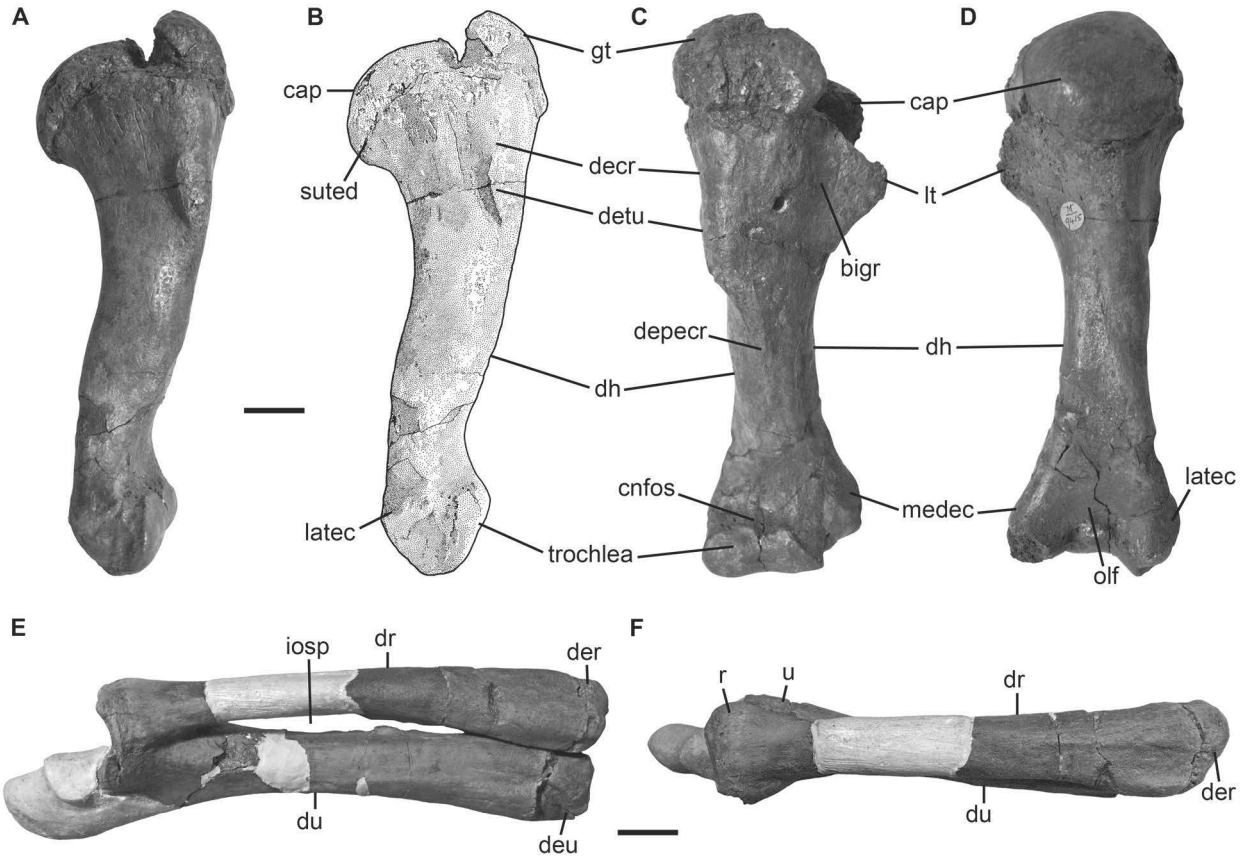

Figure 30. Stylopod and zeugopod of gen. nov. 2 spec. nov. 1. **A–D**, right humerus of NHMUK PV M9415. **A**, photography in lateral view. **B**, drawing in lateral view. **C**, photography in anterior view. **D**, photography in posterior view. **E–F**, right radius and ulna of HLMD-WT 420 in lateral (E) and anterior (F) views. White areas indicate either missing or reconstructed parts. Scale bars equal 2 cm.

half the length of the humerus shaft. The caput is rounded and flanked ventromedially by the lesser tubercle. Distally, the articulation facet for the radius and ulna is bisymmetrical and nearly perpendicular relative to the proximodistal axis of the humerus (191[0]). Dorsoanterior and dorsoposterior to the trochlea (Fig. 30C, D) the coronoid fossa and the olecranon fossa are distinct and deep.

Radius and ulna: Radius and ulna are known from HLMD-WT 420, however incompletely preserved (Fig. 30E, F). The radius lacks a piece from its shaft and the ulna is missing the olecranon including the proximal half of its articulation surface for the humerus. Both elements belong to the right side and are fused proximally as well as in the distal half of the interosseus space (Fig. 30E). The radial and ulnar diaphyses are straight (194[0]) and attached with their distal epiphyses, but still separated from these by visible sutures. The epiphyses are trapezoidal in shape and bear the articular facets for the adjacent carpals. In a direct comparison, the diaphysis of the ulna does not extend as far ventrally as that of the radius, but the ulnar epiphysis is longer than that of the radius and, consequently, both bones terminate at the same level. The anteroposterior thickness of the ulnar diaphysis exceeds that of the radius in lateral view (192[0]), but the diaphyses of both elements reach a similar length in transversal plane below the level of the proximal epiphyses (193[1]; Fig. 30F).

Manus: Neumann (1936) described the incomplete autopod of two specimens from the lower Oligocene of Flörsheim (West Germany) and provided comprehensive data on this very rarely preserved part of the sirenian skeleton. While Neumann's (1936: 258) "skeleton II" was no more available for personal investigations in the collections of the FIS, his "skeleton I" was in part accessible in Mainz (MNHM PW 1910/1). However, the identification of the latter specimen as belonging to gen. nov. 2. spec. nov. 1 is not certain due to distortion and damage by fire to most of the bones. Either way, Neumann's (1936) study gives a benchmark for evaluating the morphology of the autopod of lower Oligocene sirenians from Germany and is the basis of the following description. The terminology provided by Kaiser (1974) is applied here in order to avoid confusion in the use of different terms for the same parts.

Of all specimens certainly assigned to gen. nov. 2. spec. nov.1, HLMD-WT 420 preserves a nearly complete autopod from the right side comprising 17 elements (four carpals, five metacarpals and eight phalanges). Therefore, these rare elements of the sirenian skeleton are described in detail here though currently not relevant for the phylogenetic part of this study pending additional material of comparable taxa. Following Neumann (1936), only three carpals are missing, the scaphoid, the fused trapezium-trapezoid, and the pisiform. The carpals are arranged in two rows, a proximal and a distal row, each consisting of originally three single elements.

The triquetrum forms a discoid bone and articulates with five elements: the ulna

proximally, the hamate and metacarpal V distally, the pisiform posteriorly (on the ulnar side) and the lunate anteriorly (on the radial side). The ulnar facet has a triangular form and is saddle-shaped. The distal facet for the hamate is nearly flat, subtriangular in shape and larger than its proximal counterpart, because the distal side of the triquetrum has a posterior bony extension. A narrow, suboval articulation surface on the posterior side that also slightly overlaps the lateral side serves as attachment for the metacarpal V and is continuous with the distal facet. In lateral view, the triquetrum forms a strip-shaped area positioned transversely to the longitudinal axis of the wrist. This area measures 7 mm centrally and widens up to 9 mm anteriorly and posteriorly. In proximal and posterior views, the ulnar side is characterised by an irregularly shaped concave facet for the articulation with the pisiform. The distal edge on the radial side bears a narrow, mediolaterad extending ridge that articulates with the lunate.

The lunate roughly has the form of a cuboid that is transversely directed relative to the longitudinal axis of the wrist. Its proximal facet is nearly flat, delimited by roughly parallel extending ulnar and radial edges, and articulates with the radius. Its distal counterpart is kidney-shaped and serves as attachment for the capitate. The distal articulation surface has a smooth s-shaped flexure in transversal plane, slightly convex laterally and concave medially. The ulnar or posterior side of the lunate is trapezoid and bears a prominent dorsoproximal corner. A distinct facet that is narrow and elongated extends along the distal edge of the ulnar side to articulate with the triquetrum. Distad, this facet continues with the articulation surface for the capitate. A less distinct facet for the articulation with the scaphoid is present proximally on the radial or anterior side of the lunate and is continuous with the articulation surface for the radius. The medial or volar side is smoothly convex, whereas, laterally, the lunate has a smoothed, but uneven surface.

The hamate is a wedge-shaped bone that essentially articulates with the triquetrum proximally, the capitate anteriorly and the metacarpals III, IV and V distally. The proximal articulation surface is roughly triangular, smooth and slightly concave. It is larger than all other hamate facets and mainly serves as attachment for the distal facet of the triquetrum. Only the anteromedial corner bears a very small facet to articulate with the lunate. The distal side is characterised by three continuous facets, all being slightly concave and smooth-surfaced. The articulation facet for the metacarpal IV dominates the distal side. It is roughly rectangular in shape and meets the narrow, mediolaterally elongated facet for the metacarpal III at an angle of about 130°. The facet for the metacarpal V is present on the ulnar side, trapezoid in shape and the smallest of all distal facets. It forms an angle of about 135° with the main distal facet and meets the proximal articulation surface in a sharp edge at an angle of about 85°. The radial side of the hamate bears the mediolaterally elongated, but irregularly shaped articulation surface for the capitate. This facet is located more proximally. Another articulation with the capitate is present distally in the form of a slight ridge that is part of the distal facet for the metacarpal III. Both, the medial and lateral

sides of the hamate are convex and separated by sharp edges from the remaining surfaces. The lateral side is smooth-surfaced, while the medial side is knob-like and uneven.

The capitate shows an overall trapezoid shape mainly caused by the distinctly trapezoid radial and ulnar surfaces. This bone articulates with the lunate proximally, the metacarpal III distally, the fused trapezium-trapezoid and metacarpal II on the radial side and the hamate on the ulnar side. The proximal articulation surface is smooth and nearly flat and the distal complement slightly concave. The radial surface possesses three facets. One facet extends as an average 4 mm wide band along the proximal margin to articulate with the trapezium-trapezoid. The other two facets form semicircular areas on the distal margin for the articulation with the metacarpal II, with the larger facet laterally and the smaller one medially. Both facets are continuous with the distal articulation surface for the metacarpal III. The ulnar side of the capitate bears proximally the articulation facet for the hamate that corresponds in shape and size with the facet of the adjacent bone. The same applies for a further articulation with the hamate, which is present distally in the form of a slight ridge that is part of the distal facet for the metacarpal III. In lateral view, the capitate is flat to slightly convex having a smooth surface. Medially, the capitate is knob-like and uneven.

According to the descriptions of Neumann (1936) and specimen MNHM PW 1910/1, a similar morphology for the carpals missing in HLMD-WT 420 can be expected for gen. nov. 2 spec. nov. 1. Neumann (1936) described the scaphoid to form a thick bony plate that is attached to the radius proximally, the trapezium-trapezoid distally and the lunate on the ulnar side. The trapezium-trapezoid represents the smallest bone of all carpals (Neumann 1936) and articulates with the scaphoid proximally, the metacarpal I and II distally and the capitate on the ulnar side. The pisiform represents a 25 mm long, ovoid, but mediolaterally flattened bone bridging both rows of carpals (Neumann 1936). It has proximally a large facet for the articulation with the triquetrum and a small distal facet for the metacarpal V.

The metacarpals form elongated bones all bearing proximally the articulation facets for the adjacent carpals. Simple facets for the phalanges are present on their distal ends with the exception of metacarpal I, which terminates into a blunt conical tip indicating that no phalange is attached to this bone.

Metacarpal I measures 39 mm in total length, is distinctly curved in ulnar direction and triangular in cross section. In anterior view, this bone has a distinct ridge. The diaphysis and proximal epiphysis are fused, but the epiphyseal suture is still visible on the volar side. Laterally and on the ulnar side of the proximal end, a flat articulation surface for the metacarpal II is present. The proximal epiphysis bears a convex, subtriangular facet for the attachment of the trapezium-trapezoid.

Metacarpal II is broken into two pieces in HLMD-WT 420, but is otherwise complete measuring about 56 mm in length. The texture of its outer surface is smooth and, especially on the proximal end, moderately rugose. The lateral side of the diaphysis is

less concave compared to the medial or volar side. The anterior or radial side is characterised by a longitudinal ridge that rises distally into a blunt tuberosity. In posterior view or on the ulnar side, the lateral and medial sides converge to form a gentle keel at about half the length of the diaphysis extending in distal direction. The proximal end of metacarpal II is triangular in cross section and bears the articulation surfaces for the metacarpal I and III, the trapezium-trapezoid and the capitate. The facet for the metacarpal I is flat and roughly triangular on the lateroradial side. It is continuous with the attachment for the trapezium-trapezoid, which extends mediolaterally along the proximal surface and is narrow, irregularly shaped laterally and wider, trapezoid medially. The main facet for the trapezium-trapezoid, in turn, continues into a slightly smaller, roughly rectangular facet on the ulnar side by forming an angle of about 130°. The latter facet is the attachment for the capitate as does a semicircular facet on the lateroulnar side. Both facets incline in an angle of approximately 90° onto the ulnar side of metacarpal II to form small semicircular facets for the metacarpal III. Metacarpal II tapers in distal direction by showing a varying cross section, which is elliptical at mid-length of the diaphysis and triangular at its distal end. Both, the diaphysis and distal epiphysis are fused with the epiphyseal suture still visible on the ulnar side. The distal end of metacarpal II is convex and bears a subcircular articulation surface for the proximal phalange.

Metacarpal III is 65 mm long and differs only slightly from the morphology of metacarpal II. It is rectangular to trapezoid in cross section proximally and elliptical centrally and distally. The proximal end of metacarpal III bears two nearly rectangular and flat articulation surfaces that are continuous with each other and meet at an angle of about 120°. Of both, the larger facet faces the radial side and articulates with the capitate. The smaller, much narrower facet lies on the ulnar side and serves as attachment for the distoradial side of the hamate. The latter surface is inclined in an angle of about 90° to form two semicircular articulation facets on the ulnar side of the proximal end. Both facets are fused centrally and articulate with the metacarpal IV. Two small and separated facets are present on the radial side for the attachment of the metacarpal II. Distally, the epiphysis is connected with the diaphysis, but the epiphyseal suture is clearly visible. The distal end is convex and bears a nearly circular articulation facet for the proximal phalange in an oblique proximodistal axis.

Metacarpal IV is morphologically similar to metacarpal III. It measures 58 mm in length lacking the distal epiphysis, but most likely resembled metacarpal III also in size considering the distal epiphysis to be included. The proximal end of metacarpal IV is rectangular in cross section and flat to slightly convex bearing the articulation surface for the hamate. The radial side shows an irregularly shaped facet, which articulates with the metacarpal III. A triangular concavity is present on the ulnar side for the attachment of the metacarpal V. According to MNHM PW 1910/1, the top of the distal epiphysis was most likely developed in the form of a smooth facet for the proximal phalange.

Metacarpal V also lacks its distal epiphysis and is 55 mm long. This bone is distinctly flattened mediolaterally and suboval in cross section. Its proximal end shows a bony extension in ulnar direction, which bears a small facet for the pisiform. The main proximal articulation surface is more or less flat in an oblique anteroposterior axis comprising three continuous facets. The posteriormost facet articulates with the triquetrum, the facet located in radial direction is attached to the hamate, and, on the radial side, a subtriangular facet for the articulation with the metacarpal IV is present. A smooth facet to articulate with the proximal phalange was also present on the distal epiphysis, according to the preserved situation in MNHM PW 1910/1.

Eight phalanges form the distal parts of the hand skeleton in HLMD-WT 420. As already mentioned above, the metacarpal I bears no phalange. Metcarpal II-V each comprises two phalanges with the distal phalange distinctly shorter than the proximal one forming a small, plate-like bone.

The proximal phalange of metacarpal II is 19 mm long. Its width varies from 9 mm proximally over 7 mm centrally to 8 mm distally. The lateral side is nearly flat and the medial side concave. In proximal and distal views, small, subcircular facets for the adjacent metacarpal and distal phalange are present. The distal phalange is morphologically similar to the proximal one, but the smallest of all measuring 9 mm in length and constantly 7 mm in width. It shows an oval proximal articulation surface and has a smooth, flat distal end. The radial side is slightly shorter than the ulnar side so that the distal margin is somewhat oblique in an anteroposterior axis.

The two phalanges of metacarpal III only differ in size from those of metacarpal II. The proximal phalange is 20 mm long, 11 mm wide proximally, 8 mm wide centrally, and 9 mm wide distally. The distal phalange is about as long as wide measuring 11 mm in maximum dimensions.

The proximal phalange of metacarpal IV also corresponds to those of metacarpal II and III. It is only larger measuring 29 mm in length and has a width that amounts to 19 mm proximally, 12 mm centrally and 13 mm distally. The distal phalange is distinct in being wider than long measuring 11 mm in maximum length and 15 mm in maximum width. Its distal margin is straight anteroposteriorly.

The proximal phalange of metacarpal V is only preserved with its 29 mm long distal half indicating that it is the largest of all phalanges. This is in accord to Neumann (1936: 273), who gives a length of 41 mm for the proximal phalange of his “skeleton II”. The proximal phalange in HLMD-WT 420 is characterised by a distinct mediolateral flattening causing a semicircular cross section of the bone. The volar side is flat and the lateral side convex. Laterally, the distal epiphyseal suture is still visible. The distal surface bears a flat, semicircular facet as supposedly did the proximal end, according to Neumann (1936). The distal phalange resembles the first phalange. It is slightly longer than wide measuring 17 mm x 15 mm in maximum dimensions. The volar side is flat and smooth and the lateral

side flat to slightly convex. The radial side is longer than the ulnar side causing a slight inclination of the distal margin in anteroposterior direction.

Innominate: Either the right or left half of this paired bone is known from several specimens (NHMUK PV M9415 (Fig. 31A), BSPG 1956 I 540, CDGG S3 (Fig. 31B), PMN SSN12EC55) and both elements are preserved in HLMD-WT 420 (Fig. 31C, D), which are also illustrated in Schmidtgen (1912: pl. 29: figs. 4, 5). The pelvis shows a uniform morphology lacking distinct individual variation. It is composed of three continuous parts, all firmly fused in adults, but loosely attached with each other in juveniles (FMD SRK Eck 124).

The ilium forms a long and slender bone that is rounded in cross section. Its proximal end is slightly swollen and bears dorsomedially a 20 mm to 30 mm long depression that serves for the cartilaginous attachment of the ligaments connecting the pelvis with the sacral vertebra. In lateral view (Fig. 31A–C), the pubic bone is a short and triangular extension on the ventral side of the elongated pelvis. Its ventral tip is moderately rugose. Anterodorsal to the pubis, a rounded and distinctly concave *acetabulum* is present (198[0]) suggesting the presence of a rudimental femur.

The ischium is transversally flattened and plate-like forming the widest element of the pelvis due to its oblique dorsoventral expansion. Its distal end is thickened with a rugose area. Otherwise, the texture of the pelvic surfaces is smooth. In ventral view, the pubis is inflected mediad while the posterior end of the ischium inclines laterad. The ilium maintains its elongated form anteroposteriorly. A *foramen obturatum* is generally not developed. However, of all specimens personally investigated HLMD-WT 420 reveals a small *foramen obturatum* to be present on the left and right pelvis ventroposterior to the *acetabulum* (Fig. 31C, D). The anteroventral bony margin of the foramen is broken out on both pelvic elements, but its maximum dimensions amount up to about 5 mm x 7 mm. On the basis of this observation, character 199 is scored polymorphic (199[0/1]) indicating individual variation in this respect.

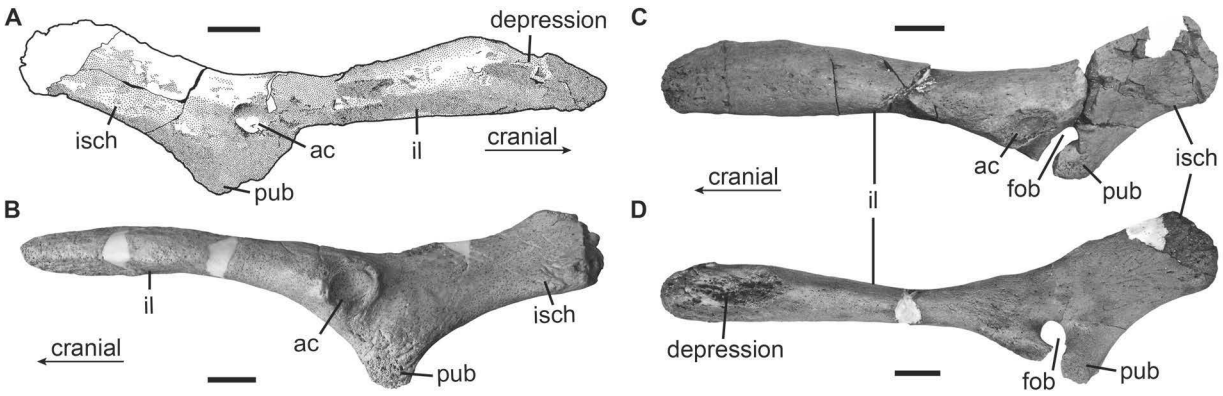

Figure 31. Innominates of gen. nov. 2 spec. nov. 1. **A**, drawing of the right pelvis of NHMUK PV M9415 in lateral view. **B**, left pelvis of CDGG S3 in lateral view. **C**, left pelvis of HLMD-WT 420 in lateral view. **D**, right pelvis of HLMD-WT 420 in medial view. White areas indicate either missing or reconstructed parts. Scale bars equal 2 cm.

Femur: A number of isolated femura from the lower Oligocene of Germany and Belgium is known from different collections (e.g., HLMD, MNHM, IRSNB). However, none of these elements is associated to skeletal remains enabling a clear taxonomic assignment to gen. nov. 2 spec. nov. 1. These isolated finds resemble those of gen. nov. 1 *taulannense* and represent slender elements with rounded proximal epiphyses and tapered distal ends lacking any articulation for the zeugopod. This is also in accordance to the pelvic morphology and the size of the *acetabulum* allowing the indirect determination of the femur to be rudimental.

Remarks

Taxonomic remarks: The establishment of the taxon gen. nov. 2 spec. nov. 1 results from the revision of the German and Belgian sirenians originally assigned to *H. schinzii* Kaup, 1838. As mentioned above, *H. schinzii* is the type species of the genus *Halitherium*, which was established on the basis of a single premolar (Kaup, 1838). This tooth (HLMD-WT Az 48; Fig. 32) is single-rooted, but the root itself is no more preserved. Voss (2010) already indicated the lack of a diagnosis for the species *H. schinzii* due to the inappropriateness of its holotype. This is corroborated in this study on the basis of comparative investigations. The holotype premolar is not certainly assignable to any taxon, because it does not yield any significant defining characters for both the genus and the species. This conclusion is partly based on its high degree of wear that precludes an unambiguous identification of this premolar. Its preserved crown measuring 11 mm in maximum diameters shows a worn central cusp whose smooth and convex side faces labially. Lingually, five accessory cuspules are present and another one mesially or distally depending on the side and locus it inhabits within the jaw. Compared to gen. nov. 1 *taulannense*, known by upper and lower premolars, and specimen BSPG 1956 I 540, comprising the right P2 and left P3–P4, HLMD-WT Az 48 most likely represents an upper posterior premolar. Using P3–P4 of BSPG 1956 I 540 as reference points, HLMD-WT Az 48 could have occupied either the third or the fourth locus based on its complex cusp pattern, which resembles that of the reference teeth. However, a clear assignment of HLMD-WT Az 48 to P3–P4 of BSPG 1956 I 540 or any upper premolars observable in gen. nov. 1 *taulannense* is not possible due to the special morphology of its crown. The overall shape of HLMD-WT Az 48 resembles a clenched

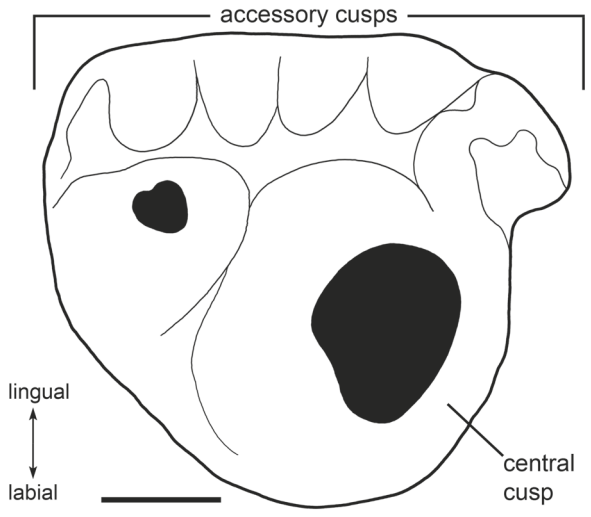

Figure 32. Isolated premolar and holotype specimen of *Halitherium schinzii* HLMD-Az 84 in occlusal view. Scale bar equals 0.25 cm.

fist, which tempted Kaup (1838: 319) to introduce for this taxon the new genus *Pugmeodon* ("Faustzahn"). This feature is found neither in isolated nor associated premolars even of a comparable degree of wear. Apart from BSPG 1956 I 540, complete series of upper premolars are unknown in specimens hitherto assigned to *H. schinzii* and other fossil sirenian taxa (e.g., Spillmann, 1959; Sagne, 2001a) making further comparative studies difficult. Therefore, it remains unresolved whether HLMD-WT Az 48 belongs to the left or the right quadrant of the jaw and the identification of its exact position within the tooth arcade is still an open question.

In conclusion, the relation of HLMD-WT Az 48 to the nominal species *H. schinzii* is doubtful and cannot be established based on its lack of diagnostic value. Consequently, *"H. schinzii"* is a *nomen dubium* and considered invalid, as is the genus *"Halitherium"* and, as a further consequence, the respective subfamily "Halitheriine". Therefore, the Oligocene sirenian material especially from Germany and Belgium is revised and redefined taking into account that the genus and species name of *"H. schinzii"* is no more available for further taxonomic purposes.

Geological and palaeogeographical remarks: Gen. nov. 2 spec. nov. 1 is abundantly known from its type locality (Mainz Basin, West Germany) mainly by ribs, vertebrae, and cranial fragments, and occasionally by partial skeletons comprising nearly complete skulls and mandibles. Apart from the Mainz Basin, this species is also known from the Antwerp and East Flanders Provinces in North Belgium (Sickenberg, 1934a). Voss (2008) described a partial skeleton from the Lower Rhine area in western Germany that is also assigned to this taxon now. Sirenian finds from the Paris Basin, which were originally referred to *"H. schinzii"* (Bizzarini, 1995; Bizzarini & Reggiani, 2010), are identified as belonging to gen. nov. 2 spec. nov. 1 in this study indicating the widespread distribution of this taxon in Central Europe (Fig. 33). Skeletal material possibly referable to gen. nov. 2 spec. nov. 1 is also reported from the Bay of Leipzig as part of the eastern North-German Plain (Böhme, 2001), Switzerland (Pilleri, 1987) and Hungary (pers. obs.). Uncertainty about the taxonomic assignment of these finds is based on the lack of cranial material reflecting the characteristic features for the species identification.

The Mainz Basin occupies only about 1,850 km² between the Rhenish Massif in the north, the Ortho-Upper-Rhine-Rift in the east, the Pfälzer Wald in the west, and the Haardt in the south (Grimm & Grimm, 2003). According to Rothausen & Sonne (1984), the Mainz Basin represents a "hanging" fault ridge in the overlap area between the Ortho-Graben and the northwest directed Para-Graben in the intersection of the Upper-Rhine-Rift and the Permo-Carboniferous Saar-Nahe-Basin.

In the early Oligocene, fully marine conditions prevailed in the Mainz Basin during the second or late Rupelian transgression event (Berger *et al*., 2005a, b; Pirkenseer *et al*., 2010). The North Sea extended to the Lower Rhine and today's German low mountain range (Meulenkamp & Sissingh, 2003), and northern Belgium was part of the southern

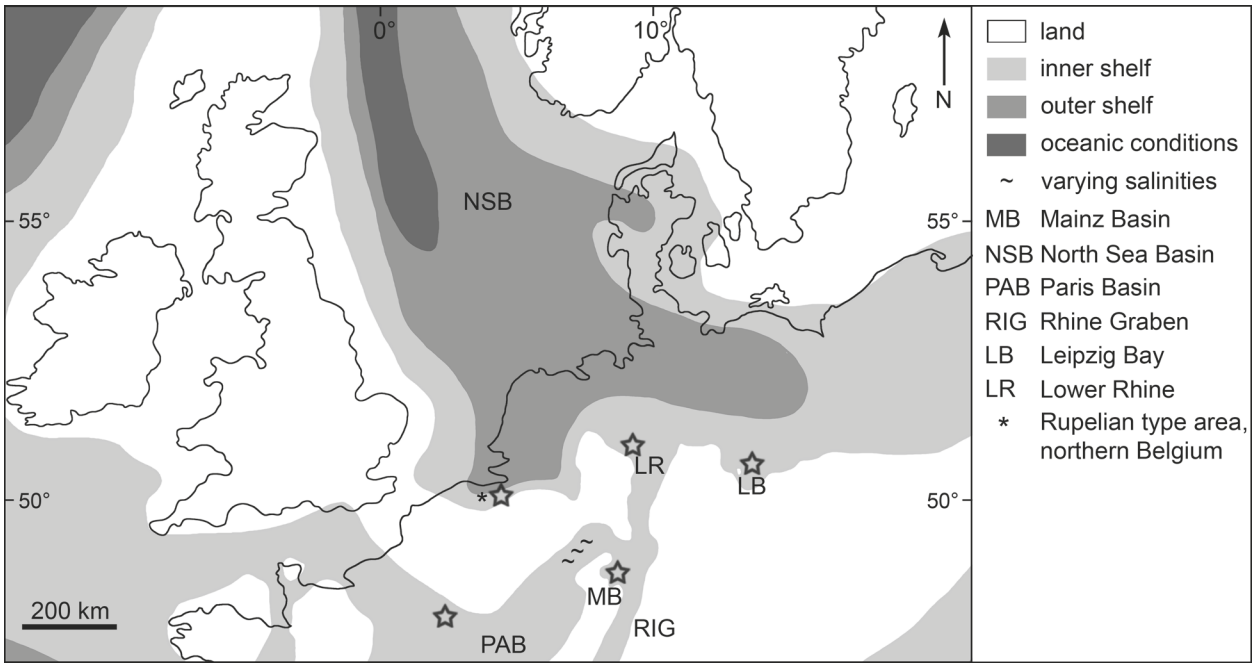

Figure 33. Geographic setting of sirenian sites and palaeogeography during the early Oligocene of Central Europe (modified after Meulenkamp & Sissingh 2003; Gürs & Janssen 2004). Asterisks indicate estimated find localities of the sympatric species gen. nov. 2 spec. nov. 1 and gen. nov. 2 *bronni*.

North Sea Basin (e.g., De Man *et al*., 2004; Van Simaeys *et al*., 2004; Vandenberghe *et al*., 2004). The almost N-S-trending Rhine-Graben is about 300 km long and 35–40 km wide and began to subside during the middle Eocene (Lutetian; Sissingh, 1998). Due to the generally assumed rift-controlled tectonic subsidence and regional relative sea-level rise (Rousse *et al*., 2012), the Rhine-Graben has two marine connections: one to the North Sea Basin and the other to the Paratethyan Molasse Basin via the Raurachian Depression (Sissingh, 1998; Rögl, 1999; Spiegel *et al*., 2007). Consequently, a continuous sedimentation area was established from the North Sea to the Paratethys via the Bay of Kassel, the Hessian Depression and the Upper-Rhine-Graben, the latter including the Mainz Basin (e.g., Rothausen & Sonne, 1984; Sissingh, 1998; Grimm & Grimm, 2003; Meulenkamp & Sissingh, 2003; Pirkenseer *et al*., 2010). A faunal interchange took place and is supported by, for example, the fish *Aeoliscus heinrichi* characteristic for the Paratethys (Sissingh, 1998) and the basking shark *Cetorhinus parvus* that immigrated from the North Sea (Grimm *et al*., 2002). According to Meulenkamp & Sissingh (2003), a marine brackish connection also existed to the Paris Basin. In the Rhine-Graben the main current system was originally directed southwards (Martini & Müller, 1971), however a northwards direction is indicated from the middle late Rupelian onwards (Martini, 1982; Spiegel *et al*., 2007).

The material collected from the Mainz Basin in the past is predominantly stored in different scientific collections, unfortunately often missing precise stratigraphic information. For example, the label of specimen NHMUK PV M9415 only indicates *"Halitherium,*

Bodenheim, Germany, Oligocene". By contrast, the available information for the new holotype specimen (BSBG 1956 I 540) is more precise. Barthel (1962: 65) stated that this partial skeleton comes from the "middle" Oligocene marine sands ("Meeressanden") (today: Rupelian, lower Oligocene according to Grimm *et al.,* 2000) of a gravel pit in Eckelsheim near Alzey (Mainz Basin). Despite the fact that many sirenian specimens from the Mainz Basin lack sufficient data on their discovery, it is commonly accepted that fossil remains of sea cows are only known from sandy and clayey marine sediments that were deposited during the second lower Oligocene transgression (e.g., Wilhelm, 1962; Bahlo & Tobien, 1982; Rothausen & Sonne, 1984; Grimm & Grimm, 2003; Pirkenseer *et al*., 2010; Rousse *et al*., 2012). The most recent stratigraphic framework of the Mainz Basin was established by e.g. Grimm *et al.* (2000), Grimm & Grimm (2003) and Grimm (2005), who also introduced the Alzey Formation for the marine coastal sands and the Bodenheim Formation for the clayey offshore sediments. Both, the Alzey Formation and the Bodenheim Formation represent the lower section of the Selztal-Group and are lower Oligocene (Rupelian) in age.

The Alzey Formation, originally named "Lower Marine Sand" (e.g, Rothausen & Sonne, 1984; Sissingh, 1998; Grimm *et al*., 2000), unconformably overlies the Permian bedrock (Rousse *et al*., 2012). It represents the coastal facies and corresponds to the basin facies of the Bodenheim Formation (Grimm, 1998; Grimm *et al*., 2000; Grimm & Grimm, 2003). The Alzey Formation is mainly composed of coarsely grained sands and gravels of yellow to white or grey colour, which locally appear reddish and greenish. Sometimes, there are also shell layers, carbonate and silt observable (Grimm *et al*., 2000; Grimm & Grimm, 2003). Based on biostratigraphy, the Alzey Formation can be assigned to two standard calcareous nannoplankton zones, the mid to higher part of NP23 and the lower part of NP24, respectively (Sissingh, 1998; Grimm *et al*., 2000). Additionally, two foraminiferal zones can be distinguished within this formation; at the base the *Planorbulina* zone and the Miliolid zone at the top (Grimm, 1998; 2002). Radioisotope data obtained from $^{87}Sr/^{86}Sr$ values of a single shell from the lower Miliolid zone reveal a date of 30.1 +/- 0.1 Ma (Grimm & Grimm, 2003). The marine sands of the Alzey Formation are very fossiliferous and yield the sometimes nearly complete remains of sirenians as is also stated by Bahlo & Tobien (1982). Sirenian skeletons from the Alzey Formation are light-coloured in accordance with the colour of the neighbouring sea sands, and can be distinguished from the dark-coloured skeletons of the Bodenheim Formation.

The Alzey Formation laterally interfingers with the clays of the Bodenheim Formation (Grimm & Grimm, 2003). It is replaced to the basin by the Bodenheim Formation, which was formerly called the "Rupel Clay" (e.g., Rothausen & Sonne, 1984; Sissingh, 1998; Grimm *et al*., 2000). Today, the Bodenheim Formation is subdivided into the Wallau Subformation at the base, the Hochberg Subformation, and the Rosenberg Subformation at the top (Grimm & Grimm, 2003).

The Wallau Subformation largely corresponds to the “Foraminifera Marls” or “Lower Rupel Clay” (Rothausen & Sonne, 1984; Grimm & Grimm, 2003). This subformation is composed of moderately to poorly stratified clays of mainly light grey to greenish colour. Partially, carbonate silty clays and traces of sand layers are intercalated. The sediments of the Wallau Subformation are not developed in all parts of the Mainz Basin, but attain a maximum thickness of about 36 m (Grimm & Grimm, 2003). The lower limit of the Wallau Subformation is determined to be 31 Ma in age (Grimm *et al*., 2000) based mainly on the chronostratigraphic correlation of foraminiferal and dinoflagellate cyst zones.

The Hochberg Subformation largely corresponds to the “Fish Shale” or “Middle Rupel Clay” (Rothausen & Sonne, 1984; Grimm *et al*., 2000; Grimm, 2002). It is characterised by dark-coloured, finely stratified to laminated, bituminous clays and marls, which transgress locally on the coastal deposits of the Alzey Formation. This subformation was deposited in water depths of up to 150 m in the Mainz Basin and represents the most prominent unit of the Bodenheim Formation with a maximum thickness of 80 m (Grimm *et al*., 2000; Grimm & Grimm, 2003). Sirenian remains found in the lower Oligocene clays of the Mainz Basin originate from the Hochberg subformation (Rothausen & Sonne, 1984). The skeletal remains are typically dark-coloured as it is the case in NHMUK PV M9415 from Bodenheim and HLMD-WT 420 from Flörsheim, for example.

According to Grimm (1994, 1998, 2002), seven foraminifera zones can be distinguished from bottom to top within the Hochberg Subformation. These biostratigraphic data allow an excellent correlation with the sediments of the Upper-Rhine-Graben and the Rupelian stratotype in northern Belgium (Grimm & Steurbaut, 2001). The Rupelian stage of Northwest Belgium is mainly composed of clays cropping out along the river Rupel. These clays are lithostratigraphically referred to as the Boom Clay Formation (De Man *et al*., 2004; Van Simaeys *et al*., 2004). Numerous sirenian specimens have been reported from theses strata and were extensively described by Sickenberg (1934a). Some of these specimens (e.g., IRSNB M.137 and IRSNB Reg. 4005) are assigned to gen. nov. 2 spec. nov. 1. in this study. The Boom Clay Formation also can be correlated biostratigraphically with the Ratingen Member in the Lower Rhine area (Vandenberghe *et al*., 2001), from where specimen NMDU-Geo 0001 is reported (Voss, 2008).

The boundary between the Hochberg Subformation and the overlying Rosenberg Subformation corresponds to the boundary between NP23 and NP24 (29.9 Ma; Grimm & Grimm, 2003). The Rosenberg Subformation corresponds to the “Upper Rupel Clay” (Rothausen & Sonne, 1984; Grimm, 2002). It is up to 15 m thick and composed of fine-layered, light grey clays, silts, marls, and carbonate silts with occasionally occurring layers of fine-grained sands (Grimm *et al*., 2000).

The Alzey and Bodenheim Formation, and especially the Hochberg Subformation, were deposited in a subtropical to Mediterranean climate (Grimm & Grimm, 2003). This is indicated for example by plant remains like palm trees near Flörsheim and cones of

conifers near Eckelsheim (Schaarschmidt, 1982).

Gen. nov. 2 *bronni* (Krauss, 1858)

Halitherium schinzi (Kaup); Bronn, H.G. (1853–1856): 780, pl. 48: fig. 9.
Halitherium bronni; Krauss, 1858: 530, pl. 20.
Halitherium schinzi Kaup *forma delheidi*; Sickenberg, 1934a: 271, fig. 2b.
Halitherium schinzi (Kaup); Fischer & Krumbiegel, 1982: 73, photo 1.
Halitherium (Kaup); Voss, 2012: 207, figs. 2–10.

Holotype: SMNS 1539, a natural endocranial cast and associated skull roof comprising the frontal, parietal and supraoccipital, both nasals broken in the median plane and remnants of the ethmoid and vomer.

Referred material: For detailed listing of the preserved skeletal parts see Appendix 1.

Type horizon and locality. Alzey Formation of the Selztal-Group (lower Oligocene) from Flonheim (Mainz Basin, West Germany).

Range and distribution: Known only from lower Oligocene deposits of the Mainz Basin, Germany (Alzey Formation and Hochberg Subformation (Bodenheim Formation)); the southern Münsterland, western Germany (upper Ratingen Member); the Bay of Leipzig, East Germany (phosphorite nodule horizon of the Böhlen Formation); and the Antwerp and East Flanders Provinces, North Belgium (Boom Clay Formation). Most likely also known from the early Oligocene of Hungary and Switzerland.

Emended diagnosis: Represents a species of gen. nov. 2 that is characterised by the combination of the following characters: infraorbital foramen rounded, about as wide as high; temporal crests as prominent on frontal as on parietal and distinctly converge at centre of skull roof; supraorbital process of frontal dorsoventrally flattened with its dorsal surface gently inclined ventrolaterad; frontal processes of parietal long, exceeding half the length of frontal; cranial roof slightly shortened relative to supraoccipital width; no contact between lacrimal and premaxilla; supraoccipital enlarged transversely; nuchal crest notched in median plane; external occipital protuberance indistinct; exoccipital meet in a suture dorsal to *foramen magnum*; supracondylar fossa of exoccipital deep and extending across entire width of occipital condyle; ventral border of horizontal mandibular ramus moderately concave and sharply downturned anteriorly; absence of P2/p2; and pelvis reduced with *acetabulum* still well developed.

Character states: 30[1]; 56[1]; 57[0]; 54[0]; 55[1]; 43[1]; 44[0]; 45[0]; 63[1]; 64[1]; 74[0]; 112[1]; 115[1]; 116[1]; 121[0]; 123[1]; 144[1]; 168[1]; 198[0]; 199[1].

Differential diagnosis: Differs from gen. nov. 2 spec. nov. 1 in the following characters: the infraorbital foramen is not oval, higher than wide; the cranial roof is not elongated relative to the transversal extension of supraoccipital; there is no contact between the lacrimal and premaxilla; and the successive P2/p2 are not developed. Differs from gen. nov. 2 spec. nov. 1 and gen. nov. 2 *alleni* in that the external occipital protuberance is not prominently developed, neither rising above the parietal plane nor bulging caudally; and that the frontal processes of parietal are not shortened.

Description

Figures 34–46; Appendix 3

The following description is mainly based on the holotype specimen and the partial skeleton CDGG S1 including a nearly complete skull. Additional information are received from referred specimens like MCZ 8829 and MHNM PW 1984/37-1.

Premaxilla: In dorsal view (Fig. 34), the rostrum is laterally compressed and has a middorsal ridge that is upraised to form a boss posteriorly (9[1]; 10[1]). Behind the upraised summit of the premaxillary symphysis, the mesorostral fossa is retracted and enlarged reaching to the level of the anterior margin of the orbit (2[1]). Lateral indentations by the nasal processes are not developed in the anterior half of the mesorostral fossa (11[1]). The premaxillary symphysis is longer than half of the total length of the premaxilla (5[1]) and it is generally enlarged relative to the condylobasal length of the skull (4[1]). The nasal processes are thin and taper at their posterior ends by lengthy overlapping the frontals and nasals (17[0]; 20[1]). In lateral view (Fig. 35B), the symphysis is strongly downturned forming an angle with the horizontal plane of about 57° (12[1]). The anteroventralmost sutural contact to the maxilla lies perpendicular to the posterior end of the symphysis (7[1]). Ventrally on the lanceolate masticating surface (14[1]), the *foramen incisivum* occupies the area between both premaxillae and opens anteriorly without sharp demarcation (15[0]; Fig. 36). The palatal roof tapers distinctly in posterior direction and widens again at the level of the infraorbital foramen (13[0]). A dentiform process is absent (16[0]).

Nasal: Small nasals extend anteromedial to the frontals (Fig. 34), which is indicated by the internasal suture that, unless it is broken (Fig. 37A, D), reaches less than half the length of the interfrontal suture (39[1]). Both elements meet in midline posteriorly (40[0]) and are separated from each other anteriorly. A nasal incisure is present at the posterior end of the mesorostral fossa, but small and does not extend posterior to the supraorbital processes of the frontal (42[1]).

Ethmoidal region: The ethmoidal region is quite well preserved in the holotype specimen (SMNS 1539; Fig. 37B) and associated with the vomer, which projects as a ventral keel. As in gen. nov. 2 spec. nov. 1, the mesethmoid forms a prominent perpendicular plate

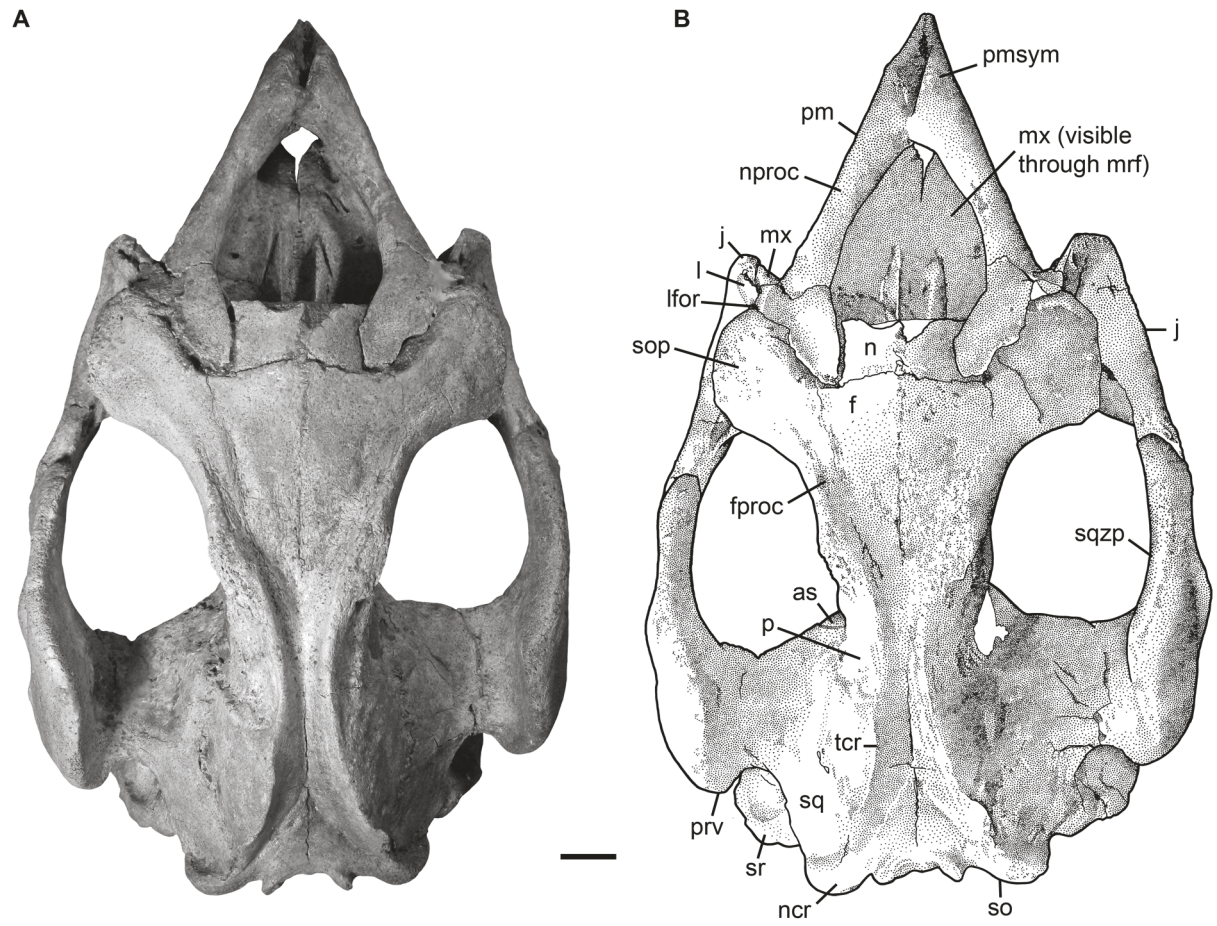

Figure 34. Cranium of gen. nov. 2 *bronni* (CDGG S1) in dorsal view. **A**, photography. **B**, drawing. White areas indicate either missing or reconstructed parts. Scale bar equals 2 cm.

that measures 10 mm to 15 mm in width by becoming narrower dorsally, ventrally and posteriorly. The mesethmoid is fused posteriorly with the presphenoid to form a distinct *crista galli*, which extends up to the roof of the cranial cavity by tapering mediolaterally. The cribiform plates of the exethmoids are well visible on the holotype skull roof. They are deeply recessed from the cranial cavity forming oval grooves for the olfactory nerves. A large ethmoturbinal (*concha maxima ethmoidalis* (Kaiser, 1974)) flanks the frontal medially below the nasal. Though broken ventrad, a thin *lamina papyracea* is preserved on the lateral side of the ethmoturbinal and also on the ventromedial side of the supraorbital process of the frontal.

Vomer: The vomer is well visible on the ventral side of the holotype (Fig. 37B), though incompletely preserved. It forms a v-shaped bone as in other sirenians and is firmly fused with the ethmoid dorsally. The vomer is broken anteriorly and posteriorly, but it was connected to the median crest of the presphenoid and to the maxilla in the animal's lifetime. The contact with the presphenoid can be judged from specimen CDGG S1, where the vomer is visible through the orbit (Fig. 35B), because the lateral wall of the frontal is

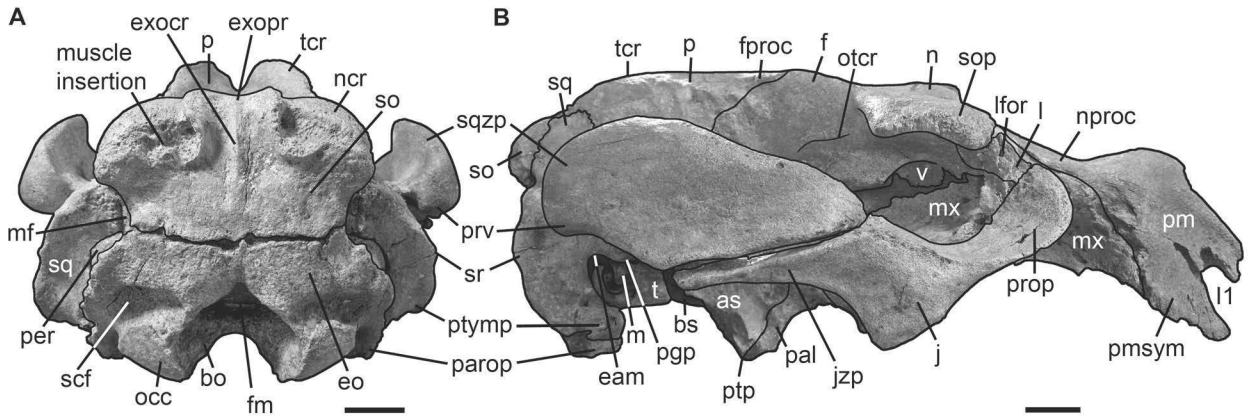

Figure 35. Cranium of gen. nov. 2 *bronni* (CDGG S1). **A**, in caudal view. **B**, in right lateral view. Scale bars equal 2 cm.

damaged. Additionally, the dorsal longitudinal groove of the maxilla that housed the anterior extension of the vomer is competely preserved in CDGG S1 and well visible through the mesorostral fossa (Fig. 34).

Lacrimal: The lacrimal fills a considerable space between the jugal and frontal (73[0]; Fig. 35B). It is not in contact with the premaxilla (74[0]), because the maxilla is interposed reaching up to the anterior tip of the supraorbital process of the frontal. This condition is best visible on the left side in specimen CDGG S1 (Fig. 34), where the lacrimal is completely preserved including a distinct nasolacrimal canal (75[0]). It has a maximum anteroposterior length of 33 mm and the lacrimal foramen measures 3.7 mm in maximum diameter.

Frontal: The frontal roof is flat between the temporal crests (52[0]) and bears no knoblike boss (53[0]; Fig. 34). Anteriorly, a small internasal process is present (43[1]), which is slightly projecting between the nasals posteriorly. The temporal crests form distinct keels (57[0]) that are as prominent on the frontal as on the parietal (56[1]). Considering the skull roof as a whole, the intertemporal constriction is strong and reaches its maximum at the centre of the skull roof (54[0]; 55[1]). On the lateral side of the frontal (Fig. 35B), the orbitotemporal crest forms a slight ridge (58[0]; 59[1]). The *lamina orbitalis* is thin and significantly less than 10 mm thick (60[0]). The supraorbital process is dorsoventrally flattened (44[0]) with its dorsal surface inclined gently ventrolaterad (45[0]). Its lateral margin is not divided (46[0]), but a prominent corner is present posterolaterally (47[1]; 48[0]; 49[1]).

Parietal: The parietal roof (Figs. 34, 37A, D) is flat and delimitated by the prominent and lyriform temporal crests (61[1]; 62[1]). In adult specimens of advanced age like CDGG S1 (Fig. 34) and SMNS 47736, the parietal roof tends to be concave between highly

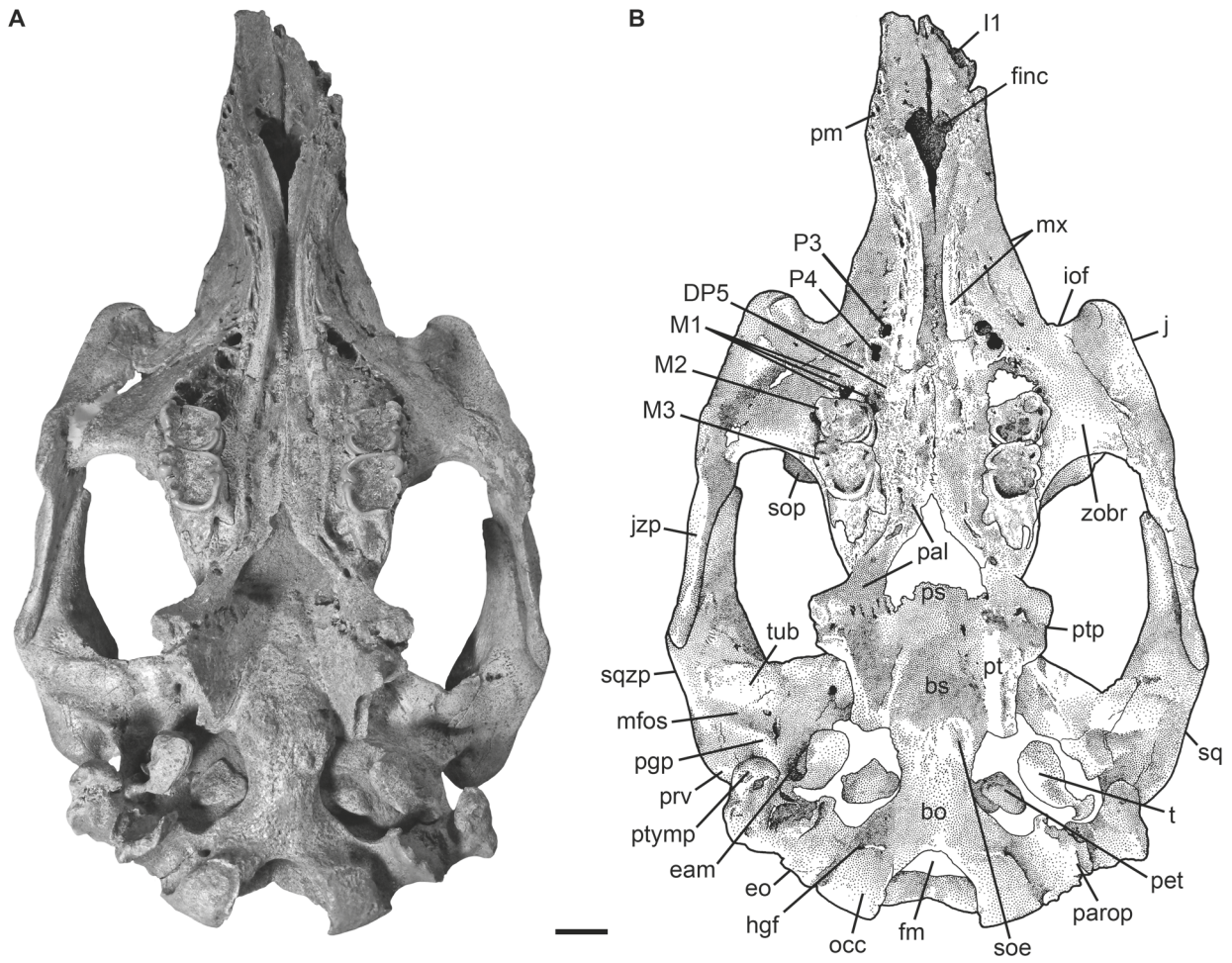

Figure 36. Cranium of gen. nov. 2 *bronni* (CDGG S1) in ventral view. **A**, photography. **B**, drawing. White areas indicate either missing or reconstructed parts. Scale bar equals 2 cm.

rising temporal crests. The frontal processes of the parietal are long exceeding half the length of the frontal (63[1]). The parietal is longer than the frontal (65[0]) and the overall proportions of the cranial roof indicate a slight brachycephaly according to the ratio l_{FP}/w_{SO} that is about 1.93 in this taxon (64[1]). Due to the distinct intertemporal constriction, the lateral sides of the parietal bulge.

Internally (Fig. 37B, E), the bony *falx cerebri* flattens out anteriorly (69[0]) and extends from a prominent tentoric process (71[0]). The *tentorium osseum* is well developed (72[1]) and an occipital spine is present between the parietal and supraoccipital (70[1]). The endocranial parietal surface is flat and slightly depressed on both sides of the bony *falx*.

Supraoccipital: The supraoccipital forms the upper part of the occipital region and is firmly fused with the parietals in the angle of the lambdoid suture (Figs. 34, 35A). According to the ratio width to height, which exceeds 1.5 in this species, this skull element is distinctly wider than high (112[1]). In dorsal view, the external lamina is concave and delimited by a convex nuchal crest forming the thickened dorsolateral ends of the supraoccipital

(113[1]); 114[0]). Medially, the nuchal crest shows a distinct notch (115[1]), but without the supraoccipital projecting onto the cranial roof (Figs. 34, 35A, 37A, C, D, F). The external occipital protuberance is only weakly developed (116[0]), and never rises above the level of the parietal roof. Additionally, the protuberance is not differentiated from the external occipital crest. The latter forms a median ridge (118[0]) that can be either distinct (SMNS 1539; Fig. 37C) or low (e.g., MCZ 8829; Fig. 37F) and diffusely flattens out about halfway of the external lamina (119[0]). Both, the protuberance and the median ridge, are distinctly indented rostrad (e.g., MCZ 8829 (Fig. 37D, F), IRSNB 8289), though to a lesser extent in the type specimen (SMNS 1539; Fig. 37A, C), as a consequence of the rostrad notching nuchal crest. Comparable to the observations in some representatives of gen. nov. 2 spec. nov. 1, the entry of a vessel passage is visible at about mid-length of the external occipital crest in MCZ 8829 (Fig. 37F) and QB 4/12.721 (Voss, 2012: fig. 3), for example. On both sides of the external occipital crest and below the nuchal crest, rugose muscle insertions of irregular shape are present for the insertion of the semispinal muscle (117[1]). The ventral margin of the supraoccipital is slightly pointed medially, forming an angle of about 140° (SMNS 1539 (Fig. 37C), CDGG S1 (Fig. 35A), MCZ 8829 (Fig. 37F)).

On the endocranial surface of the bone (Fig. 37B, E), the parietooccipital suture is indicated as a deep transverse sulcus (120[0]) that extends dorsad from the sloped lateral ends of the posterior edge of the parietals and slopes ventrally again at the parietal median tip. Below the transverse sulcus, the relief of the internal lamina is usually characterised by a narrow furrow in the median plane and relatively flat, terete bulges on both sides of the furrow.

Exoccipital: These paired elements meet in a suture of about 10 mm length dorsal to the *foramen magnum* (121[0]) and extend as plate-like elements with a slightly uneven outer surface ventrolaterad (Fig. 35A). The dorsolateral border of the exoccipital is rounded, more or less smooth and not flange-like (124[0]). Ventrolaterally (Fig. 35), the exoccipitals end in long paroccipital processes that either reach as far ventrally as the occipital condyles or exceed that level (131[0]). The *foramen magnum* is triangular in shape (130[1]) with its dorsal peak above the level of the condyles (129[1]). The supracondylar fossae are deep and extend across the entire width of the condyles (123[1]). In ventrolateral view (Fig. 36), a hypoglossal (condyloid) foramen is present lateral to each condyle and completely surrounded by bone (127[0]).

Basioccipital: This single element contributes to the occipital condyles ventrolaterally and, additionally, forms a short, columnar bone on the basicranial surface of the skull (Fig. 36). It is characterised by convex sphenooccipital eminences (128[1]) for the *longus capitis* muscles. Anteriorly, the basioccipital is firmly fused with the basisphenoid indicating adulthood.

Basisphenoid, presphenoid, orbitosphenoid: With the exception of the pre- and orbitosphenoid, which are not completely preserved, the sphenoidal region is well visible in CDGG S1. The basi- and presphenoid are firmly fused with each other and the surrounding elements (orbitosphenoid, alisphenoid and pterygoid) with the sutures to the palatines

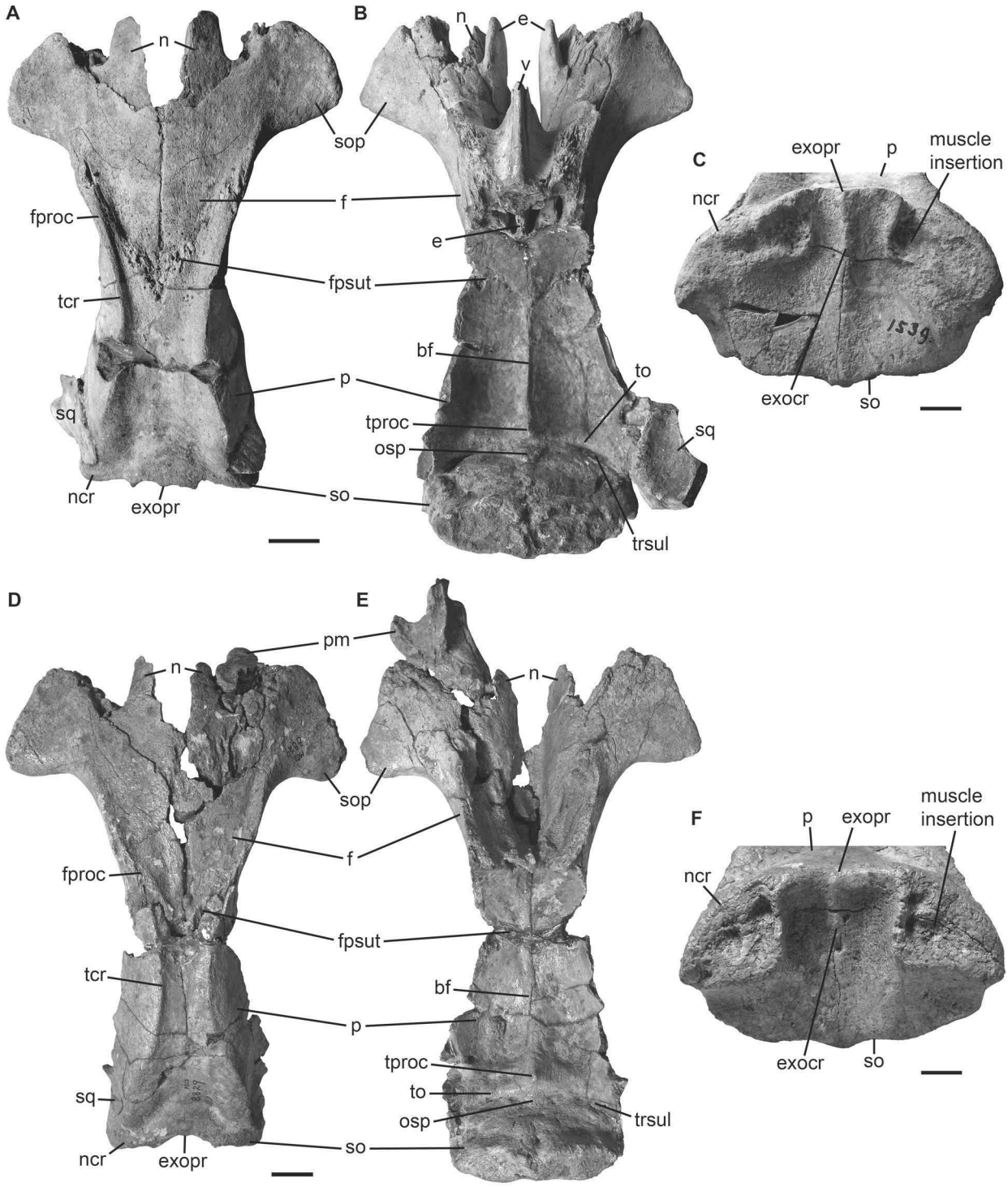

Figure 37. Selection of skullcaps of gen. nov. 2 *bronni*. **A–C**, holotype specimen SMNS 1539 in dorsal (A), ventral (B) and caudal (C) views. **D–F**, referred specimen MCZ 8829 in dorsal (D), ventral (E) and caudal (F) views. Scale bars equal 2 cm in A–B and D–E, and scale bars equal 1 cm in C and F.

remaining visible (Fig. 36). The basiphenoid has a distinct slope, being higher posteriorly than anteriorly, and continues with its flat ventral surface into the presphenoid, which has a lesser slope. The median crest of the presphenoid is visible in specimen MHNM PW 1984/37-1, but its continuation into the vomer is covered by sediment.

Alisphenoid: The alisphenoid forms the posterolateral side of the wing-shaped pterygoid process and has a more or less flat outer surface (Fig. 35B). An alisphenoid canal is absent (132[1]) as is the *foramen ovale* that is opened to form a notch or incisure (133[1]).

Pterygoid: Ventrolaterally, the paired pterygoid processes arise from the basisphenoid, whose posteromedial sides are formed by the pterygoids (Fig. 36). The pterygoid sutures to the surrounding bones are obliterated. The pterygoid fossa extends posteriorly above the level of the roof of the internal nares (134[0]). Medial to the distal end of the pterygoid process, a hook-shaped hamuli process is present (135[1]).

Palatine: This flat intermediary skull element between the maxilla extends anteriorly beyond the posterior edge of the zygomatic-orbital bridge (33[0]) up to the anterior margin of the DP5 alveolus in CDGG S1 (Fig. 36). Its posterior border is incised (35[1]). Medial to the right M3 of CDGG S1 a small foramen is present. Both palatines meet in midline and diverge posteriorly to form the anteromedial sides of the pterygoid processes. All sutures to the surrounding elements (pterygoid, alisphenoid and maxilla) remain visible. The palatines contribute to a posterior wall between the internal nares and the temporal fossa in that they curve anteromediad and join the presphenoid and orbitosphenoid.

Maxilla: The zygomatic-orbital bridge of the maxilla (Fig. 36) is anteroposteriorly long (22[0]) and nearly on the level of the palate (21[1]). Its posterior end is thickened in comparison to the very thin anterior margin (23[0]; 24[1]). In anteroventral view, a small infraorbital foramen is present on both sides of the skull, which is rounded and less than 200 mm² in cross section (25[0]; 30[1]). The infraorbital canal is not obstructed (31[0]). The palate is broad between lyriform tooth arcades, but thin at the level of the penultimate cheek tooth (32[0]).

Squamosal: The principal part of the squamosal forming the cheek region of the skull (Figs. 34, 35B) extends up to the temporal crests (87[1]). Distinct indentations of the squamosal limit posteriorly the course of the temporal crests and separate these from the nuchal crest (88[1]). The mastoid portion of the squamosal defines the mastoid foramen anteriorly (110[1]) while its posterodorsal limitations are formed by the lateral edge of the exoccipital and the ventral margin of the supraoccipital (111[0]; Fig. 35A). Laterally (Fig. 35B), the sigmoid ridge rises prominently up to the ventral margin of the supraoccipital (99[1]; 100[1]). The posttympanic process extends posteroventrally with its ventral tip projecting rostrad and forming a concave anterior surface for the attachment of

the sternomastoid muscle (108[0]; 109[0]). The external auditory meatus is short mediolaterally (104[0]) and about as wide as high (106[1]).

Lateral to the skull, the zygomatic process is triangular and tapers anteriorly (89[1]), often with a slightly dorsad rising tip (Fig. 35B). Its posterodorsal end is straight to concave (98[0]) and the ventral margin extends relatively straight with the exception of a distinct convexity posteroventrally just in front of the *processus retroversus*. This posterior end of the zygomatic process is moderately inclined inwards (101[1]; Fig. 36). On the ventral surface of the zygomatic process, transversely directed elements are present for the squamosomandibular articulation (93[0]). A deep mandibular fossa is limited anteriorly by a broad, prominent *tuberculum* (94[1]; 95[1]) and posteriorly by a fairly higher, knob-like postglenoid process (96[0]; 97[1]). The lateral and medial sides of the zygomatic process are flat to concave (90[0]) and demarcated by a sigmoid dorsal margin (91[1]; Fig. 34). The posterior end of the zygomatic root in the transition to the temporal part of the squamosal bears a distinct notch (92[1]).

Jugal: A thin preorbital process of the jugal (Fig. 35B) contacts the lacrimal (76[1]; 77[0]; 79[1]) and the maxilla, but has no connection to the premaxilla (78[0]). The central part of the jugal is characterised by a ventral extremity, lying approximately under the posterior edge of the orbit (81[1), and a postorbital process dorsally (84[1]), which does not converge with the frontal (85[0]). The ventral rim of the orbit is not overhanging (86[0]). Posteriorly, the zygomatic process of the jugal exceeds the length of the orbital diameter (83[0]) and extends up to the anterior margin of the *tuberculum* on the ventral side of the zygomatic process of the squamosal.

Ear region: The ear region is best preserved in MCZ 8829 (Fig. 38) and CDGG S4, both comprising the whole periotic, whereby CDGG S4 additionally shows the tympanic and auditory ossicles. Generally, the periotic does not differ morphologically from gen. nov. 2 spec. nov. 1. It is not fused with any other skull bone, but set in a closely fitting socket of the squamosal (136[1]). The mastoid bears an oval *processus fonticulus* with a roughened surface that is visible through the mastoid foramen on the posterolateral side of the skull (Fig. 35A). Anteriorly, the mastoid is confluent with the *tegmen tympani*, both similar in size and showing a smooth texture of their surfaces (Fig. 38). The *tegmen tympani* forms a convex, kidney-like shaped bone that distinctly tapers anteromedially into a blunt end.

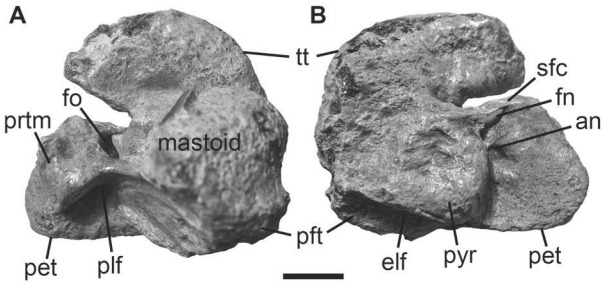

Figure 38. Periotic of gen. nov. 2 *bronni* (MCZ 8829). **A**, in ventral view. **B,** in dorsal view. Scale bar equals 1 cm.

The petrosal is wedge-shaped with a roughly convex medial extremity. On its ventral side (Fig. 38A) an inflated and smooth-

surfaced promontorium is present giving the petrosal a subconical cross section. The promontorium houses a circular-shaped oval window (*fenestra ovalis*) anterolaterally and an oval perilymphatic foramen posteromedially. Posterolaterad, the promontorium tapers to form a promontorial ridge that terminates at the level of the squamosoexoccipital suture. In endocranial view (Fig. 38B), the *pars canalicularis* of the petrosal bears an inflated and rounded pyramid. This area corresponds to the cerebral part (Robineau, 1969) that continues laterad with the endocranial surface of the *tegmen tympani*. The remaining cerebellar part is plane and rather square. Two foramina open near the anteromedial edge of the cerebellar surface providing passage for the facial (VII) and auditory (VIII) nerves. Both openings lie in an oval and concave area corresponding to the internal auditory meatus. The most anteromedial located foramen, the facial foramen, is delimited by a distinct suprafacial commissure. Towards the mastoid region, in the posterolateral wall of the pyramid, a narrow and slit-like endolymphatic foramen is situated.

An isolated right tympanic with the anterior and posterior branches broken is preserved in CDGG S4. In CDGG S1 both tympanics are preserved *in situ* showing the anterior branch to be distinctly shorter than the posterior one (Fig. 36), although most of the ear region is filled with matrix. The tympanic forms an asymmetrical and v-shaped arch that is swollen towards its medioventrally directed apex. Its posterior attachment is still connected to the anteromedial side of the posttympanic process. The whole extent of the attachment surface is visible revealing a large, oval plate that faces the mastoid posterodorsally and the top of the external auditory meatus of the squamosal anterodorsally. The imprints of the smaller and rounded anterior attachment are visible on the anteroventral side of the *tegmen tympani*. A ridge and groove along the proximolateral edge of the anterior branch most likely served as attachment area for the tympanic membrane.

The malleus is also *in situ* preserved in CDGG S1 filling the lumen of the right tympanic arch (Fig. 35B). Laterally, a sharp horizontal ridge is visible that rises from the otherwise smooth surface. The right malleus from CDGG S4 is isolated and represents a stout element. Its posterior end bears a convex swelling, the orbicular apophysis. The *processus muscularis* is enlarged and massive forming a rounded protuberance. The tip of the process appears to be separated from the anterior branch of the tympanic only by a few millimetres in CDGG S1 indicating a short *musculus tensor tympani*. On the lateral side of the malleus, the sharp horizontal ridge originates from the dorsal end of the manubrium and extends in anterior direction. Its dorsal and ventral surfaces are flat, and the anterior and posterior margins converge causing a heart-shaped outline of this ridge. The external edge of the manubrium is slightly convex. The articulation surface with the incus comprises two facets, a larger anterior and a smaller posterior facet. Both facets are roughened and raised above the body of the malleus.

In specimen CDGG S4, the right incus and stapes are *in situ* preserved. The incus is only visible in ventromedial view protecting the *crus breve* from sight, but revealing the

concave articular facets for the malleus. Anteroventrally, the surface of the incudal body bears two slight concavities. The *crus longus* is short and stout. Its medial end is formed by the *processus lenticularis* that sharply curves inward just a few millimetres behind the *corpus incudis* and articulates with the head end of the stapes. The visible length of the stapes measures about 8 mm. The stapedial foramen is well developed just lateral to the basal end, which is attached with the oval window.

Mandible: The mandibular symphysis is broad (137[1]) and has a narrow and flat masticating surface scarcely wider than the two rows of tooth alveoli it bears (138[0]; 139[0]; Fig. 39C, D). In lateral view (Fig. 39A, B), the symphysis is higher than long (142[1]). The mental foramen is placed at the level of the symphysis (141[0]) accompanied by several accessory mental foramina dorsoposteriorly (140[0]). The horizontal mandibular ramus is slender (156[0]) with its ventral border moderately concave and sharply downturned anteriorly (144[1]) and not tangent to the angle posteriorly (147[1]). The posterior margin of the mandible has no distinct *processus angularis superior*, but a broadly convex out-

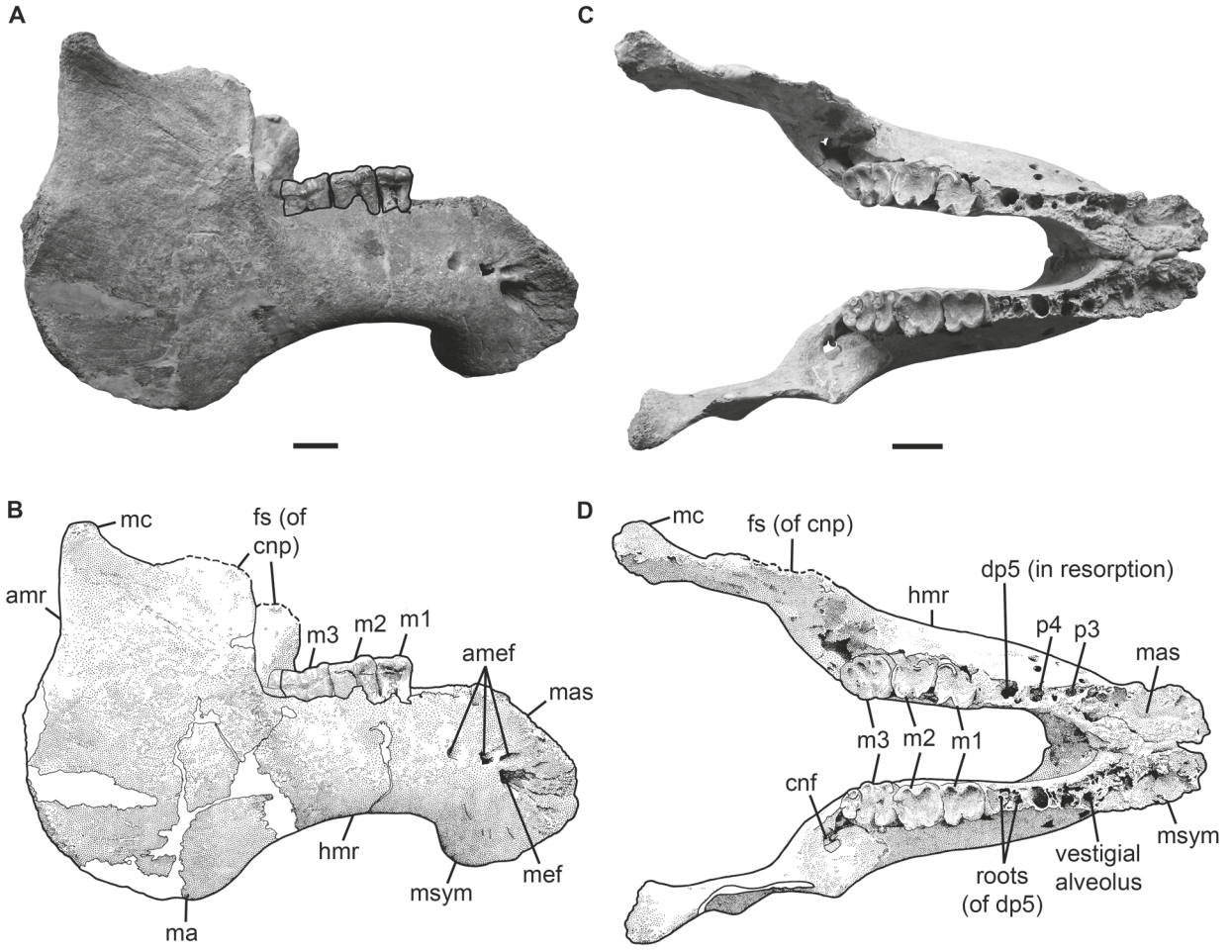

Figure 39. Mandible of gen. nov. 2 *bronni* (SMNS 47736). Photography and corresponding drawing in right lateral (**A–B**) and occlusal (**C–D**) views. White areas indicate either missing or reconstructed parts. Scale bars equal 2 cm.

line beginning well below the condyle (149[1]). The condyle occupies a position below the level of the coronoid process and bears an articulation surface that is as broad medially as laterally (148[0]; Fig. 39C, D). The anterior border of the coronoid process extends slightly anterad (151[1]) and houses an enlarged coronoid foramen of about 5 mm in diameter on its basis (153[1]). In ventromedial view, the mandibular foramen is undivided (154[0]) and reveals the dental capsule of the m3 to be exposed posteroventrally (155[1]).

Dentition: The dentition is mainly known by the alveoli in most specimens with the exception of FIS M8385, in which the complete upper cheek tooth series is preserved although heavily worn. The lifetime dental formula was most likely I1, C0, P3–4, DP5, M1–3 in the upper jaw, and i0, c0, p3–4, dp5, m1–3 in the lower jaw (164[1]; 166[1]; 167[1]; 168[1]; 169[0]; 170[0]; 180[0]; 181[0]).

Upper dentition: Both premaxillae each bear one alveolus for the incisor tusk (I1) that is about 10 cm long and extends approximately half the length of the premaxillary symphysis (158[1]; Fig. 35B).The best preserved first incisors are known from MCZ 8829 (Fig. 40B) and reveal a conical shaped crown enamelled on all sides (160[0]) that is distinctly separated from its root (165[0]). The crown has a suboval or subelliptical cross section (161[0]) and protruded about 20 mm from the premaxillae.

The permanent premolars P3–4 are single-rooted (173[1]) and best known from specimen FIS M8385, where these premolars are still fixed in the alveoli of the left and right maxilla. However, P3–4 are heavily worn with a flat to concave occlusal surface on P3 and a slightly differentiated one on P4 indicating a tall laterocentral cusp and several smaller cusps surrounding it mesiodistally.

In the subadult specimen MWNH-TER-1 (Fig. 41), the special case of labially positioned permanent premolars is observable as already described by Sagne (2001b) for gen. nov. 1 *taulannense*. There, a vestigial alveolus of the supposedly deciduous DP3 is still present on the mesiolingual side of the left and right P3. Additionally, a vestigial alveolus approximately 10 mm distant from P3 is clearly visible on the left side of the maxilla and indistinctly preserved on the right side. This alveolus is interpreted here to represent the locus for DP2, which, however, is no more replaced in this species.

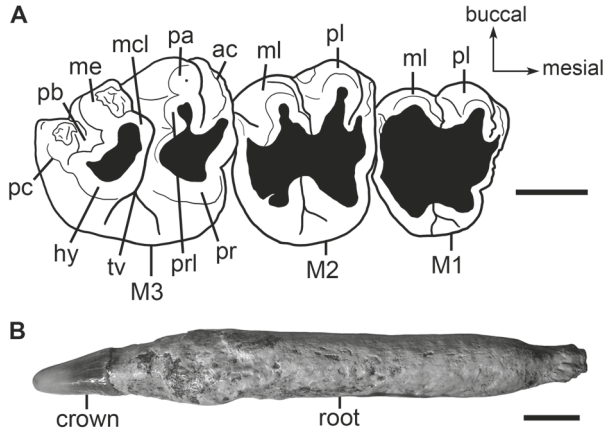

Figure 40. Dentition of gen. nov. 2 *bronni*. **A**, the right M1–3 of MWNH-TER-1 in occlusal view. **B**, first upper incisor (supposedly the right I1) of MCZ 8829 most likely in mesial view. Scale bars equal 1 cm.

In FIS M8385, the alveolus of the upper fifth premolar houses a three-rooted molariform tooth indicating that no replacement occurs at this locus (171[0]). DP5 is distinctly taller than the preceding per-

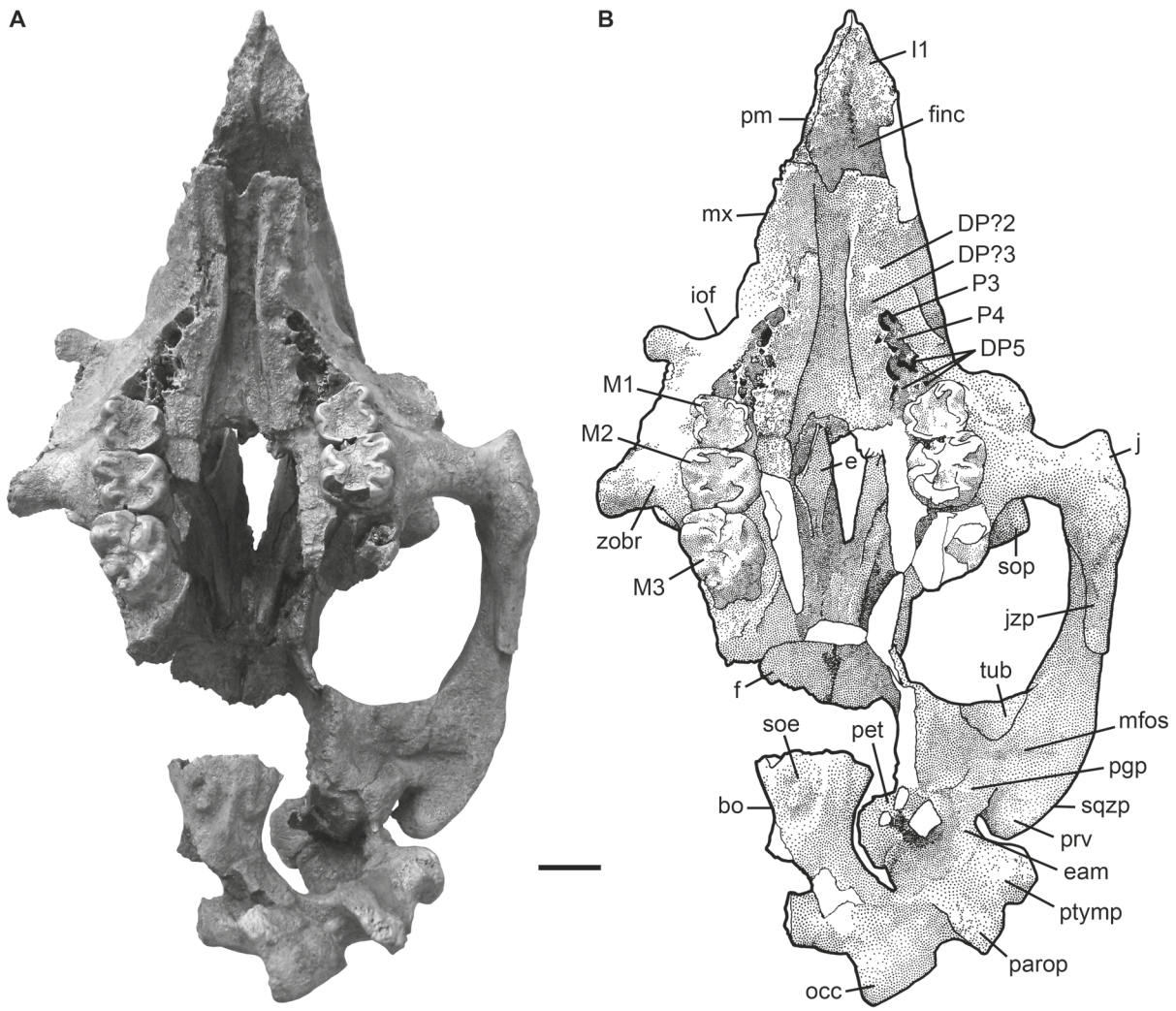

Figure 41. Cranium of gen. nov. 2 *bronni* (MWNH-TER-1) in ventral view. **A**, photography. **B**, drawing. White areas indicate broken parts. Scale bar equals 2 cm.

manent premolars, but slightly smaller than M1. Its crown has a roughly heart-shaped outline and is composed of two transverse ridges with their lingual sides pointed. The cusp pattern of DP5 cannot be further characterised due to the intense wear of its occlusal surface. The tooth is fixed in the alveoli by a large root lingually and two smaller ones mesiolabially and distolabially.

In specimen CDGG S1 (Fig. 36), the alveoli for DP5 are best preserved and visible on the right side. However, only the distolabial and lingual alveoli are clearly identifiable, whereas the mesiolabial alveolus is barely present. Therefore, DP5 is interpreted here to be in the state of resorption, which would be in accordance to the advanced age of the individual.

The molars (Figs. 36, 40A, 41) are well developed, not reduced in size relative to the skull (182[0]), and covered by smooth and thick enamel of about 2 mm in average. They slightly increase in size distad, while their tooth wear is usually decreasing in this direction according to the successive tooth eruption. Only in aged individuals (CDGG S1) all molars

are strongly and almost uniformly worn (Fig. 36). Where M1 and M2 are present, their crowns usually show wear to such an extent that no detailed description of their cusp pattern is possible. Both transverse ridges, the mesial protoloph and distal metaloph, are mostly indicated as well as remains of the *pre-* and *postcingula* that are connected lingually to the proto- and metaloph and open buccally (MWNH-TER-1 (Fig. 40A), HLMD-WT Az 100). On the M2 of specimen HLMD-WT Az 100, the cusps of the paracone and metacone are detectable. Both cusps are slightly to moderately worn, rounded and subequal in size. Additionally, the protoconule and protocone of the protoloph, and the metaconule and hypocone of the metaloph are still discernable. The transverse valley separating the protoloph from the metaloph is wide and deep on the lingual and labial sides, but it is obstructed centrally by the metaconule (178[1], 179[1]). Besides their greater size, the morphology of M1 and M2 does not differ from that of DP5 described above.

The M3 is the largest of all upper molars, which is already indicated by its strongly developed three roots with the distolabial root jutting out far from the maxilla in very old specimens (CDGG S1; Fig. 36). Fully erupted, the crown of M3 is characterised by the protoloph and the metaloph each composed of three main cusps, which are still roughly identifiable in specimen MWNH-TER-1 (Fig. 40A). The paracone and metacone are less worn of all cusps indicating that the occlusal surface is labially (or buccally) higher than lingually as is characteristic for all upper molars. Centrally, the rounded outlines of the protoconule and metaconule are still discernible before the wear surfaces of both cusps merge lingually with the heavily worn surfaces of the protocone and hypocone. The hypocone and metaconule of M3 are evidently not coalesced, which is indicated by a distinct furrow between both cusps (177[1]). The transverse valley is widest and deepest labially and, clearly obstructed centrally by the metaconule. The latter is distinctly shifted anterad to form a mesially convex arch with the metacone and hypocone. Distally, the posterior basin is large, enclosed by at least two cingular cusps (MWNH-TER-1 (Fig. 40A), FMD SRK Eck-Rat 43; 175[1]). The *postcingulum* is attached to the hypocone and opens labially. By contrast, the anterior basin is narrower and surrounded by a smooth *precingulum* that also opens labially. The overall outline of the M3 crown is heart-shaped, but not in the same way as DP5–M2. Here, the distal loph is distinctly shorter transversally than the anterior one resulting in a lingual tip shifted more mesially.

Lower dentition: The most complete mandibles providing information on both, the tooth morphology and lower dental formula, belong to the specimens MNHM PW 1984/37-1, SMNS 47736 (Fig. 39), CDGG S2, and FMD SRK Eck-Rat 43. In case of preservation the teeth are heavily worn and their presence is mainly indicated by their alveoli.

The mandibular symphysis bears a spongy and roughened masticating surface with irregularly formed and shallowly concave alveoli. Usually, there are two closely spaced rows of alveoli discernible, four on each side that may have housed three pairs of vestigial incisors and one pair of vestigial canines.

The presence of the permanent p3 and p4 is indicated by their single alveoli, which are clearly determinable in most cases. Numerous isolated and single-rooted premolars from the lower Oligocene of Germany are housed in the collections of HLMD and MNHM, for example, but no premolar is known associated with the individuals and partial skeletons assigned to gen. nov. 2 *bronni*. Specimen CDGG S2 preserves dp5 to m3 from both tooth arcades. All teeth have worn crowns and therefore the description of their cusp pattern and overall morphology is generalised and summarised in the following.

The teeth possess two roots and mesiodistally elongated crowns. The dp5 is molariform and the smallest tooth within the cheek tooth row. Usually, the bipartite alveoli of dp5 are discernable (MNHM PW 1984/37-1, CDGG S1), but some specimens show the alveoli of this unreplaced premolar in the state of resorption (FMD SRK Eck-Rat 43, SMNS 47736). In specimen SMNS 47736 (Fig. 39C, D), the special case of irregular resorption can be observed. While the two dp5 roots are still preserved on the right side, the corresponding alveoli on the left side are already fused. Only the remains of the lingual bony interseptum and, deep inside the alveolus, also the interseptum from the labial side indicate that this alveolus was divided once.

Distad within the tooth arcade, the crowns progressively increase in size revealing m3 to be the tallest molar. Characteristically, the crowns have a mesial protolophid and a distal hypolophid, both apparently separated by a transverse valley, which is indicated by the lingual and labial incisures in the centre of the crown. The two main transverse lophs are approximately perpendicular to the longitudinal axis of the tooth arcade and appear to be equal in size. The occlusal surfaces are flattened and higher lingually than labially. Mesiolabially, the indistinct remains of a *precingulum* are discernible at least on m2 and m3 of SMNS 47736 as well as a *postcingulum* enclosing a moderately wide talonid basin on m2 and forming a distinct hypoconulid lophule on m3.

Of all molars, the m3 crown in SMNS 47736 is best preserved (Fig. 39C, D). It is oval and distinctly elongated mesiodistally by the presence of a large protolophid and hypolophid in addition to the hypoconulid, which forms the distal tapered end of this tooth. The protolophid is only slightly larger than the hypolophid. Both lophs are parallel to each other, but not perpendicular to the mesiodistal axis of the tooth row, because they form mesially slight convexities. The cusps of the metaconid and entoconid are still identifiable on the left side on the otherwise worn proto- and hypolophid, respectively. Both, the meta- and entoconid are subequal in size and shape. The transverse valley is deep forming a furrow labially and widens lingually, where it also reaches its maximum depth. Centrally, the transverse valley is obstructed, but it is not clear whether this results from a hypoconid accessory cuspule or from a distointernal accessory cuspule of the protolophid. The hypoconulid comprises a minimum of two cusps rather three as is indicated on the right m3 of SMNS 47736. It encloses a talonid basin of variable width.

Hyoid apparatus: Not known from any available specimen assignable to gen. nov. 2 *bronni*.

Vertebral column: Several partial vertebral columns are known from gen. nov. 2 *bonni*, one of which is QB-4/12.721 already described and illustrated by Voss (2012). This specimen comprises 20 vertebrae representing all segments of the column. Considering the fact that no morphological differences of the vertebral column are discernible between gen. nov. 2 spec. nov. 1 and gen. nov. 2 *bronni*, and that vertebral characters are not considered for the systematic treatment of this species in this study, reference is given to the description of gen. nov. 2 spec. nov. 1 and Voss (2012). The following morphological data complement the knowledge on this species.

A putative nearly complete vertebral column is known from specimen SMNS 47736 comprising seven single cervicals, 20 thoracics, two lumbars, one sacral and 17 caudals. However, some of the postcranial elements were replaced from a second specimen and it is not sure which ones exactly (pers. comm. R. Ziegler). Therefore, it also cannot be ascertained if the number of vertebrae especially from the thoracic and lumbar segments was correctly determined. However, this specimen supports the assumption that the cervical column is composed of seven individual vertebrae without fusion between the axis and C3. This can also be observed in specimen MNHM PW 1984/37-1, where a craniocaudal series of C2 to C4 is preserved. The complete cervical columns of CDGG S1 and CDGG S2, on the other hand, show the special feature of a fused axis and C3 as is already described for gen. nov. 2 spec. nov. 1 (BSPG 1956 I 540).

In contrast to 20 thoracic vertebrae assessed for SMNS 47736, specimen CDGG S2 reveals only 16 thoracics. Even if 19 thoracics are taken to be generally present as is in gen. nov. 2 spec. nov. 1, this might indicate intraspecific morphological variation comparable to the observations in extant *Trichechus* species (Domning & Hayek, 1986).

The lumbar vertebrae characteristically have the mediolaterally long, wing-shaped transverse processes with blunt and swollen distal ends. In specimen CDGG S2, the number of the lumbars and sacrals seems to be also variable in comparison with gen. nov. 2 spec. nov. 1. Here, four lumbars with the caudalmost one serving as sacral vertebra are identified. This is in accordance to the observations in QB-4/12.721 (Voss, 2012), where four vertebrae are described and assigned to the lumbar and sacral region on the basis of four pairs of large transverse processes.

Caudals 1–3 still have long and nearly horizontally directed transverse processes resembling those of the lumbar region. The lack of markedly roughened distal ends on their transverse processes and the presence of articulation facets for chevrons on the ventral side of the centrum distinguish those caudals from the preceding lumbars. From Ca4 onwards, the caudad inclination of the transverse processes begins. Considering the total number of 26 caudal vertebrae in gen. nov. 2 spec. nov. 1 (NHMUK PV M9415), the caudal series in gen. nov. 2 *bronni* is not completely known.

Chevrons: A number of isolated chevron bones are known from CDGG S1 not differing from gen. nov. 2 spec. nov. 1 (HLMD-WT 420).

Ribs: The ribs do not differ morphologically from those described for gen. nov. 2 spec. nov. 1. Furthermore, Voss (2012) already described the ribs of specimen QB-4/12.721. Therefore, only the systematically important features are mentioned in the following referring to Voss (2012) for more detailed information. The ribs are compact and voluminous with a great anteroposterior width as is also the case in CDGG S1. In QB-4/12.721, however, the ribs have a more slender overall shape. In each case, the rib shafts are flattened mediolaterally and elliptical in cross section (197[0]). The first rib (Fig. 42) has a protuberance ventral to its *capitulum* (195[1]) and shows a remarkable extension of its distal extremity (196[1]).

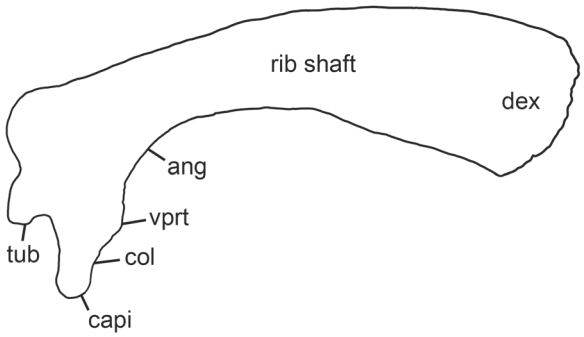

Figure 42. Outline drawing of the left first rib of gen. nov. 2 *bronni* (MB Ma. 49618) in anterior view. The exact scale of the original was not determinable, because the respective skeleton is on display.

Sternum: The sternum of gen. nov. 2 *bronni* is completely known, but not from a single individual (Fig. 43). Specimen MCZ 8829 preserves the manubrium, which is similar to that of CDGG S1, where also the corpus is present (Fig. 43A). MNHM PW 1984/37-1 includes the corpus and the xiphisternum (Fig. 43B). Summarising, the sternum is composed of three elements (200[0]).

The manubrium has a nearly constant mediolateral width along its anteroposterior length. The cranial edge is straight to slightly rounded without forming an anterior process (201[1]). Both, the dorsal and ventral surfaces are smooth in CDGG S1, whereas MCZ 8829 reveals a ventromedial knob on its anterior half. However, a ventral sternal keel is missing (202[0]). While MCZ 8829 is flat to slightly concave dorsally and convex ventrally, CDGG S1 differs from this condition being double-curved in lateral views. There, the dorsal surface is concave anteriorly and flat to slightly convex posteriorly. Accordingly, the ventral surface is flat to convex anteriorly and flat to slightly concave posteriorly. The manubrium reaches its

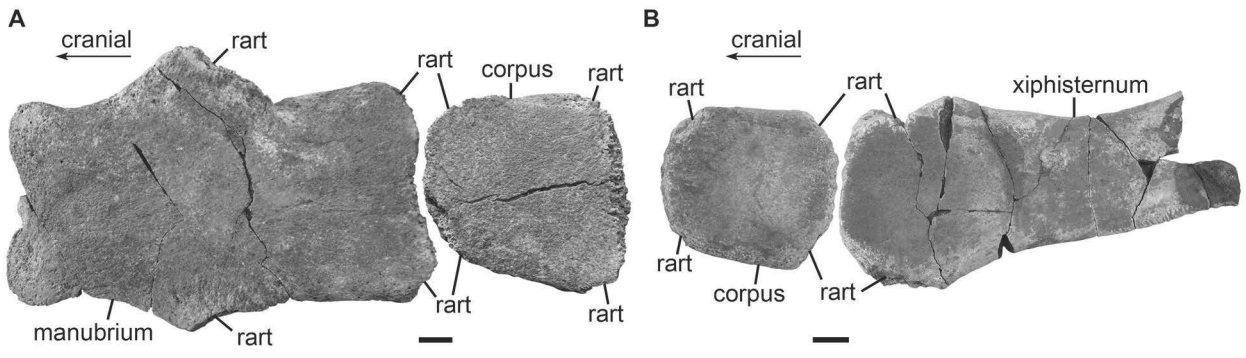

Figure 43. Sternal elements of gen. nov. 2 *bronni*. **A**, manubrium and corpus of CDGG S1 in ventral view. **B**, corpus and xiphisternum of MNHM PW 1984/37-1 in ventral view. Scale bars equal 1 cm.

greatest mediolateral width at about half its length, from where the large and concave, paired rugosities for the articulation with the first ribs extend laterodistad. A smaller and less concave rib articulation each lies caudally at the junction of the manubrium and the corpus indicated by chamfered posterolateral edges of the former. The caudal margin of the manubrium is thickened and slightly concave for the cartilaginous articulation with the corpus.

The corpus is compact forming the smallest element intermediate between the manubrium and xiphisternum. Its dorsal and ventral surfaces are smooth and flat. All edges are radiused and chamfered for the appropriate rib articulation that it forms together with the adjacent sternal elements. As a result, the corpus receives a roughly octagonal shape.

The xiphisternum only has an articulation facet for the respective rib at its anterolateral corner. This indicates that, in total, three pairs of the anteriormost ribs articulate with the whole sternum, which is consistent with the rugose distal texture of R1–3. The anterior part of the xiphisternum resembles the corpus in shape and size, but it tapers distad to form a long posterior process. Although its distal end is broken in MNHM PW 1984/37-1, this process is clearly divided.

Scapula: The scapula is sickle-shaped (187[0]), broader proximally than distally. In lateral view (Fig. 44), the scapular spine forms a prominent, caudally overhanging flange separating a concave infraspinous fossa from a distinctly wider and flatter supraspinous fossa (186[1]). The scapular spine is shortened and does not exceed half the length of the outer surface (184[1]). A proximal rugosity of the spine is minor (CDGG S1) or not (MCZ 8829) developed (183[1]). Although the distal end of the acromion is broken in all specimens, its position at the level of the scapular neck, i.e. the *collum scapulae*, is clearly determinable (188[0]). The glenoid cavity is moderately concave and oval in outline with its longitudinal axis extending anteroposteriorly. Anterodorsal to and not disjoint from the anterior apex of the articular glenoid, a moderately developed and medially inclined coracoid process is present (185[0]). The costal surface of the scapula is smooth and flat to slightly concave.

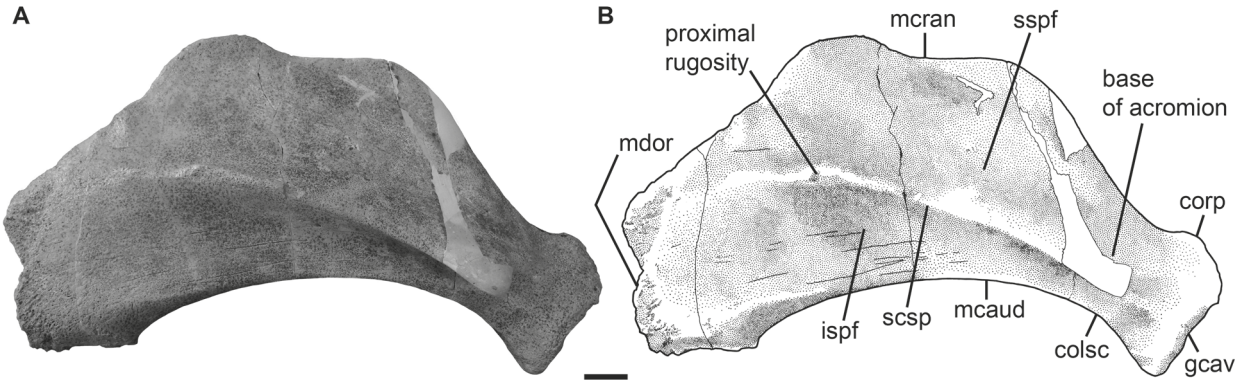

Figure 44. Right scapula of gen. nov. 2 *bronni* (CDGG S1). Photography (**A**) and corresponding drawing (**B**) in lateral view. White areas indicate either missing or reconstructed parts. Scale bar equals 2 cm.

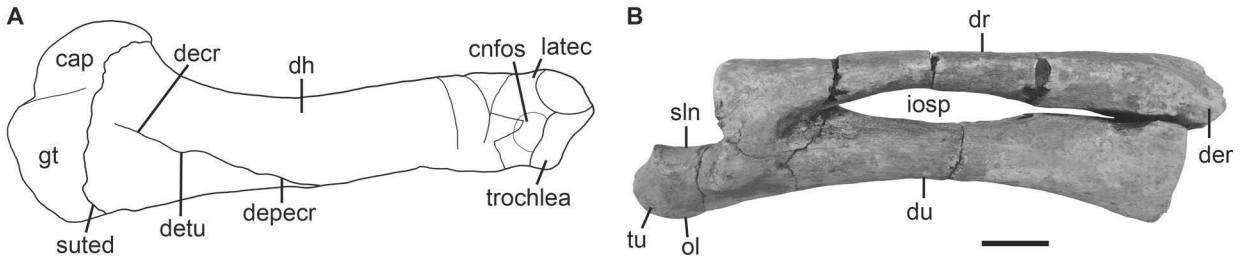

Figure 45. Stylopod and zeugopod of gen. nov. 2 *bronni*. **A**, outline drawing of left humerus (CDGG S2) in anterolateral view. The exact scale of the original was not determinable, because the respective skeleton is on display. **B**, photography of left radius and ulna of MNHM PW 1945/233 in lateral view. Scale bar equals 2 cm.

Humerus: The left humerus is preserved in the partial skeleton CDGG S2 (Fig. 45A). It forms a compact bone with distinctly developed epiphyses (189[1]) although the suture between the proximal epiphysis and humerus shaft is not obliterated indicating that this animal was not very old. The greater tubercle is elevated above the level of the rounded caput (190[1]). Anteromedially, the lesser tubercle occupies a position distinctly below the top of the caput. In anterior view, the diaphysis is characterised by a triangular deltoid crest that is separated from the greater tubercle by the proximal suture. The deltoid crest is slightly overhanging laterally at the level of the deltoid tuberosity and continues distad into a narrow deltopectoral crest at about half the length of the humerus shaft. The distal articulation facet for the radius and ulna is only slightly inclined and nearly perpendicular to the proximodistal axis of the humerus (191[0]). Both, the coronoid and olecranon fossae, are distinctly developed.

Radius and ulna: The right articulated radius-ulna complex is known from MNHM PW 1945/233 (Fig. 45B). The diaphyses of both elements are straight (194[0]), fused proximally and distally. In medial and lateral views, the diaphysis of the ulna is thicker anteroposteriorly than the diaphysis of the radius (192[0]). Both lack their distal epiphyses and the ulna shaft is shorter than the radius differing in length by about 10 mm. In anterior and posterior views, the ulnar diaphysis is transversally as long as the radial diaphysis just below the level of their proximal epiphyses (193[1]). The articulation surface for the humerus has a semilunar shape on the ulna, but is flat on the radius. The anterior margin of the olecranon is tilted back and forms an angle of about 50° with the axis of the ulna shaft. Proximally, the olecranon is thickened and bears a tuberosity.

Manus: Elements of the autopod unquestionably referable to gen. nov. 2 *bronni* are known by two fragments (QB-4/12.721-PH) that most likely represent middle phalanges and are already described by Voss (2012). Additionally, a single metacarpal, 62 mm long with its distal end broken, is preserved in IRSNB Reg. 4006. It most likely represents the third metacarpal from the left side according to comparisons with the autopod from gen.

nov. 2 spec. nov. 1. The proximal end has two facets, a larger, anterodorsally directed facet semicircular in shape for the articulation with the capitate, and a smaller, posterodorsally directed facet for the articulation with the hamate. The posterodorsal part of the proximal articulation surface extends over the posterior edge of the diaphysis. Just below the articulation with the adjacent carpals, the anterior and posterior sides are rugose serving as attachment areas for the second and fourth metacarpals, respectively. Both surfaces are slightly concave with the contact for the fourth metacarpal slightly more depressed than its anterior counterpart. In posterior and lateral views, the diaphysis of the metacarpal III is smoothly convex. Its anterior side is characterised by a ridge that extends from the proximomedial corner and curves distad along the shaft. The medial side also possesses a longitudinal ridge that comes from the distal extremity and divides proximally to enclose a longitudinal groove.

Innominate: Pelvic remains associated with partial skeletons of gen. nov. 2 *bronni* are known from QB-4/12.721 and CDGG S1, the latter of which preserves the complete pelvis of the right side (Fig. 46). It comprises the ilium anteriorly, the pubis posteroventrally and the ischium dorsoposteriorly without a clear boundary between these three parts.

The ilium is characteristically elongated, slender and rounded in cross section in its posterior half, but thickened anteroproximally having dorsomedially a longish, concave and pitted area for the attachment to the sacral vertebra. In lateral view of the pelvis (Fig. 46A, B), a distinct *acetabulum* is present anterodorsal to the pubic bone. The acetabular edges are raised causing a suboval shape of this concavity (198[0]). The pubis forms a short and triangular bone having a roughened outer surface and a blunt ventral tip. In ventral view, the pubis is slightly inflected mediad.

The ischium is flattened mediolaterally, plate-like, but not wider dorsoventrally than the ilium in an oblique sagittal plane. Its medial surface is flat to slightly concave (Fig. 46C, D), its lateral side is slightly convex (Fig. 46A, B). The posterior end of the ischium is neither markedly thickened nor flaring laterad. A rugose protuberance pointing posterolaterad is present on the dorsal edge of the ischium and perpendicular to the ventralmost pubic extension. Another protuberance occurs on the ventromedial edge of the acetabular region about 20 mm anterodorsal to the ventral tip of the pubis (Fig. 46C, D). This protuberance is inclined inward similar to the pubis. A *foramen obturatum* is missing (199[1]).

Femur: Specimen IRSNB Reg. 4006 comprises the left femur lacking its distal end and measuring 88 mm in preserved length. Although the femur forms a gracile element, its proximal end is distinctly developed. The femur head is rounded and flanked laterally by the greater trochanter, which forms an oval tuberosity well below the top of the head. The neck of the femur is indistinct. Anteroventral to the neck, a slight prominence is present, which corresponds to the lesser trochanter. The femur shaft is slender, transversally rounded and tapering distad.

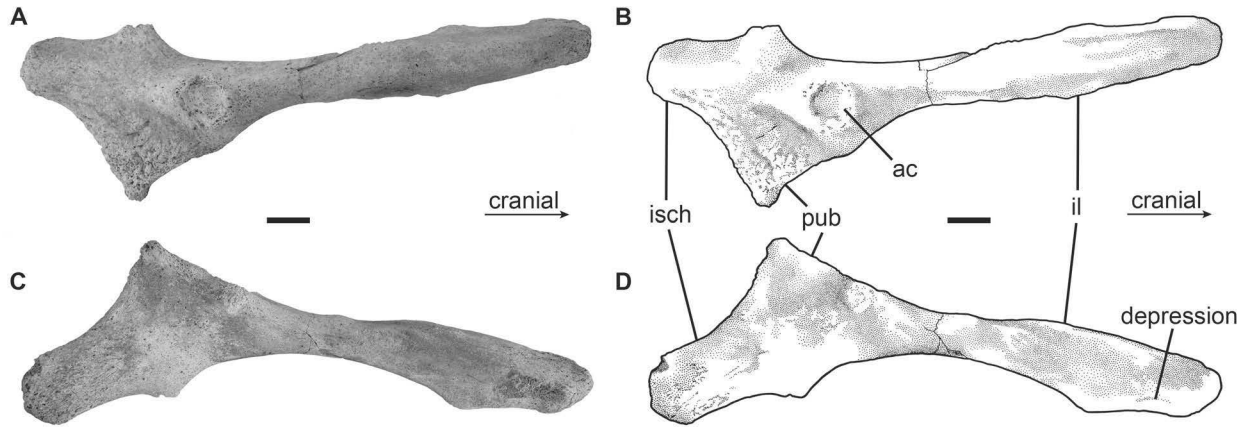

Figure 46. Right innominate of gen. nov. 2 *bronni* (CDGG S1). Photography and corresponding drawing in right lateral (**A–B**) and medial (**C–D**) views. Scale bars equal 2 cm.

Taxonomic remarks

Since the establishment of the extinct species *"Halitherium schinzii"* by Kaup (1838), sirenian remains from the early Oligocene of Germany and Belgium in particular have been assigned to this taxon. This is largely based on the assumption that a single species inhabited the early Oligocene sea. Nevertheless, inter- and intraspecific morphological variation has been indicated for this taxon since the middle of the 19th century. This resulted either in the description of new species (e.g., Krauss, 1858; Hartlaub, 1886) or the establishment of different morphotypes (Sickenberg, 1934a). One of the first attempts to figure out morphological distinctions on the species level were undertaken by Krauss (1858). He erected the species *"Halitherium" bronni* on the basis on his specimen "Nro. I" (Krauss, 1858: 523), a skullcap (SMNS 1539) from Flonheim (Mainz Basin, West Germany) and the holotype of gen. nov. 2 *bronni* in this study. Until today, this species was regarded as synonymous with *"H. schinzii"* as is the case with all other subsequently established species (Domning, 1996).

However, a morphological and/or phylogenetical approach for a synonymy of species with *"H. schinzii"* on an objective basis is still missing. Therefore, sirenian material, especially from the lower Oligocene of Germany and Belgium, was (re-)examined for the present study. The morphological re-evaluation proved particularly necessary after the recognition of *"H. schinzii"* as a *nomen dubium* as already outlined above. Additionally, significant morphological differences amongst putative representatives of *"H. schinzii"* have recently been observed and were mentioned numerous times (e.g., Voss, 2007, 2008, 2009a, b, 2010). In the latest treatment, Voss (2012) rekindled the debate on the splitting of species currently lumped under *"H. schinzii"* and hypothesised about the validity of Krauss' (1858) species *bronni*.

Although Krauss (1858) justified the implementation of the new species on a morphological misinterpretation of the frontonasal area, he also recognised a specific

morphology of the supraoccipital that was again observed by Voss (2012) in specimen QB 4/12.721 from western Germany. In contrast to the very prominent superficial anatomy of specimens now assigned to gen. nov. 2 spec. nov. 1, the supraoccipital of gen. nov. 2. *bronni* shows an anteriorly concave nuchal crest in the median plane and a reduced external occipital protuberance. These features are remarkably well developed in specimen MCZ 8829 (Bronn, 1853–1856: pl. 48: fig. 9a; Fig. 37D, F). In combination with a rostrad extending external occipital crest and protuberance, the notched nuchal crest reflects a completely opposite anatomical structure as is in gen. nov. 2 spec. nov. 1. Therefore, the specific supraoccipital morphology is classified as one of the main distinguishing characters on species level considering the fact that most specimens preserve the skull roof only.

The hypothesis of the presence of two sirenian morphospecies in the early Oligocene of Central Europe is corroborated by the cladistic analyses performed in the present thesis. In addition to the features referring to the supraoccipital, the separation of the lacrimal from the premaxilla, an infraorbital foramen that is rounded instead of oval, and the absence of P2/p2 provide further morphological criteria for the establishment of gen. nov. 2 *bronni* and its distinction from gen. nov. 2 spec. nov. 1.

In previous studies, the quantitative assessment of the dental formula within Sirenia yielded different results for the absence or presence of the second permanent upper and lower premolars. In his monograph on *"Halitherium schinzii"* from the Mainz Basin, Lepsius (1882) distinguished individuals with two sequential, single alveoli for P3/p3 and P4/p4 in front of DP5/pd5 from those with an additional alveolus for a single-rooted P2/p2 slightly distant to P3/p3. This indication of intraspecific variation is taken up by e.g. Barthel (1962), who postulated that the loss of the right upper P2 in the adult specimen BSPG 1956 I 540 now assigned to gen. nov. 2 spec. nov.1 has to be expected during the animal's lifetime. However, the subsequent loss of a tooth belonging to the secondary dentition is not documented neither for fossil nor extant sirenian taxa. Instead, the morphological review of specimens that were originally assigned to *"H. schinzii"* reveals the distinction of two species also by the absence or presence of P2/p2.

This is best observable by the comparison of the upper dentition of specimen BSPG 1956 I 540 (gen. nov. 2 spec. nov. 1; Fig. 20) and CDGG S1 (gen. nov. 2 *bronni*; Fig. 36), representing similar growth stages. Both individuals have an obliterated basioccipital-basisphenoid suture indicating adulthood (Pocock, 1940; Mitchell, 1973). Additionally, M3 is fully erupted showing a similarly high degree of wear, which indicates that these individuals died of old age. While the right P2 is still preserved *in situ* in BSPG 1956 I 540, though heavily worn, the tooth arcade in CDGG S1 exhibits no further alveoli or remains of P2 in front of P3. This difference is also observable in subadults like MWNH-TER-1 (gen. nov. 2 *bronni*) and FIS M2597 (gen. nov. 2 spec. nov.1.) of approximately similar age (Fig. 47). Both specimens are characterised by an unfused basioccipital-basisphenoid

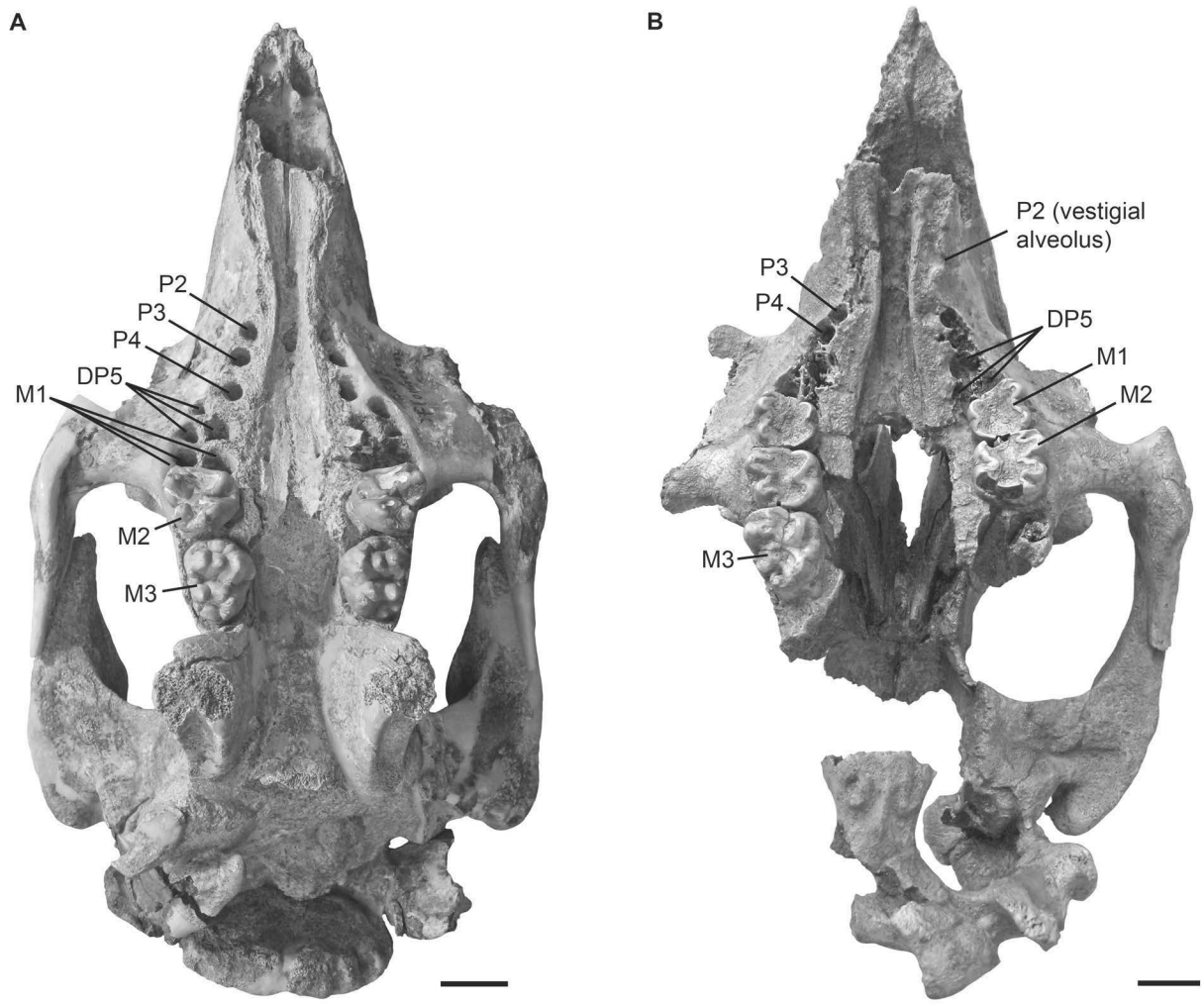

Figure 47. Comparison of dentition within gen. nov. 2. **A**, gen. nov. 2 spec. nov. 1 (FIS M2597) in ventral view. **B**, gen. nov. 2 *bronni* (MWNH-TER-1) in ventral view. Scale bars equal 2 cm.

suture associated with a M3 that either is fully erupted and slightly to moderately worn (MWNH-TER-1; Fig. 47B) or nearly fully erupted and almost unworn (FIS M2597; Fig. 47A). FIS M2597 preserves three isolated and deep alveoli in front of DP5 in each quadrant of the upper jaw, which housed single-rooted P2–4 in the animal's lifetime. Specimen MWNH-TER-1 also still retains a single, but small alveolus circa 10 mm in front of P3 on the left and probably also on the right side of the maxilla. This alveolus is, additionally, rather shallow and not sharply defined and considered to be in a state of resorption. A permanent second upper premolar was certainly not developed in this specimen.

Lepsius (1882) already observed resorption at the position of DP2/dp2 for some specimens of *"H. schinzii"*, however, without drawing any consequences for the taxonomic treatment of the respective specimens. Following Luckett's (1993) observations of rudimentary deciduous teeth lacking successors in mammals, the indication of an extra premolar position in front of P3 in MWNH-TER-1 is interpreted here to represent instead remnants of the first premolar generation that is not replaced at the DP2 locus.

Whether the tooth at the DP2 locus was a vestigial diminutive premolar or still functional can be only tentatively concluded considering the fact that even in extant taxa the decision on whether or not to consider a tooth as vestigial is sometimes difficult and not entirely objective (Van Nievelt & Smith, 2005). These authors consider a tooth as vestigial if it did not consistently pierce the gingival or was shed after a short period. At least the latter can be hypothesised for MWNH-TER-1, because the deciduous premolar was lost in a subadult stage of the individual. The issue of suppression of tooth replacement is a complex matter and it is not yet well investigated within living and fossil sirenians. The present thesis does not attempt to resolve this issue. However, it should be emphasised that the extant dugong, which is characterised by a highly derived dentition, comprises only teeth belonging to the first ("milk") generation. Heuvelmans (1941) dental formula of the cheek tooth rows in the dugong recognises three premolars and three molars as functional teeth. The premolars, which are presumably the posterior three deciduous premolars (Lanyon & Sanson, 2006), are not replaced, but progressively fall out or are partially resorbed. In contrast the molars, which by definition are never replaced, erupt posteriorly during growth (Mitchell, 1973). Hence, a deciduous tooth does not necessarily need to be vestigial to remain unreplaced.

Van Nievelt & Smith (2005) documented a wide range of tooth replacement patterns in therians and point out that the loss of deciduous teeth at various loci is fairly common in diverse eutherian groups. One of the hypotheses presented by Van Nievelt & Smith (2005) is that dental replacement may be lost in the process of full elimination of, respectively, a tooth or locus, at any given position. Loci that are reduced in size may then lead to the suppression of replacement of deciduous teeth as an intermediate stage. Although Van Nievelt & Smith (2005) argued that no single hypothesis is adequate to explain the full range of observed tooth replacement patterns, the hypothesis presented above could well match with the observations in subadult and adult individuals of gen. nov. 2 *bronni* considering a reduced antemolar dentition in both extant genera: *Trichechus* (e.g., Domning, 1982) and *Dugong* (e.g., Lanyon & Sanson, 2006). Consequently, intraspecific variation with respect to the absence and presence of P2/p2 within the specimens traditionally assigned to *"H. schinzii"* is refuted in this study.

In conclusion, gen. nov. 2 *bronni* is considered here to be the sister taxon of gen. nov. 2 spec. nov. 1 and a sympatric species according to the concordant geographic and stratigraphic occurrence (Fig. 33). Both taxa are early Oligocene in age and well known from the Alzey Formation and Hochberg Subformation (Bodenheim Formation) of their type locality, the German Mainz Basin. In addition to the type locality, gen. nov. 2 *bronni* is also known from the upper Ratingen Member of the southern Münsterland in western Germany (Voss, 2012). Fischer & Krumbiegel (1982) described and illustrated a specimen (Ru 26) from the phosphorite nodule horizon of the Böhlen Formation, which is Rupelian according to Böhme (2001), of the Bay of Leipzig, East Germany. This specimen can

be clearly assigned to gen. nov. 2 *bronni* due to a significant supraoccipital morphology. Furthermore, the specimens IRSNB Reg. 4006 and 4011 from the Boom Clay Formation of the Antwerp and East Flanders Provinces (North Belgium) can be also taxonomically referred to gen. nov. 2 *bronni*.

Gen. nov. 2 *alleni* (Simpson, 1932a)

Halitherium antiquum (Leidy); Allen, *sensu* Allen, 1926: 455, pl. 2: figs. 1, 2.
Halitherium alleni; Simpson, 1932a: 445.
Felsinotherium alleni (Simpson); Kellogg, 1966: 91.
M[etaxytherium]. alleni (Simpson); Fondi & Pacini, 1974: 45.

Holotype: MCZ 17142, a parietal-supraoccipital skullcap.

Referred material: Parietal-supraoccipital skullcaps MCZ 16484 and YPM 21335. For detailed listing of the preserved skeletal parts see Appendix 1.

Questionably referred material: USNM: 299830, 23394, unnumbered cast of a right maxillary fragment with M2–3. MCZ: 17145, 16683, 16684, 17141, 16485, 16496. For detailed listing of the preserved skeletal parts see Appendix 1.

Type horizon and locality: Ashley River phosphate deposits near Charleston, South Carolina (USA). Probably the Chandler Bridge Formation (late Oligocene) after Domning (1996) and/or the Hawthorne Formation (early Miocene) according to the collection data of YPM 21335.

Range and distribution: Known only from type locality.

Emended diagnosis: Represents a gen. nov. 2 species that is characterised by the following characters: nuchal crest convex; external occipital protuberance and external occipital crest prominent; frontal roof flat; intertemporal constriction strong at centre of skull roof; temporal crests prominent on frontal and parietal and separated from nuchal crest by squamosal; squamosal forms deep indentations in posterior corners of parietal; parietal roof flat; and bony *falx cerebri* flattens out in anterior direction.

Character states: 114[0]; 116[1]; 118[0]; 52[0]; 54[0]; 55[1]; 56[1]; 57[0]; 87[1]; 88[1]; 61[1]; 69[0].

Differential diagnosis: Differs from gen. nov. 2 spec. nov. 1 and gen. nov. 2 *bronni* in the following features: the parietosquamosal indentations are conspicuously deep and pronounced and the supraoccipital bears a broad, triangular occipital spine of the bony *falx cerebelli* on its endocranial surface.

Description of referred material
Figures 48, 49; Appendix 3

Taxon gen. nov. 2 *alleni* is represented by three individuals including the holotype and is mainly known by parietal-supraoccipital skullcaps all coming from the phosphate Ashley River deposits.

Frontal: Specimen YPM 21335 (Fig. 48) preserves the posterior portion of the frontal. The temporal crests are prominent forming distinct keels that are as strong as on the parietal (56[1]; 57[0]). Starting on the frontal, the lyriform temporal crests distinctly converge towards the centre of the skull roof (54[0]); 55[1]), where they reach their minimum distance, and then diverge again in caudal direction. The frontal roof is flat (52[0]) and has no knoblike bosses medial to the temporal crests (53[0]).

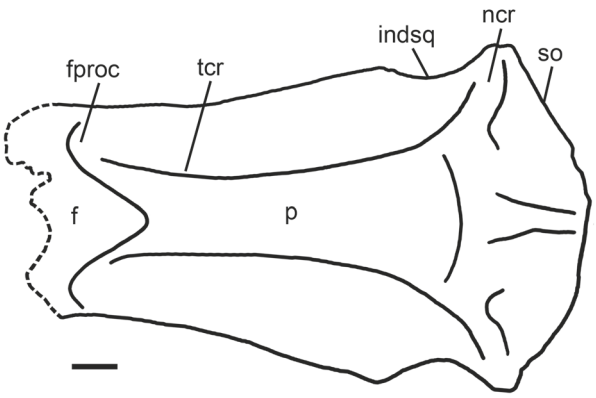

Figure 48. Outline drawing of parietal-supraoccipital skullcap of gen. nov. 2 *alleni* (YPM 21335) in dorsal view. Dashed lines indicate broken parts. Scale bar equals 1 cm.

Parietal: The parietal roof lacks an external sagittal crest (62[1]), but is flat between high and thickened temporal crests (61[1]). In YPM 21335 (Fig. 48), the frontal processes of the parietal already end at about half the length of the preserved frontal roof. Therefore, it can be assumed with certainty that these processes did not exceed half the length of the original frontal roof and are scored to be short (63[1]). Dorsolaterally (Fig. 49A), the parietal reveals conspicuous indentations formed by the cranial parts of the squamosal. The latter itself is not preserved, but, judging from its imprints, the squamosal extends to the temporal crests (87[1]) and separates these from the nuchal crest of the supraoccipital by occupying the posterolateral corners of the parietal (88[1]).

On the interior aspect of the bone (Fig. 49B), a broad and triangular occipital spine is present in the median plane at the parietosupraoccipital junction (70[1]). The tentoric process and *tentorium osseum* are well developed (71[0]; 72[1]) with a prominent bony *falx cerebri* that extends rostrad and flattens out just before the frontoparietal suture (69[0]).

Supraoccipital: This upper element of the occipital surface (Fig. 49C) is enlarged transversally given by the ratio width to height that equals 1.56 in the holotype specimen (112[1]). The nuchal crest is thickened and convex forming the dorsolateral ends of the supraoccipital (113[1]; 114[0]). The external occipital protuberance rises slightly above the dorsal surface (116[1]) and releases ventrad the external occipital crest, which forms a distinct median ridge well exceeding half the length of the supraoccipital (118[0]; 119[0]). Dorsolateral to the median ridge and below the nuchal crest, flattish and roughened

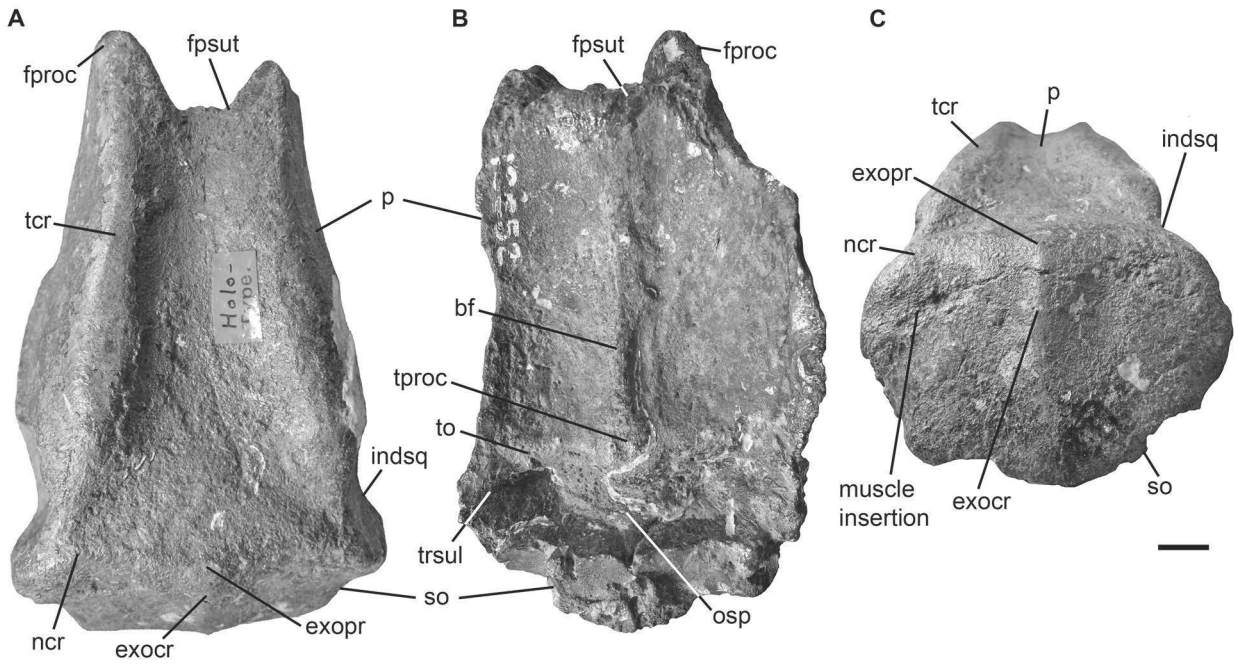

Figure 49. Parietal-supraoccipital skullcap of gen. nov. 2 *alleni* (MCZ 17142, holotype). **A**, in dorsal view. **B**, in ventral view. **C**, in caudal view. Scale bar equals 1 cm.

muscle insertions of indistinct outline are present (117[1]). Lateral to the occipital spine (Fig. 49B), the internal supraoccipital surface is smooth. The transverse sulcus is indicated dorsolaterally by deep pits (120[0]).

Description of the questionably referred material

In the following, known specimens hitherto assigned to *"Halitherium" alleni* and possibly referable to gen. nov. 2 *alleni* are described. The given scoring of characters for these elements is not included in the cladistic analyses conducted in this study, because of the only questionable taxonomic assignment of these specimens.

Premaxilla: This skull element is only known by the posterior ends of the nasal processes articulated with frontal USNM 23394, but gives evidence for a sutural contact between both, the premaxilla and the frontal (20[1]). Additionally, it reveals the external nares to be retracted and enlarged reaching to the level of the anterior margin of the orbit (2[1]). The nasal processes are thin and tapering at their posterior ends, having lengthy overlap with the frontal and/or nasal (17[0]).

Nasal: In USNM 23394, parts of both nasals are set in a socket of the frontal medial to the articulating premaxilla (37[0]; 38[0]). The estimated internasal suture is distinctly shorter than half the length of the interfrontal suture exposed (39[1]). A nasal incisure is present at the posterior end of the mesorostral fossa, but it is small and does not extend posterior to the supraorbital processes of the frontal (42[1]). The nasals are broken in midline and

it is not detectable if they meet each other.

Frontal: The cranial roof of specimen USNM 23394 supplements the potential information on the frontal. An internasal process (43[1]) is present on the anterior margin possibly separating the nasal bones posteriorly. The supraorbital process is dorsoventrally flattened (44[0]) with the dorsal surface inclined gently ventrolaterad (45[0]). Its lateral margin is smooth, not indented by dorsoventral grooves (46[0]). The posterolateral corner of the supraorbital process is prominent (47[1]; 49[1]), but not projecting posteriorly (48[0]).

Maxilla: A right maxillary fragment with a heavily worn M2 and a moderately worn M3 is known. The fracture surface of the broken zygomatic-orbital bridge indicates its position nearly at level with the palate (21[1]).

Squamosal: The only squamosal element known is a right isolated zygomatic process (MCZ 17145) that is triangular in lateral outline and tapered anteriorly (89[1]). Its postero-dorsal end is straight (98[0]), the medial side flat (90[0]) and the dorsal margin inclined inward forming a sigmoid ridge (91[1]). Ventrally, the *tuberculum* and glenoid fossa form a distinct and transversely elongated relief for the articulation with the lower jaw (93[0]; 94[1]; 95[1]). This articulation surface is defined posteriorly by the postglenoid process that is, although broken, still detectable to be prominent and knob-like (96[0]; 97[1]). A *processus retroversus* is present and moderately inflected (101[1]).

Dentition: Only the right M2 and M3 associated with a maxillary fragment (cast USNM unnumbered) are known (180[0]; 181[0]; 182[0]). Both teeth are three-rooted, fully erupted and show heavy (M2) to moderate (M3) wear.

On M2, the protoloph mesially and metaloph distally have a constant transversal width. Mesially, remnants of the *precingulum* are present that enclose a narrow anterior basin. No cusp pattern is identifiable yet, but the presence of a deep transverse valley and a large posterior basin enclosed by a smooth *postcingulum*.

On M3, paracone, protoconule and protocone form a transversally arranged protoloph that is larger than the metaloph. Mesially, a *precingulum* originates from the protocone and is sloping and open labially. The paracone and protoconule are about equal in size, but smaller than the protocone. The transverse valley is obstructed lingually apparently by a posterolingual accessory cuspule from the protocone. On the metaloph, the hypocone is slightly shifted backwards and larger than the metacone due to the fact that the metaconule is fused with the hypocone forming a hypocone-metaconule cusp (176[0]). The overall shape of the metaloph is convex mesially. Distally, a bicuspid *postcingulum* encloses a relatively large posterior basin that is closed labially and opened lingually (175[1]). Both, the anterior and posterior basin are about equal in size.

Vertebral column: Centrum MCZ 16485 is of rounded shape and most likely had occu-

pied a position within the anterior part of the caudal column. Anteroventral to the centrum, slight imprints of the chevron bones characterise this vertebra. The bases of the broken transverse processes indicate a slight ventral slope. The neural arch and spine are missing.

Ribs: A single rib fragment (MCZ 16496) from the right half of the thorax is preserved. The distance between the *capitulum* and *tuberculum*, i.e. the *collum* of the rib, is 43 mm long indicating an anterior position within the thorax. The rib shaft is broken about half its estimated total length revealing an oval cross section (187[0]).

Humerus: Three proximal fragments of the humerus are known only missing the distal articulation facet in MCZ 16683. The humerus is a compact element with a massive shaft and distinctly developed epiphyses (189[1]). The greater tubercle is distinctly elevated above the level of the rounded caput (190[1]).

Remarks

Taxonomic remarks: In this study, taxon gen. nov. 2 *alleni* is regarded to represent one of two valid sirenian species known from the phosphate deposits near Charleston (Fig. 50), which was originally designated as *Halitherium alleni* by Simpson (1932a) on the basis of the holotype MCZ 17142.

The distinction of two associated sirenian taxa had already been postulated by Allen (1926) and later supported by Simpson (1932a) and Kellogg (1966). The species division is mainly based on size differences resulting in the grouping of assorted remains to a

Figure 50. Geographic setting of the sirenian site on the Ashley River near Charleston, South Carolina, USA. Asterisk indicates estimated locality of species gen. nov. 2 *alleni*. *Abbreviations*: **E**, Lake Erie; **FL**, Florida; **GA**, Georgia; **M**, Lake Michigan; **SC**, South Carolina.

relatively small sirenian, *"Halitherium" alleni* Simpson, 1932a, on the one hand, and to a larger species, *Dioplotherium manigaulti* Cope, 1883, on the other.

Most sirenian specimens belonging to the smaller size category are represented by skullcaps and humeri. On the basis of morphological comparisons with European taxa, Allen (1926) assigned this material to the genus *Halitherium*, which Simpson (1932a) regarded as well justified considering the inadequacy of the material. According to Domning (1989a), the material of both taxa is fragmentary, probably reworked and in need of revision. Considering these facts, the species *Dioplotherium manigaulti* was carefully and convincingly reviewed by Domning (1989a) and, therefore, this study provides guidance here. Consequently, only comparable specimens that are morphologically similar and/or represent associated elements are considered and assigned to gen. nov. 2 *alleni*.

The parietal-supraoccipital skullcaps in question most likely represent a single species, due to two morphological characters that are distinct in *D. manigaulti*. These characters refer to the parietal and include the temporal crests that do not come closest behind, but instead at the centre of the skull roof in gen. nov. 2 *alleni*. Furthermore, all parietal-supraoccipital skullcaps assigned to gen. nov. 2 *alleni* are characterised by very deep indentations by the squamosal that are less pronounced in *D. manigaulti*. Additionally, the cladistic analyses performed in this study reveal gen. nov. 2 *alleni* to form a monophyletic group with gen. nov. 2 spec. nov. 1 and gen. nov. 2 *bronni*. Its position within this grouping is not consistent as it will be outlined and discussed later in the chapters "Phylogenetic analyses" and "Discussion". However, it is well proven to represent a valid taxon within the stem group distinguishable from *D. manigaulti* that is proven to represent a crown group sirenian.

Cranial and postcranial materials questionably assigned to gen. nov. 2 *alleni* and excluded from cladistic treatment are described here with the intention of summarising those skeletal elements potentially referable to this species based on the hypothesis of two different sized taxa hitherto known from the phosphate beds near Charleston. However, Domning (1989a) suggested the presence of at least two unnamed sirenian genera in the same deposits in addition to those mentioned above. This hypothesis has yet to be substantiated, but must still be taken into consideration. Either way, this grouping of fossil material is provisional and pending further investigations on more complete specimens of known geological age, which might permit a substantial review of the species in the manner of Domning (1989a) on *D. manigaulti*.

Geological remarks: The mammalian specimens obtained during the phosphate dredging operations on the Ashley, Cooper, and Wando River near Charleston (South Carolina) were collected mainly in the 19th century and comprise a mixed assemblage of different geological ages (e.g., Allen, 1926; Simpson, 1932a; Kellogg, 1966; Domning, 1989a). Accordingly, the stratigraphic provenance for none of the sirenian specimens referred to gen. nov. 2 *alleni* is known for certain. Therefore, the taxonomic, systematic and stratigraphic

assignment of these specimens should be taken as a provisional and rather cautious interpretation.

According to Kellogg (1966), the river phosphate deposits northwest of Charleston unquestionably comprise an overlying succession from the upper Eocene to the Pleistocene. In view of the mixed assemblage of fossil vertebrates, Simspon (1932a) estimated the stratigraphic provenance of gen. nov. 2 *alleni*, his *"Halitherium" alleni*, to the lower Miocene or earlier, according to his conclusion that *"Halitherium"* does not occur in later deposits. Domning (1989a) took up the issue on the stratigraphy of the river sediments in the Charleston area and named several geological formations as possible source beds of the sirenian specimens. These include, amongst others, the late Eocene portion of the Cooper Formation, the early Chattian Ashley Formation and the middle Chattian Chandler Bridge Formation. Although most of the mined sirenian material had been reworked, Domning (1989a) stated that it probably included some phosphatised sediments from the Ashley Formation and the Chandler Bridge Formation, both late Oligocene in age. These are exactly the formations that Domning (1996) considers to be the probable stratigraphic horizon of *"Halitherium" alleni*, which also corresponds to the collection data of parietal USNM 299830. However, this specimen is too fragmentarily preserved and therefore only questionably referred to gen. nov. 2 *alleni*. Another specimen, the parietal-supraoccipital skullcap YPM 21335, is recorded as coming from the Hawthorn Formation, which is raised to group status by Scott (1988). The Hawthorn Group unconformably overlies the Cooper Formation in South Carolina (Ernissee *et al*., 1977; Scott, 1990) and its Miocene age has been well accepted until today (e.g., Green *et al*., 2008, 2009). The indication of a Miocene provenance is consistent with the collection data of specimen MCZ 16484. A supposedly lower Miocene provenance is indicated for the type specimen and some of the questionably referred material. Notwithstanding the uncertainty of stratigraphic determinations of components of mixed assemblages an early Miocene age is favoured for gen. nov. 2 *alleni*.

Genus nov. 3

Type species: Halitherium cristolii (Fitzinger, 1842).

Included species: Gen. nov. 3 *cristolii*.

Generic diagnosis: Sirenian with external nares that are retracted and enlarged, reaching beyond the anterior margin of the orbit. Rostrum strongly downturned. Nasals reduced and do not meet in midline. Temporal crests prominent on frontal and parietal reaching the nuchal crest. Intertemporal constriction strong with its maximum behind the centre of the skull roof. Posterolateral corner of supraorbital process projects posteriorly. Frontal processes of parietal short and do not exceed half the length of the frontal. Orbitotem-

poral crest present and prominent. *Tuberculum* at ventral side of zygomatic process of squamosal forms low convexity. *Processus retroversus* moderately inflected. Mastoid foramen defined by squamosal, exoccipital and supraoccipital. Height of supraoccipital distinct. Both, external occipital protuberance and external occipital crest, distinct. Nuchal crest narrow and sharp-edged. Bony *falx cerebri* prominent and flattens out in anterior direction just in front of the frontoparietal suture. Mandibular symphysis and masticating surface broad. Horizontal mandibular ramus with strongly concave ventral border. Anterior border of coronoid process extends slightly anterad and posterior border of mandible without distinct *processus angularis superior*. Permanent fifth premolar absent.

Character states: 3[1]; 12[1]; 39[1]; 40[1]; 56[1]; 57[0]; 88[0]; 54[0]; 55[0]; 48[1]; 63[0]; 58[0]; 59[0]; 95[0]; 101[1]; 111[0]; 112[0]; 116[1]; 118[0]; 113[0]; 69[0]; 137[1]; 138[1]; 146[1]; 151[1]; 149[1]; 171[0].

Differential diagnosis: Differs from all stem group representatives in possessing the synapomorphic character of a strongly concave ventral border of the horizontal mandibular ramus. Differs from all crown group representatives in lacking the following synapomorphies: paroccipital process of exoccipital short; absence of P3/p3 and P4/p4; strongly developed coracoid process of scapula; and presence of a ventral manubrial keel.

Gen. nov. 3 *cristolii* (Fitzinger, 1842)

Halitherium cristolii; Fitzinger, 1842: 71, pl. 1.
M[anatus]. christolii (Fitzinger); De Blainville, 1844: 122.
Met[axytherium]. christolii (Fitzinger); Laurillard, 1846: 172.
Halianassa collinii; Meyer [partim], *sensu* Meyer, 1847: 189, 578.
Halianassa collinii (Meyer); Ehrlich, 1855: 3, corresponding figures on page 14–17, pls. 1, 2.
Halitherium schinzi; Kaup, *sensu* Peters, 1867: 310.
Halitherium schinzi; Kaup [partim], *sensu* Lepsius, 1882: 164.
Metaxytherium(?) pergense; Toula, 1899: 459, pl. 12.
Halitherium christoli (Fitzinger); Abel, 1904: 25, fig. 1, pl. 1: figs. 12, 13, pl. 2: figs. 4, 11, 17, pl. 5: fig. 8.
Halitherium pergense (Toula); Spillmann, 1959: 11, figs. 6, 7.
Halitherium christoli (Fitzinger); Spillmann, 1959: 17, figs. 8–18, 21, 23, 28, 29a, 30, 33a.
Halitherium abeli; Spillmann, 1959: 36, figs. 19, 20, 22, 24–27, 29b, 31, 32, 33b, 34, pls. 1–4.
Halitherium pergense (Toula); Spillmann, 1969: 61, fig. 1.
Halitherium christoli (Fitzinger); Spillmann, 1969: 62, fig. 2, pl. 8.
Halitherium abeli (Spillmann); Spillmann, 1969: 62, fig. 3, pl. 9.
Halitherium pergense (Toula); Spillmann, 1973: 197, figs. 1, 2, pl. 39.

Halitherium christoli (Fitzinger); Spillmann, 1973: 198, fig. 4, pl. 40.
Halitherium abeli (Spillmann); Spillmann, 1973: 205.

Lectotype, present designation: A mandible (LI 2012/1) with left dp5–m2 and right m1–3.

Paralectotype: Fragment of right maxilla with worn M1 crown and remnants of DP5 roots (LI 2012/2), and an isolated crown of M3 (LI 2012/3) from the right side.

Referred material: LI: 2012/4, 2012/5, 2012/6, 2012/7, 1992/118, 1931/21, 1931/263, 1928/82, 1927/200, 1926/394, 1926/395, 1854/327, 1899/11, 1917/7, 1921/71, 1939/257, 1948/33, 2013/1. For detailed listing of the preserved skeletal parts see Appendix 1.

Type horizon and locality: Sicherbauer-Gestätte sand quarry, Linz (Upper Austria). Linz-Melk Formation, Linzer Sande (= Linz sands), late Oligocene, Egerian (Chattian).

Range and distribution: Known only from the late Oligocene of Linz and the area around Linz.

Emended diagnosis: As for the genus.

Remarks: Taxon gen. nov. 3 *cristolii* is originally based on a type series according to Fitzinger (1842). This type series is composed of a mandible with left dp5–m2 and right m1–3 (LI 2012/1), two isolated molars (LI 2012/2 + 3), an isolated m3, ribs and vertebrae. In the interest of nomenclatural stability, the mandible is designated as lectotype, because the type series material is not certainly assignable to a single specimen. Accordingly, the remaining skeletal elements associated with the species erection by Fitzinger (1842) represent paralectotypes. The ribs and vertebrae mentioned by Fitzinger (1842) are no more traceable in the Oberösterreichisches Landesmuseum Linz. Additionally, an isolated m3 supposed to be housed in the Naturhistorisches Museum Wien (NHMW) according to Fitzinger (1842) is neither listed in the catalogue of Pia & Sickenberg (1934) nor present in the NHMW collections itself (pers. comm. U. Göhlich). These elements are now considered to be lost.

Furthermore, it is proposed in this study to maintain the original spelling of the species name *cristolii* as it was established by Fitzinger (1842). No uniform spelling of this specific epithet exists until today. For example, Ehrlich (1855: 11) spelled the epithet *"cristolii"* while Abel (1904: 25) and Spillmann (1959: 17) used *"christoli"*. Originally, Fitzinger (1842) established this species in honour of Jules de Christol. He spelled the name "de Cristol" and consistently applied the spelling *"cristolii"* throughout his entire work. Therefore, *"cristolii"* (Fitzinger, 1842: 71) is the "correct original spelling" according to Articles 32.1. and 32.2. of the IKZN (2000) and is not to be considered as a spelling that must be corrected following Articles 32.5. and 32.5.1.

Description

Figures 51–59, Appendix 3

This taxon is quite well known from cranial and postcranial elements. However, the premaxilla and lacrimal are not known at all as are the pelvis, zeugopod and autopod. The following description is mainly based on a partial skull (LI 1926/394) and two mandibles (LI 1939/257 and LI 2012/1).

Premaxilla: The premaxilla is in no specimen preserved, but some characters can be scored by indirect observations. The external nares are retracted and enlarged (Fig. 51) as in all sirenians and reach beyond the anterior margin of the orbit (3[1]). Judging from the recesses in the anterior margin of the frontal, the nasal processes are not broadened and bulbous at their posterior ends (19[0]), but taper having lengthy overlap with the frontals (20[1]). The angle of the rostrum most likely exceeds 50° (12[1]) considering the deflection of the mandibular symphysis of about 60° (Fig. 56).

Nasal: The exact status of the nasals cannot be determined without doubt according to the poor preservation of the nasal area in specimen LI 1926/394 (Fig. 51). Therefore, it is left open if the nasals are fused or coalesced with the frontals. However, judging from the right anterior margin of the frontals that is not damaged, but smoothed without an attachment area for the nasals, these elements are considered to be small (39[1]) without meet-

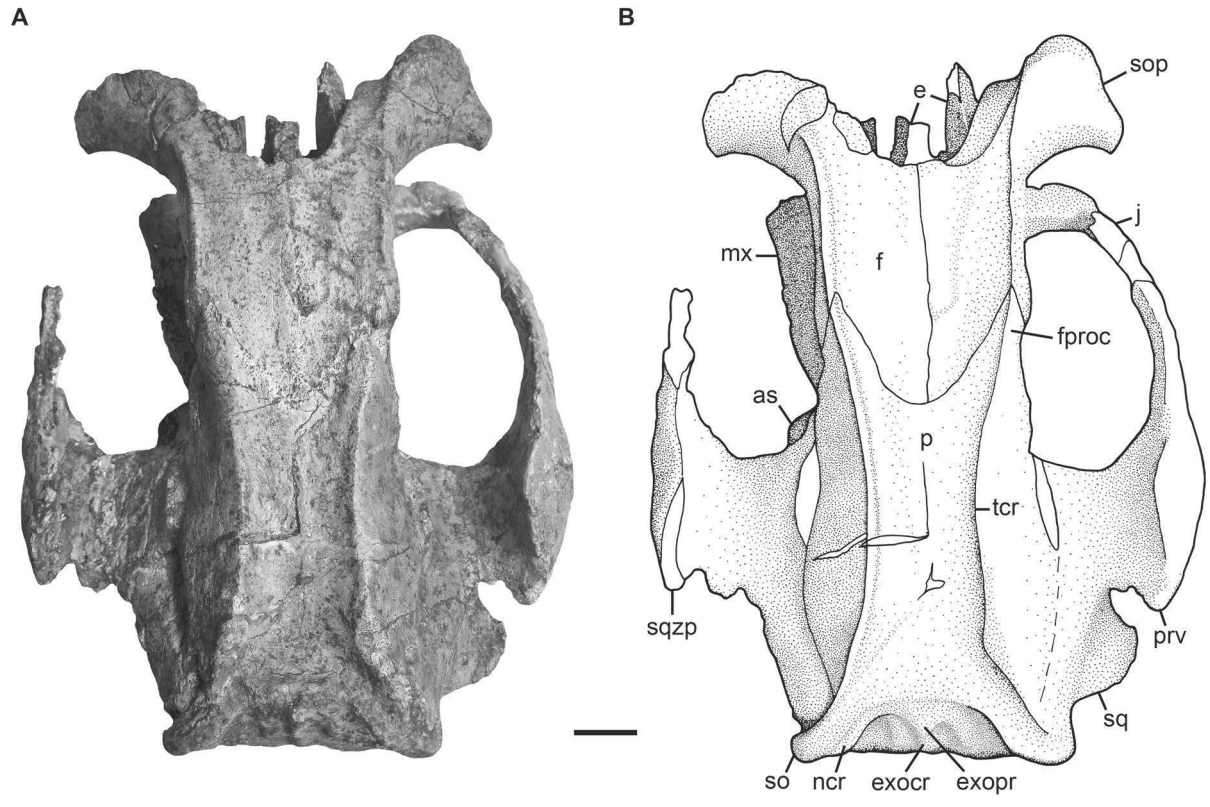

Figure 51. Cranium of gen. nov. 3 *cristolii* (LI 1926/394) in dorsal view. **A**, photography. **B**, drawing. White areas indicate either missing or reconstructed parts. Scale bar equals 2 cm.

ing in midline (40[0]). A nasal incisure is present at the posterior end of the mesorostral fossa and deep extending posterior to the supraorbital processes of the frontal (41[1]).

Ethmoidal region: The ethmoid is incompletely preserved and not easily observable in all aspects. A prominent perpendicular plate of the mesethmoid is visible in dorsal and anterior views of the skull LI 1926/394 (Fig. 51). This vertical wall measures 10 mm to 15 mm in width, is narrower dorsally and ventrally, and apparently also becomes thinner posteriorly. Ventrally, the perpendicular plate is fused with the likewise distinctly developed vomer. On the right side of the skull and medial to the frontal (Fig. 51), the almost complete large ethmoturbinal (*concha maxima ethmoidalis* (Kaiser, 1974)) extends nearly parallel to the mesethmoid. Its left counterpart is only fragmentarily preserved. The *crista galli* and *lamina papyracea* are either not preserved or not visible.

Vomer: The vomer is exposed on the ventral side of the skull LI 1926/394, but broken anteriorly (Fig. 52). It is fused with the presphenoid posteriorly and forms the cranial extension of its median crest. The vomer is triangular in cross section, firmly fused with the ethmoid via its flat dorsal surface and contacts the maxilla laterally. In lateral view (Fig. 53B), the vomer is also visible through the orbit due to the incomplete preservation of the skull.

Frontal: In dorsal view (Fig. 51), the frontal roof is flat between the temporal crests (52[0]) and bears no knoblike bosses (53[0]). The straight to slightly concave anterior margin of the frontal has no internasal process (43[0]). The temporal crests form distinct keels (57[0])

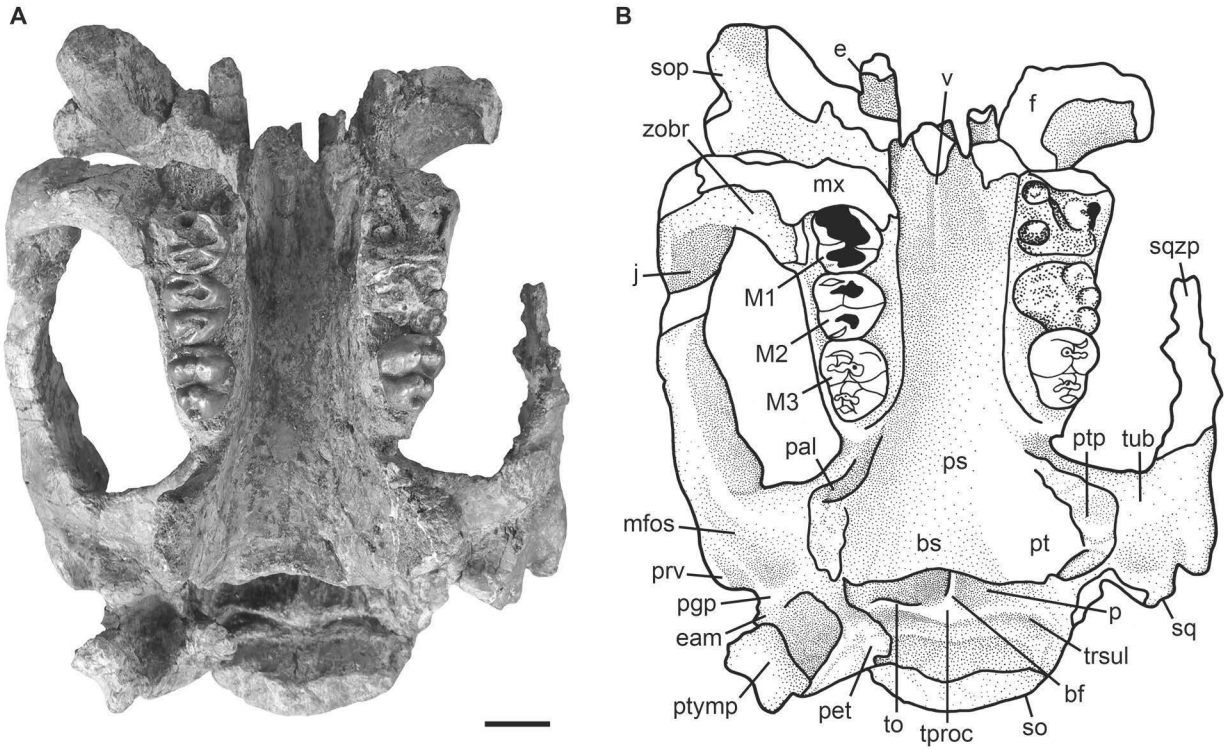

Figure 52. Cranium of gen. nov. 3 *cristolii* (LI 1926/394) in ventral view. **A**, photography. **B**, drawing. White areas indicate either missing or reconstructed parts. Scale bar equals 2 cm.

and are as prominent on the frontal as on the parietal (56[1]). In lateral view (Fig. 53B), the supraorbital process is dorsoventrally flattened (44[0]) with its dorsal surface inclined gently ventrolaterad (45[0]). Its lateral margin is not divided (46[0]) having a prominent posterolateral corner that projects posteriorly (47[1]; 48[1]; 49[1]). An orbitotemporal crest forms a distinct craniocaudally extending ridge (58[0]; 59[0]). The *lamina orbitalis* is significantly less than 10 mm thick (60[0]).

Parietal: The parietal roof (Fig. 51) is flat between the temporal crests (61[1]) and characterised by a strong intertemporal constriction that reaches its maximum behind the centre of the skull roof with the parietal bulging laterally (54[0]; 55[0]). An external sagittal crest is not developed (62[1]). The frontal processes of the parietal are short and do not exceed half the length of the frontal in midline (63[0]). The parietal is longer than the frontal (65[0]) and the overall proportions of the cranial roof indicate a slight brachycephaly according to the ratio l_{FP}/w_{SO} that is below 2 (64[1]).

In endocranial view (Fig. 52), the bony *falx cerebri* extends from a prominent tentoric process (71[0]) and flattens out anteriorly before reaching the frontoparietal suture (69[0]). The *tentorium osseum* is well developed (72[1]), an internal occipital spine is missing (70[0]). On both sides of the bony *falx*, the flat internal parietal surface shows the depressions for the superior parts of the brain hemispheres.

Supraoccipital: The height of the supraoccipital is distinct indicating that this element is only slightly wider than high (112[0]; Fig. 53A). Dorsally, the nuchal crest is constantly narrow along its transversal length and relatively sharp-edged (113[0]). It makes up the dorsolateral margin of the supraoccipital (114[0]). The external occipital protuberance rises above the parietal roof (116[1]) and is also prominent in posterior direction (115[0]). Ventrad, the protuberance releases the external occipital crest that forms a distinct ridge,

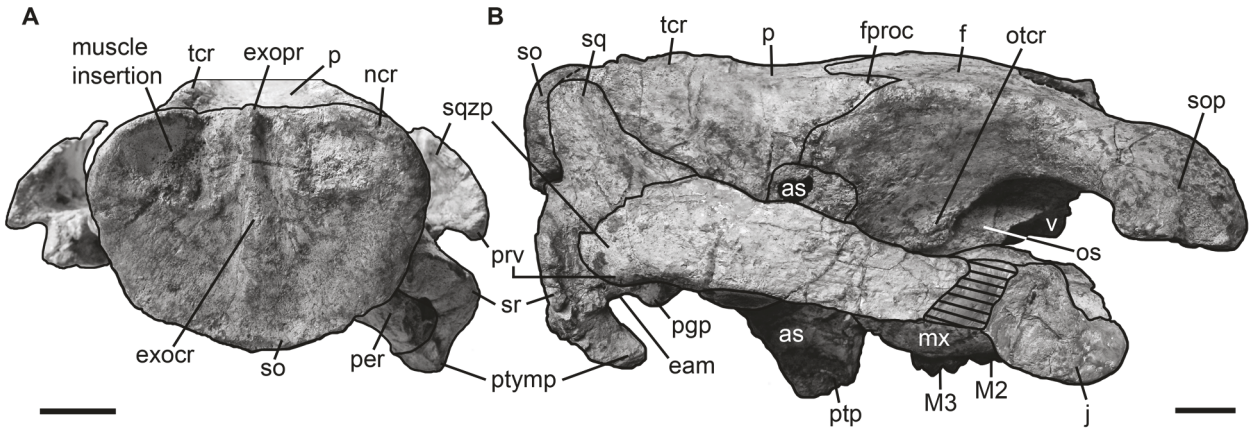

Figure 53. Cranium of gen. nov. 3 *cristolii* (LI 1926/394). **A**, in caudal view. **B**, in right lateral view. Shaded area indicates either missing or reconstructed part. Scale bars equal 2 cm.

which slightly flattens out after one third of the supraoccipital's height entering imminently its ventral margin (118[0]; 119[0]). Dorsolateral to this median ridge, the deep and large insertions for the semispinal muscle occupy about the upper third of the external lamina. The area of the muscle insertion is triangular in shape and defined by distinct ridges medioventrally and the nuchal crest dorsolaterally (117[1]). The ventral margin of the supraoccipital is slightly tapered to an angle of approximately 135° in specimen LI 1926/394.

Specimen LI 1899/11 (Fig. 54), formerly designated as the holotype of *"Halitherium" pergense*, but now referred to gen. nov. 3 *cristolii*, also shows a distinct nuchal crest. However, the protuberance, median ridge and definitions of the muscle insertions are less prominently developed than in LI 1926/394 indicating its juvenile status.

In interior view (Fig. 52), the supraocciptal is flat with the exception of longitudinal bulges dorsolaterally that are merged in the median plane and separated by a deep transverse sulcus from the *tentorium osseum* (120[0]). Posterolaterally, the parietals extend between the supraocciptal and squamosal forming a short flange.

Exoccipital: The dorsal parts of these paired elements are not preserved in any specimen. However, the total length of the ventral margin of the supraoccipital in LI 1926/394 (Figs. 52, 53A) reveals the articulation surface for the exoccipitals indicating that these bones evidently meet in a suture dorsal to the *foramen magnum* (121[0]). Additionally, specimen LI 1939/257 (Spillmann, 1959: fig. 19) preserves the ventralmost parts of the exoccipitals with the paroccipital processes that are long and project as far ventrally as the occipital condyles (131[0]). Medioventral to the paroccipital processes, the hypoglossal foramen is not opened to form a notch or incisure, but is well surrounded by bone (127[0]). The supracondylar fossae are distinct and define the occipital condyles across their entire width (123[1]).

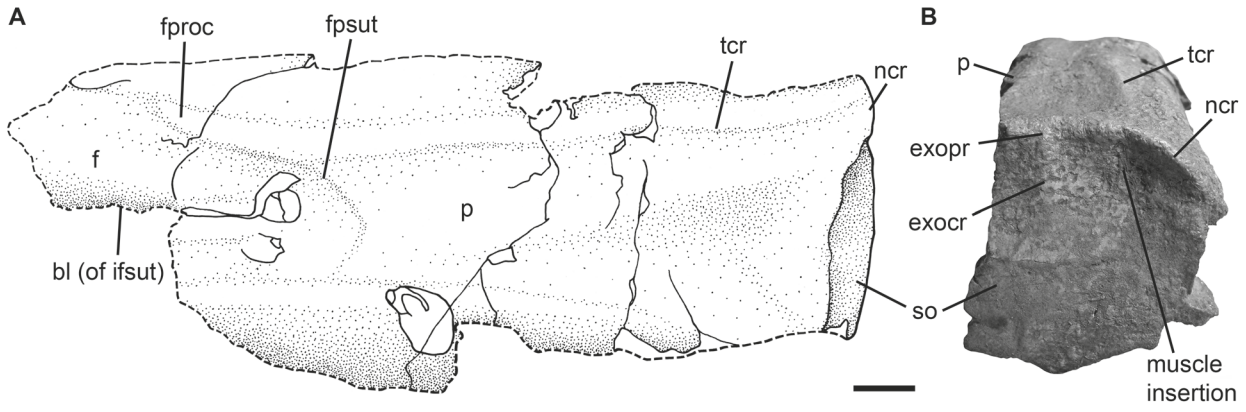

Figure 54. Parietal-supraoccipital skullcap of gen. nov. 3 *cristolii* (LI 1899/11, holotype of *"Halitherium" pergense*). **A**, drawing in dorsal view. **B**, photography in caudal view. White areas indicate either missing or reconstructed parts. Dashed lines pertain to broken parts. Scale bar equals 1 cm.

Basioccipital: An isolated basioccipital fused with the lower parts of the exoccipital is preserved in specimen LI 1939/257 (Spillmann, 1959: fig. 19). It contributes to the occipital condyles ventrolaterally and extends craniad as a short, columnar bone. On its ventral side, the sphenooccipital eminences for the *longus capitis* muscles are concave and separated by a short, but distinct ridge (128[0]). Specimens LI 1939/257 and LI 1926/394 (Fig. 52) that either preserve the basioccipital or basisphenoid show smoothed attachment areas for the adjacent bone indicating hat the basioccipital and basisphenoid were not fused. On that basis, both specimens can be determined as subadults.

Basisphenoid, presphenoid, orbitosphenoid: In specimen LI 1926/394, the sphenoidal region is well observable (Fig. 52). The basisphenoid has a flat ventral surface that is defined laterally by anteroposteriorly broad pterygoid processes. Cranially, the basisphenoid continues with a slight anterodorsal slope into the presphenoid. Both bones are firmly fused with each other and with the orbitosphenoid anterolaterally, the alisphenoid dorsolaterally and the pterygoid posterolaterally. The median crest of the presphenoid is not prominently developed, which might be related to the state of preservation of the skull in this area, and only becomes distinct at the level of the adjacent vomer. On the lateral side of the skull (Fig. 53B), the orbitosphenoid is exposed and contributes to the anterior medial wall of the temporal fossa. The orbitosphenoid is defined by the frontal dorsally, the alisphenoid posterodorsally and apparently by the maxilla ventrally. Its sutures with the palatine are not detectable.

Alisphenoid: The alisphenoid is well visible in lateral view of the skull (Fig. 53B). Its sutural contact to the frontal, parietal and squamosal can be clearly determined. Furthermore, the alisphenoid forms the slightly uneven posterolateral side of the pterygoid process. An alisphenoid canal is absent (132[1]) and the *foramen ovale* is opened to form a notch or incisure (133[1]).

Pterygoid: As in other sirenians, the pterygoid is present on the posteromedial side of the pterygoid process, but fully fused with the surrounding bones (Fig. 52). Though not well preserved in LI 1926/394, the wing-shaped pterygoid processes each bear a dorsoventrally long fossa posteriorly that extends above the level of the roof of the internal nares (134[0]). The distal ends of both pterygoid processes are somewhat damaged, but the distomedial angle of the right pterygoid process is still distinct and indicates a hamuli process (135[1]).

Palatine: Only the posteriormost parts of the palatines are preserved in LI 1926/394 and best observable on the right side (Fig. 52). There, the palatine forms the anteromedial margin of the pterygoid process. Its sutures with the surrounding bones are only hardly visible on the distal and medial sides of the pterygoid process and on the posterior side of the maxillary alveolar margin.

Maxilla: The zygomatic-orbital bridge (Fig. 52) is not completely preserved in any specimen. However, in the maxillary fragment of LI 1939/257 its dimensions are 47 mm in minimum length and 17.5 mm in nearly original height (Spillmann, 1959: fig. 20). On the basis of these data, the zygomatic-orbital bridge can be clearly determined to be long anteroposteriorly (22[0]). Additionally, it is only slightly elevated above the alveolar margin (21[1]) and its posterior end is thickened (23[0]; 24[1]). Remnants of the infraorbital canal reveal no obstruction (31[0]).

Squamosal: The cranial part of the squamosal (Figs. 51, 53B) extends up to the temporal crests (87[1]), but does not interrupt the course of the temporal crests so that these reach the occipital nuchal crest (88[0]). The posttympanic process is not clublike distally (Fig. 53B), but concave anteroventrally for the attachment of the sternomastoid muscle (108[0]; 109[0]). In posterior view of the skull (Fig. 53A), a prominent sigmoid ridge is visible forming the laterocaudal margin of the squamosal (99[1]; 100[1]). Posterolaterally, the mastoid foramen is present (110[1]), filled by the periotic and enclosed by the squamosal anteriorly, the exoccipital posteriorly, and the supraoccipital dorsally (111[0]).

Lateral to the skull (Figs. 51, 53B), each of the zygomatic processes projects from a zygomatic root that, though partially broken, is characterised by a distinct notch posteriorly (92[1]). The zygomatic process is triangular in shape tapering in anterior direction (89[1]). Its lateral and medial sides are flat to concave (90[0]) with the dorsal margin distinctly inclined inwards to form a sigmoid ridge (91[1]). The posterodorsal end of the zygomatic process is straight to concave (98[0]). The external auditory meatus is short mediolaterally (104[0]) and about as wide anteroposteriorly as high (106[1]). Ventrally (Fig. 52), the elements of the mandibular articulation surface are elongated transversely (93[0]). The mandibular fossa forms a distinct depression (94[1]) relative to the slightly convex *tuberculum* anteriorly (95[0]). Posterior to the mandibular fossa, the postglenoid process rises as a prominent knob (96[0]; 97[1]). The posterior end of the zygomatic process, the *processus retroversus*, shows a moderate inwards directed inflection (101[1]).

Jugal: Only a fragmentarily preserved middle part of the right jugal is known from specimen LI 1926/394 (Fig. 53B) indicating that a postorbital process is supposedly present (? 84[1]). Considering the position and shape of the supraorbital processes of the frontal the development of a postorbital bar can be excluded (85[0]). The zygomatic process of the jugal is not preserved, but according to its imprints on the ventral side of the zygomatic process of the squamosal, it reaches the *tuberculum* exceeding the diameter of the orbit (83[0]).

Ear region: In specimen LI 1926/394, the right periotic is poorly preserved (Figs. 52, 53A). It is not fused with the adjacent skull bones and set in a closely fitting socket in the squamosal (136[1]). The *tegmen tympani* is only indicated by its imprints on the dorsolateral side of

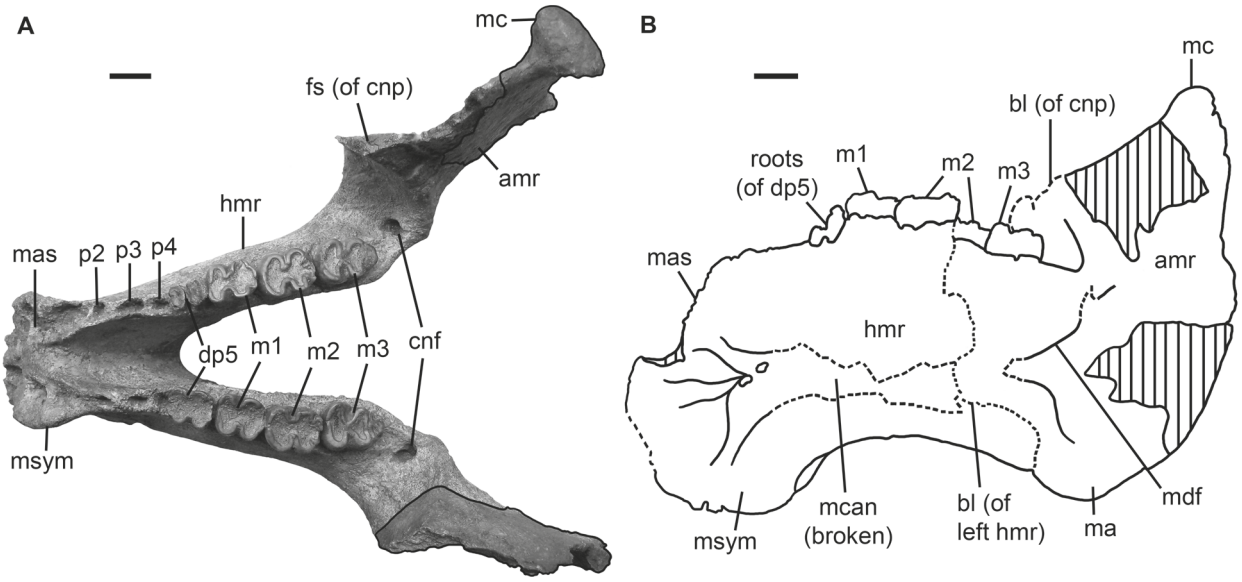

Figure 55. Mandibles of gen. nov. 3 *cristolii*. **A**, photography of LI 1939/257 (holotype of *"Halitherium" abeli*) in occlusal view. **B**, outline drawing of LI 2012/1 (lectotype) in left lateral view revealing information on the medial side of the right mandible. Dashed lines indicate broken parts. Both, framed (A) and shaded (B) areas, indicate either missing or reconstructed parts. Scale bars equal 2 cm.

the squamosal. It was most likely about as big as the mastoid or slightly smaller. The petrosal is fragmentarily preserved medioventrally with the perilymphatic foramen supposedly not separated into a *fenestra rotunda* and *cochlea caniculus*. The *processus fonticulus* fills the mastoid foramen posteriorly (Fig. 53A). The auditory ossicles are unknown.

Mandible: The mandibular symphysis is broad as is the masticating surface that is lacking a median furrow and houses four large and shallow alveoli for vestigial incisors and canines (137[1]); 138[1]; 139[0]). This is best visible in LI 1939/257 (Fig. 55A) that exhibits a completely preserved masticating surface, whereas in LI 2012/1 (Figs. 55B, 56A) the ventralmost end is broken. In lateral view (Fig. 56), the symphysis is higher than long (142[1]) and bears the mental foramen laterally (141[0]), which is joined dorsoposteriorly by two large accessory mental foramina on each side in specimen LI 1939/257 (140[0]; Fig. 56B). In the lectotype (LI 2012/1; Fig. 56A), the mental foramen is broken off dorsoposteriorly and therefore the single accessory mental foramina are not identifiable, but their open canals are merged with the main foramen. The overall build of the horizontal mandibular ramus appears to be broad dorsoventrally, but it is evaluated to be slender on the basis of its minimum dorsoventral height that is smaller than 0.25 x length of the mandible (156[0]). Its ventral border is strongly concave and not tangent to the angle posteriorly (146[1]; 147[1]). The ascending mandibular ramus is incomplete lacking most of the coronoid process, but still reveals a slight slope of it in anterior direction (151[1]). Posteriorly, the mandible is missing a distinct *processus angularis superior* and rather

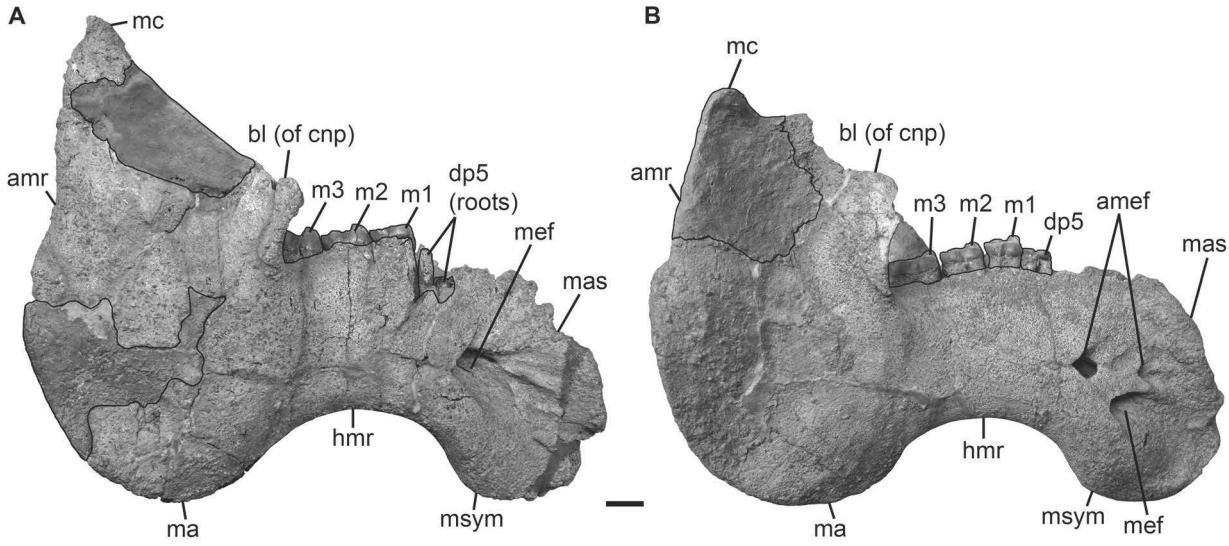

Figure 56. Mandibles of gen. nov. 3 *cristolii* in right lateral views. **A**, LI 2012/1 (lectotype). **B**, LI 1939/257 (holotype of *"Halitherium" abeli*). Framed areas of the ascending mandibular rami (amr) indicate either missing or reconstructed parts. Scale bar equals 2 cm.

has a broadly convex outline (149[1]). The mandibular condyle is well preserved in both specimens with an articulation surface of even elliptical outline in a mediolateral axis (148[0]). In LI 1939/257 (Fig. 55A), the condyle is partially covered by plaster today, but it is originally preserved as is also stated by Spillmann (1959: 44, fig. 25). Behind m3 at the basis of the ascending ramus (Fig. 55A), the coronoid foramen is enlarged and varies between 7.5 mm and 9.5 mm in maximum diameters (153[1]). In medial view (Fig. 55B), a single and undivided mandibular foramen (154[0]) reveals the dental capsule of m3 to be exposed posteroventrally (155[1]).

Dentition: The premaxilla and anterior part of the maxilla are missing and therefore no conclusion on the absence or presence of incisor tusks can be drawn. However, the complete lower tooth arcade is preserved in two mandibles, one of which representing the lectotype (LI 2012/1). Accordingly, the dental formula in the lower jaw is determined to be i0, c0, p2–4, dp5, m1–3. Considering the logical occlusion pattern and the conditions in similarly derived sirenians, the second and third upper incisors are considered to be absent as are the upper canines (164[1]; 166[1]) while the permanent premolars P2–4 and the persistent DP5 are present (167[1]; 168[0]; 169[0]; 170[0]). Consequently, the lifetime dental formula in the upper jaw is estimated to have been most likely ?I1, C0, P2–4, DP5, M1–3 (180[0]; 181[0]).

Upper dentition: Besides the paralectotypes LI 2012/2 and LI 2012/3, only two specimens have upper teeth or parts of these preserved. For example, LI 1939/257 preserves a right maxillary fragment exhibiting the broken crowns and roots from M1–3, DP5, P4, P3, and most likely also P2 (Spillmann, 1959: fig. 20). The permanent premolars are single-

rooted (173[1]) and DP5 is three-rooted, as is characteristic for a molariform premolar that remains unreplaced (171[0]).

The skull of specimen LI 1926/394 reveals M1–3 from the right tooth arcade, the left M3, and the roots of the left M1–2, and therefore is the principal reference for the following description (Figs. 52, 57). The molars are three-rooted, not reduced in size relative to the skull (182[0]) and have well developed enamel of about 2 mm thickness in average.

Mesiolabially, the right M1 is broken where the anterior *cingulum* might have been present, but it can be clearly identified as the smallest molar. M1 is strongly worn in LI 1926/394 as is the paralectotype LI 2012/2 preventing any description of its cusp pattern except for the presence of two transverse lophs, a supposedly deep central valley and the *postcingulum*. The crown of M1 is heart-shaped in outline as that of the slightly larger M2.

The right M2 (Fig. 57) is moderately worn and has distinct *pre-* and *postcingula* that attach to the two main transverse lophs mesio- and distolingually and open labially by decreasing in height. The anterior and posterior basin each represents a deep furrow of similar size. Centrally, a deep transverse valley separates the protoloph from the metaloph, but without being obstructed by the metaconule (179[0]). The protoloph bears a continuous wear surface connecting the paracone labially, the protoconule centrally and the protocone lingually, which each are still discernable as single cusps. The metaloph is slightly less worn and reveals the nearly transverse row consistent of metacone and hypocone from labial (or buccal) to lingual with the metaconule in between only very slightly shifted anterad (178[0]). Despite tooth wear, these posterior cusps still can be clearly distinguished from each other.

The right upper M3 is well preserved in specimen LI 1926/394 and only slightly worn (Fig. 57). This stands in contrast to the state of preservation of the paralectotype LI 2012/3, an isolated right M3 that shows a strongly worn protoloph and is broken distolingually. However, both teeth resemble in shape and are also similar in their preserved morphology. The M3 is larger than M2 with its crown in the shape of an elongated heart due to the distal metaloph being transversally shorter than the mesial protoloph. Proto- and metaloph are each characteristically composed of three cusps. Accessory cusps or cuspules are not present. The main cusps of the protoloph form a transverse row and are clearly separated and distinct from each other. Lingually, the protocone represents the largest and highest cusp followed in labial direction by the smaller protoconule and paracone, both of about the same size. A cuspid *precingulum* is at-

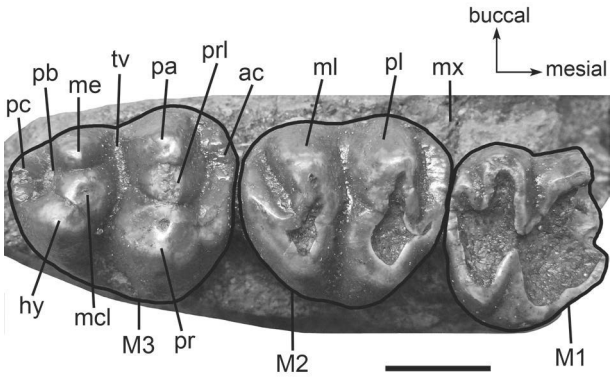

Figure 57. The right upper molars M1–M3 of gen. nov. 3 *cristolii* (LI 1926/394) in occlusal view. Scale bar equals 1 cm.

tached mesiolingual to the protocone and opens labially by decreasing in height. The anterior basin forms a deep furrow. Proto- and metaloph are separated by a distinct transverse valley that is somewhat obstructed, but not closed by the slightly anterad shifted metaconule. The hypocone is slightly larger than the subequally sized metaconule and metacone, and closely spaced with the metaconule, but still separated from it by a distinct furrow (177[1]). The posterior basin is large and deep enclosed by two cingular cusps (175[1]) that form the *postcingulum*, which is connected to the hypocone lingually and open labially.

Lower dentition: Two specimens of approximately the same age or state of tooth wear reveal the lower dentition. Mandible LI 1939/257 preserves both tooth arcades (Fig. 55A) and the lectotype specimen LI 2012/1 has only the right arcade complete while the left one is broken behind m2 (Figs. 55B, 56A). The masticating surface of the mandibular symphysis (Fig. 55A) bears four large and irregularly rounded alveoli that are not very deep and may have housed three pairs of vestigial incisors and one pair of vestigial canines. The teeth themselves are not known as are the permanent premolars p2–4, for which separated and deep alveoli of clear outline are present in both specimens (173[0]). A further alveolus is present at the junction between the masticating surfaces of the horizontal mandibular ramus and the mandibular symphysis. It resembles in size and outline the alveoli for the vestigial lower incisors and canines and is interpreted here to may have housed a vestigial p1, which is not replaced at this locus. The paired roots of dp5 are preserved in both mandibles, but in specimen LI 1939/257 (Fig. 55A), though heavily worn, the left crown is present indicating a molariform tooth (171[0]). Its protolophid and hypolophid have about the same transversal length.

Molars m1–3 are preserved in both specimens and characterised by having two roots and mesiodistally elongated crowns that slightly increase in size from anterior to posterior within the tooth arcade (Fig. 55A). All crowns are moderately to strongly worn preventing most details on their cusp pattern except for the two main transverse lophs that are separated by a deep transverse valley. The protolophid and hypolophid are nearly perpendicular to the longitudinal axis of the tooth arcade. In the lectotype specimen, m2 and m3 are slightly less worn than in specimen LI 1939/257 and reveal the transverse valley to be obstructed by an accessory cuspule that is connected to the hypoconid mesiointernally. This might have been also the case on m1, however, which is too heavily worn to draw unambiguous conclusions. While the protolophid is about as large transversally as the hypolophid on m1, the hypolophid decreases in size from m2 onwards and becomes distinctly shorter on m3. Additionally, the bicuspid morphology of the protolophid and hypolophid is still discernable on m3. This becomes more obvious in a nearly unworn isolated m3 (LI 2012/6) from the left side (Abel, 1904: pl. 1: fig. 13). There, the metaconid forms a prominent lingual cusp that is slightly larger than the protoconid on the labial side. On the hypolophid, the entoconid is about as large as the hypoconid. Also

the isolated m3 (LI 2012/6) reveals a mesiointernal accessory cuspule of the hypoconid. A *precingulum* is not detectable on any molar. The hypoconulid lophule distally is composed of two cusps in LI 2012/1 that are roughly observable also in LI 1939/257 (Fig. 55A). Specimen LI 2012/6 shows two additional cuspules between the two cusps that might be no more observable in the former two specimens due to wear.

Hyoid apparatus: Not preserved in any specimen.

Vertebral column: The vertebral column is only incompletely known by a few cervicals, several thoracics, some lumbars, and caudals. Most of the vertebral remains are associated with two partial skeletons, LI 1854/327 and LI 2013/1. The ribs and vertebrae of specimen LI 2013/1 are lost today and only documented in Spillmann (1959: fig. 2). Otherwise, the vertebrae are only known by fragments as also indicated by Spillmann (1959), but these also seem to be no more available in the collections of the Oberösterreichisches Landesmuseum Linz. Relative correlation to a position within the column is partly possible.

Cervicals: The atlas is almost completely preserved in specimen LI 1939/257. Both cranial articular facets are well defined and form concave and kidney-shaped areas for the articulation with the occipital condyles. The caudal articular facets are slightly flatter and have a rounded outline without the large dorsoventral extension as is in their cranial counterparts. The lateral margins of the articular facets flare out so that the articular surfaces are somewhat directed medially into direction of the vertebral canal. The vertebral foramen is large, occupying the centre of the atlas, and partially obstructed about half its height by a small bony knob on the right side. This knob certainly was present also on the left side, but it is no more preserved and this area is replaced by plaster now. The neural arch is a low ridge with a small triangular surface anterodorsally that possesses a narrow and low median keel about 10 mm long. The anterior surface slightly rises in dorsocaudal direction whereas dorsocaudally the neural arch is not inclined, but forms a smooth and rounded ridge.

Laterally, the atlas shows caudad projecting aliform transverse processes, the left one broken to its base. Ventral and medial to the transverse processes, the *foramen transversarium* is located measuring about 2 mm in diameter. The vertebral foramen is defined ventrally by a bony bridge about 10 mm long anteroposteriorly and missing the caudad projecting articulation surface for the second cervical, the area of which is replaced by plaster now.

Specimen LI 1939/257 and LI 1854/327 preserve a further vertebra from the cervical series, the latter only observable in caudal view and missing the transverse and caudal articular processes. Both vertebrae represent elements commencing C3–7, but their exact position within the cervical column cannot be determined. Both centra are short anteroventrally and form the flat basis of the vertebral foramen that is overall rounded, but slightly peaked dorsally. Dorsal to the centra, the neural arch is preserved with the

neural spine rising straight up and having a slight keel cranially and a somewhat concave surface caudally.

In specimen LI 1939/257, the cranial and caudal epiphyses are more or less equal in size, but flat to concave cranially and slightly convex caudally. Lateral to the centrum, wing-shaped transverse processes are present, the right one broken to its base. The left transverse process extends laterad with a slight slope in caudal and ventral directions. The rear side of the process is flat to slightly concave. In cranial view, the prezygapophyses are flat dorsally and directed anterolaterad. In caudal view, the right postzygapophysis is present dorsal to the transverse process at a somewhat higher level than the prezygapophyses. Though the posterior tip is broken, it can be clearly determined that the articular facet for the adjacent cervical is directed ventrad and posteromediad.

Thoracics: Both partial skeletons, LI 1854/327 and LI 2013/1, preserve thoracic vertebrae. Their morphology does not importantly differ from that of gen. nov. 2 spec. nov. 1 and gen. nov. 2 *bronni* and, therefore, the description is generalised in the following.

The thoracic centra represent compact elements characterised by a roughly heart-shaped outline that is caused by a more or less pronounced ventral crest and a shallow longitudinal depression dorsally. Dorsolaterally, the centra show deeply concave cranial and caudal articular facets for the *capitulum* of the corresponding ribs while the remaining lateral surface is flat to slightly concave. The cranial and caudal extremities are flat and always wider than high. Lateral to the base of the neural arch, the transverse processes originate as very short and wedge-shaped elements with a slight dorsad slope. In ventral view, the transverse processes bear the rounded articular facets for the *tuberculum* of the corresponding ribs. The mammillary processes form prominent knobs on the cranial sides of the transverse processes. Dorsal to the rounded and keyhole-shaped vertebral foramen, the cranial and caudal zygapophyses are present with the former flattened dorsally and the latter flattened ventrally. The preserved neural spines are about as long anteroposteriorly as the centra they are belonging to and rise straight up with their lateral surfaces keeled cranially and cleaved caudally. The summit of the neural spine bears a tuberosity. Vascular canals can be variably present on the vertebrae, especially on the ventrolateral and dorsal surfaces of the centra.

Lumbars: Specimen LI 1854/327 reveals a single centrum including the transverse processes and is assigned to the lumbar region. This vertebra is only observable in cranial view. The vertebral body represents a massive element with an oval outline being wider than high. Its lateral and ventral surfaces are flat and the cranial epiphysis is slightly concave. The neural arch is not preserved. Though partially broken on the left side, the transverse processes are long mediolaterally and attach with craniocaudally broad bases lateral to the mid-section of the centrum. In cranial view, they extend more or less horizontally and show only a slight ventrocaudad inclination. The dorsal and ventral surfaces of the transverse processes are smooth and terminate in narrow and blunt distal ends.

Therefore, this vertebra is not considered to represent a sacral vertebra as it supposedly did not serve for the attachment of the pelvic tendons, but has to be assigned to the presacral lumbars. Its exact position within the lumbar segment remains, however, uncertain.

Caudals: Some caudal vertebrae have been present in the partial skeleton LI 2013/1 with certainty, which is the only reliable information up to now. As mentioned above, this specimen is no more available in the LI collections. Additionally, the caudals are only recorded in Spillmann (1959), but neither described in detail nor illustrated except for the schematic documentation of the find situation of the respective specimen, which, however, only barely reflects on these elements.

Chevrons: Not known in any specimen assignable to gen. nov. 3 *cristolii*.

Ribs: Abundant rib fragments are known, but the two partial skeletons LI 1854/327 and LI 2013/1 (now lost) provide several complete ribs. Most elements are known from specimen LI 1854/327, which preserves 34 ribs and rib fragments. However, none of these specimens preserve the first rib. Additonally, specimen LI 1854/327 is reconstructed in the original find situation and, therefore, no measurements could be taken from the preserved ribs. Nonetheless, the ribs can be clearly determined to have an elliptical cross section (197[0]) forming long, slightly arching elements composed of compact bone tissue. They do not differ from the formerly described ribs of gen. nov. 2 spec. nov. 1 and gen. nov. 2 *bronni* and, therefore, reference are given to these taxa.

Sternum: Two sternal fragments are preserved, LI 2012/5 (Fig. 58C) and LI 1948/33. Specimen LI 1948/33 was found in 1944 as was the partial skeleton LI 2013/1. However, it is not certain if both belong to a single specimen, which is also indicated by a separate collection number for the sternal part. Therefore, LI 2013/1 and LI 1948/33 are treated here as two different specimens.

Specimen LI 2012/5 measures 84 mm in maximum length and 65 mm in maximum width and is the smallest of both sternal fragments, but also the best preserved one (Fig. 58C). Abel (1904: 36) identifies that element to belong to the *“processus ensiformis”* of the xiphisternum. This part of the sternum, however, bears no facets for the attachment of the ribs. Spillmann (1959) considered it to be part of the corpus. Here, this element and also LI 1948/33 are considered to represent the anterior parts of the manubrium (200[0]). The manubrium has smooth dorsal and ventral surfaces, the former slightly convex and the latter slightly concave. A ventral keel is not present (202[0]). In caudal direction the manubrium slightly widens while anteriorly, a blunt process is present (201[1]). The lateral margins are thickened anteriorly, each characterised by originally three articulation facets for the attachment of the anteriormost ribs. The lateral margins become thinner caudally forming sharp edges.

Scapula: Three scapular remains were described by Spillmann (1959), one of which re-

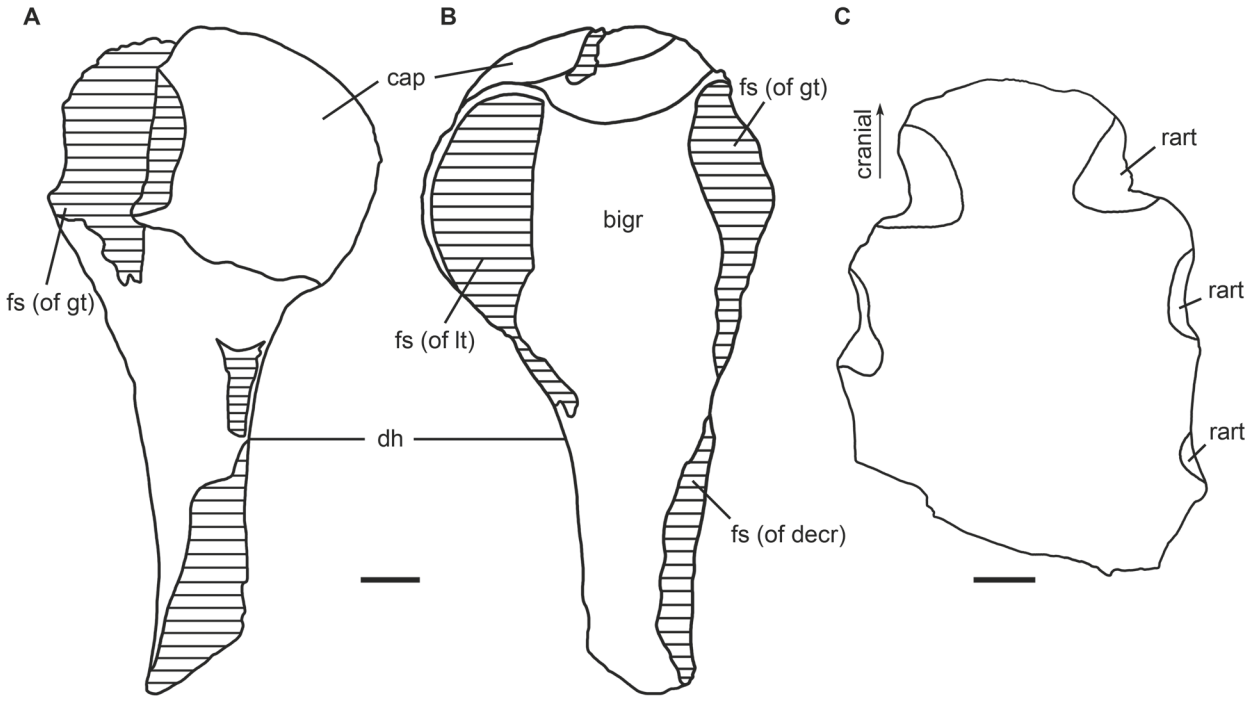

Figure 58. Outline drawings of the left humerus LI 2012/4 and the manubrium LI 2012/5 of gen. nov. 3 *cristolii*. **A**, humerus in posterior view. **B**, humerus in anterior view. **C**, manubrium of sternum in ventral view. Shaded areas indicate missing parts. Scale bars equal 1 cm.

presenting the distal two thirds of the left element (LI 1854/327; Fig. 59). Additionally, the partial skeleton LI 2013/1 preserves parts of the left scapular blade. The right element of LI 2013/1 was originally present (Spillmann, 1959), but is now lost.

The scapular blade is sickle-shaped (187[0]) defined by the *margo cranialis* anteriorly, the *margo dorsalis* proximally and the *margo caudalis* posteriorly. The anterior margin steeply rises craniodorsad with an angle of about 50° from the *collum scapulae*, i.e. the scapular neck, and turns nearly rectangular to run more or less straight dorsad for about 100 mm. Specimen LI 1854/327 is broken at this level (Fig. 59), but the left scapula of LI 2013/1 (Spillmann, 1959: fig. 31) preserves the proximal end that shows a dorsocaudal slope of about 45° into the *margo dorsalis*. The latter extends approximately 100 mm almost parallel to the vertebral column and, finally, forms an angle of about 90° with the *margo caudalis*. The posterior margin is largely convex cranially and converges distad together with the *margo cranialis* to form the long and slender *collum* of about 50 mm in dorsoventral length, which is best visible in LI 1854/327 (Fig. 59).

The external surface (Fig. 59A) is separated by the scapular spine into a large and shallow supraspinous fossa and a narrow and more concave infraspinous fossa (186[1]). The scapular spine forms a rounded flange without a proximal rugosity (183[1]) and does not exceed half the length of the scapular blade (184[1]). It starts with a broad basis at about the middle portion of the blade, and rises slightly, but steadily towards its distal end. The spine becomes narrower in distal direction by sloping slightly caudad and, finally,

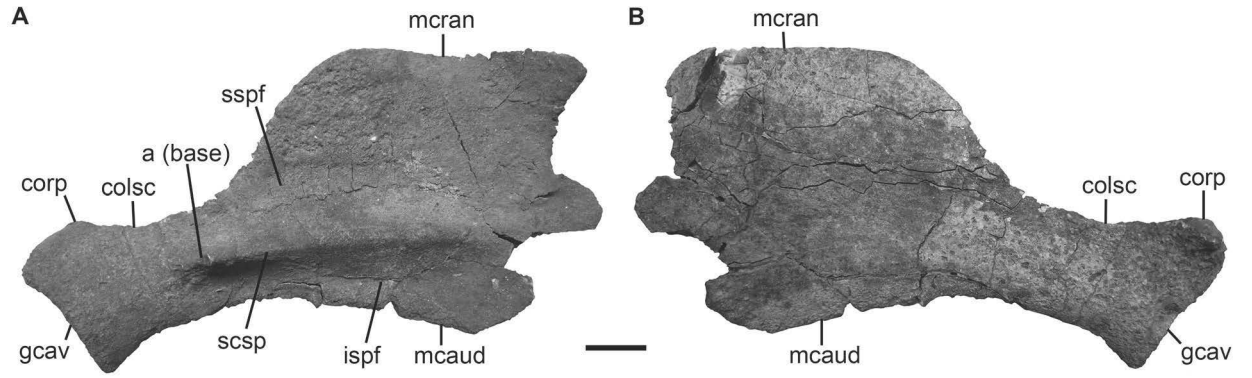

Figure 59. Left scapula gen. nov. 3 *cristolii* (LI 1854/327). **A**, in lateral view. **B**, in medial view. Scale bar equals 2 cm.

enters into the acromion. Although, the acromion is broken in all specimens, it can be clearly stated that it does not exceed the level of the glenoid cavity (188[0]). The coracoid process is moderately developed (185[0]), inclined medially and does not disjunct from the anterior apex of the articular glenoid (Fig. 59B). The glenoid cavity is shallow and oval-shaped, narrower mediolaterally and wider anteroposteriorly, about 25 mm x 48 mm in LI 1854/327. Medially (Fig. 59B), the costal surface is overall flat and smooth, only slightly convex in its central part according to the curvature of the ribs.

Humerus: Two single fragments of the left humerus from different individuals are known. Specimen LI 2012/4 represents a left proximal half of 115 mm length in its maximum dimensions (Fig. 58A, B) and specimen LI 2013/1 preserves a distal fragment that was excavated together with the partial skeleton in 1944.

Although incompletely preserved, the humerus is identified to be compact having distinctly developed epiphyses (189[1]). The diaphysis forms a strong shaft, but it is broken in both specimens and preserves only remnants of the deltoid crest anteriorly in LI 2012/4 (Fig. 58B). The humerus head is rounded and separated by a deep furrow from the lesser tubercle. Both, the lesser and greater tubercle are broken. The bicipital groove is deep and wide serving for the attachment of the biceps muscle. On the distal fragment (Spillmann, 1959: fig. 32), the lateral and medial epicondyles are barely preserved. However, the trochlea can be identified as a sandglass-shaped and smooth articulation surface for the radius and ulna. Its inclination relative to the shaft appears to be perpendicular, but cannot be determined without doubt due to the incomplete state of preservation.

Remarks

Taxonomic remarks: Taxon gen. nov. 3 *cristolii* is well defined basal to the crown group (see chapter “Phylogenetic analyses”). This species is only known from the Linz Basin (Fig. 60) and was described as *“Halitherium” cristolii* by Fitzinger (1842), Abel (1904) and Spillmann (1959). Toula (1899) erected a new species for a sirenian find from Perg in Upper

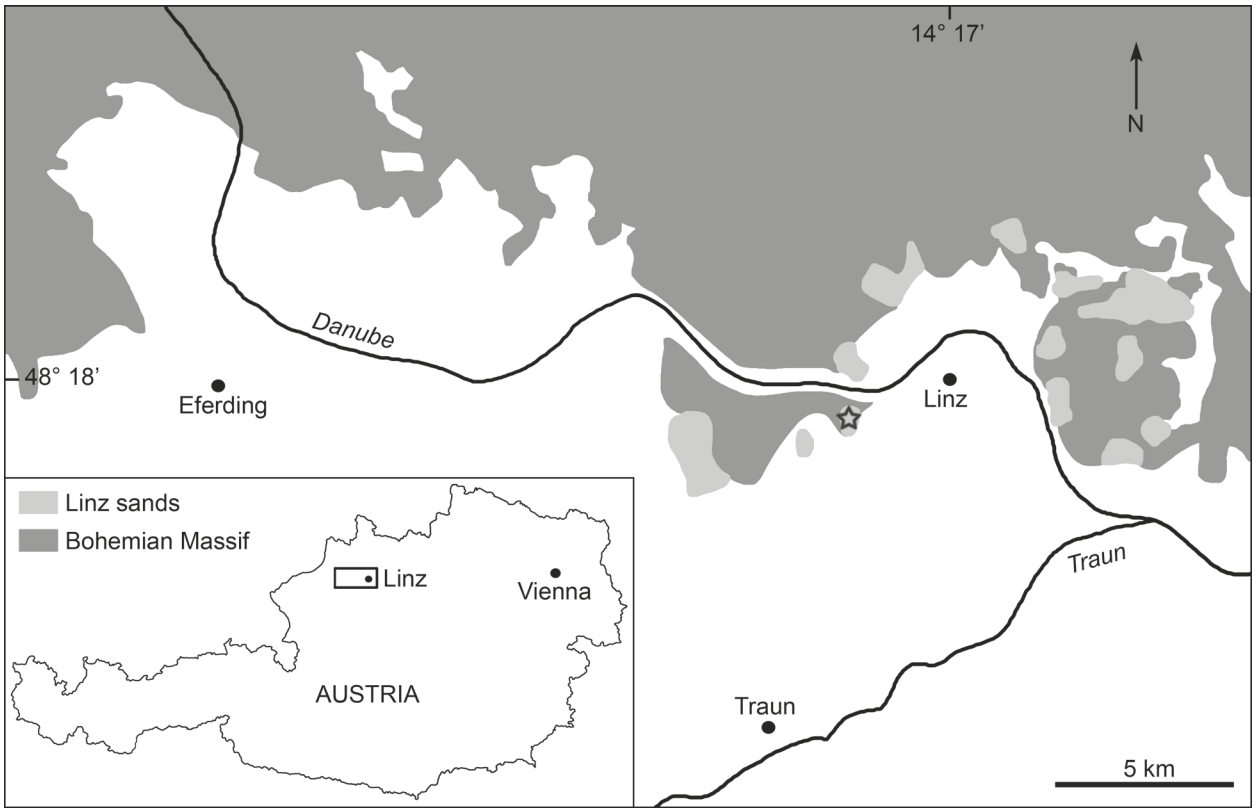

Figure 60. Geographic and geologic overview of the location of Linz, Upper Austria (modified after Spillmann, 1959 and Faupl & Roetzel, 1990). Asterisk indicates estimated locality of species gen. nov. 3 *cristolii*.

Austria supposedly belonging to *Metaxytherium*, *M. pergense*, which Spillmann (1959) confirmed and re-named into *"Halitherium" pergense*. Furthermore, Spillmann (1959) established the new species *"Halitherium" abeli* for some skeletal finds from the Linz area. Both taxa were subjectively synonymised under *"H." cristolii* by Domning (1996). This seems to be well supported, because the sirenian material from the Linz Basin does not yield such morphological differences that would suggest the presence of different morphospecies as is the case for example in the Mainz Basin. However, this synonymy has not proven until today. Therefore, the three species last hypothesised by Spillmann (1959) were treated independently in the cladistic analyses first in order to gain a largely objective basis for the splitting or lumping of taxa. As will be discussed later in this thesis, the cladistic analyses based on individuals reveal no morphological differences on the species level supporting the presence of a single taxon, gen. nov. 3 *cristolii*.

Geological and palaeogeographical remarks: The synonymy of the sirenian species *pergense* and *abeli* with gen. nov. 3 *cristolii* that was already stated by Domning (1996) is well justified also by geological and biostratigraphical data. The area around Linz (Fig. 60) is geologically situated in the Molasse Zone of Upper Austria between the crystalline basement of the Bohemian Massif in the north and the main overthrust of the

Alpine orogenic front in the south (e.g., Peschel, 1982; Steininger *et al*., 1996; De Ruig & Hubbard, 2006). It forms part of the North Alpine foreland basin (NAFB) and is a classical asymmetric foredeep that was formed as a result of the collision between the Apulian continental microplate and the North European craton (De Ruig & Hubbard, 2006; Steininger *et al*., 1996). The Molasse Basin in Upper Austria contains a thick succession of Oligocene to early Miocene deposits. In the Egerian, significant amounts of well sorted, shallow-marine and deltaic sands derived from the Bohemian Massif (Peschel, 1982) were deposited along the northern margin of the eastern NAFB (Papp *et al*., 1978), where they were tidally reworked (Kuhlemann & Kempf, 2002). These sands are known as the "Linzer Sande" and "Melker Sande" of the Linz-Melk Formation (Rupp, 2008: 56). At the same time, the deep-marine Puchkirchen Formation was accumulated in the southern margin of the NAFB at the active front of the rising Alps (e.g., Rötzel *et al*., 1983; De Ruig & Hubbard, 2006; Rupp, 2008).

The beach facies of the Puchkirchen Formation in the area around Linz, the Linz sands, yielded the skeletal finds now assigned to gen. nov. 3 *cristolii* (Fig. 60). These sediments reach a thickness of 50 m on average and consist of white, predominantly fine-grained and very mature quartz sands interrupted by local, fluviatile remodelled sediments often characterised by cross-bedded gravels (Peschel, 1982). An up to date geological and stratigraphical overview of the Linz area is provided by Kuhlemann & Kempf (2002) and Piller *et al.* (2004), for example, who consider the new division of the Upper Oligocene and Miocene of the Austrian Paratethys following Papp *et al.* (1968). According to these studies, the Egerian comprises the Chattian and Aquitanian of the German Molasse, and the Puchkirchen Formation is subdivided into a lower, Chattian, and an upper, Aquitanian, part (e.g., Kuhlemann & Kempf, 2002; Hubbard *et al*., 2005; De Ruig & Hubbard, 2006). The Linz sands that facially and stratigraphically correspond to the Melk sands of Lower Austria (Papp *et al*., 1978; Rötzel *et al*., 1983) are considered to belong to the lower Puchkirchen Formation and are of upper Oligocene (Chattian) age (Papp *et al*., 1968). The stratigraphic assignment of the Linz sands is supported for example by Grill (1935) and Rögl & Steininger (1969), who already stated a Chattian mollusc fauna in the Linz sands of the Gallneukirchen Basin. Sickenberg (1934b) and Thenius (1960) dated the Linz sands at Chattian in age on the basis of the faunal assemblages of terrestrial mammals. With the find of the larger foraminifera *Miogypsina formosensis* in Plesching near Linz the microfossil evidence for the Chattian type from Astrup and Doberg (northern Germany), and Eger (Hungary) was delivered (Rögl & Steininger, 1969).

Notwithstanding the uniformly reported Chattian age of the Linz sands, Spillmann (1959) justified the erection of three different sirenian species in the Linz Basin on the basis of different discovery localities and beach terraces. However, the assessment of Spillmann's (1959) careful review of the history of the discovery of the single sirenian finds does not corroborate his conclusions. According to Spillmann (1959), all specimens

assigned to *"H." cristolii* mainly come from three very closely spaced sand quarries near Linz. This information also corresponds to the records of Fitzinger (1842) on the sand quarries present around 1840. *"Halitherium" abeli* is known from another sand quarry, the "Lemonikeller" (Spillmann, 1959: 5), which however is only 400 m away from the find locality of *"H." cristolii*. The only known sirenian find outside Linz is a single skullcap and natural endocranial cast from Perg, *"H." pergense* (Toula, 1899), located about 30 km westwards from Linz. In the area around Perg the Linz sands are modified to a crystalline sandstone (Fuchs & Thiele, 1987). These sandstones have been already correlated with the Linz sands and, accordingly, are considered to be of Chattian age too (Grill, 1935).

In conclusion, all sirenian specimens from the Linz Basin can be correlated to Egerian (upper Oligocene) sediments and represent a single species.

Suborder nov. 1

Included genera: Bharatisiren Bajpai & Domning, 1997; *Corystosiren* Domning, 1990; *Crenatosiren* Reinhart, 1959; *Dioplotherium* Cope, 1883; *Domningia* Thewissen & Bajpai, 2009; *Dugong* Lacépède, 1799; *Kutchisiren* Bajpai *et al.,* 2010; *Nanosiren* Domning & Aguilera, 2008; *Rytiodus* Lartet, 1866; *Xenosiren* Domning, 1989b; gen. nov. 4.

Stratigraphical range: Latest Oligocene – recent.

Geographical range: India, Mexico, Venezuela, USA, France, Italy, Indo-Pacific (sub-) tropical regions.

Diagnosis: The monophyly of the new suborder is strongly supported by all of the various analyses conducted in this study and defined by five synapomorphies: frontal roof deeply concave or depressed overall (with or without a small median convexity) between temporal crests, but not sloping ventrad anteriorly; frontal roof bears a bilateral pair of knoblike bosses, more or less cylindrical in shape and directed anterad, or at least a distinct longitudinal ridge or swelling medial and parallel to, and distinct from, each temporal crest; preorbital process of jugal thick and robust (breadth ≤ thickness); ventral rim of orbit does distinctly overhang; and the *processus retroversus* is strongly inflected. Additionally, this clade is characterised by the absence of second and third upper incisors, canines, and permanent premolars.

Character states: 50[1]*; 53[1]*; 77[1]*; 86[1]*; 102[1]*; 164[1]; 166–170[1]; 171[0]; 172[1]; 173[0]; (* = synapomorphy).

Family nov. 1

Type genus: Nanosiren Domning & Aguilera, 2008.

Included genera: Only *Nanosiren* Domning & Aguilera, 2008.

Stratigraphical range: Early Miocene to early Pliocene.

Geographical range: Western Atlantic Ocean, Caribbean Sea, Gulf of Mexico, and possibly eastern Pacific Ocean.

Diagnosis: Represents a group of small sirenian species that is characterised by the combination of the following features: frontal roof deeply concave with a bilateral pair of knoblike bosses; maximum intertemporal constriction at centre of skull roof; internal sagittal crest keeping its height along the length of parietal; preorbital process of jugal thick and robust; ventral rim of orbit distinctly overhanging; *processus retroversus* strongly inflected; paroccipital process of exoccipital long, reaching as far ventrally as occipital condyle; and depth of I1 alveolus distinctly less than half the length of premaxillary symphysis.

Character states: 50[1]; 53[1]; 55[1]; 68[1]; 77[1]; 86[1]; 102[1]; 131[0]; 157[0].

Differential diagnosis: Differs from *Crenatosiren* in that the zygomatic-orbital bridge is shortened; the exoccipitals do not meet in a suture dorsal to *foramen magnum*; the hypoglossal foramen is replaced by a groove or forms a notch; and the I1 is smaller.

Differs from the Dugongidae in lacking the following synapomorphies: first upper incisor (I1) with enamel mainly on medial side; and I1 with enamel extending entire length of tusk. Distinguished from all stem group sirenians in having a deeply concave frontal roof that bears a bilateral pair of knoblike bosses; a thickened and robust preorbital process of jugal; a distinctly overhanging ventral rim of orbit; and a strongly inflected *processus retroversus*.

Dugongidae Gray, 1821

Type genus: Dugong Lacépède, 1799.

Included genera: Bharatisiren Bajpai & Domning, 1997; *Corystosiren* Domning, 1990; *Dioplotherium* Cope, 1883; *Domningia* Thewissen & Bajpai, 2009; *Dugong* Lacépède, 1799; *Kutchisiren* Bajpai *et al.*, 2010; *Rytiodus* Lartet, 1866; *Xenosiren* Domning, 1989b; gen. nov. 4.

Stratigraphical range: Late Oligocene – recent.

Geographical range: India, Mexico, USA, France, Italy, Indo-Pacific (sub-) tropical regions.

Emended diagnosis: Sirenians that possess the following characters: anteroventralmost maxillopremaxillary suture perpendicular to posterior end of symphysis; ventral extremity of jugal lies ventral to orbit; sphenooccipital eminences convex; I1 alveolus extends more

than half the length of the symphysis; first upper incisor (I1) with enamel mainly on medial side; and I1 with enamel extending entire length of tusk.

Character states: 7[1]; 82[1]; 128[1]; 159[1]; 160[1]*; 165[1]*; (* = synapomorphy).

Differential diagnosis: Differs from all other sirenians in having the unique characters of a first upper incisor (I1) with enamel mainly on medial side; and enamel extends along entire length of I1 tusk.

Dugonginae (Gray, 1821) Simpson, 1932a

Type genus: Dugong Lacépède, 1799.

Included genera: Only *Dugong* Lacépède, 1799.

Stratigraphical range: Recent.

Geographical range: Indo-Pacific (sub-)tropical region from the western Pacific islands to the Red Sea.

Emended diagnosis: Sirenians characterised by the following combination of features: mesorostral fossa indented anteriorly; palate more than 1 cm thick at level of penultimate cheek tooth; presence of internasal process of frontal; supraorbital process of frontal devided by one or more distinct, deep dorsoventral grooves indenting its lateral margin; prominent posterolateral corner of supraorbital process of frontal; frontal about as long as parietal in midline; contact between jugal and premaxilla; external occipital protuberance weakly developed; external occipital crest broad and undefined; mental foramen not at level of mandibular symphysis, but far back caudally; M2 without an approximately transversally directed hypocone and metaconule.

Character states: 11[0]; 32[1]; 43[1]; 46[1]; 49[0]; 67[1]; 78[1]; 116[0]; 118[1]; 141[1]; 178[1].

Differential diagnosis: Distinguished from Rytiodontinae in lacking the synapomorphic character of a supraorbital process of frontal that is turned markedly downward, with its dorsal surface inclined strongly ventrolaterad. Differs from all other sirenians in possessing a first upper incisor (I1) with enamel mainly on medial side and enamel extending along entire length of I1 tusk.

Rytiodontinae Abel, 1914

Type genus: Rytiodus Lartet, 1866.

Included genera: Bharatisiren Bajpai & Domning, 1997; *Corystosiren* Domning, 1990;

Dioplotherium Cope, 1883; *Domningia* Thewissen & Bajpai, 2009; *Kutchisiren* Bajpai *et al.*, 2010; *Rytiodus* Lartet, 1866; *Xenosiren* Domning, 1989b; gen. nov. 4.

Stratigraphical range: Late Oligocene – early Pliocene.

Geographical range: Kachchh (= Kutch, India), Yucatan and Baja California Sur (Mexico), California (USA), France, Italy.

Emended diagnosis: Represents a group of derived sirenians lacking a thin nasal process that tapers at its posterior end and has lengthy overlap with frontal and/ or nasal. The supraorbital process of frontal is turned markedly downward, with its dorsal surface inclined strongly ventrolaterad. Concavity of frontal roof not overall between the temporal crests, but increasing to anterior margin by sloping steadily ventrad. Frontal processes of parietal long, extend half the length of interfrontal. Ventral rim of orbit does distinctly overhang. *Processus retroversus* moderately inflected. Cross section of I1 crown is not suboval or subelliptical. M3 with small posterior basin enclosed by a single cusp or ridge only.

Character states: 17[1]; 45[1]*; 50[0]; 51[1]; 63[1]; 88[0]; 101[1]; 161[1]; 174[0]; (* = synapomorphy).

Differential diagnosis: Differs from all other sirenians in possessing the synapomorphy of a supraorbital process of frontal that is turned markedly downward, with its dorsal surface inclined strongly ventrolaterad.

Genus nov. 4

Type species: Halitherium bellunense (De Zigno, 1875).

Included species: Gen. nov. 4 *bellunense.*

Generic diagnosis: Sirenian having the combination of the following characters: angle of rostrum great, about 60°; nasal process of premaxilla broadened and bulbous at posterior end, having more or less vertical joint surface in contact with frontal; zygomatic-orbital bridge of maxilla shortened and thickened posteriorly, but not transformed into vertical wall; frontal roof more or less flat and bears no knoblike boss medial to temporal crests; intertemporal constriction weak with its maximum behind centre of skull roof; temporal crests prominent and not interrupted by squamosal reaching nuchal crest; ventral extremity of jugal lies ventral to orbit; ventral rim of orbit not overhanging; zygomatic process of squamosal triangular in shape with dorsal margin distinctly inclined inward and posterodorsal end convex; *processus retroversus* moderately inflected; height of supraoccipital distinct; first upper incisor with enamel on all sides, and canines and permanent premolars absent.

Character states: 12[1]; 19[1]; 22[1]; 23[0]; 24[1]; 51[0]; 52[0]; 53[0]; 54[1]; 55[0]; 57[0]; 87[0]; 88[0]; 81[0]; 82[1]; 86[0]; 89[1]; 91[1]; 98[1]; 101[1]; 112[0]; 160[0]; 166[1]; 167[1]; 168[1]; 169[1]; 170[1].

Differential diagnosis: Differs from most sirenian taxa in that the nasal process of the premaxilla is broadened and bulbous at its posterior end having a more or less vertical joint surface in contact with the frontal (but not *Corystosiren, Potamosiren* and *Ribodon*, in which this character is not preserved, and not *Rytiodus*, *Dioplotherium* and *Xenosiren,* which share this character with gen. nov. 4 *bellunense*). Differs from all stem group representatives in showing two synapomorphies of the crown group: absence of both, the successive P3/p3 and P4/p4. Differs from gen. nov. 2 *alleni*, in which none of the characters mentioned above is preserved, in that the squamosal does not extend up to the temporal crests. Differs from *Dioplotherium* in lacking an anteroposteriorly elongated zygomatic-orbital bridge of the maxilla. Differs from *Xenosiren* in showing no transverse vertical wall formed by the zygomatic-orbital bridge of the maxilla. Differs from *Rytiodus* and *Corystosiren* in that the I1 crown is not broad and extremely flattened mediolaterally in cross section. Differs from *Ribodon* and *Potamosiren* in that the rostrum is strongly deflected.

Gen. nov. 4 *bellunense* (De Zigno, 1875)

Halitherium bellunense; De Zigno, 1875: 12, pls. 1, 2.
Halitherium bellunense (De Zigno); De Zigno, 1878: 3.
Metaxytherium bellunense (De Zigno); Lepsius, 1882: 180.
Halitherium bellunense (De Zigno); De Zigno, 1887: 728.
Halitherium bellunense (De Zigno); Abel, 1905: 393, fig. 1.
Halitherium bellunense (De Zigno); Domning, 1989a: 424, fig. 6.

Holotype. MGPD-18Z associated skullcap, MGPD-19Z left premaxilla with tusk, MGPD-20/21Z fragment of left maxilla with DP5-M2, MGPD-22Z left and MGPD-23Z right zygomatic processes, MGPD-7384Z fragment of left jugal, MGPD-7385/6Z fragment of right maxilla with DP5 and M1, MGPD-7387Z an isolated fragment of a molar, MGPD-7383Z a fragment of a lower molar, seven fragments of vertebrae (MGPD-7362Z, -7367Z, -7368Z, -7369Z, -7374Z, -7375Z, -7376Z), and six rib fragments (MGPD-7358/9Z, -7363Z, -7364Z, -7366Z, -7381Z) of a juvenile specimen.

For detailed listing of the preserved skeletal parts see also Appendix 1.

Referred material: Only the holotype is known.

Type horizon and locality: Cavarzano, Valle delle Guglie, near Belluno, Italy. Basal portion of the Belluno Glauconitic Sandstone Formation according to Sorbi (2007: 74), latest late Oligocene (upper Chattian) in age.

Range and distribution: Known only from type locality.

Emended diagnosis: As for the genus.

Description

Figures 61–64, Appendix 3

This taxon was described and illustrated by De Zigno (1875) and Abel (1905). Sorbi (2007) supplemented the previous studies by essentially following Domning's (1994) character list. Here, the holotype material is set into a broader context of anatomical characters contributing to new and more comprehensive indications of the taxon's skeletal morphology. The description part deals with the preserved material only, and hence skeletal elements not mentioned are unknown.

Premaxilla: The left premaxilla is preserved embedded in sedimentary matrix mediorostrally and posteriorly, partly surrounding the posterior end of the nasal process (Fig. 61). The total preserved length of the premaxilla measures 178 mm, the rostrum reaches 94 mm in length and is, according to the ratio l_{SYM}/l_{PM} of 0.53, longer than half the total length of the premaxilla (5[1]). Taking into account the conditions in the taxa for comparison with similar ratios, the symphysis is considered to be overall enlarged (4[1]). In lateral view, the premaxillary symphysis is compressed to form a low middorsal ridge and a slight boss at the summit (9[1]; 10[1]). The angle of the rostrum is estimated to be 60° (12[1]). The first incisor tusk is preserved and present in the symphysis indicating that a dentiform process is missing medially (16[0]). Lateroposteriorly, the maxillopremaxillary suture is indicated and perpendicular to the posterior end of the symphysis (7[1]).

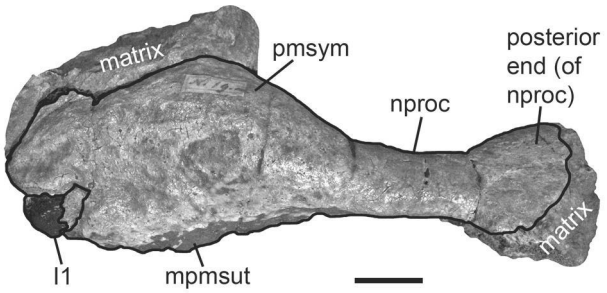

Figure 61. Premaxilla (MGPD-19Z) of gen. nov. 4 *bellunense* in left lateral view. Scale bar equals 2 cm.

Anteromedial to the nasal process, the mesorostral fossa shows no indentations (11[1]) and extends retracted and enlarged dorsoposterad (1[1]). If the external nares exceed the level of the anterior margin of the orbit cannot be determined due to the missing facial part of the skull. The posterior end of the nasal process is broadened and bulbous having more or less a vertical joint surface in contact with the frontal (19[1]; 20[1]).

Frontal: The associated skullcap (MGPD-18Z) preserves the posterior part of the frontal roof with most of its surface eroded (Fig. 62A). Its dorsolateral parts that supposedly bear the temporal crests are broken. Posteriorly, the dorsal surface is nearly undamaged and reveals the frontal roof to be flat (51[0]) without knoblike bosses (53[0]). The interior aspect of the frontal and of the preserved skullcap at all, remains undescribed due to adhered sediment.

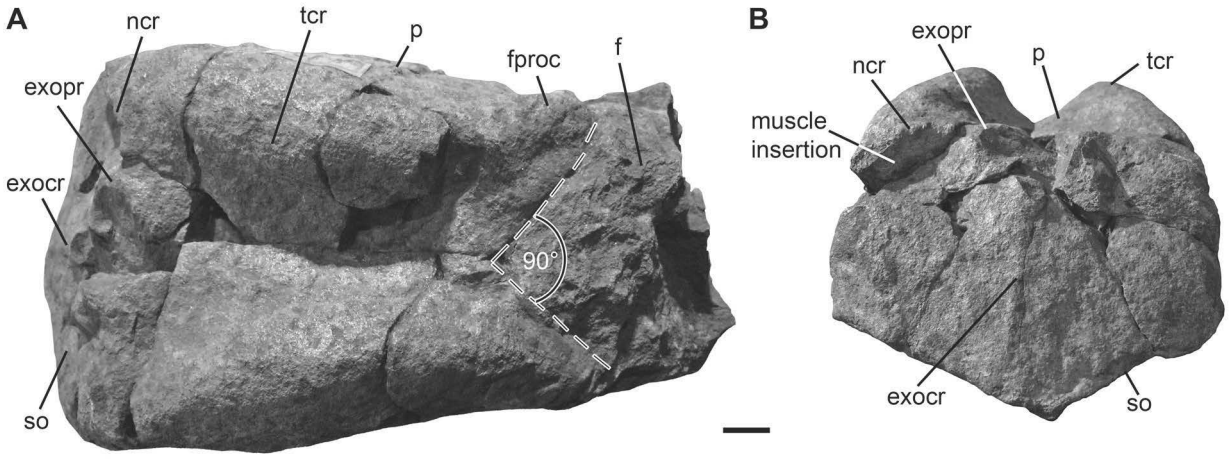

Figure 62. Parietal-supraoccipital skullcap (MGPD-18Z) of gen. nov. 4 *bellunense*. **A**, in dorsal view. **B**, in caudal view. Scale bar equals 1 cm.

Parietal: The parietal roof (Fig. 62A) lies more or less flat between the temporal crests and is slightly concave centrally where the temporal crests reach their maximum height and constriction (55[0]). Generally, the intertemporal constriction is weak (54[1]) with the temporal plane of the parietal sloping as a flat wall laterally. The temporal crests form prominent and thickened lyriform keels (57[0]) that are bulging medially at the centre of the parietal roof. They diverge anteriorly and posteriorly by decreasing in height. The course of the temporal crests is not interrupted by the squamosal dorsoposteriorly, so they reach the nuchal crest (88[0]). Anteriorly, the frontal processes of the parietal are separated by an angle of about 90° and supposedly extend only a short distance on the frontal roof.

Supraoccipital: Small parts of the supraoccipital are missing on the left dorsolateral and dorsomedial sides, and the left and right thirds of this skull element are separated from its mid-portion by fractures (Fig. 62B). Nevertheless, the supraoccipital can be determined to form a compact wall dorsoposterior to the brain, being distinct in height according to the width/height ratio of about 1.36 (112[0]). In lateral view, the supraoccipital meets the parietal roof at an angle of about 115°. The nuchal crest is narrow and sharp-edged, and extends as a convex ridge dorsolaterad (113[0]; 114[0]). Though eroded partially, the nuchal crest shows no notch in the median plane (115[0]), but an external occipital protuberance that forms a prominent knob rising above the parietal roof (116[1]). Lateral to the protuberance, rounded muscle insertions are present for the attachment of the semispinal muscle (117[0]). The external occipital protuberance extends ventrad as a distinct, but low median ridge (118[0]), somewhat shifted to the left side. It exceeds half the height of the supraoccipital and almost ends in its ventral tip (119[0]). The ventral margin of the supraoccipital is pointed in the median plane, meeting at an angle of about 132°. The internal surface of the supraoccipital is covered by sediment preventing any morphological observations.

Maxilla: Two maxillary fragments associated with the cheek dentition are preserved. On the lateral side of the left fragment (MGPD-20/21Z; De Zigno, 1875: pl. 2: fig. 4), the broken base of the zygomatic-orbital bridge is observable indicating that it extends slightly above the alveolar margin, elevated about 1 cm (21[1]). According to its length and height, the zygomatic-orbital bridge is clearly shortened anteroposteriorly and thickened posteriorly (24[1]), but not transformed into a transverse vertical wall (22[1]; 23[0]).

Squamosal: The cranial portion of the squamosal is not preserved, but its attachment areas lateral to the parietal show that it does not extend to the temporal crests (87[0]; Fig. 62A). Only the single left and right zygomatic processes (MGPD-22Z (Fig. 63) and MGPD-23Z) are present, with the left one having preserved the posterolateral part of the zygomatic root indicating a distinct notch (92[1]). In lateral view (Fig. 63A), the zygomatic process has a flat surface and is roughly triangular in shape, dorsoventrally high posteriorly and tapering anteriorly (89[1]). Its posterodorsal end is convex in outline (98[1]). The *processus retroversus* forms the posterior end of the zygomatic process and is moderately inflected without projecting below the jugosquamosal suture (101[1]). The ventral margin of the zygomatic process is straight, except for a distinct convexity just in front of the *processus retroversus*, and reveals no information on the mandibular articulation surface. Medially (Fig. 63B), the zygomatic process is slightly concave with the dorsal margin inclined inward forming a sigmoid ridge (90[0]; 91[1]).

Jugal: An isolated middle part of the left jugal is preserved (Fig. 63A) with the preorbital and zygomatic processes present, but broken anteriorly and posteriorly (76[1]). The zygomatic process of the jugal may have been as long as the diameter of the orbit considering the corresponding attachment area on the ventral margin of the zygomatic process of the squamosal that reaches as far posteriorly as to the beginning of its ventral convexity. However, the orbital area of the skull is too scarcely preserved in order to score character 83 unambiguously. Ventral to the orbit, the dorsal margin of the jugal is thick, but not overhanging laterally (86[0]). The ventralmost extremity of the jugal is positioned under the orbit (82[1]). Anterior to the tip of the squamosal zygomatic process, the postorbital process bulges (84[1]), but without rising high enough to form a postorbital bar with the frontal (85[0]).

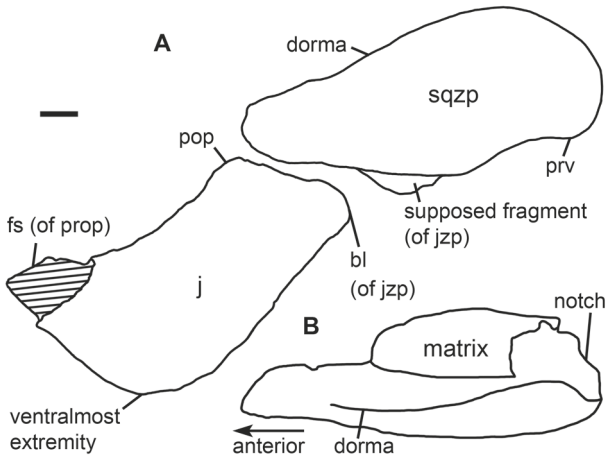

Figure 63. Outline drawings of left zygomatic process of squamosal (MGPD-22Z) and left jugal (MGPD-7384Z) of gen. nov. 4 *bellunense*. **A**, both elements in lateral view. **B**, zygomatic process of squamosal in dorsal view. Shaded area indicates missing part. Scale bar equals 1 cm.

Mandible: A bone fragment of about 40 mm in its maximum dimensions is referred to the lower jaw due to the presence of a two-rooted molar or molariform premolar (MGPD-7383Z). The tooth crown is only fragmentarily preserved hampering any detailed descriptions.

Dentition: Besides two poorly preserved tooth remains (MGPD-7383Z and -7387Z) that do not provide any information except for their presence, morphologically valuable records are the left premaxilla including the first incisor tusk and the left and right maxillary fragments. The upper lifetime dental formula is interpreted to be I1, C0, P0, DP5, M1–3 (180[0]; 181[0]; 182[0]).

De Zigno (1875: pl. 2: fig. 1) illustrated the first incisor tusk being complete and unworn with a lateral exposure in the premaxilla of about 30 mm. Though the anteriormost tip of about 10 mm is broken today (Fig. 61), the original state of preservation reveals this tusk to be most likely unerupted. In cross section, the crown is lens-shaped (162[1]) with sharp anterior and posterior edges measuring 17 mm x 8 mm in diameter. The crown is covered by black enamel on all sides (160[0]), but no conclusions can be drawn on the extension of the enamel, i.e. either along the entire length of the tusk or being distinct from the root. The slightly swollen lateral sides of the premaxillary symphysis indicate a length of the tusk alveolus that is not restricted to less than half the length of the premaxillary symphysis (157[1]). However, if the alveolus extends about half the length of the symphysis or does even exceed that level remains uncertain. The clarification of these characters should wait until more and better preserved material is known, particularly from adult specimens.

The cheek dentition is qualitatively and quantitatively best preserved in the maxillary fragment MGPD-20/21Z, and therefore it is the basis for the following description (Fig. 64). Three cheek teeth are preserved and interpreted here to represent DP5, M1 and M2. Abel (1905) and Sorbi (2007) interpret a small rounded tooth fragment mesiolingual to the incomplete DP5 crown as remains of the fifth premolar or the fourth deciduous premolar, respectively. Here, this tooth fragment is considered to be part of the broken DP5 crown. This observation is supported by the original extend of the DP5 alveolus still discernable mesially, lingually and distally by imprints in the maxillary bone. The area that might have been covered by the complete crown includes that fragment, which additionally corresponds to the tight positioning of the cheek teeth that barely would have given space for a premolar

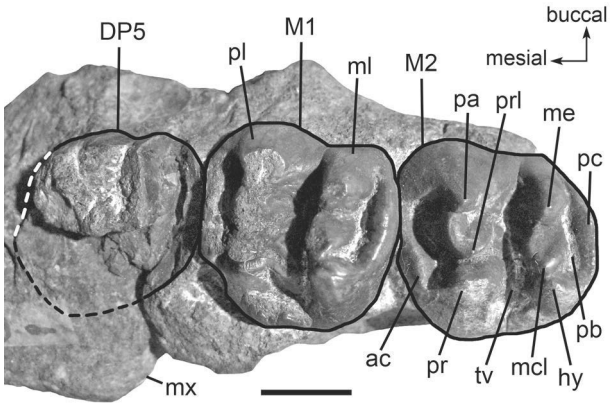

Figure 64. Fragment of left maxilla with DP5-M2 (MGPD-20/21Z) of gen. nov. 4 *bellunense* in occlusal view. Dashed lines indicate the supposed outline of DP5. Scale bar equals 1 cm.

at this place. Accordingly, DP5 is only slightly smaller than the subsequent molars and similar in having a slightly heart-shaped crown as it also can be generally observed in taxa for comparison. The fracture surfaces of the crown provide insights to the broken lingual and distolabial roots identifying this tooth to be a three-rooted molariform premolar (171[0]). Anterior to DP5, no traces of alveoli are preserved. Therefore, the premolars are considered to be absent as are the canines, and the second and third incisors in correspondence to the taxa for comparison showing similarly derived conditions of gen. nov. 4 *bellunense* (164[1]; 166[1]; 167[1]; 168[1]; 169[1]; 170[1]).

The left M1 is fully erupted and only slightly worn with the uppermost tips of the main cusps flattened. Its cups pattern does not differ from that of M2 and is summarised in the description below.

The left M2 is not completely erupted inhabiting a slightly lower position relative to M1. Its crown is entirely unworn revealing the two main transverse lophs each bearing three cusps that are clearly separated from each other. The *precingulum* transversally slopes from the lingual (or buccal) to the labial side and encloses a narrow anterior cingular valley that opens anterolabially. The protoloph is composed of the paracone mesiolabially and the protocone mesiolingually, both enclosing the protoconule to form a transverse ridge. While the protocone forms a prominent vertically rising cusp the paracone and protoconule slope in lingual direction. The transverse valley is deep and not obstructed by the metaconule, whereby the latter is nearly transversally directed with the hypocone and metacone to form the metaloph (178[0]; 179[0]). As on the protoloph, the metacone and metaconule are inclined lingually, but the hypocone slopes labially. A posterior *cingulum* is attached to the hypocone and encloses a posterior basin of moderate size that opens labially.

Vertebral column: Besides four vertebral fragments (MDPD-7362Z, -7374Z, -7375Z, -7376Z) that are not further assignable, three centra (MGPD-7367Z, -7368Z, -7369Z) are identified to represent thoracics and one centrum (MGPD-7383Z) is allocated to the lumbars. All centra are lacking the transverse processes and neural arches. The thoracic centra show a slight heart-shaped outline while the lumbar centrum is oval-shaped. The proximal and distal extremities are flat and slightly concave medially.

Ribs: Six rib fragments are present; thereof MGPD-7358/9Z is the largest one. It is composed of originally two single fragments that are now glued representing the distal part of the rib shaft. This element measures about 240 mm in maximum preserved length and has a more or less constant anteroposterior width that diminishes slightly only in the last 70 mm of the somewhat inclined distal extremity. Cemented gravels and shells cover the rib fragment, but the fracture surface of its shaft reveals a clearly elliptical cross section with 50 mm in maximum and 30 mm in minimum diameters (197[0]). According to the slope of the distal end, the rib is allocated to the left side of the thorax and may have had occupied a position in the anterior part of the thorax.

Another noteworthy element is a proximal fragment of about 128 mm length most likely belonging to the left first rib (MGPD-7366Z). The *capitulum* and *tuberculum* have a distance of 42 mm indicating a long *collum* typical for the anteriormost ribs. Ventral to the *capitulum*, a protuberance is missing (195[0]).

Remarks

Taxonomic and morphological remarks: This taxon is well placed within the crown group (see chapter “Phylogenetic analyses”), but conclusions on its taxonomic and systematic establishment requires caution for two reasons. On the one hand, this species is not well known by its morphological characters, which is indicated by approximately 62 % question marks for this taxon in the present data matrix (Appendix 4). Second, this taxon is identified as representing a young animal. This is indicated by the most likely unerupted and unworn incisor tusk of the left premaxilla (Fig. 61), and by the state of wear and eruption of the preserved molars (Fig. 64). In contrast to De Zigno (1875) and Abel (1905), the preserved molars certainly do not represent the left DP5–M3 (MGPD-20/21Z) and right M1–2 (MGPD-7385/6Z), but the left DP5–M2 and the right DP5-M1. Sorbi (2007) also reached the same conclusion on the maxillary remains except for the presence of a DP4 lingual to the left DP5 in MGPD-20/21Z, which is interpreted here as a fragment belonging to DP5 (Fig. 64).

Usually, the upper M3 is larger than M2 and has an elongated shape with the metaloph transversally shorter than the protoloph, but this is not the case in the last preserved molar in the present material. Here, the left M2 is nearly as large as M1, both showing a slightly heart-shaped outline with the protoloph as large as the metaloph. Additionally, the left M2 occupies a position behind the zygomatic-orbital bridge, which however, would be more or less at the level of its posterior end in adult individuals. Considering the cheek-tooth succession in young dugongs reported for example by Mitchell (1973) and Marsh (1980), the relative age of this animal is estimated between three and four years indicating immaturity.

Geological and palaeogeographical remarks: The stratigraphic provenance of gen. nov. 4 *bellunense* was already outlined and amended by Sorbi (2007) and determined to be upper Oligocene (Chattian). For the sake of completeness, the stratigraphy of the taxon’s type locality is summarised and verified below.

According to De Zigno (1875), gen. nov. 4 *bellunense* was found in Cavarzana, near Belluno in northern Italy (Fig. 65), which was subsequently adjusted into Cavarzano by Sorbi (2007). The holotype specimen was embedded in dark green, glauconitic, and shell-rich sandstones overlain by grey sandstone layers. The glauconitic sandstones were considered to be early Miocene in age by De Zigno (1875). This stratigraphic assignment has been maintained ever since until quite recently (e.g., Lepsius, 1882; Abel, 1905; Pilleri,

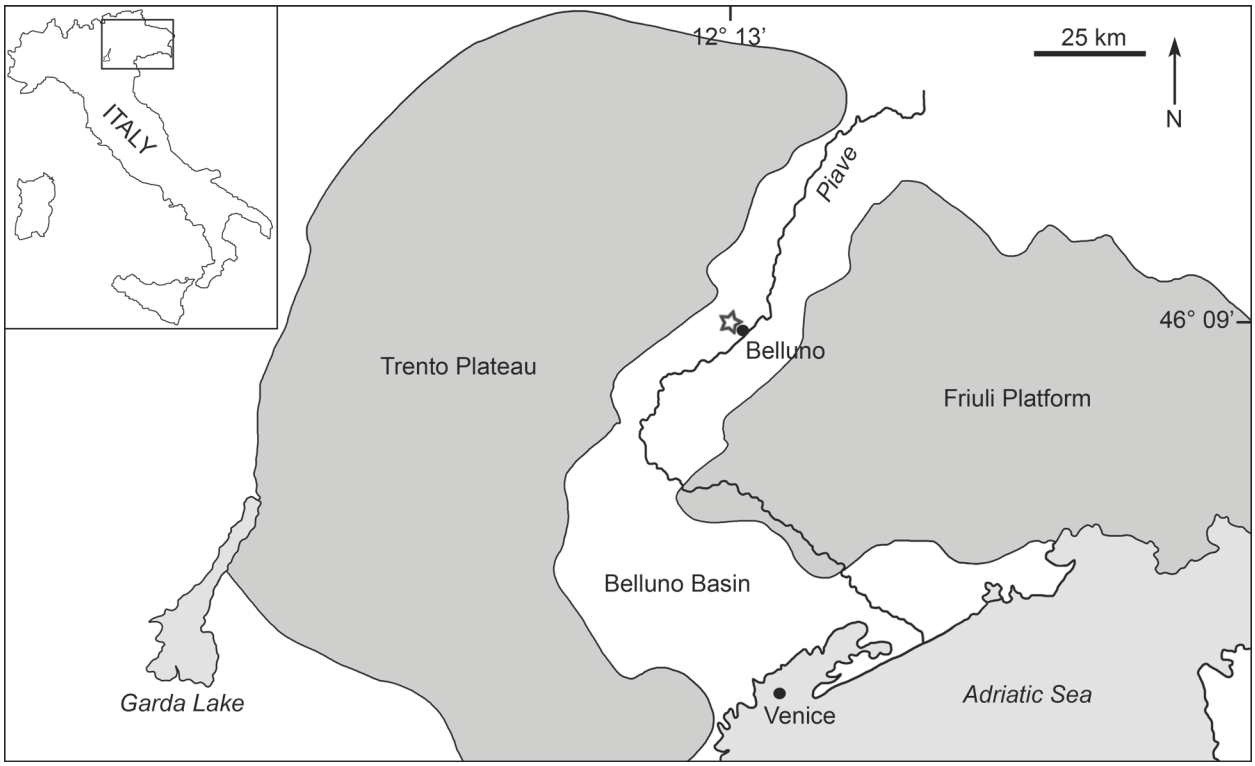

Figure 65. Geographic setting and sketch map of the location of Cavarzano, Valle delle Guglie, near Belluno, Italy (modified after Bosellini *et al.,* 1981 and Dallanave *et al.,* 2009). Asterisk indicates estimated locality of species gen. nov. 4 *bellunense*.

1985; Domning, 1996).

Today, these sediments are identified as belonging to the lowermost sequence (upper Chattian – lower Aquitanian) of the Venetian Molasse Basin in the Belluno syncline, between the Trento Platform in the north-west and the Friuli Platform in the east (Bosellini *et al.*, 1981; Dallanave *et al*., 2009), and unconformably overlie the Eocene Belluno Flysch of Ypresian age (Ghibaudo *et al*., 1996; Zampieri & Grandesso, 2003). The transgressive systems tract of the lower sequence comprises a basal, condensed, glauconitic and fossiliferous sand sheet, the so-called Belluno Glauconitic Sandstone, which corresponds to De Zigno's (1875) type horizon of gen. nov. 4 *bellunense*. The top of the transgressive event is built by the lower part of the Bastia Siltstone, De Zigno's (1875) overlaying grey sandstone that represents a finer-grained, essentially muddy unit.

The determination of the type stratum of gen. nov. 4 *bellunense* is uncertain, but can be limited. According to Ghibaudo *et al.* (1996), the Belluno Glauconitic Sandstone is 11 m thick and can be subdivided, from base to top, into a shell-rich, gravelly glauconitic sandstone facies followed by glauconitic sandstones characterised by an alignment of bioclasts, which are topped by a bioturbated glauconitic sandstone facies. Only the first and second facies of the Belluno Glauconitic Sandstone contain bioclasts, mainly pectinids, and therefore have relevance as to the type stratum of gen. nov. 4 *bellunense*. De Zigno (1875) did not mention the shell-pavements characteristic for the 68 cm thick

second facies. Based on that, it could be inferred that gen. nov. 4 *bellunense* comes from the first facies that commences at an interval of 15-35 cm thickness. Either way, this stratigraphic assignment is only subtle and the type stratum of gen. nov. 4 *bellunense* can be limited at least to the basal 83 cm to 103 cm of the Belluno Glauconitic Sandstone.

Both units, the Belluno Glauconitic Sandstone and the lower part of the Bastia Siltstone, are illustrated as representing the upper section of the Chattian stage (Ghibaudo *et al*., 1996). This precise and clearly defined stratigraphic determination is supported by the subsidence analysis by Mellere *et al.* (2000), who date the molasse deposits of the Belluno Glauconitic Sandstone to 27–25 Ma and the Bastia Siltstone to 25–22.5 Ma on the basis of planktic foraminifera. Foraminifera assemblages and facies associations also reveal both units to represent deposits of a shallow marine environment, dating paleobathymetrically the Belluno Glauconitic Sandstone to the inner neritic and the Bastia Siltstone to the offshore inner-shelf level (Mellere *et al*., 2000).

In conclusion, gen. nov. 4 *bellunense* comes from the basal part of the Belluno Glauconitic Sandstone Formation corresponding to Sorbi (2007: 74) and is upper Chattian in age.

Suborder nov. 2

Included genera: Anomotherium Siegfried, 1965; *Caribosiren* Reinhart, 1959; *Dusisiren* Domning, 1978; *Hydrodamalis* Retzius, 1794; *Metaxytherium* De Christol, 1840; *Miosiren* Dollo, 1889; *Potamosiren* Reinhart, 1951; *Ribodon* Ameghino, 1883; *Trichechus* Linnaeus, 1758.

Stratigraphical range: Middle or late Oligocene – recent.

Geographical range: Tropical and subtropical regions worldwide and North-Pacific.

Diagnosis: The monophyly of this new clade is supported by the combination of the following features: posterolateral corner of supraorbital process not prominent; external auditory meatus long mediolaterally (> 1 cm); I1 alveolus extends less than half the length of the premaxillary symphysis; hypocone and metaconule of M2 not transversally directed, but metaconule obstructing the transverse valley; anteroposterior flattening of diaphysis of radius weak, radius as thick as ulna.

Character states: 49[0]; 104[1]; 157[0]; 178[1]; 179[1]; 192[1].

Trichechidae Gill, 1872 (1821)

Type genus: Trichechus Linnaeus, 1758.

Included genera: Anomotherium Siegfried, 1965; *Miosiren* Dollo, 1889; *Potamosiren* Reinhart, 1951; *Ribodon* Ameghino, 1883; *Trichechus* Linnaeus, 1758.

Stratigraphical range: Late Oligocene – recent.

Geographical range: Central Europe, Colombia, Argentinia, Rivers Amazon and Orinoco (South America), West Indies, southeastern USA, Central American coasts and northern South America, West African Rivers and coastal region from Senegal to Angola.

Emended diagnosis: Crown group sirenians having the combination of the following characters: rostrum small relative to cranium; premaxillary symphysis shorter than half the total length of premaxilla; anteroventralmost maxillopremaxillary suture in the rear of posterior end of symphysis, below mesorostral fossa; anterior palatal roof in front of infraorbital foramina broad, only slightly narrower than the posterior palatal roof; rostral masticating surface straight; *foramen incisivum* sharply demarcated anteriorly; infraorbital foramen rounded, about as wide as high; palate more than 1 cm thick at level of penultimate cheek tooth; posterior end of zygomatic root without distinct notch; postglenoid process of squamosal weak; external auditory meatus very broad and shallow, wider anteroposteriorly than high; nuchal crest short, reaching as far as squamososupraoccipital suture; exoccipitals meet in a suture dorsal to *foramen magnum*; transverse valley of M2 not obstructed by metaconule; first rib without protuberance ventral to *capitulum*.

Character states: 4[0]; 5[0]; 6[0]; 13[1]; 14[0]; 15[1]; 30[1]; 32[1]; 92[0]; 96[1]; 107[1]*; 114[1]; 121[0]; 179[0]; 195[0]; (* = synapomorphy).

Differential diagnosis: Differs from all other sirenians in possessing the synapomorphic character of a very broad and shallow external auditory meatus that is wider anteroposteriorly than high.

Miosireninae Abel, 1919

Type genus: Miosiren Dollo, 1889.

Included genera: Anomotherium Siegfried, 1965; *Miosiren* Dollo, 1889.

Stratigraphical range: Late Oligocene – early Miocene.

Geographical range: Germany and Belgium (Central Europe).

Emended diagnosis: Sirenians that possess the combination of the following features: external nares retracted and enlarged, reaching to the level of the anterior margin of the orbit; nasals well developed, length of internasal suture longer than half the length of interfrontal suture exposed dorsally; nasals meet in midline; nasal incisures absent; *lamina orbitalis* of frontal thickened; parietal roof convex; nuchal crest convex, forming dorsolateral ends of supraoccipital; supracondylar fossa of exoccipital deep and extending

across entire width of occipital condyle; paroccipital process of exoccipital long, reaching as far ventrally as occipital condyle or longer; presence of P4/p4; all permanent premolars single rooted; hypocone and metaconule of upper M2 nearly transversally directed.

Character states: 2[1]; 39[0]; 40[0]; 42[0]; 60[1]*; 61[0]; 114[0]; 123[1]; 131[0]; 170[0]; 173[1]; 178[0]; (* = synapomorphy).

Differential diagnosis: Differs from all other sirenians in having the synapomorphic character of a thickened *lamina orbitalis* of frontal.

Trichechinae (Gill, 1872 [1821]) Domning, 1994

Type genus: Trichechus Linnaeus, 1758.

Included genera: Potamosiren Reinhart, 1951; *Ribodon* Ameghino, 1883; *Trichechus* Linnaeus, 1758.

Stratigraphical range: Middle Miocene – recent.

Geographical range: Colombia, Argentinia, Rivers Amazon and Orinoco (South America), West Indies, southeastern USA, Central American coasts and northern South America, West African Rivers and coastal region from Senegal to Angola.

Emended diagnosis: Crown group sirenians that are characterised by the combination of the following features: angle of premaxillary symphysis weak; mandibular symphysis broad transversally; accessory mental foramina present in addition to and usually posterior to the large principal foramen; mandibular symphysis as long as high or longer; horizontal mandibular ramus slender; incisors, canines, and all permanent premolars absent.

Character states: 12[0]; 137[1]; 140[0]; 142[0]; 156[0]; 160[0]; 161[1]; 162[0]; 163[0]; 164[1]; 165[0]; 166–170[1]; 171[0]; 172[1]; 173[0].

Differential diagnosis: Distinguished from most stem group sirenians (*Prorastomus, Pezosiren, Protosiren, Eosiren, Eotheroides*, *Prototherium*, and gen. nov. 1) in that no canines are developed. Differs from *Sirenavus hungaricus* in that the anterior border of the coronoid process is not approximately vertical. Differs from the stem group representatives gen. nov. 2 spec. nov. 1, gen. nov. 2 *bronni*, and gen. nov. 3 in that the mandibular symphysis is not higher than long. Distinguished from gen. nov. 2 *alleni* in showing no strong intertemporal constriction at the centre of the skull roof. Differs from all crown group sirenians except for the genus *Hydrodamalis* in possessing a mandibular symphysis that is as long as high or longer. Distinguished from *Hydrodamalis* in having accessory mental foramina in addition to the large principal foramen and functional teeth in adult.

Family nov. 2

Type genus: Hydrodamalis Retzius, 1794.

Included genera: Dusisiren Domning, 1978; *Hydrodamalis* Retzius, 1794.

Stratigraphical range: Early middle Miocene – recent.

Geographical range: Baja California and Baja California Sur (Mexico), California (USA), Japan, Aleutian and Commander Islands, North-Pacific.

Diagnosis: Large sirenians that possess the following combination of characters: external nares, retracted and enlarged, reaching beyond the anterior margin of the orbit; premaxillary symphysis laterally compressed, bearing a middorsal ridge that is upraised to form a boss posteriorly; angle of rostrum weak or moderate, below 50°; supraorbital process of frontal dorsoventrally thickened; frontal roof more or less flat between temporal crests; supraoccipital enlarged transversally; incisors, canines, and permanent premolars absent.

Character states: 3[1]; 9[1]; 10[1]; 12[0]; 44[1]; 52[0]; 112[1]; 160[0]; 161[1]; 162[0]; 163[0]; 164[1]; 165[0]; 166–170[1]; 171[0]; 172[1]; 173[0].

Differential diagnosis: Differs from all stem group representatives except for *Eosiren imenti* and gen. nov. 3 *cristolii* in having external nares that are retracted and enlarged, reaching beyond the anterior margin of the orbit. Differs from *Eosiren imenti* and gen. nov. 3 *cristolii* in that the supraorbital process of frontal is not flattened dorsoventrally. Distinguished from all crown group sirenians except for the Trichechidae, gen. nov. 4 *bellunense*, and the genus *Metaxytherium* in lacking a concave frontal roof. Differs from gen. nov. 4 *bellunense* and the genus *Metaxytherium* in lacking a first upper incisor. Differs from Trichechidae in that the external auditory meatus of squamosal is about as wide anteroposteriorly as high.

Hydrodamalinae (Palmer, 1895 [1833]) Simpson, 1932a

Type genus: Hydrodamalis Retzius, 1794.

Included genera: Hydrodamalis Retzius, 1794.

Stratigraphical range: Middle Pliocene – recent.

Geographical range: Baja California (Mexico), California (USA), Aleutian and Commander Islands, North-Pacific.

Emended diagnosis: Anterior palatal roof in front of infraorbital foramina broad, slightly narrower than the posterior palatal roof; rostral masticating surface straight; dentiform process of premaxilla present; zygomatic-orbital bridge of maxilla shortened; maximum

intertemporal constriction behind centre of skull roof; contact between lacrimal and premaxilla present; glenoid fossa shallow; postglenoid process of squamosal weak; absence of functional teeth in adult; medially curved diaphyses of radius and ulna.

Character states: 13[1]; 14[0]; 16[1]*; 22[1]; 55[0]; 74[1]; 94[0]; 96[1]; 181[1]*; 194[1]*; (* = synapomorphy).

Differential diagnosis: Distinguished from all other sirenians by the following synapomorphies: presence of dentiform process of premaxilla; functional teeth absent in adult; diaphyses of radius and ulna curved medially.

Sirenia incertae sedis

Halitherium antillense Matthew, 1916

Holotype: AMNH 9844, posterior part of left mandible with m1–3 and one cervical and one thoracic vertebra.

Referred material: Only the holotype is known.

Type horizon and locality: Bluff, west bank of Rio Jacaguas, 1 km N and 1 km W of Juana Diaz, Puerto Rico. Principal reference section of the Juana Diaz Formation (Monroe, 1980: 68) within the higher *Globigerina ampliapertura* zone (Moussa & Seiglie, 1970: 1892), lower Chattian, late Oligocene.

Range and distribution: Known only from type locality.

Description

Mandible: Although broken anteriorly (Fig. 66), the horizontal mandibular ramus appears to be slender (156[0]) with its ventral border moderately concave (143[1]; 146[1]) and not tangent to the angle (147[1]). The anterior border of the coronoid process extends slightly anteriorly (151[1]) having an enlarged coronoid foramen at its basis (153[1]). The mandibular foramen is undivided (154[0]) revealing the dental capsule exposed posteroventrally (155[1]; Fig. 66B).

Dentition: In front of the heavily worn m1–3 (180[0]; 181[0]; 182[0]), the alveoli for a three-rooted dp5 are present indicating no tooth replacement at this locus (171[0]). Anteriorly to dp5, two alveoli are interpreted to represent p3 and p4 (169[0]; 170[0]), which are single-rooted (173[1]).

Vertebral column: Two vertebrae, one cervical and one thoracic, are present mainly via the vertebral body, which is flat and oval in the first and thick and heart-shaped in the latter.

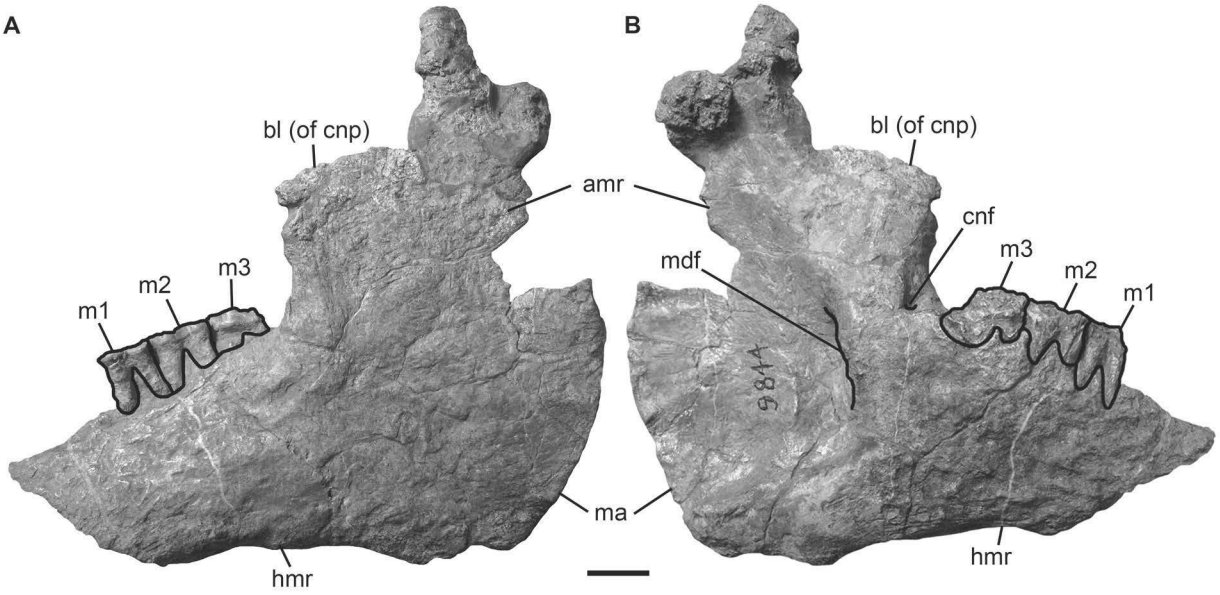

Figure 66. Posterior part of left mandible and holotype specimen of *"Halitherium antillense"* AMNH 9844. **A**, in lateral view. **B**, in medial view. Scale bar equals 2 cm.

Remarks

Matthew (1916) provisionally referred this sirenian to the genus *"Halitherium"*. As it will be pointed out later in this thesis, the cladistic treatment of this species doesn't lead to a reliable phylogenetic signal. Additionally, the holotype bears no diagnostic features for any species distinction and, therefore, *"H. antillense"* is considered a *nomen dubium*.

PHYLOGENY

Anatomical character data

The character list below comprises 43 new features, the remainder are mainly based on Domning (1994) and the following sources: Domning & Thomas (1987), Domning *et al.* (1994), Bajpai & Domning (1997), Sagne (2001b), Furusawa (2004), Sorbi (2007), Domning & Aguilera (2008), Bajpai *et al.* (2010), and Velez-Juarbe et al. (2012). The references listed with each character are not necessarily the first use of it, but the primary source for the interpretation of this character here. Modifications of characters in the form of corrections and additions, for example, are commented upon if they are not self-explanatory. The symbol "#" stands for referred character numbers of other publications.

Premaxilla

1. External nares not retracted and enlarged: [0] present; [1] absent (modified after Domning, 1994: #8).
2. External nares retracted and enlarged, reaching the level of the anterior margin of the orbit: [0] absent; [1] present (modified after Domning, 1994: #8).
3. External nares, retracted and enlarged, reaching beyond the anterior margin of the orbit: [0] absent; [1] present (modified after Domning, 1994: #8).

Notes/remarks: Characters two and three represent the redefined character state 8[1] from Domning (1994). This character split enhances the subdivision within Sirenia and was already adopted by Sorbi (2007).

4. Rostrum: [0] small relative to cranium; [1] enlarged (length of premaxillary symphysis > 0.27 x condylobasal skull length) (Domning, 1994: #3).
5. Premaxillary symphysis: [0] shorter than half the total length of premaxilla; [1] as long as or longer than half the total length of premaxilla (**new**, similar to Velez-Juarbe *et al*., 2012).

Notes/remarks: This character is newly introduced to provide more objective criteria for the evaluation of the proportionality between the nasal process and the symphysis of the premaxilla (Table 1) according to the descriptions in Sickenberg (1934a) and Savage *et al.* (1994). The ratio of length of symphysis to length of premaxilla (l_{SYM}/l_{PM}) is used, which was already introduced by Sagne (2001b). While Sagne (2001b) applied this ratio to evaluate alternatively the size of the premaxillary symphysis according to character 3 from Domning (1994), the calculation of l_{SYM}/l_{PM} is used here to avoid the subjective division into a "long" and "very short" nasal process by Domning (1994: #7).

6. Anteroventralmost maxillopremaxillar suture in the rear of posterior end of symphysis, below the mesorostral fossa: [0] present; [1] absent (modified after Sagne, 2001b: #3).

7. Anteroventralmost maxillopremaxillar suture perpendicular to posterior end of symphysis: [0] absent; [1] present (modified after Sagne, 2001b: #3).
8. Anteroventralmost maxillopremaxillar suture forward to posterior end of symphysis: [0] absent; [1] present (**new**).

Notes/remarks: This character is an addition to Sagne's (2001b) observations according to personal studies on sirenian taxa for comparison and comprises corrections as to the scoring of some taxa.

Table 1. Examples of the ratio l_{SYM}/l_{PM} for selected taxa. Measurements in mm (preserved length in parentheses); "e" indicates estimated dimensions.

Taxon	Collection number	l_{SYM}	l_{PM}	Ratio
Prorastomus sirenoides	NHMUK PV M44897	(60)	(118)	(0.51)
Protosiren fraasi	SMNS 10576	(50)	(140)	(0.34)
Protosiren smithae	USNM 94810	68	176	0.38
Eosiren stromeri	SMNS 44007	114	20e	0.57
Eosiren libyca	SMNS 44008	109	191	0.57
	NHMUK PV M10910	99	182	0.54
Eosiren imenti	CGM 40210	(107)	(195)	(0.55)
Eotheroides lambondrano	UA 9046	(50)	(131)	(0.38)
Prototherium veronense	MGPD-10Z	(98)	(186)	(0.53)
Prototherium intermedium	MGPD-28997	85	165	0.52
Gen. nov. 1 *taulannense*	RGHP D040	106	155	0.68
Gen. nov. 2 *bronni*	CDGG S1	(97.5)	(190)	(0.51)
	FIS M8385	(83)	(143)	(0.58)
Gen. nov. 2 spec. nov. 1	BSPG 1956 I 540	(89)	(178)	(0.5)
	FIS M2597	(65)	(126)	(0.52)
	LS RLP PW 2005/5042-LS	(85)	(170)	(0.5)
Gen. nov. 4 *bellunense*	MGPD-18Z–23Z, 7358Z–7387Z	(94)	(178)	(0.53)
Miosiren kocki	IRSNB M.136	121	275	0.44
Trichechus inunguis	MCZ 1079	33	108	0.31
Trichechus senegalensis	MNHN 1945–235	65	160	0.41
Trichechus manatus	MCZ 1791	56	145	0.39
	MCZ B7432	91	198	0.46
Caribosiren turneri	UCMP 38722	128	209	0.61
Metaxytherium serresii	GU 26P115B	130	217	0.59
Metaxytherium crataegense	AMNH 26838	128	239	0.54
Metaxytherium floridanum	USNM 377509	172	284	0.61
Crenatosiren olseni	UF/FGS V6094	107	185	0.58
Bharatisiren kachchhensis	LUVP/MP 1032	(139)	(272)	(0.51)
Dugong dugon	MCZ 5310	190	274	0.69
	MNHN 1945–227	195	283	0.69
Dusisiren jordani	UCMP 77037	198	385	0.51
	UCMP 3794	183	360	0.51
Hydrodamalis gigas	USNM 22999	226	393	0.57

Table 2. Examples of the rostral angle (in degree) for selected taxa.

Taxon	Collection number	Rostral deflection (∠)
Prorastomus sirenoides	NHMUK PV M44897	< 10°
Protosiren fraasi	SMNS 10576	~ 20°
Protosiren smithae	USNM 94810	~ 40°
Eosiren stromeri	SMNS 44007	< 30°
Eosiren imenti	CGM 40210	~ 45°
Eotheroides lambondrano	UA 9046	~ 35°
Prototherium veronense	MGPD-10Z	< 40°
Prototherium intermedium	MGPD-28997	~ 40°
Gen. nov. 1 *taulannense*	RGHP D040	~ 57°
Gen. nov. 2 spec. nov. 1	FIS M2597	~ 56°
	BSPG 1956 I 540	~ 58°
Gen. nov. 2 *bronni*	MWNH-TER-1	~ 57°
	CDGG S1	~ 55°
Gen. nov. 4 *bellunense*	MGPD-18Z–23Z, 7358Z–7387Z	~ 60°
Miosiren kocki	IRSNB M.136	< 30°
Trichechus manatus	MCZ 1791	~ 20°
Metaxytherium serresii	GU 26P115B	55°–60°
Metaxytherium floridanum	USNM 377509	~ 70°
Crenatosiren olseni	UF/FGS V6094	~ 55°
Bharatisiren kachchhensis	LUVP/MP 1032	30°–40°
Nanosiren sanchezi	UNEFM-VF-041	~ 77°
Dugong dugon	MCZ 5310	~ 70°

9. Premaxillary symphysis: [0] not laterally compressed to form a middorsal ridge; [1] laterally compressed, bearing a middorsal ridge (modified after Bajpai & Domning, 1997: #10).
10. Summit of premaxillary symphysis: [0] flattened; [1] upraised to form a boss in lateral view (modified after Bajpai & Domning, 1997: #10).
11. Mesorostral fossa: [0] indented anteriorly; [1] not indented anteriorly (**new**).
12. Angle of rostrum: [0] weak or moderate; [1] strong (≥ 50°) (modified after Sagne, 2001b: #4; Table 2).
13. Anterior palatal roof in front of infraorbital foramina: [0] very narrow compared to posterior palatal roof; [1] broad, almost as broad as the posterior palatal roof (modified after Sagne, 2001b: #5).
14. Rostral masticating surface: [0] straight; [1] lanceolate (**new**).
15. *Foramen incisivum*: [0] not sharply demarcated anteriorly; [1] sharply demarcated anteriorly (**new**).
16. Dentiform process of premaxilla: [0] absent; [1] present (**new**).

Notes/remarks: Characters 14–16 are newly established in order to accommodate features that Domning (1978) recorded for the genera *Dusisiren* and *Hydrodamalis* in particular.

17. Nasal process thin and tapering at posterior end, having lengthy overlap with frontal and/or nasal: [0] present; [1] absent (modified after Domning, 1994: #6).
18. Nasal process tapering but thickened at posterior end, with long overlap of frontal and/or nasal: [0] absent; [1] present (modified after Bajpai & Domning, 1997: #6).
19. Nasal process broadened and bulbous at posterior end, having more or less vertical joint surface in contact with frontal: [0] absent; [1] present (modified after Domning, 1994: #6).
20. Contact between premaxilla and frontal: [0] absent; [1] present (Domning, 1994: #9).

Maxilla

21. Zygomatic-orbital bridge: [0] elevated above palate, with its ventral surface lying > 15 mm above the alveolar margin; [1] nearly level with palate or slightly above alveolar margin (modified and redefined after Domning, 1994: #11).

Notes/remarks: Sagne (2001b: #6) already noted intraspecific variability within the extant Sirenia and the fossil representatives *Metaxytherium floridanum* and *"Halitherium" taulannense* with respect to the elevation of the zygomatic-orbital bridge. Domning (1994) considered a zygomatic-orbital bridge to be elevated when exceeding the alveolar margin by about 10 mm. This elevation level was adjusted to 15 mm by Sagne (2001b), which accords well with personal observations in the German Oligocene Sirenia and is, therefore, adopted here. In contrast to Domning (1994) and similar to Sagne (2001b), the plesiomorphic and derived states are converse due to the outgroup choice.

22. Zygomatic-orbital bridge: [0] long anteroposteriorly (vertical thickness < 0.40 x minimum length); [1] shortened (thickness ≥ 0.40 x length) (modified after Domning, 1994: #14).
23. Zygomatic-orbital bridge transformed into transverse vertical wall: [0] absent; [1] present (modified after Domning, 1994: #14).

Notes/remarks: The zygomatic-orbital bridge in the form of a transverse vertical wall designates an autapomorphy of *Xenosiren yucateca* (Domning, 1989b, 1994) and is a special variant of character state 22[1]. The original multistate character 14 from Domning (1994) is split here in order to avoid repetition of his character state "short".

24. Posterior end of zygomatic-orbital bridge thickened, thickness not constant anteroposteriorly: [0] absent; [1] present (modified after Sagne, 2001b: #7 and Velez-Juarbe *et al.*, 2012: #22).
25. Infraorbital foramen small, does not exceed 200 mm² in adults: [0] present; [1] absent (modified and redefined after Domning, 1994 and Bajpai & Domning, 1997: #13).
26. Infraorbital foramen large, taller than 200 mm², but less than 500 mm² in adults: [0] absent; [1] present (modified and redefined after Domning, 1994 and Bajpai & Domning, 1997: #13).

27. Infraorbital foramen very large, exceeding 500 mm² in adults: [0] absent; [1] present (modified and redefined after Bajpai & Domning, 1997: #13).

Notes/remarks: The objective evaluation of the size of the infraorbital foramen relative to intraspecific variability observable in certain taxa reveals difficulties since the introduction of this character by Domning (1994). The application of this character to individuals whose adulthood is quite certain comprises one of the modifications designated here in order to limit the impact of intraspecific variability. For example, the extant *Dugong* varies in having an infraorbital foramen that can be either large or very large. However, all adult individuals personally examined reveal the very large condition, while juveniles or even some subadults tend to show a large foramen that does not reach 500 mm². Additionally, subsequent studies like Bajpai & Domning (1997) deal with the adjustment of this character aiming at a more precise subdivision into “small”, “large” and “very large”. Nevertheless, the diameters of “15 mm x 10 mm” given by Domning (1994) to distinguish a small infraorbital foramen from a large one remain subjective, as are the readjusted diameters of “15 mm x 15 mm” provided by Sagne (2001b). In this study, area measurements of an ellipse (A=¼Π*D*d with D equals the tall diameter and d equals the small diameter) are used to calculate the size of the infraorbital foramen (Table 3) leading to more objective data (Fig. 67).

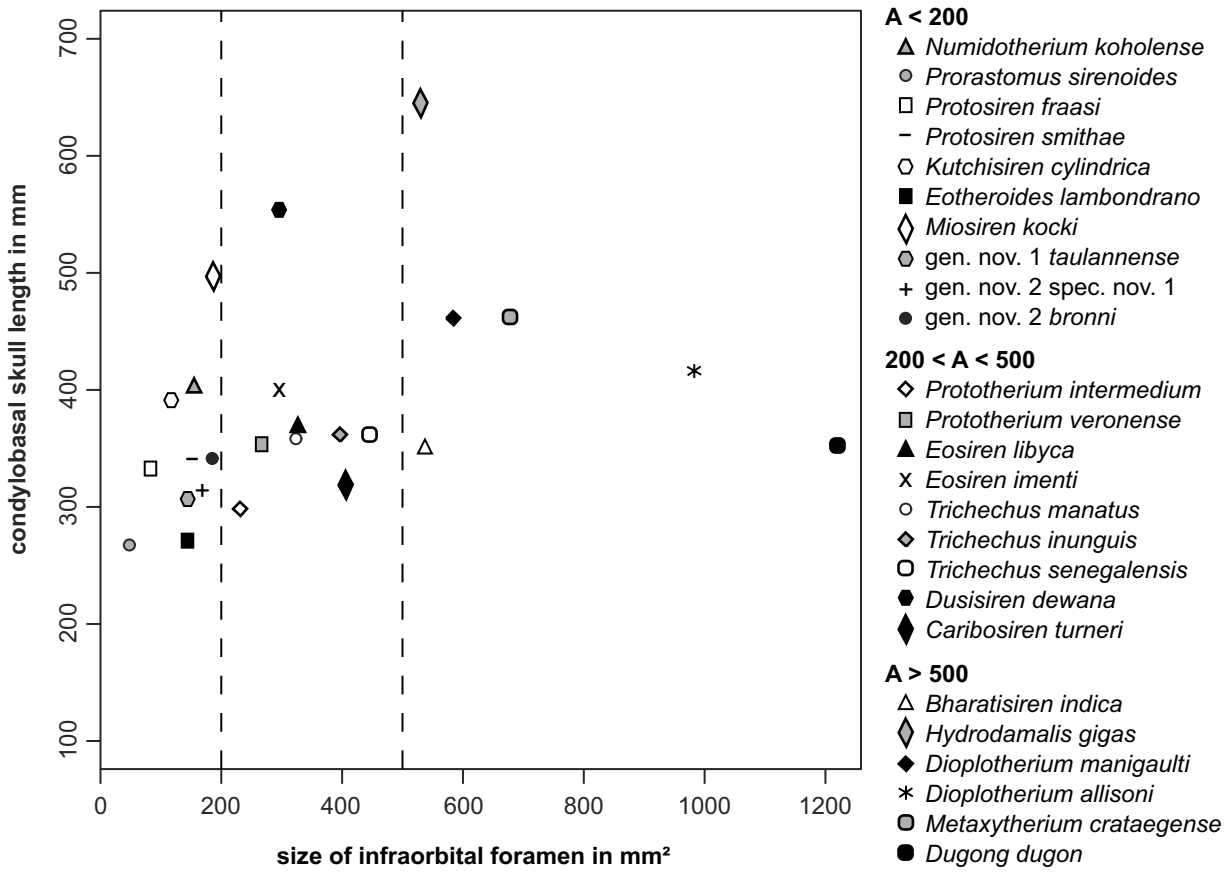

Figure 67. Graphical presentation of the size of the infraorbital foramen in relation to the condylobasal skull length for selected taxa.

Table 3. Examples of area measurements ("A") of the infraorbital foramen for selected taxa. Height and width or small and large diameter, respectively, are given in mm (preserved diameter in parentheses), and "A" in mm².

Taxon	Collection number	Height	Width	A
Prorastomus sirenoides	NHMUK PV M44897	5.6	11	48
Protosiren fraasi	SMNS 10576	9.5	11	82
Protosiren smithae	USNM 94810	16	12	151
Eosiren libyca	SMNS 44008	21.5	(19.7)	(333)
	NHMUK PV M10910	19.5	18	276
Eotheroides aegyptiacum	SMNS 43990	17	10	134
Eotheroides lambondrano	UA 9046	13	14	143
Eosiren imenti	CGM 40210	22	17	294
Prototherium veronense	MGPD-10Z	24	14	264
Prototherium intermedium	MGPD-28997	19	(15)	(224)
	MGPD-26300	(22)	(20)	(346)
Gen. nov. 1 *taulannense*	RGHP D040	13	15	153
Gen. nov. 2 spec. nov. 1	BSPG 1956 I 540	17	13	173
	FIS M2597	16	9	113
	FIS M8002	18	12.5	177
Gen. nov. 2 *bronni*	CDGG S1	16	15.5	195
	FIS M8385	13	12	156
	MWNH-TER-1	11.5	11	99
Trichechus manatus	MB Ma. 17377	20	21	330
Trichechus senegalensis	MB Ma. 69335	24.5	23	443
Trichechus inunguis	MB Ma. 35807	23	22	397
Miosiren kocki	IRSNB M.136 (right)	16.2	15	191
	IRSNB M.136 (left)	13.5	13	137
Caribosiren turneri	UCMP 38722	(24)	21.4	(403)
Metaxytherium crataegense	USNM 16757	(39)	(22)	(674)
Dioplotherium allisoni	MPEG 63-V	32	39	981
Dioplotherium manigaulti	UF 95615	24	31	584
Bharatisiren indica	IITR-SB 2893	26	26	531
Kutchisiren cylindrica	GSI-K60/998	> 15	> 10	> 117
Dugong dugon	MCZ 5310	33	47	1218
	MB Ma. 69313	25	31	608
Dusisiren dewana	Holotype uncatalogued	21	18	297
Hydrodamalis gigas	MNHN 1886-501	28	24	527

28. Infraorbital foramen oval, distinctly higher than wide: [0] absent; [1] present (modified after Sagne, 2001b: #9).
29. Infraorbital foramen oval, distinctly wider than high: [0] present; [1] absent (modified after Sagne, 2001b: #9)
30. Infraorbital foramen rounded, about as wide as high: [0] absent; [1] present (modified after Sagne, 2001b: #9).

31. Infraorbital canal: [0] not obstructed; [1] partly obstructed by a transverse bony ridge (Domning & Aguilera, 2008: #20).
32. Palate: [0] thin or incomplete at level of penultimate cheek tooth or posterior end of zygomatic-orbital bridge, respectively; [1] > 10 mm thick at level of penultimate cheek tooth or posterior end of zygomatic-orbital bridge, respectively (modified after Domning, 1994: #16).

Notes/remarks: The modification of this character is related to its application to toothless sirenian taxa like *Hydrodamalis*. The level of the penultimate cheek tooth corresponds well with the posterior end of the zygomatic-orbital bridge in adults, and therefore the latter is supplemented.

Palatine

33. Palatines: [0] extend anteriorly beyond posterior edge of zygomatic-orbital bridge: [1] behind posterior edge of zygomatic-orbital bridge (Domning, 1994: #99).
34. Posterior border of palatine not incised, merely shallowly concave: [0] present; [1] absent (modified after Domning, 1994: #97).
35. Posterior border of palatine incised or deeply indented, but not as far forward as level of M1 or the central part of the zygomatic-orbital bridge: [0] absent; [1] present (modified after Domning, 1994: #97).
36. Posterior border of palatine very deeply incised, to as far forward as level of M1 or the central part of the zygomatic-orbital bridge: [0] absent; [1] present (modified after Domning, 1994: #97).

Notes/remarks: As has been done with character 32, the characters 35 and 36 are adjusted to enhance their application to toothless sirenian taxa. The level of M1 is approximately consistent with the middle section of the zygomatic-orbital bridge in adults; the latter is thus added to the character definition.

Nasal

37. Nasals fused with frontals and/or ethmoid, but not coalesced: [0] absent; [1] present (**new**).
38. Nasals coalesced with frontals and/or ethmoid: [0] absent; [1] present (**new**).

Notes/remarks: Characters 37 and 38 include the revision and amendment of the character states 31[1] and 32[1] from Domning (1994). Both of Domning's (1994) character states encompass two completely different conditions of the nasals, which are characterised to be either separated in the midline or absent. The introduction of the terms fused and coalesced facilitates the distinction between nasals being small, but either still visible by sutures to the adjacent bones or completely merged without trackable sutures, in other words absent.

39. Nasals well developed (length of internasal suture ≥ 0.5 x length of interfrontal suture exposed dorsally): [0] present; [1] absent (modified after Domning, 1994: #32).
40. Nasals meet in midline: [0] present; [1] absent (modified after Domning, 1994: #31).
41. Nasal incisure at posterior end of mesorostral fossa deep and narrow (extends posterior to the supraorbital process): [0] absent; [0] present (modified after Domning, 1994: #37).
42. Nasal incisure at posterior end of mesorostral fossa small (does not extend posterior to the supraorbital process): [0] absent; [1] present (modified after Domning, 1994: #37).

Frontal

43. Internasal process of frontal: [0] absent; [1] present (modified after Domning, 1994: #37).

Notes/remarks: This character is the revised form of Domning's (1994) character state 37[2], whose median convexity of the anterior frontal margin corresponds with the internasal process of the frontal. This character split was already performed by Sagne (2001b: #14) and is adopted here.

44. Supraorbital process of frontal: [0] dorsoventrally flattened (less than about 2 cm thick); [1] dorsoventrally thickened (more than about 2 cm thick) (modified after Domning, 1994: #36 and #43 and the redefined #36 from Bajpai *et al*., 2010).
45. Supraorbital process of frontal: [0] with dorsal surface inclined gently ventrolaterad; [1] turned markedly downward, with dorsal surface inclined strongly ventrolaterad (modified after Domning, 1994: #43).
46. Supraorbital process of frontal: [0] not divided; [1] divided by one or more distinct, deep dorsoventral grooves indenting its lateral margin (Bajpai & Domning, 1997: #44).
47. Posterolateral corner of supraorbital process: [0] absent; [1] present (modified after Domning, 1994: #36).
48. Posterolateral corner of supraorbital process projecting posteriorly: [0] absent; [1] present (modified after Domning, 1994: #43).
49. Posterolateral corner of supraorbital process prominent: [0] absent; [1] present (modified after Domning, 1994: #36).
50. Frontal roof deeply concave or depressed overall (with or without a small median convexity) between temporal crests, but not sloping ventrad anteriorly: [0] absent; [1] present (modified after Domning & Aguilera, 2008: #42).
51. Frontal roof deeply concave or depressed, sloping steadily ventrad to anterior margin: [0] absent; [1] present (modified after Domning, 1994: #42).
52. Frontal roof more or less flat between temporal crests: [0] present; [1] absent (modified after Domning, 1994: #42).

53. Frontal roof: [0] bears no knoblike boss; [1] bears a bilateral pair of knoblike bosses, more or less cylindrical in shape and directed anterad; or at least a distinct longitudinal ridge or swelling medial and parallel to, and distinct from, each temporal crest (Domning & Aguilera, 2008: #45).
54. Intertemporal constriction: [0] strong, intertemporal region distinctly constricted, narrower than cranial cavity; [1] weak, intertemporal region wide and about as broad as cranial cavity (modified after Domning & Thomas, 1987: #1).
55. Maximum intertemporal constriction: [0] behind the centre of the skull roof; [1] approximately at the centre of the skull roof (modified after Domning & Thomas, 1987: #1).
56. Temporal crests: [0] more prominent on parietal than on frontal; [1] as prominent on frontal as on parietal (modified after Sagne, 2001b: #17).
57. Temporal crests: [0] prominent, forming distinct keels; [1] weak, only slightly pronounced (Sagne, 2001b: #16).
58. Orbitotemporal crest: [0] present; [1] absent (modified after Sagne, 2001b: #18 and Domning *et al*., 1994: #41).
59. Orbitotemporal crest prominent forming a distinct ridge: [0] present; [1] absent (modified after Sagne, 2001b: #18).
60. *Lamina orbitalis* of frontal thickened (about 1 cm) forming the anterior medial wall of temporal fossa: [0] absent; [1] present (modified after Domning, 1994: #38).

Parietal

61. Parietal roof: [0] convex; [1] more or less flat between temporal crests (modified after Sorbi, 2007: #45).
62. External sagittal crest: [0] present; [1] absent (Domning, 1994: #51).
63. Frontal processes of parietal: [0] short, do not exceed half the length of interfrontal; [1] long, do extend half the length of interfrontal (Sagne, 2001b: #20).
64. Proportions of cranial roof according to ratio l_{FP}/w_{SO}: [0] exceeding ratio of 2; [1] below ratio of 2 (Sagne, 2001b: #22; Table 4).
65. Parietal longer than frontal in midline: [0] present; [1] absent (**new**).
66. Frontal longer than parietal in midline: [0] absent; [1] present (**new**).
67. Frontal as long as parietal in midline: [0] absent; [1] present (**new**).
68. Bony *falx cerebri* keeping its height along the length of parietal: [0] absent; [1] present (**new**).
69. Bony *falx cerebri* flattening out in anterior direction: [0] present; [1] absent (**new**).
70. Internal occipital spine of *falx cerebelli*: [0] absent; [1] present (**new**).
71. Tentoric process and *tentorium osseum*: [0] present; [1] absent (**new**).
72. *Tentorium osseum* well developed forming a transverse ridge: [0] absent; [1] present (**new**).

Table 4. Examples of the ratio l_{FP}/w_{SO} (frontoparietal length / supraoccipital width) for selected taxa. Measurements in mm (preserved dimensions in parentheses); "e" indicates estimated dimensions.

Taxon	Collection number	l_{FP}	w_{SO}	Ratio
Prorastomus sirenoides	NHMUK PV M44897	125	(56)	(2.23)
Protosiren fraasi	FIS M3742	140	76	1.8
	FIS M3743	(133)	78	(1.7)
Protosiren smithae	USNM 94810	160	90	1.77
Eosiren libyca	SMNS 44008	(164)	(64)	(2.56)
Eotheroides lambondrano	UA 9046	(107)	52	(2.1)
Eotheroides aegyptiacum	SMNS 44000	133	56	2.4
Ashokia antiqua	GIS K60/448	195	(78)	(2.5)
Prototherium veronense	MGPD-10Z	157	63	2.5
Trichechus manatus	MB Ma. 17377	153	95	1.6
Trichechus senegalensis	MB Ma. 69335	177	106	1.7
Trichechus inunguis	MB Ma. 35807	138	81	1.7
Anomotherium langewieschei	DM 327	(155)	(110)	(1.4)
Miosiren kocki	IRSNB M.136	(210)	(99)	(2.12)
Gen. nov. 1 *taulannense*	RGHP D040	147	73	2.02
Gen. nov. 2 *bronni*	SMNS 1539	154	80	1.93
	CDGG S1	173	89.5	1.93
Gen. nov. 2 spec. nov. 1	BSPG 1956 I 540	141	68	2.07
	FIS M8002	189	72	2.6
Gen. nov. 3 *cristolii*	LI 1926/394	165	85	1.94
Corystosiren varguezi	IGM 4569	180	128e	(1.4)
Dioplotherium allisoni	MPEG 63-V	(146)	84e	(1.7)
Caribosiren turneri	UCMP 38722	137	(61)	2.25
Metaxytherium floridanum	SDSM 12470	172	84	2.04
Metaxytherium arctodites	FCM 3639	(162)	90	(1.8)
Metaxytherium crataegense	AMNH 26838	143	89	1.6
Crenatosiren olseni	UF/FGS V6094	112	70	1.6
	ChM PV5437	119	61	1.95
Dioplotherium manigaulti	UF 95615	176	80	2.2
Dugong dugon	MB Ma. 69313	140	81	1.7
Bharatisiren kachchhensis	LUVP/MP 1032	(183)	97	(1.89)
Hydrodamalis cuestae	UCMP 86433	240	131	1.8
Hydrodamalis gigas	AMNH 14271	210	167	1.25

Lacrimal

73. Lacrimal: [0] well developed filling the space between frontal and jugal; [1] reduced, present in the anterodorsal rim of the orbit (modified after Domning, 1994: #91).
74. Contact between lacrimal and premaxilla: [0] absent; [1] present at lateral surface of nasal process of premaxilla (Sagne, 2001b: #24; corresponds to newly introduced #93 from Bajpai *et al*., 2010).
75. Nasolacrimal canal: [0] present; [1] absent (modified after Domning, 1994: #91).

Jugal

76. Preorbital process of jugal: [0] absent; [1] present (modified after Sorbi, 2007: #88).
77. Preorbital process of jugal thick and robust (breadth ≤ thickness): [0] absent; [1] present (modified after Domning, 1994: #88).
78. Contact between jugal and premaxilla: [0] absent; [1] present (Domning, 1994: #87).
79. Contact between jugal and lacrimal: [0] absent; [1] present (**new**).
80. Ventral extremity of jugal lies posterior to orbit: [0] present; [1] absent (modified after Domning, 1994: #85).
81. Ventral extremity of jugal lies approximately under posterior edge of orbit: [0] absent; [1] present (modified after Domning, 1994: #85).
82. Ventral extremity of jugal lies ventral to orbit: [0] absent; [1] present (modified after Domning, 1994: #85).
83. Posterior (zygomatic) process of jugal: [0] as long as or longer than diameter of orbit; [1] shorter than diameter of orbit (Domning, 1994: #89).
84. Postorbital process of jugal: [0] absent; [1] present (modified after Domning, 1994: #85).
85. Orbit nearly or completely closed by frontojugal (postorbital) bar: [0] absent; [1] present (**new**).
86. Ventral rim of orbit: [0] does not distinctly overhang lateral surface of jugal, where such a surface is present below orbit; [1] does distinctly overhang (Bajpai & Domning, 1997: #90).

Squamosal

87. Squamosal: [0] does not extend to temporal crest; [1] extends to temporal crest (Domning, 1994: #76).
88. Temporal crests: [0] reach nuchal crest, not interrupted by squamosal; [1] interrupted by squamosal, which form conspicuous indentations in posterior corners of parietal roof (Domning & Thomas, 1987: #8).
89. Lateral shape of zygomatic process: [0] longish to oval, does not taper in anterior direction; [1] triangular and tapering in anterior direction (redefined after Sagne, 2001b: #29).
90. Medial side of zygomatic process: [0] flat to concave; [1] markedly swollen forming a vertical wall (modified after Domning, 1994: #84).
91. Dorsal margin of zygomatic process: [0] not distinctly inclined inward forming a nearly straight ridge; [1] distinctly inclined inward forming a sigmoid ridge (modified after Domning, 1994: #84).
92. Posterior end of zygomatic root having a distinct notch: [0] absent; [1] present (modified after Furusawa, 2004: #17).
93. Arrangement of glenoid fossa and *tuberculum* on ventral articulation surface of zygomatic process: [0] elongated transversely; [1] rounded (**new**).

94. Glenoid fossa: [0] shallow, ventral articulation surface nearly flat; [1] deep concavity (**new**).
95. *Tuberculum*: [0] low convexity, only slightly differentiated from ventral articulation surface; [1] prominent bump rising above level of ventral articulation surface (**new**).
96. Postglenoid process: [0] distinct; [1] weak forming a slight swelling (**new**).
97. Shape of postglenoid process: [0] longish in transversal plane; [1] knob-like (**new**).
98. Posterodorsal end of zygomatic process: [0] straight to concave; [1] convex (modified after Domning & Thomas, 1987: #16).
99. Sigmoid ridge of squamosal: [0] absent; [1] present (modified after Domning, 1994: #74).
100. Sigmoid ridge of squamosal prominent, visible in posterior view of the skull: [0] absent; [1] present (modified after Domning, 1994: #74).
101. *Processus retroversus* moderately inflected: [0] absent; [1] present (modified after Domning, 1994: #77).
102. *Processus retroversus* strongly inflected: [0] absent; [1] present (modified after Domning & Aguilera, 2008: #77).

Notes/remarks: The evaluation of the conditions “moderately” and “strongly” inflected appears to be somewhat subjective, because the degree of inflection of the *processus retroversus* cannot be set in relation to a specific parameter. However, the investigated taxa and specimens that are the subjects of the present study reveal that an unambiguous distinction between both characters is possible and hence the taxa themselves provide a proper benchmark. A moderate inflection of the *processus retroversus* is the case in the taxa and specimens belonging to the *“Halitherium”*-species complex, for example. By contrast, the crown group sirenians *Dugong* and *Nanosiren* possess a *processus retroversus* that is strongly inflected indicated by an anterotransversal notch on the posterior ventral side of the zygomatic process.

103. *Processus retroversus* not inflected: [0] absent; [1] present (modified after Domning, 1994: #77).
104. External auditory meatus: [0] short mediolaterally (≤ 1 cm); [1] long mediolaterally (> 1 cm) (redefined after Domning, 1994: #75).
105. External auditory meatus narrow and slitlike (anteroposterior breadth less than dorsoventral height): [0] present; [1] absent (modified after Domning, 1994: #82).
106. External auditory meatus about as wide anteroposteriorly as high: [0] absent; [1] present (modified after Domning, 1994: #82).
107. External auditory meatus very broad and shallow (wider anteroposteriorly than high): [0] absent; [1] present (modified after Domning, 1994: #82).
108. Posttympanic process: [0] present, with ventral extremity projecting ventrad or anteroventrad for sternomastoid muscle; [1] absent, sloping against the paroccipital process of the exoccipital (modified after Domning, 1994: #73).

109. Posttympanic process enlarged and clublike: [0] absent; [1] present (modified after Domning, 1994: #73).

Notes/remarks: An enlarged and clublike posttympanic process defines an autapomorphy of *Miosiren kocki* and is a special variant of character state 108[0]. In this condition the process is very clearly present with its extremity for the sternomastoid muscle not projecting anteroventrad, but ventrad. Consequently, it is distinctly separated from the paroccipital process. Therefore, Domning's (1994) original multi-state character 73 is split into two binary characters that are treated separately in the cladistic analyses performed in this study.

110. Mastoid foramen: [0] absent; [1] present (**new**).
111. Mastoid foramen defined by squamosal and exoccipital under exclusion of supraoccipital: [0] absent; [0] present (**new**).

Occipital

112. Size of supraoccipital: [0] height distinct, only slightly wider than high (w/h < 1.5); [1] enlarged transversally, wider than high (w/h > 1.5) (Sagne, 2001b: #34).

Notes/remarks: To differentiate between a transversally wide or narrow supraoccipital, the ratio of width to height of this bone introduced by Domning (e.g., 1988, 1989a) is used. For some taxa, like *Metaxytherium floridanum* (Domning, 1988) or *M. krahuletzi* (Domning & Pervesler, 2001), intraspecific variability is stated with ratios that vary from 1.3 to 1.92 and from 1.16 to 1.63, respectively. Therefore, this potential character might not have been applied in the phylogenetic analysis by Domning (1994). However, all taxa but one can be scored unambiguously in this study (Appendix 4). The reassessment of taxa during this project does not confirm a range of the width to height ratio of the supraoccipital to such an extent as proposed in the studies by Domning (1988) and Domning & Pervesler (2001), for example. Supraoccipitals of *M. floridanum* are known from several specimens, for which ratios are calculated that slightly exceed 1.5 at least. Variation of the ratio is constricted when non-adult individuals and only estimated measurements that may disguise the real conditions are excluded from the calculation. Therefore, mainly individuals of adult age and measurements reflecting complete distances were considered (Table 5). *Metaxytherium krahuletzi* is scored polymorphic according to personal investigations on a limited number of accessible supraoccipitals and, hence, supplemented by data from literature.

113. Nuchal crest: [0] narrow and sharp-edged; [1] thickened (**new**).
114. Nuchal crest: [0] convex (forming the dorsolateral ends of the supraoccipital); [1] short, reaching as far as squamososupraoccipital suture (modified after Domning & Thomas, 1987: #15).
115. Nuchal crest notched in median plane: [0] absent; [1] present (**new**).
116. External occipital protuberance: [0] weak, not differentiated from external occipital crest; [1] prominent knob (**new**).

Table 5. Examples of the ratio width to height of the supraoccipital for selected taxa. Measurements in mm (preserved dimensions in parentheses).

Taxon	Collection number	Width	Height	Ratio
Eotheroides lambondrano	UA 9046	52	44	1.18
Eotheroides aegyptiacum	SMNS 44000	56	42	1.3
Ashokia antiqua	GIS K60/448	(78)	(52)	(1.5)
Prototherium veronense	MGPD-10Z	(63)	(63)	(1)
Prototherium intermedium	MGPD-28997	62	48	1.29
Gen. nov. 1 *taulannense*	RGHP D040	73	44	1.65
Gen. nov. 2 *alleni*	MCZ 17142	75	48	1.56
	YPM 21335	(75)	(50)	(1.5)
Gen. nov. 2 spec. nov. 1	BSPG 1956 I 540	68	(45)	(1.51)
	FIS M2597	65	37	1.75
	MNHM PW 1949/157	68	44	1.55
	MNHM PW 1991/66-LS	75	45	1.66
Gen. nov. 2 *bronni*	CDGG S1	88	50	1.76
	FMD SRK Eck-Rat 43	90	55	1.64
	SMNS 1539	80	49	1.63
	FIS M8385	78	50	1.56
Gen. nov. 3 *cristolii*	LI 1926/394	83	61	1.36
Gen. nov. 4 *bellunense*	MGPD-18Z–23Z, 7358Z–7387Z	83	61	1.36
Anomotherium langewieschei	DM 327	(110)	60	(1.8)
Miosiren kocki	IRSNB M.136	(99)	(40)	(2.5)
Trichechus manatus	MCZ 1791	98	47	2.1
Trichechus senegalensis	MNHN 1885-673	103	51	2.0
Dioplotherium allisoni	MPEG 64-V	93	65	1.4
Dioplotherium manigaulti	UF 95615	80	62	1.29
Metaxytherium floridanum	USNM G-544	101	62	1.63
Metaxytherium arctodites	FCM 3639	90	64	1.4
Metaxytherium crataegense	AMNH 26838	89	56	1.59
Bharatisiren kachchhensis	LUVP/MP 1032	97	(56)	(1.7)
Crenatosiren olseni	UF/FGS V6094	70	50	1.4
Nanosiren sanchezi	UNEFM-VF-041	63	39	1.6
Kutchisiren cylindrica	GSI-K60/998	(76)	(68)	(1.1)
Dugong dugon	MB Ma. 69313	86	48	1.79
Dusisiren takasatensis	TA 1–5	142	39	3.6

117. Muscle insertions: [0] rounded; [1] indistinct (**new**).
118. External occipital crest: [0] forming a distinct ridge; [1] relatively broad and undefined laterally (**new**).
119. Length of external occipital crest: [0] exceeds half the height of supraoccipital or even longer ending in ventral margin; [1] reaching half the height of supraoccipital or less (**new**).

120. Transverse sulcus: [0] present; [1] absent (modified after Furusawa, 2004: #20).
121. Exoccipitals: [0] meet in a suture dorsal to *foramen magnum*; [1] do not meet in a suture (Domning, 1994: #66).
122. Supracondylar fossa of exoccipitals shallow, only slightly differenciated from rear surface of exoccipitals above condyle, and not extending across entire width of occipital condyle: [0] absent; [1] present (modified after Domning, 1994: #67).
123. Supracondylar fossa of exoccipitals deep, forming distinct concavity on rear surface of exoccipitals above condyle, and extending across entire width of occipital condyle: [0] absent; [1] present (modified after Domning, 1994: #67).
124. Dorsolateral border of exoccipital rounded and more or less smooth, not flangelike: [0] present; [1] absent (modified after Domning, 1994: #70).
125. Dorsolateral border of exoccipital thick and overhanging posteriorly as a flange: [0] absent; [1] present (modified after Domning, 1994: #70).
126. Dorsolateral border of exoccipital greatly thickened, forming rugose overhanging flange: [0] absent; [1] present (modified after Domning, 1994: #70).
127. Hypoglossal (= condyloid) foramen: [0] surrounded by bone; [1] having the tendency to be replaced by a shallow groove or forming a notch (modified after Domning & Aguilera, 2008: #72).
128. Sphenooccipital eminences: [0] concave; [1] convex (modified after Sagne, 2001b: #37).
129. Dorsal limit of *foramen magnum*: [0] at level of occipital condyles; [1] above level of occipital condyles (Sagne, 2001b: #38).
130. *Foramen magnum*: [0] rounded; [1] triangular, having a dorsal peak (modified after Furusawa, 2004: #12).
131. Paroccipital process of exoccipital: [0] long, does reach as far ventrally as occipital condyle or longer; [1] short, does not reach as far as occipital condyle (modified after Sorbi, 2007: #65).

Sphenoid

132. Alisphenoid canal: [0] present; [1] absent (Domning, 1994: #101).
133. *Foramen ovale*: [0] enclosed by bone; [1] opened to form a notch or incisure (Domning, 1994: #103).

Pterygoid

134. Pterygoid fossa: [0] extending above level of roof of internal nares; [1] confined to below roof of internal nares (modified after Bajpai & Domning, 1997: #102).
135. Hamuli processes: [0] absent; [1] present (Sagne, 2001b: #42).

Periotic

136. Periotic: [0] fused to alispenoid; [1] not fused with any other skull bone, set in closely fitting socket in squamosal (Domning, 1994: #115).

Mandible

137. Mandibular symphysis: [0] laterally compressed; [1] broad, forming a bulbous chin (modified after Domning, 1994: #121).
138. Masticating surface: [0] narrow, scarcely wider than the two rows of tooth alveoli it bears; [0] broad (modified after Domning, 1994: #121).
139. Masticating surface with a median furrow: [0] absent; [1] present (modified after Sagne, 2001b: #48).
140. Accessory mental foramina: [0] present, in addition to and usually posterior to the large principal foramen; [1] absent (Domning, 1994: #123).
141. Mental foramen: [0] at level of symphysis; [1] far back caudally (Furusawa, 2004: #31).
142. Size of symphysis: [0] as long as high or longer; [1] higher than long (Sagne, 2001b: #50; Table 6).

Table 6. Examples of dimensions of the mandibular symphysis for selected taxa. Measurements in mm (preserved lengths in parentheses).

Taxon	Collection number	Length	Height
Prorastomus sirenoides	NHMUK PV M44897	73	39
Protosiren smithae	USNM 94810	(70)	(64)
Eosiren libyca	SMNS 44008	79.5	79
Prototherium intermedium	MGPD-28997	(40)	(66)
Gen. nov. 1 *taulannense*	RGHP C001	64	77
	RGHP E.7.096a	69	81
Gen. nov. 2 *bronni*	CDGG S1	(63)	89
	SMNS 47736	69	82
Gen. nov. 2 spec. nov. 1	BSPG 1956 I 540	64	75
	CDGG S3	62	(63)
Gen. nov. 3 *cristolii*	LI 2012/1	(82)	110.5
	LI 1939/257	90	120
Anomotherium langewieschei	DM 327	83	100
Trichechus manatus	MCZ 1791	81	69
Trichechus senegalensis	MNHN 1885-673	95	71
Metaxytherium arctodites	FCM 3639	107	144
Metaxytherium crataegense	AMNH 26838	(67)	87.5
Kutchisiren cylindrica	GSI-K60/998	(81)	115
Dugong dugon	MB Ma. 69313	79	122
Dusisiren jordani	UCMP 77037	126	141
Hydrodamalis cuestae	UCMP 23001	172	147
Hydrodamalis gigas	NRM A608459	161	137

143. Straight or only slightly concave ventral border of horizontal mandibular ramus: [0] present; [1] absent (modified after Domning, 1994: #122).
144. Moderately concave and anteriorly sharply downturned ventral border of horizontal mandibular ramus: [0] absent; [1] present (modified after Domning, 1994: #122).
145. Moderately and evenly concave ventral border of horizontal mandibular ramus: [0] absent; [1] present (modified after Domning, 1994: #122).
146. Strongly concave ventral border of horizontal mandibular ramus: [0] absent; [1] present (modified after Domning, 1994: #122).
147. Ventral border of horizontal ramus of mandible: [0] tangent to angle; [1] not tangent to angle (Domning, 1994: #129).
148. Articulation surface of condyle: [0] as broad medially as laterally; [1] narrower medially than laterally (Sagne, 2001b: #53).
149. Posterior border of mandible: [0] with a distinct steplike process (*processus angularis superior*) below condyle; [1] without a distinct *processus angularis superior*, but with broadly convex outline beginning well below condyle (modified after Domning, 1994: #125).

Notes/remarks: Domning (1994) originally established a multi-state character for the evaluation of the posterior border of the mandible. The plesiomorphic character state "descends ventrally or posteroventrally from condyle without marked interruption or abrupt change of direction" designates an autapomorphy of *Prorastomus sirenoides* in Domning's (1994) phylogenetic study. However, Savage *et al.* (1994) and personal observations reveal the posterior mandibular border in *Prorastomus* to be broken to such an extent that no judgement on its direction can objectively be made. As a consequence, Domning's (1994) multi-state character is treated here as binary by scoring *Prorastomus* 149[?].

150. Anterior border of coronoid process approximately vertical: [0] present; [1] absent (modified after Domning, 1994: #126).
151. Anterior border of coronoid process extends slightly anterior to base of process: [0] absent; [1] present (modified after Domning, 1994: #126).
152. Anterior border of coronoid process extends very far anterior to base of process, forming an angle of about 45° towards the longitudinal axis of the tooth arcade: [0] absent; [1] present (modified after Domning, 1994: #126).
153. Size of coronoid foramen: [0] reduced; [1] enlarged, diameter > 3 mm (modified after Sagne, 2001b: #56).
154. Mandibular foramen: [0] undivided; [1] having the tendency to separation (modified after Sagne, 2001b: #57).
155. Mandibular dental capsule: [0] completely enclosed by bone of mandible; [1] exposed posteroventrally (modified after Domning, 1994: #127).

156. Horizontal ramus of mandible: [0] slender (minimum dorsoventral height < 0.25 x length of mandible); [1] broad dorsoventrally (height ≥ 0.25 x length of mandible) (Domning, 1994: #128).

Dentition

157. I1 alveolus extends less than half the length of the premaxillary symphysis: [0] present; [1] absent (modified after Domning, 1994: #140).
158. I1 alveolus extends about half the length of the premaxillary symphysis: [0] absent; [1] present (modified after Domning, 1994: #140).
159. I1 alveolus extends more than half the length of the premaxillary symphysis: [0] absent; [1] present (modified after Domning, 1994: #140).
160. First upper incisor with enamel mainly on medial side, not forming a complete crown with enamel on all sides: [0] absent; [1] present (modified after Domning, 1994: #142).

Notes/remarks: Domning (1994) introduced a further character (#136) considering a first upper incisor with enamel mainly on the lateral side as an autapomorphy of *Prorastomus sirenoides*. This character doesn't find consideration in this study, because it was established on the basis of an isolated find of a tusk from Jamaica that was referred to *P. sirenoides* by Savage *et al.* (1994). As outlined before, this tusk is neither known from the type locality of *P. sirenoides* nor is an incisor tusk preserved in the holotype specimen and, therefore, it cannot be certainly assigned to this taxon. Additionally, Savage *et al.* (1994) only tentatively identified the fragment of a tooth as representing the right upper incisor. For these reasons, this tooth is excluded for the evaluation of *P. sirenoides* as is the character 136 from Domning (1994).

161. I1 with suboval or subelliptical cross section of crown: [0] present; [1] absent (modified after Domning, 1994: #141).
162. I1 with lens-shaped or lozenge-shaped cross section of crown: [0] absent; [1] present (modified after Domning, 1994: #141).
163. I1 with broad and extremely mediolaterally flattened cross section of crown: [0] absent; [1] present (modified after Domning, 1994: #141).
164. Second and third upper incisors: [0] present; [1] absent (modified after Domning, 1994: #143).

Notes/remarks: Domning's (1994) character 143 also considers the presence (at least in part) and absence of the lower first to third incisors. In this study, the evaluation of the lower incisors is disregarded for two reasons. The masticating surface of the mandible often does not preserve the single alveoli in such quality that definitive judgement especially on the partial absence or presence of lower incisors is possible. Therefore, the lower dental formula is evaluated under reserve only, mainly distinguishing between alveoli for permanent or vestigial teeth. On the contrary, the single alveoli are mostly well identifiable

on the upper jaw or premaxilla, respectively. As character 164 reflects indirectly on the development of first incisor tusks in toothed sirenians focus is lain here only on the evaluation of the upper premaxillar dentition.

165. First upper incisor with enamel extending entire length of tusk, without enamel crown distinct from root: [0] absent; [1] present (modified after Domning, 1994: #137).
166. Canines: [0] present; [1] absent (modified after Domning, 1996: #144).
167. Permanent P1/p1: [0] present; [1] absent (modified after Domning, 1994: #157 and Domning *et al*., 1994: #145).
168. Permanent P2/p2: [0] present; [1] absent (modified after Domning, 1994: #157 and Domning *et al*., 1994: #145).
169. Permanent P3/p3: [0] present; [1] absent (modified after Domning, 1994: #157 and Domning *et al*., 1994: #145).
170. Permanent P4/p4: [0] present; [1] absent (modified after Domning, 1994: #157 and Domning *et al*., 1994: #145).
171. Permanent P5/p5: [0] absent; [1] present (modified after Domning, 1994: #146).

Notes/remarks: Several studies, such as Savage *et al.* (1994), noted that it is still debated whether the presence of a fifth permanent premolar in some Eocene Sirenia is a synapomorphy of the order and represents a reversal of a previous loss of P5/p5 as assumed by Domning (1994), or a retention of a plesiomorphic eutherian condition (e.g., Domning *et al*., 1982, 1986). In contrast to the results of his cladistic analysis on Sirenia, Domning (1994) designated the presence of a fifth permanent premolar as the plesiomorphic condition of his character 146. This would imply that the outgroup taxa chosen by Domning (1994), the proboscidean *Moeritherium* and the desmostylian *Paleoparadoxia*, possess five premolars as well. However, this is not the case (e.g., Gheerbrant, 2009; Domning & Pyenson, 2008). Additionally, Domning's (1994) interpretation of a permanent fifth premolar as a synapomorphy of the order Sirenia cannot be maintained according to his scoring of the two outgroup members (#146[0]), which instead argues for the hypothesis of the retention of P5/p5 as a plesiomorphic trait.

In this study, the absence of P5/p5 within toothed Sirenia is defined by no replacement at the P5/p5 loci according to the definition of a permanent premolar and Domning's (1994) character state 146[1]. As a result, single-rooted P5/p5 are not developed, but instead the three-rooted deciduous and molariform DP5/dp5 are retained.

Character 171 also contains the revision of Domning's (1994) character 155 on the postcanine dental formula. Therein, Domning (1994: 180) designates the plesiomorphic condition to be "P1–4, M1–3" and the derived state, characterising the order Sirenia, to be "P1–5, M1–3, or secondarily reduced from this condition by loss of anterior premolars". The latter does not only stand in contradiction to Domning's (1994) character 146, wherein he scores the fifth permanent premolar to be the retention of a plesiomorphic trait. Furthermore, the definition of that character state contains a subjective *á priori* interpretation.

172. Some permanent premolars double- or triple-rooted: [0] present; [1] absent (modified after Domning, 1994: #157).
173. All permanent premolars single-rooted: [0] absent; [1] present (modified after Domning, 1994: #157).
174. M3 with small posterior basin enclosed by a single cusp or ridge only: [0] present; [1] absent (modified after Sagne, 2001b: #63).
175. M3 with large posterior basin enclosed by several cusps: [0] absent; [1] present (modified after Sagne, 2001b: #63).
176. Hypocone and metaconule of M3 coalescent: [0] present; [1] absent (modified after Sagne, 2001b: #64).
177. Hypocone and metaconule of M3 separated by a distinct furrow: [0] absent; [1] present (modified after Sagne, 2001b: #64).

Notes/remarks: The cusp pattern of the sirenian molars was shown to be variable according to the studies by, for example, Domning (1988) and Domning & Pervesler (2001). Therefore, these authors stated discrepancies with regard to the cusps homologies. Characters 176 and 177 refer to the distal transverse ridge, the metaloph, of M3 consisting of the hypocone lingually, the metacone buccally and the central metaconule following the general terminology of mammalian molars provided by Thenius (1989). This is supported by Domning (1978), who used the study from Reinhart (1959) as a basis of comparison to clarify his terminology. In contrast to Reinhart (1959), Domning (1978) considered the three cusps of the metaloph of M3 to form a more or less transverse arrangement that does not include posterior cingular cusps that often define a posterior basin. This terminology was not consistently applied by, for example, Domning & Pervesler (2001), who omitted clarification of the homology of the cusps of M3 in *Metaxytherium krahuletzi*. However, personal investigations argue for a clear and merely descriptive terminology according to Thenius (1989) and Domning (1978), especially when fully erupted and unambiguously determined third upper molars are used. Accordingly, the metaconule is considered to be coalesced with the hypocone when the metaloph consists of only two cusps by omitting any posterior cingular cusps that might be present.

178. Hypocone and metaconule of M2 nearly transversally directed: [0] present; [1] absent (modified after Sagne, 2001b: #65).
179. Transverse valley of M2 obstructed by metaconule: [0] absent; [1] present (modified after Sagne, 2001b: #65).
180. Supernumerary molars: [0] absent, [1] present and replenished indefinitely by horizontal replacement (Domning, 1994: #150).
181. Functional cheek teeth in adult: [0] present; [1] absent (modified after Domning, 1994: #151).
182. Molars conspicuously reduced in size relative to skull and mandible: [0] absent; [1] present (modified after Domning, 1994: #158).

Scapula

183. Proximal rugosity of scapular spine: [0] thickened; [1] hardly or not differentiated from scapular spine (Sagne, 2001b: #67).
184. Relative length of scapular spine: [0] elongated, exceeding half the total length of scapular blade and nearly reaches dorsal margin; [1] shortened, ending well before dorsal margin, confined to about half the length of scapular blade (modified after Sagne, 2001b: #68).
185. Coracoid process: [0] weak or moderately developed forming a slight bump; [1] strongly developed forming a true process (modified after Sagne, 2001b: #69).
186. Supraspinous fossa: [0] only slightly larger than or nearly as large as infraspinous fossa; [1] distinctly larger than infraspinous fossa (modified after Sagne, 2001b: #70).
187. Shape of scapula: [0] relatively slender, longish or sickle-shaped; [1] anteroposteriorly broad and plate-like (**new**).
188. Acromion: [0] at level of the neck; [1] extends up to glenoid cavity (Furusawa, 2004: #18).

Humerus

189. Size of humerus: [0] slender with tapered epiphyses; [1] compact with distinctly projecting epiphyses (Sagne, 2001b: #71).
190. Height of greater tubercle: [0] at level of humerus head; [1] distinctly elevated above humerus head (Sagne, 2001b: #71).
191. Inclination of distal articulation facet from proximodistal axis: [0] weak, distal articulation facet almost perpendicular; [1] strong (Sagne, 2001b: #73).

Radius and Ulna

192. Anteroposterior flattening of diaphysis of radius: [0] strong, radius more slender anteroposteriorly than ulna; [1] weak, radius as thick as ulna (Sagne, 2001b: #74).
193. Transversal length of diaphysis of radius (below proximal epiphysis): [0] distinctly shorter than ulna; [1] as long as or even longer than ulna (Sagne, 2001b: #75).
194. Diaphyses of radius and ulna: [0] straight; [1] curved medially (Furusawa, 2004: #11).

Ribs

195. First rib with protuberance ventral to *capitulum*: [0] absent; [1] present (Sagne, 2001b: #77).
196. First rib with extension of distal extremity: [0] strong; [1] weak or even absent (Sagne, 2001b: #78).
197. Rib in cross section: [0] flat ellipse; [1] rounded ellipse (Furusawa, 2004: #3).

Innominate

198. *Acetabulum*: [0] present, forming a distinct concavity; [1] reduced (**new**).
199. *Foramen obturatum*: [0] present; [1] absent (**new**).

Sternum

200. Sternum: [0] consisting of sternebrae; [1] fused to a single element. (**new**)
201. Anterior process of manubrium: [0] present; [1] absent (modified after Furusawa, 2004: #5).
202. Ventral keel of manubrium: [0] present; [1] absent (**new**).

Phylogenetic analyses

The following section offers six phylogenies documenting the process by which the results of cladistic treatment of the sirenian taxa under consideration in this study were obtained. The phylogentic analyses A–C are based on cranial and dental characters for direct comparison with the analysis developed by Domning (1994) and the subsequent phylogenetic analyses D–F. The latter are expanded to include postcranial characters as well. The phylogenetic approach F represents the final sirenian analysis employing 202 binary characters and 52 ingroup taxa in addition to one outgroup-complex.

As indicated in chapter “Material and Methods”, the original dataset contains 56 sirenian species, including three invalid species (*“H.” bronni*, *“H.” abeli* and *“H.” pergense*), and ten specimens originally assigned to *“H. schinzii”*. In addition to *M. subapenninum*, this dataset was reduced by three species that were successively deleted *á posteriori* before the final analysis of the sirenian interrelationships. The respective taxa *Eotheroides babiae* and *“Halitherium antillense”* are known only from a few mandibular and dental characters, whereas the invalid species *“Halitherium” pergense* is based on an incomplete skull roof. When these three species were retained in the analysis, results showed varying topologies and an unusually high number of cladograms (up to 1,000 cladograms result from a heuristic search with 1,000 trees kept). Additionally, the ingroup is characterised by a high degree of polytomies, which is related to the paucity of morphological information in the respective species (see Appendix 4).

The phylogenetic analyses A–F are preceded by a test of the analysis of Sirenia presented by Domning (1994) in order to show what results can be expected by applying criteria that are as objective as possible.

Test of Domning’s (1994) cladistic analysis

Domning (1994) presented the most comprehensive cladistic analysis of the Sirenia so far including 36 species and subspecies and 62 informative cranial and dental charac-

ters. By means of the Hennig86 software, 60 equally most parsimonious trees (MPTs) were produced with a tree length (TL) of 152 steps, a consistency index (CI) of 0.55, and a retention index (RI) of 0.91. By successive character weighting and ordering of all multistate characters except for three, Domning (1994) reduced the tree number to six MPTs, of which he finally presents the Nelson consensus tree with a TL of 162, a CI of 0.76, and a RI of 0.91. Domning (1994) also introduced a statistically-based method for scoring intraspecific variation, because Hennig86 does not accept multiple states of a character for a given taxon. This procedure resulted in the arbitrary scoring of some characters. The method of scoring polymorphisms unambiguously as one of two states is arbitrary and does not reflect the “true” evolutionary history of a respective taxon. As outlined before, another source for subjectivity is that Domning (1994) also considered skeletal material, which is not certainly assignable to any particular taxon.

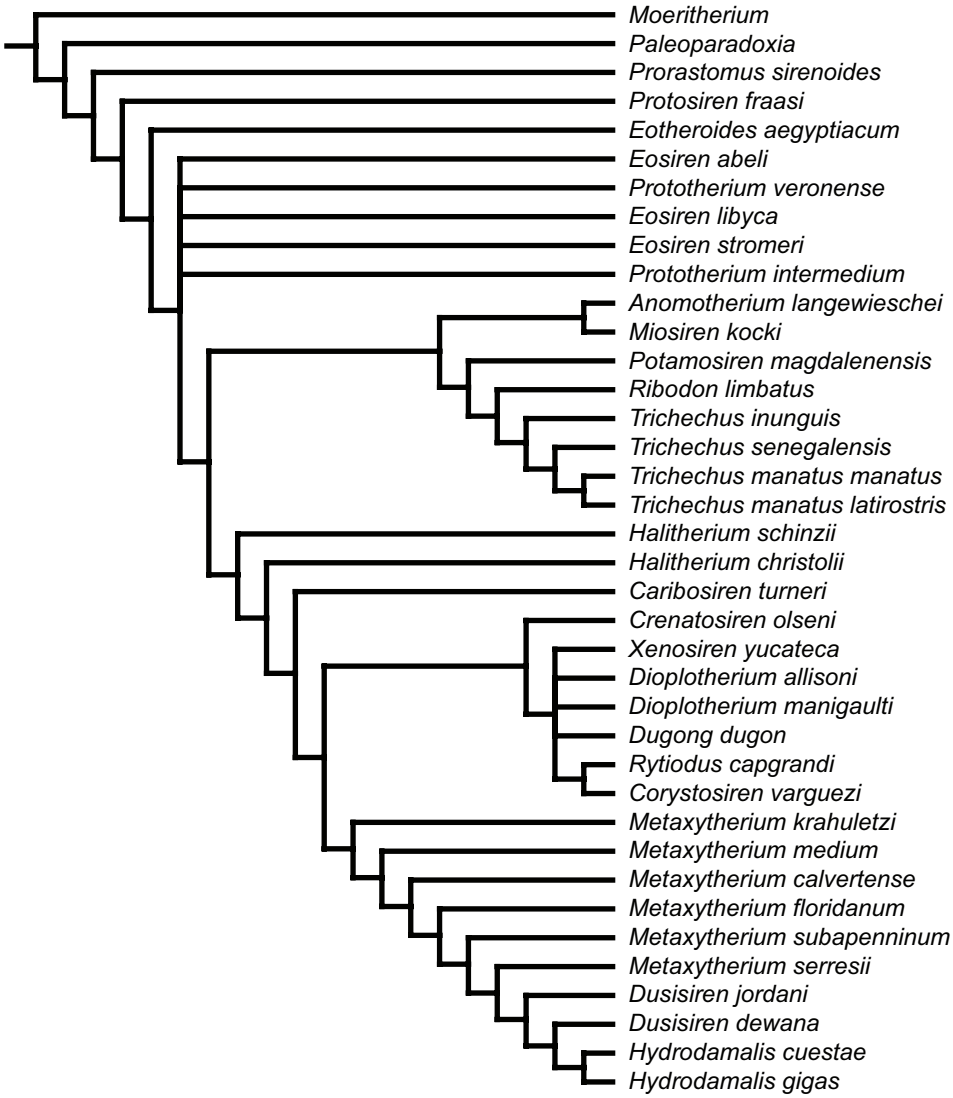

Figure 68. The strict consensus tree from 25 equally most parsimonious trees resulting from a test of Domning’s (1994) phylogenetic analysis employing unweighted and unordered characters (TL = 151, CI = 0.53, RI = 0.79).

Although Domning (1994) stated that his analysis was of a provisional nature and in need of revision in many parts, the resulting classification was retained nearly unrevised in systematic studies of Sirenia up to now. Accordingly, the starting point for a revision of sirenians in general and the genus *Halitherium* in particular was to test Domning's (1994) analysis. This test was conducted using WinClada software implementing NONA by employing the most objective cladistic principles indicating unweighted and unordered characters. Three uninformative characters out of 62 of the original data matrix were found and deleted before analysing the interrelationships of Sirenia. The heuristic search produced 25 MPTs. The strict consensus tree (Fig. 68) has a TL of 151, a CI of 0.53 and a RI of 0.79.

Compared to Domning's (1994) Nelson consensus tree (Fig. 2), the tree length of the test is shorter, indicating that less transformation steps lead to a similar topology. Major differences to the phylogeny of Domning (1994) are the unresolved interrelationships of the Eocene dugongids (*Eosiren* and *Prototherium*) and the Neogene Dugonginae comprising, amongst others, the only living representative, the dugong. The topology of the clade Trichechidae, including the extant genus *Trichechus*, resembles that in Domning's (1994) analysis and is well resolved. Regarding the genus *Metaxytherium*, the tree topology of the test is slightly less polytomous or instable between *M. medium*, *M. calvertense*, and *M. floridanum* than it is in Domning (1994). Still, the genus *Metaxytherium* remains paraphyletic as is the genus *"Halitherium"*.

In conclusion, the phylogeny resulting from the test is more objective, but also more homoplastic and less robust than Domning's (1994) analysis. A lower CI indicates the relative high degree of homoplasies (parallelisms and reversals) in the dataset. The low robustness is revealed by the bootstrap data below 50 % for most of the clades indicating that the respective nodes and monophyletic groups within this phylogeny have statistically only weak support. Additionally, many terminal taxa like *"H." cristolii* and most *Metaxytherium* species are not defined by characters or character combinations, and therefore have the status of paraphyletic meta-species (Rieppel, 1999).

Phylogenetic analysis A

This analysis was conducted with 182 cranial and dental characters applied to an outgroup-complex (*Phosphaterium escuilliei* and *Numidotherium koholense*) and 62 ingroup members including 52 species, two of which are regarded as invalid (*"H." bronni* and *"H." abeli*), and ten specimens traditionally assigned to *"H. schinzii"*. Seven characters were uninformative (characters 1, 20, 23, 76, 79, 109, 110) and therefore deleted. The heuristic search resulted in 12 MPTs. The strict consensus tree (Fig. 69) has a TL of 709 steps, a CI of 0.24 and a RI of 0.67. When repeating the analysis, the number of nodes that collapsed in the strict consensus tree varies between six and eleven resulting in a slightly

different arrangement of species and specimens originally assigned to *"H. schinzii"* (node 15). However, neither the distribution of characters nor the properties of the phylogeny (TL, CI, RI) are affected. Figure 69 shows the strict consensus tree with eight nodes collapsed.

The phylogenetic hypothesis presented here defines the clade Sirenia (node 1) by five synapomorphies (characters 1, 20, 76, 79, 110) such as retracted and enlarged external nares, contact between premaxilla and frontal, and the presence of a preorbital process of the jugal. These synapomorphies thus revealed to be uninformative and were excluded from the analysis. As a result of the cladistic analysis, the Sirenia are divided into a stem group (nodes 1–22) and a crown group (node 23).

The stem group comprises, amongst others, the extinct genera *Prorastomus, Pezosiren, Protosiren, Ashokia, Sirenavus, Eotheroides, Anomotherium*, *Miosiren, Eosiren* and *Prototherium*. Most of the main nodes (2, 3, 5–8, 11, 16, 20) are partially supported by several synapomorphies. In contrast to previous studies (e.g., Domning, 1994), the genera *Protosiren* (node 4) and *Prototherium* (node 19) are revealed to be monophyletic, whereas *Eotheroides* and *Eosiren* remain paraphyletic. The sister grouping of *Anomotherium* and *Miosiren* (node 9) corroborates the clade Miosireninae Abel, 1919 based on e.g. the uniquely derived feature of a thickened *lamina orbitalis* of the frontal (60[1]). However, the clade Trichechidae comprising the Miosireninae and Trichechinae (node 47) as understood by Domning (1994, 1996) is not supported by this analysis.

Additionally, the stem group includes two clades (nodes 12, 22) composed of species and specimens, which were originally referred to the genus *"Halitherium"*. The monophyletic grouping above node 12 defines the species gen. nov. 1 *taulannense* to be the basal sister taxon to a clade (node 13), which includes two monophyletic groups (nodes 14, 15) based on seven derived characters. Node 14 unites five specimens traditionally assigned to *"H. schinzii"* on the basis of one derived and two plesiomorphic characters. The terminal branches of each specimen as well as the sister groupings between the specimens are not defined by characters. The same applies to the grouping above node 15, which is entirely or partially polytomous depending on the results of the repeated analysis and the number of nodes that collapsed in the strict consensus tree. This grouping is characterised by a combination of one plesiomorphic and three derived characters. The polytomy comprises six specimens originally referred to *"H. schinzii"*, one of these representing the species *bronni* (holotype: SMNS 1539). A further branch within this polytomous arrangement is defined by two characters and identifies the species gen. nov. 2 *alleni* originally lumped into the genus *"Halitherium"*.

Node 22 represents the most derived stem group representatives in this phylogenetic hypothesis and unites the species gen. nov. 3 *cristolii* and *abeli* (LI 1939/257 including the holotype) on the basis of one plesiomorphic character. Both terminal branches are not defined by characters.

The crown group (node 23) is subdivided in two major clades, which are united by two synapomorphies referring to a short paroccipital process of the exoccipital and the lack of a fourth permanent premolar. Node 24 defines the first major clade, the Dugonginae as generally understood (Domning, 1994; Domning & Aguilera, 2008). This monophyletic group is composed of 11 taxa: *Crenatosiren, Nanosiren, Dugong, Rytiodus, Corystosiren, Bharatisiren, Domningia, Kutchisiren, Dioplotherium, Xenosiren,* and the species gen. nov. 4 *bellunense*; the latter also previously referred to the genus *Halitherium*. The monophyly of the dugongines is well supported by five synapomorphies, e.g. a frontal roof with a bilateral pair of knoblike bosses, a preorbital process of the jugal that is thick and robust, and a strongly inflected *processus retroversus* of the zygomatic process of the squamosal. The living dugong is well nested within the dugongines as a basal sister taxon to a monophyletic clade above node 28. The sister relationship between the *Dugong* and all dugongines other than *Crenatosiren* and *Nanosiren* (node 27) is uniquely identified by a first upper incisor with enamel mainly on the medial side and enamel extending the entire length of the tusk. Above node 28, a polytomy indicates unresolved interrelationships of *Corystosiren*, *Rytiodus*, and two monophyletic groups (nodes 29, 32), each of the latter defined by one synapomorphy.

The second major clade (node 35) is based on a combination of homoplastic cranial and dental characters such as a small nasal incisure at the posterior end of the mesorostral fossa and a transverse valley of the upper M2 obstructed by the metaconule. This clade includes the paraphyletic genus *Metaxytherium* as already indicated in previous studies (e.g. Domning & Thomas, 1987; Domning, 1994; Sorbi *et al*., 2012), the monospecific genus *Caribosiren*, and two subfamilies as understood by e.g. Domning (1994): the Hydrodamalinae (node 42) and the Trichechinae (node 47). The Hydrodamalinae encompassing the genera *Dusisiren* and *Hydrodamalis* are parapyletic here, in contrast to the phylogenetic results of Domning (1994). While the interrelationships within *Dusisiren* are not completely resolved, which is indicated by a trichotomy above node 43, *Hydrodamalis* is monophyletic (node 46) based on homoplastic and synapomorphic (e.g. presence of a dentiform process) features. In the analysis presented here, *Hydrodamalis* forms the sister group to the Trichechinae (node 45), which is substantiated by a combination of plesiomorphic and apomorphic characters. The Trichechinae (node 47) are monophyletic. Within the Trichechinae, the presence of supernumerary molars characterises the extant genus *Trichechus* and the extinct genus *Ribodon*, both forming a sister group (node 48).

Figure 69. Phylogenetic hypothesis of sirenians conducted by using the heuristic search function with tree-bisection-reconnection of branch swapping. The strict consensus tree of analysis A (TL = 709, CI = 0.24, RI = 0.67) was received from 12 equally most parsimonious trees. Representatives of the former *"Halitherium"*-species complex in bold.

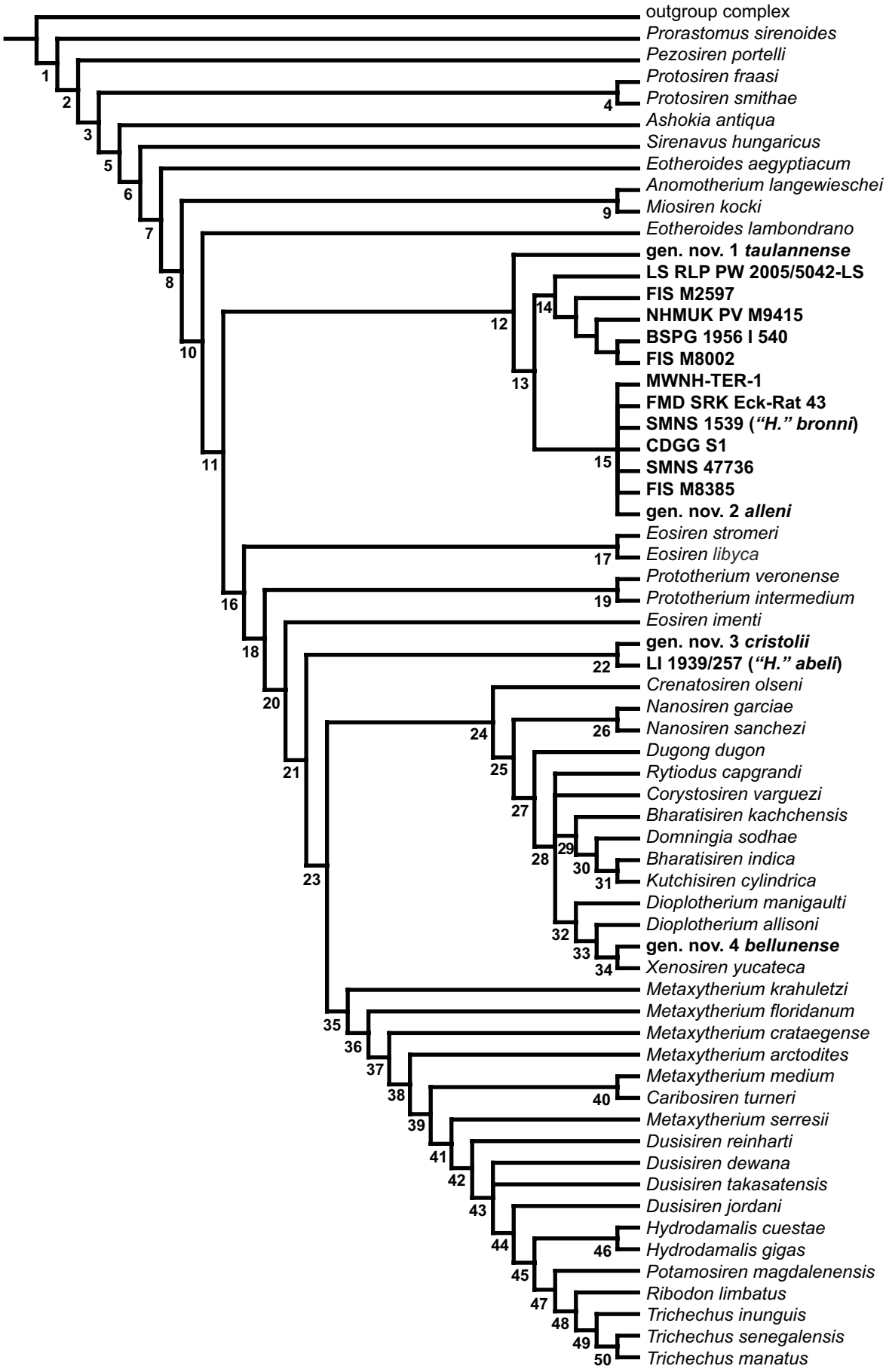
outgroup complex
Prorastomus sirenoides
Pezosiren portelli
Protosiren fraasi
Protosiren smithae
Ashokia antiqua
Sirenavus hungaricus
Eotheroides aegyptiacum
Anomotherium langewieschei
Miosiren kocki
Eotheroides lambondrano
gen. nov. 1 taulannense
LS RLP PW 2005/5042-LS
FIS M2597
NHMUK PV M9415
BSPG 1956 I 540
FIS M8002
MWNH-TER-1
FMD SRK Eck-Rat 43
SMNS 1539 ("H." bronni)
CDGG S1
SMNS 47736
FIS M8385
gen. nov. 2 alleni
Eosiren stromeri
Eosiren libyca
Prototherium veronense
Prototherium intermedium
Eosiren imenti
gen. nov. 3 cristolii
LI 1939/257 ("H." abeli)
Crenatosiren olseni
Nanosiren garciae
Nanosiren sanchezi
Dugong dugon
Rytiodus capgrandi
Corystosiren varguezi
Bharatisiren kachchensis
Domningia sodhae
Bharatisiren indica
Kutchisiren cylindrica
Dioplotherium manigaulti
Dioplotherium allisoni
gen. nov. 4 bellunense
Xenosiren yucateca
Metaxytherium krahuletzi
Metaxytherium floridanum
Metaxytherium crataegense
Metaxytherium arctodites
Metaxytherium medium
Caribosiren turneri
Metaxytherium serresii
Dusisiren reinharti
Dusisiren dewana
Dusisiren takasatensis
Dusisiren jordani
Hydrodamalis cuestae
Hydrodamalis gigas
Potamosiren magdalenensis
Ribodon limbatus
Trichechus inunguis
Trichechus senegalensis
Trichechus manatus
1
2
3
4
5
6
7
8
9
10
11
12
13
14
15
16
17
18
19
20
21
22
23
24
25
26
27
28
29
30
31
32
33
34
35
36
37
38
39
40
41
42
43
44
45
46
47
48
49
50

Phylogenetic analysis B

For the sirenian analysis B, the species gen. nov. 2 *alleni* was removed from the ingroup to check its impact on the polytomy above node 15. Although the relationships between gen. nov. 2 *alleni* and the specimens traditionally assigned to *"H. schinzii"* remain unresolved in analysis A, the taxonomic autonomy of gen. nov. 2 *alleni* is supported by two characters distinguishing this species from the specimens that bear no characters on their terminal branches (MWNH-TER-1, FMD SRK Eck-Rat 43, SMNS 1539, CDGG S1, SMNS 47736, FIS M8385). The taxon *alleni* is additionally supported by its geographic and presumed stratigraphic provenance that differs from that of the specimens originally referred to *"H. schinzii"*. Accordingly, the ingroup is reduced here to 51 taxa and ten specimens. In all other respects analysis B is derived from analysis A. As in analysis A, seven characters were found uninformative and were deleted accordingly (characters 1, 20, 23, 76, 79, 109, 110 of analysis A). The strict consensus tree (Fig. 70) was calculated from 4 MPTs, which has a TL of 707 steps, a CI of 0.24 and a RI of 0.67; three nodes collapsed.

The result of phylogenetic analysis B is congruent with that of analysis A in its topology and character distribution. The only difference refers to the completely resolved interrelationships between the single specimens originally referred to *"H. schinzii"* above node 15. Sister groupings between the specimens and the terminal branches are not defined by characters, which is in accordance to analysis A. Additionally, the monophyletic grouping above node 15 is supported by the same combination of characters as in analysis A.

Phylogenetic analysis C

According to the results of analysis B, a third analysis was conducted by re-inclusion of the species gen. nov. 2 *alleni*. With the exception of gen. nov. 2 *alleni*, the species and specimens above nodes 14, 15 and 22 (in analysis A and B) that were originally referred to the genus *"Halitherium"* are each lumped together, because they are considered to represent single monophyletic taxa based on corresponding and complementing characters in the used data matrix (Appendix 4). The character distribution and corresponding states for that analysis are listed in the Appendix 5.

The third phylogenetic analysis included 52 taxa in addition to the outgroup-complex. Seven uninformative characters (1, 20, 23, 76, 79, 109, 110 of analysis A) were removed from the analysis. The heuristic search resulted in 4 MPTs. The strict consensus tree is presented in Figure 71 with a TL of 707 steps, a CI of 0.24 and a RI of 0.64; three nodes collapsed.

Figure 70. Phylogenetic hypothesis of sirenians excluding the species gen. nov. 2 *alleni*. The strict consensus tree of analysis B (TL = 707, CI = 0.24, RI = 0.67) was received from four equally most parsimonious trees and conducted by using the heuristic search function with tree-bisection-reconnection of branch swapping. Representatives of the former *"Halitherium"*-species complex in bold.


outgroup complex
Prorastomus sirenoides
Pezosiren portelli
Protosiren fraasi
Protosiren smithae
Ashokia antiqua
Sirenavus hungaricus
Eotheroides aegyptiacum
Anomotherium langewieschei
Miosiren kocki
Eotheroides lambondrano
gen. nov. 1 taulannense
LS RLP PW 2005/5042-LS
FIS M8002
NHMUK PV M9415
BSPG 1956 I 540
FIS M2597
CDGG S1
FIS M8385
FMD SRK Eck-Rat 43
SMNS 47736
MWNH-TER-1
SMNS 1539 ("H." bronni)
Eosiren stromeri
Eosiren libyca
Prototherium veronense
Prototherium intermedium
Eosiren imenti
gen. nov. 3 cristolii
LI 1939/257 ("H." abeli)
Crenatosiren olseni
Nanosiren garciae
Nanosiren sanchezi
Dugong dugon
Rytiodus capgrandi
Corystosiren varguezi
Bharatisiren kachchhensis
Domningia sodhae
Bharatisiren indica
Kutchisiren cylindrica
Dioplotherium manigaulti
Dioplotherium allisoni
gen. nov. 4 bellunense
Xenosiren yucateca
Metaxytherium krahuletzi
Metaxytherium floridanum
Metaxytherium crataegense
Metaxytherium arctodites
Metaxytherium medium
Caribosiren turneri
Metaxytherium serresii
Dusisiren reinharti
Dusisiren dewana
Dusisiren takasatensis
Dusisiren jordani
Hydrodamalis cuestae
Hydrodamalis gigas
Potamosiren magdalenensis
Ribodon limbatus
Trichechus inunguis
Trichechus manatus
Trichechus senegalensis

Figure 71. Phylogenetic hypothesis of sirenians re-including the species gen. nov. 2 *alleni*. The strict consensus tree of analysis C (TL = 707, CI = 0.24, RI = 0.64) was received from four equally most parsimonious trees and conducted by using the heuristic search function with tree-bisection-reconnection of branch swapping. Numbers above branches reflect bootstrap estimates. Representatives of the former *"Halitherium"*-species complex in bold.

In the present phylogenetic tree (Fig. 71), the combined species and specimens originally referred to *"Halitherium"* are arranged on species level. In particular, node 13 defines a clade comprising three taxa with resolved interrelationships in contrast to the previous analyses. Node 13 is supported by two derived characters. The species gen. nov. 2 *alleni* is sister to a clade (node 14) comprising two different species, gen. nov. 2 spec. nov. 1 and gen. nov. 2 *bronni*, according to the morphological revision of the skeletal remains originally referred to *"H. schinzii"*. Whereas the species gen. nov. 2. *alleni* is not at all defined by characters, both terminal branches above node 14 are characterised by a number of plesiomorphies and apomorphies. However, the sister grouping represented by node 14 is not defined.

When repeating the analysis, the position of gen. nov. 2 *alleni* is revealed to be unstable, because this species can also group together with either of the species above node 14. In both cases, the clade above node 13 is not only defined by two, but seven derived characters, which are the same that define this node in the analyses A and B. Additionally, the distribution of characters varies slightly in the terminal branches of gen. nov. 2 spec. nov. 1 and gen. nov. 2 *bronni* depending on the sister grouping that either of the respective species forms with gen. nov. 2 *alleni*. The terminal branch of the species gen. nov. 2 *alleni* remains undefined in each result of the third analysis.

The variable topology above node 13 is related to the limited number of skeletal remains available for gen. nov. 2 *alleni* resulting in missing morphological information (see Appendix 4). Either way, a monophyletic clade (node 13) that comprises three taxa with resolved interrelationships is supported. In this analysis, a sister group relationship between gen. nov. 2 spec. nov. 1 and gen. nov. 2 *bronni* with gen. nov. 2 *alleni* as the basal sister taxon is favoured. This is supported by the geographic and stratigraphic distribution of gen. nov. 2 *alleni*, which differs from that of gen. nov. 2 spec. nov. 1 and gen. nov. 2 *bronni* and will be pointed out in detail in the discussion of the results.

As another result of analysis C, the most derived stem group representatives united by node 22 (in analysis A and B) are lumped together to gen. nov. 3 *cristolii* based on congruent character distribution. Here, taxon gen. nov. 3 *cristolii* is defined by one derived and four plesiomorphic characters and is sister to a clade (node 21) comprising all crown-group taxa. This sister grouping (node 20) is supported by the same combination of ten plesiomorphic and derived characters as in analysis A and B. The arrangement of the remaining sirenian taxa and distribution of characters are congruent to that in the analyses A and B.

Phylogenetic analysis D

This analysis is conducted analogous to analysis A and was developed for 52 taxa, ten specimens originally assigned to *"H. schinzii"* and one outgroup-complex (*Phospha-*

therium escuilliei and *Numidotherium koholense*). The data matrix included 182 cranial and dental characters in addition to 20 postcranial characters. Seven uninformative characters were found (characters 1, 20, 23, 76, 79, 109, 110 of analysis A) and deleted before exploring the interrelationships of the Sirenia. The heuristic search resulted in 36 MPTs with a strict consensus tree shown in Figure 72 (TL: 779, CI: 0.25, RI: 0.67; 12 nodes collapsed).

As in analysis A, the clade Sirenia (node 1) is defined by five synapomorphies (characters 1, 20, 76, 79, 110) and divided into a stem group (nodes 1–19) and a crown group (node 20). Within the stem group representatives the extinct genera *Protosiren* (node 4) and *Prototherium* (node 10) are resolved as monophyletic. In contrast to analysis A, each of the main nodes (2, 3, 5–9, 11, 13, 15 and 18) of the stem group is well supported by synapomorphies with the only exception of node 14, which is defined by a combination of plesiomorphic and derived characters. Node 14 includes the species gen. nov. 1 *taulannense*, which is, in contrast to analysis A, not part of a monophyletic group only composed of *"Halitherium"* species. However, it is the sister taxon to a clade (node 15) comprising all other species and specimens traditionally referred to *"Halitherium"* including the species *bronni* (SMNS 1539) and *abeli* (nodes 16, 17, 19) and the crown group (node 20). Node 15 is strongly supported by four synapomorphies like the absence of canines (166[1]) and P1/p1 (167[1]), and the presence of a ventral protuberance on the first rib (195[1]).

The species and specimens that were originally lumped into *"H. schinzii"* are arranged above nodes 16 and 17, each characterised by a polytomy and defined by a number of homoplasies. The entire polytomous arrangement of species and specimens above nodes 16 and 17 is the result of a strict consensus tree with 12 nodes collapsed as it is presented here (Fig. 72). Similar to analysis A, the number of collapsed nodes can vary between nine and twelve in the strict consensus tree when repeating the analysis. This merely affects the interrelationships of the single individuals either above node 16 or 17 that can be partially arranged in a dichotomy. However, the character distribution and properties of the phylogeny (TL, CI, RI) remain unchanged. Additionally, node 17 includes the North-American species gen. nov. 2 *alleni*, which represents the only terminal branch in the polytomy that is defined by two characters (115[0], 116[1] of analysis A). All other terminal species and specimens united by nodes 16 and 17 are undefined.

Also in this phylogenetic hypothesis the species gen. nov. 3 *cristolii* and *abeli* form sister taxa (node 19) based on a single plesiomorphic character (95[0] of analysis A),

Figure 72. Phylogenetic hypothesis of sirenians conducted by using the heuristic search function with tree-bisection-reconnection of branch swapping. The strict consensus tree of analysis D (TL = 779, CI = 0.25, RI = 0.67) was received from 36 equally most parsimonious trees. Representatives of the former *"Halitherium"*-species complex in bold.

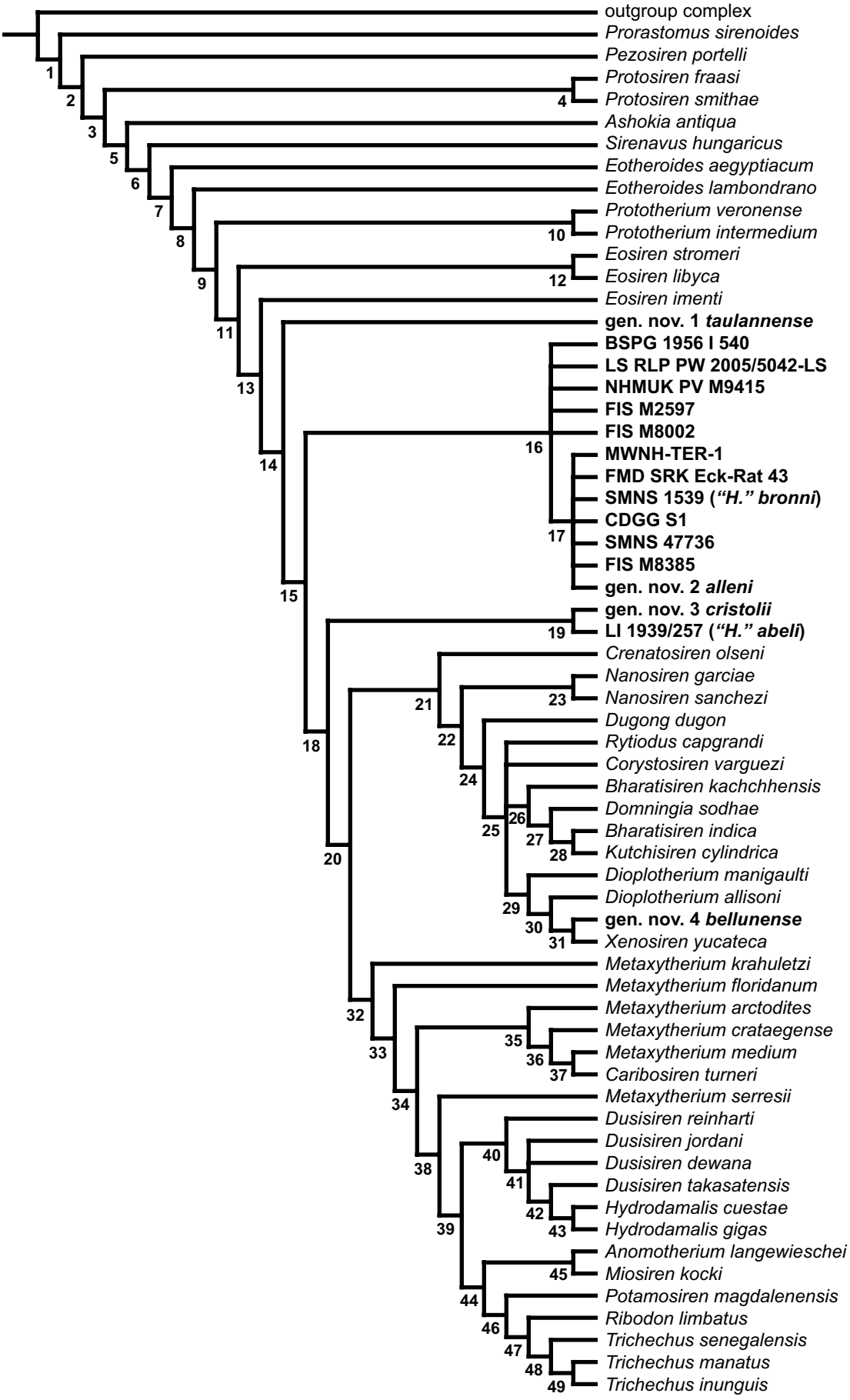
outgroup complex
Prorastomus sirenoides
Pezosiren portelli
Protosiren fraasi
Protosiren smithae
Ashokia antiqua
Sirenavus hungaricus
Eotheroides aegyptiacum
Eotheroides lambondrano
Prototherium veronense
Prototherium intermedium
Eosiren stromeri
Eosiren libyca
Eosiren imenti
gen. nov. 1 taulannense
BSPG 1956 I 540
LS RLP PW 2005/5042-LS
NHMUK PV M9415
FIS M2597
FIS M8002
MWNH-TER-1
FMD SRK Eck-Rat 43
SMNS 1539 ("H." bronni)
CDGG S1
SMNS 47736
FIS M8385
gen. nov. 2 alleni
gen. nov. 3 cristolii
LI 1939/257 ("H." abeli)
Crenatosiren olseni
Nanosiren garciae
Nanosiren sanchezi
Dugong dugon
Rytiodus capgrandi
Corystosiren varguezi
Bharatisiren kachchhensis
Domningia sodhae
Bharatisiren indica
Kutchisiren cylindrica
Dioplotherium manigaulti
Dioplotherium allisoni
gen. nov. 4 bellunense
Xenosiren yucateca
Metaxytherium krahuletzi
Metaxytherium floridanum
Metaxytherium arctodites
Metaxytherium crataegense
Metaxytherium medium
Caribosiren turneri
Metaxytherium serresii
Dusisiren reinharti
Dusisiren jordani
Dusisiren dewana
Dusisiren takasatensis
Hydrodamalis cuestae
Hydrodamalis gigas
Anomotherium langewieschei
Miosiren kocki
Potamosiren magdalenensis
Ribodon limbatus
Trichechus senegalensis
Trichechus manatus
Trichechus inunguis
1
2
3
4
5
6
7
8
9
10
11
12
13
14
15
16
17
18
19
20
21
22
23
24
25
26
27
28
29
30
31
32
33
34
35
36
37
38
39
40
41
42
43
44
45
46
47
48
49

although the terminal branches of both species are also not defined. Nevertheless, they represent the most derived stem group representatives.

In accordance to analysis A, the crown group (node 20) is subdivided in two major clades (nodes 21, 32). However, this grouping is supported here by five instead of two synapomorphies that not only refer to the cranium and dentition, but also to the postcranium (characters 131, 169, 170, 185, 202). The postcranial character 202 reflects the plesiomorphic condition for defining the crown group, which is by definition the opposite of a synapomorphic state. Beside the rare distribution of this character within Sirenia, this is related to the inconsistency between the polarity of this character determined by ingroup comparison and the fossil record. Although character 202 is not known for the earliest fossil sirenian, but is for the slightly older *Pezosiren portelli*, a test was conducted by applying a reversed polarity for this character. The topology and character distribution of the phylogeny resulting from a repeated analysis D remained unchanged. The consistency index and retention index also remained the same while the tree length (TL) of 778 indicated one transformation step less. Only the status of character 202 has changed to a homoplasy defining the crown group with the derived condition. Therefore, character 202 is only provisionally treated as a synapomophy for the crown group in this study. Additionally, the polarity of four further characters (71, 120, 196, 197) revealing the same conflict with the fossil record was tested. All of these characters originally occurred as homoplasies in the phylogeny resulting from analysis D. In the repetition of analysis D, each character maintained the status of a homoplasy, but in the reversed polarity. The topology and character distribution of this tree remained unaffected while its properties slightly changed (TL = 777, CI = 25, RI = 63).

The topology of the Dugonginae (node 21) as defined by Domning (1994) is unchanged in comparison to analysis A as well as the distribution of characters, which differs only slightly in the absence or presence of a few characters. However, this is not the case of the resulting topology and character distribution of the second clade (node 32) within the crown group.

A major difference to analysis A refers to the position of *Anomotherium* and *Miosiren* (Miosireninae, node 45), which are not arranged in the stem group here, but plot well within the crown group. This phylogenetic hypothesis of analysis D additionally supports a sister group relationship between the Miosireninae and the Trichechinae (node 46) as was already indicated by previous studies (Domning, 1994). The resulting clade (node 44), the Trichechidae as understood by Domning (1994), is uniquely defined by, amongst other features, an external auditory meatus that is very broad anteroposteriorly and shallow (60[1]). With respect to the Trichechinae, the interrelationships and distribution of characters also slightly differ in comparison to analysis A. While *Potamosiren* and *Ribodon* remain the most plesiomorphic representatives of the Trichechinae as in analysis A, a sister

grouping between *T. manatus* and *T. inunguis* with *T. senegalensis* as basal sister taxon is favoured here instead of the grouping [[*T. manatus* + *T. senegalensis*] + *T. inunguis*].

A further difference to analysis A and a likewise unique result of a phylogenetic analysis of Sirenia so far, is that the Trichechidae (node 44) form the sister group to the Hydrodamalinae (node 40). In addition to seven plesiomorphic characters, this sister relationship (node 39) is defined by the extension of the acromion of the scapula up to the glenoid cavity, which is a synapomorphic postcranial character. The Hydrodamalinae are monophyletic here, as already outlined by Domning (1994), however no character defines this clade. A trichotomy above node 41 characterises the unresolved interrelationships within *Dusisiren* similar to node 43 in analysis A. However, the present phylogenetic hypothesis supports a sister grouping between *D. takasatensis* and *Hydrodamalis* rather than *D. jordani* being sister to *Hydrodamalis*. The monophyly of the bispecific genus *Hydrodamalis* (node 43) is not only characterised by the unique features of a dentiform process (16[1]) and the absence of functional cheek teeth in adults (181[1]) as in analysis A, but also by the postcranial synapomorphy of a medially curved radial and ulnar diaphysis (194[1]).

The remaining parts of the clade above node 32 are only supported by homoplasies and comprise the still paraphyletic genus *Metaxytherium* and *Caribosiren turneri*. However, in contrast to analysis A, a monophyletic clade (node 35) including *Caribosiren* and three *Metaxytherium* species is supported by this phylogenetic hypothesis. Here, *C. turneri* is sister to *M. medium* (node 37) on the basis of three plesiomorphic and two derived characters. The taxa *M. krahuletzi* and *M. floridanum* have the most basal position within the clade above node 32. *Metaxytherium serresii* is the most derived representative of the genus *Metaxytherium* and sister taxon to the clade comprising the Trichechidae (node 44) and the group including the genus *Hydrodamalis* (node 40).

Phylogenetic analysis E

In order to clarify the sister grouping of the specimens originally assigned to *“Halitherium schinzii”*, the taxon gen. nov. 2 *alleni* was removed from the analysis, as was done for analysis B. Therefore the data set includes 51 taxa and 10 specimens in addition to the outgroup-complex. Seven uninformative characters out of 202 total characters from the original data matrix were found (characters 1, 20, 23, 76, 79, 109, 110 of analysis A) and deleted before analysing the interrelationships of the ingroup. The heuristic search resulted in 12 MPTs. The strict consensus tree (Fig. 73) has a TL of 777, a CI of 0.25, and a RI of 0.67; seven nodes collapsed.

The phylogenetic hypothesis presented here resembles that of analysis D with respect to the topology and distribution of characters. The only difference refers to node 17, which defines a monophyletic group with resolved interrelationships between the species *bronni* (SMNS 1539) and five specimens that were traditionally assigned to *“H. schinzii”*.


outgroup complex
Prorastomus sirenoides
Pezosiren portelli
Protosiren fraasi
Protosiren smithae
Ashokia antiqua
Sirenavus hungaricus
Eotheroides aegyptiacum
Eotheroides lambondrano
Prototherium veronense
Prototherium intermedium
Eosiren stromeri
Eosiren libyca
Eosiren imenti
gen. nov. 1 taulannense
FIS M8002
LS RLP PW 2005/5042-LS
NHMUK PV M9415
BSPG 1956 I 540
FIS M2597
MWNH-TER-1
FIS M8385
FMD SRK Eck-Rat 43
SMNS 1539 ("H." bronni)
CDGG S1
SMNS 47736
gen. nov. 3 cristolii
LI 1939/257 ("H." abeli)
Crenatosiren olseni
Nanosiren garciae
Nanosiren sanchezi
Dugong dugon
Rytiodus capgrandi
Corystosiren varguezi
Bharatisiren kachchhensis
Domningia sodhae
Bharatisiren indica
Kutchisiren cylindrica
Dioplotherium manigaulti
Dioplotherium allisoni
gen. nov. 4 bellunense
Xenosiren yucateca
Metaxytherium krahuletzi
Metaxytherium floridanum
Metaxytherium arctodites
Metaxytherium crataegense
Metaxytherium medium
Caribosiren turneri
Metaxytherium serresii
Dusisiren reinharti
Dusisiren jordani
Dusisiren dewana
Dusisiren takasatensis
Hydrodamalis cuestae
Hydrodamalis gigas
Anomotherium langewieschei
Miosiren kocki
Potamosiren magdalenensis
Ribodon limbatus
Trichechus senegalensis
Trichechus manatus
Trichechus inunguis

This grouping is based on the same combination of characters as in analysis D. Additionally, the sister relationships between the single specimens remain undefined as are the terminal branches, which is also in accordance with analysis D. Other specimens that also have originally been referred to *"H. schinzii"* are arranged in a polytomy at the base of the clade above node 16. When repeating analysis E, the number of nodes that collapsed in the strict consensus tree varies slightly. For example, in a variant with six nodes collapsed two specimens within this polytomy form a sister group. However, the combination of characters defining node 16 is not affected by the changed topology, as are the tree length, consistency index and retention index. Additionally, the dichotomy and terminal branches within the polytomy remain undefined as in analysis D.

Phylogenetic analysis F

By comparing the character distribution and corresponding states of the species and specimens originally assigned to the genus *"Halitherium"* above nodes 16, 17 and 19 of analysis E, the sirenians above each of these nodes could be lumped together to form a single taxon. Following the procedure of analysis C, the species gen. nov. 2 *alleni* was included again. Hence, analysis F was conducted for 52 taxa in addition to the outgroup-complex. Seven uninformative characters out of 202 were found (characters 1, 20, 23, 76, 79, 109, 110 of analysis A) and deleted before analysing the interrelationships of fossil and extant taxa assigned to Sirenia. The heuristic search resulted in 4 MPTs. The strict consensus tree (Fig. 74) has a TL = 776, CI = 0.25, RI = 0.63; three nodes collapsed. The character distribution and corresponding states for that analysis are listed in the Appendix 6.

As in analysis C, the species gen. nov. 2 *alleni* is sister to a clade (node 17) comprising gen. nov. 2 spec. nov. 1 and gen. nov. 2 *bronni* originally referred to *"H. schinzii"*. The sister grouping above node 16 is supported by a single derived character. The species gen. nov. 2 *alleni* is not defined by characters as is the sister grouping above node 17. However, both species, gen. nov. 2 spec. nov. 1 and gen. nov. 2 *bronni,* are defined by several plesiomorphic and apomorphic characters. When repeating the analysis, the position of gen. nov. 2 *alleni* can vary in so far that it is either sister to gen. nov. 2 spec. nov. 1 or gen. nov. 2 *bronni*. In both cases, the unstable position of gen. nov. 2 *alleni* results in a slightly different distribution of characters in the terminal branches of gen. nov. 2 spec. nov. 1 and gen. nov. 2 *bronni*. Therefore, four instead of one consistent characters

Figure 73. Phylogenetic hypothesis of sirenians excluding the species gen. nov. 2 *alleni*. The strict consensus tree of analysis E (TL = 777, CI = 0.25, RI = 0.67) was received from 12 equally most parsimonious trees and conducted by using the heuristic search function with tree-bisection-reconnection of branch swapping. Representatives of the former *"Halitherium"*-species complex in bold.

Figure 74. Phylogenetic hypothesis of sirenians re-including the species gen. nov. 2 *alleni*. The strict consensus tree of analysis F (TL = 776, CI = 0.25, RI = 0.63) was received from four equally most parsimonious trees and conducted by using the heuristic search function with tree-bisection-reconnection of branch swapping. Numbers above branches reflect bootstrap estimates. Representatives of the former *"Halitherium"*-species complex in bold.

support node 16. The terminal branch of the species gen. nov. 2 *alleni* remains undefined in each topological position.

This observation resembles that in analysis C and is likewise explained by the high degree of missing morphological information for gen. nov. 2 *alleni*. A sister grouping [gen. nov. 2 spec. nov. 1 + gen. nov. 2 *bronni*] with gen. nov. 2 *alleni* as the basal sister taxon is also favoured in this phylogenetic hypothesis due to the geographic and stratigraphic distribution of gen. nov. 2 *alleni* that differs from that of gen. nov. 2 spec. nov. 1 and gen. nov. 2 *bronni*.

In accordance with analysis C, taxon gen. nov. 3 *cristolii* resulted from the lumping of the two terminal species above node 19 of analysis D and E. Here, the species *cristolii* occupies the most derived position within the stem group basal to the crown group (node 19) and is defined by one derived and three plesiomorphic characters. Unlike analysis C, this sister grouping between gen. nov. 3 *cristolii* and the crown group (node 18) is supported amongst other features by one synapomorphy that refers to the presence of a strongly concave ventral border of the horizontal mandibular ramus (146[1]). The distribution of characters and topology of the remaining parts of the phylogenetic tree presented here are congruent to that in analyses D and E.

In a final step, the data set of analysis F was complemented for the taxa gen. nov. 2 spec. nov. 1 and gen. nov. 2 *bronni* by employing specimens now clearly assignable to one of the two species. In this process, three characters (192–194) were completed for gen. nov. 2 spec. nov. 1 and eight characters (178–179 and 189–194) for gen. nov. 2 *bronni*. Additionally, a single character (199) was scored polymorphic for gen. nov. 2 spec. nov. 1 referring to the *foramen obturatum* of the pelvic bone that is usually absent, but present in a single specimen (HLMD-WT 420). The repeat of analysis F resulted in a phylogeny having the same topology and properties (CI, RI) as that of analysis F (Fig. 74) with an uncompleted data set except for the tree length that then counts 777 steps.

DISCUSSION

Phylogeny and systematics of the order Sirenia

The monophyly of sirenians is beyond debate and well supported by morphological (e.g., Novacek & Wyss, 1986; Domning, 1994) and molecular (e.g., Lavergne *et al*., 1996) data. The morphology based phylogenetic analysis of the Sirenia by Domning (1994), which was the most comprehensive study up to now, identified four synapomorphies defining sirenian monophyly. Combination and re-assessment of different data sets and the inclusion of new morphological characters in this study, however, reveal five synapomorphies verifying this clade. Both, the quality and quantity of sirenian synapomorphies, are consistent when only cranial (analysis C; Appendix 5) or cranial and postcranial features (analysis F; Appendix 6) are applied. Two of these features were previously detected by Domning (1994) and encompass the external nares being retracted and enlarged, and the premaxilla contacting the frontal. Another character that was not included in Domning's (1994) analysis, but noted in support of the Sirenia pertains to the presence of a mastoid foramen through which the posterior part of the periotic, the mastoid, is exposed (see also Novacek & Wyss, 1986).

Apart from that, two further synapomorphies introduced by Domning (1994) are refuted here. On the one hand, the absence of a sagittal crest has become obsolete given that in *Pezosiren*, which is considered in a cladistic analysis for the first time, a weak crest is still present (Domning, 2001c). On the other hand, the results obtained through this study do not sustain a permanent fifth premolar as unique for sirenians. This feature was only provisionally treated as a synapomorphy by Domning (1994). As indicated before, Domning's (1994) character state 155[1] on the postcanine dental formula of sirenians includes the *á priori* statement of a secondary reduction from the condition "P1–5, M1–3" postulated for later sirenians. However, this reflects an interpretation that can only be made of a cladistic analysis *á posteriori*. Additionally, the meaning of a fifth permanent premolar in some Eocene Sirenia is still under debate (Savage *et al*., 1994). Although the present study does not attempt to resolve this problem, it can be stated that a synapomorphic status of the permanent fifth premolar is refuted on the basis of the present results. Neither the hypothesis of a reversal of a previous loss of P5/p5 (e.g., Domning, 1994), nor a retention of a plesiomorphic eutherian condition (e.g., Domning *et al*., 1982, 1986) can be excluded here to explain the presence of the extra premolar locus. In addition to the synapomorphies mentioned above, the presence of a preorbital process of the jugal and its contact with the lacrimal are found in this study to further characterise the monophyly of sirenians.

With respect to the higher-level interrelationships of Sirenia, there are significant differences compared to the results of Domning (1994). Additionally, the topology varies in part when either only cranial or cranial and postcranial features are considered. In this

study, a new systematic framework is provided according to the results of the cladistic approach that is stepwise documented in the analyses A to F. In the following discussion, reference is given to analysis C (Fig. 71) and F (Fig. 74) when only cranial or cranial and postcranial features, respectively, support the phylogenetic hypotheses presented here. According to these analyses, the order Sirenia can be clearly distinguished into a stem and a crown group.

The stem group Sirenia

Beside the species previously assigned to the genus *"Halitherium"* that will be discussed later, the arrangement of the stem group is more or less in agreement in analyses C and F. The Prorastomidae comprising *Prorastomus* and *Pezosiren* as understood by Domning (2001c) are confirmed to be paraphyletic in both analyses as was postulated previously by Domning (1994, 2001c). Accordingly, *Prorastomus* and *Pezosiren* are considered as the most basal stem group representatives, but without forming a clade. It is therefore suggested that the family "Prorastomidae" will be refuted based on the lack of defining characters.

Significantly, the genus *Protosiren* forms a monophyletic group, which is supported by nine homoplasies when only cranial features are considered or, alternatively, ten homoplasies when the analysis is expanded by postcranial features. Synapomorphies are not found to define this genus, but high bootstrap values of 95 % (analysis C) and 97 % (analysis F) further confirm this clade. Additionally, this result may corroborate a monophyletic family Protosirenidae according to Domning (1996) and Domning & Gingerich (1994), and provides objective arguments for such a clade for the first time. Beside the fact that the protosirenids are only monospecifically represented with *P. fraasi* in Domning's (1994) analysis, this group has been stated several times to be probably paraphyletic (Domning, 1994; Bajpai *et al*., 2009).

Another remarkable result derived from the phylogenetic analyses presented here supports the monophyly of the genus *Prototherium*. A sister group relationship between *P. intermedium* and *P. veronense* is confirmed in this study by a number of homoplasies, and bootstrap values of 61 % (analysis C) and 57 % (analysis F). However, this is in contrast to Domning's (1994) phylogenetic hypothesis. According to Domning (1994), *Prototherium* is paraphyletic with *P. veronense* being sister to *Eosiren abeli* and *P. intermedium* placed basal to a clade comprising the Trichechidae and all other derived Sirenia.

Additionally, *Eosiren libyca* is sister to *E. stromeri* when cranial and also postcranial characters are employed. This sister grouping is supported by three consistent homoplasies and contrasts with Domning's (1994) result, in which both taxa are part of a trichotomy. However, in agreement with Domning (1994), the monophyly of the genus *Eosiren* could not be confirmed in this study. In the present case, this results from the inclusion of a third species, *E. imenti*, that resolves phylogenetically in a slightly more derived position than [*E. libyca* + *E. stromeri*].

The crown group Sirenia

As in Domning (1994), the Miosireninae [*Anomotherium* + *Miosiren*] are uniquely defined by a thickened *lamina orbitalis* of the frontal. Additionally, this clade is strongly supported by bootstrap values of 92 % (analysis C) and 95 % (analysis F) in this study. However, the analyses performed here reveal two alternative hypotheses about their systematic position. Miosirenines are arranged within the stem group when only cranial features are employed (analysis C; Fig. 71). Their position between the late and middle Eocene species *Eotheroides aegyptiacum* and *E. lambondrano* favours the hypothesis of a middle Eocene origin of Trichechidae (Miosireninae and Trichechinae) as originally raised by Domning (1982) and confirmed by Sagne (2001b). However, a monophyletic grouping of miosirenines and trichechines as resolved in Domning's (1994) analysis is not supported by the analysis based on cranial characters. In the present study, the clade Trichechidae formed by miosirenines and trichechines only results when postcranial characters are also considered (analysis F; Fig. 74). In agreement with Domning (1994), this sister group relationship is then uniquely characterised by a very broad and shallow external auditory meatus rooting the Miosireninae well within one of the major clades (node 31 of analysis F) of the crown group.

One of the most novel results in this study is that Hydrodamalinae, as understood by Domning (1994), and Trichechidae form a sister group. This new clade is well supported in both analyses of the present study and well placed within one of the two major crown group clades (node 33 in analysis C (Fig. 71) and node 31 in analysis F (Fig. 74)). Trichechines and hydrodamalines (node 40 in analysis C) are, amongst other features, uniquely characterised by one synapomorphy (145[1]) when only cranial features are considered. This sister group relationship finds further support in the bootstrap analysis with a statistical probability of 58 %. It has to be recognised that in this case miosirenines are not monophyletically united with trichechines as indicated above, and hydrodamalines are paraphyletic when postcranial characters are excluded. However, even the result of analysis C suggests hydrodamalines are the closest relatives to the group encompassing the living manatees (*Trichechus*).

A more parsimonious phylogeny is provided by the analysis F (Fig. 74) of cranial and postcranial characters. In agreement with Domning (1994), this analysis recovers the Hydrodamalinae (node 39) as monophyletic and the Miosireninae (node 44) are included in the crown group forming a trichechid clade (node 43) together with the Trichechinae (node 45). In contrast to Domning (1994), the Trichechidae as sister to the Hydrodamalinae is well supported by one synapomorphy and a number of homoplasies and, therefore, results in the establishment of a new clade (node 38). A large acromion extending up to the glenoid cavity of the scapula uniquely defines this new clade and underlines the impact of postcranial features on sirenian systematics.

In light of a sister relationship between the Trichechidae and Hydrodamalinae, the

hydrodamalines are no longer recognised to be a subfamily of the Dugongidae as was proposed by Domning (1994, 1996). Moreover, this group is phylogenetically on the same level as the family Trichechidae and therefore should receive the status of a family as well. Consequently, it is suggested in this study to erect a new family name for the group encompassing the genera *Dusisiren* and *Hydrodamalis* (node 39 in analysis F). The subfamily Hydrodamalinae is nevertheless maintained in sirenian systematics, but it is suggested here to apply this term only to the taxonomic basis for this group, the genus *Hydrodamalis* (Simpson, 1932a) above node 42 (analysis F).

Below, the term Hydrodamalinae is, however, used in the same extent as defined previously (e.g., Domning, 1994, 1996) until such time as the new taxon name for the group above node 39 is published.

The interrelationships within "hydrodamalines" more or less agree with previous results. The genus *Dusisiren* is paraphyletic when either only cranial or cranial and postcranial characters are considered, which is in accordance with Domning (1994) and Furusawa (2004). Furusawa (2004) offered the sole phylogeny including all known representatives of this genus, whose interrelationships are shown to be completely resolved. While *D. reinharti* is the most basal representative also in the present study, the interrelationships of the remaining *Dusisiren* species are unclear at least in part. *Dusisiren jordani* is sister to the monophyletic genus *Hydrodamalis* and trichechines when cranial characters (analysis C; Fig. 71) are employed. However, applying postcranial characters as well (analysis F; Fig. 74) revealed *D. takasatensis* to be sister to *Hydrodamalis*, which also corresponds well with Furusawa (2004). Additionally, the bootstrap analysis of the cladistic analysis F supports the clade [*D. takasatensis* + [*H. gigas* + *H. cuestae*]] with a probability value of 50 %, whereas bootstrap support is lower than 50 % in analysis C.

The stem-lineage of the crown group clade (node 33 in analysis C, node 31 in analysis F) comprising the "Hydrodamalinae" and the group including the living manatees (*Trichechus*), is composed of a paraphyletic assemblage of taxa. This grouping predominantly includes representatives of the genus *Metaxytherium*. The paraphyly of this group has already been established in previous studies (e.g., Domning, 1994; Sorbi *et al*., 2012) suggesting that a revision is urgently needed. Although a revision of *Metaxytherium* is beyond the remit of the present study, it should be emphasised that the interrelationships of its representatives are fully resolved (Figs. 71, 74). This is in complete contrast to several studies (Domning, 1994; Velez-Juarbe *et al*., 2012; Sorbi *et al*., 2012) revealing a high degree of polytomies for that genus.

The species *M. krahuletzi* is the most basal member of this group, which corresponds to the results of previous studies (e.g., Domning & Thomas, 1987; Domning, 1994; Velez-Juarbe *et al*., 2012). Interestingly, *Caribosiren turneri* is part of a monophyletic group [*M. medium* + *C. turneri*] in analysis C (Fig. 71) and [*M. arctodites* + [*M. crataegense* + [*M. medium* + *C. turneri*]]] in analysis F (Fig. 74), each is recovered here for the first time.

This group may represent a single taxon on the genus level or an even higher category pending further studies that focus on the revision of the genus *Metaxytherium*. Additionally, *M. serresii* is verified as the most derived representative of this genus placed basal to the clade comprising the "hydrodamalines" and manatees (node 40 in analysis C and node 38 in analysis F). The derived position of this species is verified by Domning (1994), although he assumed a more basal placement for this species by stating his result to be spurious. Instead, *M. arctodites* is considered to be the most derived representative of this group as indicated by the most recent studies (Velez-Juarbe *et al*., 2012; Sorbi *et al*., 2012) contrasting the present hypothesis.

In this study, it is desisted to establish a new systematic framework for the taxa *Metaxytherium* and *Caribosiren* despite the well resolved stem-lineage of the clade above node 33 (analysis C) and node 31 (analysis F), respectively. Especially, the genus *Metaxytherium* is paraphyletic and therefore any taxonomic decision is postponed here until a subsequent revision of this genus.

The second major clade of the crown group (Fig. 71: analysis C, node 22; Fig. 74: analysis F, node 20) comprises the Dugonginae as previously understood (e.g., Domning, 1994; Velez-Juarbe *et al*., 2012) including the only living representative *Dugong dugon*. The dugongines are hitherto considered to be a subfamily of the Dugongidae. Dugongids are paraphyletic in Domning (1994) and include the Trichechidae nested within it, but they are monophyletic in the subset study of Velez-Juarbe *et al.* (2012) with trichechids being the sister group to dugongids. In this study, however, neither hypothesis could be confirmed. Here, the Dugongidae as traditionally understood would be paraphyletic if the hierarchical model provided by Domning (1994, 1996) was adopted. However, Domning (1994) regards his cladistic analysis as preliminary and his revised classification of sirenians as merely provisional. Therefore, it is not entirely followed in the present study.

Analogous to the "Hydrodamalinae", the consideration of the dugongine clade on subfamily level is refuted here. This clade is phylogenetically on the same level as the major crown group clade above node 33 (analysis C) and node 31 (analysis F), the latter of which comprises at least one family, the trichechids. Therefore, both crown group clades are recognised to represent a group of taxa on a classification level higher than that of a subfamily, for example. In this study, the status of a suborder is suggested for each of the crown group clades. However, in the following discussion the term Dugonginae is used in the traditional sense for practical reasons pending the publication of a new nominal suborder for this group.

Unlike the suborder above node 33 (analysis C) or node 31 (analysis F), the suborder above node 22 (analysis C) or node 20 (analysis F) is defined by several synapomorphies (Appendices 5, 6). Both analyses C and F consistently unite the "dugongines" by five synapomorphies such as bilateral knoblike bosses on the frontal roof, a thick and robust preorbital process of the jugal, and a strongly inflected *processus retroversus* of

the squamosal. The interrelationships within this clade are also congruent when cranial (analysis C; Fig. 71) or cranial and postcranial characters (analysis F; Fig. 74) are employed. Additionally, there is partial congruence, when these results are compared with the different existing phylogentic hypotheses of the “dugongine” interrelationships.

The phylogenetic positions of *Crenatosiren olseni*, as the most basal “dugongine”, the bispecific genus *Nanosiren* and the extant *Dugong* are in good agreement with the cladistic results of Domning & Aguilera (2008) and Velez-Juarbe *et al.* (2012). Especially, the monophyly of the recently established genus *Nanosiren*, Domning & Aguilera, 2008 is well supported here by a number of homoplasies and bootstrap values of 96 % (node 24 in analysis C) and 97 % (node 22 in analysis F), respectively. Both, a single synapomorphy and constant bootstrap value of 55 % also provide significant support for a clade uniting all remaining “dugongines” (node 26 in analysis C and node 24 in analysis F). This monophyletic grouping also agrees with the results of several previous analyses (Domning, 1994; Sorbi, 2007; Domning & Aguilera, 2008; Velez-Juarbe *et al*., 2012), although these studies employ varying data sets, in particular with regard to the included “dugongine” taxa.

On the basis of the present results and consistency of these with the phylogenetic hypotheses of previous studies, a new systematic concept is proposed for the suborder above node 22 (analysis C; Fig. 71) or node 20 (analysis F; Fig. 74). There are objective reasons to maintain the family Dugongidae. However, this term should not be used to the same extent as in previous studies (e.g., Domning, 1994), but rather be applied to the clade (node 25 in analysis C and node 23 in analysis F) comprising the taxonomic basis for this group, the living *Dugong* (Gray, 1821). According to this systematic consequence, all dugongids can be uniquely identified as having first upper incisors with enamel mainly present on the medial side (160[1]) and that the enamel extends the entire length of the tusk (165[1]). Additionally, the sister group to the Dugongidae is considered as a new family and only includes the genus *Nanosiren* (node 24 in analysis C and node 22 in analysis F).

There would be also the possibility to establish a superfamily for the clade above node 23 (analysis C) or node 21 (analysis F) and consequently for its sister group, *Crenatosiren olseni*. However, considering the fact that the latter represents a single species for which the establishment of a superfamily rank doesn’t seem to be practicable, this taxonomic procedure is not followed here.

Moreover, the present results allow distinguishing between two subfamilies within the Dugongidae. On the one hand, this refers to the monospecific *Dugong* that is placed in its own subfamily. Due to the fact that the *Dugong* already represents the taxonomic basis for the Dugonginae as indicated by Simpson (1932a; 1945), this subfamily is retained, but limited here. The *Dugong* is the only living representative of the suborder above node 22 (analysis C) or node 20 (analysis F), but it is not recovered as the most derived member of this clade in any study. This is also indicated by a long ghost-lineage of this

Figure 75. Time-calibrated phylogeny of sirenians on the basis of the strict consensus tree of analysis F (TL = 776, CI = 0.25, RI = 0.63; Fig. 74). Representatives of the former *"Halitherium"*-species complex in bold. Stratigraphic ages from Gradstein *et al.* (2004).

species when the sirenian phylogeny is applied to the fossil record (Fig. 75). Therefore, it is reasonable to assume that future sirenian finds will yield fossil representatives that are more closely related to the *Dugong* than to any other taxon and can be well placed within the Dugonginae.

On the other hand, the polytomy above node 26 (analysis C; Fig. 71) or node 24 (analysis F; Fig. 74) reconfirms the subfamily Rytiodontinae that was established by Abel (1914) on the basis of the genus *Rytiodus*. Formerly, all taxa included in the Rytiodontinae were transferred to the "Dugonginae" by Domning (1994) based on the results of his phylogenetic analysis that showed *Dugong dugon* to be placed within this clade. This extension of the "Dugonginae" is not followed in the present study. Instead, the synapomorphic character of a supraorbital process of the frontal that is turned markedly downward, with its dorsal surface inclined strongly ventrolaterad (45[1]) unites this group of derived sirenians and underlines its taxonomic autonomy. According to the results of this study, the rytiodontines comprise all taxa formerly referred to this group except for *Crenatosiren olseni* that falls outside this clade due to its basal position within the suborder above node 22 (analysis C) or node 20 (analysis F).

Having a closer look at the Rytiodontinae (node 26 in analysis C and node 24 in analysis F), the partially unresolved interrelationships of these fossil sirenians indicate that this group is still in need of revision. Additionally, the topology of this clade differs significantly from previous studies as it is the case across all of the trials, at least in part. Such discrepancies are probably related to the use of different data sets as mentioned above. The present study provides the most extensive phylogenetic analysis of fossil and extant sirenians up to now, especially due to the inclusion of several "dugongine" taxa (used in the traditional sense as provided by Domning (1994, 1996)) that were newly established.

Velez-Juarbe *et al.* (2012) recently provided a phylogenetic approach focussing on "Dugonginae". Consequently, this is a good opportunity for comparison. However, this study also revealed the most contradictions to the results presented herein. While the interrelationships of "dugongines" are completely resolved in Velez-Juarbe *et al.* (2012), a hypothesis on the phylogenetic position of *Rytiodus capgrandi* (early Miocene of France) and *Corystosiren varguezi* (early Pliocene of Mexico) can not be established from the present study. Several cladistic analyses (Domning, 1994; Sorbi, 2007; Domning & Aguilera, 2008) reveal both taxa to be closely related forming a monophyletic group. However, such a phylogenetic hypothesis is not corroborated by the analysis of Velez-Juarbe *et al.* (2012), in which both taxa are indeed closely related, but do not form a clade. The latter would be also more parsimonious considering the different geographical and stratigraphical occurrence of both taxa.

A new result and major contrast to all previous studies is the distinction of two monophyletic groups within the Rytiodontinae above node 26 (analysis C; Fig. 71) and node

24 (analysis F; Fig. 74). Both clades are strongly justified in being each uniquely characterised by a single synapomorphy in addition to several homoplasies. Moreover, both groups find significant support from the fossil record providing evidence of two “dugongine” hot spots in different ocean basins. The clade [*B. kachchhensis* + [*D. sodhae* + [*B. indica* + *Kutchisiren cylindrica*]]] above node 27 (analysis C) and node 25 (analysis F) comprises a derived group of extinct sirenians that is hitherto only known from the Indian region. Whereas, the monophylum [*D. manigaulti* + [*D. allisoni* + [gen. nov. 4 *bellunense* + *X. yucateca*]]] above node 30 (analysis C) and 28 (analysis F) includes sirenians mainly known from the West Atlantic and Caribbean Region. Within this clade, the later-discussed species gen. nov. 4 *bellunense* represents the only European species and reveals to be the sister taxon to *Xenosiren yucateca*. As a further consequence, it is well supported as a crown group member. However, a taxonomic consequence for both clades is not proceeded here, because they are part of a polytomy. Therefore any evaluation of a systematic rank is postponed pending further investigations.

New implications on the origin of the Trichechidae

The Trichechidae still have a sparse fossil record and the present study did not aim to clarify the origin of this clade. Nevertheless, it should be pointed out that the late Oligocene occurrence of *Anomotherium langewieschei* as the earliest known trichechid implies a pre-late Oligocene origin of this group. This general conclusion meets previous assumptions by, for example, Savage (1976) and Domning (1994). However, a middle Eocene (Savage, 1976; Domning, 1982; Sagne, 2001b) or late Eocene (Domning, 1994) origin of trichechids is decisively refuted here.

The cladistic evidence gleaned in this study rather supports an early Oligocene origin (Fig. 75) as was already tentatively concluded by Domning (1994). This hypothesis corresponds well with the evolution of the trichechid clade primarily in the Neogene of South America. An early Oligocene divergence finds additional support in the Central American and southern North American occurrence of the first “hydrodamalines”, which share a common ancestor with trichechids, although they are only known from the middle Miocene at the earliest. Rainey *et al.* (1984) also corroborated a post-Eocene origin of the Trichechidae and they provided the only phylogeny of living sirenians so far including the extinct *H. gigas* based on molecular data. According to the study of Rainey *et al.* (1984), the trichechid divergence is dated in the range of 17–20 Ma (early Miocene). It must be emphasised that Rainey *et al.* (1984) use the term trichechids as previously defined (e.g., Domning, 1982) comprising only the Trichechinae as understood today (e.g., Domning, 1994). Considering a middle Miocene occurrence of the first trichechine *Potamosiren magdalenensis*, the estimated divergence time is not in conflict with the actual fossil record. If the Miosireninae are also considered to be trichechids as recovered in this study, the molecular estimate by Rainey *et al.* (1984) does contradict the early Oligo-

cene divergence time hypothesised here, though not to the same extent as the Eocene estimate inferred by Domning (1982, 1994). However, Rainey *et al.* (1984) point to improvements of their analysis aiming at the consideration of rates of molecular change in constructing phylogenies, which might lead to revised results being more congruent with palaeontological data in the future.

The interrelationships of the living Trichechinae

The monophyly of the Trichechinae [*Potamosiren* + [*Ribodon* + *Trichechus*]] is well supported by bootstrap analyses (analysis C = 55 %; analysis F = 63 %). The use of different data sets, however, contradicts each other when analysing the interrelationships of the living *Trichechus* (manatees). A sister relationship between the West Indian (*T. manatus*) and West African (*T. senegalensis*) manatee is generally supported by morphological (Domning & Hayek, 1986; Domning, 1994) and cyt *b* gene (Vianna *et al*., 2006) data. In the present study, the analysis C of cranial characters (Fig. 71) also resulted in this monophyletic grouping. By contrast, analysis F (which additionally considers postcranial characters; Fig. 74) supports a sister relationship of *T. manatus* and the Amazonian manatee (*T. inunguis*) instead, indicating that both derived from a more recent common ancestor than either does with *T. senegalensis*. This phylogenetic hypothesis would be also consistent with a South American based evolution of manatees.

The first study that showed *T. manatus* as sister taxon to *T. inunguis* was provided by Lowenstein (1985). However, Domning & Hayek (1986) argue against this molecular approach in that it lacks explanations or supporting evidence and that it is supposedly based on the study of Rainey *et al.* (1984). While the latter may be true, but not necessarily an opposing argument, it can be stated here that Lowenstein (1985: 542) provided a clear outline on the "type of assay" that he "used for identifying proteins in fossils and other organic tissue", which argues for the autonomy of his study.

Further arguments for a close relationship between *T. manatus* and *T. inunguis* were raised by the mtDNA phylogeny of Vianna *et al.* (2006), who also revealed the presence of interspecific hybrids around an area of sympatry at the mouth of the Amazon River. Interestingly, Domning & Hayek (1986) contradict themselves when postulating the sister grouping between *T. manatus* and *T. senegalensis*. These authors regarded three synapomorphies to be more supportive to their hypothesis than the four synapomorphies that unite *T. manatus* and *T. inunguis*. This is explained here by the fact that Domning & Hayek (1986: 135) did not conduct a phylogenetic analysis, but rather concluded *á priori* on the basis of likely convergences, characters of doubtful polarity or "more promising characters". As a matter of fact, the conclusions by Domning & Hayek (1986) are subjectively influenced by making arbitrary assumptions on the evolutionary history of the three manatee species.

Another, more recent molecular approach (Kuntner *et al*., 2010) provides a species-level phylogeny of Afrotheria corroborating another controversial relationship of manatees

in addition to the present study. Kuntner *et al.* (2010) hypothesised that the Amazonian and West African manatee are more closely related to each other than either is with the West Indian manatee. This hypothesis is also supported by two synapomorphies (Domning & Hayek, 1986) implying that there exist informative characters shared by any two of the three species of *Trichechus*. The latter is explained with an almost simultaneous divergence of the three manatee species (Domning & Hayek, 1986). Ultimately, the perspective and scientific knowledge of the present study suggest that the application of different data sets leads to different phylogenetic hypotheses on the interrelationships of manatees, indicating the necessity of larger trials in the future.

The robustness of the sirenian phylogeny

Beside differences to Domning (1994) and several analyses on subsets of the Sirenia, the present study also reflects discrepancies between the phylogenetic hypotheses that resulted when cranial (analysis C; Fig. 71) or cranial and postcranial features (analysis F; Fig. 74) are employed. As outlined before, disagreements are mainly related to the phylogenetic position of the Miosireninae.

The evolutionary tree resulting from the cladistic analysis of cranial and postcranial data (analysis F) is argued here to represent the more parsimonious hypothesis for several reasons. This pertains to the character-based support of the stem group. In contrast to analysis C (Appendix 5), all main nodes within the stem group of analysis F (Appendix 6) are confirmed by synapomorphies. The only exception is node 14 that is characterised by a combination of homoplasies. As a further contrast to analysis C, all main nodes within the stem group of analysis F are usually supported by more than one synapomorphy. The improved fit between the tree and data is also shown in the consistency index (CI), which is, although only minimally, slightly higher in analysis F. Furthermore, the result of analysis F is better corroborated by the fossil record (Fig. 75) than that of analysis C. Especially the phylogenetic position of the Miosireninae within the crown group is more congruent with their stratigraphic occurrence in the upper Oligocene and lower Miocene, respectively, than their arrangement between Eocene taxa within the stem group.

The present study underlines the significance of a comprehensive data set with respect to both the taxa and characters employed for investigating sirenian interrelationships. This becomes evident when Domning's (1994; Fig. 2) phylogeny is compared with the one that resulted from analysis F (Fig. 74) showing that neither character weighting nor ordering are necessary cladistic tools. Beside the integral approach of the intricate *"Halitherium"*-species complex, the greatest difference to Domning (1994) refers to the position of the Trichechidae followed by several taxa that are, conversely, monophyletic. However, the overall pictures of both analyses are not so far apart that they are irreconcilable even though or precisely because different approaches and methods were applied. While Domning (1994) considered 36 sirenian taxa by focussing on cranial characters,

several of which were weighted and ordered, the cladistic analyses in this study were conducted under objective criteria and complemented with additional taxa and characters. As a consequence, the consistency index (CI) of 0.76 given by Domning (1994) is considered as artificially inflated. However, the objective test of Domning's (1994) analysis still reveals a reliable CI of 0.53, as do some recent cladistic approaches on subsets of Sirenia (e.g., Velez-Juarbe *et al*., 2012).

The strikingly lower CI of 0.25 given here (analysis F; Fig. 74) requires explanation. Primarily, it might be due to the fact that the present study provides the most extensive phylogenetic analysis with a data set that includes 16 additional sirenian taxa compared to Domning (1994) and, moreover, about three times as many informative characters. Therefore, the probability of the occurrence of homoplasies is considered to be generally increased, which is also directly indicated here by the retention index (RI) of 63 %. In this context, the availability of morphological data for some taxa is considered to have further impact. Many taxa are known from only a single specimen that, in the worst case, is additionally badly preserved and consequently often lacks information for certain characters. Especially postcranial features, which are entirely known for the extant taxa, often can be only insufficiently scored for fossil sirenians. This results in a relatively high number of question marks for the respective taxa in the data set (Appendix 4), which are considered as missing information by the software used. Nevertheless, the present study shows that it is precisely these postcranial features, which have systematic significance. Several postcranial characters have the status of a synapomorphy (Appendix 6). For example, the presence of a ventral protuberance on the *capitulum* of the first rib (195[1]) uniquely defines node 15 (analysis F; Fig. 74) within the stem group. The crown group (node 19 in analysis F) is, amongst others, characterised by a prominently developed coracoid process of the scapula (185[1]) and most likely by the synapomorphy or at least homoplasy of a ventral keel present on the sternal manubrium (202[0]). Additionally and already outlined before, the extension of the acromion of the scapula (188[1]) is a synapomorphy that unites the "Hydrodamalinae" and Trichechidae.

Finally, the relatively low CI in this study can be explained through the evolution of the Sirenia itself. The main morphological features and specialisations of sirenians, like retracted and enlarged external nares, are linked to adaptation to an aquatic life-style (Domning, 2001a; Berta et *al*., 2006). This transition took place amongst the Eocene representatives of the order. While the first sirenians were still amphibious quadrupeds (Domning, 2001c), fully aquatic forms occurred already in the late Eocene (Domning, 2001a; Berta et *al*., 2006). Therefore, from the evolutionary point of view, sirenians have changed their skeletal morphology relatively little over the last 40 Ma. As a matter of fact, the three extant genera including the subfossil *Hydrodamalis* are mainly distinguished by their entirely herbivorous food source, which is, amongst others, inferred from the degree of rostral deflection (Domning, 2001b). The *Dugong* has a strongly downturned

rostrum and tusks consistent with the dugong's nature of being an obligate bottom feeder specialised on seagrasses (Lanyon & Sanson, 2006; Domning & Beatty, 2007). By contrast manatees are generalist feeder showing a less pronounced snout-deflection and supernumerary molars pointing to a habit of browsing on diverse aquatic plants including seagrasses (Domning, 1980, 1982; Domning & Hayek, 1986). The only non-tropical species *Hydrodamalis* is characterised by another adaptive feeding strategy that involves a moderate snout deflection and the loss of teeth for consuming kelp (Domning, 1989c; Domning & Furusawa, 1994).

In conclusion, the homoplasy-based phylogeny of Sirenia as a group of mammals that commonly adapted to a life in water is not a surprising result. Consequently, improvement and optimisation of the present results may be a matter for further investigations of both, taxa and characters.

Phylogeny and systematics of the *"Halitherium"*-species complex

Traditionally, the genus *"Halitherium"* is suspected to be monophyletic, although more recently, this has never been substantiated with sufficient evidence from phylogenetic analyses. On the one hand, this may be explained by the fact that no cladistic analysis of Sirenia has been conducted so far including all known *"Halitherium"* species. Phylogenetic analyses considering Sirenia as a whole (Domning, 1994) or subsets of the order (Bajpai & Domning, 1997; Domning & Pervesler, 2001; Furusawa, 2004; Domning & Aguilera, 2008; Velez-Juarbe *et al*., 2012) only included the taxa *"H. schinzii"*, *"H." cristolii*, and, in later studies, also *"H." taulannense*. The far greater problem, however, are defining characters for the genus *"Halitherium"* amongst several other genera within the Sirenia and "Halitheriinae", in particular. Apart from Sickenberg's (1934a) conclusion that *"Halitherium"* needs to be revised, the issue of missing reliable diagnoses was recently re-raised by Sagne (2001a) in the course of the establishment of *"H." taulannense*. Sagne (2001b) integrated this new taxon in Domning's (1994) cladistic analysis, expanded the data matrix by some other informative characters and taxa, and revealed that *"H." taulannense* is morphologically more closely related to *"Halitherium"* than to any other Eocene genus. However, a monophyletic grouping and, consequently, a formal diagnosis for *"Halitherium"* was not achieved by the phylogenetic analysis of this species. Accordingly, the taxonomic assignment of *"H." taulannense* can only be approximated by expanding the set of species considered to represent the genus *"Halitherium"* in addition to the taxa established in the 19th and 20th century.

Beside the rather arbitrary taxonomic treatment of newly discovered species, another taxonomic problem remained unconsidered up to now. As detailed above, the premolar holotype (Fig. 32) of the type species *"H. schinzii"* bears no distinguishing features that could be related to a given sirenian species or even to define one. The potential of this tooth to be a holotype is definitively hampered by its lack of any meaningful diagnostic

value. As a result of the present study, the species name *"H. schinzii"* is treated as a *nomen dubium* as are consequently the genus *"Halitherium"* and the subfamily "Halitheriinae". These taxonomic terms are now deemed to be preoccupied and therefore will be no longer available for nomenclatural purposes. With this taxonomic consequence one of the main sources of sirenian paraphyla is abolished hence providing new approaches to interpret the taxa originally lumped in these categories. With respect to the former *"Halitherium"*-species complex, a new designation for the respective taxa is aspired.

The representatives of the original *"Halitherium"*-species complex are plotted at different systematic positions within Sirenia. Five of six species are arranged within the stem group (gen. nov. 1 *taulannense*, gen. nov. 2 spec. nov. 1, gen. nov. 2 *bronni*, gen. nov. 2 *alleni* and gen. nov. 3 *cristolii*), whereas one species (gen. nov. 4 *bellunense*) occupies a position within the crown group when both, only cranial characters (analysis C; Fig. 71) and cranial and postcranial characters (analysis F; Fig. 74), are considered. Hence, a monophyletic assemblage as previously assumed by several authors is not corroborated.

"Halitherium" taxa in the sirenian stem group

In the stem group, the homoplastic character of a thickened nuchal crest (113[1]) is consistent in both analyses and supports the monophyly of the genus gen. nov. 2. This clade is also well corroborated by the bootstrap analysis with values of 64 % (analysis C) or 67 % (analysis F). As indicated above, the hypothesis of gen. nov. 2 spec. nov. 1 being sister to gen. nov. 2 *bronni* with gen. nov. 2 *alleni* at the base of this sister group [[gen. nov. 2 *alleni* + [gen. nov. 2 spec. nov. 1 + gen. nov. 2 *bronni*]]] is favoured in this study. The distribution of characters differs slightly when cranial or cranial and postcranial characters are employed (compare Appendices 5, 6), but without affecting this specific topology of the taxa.

The sister group relationship between gen. nov. 2 spec. nov. 1 and gen. nov. 2 *bronni* is supported by their lower Oligocene age and similar or overlapping regional distribution in Central Europe indicating the presence of two sympatric species. Both taxa are founded on a representative sample of specimens that were originally referred to *"H. schinzii"* (Figs. 70, 73). The phylogenetic analyses in this study show that the respective individuals possess characters those allow two morphospecies to be distinguished (Appendices 4–6). The morphological distinction of both species is well supported in this study by, for example, the detailed supraoccipital anatomy and the occurrence of a second permanent premolar.

Gen. nov. 2 *alleni* also could be convincingly hypothesised to be sister to either of the Central European species according to the phylogenetic results indicating a variable arrangement of this taxon within gen. nov. 2. As already outlined above, gen. nov. 2 spec. nov. 1 and gen. nov. 2 *bronni* are considered to share a more recent common ancestor with each other than either does with gen. nov. 2 *alleni* on the basis of their similar stratigraphy and geography. This hypothesis is considered to be more parsimonious because the geographic occurrence of gen. nov. 2 *alleni* is limited to the North American continent.

Moreover, this species is stratigraphically younger than the early Oligocene sister taxa of Central Europe if an early Miocene or at least a late Oligocene age for gen. nov. 2 *alleni* is accepted. Although in this study gen. nov. 2 *alleni* is shown to be a valid taxon and morphologically identifiable, larger samples are necessary to better establish and substantiate its phylogenetic position.

A major difference between the cladistic analysis C (Fig. 71) and analysis F (Fig. 74) refers to the position of gen. nov. 1 *taulannense* within the stem group. This taxon forms a monophyletic group with gen. nov. 2 plotting at the basis of [gen. nov. 2 *alleni* + [gen. nov. 2 spec. nov. 1 + gen. nov. 2 *bronni*]] when only cranial features are considered (analysis C). A clade comprising gen. nov. 1 *taulannense* is, however, not sufficiently supported by the bootstrap analysis. This is also the case in the phylogenetic analysis F extended by postcranial characters. Here, gen. nov. 1 *taulannense* is not included into a monophyletic grouping, but placed one node below the clade [gen. nov. 2 *alleni* + [gen. nov. 2 spec. nov. 1 + gen. nov. 2 *bronni*]]. Previous studies (e.g., Domning & Aguilera, 2008) assuming a single species in the lower Oligocene of Europe (*"H. schinzii"*) never confirm a monophyletic assemblage with the species *taulannense*. Instead both taxa are shown to be closely related. Considering the comprehensive phylogenetic approach of analysis F and the results of previous studies, it is argued here that gen. nov. 1 *taulannense* is a monospecific genus distinct from gen. nov. 2.

The phylogenetic position of gen. nov. 3 *cristolii* is constant when only cranial or cranial and postcranial characters are applied (Figs. 71, 74). According to this result, gen. nov. 3 *cristolii* is shown to be the most derived stem group representative, which also agrees well with the cladistic achievements by Domning (1994) and Domning & Aguilera (2008). Additionally, this taxon is considered to be the only species present in the upper Oligocene of Austria by concluding that the species *abeli* is synonymous with gen. nov. 3 *cristolii*. This result is in agreement with previous suggestions by Domning (1996), but demonstrated here on an objective and phylogenetic basis for the first time.

The species *abeli* was founded on a nearly complete mandible (LI 1939/257; Figs. 55A, 56B) and is additionally known by some cranial elements (Spillmann, 1959). Significantly, both species *abeli* and *cristolii* absolutely correspond in their observable morphological features when *abeli* is separately analysed first for testing its status and affinities (see analyses A, B, D, E). This is reflected in the phylogenetic trees (Figs. 69, 70, 72, 73) of the present study in so far that both taxa are united by a single homoplasy, but appear as metaspecies lacking characters on their individual branches. As a matter of fact, the only potential morphological difference inferred from Domning's (1994) data matrix is discarded by the re-investigation of both species. Domning (1994) postulated the absence of accessory mental foramina in the holotype mandible (LI 2012/1) of *cristolii*. Personal observations reveal that these foramina are not lacking in the holotype, but in fact are simply not preserved. While the left lateral wall of the mandibular canal is broken along the whole

length of the horizontal ramus (Fig. 55B), the right symphyseal region is damaged to such a degree that no reliable conclusion on the absence or presence of accessory mental foramina can be drawn (Fig. 56A). Therefore, this character is not scored for the specimens representing the species *cristolii*. On the other hand, accessory mental foramina are well preserved and clearly visible on both sides of the mandibular symphysis of *abeli* (Fig. 56B). This implies a revision of this character resulting from the synonymy of the species *abeli* and *cristolii* that are now lumped under the taxon gen. nov. 3 *cristolii*.

Status and affinities of "Halitherium" bellunense

Interestingly, gen. nov. 4 *bellunense* is the only European species phylogenetically well nested within a clade above node 30 (analysis C; Fig. 71) or node 28 (analysis F; Fig. 74). This taxon is likewise the most derived representative of the previous *"Halitherium"*-species complex. In this study, gen. nov. 4 *bellunense* is sister to *Xenosiren yucateca*, a group characterised by a single homoplasy (Appendices 5, 6). Gen. nov. 4 *bellunense* was phylogenetically analysed for the first time by Sorbi (2007), who controversially resolved this species as a member of a monophyletic group including the genera *Rytiodus* and *Corystosiren*. The latter two taxa are exactly those that plot in a polytomy in the present study. Further morphological investigations and cladistic studies on these two species may contribute to a better resolution of their interrelationships in the future. As a potential consequence, this may also affect the phylogenetic arrangement of gen. nov. 4 *bellunense* though this is not corroborated by the present study. On the one hand, analysis C (Fig. 71) and F (Fig. 74) do not differ in the topology of the crown group clade encompassing gen. nov. 4 *bellunense* (node 30 in analysis C and node 28 in analysis F). Additionally, different tests like the deletion of the second major crown group clade (node 33 in analysis C and node 31 in analysis F) do not show any impact on the stability of this clade. Therefore, a reliable sister group relationship between gen. nov. 4 *bellunense* and *X. yucateca* is argued here. Apart from the differences on species level, the present study corroborates the phylogenetic hypothesis of Sorbi (2007) that gen. nov. 4 *bellunense* represents a crown group sirenian, hence providing objective support for Domning's (1996) previous suggestion.

Status and affinities of the species excluded from the phylogenetic analyses

The species *pergense* is confirmed to be a junior synonym of gen. nov. 3 *cristolii*, as was previously suggested by Domning (1996). The partial skull roof representing *pergense* (Fig. 54) is characterised by a distinctly smaller size compared to the skull (LI 1926/394; Figs. 51–53) known from gen. nov. 3 *cristolii*. Additionally, the preserved cranial structures are less pronounced in *pergense* than in gen. nov. 3 *cristolii* indicating immaturity, as it is also observable in juvenile skulls of the dugong, for example. Apart from that, the holotype of *pergense* is included separately first in the cladistic analyses performed in this study to test its status and affinities. However, the separate cladistic treatment yielded an

insufficient phylogenetic signal grouping *pergense* randomly. This is most likely related to the species' paucity of morphological features indicated by about 88 % question marks in its character matrix (Appendix 4). As a consequence, *pergense* is excluded *á posteriori* from further cladistic treatment. Direct comparisons of the compiled character matrices of gen. nov. 3 *cristolii* and *pergense* reveal no morphological differences. The only deviation consists in the less pronounced external occipital protuberance in *pergense*, which is explained by its juvenile status. In addition to that, the corresponding stratigraphic and geographic occurrences of both taxa provide no indication that more than a single species was present in the Austrian upper Oligocene.

For the species *"Halitherium antillense"* likewise no phylogenetic signal could be found. This is mainly related to the fact that this species is only insufficiently represented by a single specimen. Actually, this species is merely based on a badly preserved posterior fragment of the left mandible including m1–3 (Fig. 66), and two vertebral elements (Matthew, 1916). Accordingly, the species *"H. antillense"* covers less than 9 % of the characters contained in the data matrix (Appendix 4) implying little information for the establishment of a phylogenetic hypothesis. By including *"H. antillense"* into the phylogenetic analyses it resolved in random positions within Sirenia causing a disruptive impact on the topology of other sirenian groupings. Therefore, it is concluded that the material basis of this species bears no diagnostic characters, and this prevents any meaningful phylogenetic hypothesis for *"H. antillense"*. Additionally, it is assessed in this study that the quality of its holotype is extremely low. Neither it is possible to define a species on the holotype material that can be clearly distinguished from other taxa nor is *"H. antillense"* unambiguously assignable to any known species. Consequently, the species name *"H. antillense"* is declared a *nomen dubium* in this study.

Aspects of intraspecific variation

As a further result of the present study, the aspect of intraspecific variation that was widely speculated on with respect to *"H. schinzii"* (e.g., Sickenberg, 1934a), is refuted here. This is substantiated by observations in extant taxa, in which sexual dimorphism and ontogenetic stages for example, could only insignificantly be detected. According to Domning & Hayek (1986), sexual dimorphism in skulls of the three living *Trichechus* species (manatees) is not present. On the contrary, the monospecific *Dugong* does vary in the development of the snout region, which is related to the expansion of the male tusks (Spain & Heinsohn, 1974; Spain *et al*., 1976). However, Marsh (1980) limited the significance of these sexual differences in so far that the male tusks only erupt and wear in the postpubertal phase. Moreover, tusks are indeed present in females and can also erupt and show wear in old individuals.

Another account on intraspecific variation and sexual dimorphism was provided by Domning (1991b) on the innominate bones of *Dugong*. For example, the ischia of adults

and males often show a more pronounced dorsoventral expansion as well as processes on the ventral side in contrast to younger individuals and females. Although Domning (1991b) evaluated this variation as considerable, he likewise confirmed a broad overlap between the sexes and different ontogenetic stages making unambiguous distinctions difficult.

Although the investigation of intraspecific variation is not the focus of the present study, the results of previous approaches on this aspect in manatees and dugongs were also personally verified and can be confirmed. Intraspecific variation is also observed in fossil sirenians that were investigated in this study, particularly gen. nov. 2 spec. nov.1 and gen. nov. 2 *bronni*, and also some taxa for comparison like *Metaxytherium krahuletzi* and *M. floridanum*. Amongst these taxa, differences of the ischium are observable according to Domning (1991b; compare also Figs. 31, 46). Beside variable dimensions of bones, particularly noticeable is the height and course of the temporal crests that often change and cause different frontoparietal widths. For example, this is clearly observable in gen. nov. 2 spec. nov 1 by comparing the juvenile skull roof FMD SRK Eck 124 (Fig. 21A) with the cranium of BSPG 1956 I 540 (Fig. 18). These observations are already recognised in the extant *Dugong* by Spain & Heinsohn (1974), who documented that the temporal crests are especially variable, but do not have any obvious association with sex or other factors. Furthermore, it was personally observed that neither in extant nor in fossil sirenian taxa do the basic skeletal structures qualitatively vary as was detected for gen. nov. 2 spec. nov. 1 and gen. nov. 2 *bronni*. By concluding that intraspecific variation only plays a minor role within sirenians, features like the opposite supraoccipital morphology for the insertion of the neck muscles in taxa of gen. nov. 2 are identified as distinguishing factors on species level.

Ecomorphological considerations

As outlined above, the Central European sister taxa gen. nov. 2 spec. nov. 1 and gen. nov. 2 *bronni* can be clearly distinguished amongst other features on the basis of the supraoccipital anatomy and the occurrence of a second permanent premolar. The functional importance of these features may be tied to different feeding strategies as was suggested by Domning & Hayek (1986) with respect to some interspecific differences within manatees (*Trichechus*). The development of the insertion areas for the neck muscles and ligaments on the supraoccipital indicates differences in the use of these muscles in gen. nov. 2 spec. nov. 1 and gen. nov. 2 *bronni*. On the intraspecific level, Domning & Hayek (1986) point out that processes and protuberances tend to become more pronounced with age. This apparently correlates with the increased development and use of the muscles attached to these structures. Considering the presence of a prominent external occipital protuberance in gen. nov. 2 spec. nov. 1 (see Fig. 23) and its reduction accompanied by a large nuchal fossa in gen. nov. 2 *bronni* (Fig. 37D, F), the extension of the atlantooccipital joint was most likely different in both taxa. It is not exactly clear by

now how these different supraoccipital structures affect the direction of movement of the head. The present study does not attempt any functional morphology and/or myology, but previous suggestions on the supraoccipital morphology may provide proper explanations. For example, *T. inunguis* predominantly shows a surface-feeding habit, which is explained, amongst others, by the strong development of the species' supraoccipital that allows the skull to stand upright (Domning & Hayek, 1986). Hence, it may be conceivable that gen. nov. 2 spec. nov. 1 was more related to the water surface according to the prominent rear surface of its supraoccipital indicating strongly developed neck muscles. By contrast, gen. nov. 2 *bronni* shows an absolute opposite skeletal development and therefore may have been confined to the bottom or deeper levels in the water column, respectively.

The hypothesis of niche partitioning in sympatric fossil sirenians is also supported by the perspective of marine plant evolution (e.g., Domning, 2001b). Ancient seagrasses and other macrophytes are supposed to have been more diverse and differed ecologically in energy flow patterns compared to present aquatic floras (Domning, 1982; Velez-Juarbe *et al*., 2012). Considering sirenians as having an obligate herbivorous life-style, it is suggested that feeding-niche partitioning had structuring effects on multispecies sirenian communities (Domning & Beatty, 2007). This hypothesis was recently substantiated by a comparative study on three different sympatric sirenian assemblages commencing the past ~26 Ma (Velez-Juarbe *et al*., 2012). Velez-Juarbe *et al.* (2012) reveal features linked to sirenian dietary and foraging preferences like tusk morphology and rostral deflection that have iteratively evolved in separate ocean basins. Although substantiated studies on such ecomorphological parameters in pre-late Oligocene multispecies sirenian communities are still not available, the factor of niche partitioning is taken in this study to explain best two sympatric taxa in the lower Oligocene of Central Europe.

CONCLUSIONS

The present study introduces the hitherto most comprehensive phylogenetic analysis of the order Sirenia with an up to date set of valid taxa and morphological characters (Appendix 4). This phylogenetic approach is the first performed under maximum objective criteria employing robust cladistic principles for clarifying the status and affinities of the genus *"Halitherium"*. Based on the morphological (re-)investigation of taxa previously assigned to this group, its monophyly, interrelationships and systematic position within Sirenia is evaluated yielding the following main results:

1. The holotype of the type species *"H. schinzii"* – a premolar – is not clearly assignable to any sirenian taxon and hence identified as non-diagnostic. Consequently, the species name *"H. schinzii"* is a *nomen dubium* as are the thereon-based genus *"Halitherium"* and the subfamily "Halitheriinae".
2. The monophyly of the *"Halitherium"*-species complex that was previously assumed by several authors is not confirmed in this study. The individual species formerly referred to this group are distributed across several branches within the stem group and the crown group.
3. There is substantiated evidence for the presence of two sympatric morpho-species in the lower Oligocene especially from Germany and Belgium. Both taxa (gen. nov. 2 spec. nov. 1 and gen. nov. 2 *bronni*) are hypothesised to form a sister group within the stem group and are significantly distinguishable for example by the supraoccipital morphology and the permanent dentition. One of these species implies the validity of the species *bronni*, which was formerly assigned to be synonymous to *"H. schinzii"*.
4. This monophyletic grouping is extended by the North American species gen. nov. 2 *alleni* that occupies a significant position at the base of the Central European sister taxa forming a monophyletic Euro-American clade.
5. The species gen. nov. 1 *taulannense* is placed basal to the Euro-American-species complex showing a more plesiomorphic status.
6. The species gen. nov. 3 *cristolii* is identified as the most derived stem group representative of the order Sirenia and considered to represent the only species in the late Oligocene of Upper Austria following Domning's (1996) synonymy index. Support for a synonymy of the species *abeli* with gen. nov. 3 *cristolii* is found on the basis of cladistic analyses for the first time. Morphological and stratigraphical data result in the recognition of the species *pergense* as a junior synonym of gen. nov. 3 *cristolii*.
7. The species gen. nov. 4 *bellunense* is phylogenetically nested within the crown group supporting Domning's (1996) assumption of its derived status.

8. No phylogenetic signals were found for the Central American species *"Halitherium antillense"*. Its holotype, representing the only known specimen, provides no sufficient morphological data for a phylogenetic analysis and also lacks identifying features on species level. Therefore, the species name *"H. antillense"* is considered a *nomen dubium*.

As a further result, the revision of the *"Halitherium"*-species complex combined with the re-assessment of characters and taxa provides new implications for the taxonomy and systematics of Sirenia on a larger scale. As indicated by previous studies, the family Prorastomidae is also paraphyletic here. Therefore, it is suggested to avoid this term by considering the taxa formerly assigned to this group (*Prorastomus* and *Pezosiren*) as the most basal stem group representatives of the order Sirenia. Conversely, the Protosirenidae appear to be verified in this study. Two species representing the only genus of this group, *Protosiren*, are confirmed monophyletic by a suite of morphological characters. However, the establishment of a family rank for this genus is not proceeded here as are any taxonomic acts above the genus level for the stem group. In the sense of taxonomic consequence, the other way round would imply the establishment of a suborder for each of the stem group representatives considering the two crown group clades that each have suborder status as well. However, there is no virtue in doing so, because one half of the stem group representatives are monospecific and the other half constitutes bi- or trispecific genera (Fig. 74).

With respect to the crown group, the establishment of two new suborders is suggested in this study. This implies an expansion of the taxonomic concept of Sirenia to abandon the traditional suprageneric classification of Simpson (1945). The mere distinction of four families (Prorastomidae, Protosirenidae, Dugongidae and Trichechidae) is considered to be insufficient to sustain a proper handling of sirenian diversity known to date. The first suborder (subord. nov. 1) refers to the group comprising the living *Dugong* (node 20 in analysis F; Fig. 74). The family Dugongidae is retained in this study, but limited to the clade above node 23 (analysis F) including the *Dugong* giving the basis for this family (Gray, 1821). Moreover, the morphological information currently available enables to further subdivide this group into two subfamilies. The Dugonginae (Gray, 1821) Simpson, 1932a are maintained here, but limited to the *Dugong*. The subfamily Rytiodontinae Abel, 1914 (node 24 in analysis F) is re-established here and comprises the genera *Rytiodus, Corystosiren, Bharatisiren, Domningia, Kutchisiren, Dioplotherium, Xenosiren,* and gen. nov. 4. A further and new family (fam. nov. 1) is envisioned for the sister group to the dugongids comprising the genus *Nanosiren* (node 22 in analysis F).

The second suborder (subord. nov. 2) designates the clade above node 31 (analysis F; Fig. 74) comprising the Trichechidae (manatees in the broader sense) and a group including the recently exterminated *Hydrodamalis gigas*. The latter group (node 39 in analysis F) was hitherto known as a subfamily of the "Dugongidae", the "Hydrodamalinae"

(e.g., Domning, 1994). With the new systematic framework provided here, a new family (fam. nov. 2) is introduced for this group indicating the same rank as its sister group, the Trichechidae (node 43 in analysis F). The Hydrodamalinae are retained, but limited to the genus *Hydrodamalis* (node 42 in analysis F). The systematic of the trichechid clade as proposed by Domning (1994) is corroborated in this study and remains unchanged.

The revised classification of the order Sirenia is strongly supported by the cladistic analyses conducted in this study, because the main nodes of the resulting phylogeny are properly defined by synapomorphies (analysis F; Fig. 74; Appendix 6). However, the diagnosis of the terminal taxa is, by contrast, predominantly based on character combinations composed of homoplasies, which is also indicated by a relatively low consistency index. Additionally, not all systematic controversies could be resolved on the basis of the morphological data available by now. As already pointed out by Domning (1994), also in this study the most problematic areas are the conspicuously paraphyletic genus *Metaxytherium* as well as the incompletely resolved clade of the newly established first suborder (node 20 in analysis F; Fig. 74) formerly known as “Dugonginae” (e.g., Domning, 1996). However, molecular analyses as employed for clarifying the interrelationships of extant taxa are not possible to apply, because the group forming the focus of this study is exclusively extinct. The greatest potential to improve and optimise the present results is seen in new and clearly defined morphological characters, a better fossil record of poorly known taxa, a distinct morphological definition of taxa on species level, the establishment of sufficient holotypes by excluding juvenile and/or fragmentary material, and the revision of questionably referred material.

In conclusion, the phylogenetic analyses obtained from this study provide new information on the interrelationships of the order Sirenia. The resulting new classification concept is a very first step into a monophyla-based systematic of Sirenia and summarised at genus level as follows:

Order **Sirenia** Illiger, 1811

Stem group sirenians

Genus ***Pezosiren*** Domning, 2001c
Genus ***Prorastomus*** Owen, 1855
Genus ***Protosiren*** Abel, 1907
Genus ***Ashokia*** Bajpai, Thewissen, Kapur, Tiwari & Sahni, 2009
Genus ***Sirenavus*** Kretzoi, 1941
Genus ***Eotheroides*** Palmer, 1899
Genus ***Prototherium*** De Zigno, 1887
Genus ***Eosiren*** Andrews, 1902
Genus **“gen. nov. 1”**
Genus **“gen. nov. 2”**
Genus **“gen. nov. 3”**

Crown group sirenians

Suborder **"subord. nov. 1"**

Genus ***Crenatosiren*** Domning, 1991a

Family **"fam. nov. 1"**

Genus ***Nanosiren*** Domning & Aguilera, 2008

Family **Dugongidae** Gray, 1821

Subfamily **Dugonginae** (Gray, 1821) Simpson 1932a

Genus ***Dugong*** Lacépède, 1799

Subfamily **Rytiodontinae** Abel, 1914

Genus ***Bharatisiren*** Bajpai & Domning, 1997

Genus ***Corystosiren*** Domning, 1990

Genus ***Dioplotherium*** Cope, 1883

Genus ***Domningia*** Thewissen & Bajpai, 2009

Genus ***Kutchisiren*** Bajpai, Domning, Das, Vélez-Juarbe & Mishra, 2010

Genus ***Rytiodus*** Lartet, 1866

Genus ***Xenosiren*** Domning, 1989b

Genus **"gen. nov. 4"**

Suborder **"subord. nov. 2"**

Genus ***Caribosiren*** Reinhart, 1959

Genus ***Metaxytherium*** De Christol, 1840

Family **"fam. nov. 2"**

Genus ***Dusisiren*** Domning, 1978

Subfamily **Hydrodamalinae** (Palmer, 1895 [1833] Simpson, 1932a

Genus ***Hydrodamalis*** Retzius, 1794

Family **Trichechidae** Gill, 1872 (1821)

Subfamily **Miosireninae** Abel, 1919

Genus ***Anomotherium*** Siegfried, 1965

Genus ***Miosiren*** Dollo, 1889

Subfamily **Trichechinae** (Gill, 1872 [1821]) Domning, 1994

Genus ***Potamosiren*** Reinhart, 1951

Genus ***Ribodon*** Ameghino, 1883

Genus ***Trichechus*** Linnaeus, 1758

REFERENCES

Abel O. 1904. Die Sirenen der mediterranen Tertiärbildungen Österreichs. *Abhandlungen der Kaiserlich-Königlichen Geologischen Reichsanstalt* **19:** 1–223.

Abel O. 1905. Über *Halitherium bellunense* eine Übergangsform zur Gattung *Metaxytherium*. *Jahrbuch der Kaiserlich-Königlichen Geologischen Reichsanstalt* **9:** 393–398.

Abel O. 1907. Die Stammesgeschichte der Meeressäugethiere. *Meereskunde* **1:** 1–36.

Abel O. 1913. Die eocänen Sirenen der Mittelmeerregion. Erster Teil: Der Schädel von *Eotherium aegyptiacum*. *Paleontographica* **59:** 289–360.

Abel O. 1914. *Die vorzeitlichen Säugetiere.* Jena: Gustav Fischer.

Abel O. 1919. *Die Stämme der Wirbelthiere.* Berlin & Leipzig: W. De Gruyter & Co.

Abel O. 1925. *Geschichte und Methode der Rekonstruktion vorzeitlicher Wirbeltiere*. Jena: Gustav Fischer.

Allen GM. 1926. Fossil mammals from South Carolina. *Bulletin of the Museum of Comparative Zoology* **67:** 447–467.

Ameghino F. 1883. Sobre una colección de mamíferos fósiles del piso mesopotámico de la formación patagónica recogidos en las barrancas del Paraná por el profesor Pedro Scalabrini. *Boletim Academia Nacional de Ciencias Córdoba* **5:** 101–116.

Amrine HM, Springer MS. 1999. Maximum-likelihood analysis of the tethythere hypothesis based on a multigene data set and a comparison of different models of sequence evolution. *Journal of Mammalian Evolution* **6:** 161–176.

Andrews CW. 1902. Preliminary note on some recently discovered extinct vertebrates from Egypt. Part III. *Geological Magazine* **9:** 291–295.

Andrews CW. 1906. *A descriptive catalogue of the Tertiary Vertebrata of the Fayûm Egypt. Based on the collection of the Egyptian government in the Geological Museum Cairo and on the collection in the British Museum (Natural History).* London: London Trustees of the British Museum.

Aranda-Manteca FJ, Domning DP, Barnes LG. 1994. A new middle Miocene sirenian of the genus *Metaxytherium* from Baja California and California: Relationships and paleobiogeographic implications. In: Berta A, Deméré TA, eds. Contributions in Marine Mammal paleontology honoring Frank C. Whitmore Jr. *Proceedings of the San Diego Society of Natural History* **29:** 191–204.

Asher RJ. 2007. A web-database of mammalian morphology and a reanalysis of placental phylogeny. *BMC Evolutionary Biology* 2007 **7:** 1–10.

Asher RJ, Novacek MJ, Geisler JH. 2003. Relationships of endemic African mammals and their fossil relatives based on morphological and molecular evidence. *Journal of Mammalian Evolution* **10:** 131–162.

Bahlo E, Tobien H. 1982. Bestandsaufnahme der Säugetiere im “prä-aquitanen” Tertiär des Mainzer Beckens. *Mainzer geowissenschaftliche Mitteilungen* **10:** 131–137.

Bajpai S, Domning DP. 1997. A new dugongine sirenian from the early Miocene of India. *Journal of Vertebrate Paleontology* **17:** 219–228.

Bajpai S, Thewissen JGM, Kapur VV, Tiwari BN, Sahni A. 2006. Eocene and Oligocene sirenians (Mammalia) from Kachchh, India. *Journal of Vertebrate Paleontology* **26:** 400–410.

Bajpai S, Domning DP, Das DP, Mishra VP. 2009. A new middle Eocene sirenian (Mammalia, Protosirenidae) from India. *Neues Jahrbuch für Geologie und Paläontologie, Abhandlungen* **252:** 257–267.

Bajpai S, Domning DP, Das DP, Vélez-Juarbe J, Mishra VP. 2010. A new fossil sirenian (Mammalia, Dugonginae) from the Miocene of India. *Neues Jahrbuch für Geologie und Paläontologie, Abhandlungen* **258:** 39–50.

Barthel W. 1962. Über ein neues montiertes Skelett von *Halitherium schinzi* Kaup (Sirenia). *Mitteilungen der Bayerischen Staatssammlung für Paläontologie und Historische Geologie* **2:** 65–68.

Berger J-P, Reichenbacher B, Becker D, Grimm M, Grimm K, Picot L, Storni A, Pirkenseer C, Schaefer A. 2005a. Paleogeography of the Upper Rhine Graben (URG) and the Swiss Molasse Basin (SMB) from Eocene to Pliocene*. International Journal of Earth Sciences* **94:** 697–710.

Berger J-P, Reichenbacher B, Becker D, Grimm M, Grimm K, Picot L, Storni A, Pirkenseer C, Schaefer A. 2005b. Eocene-Pliocene time scale and stratigraphy of the Upper Rhine Graben (URG) and the Swiss Molasse Basin (SMB). *International Journal of Earth Sciences* **94:** 711–731.

Berta A, Sumich JL, Kovacs KM. 2006. *Marine Mammals: Evolutionary Biology*. Second edition. New York: Academic Press.

Bertram GCL, Bertram CKR. 1973. The modern Sirenia: their distribution and status. *Biological Journal of the Linnean Society* **5:** 297–338.

Bizzarini F. 1995. Osservazioni sull'*Halitherium schinzi* Kaup, 1838 (Sirenia, Mammalia) conservato presso il Museo Civico di Storia Naturale di Venezia. *Bollettino del Museo Civico di Storia Naturale di Venezia* **44:** 163–171.

Bizzarini F, Reggiani P. 2010. *Halitherium schinzi* nel nuovo allestimento del Museo di Storia Naturale di Venezia. *Bollettino del Museo Civico di Storia Naturale di Venezia* **61:** 131–137.

Bizzotto B. 2005. La struttura cranica di *Prototherium intermedium* (Mammalia: Sirenia) del l'Eocene superiore Veneto. Nuovi Contributi alla sua Anatomica e Sistematica. *Lavori Societá Veneziana di Scienze Naturali* **30:** 107–125.

Böhme M. 2001. Die Landsäugerfauna des Unteroligozäns der Leipziger Bucht – Stratigraphie, Genese und Ökologie. *Neues Jahrbuch für Geologie und Paläontologie, Abhandlungen* **220:** 63–82.

Bosellini A, Masetti D, Sarti M. 1981. A Jurassic "Tongue of the Ocean" infilled with oolitic sands: The Belluno Trough, Venetian Alps, Italy. *Marine Geology* **44:** 59–95.

Brandt JF. 1833. Über den Zahnbau der Stellerschen Seekuh (*Rytina stelleri*) nebst Bemerkungen zur Charakteristik der in zwei Unterfamilien zu zerfällenden Familie der pflanzenfressenden Cetaceen. *Mémoires de l'Académie impériale des sciences de St.-Pétersbourg. Sér. 6. Sciences mathématiques, physique et naturelles* **2:** 103–118.

Bronn HG. 1853-1856. *H. G. Bronn's Lethaea geognostica oder Abbildung und Beschreibung der für die Gebirgs-Formationen bezeichnendsten Versteinerungen.* Band 3: 4. Caeno-Lethaea: 6. Theil: Molassen-Periode. Stuttgart: Schweizerbart'sche Verlagshandlung und Druckerei.

Bryant HN. 2001. Character polarity and the rooting of cladograms. In: Wagner GP, ed. *The character concept in evolutionary biology.* San Diego & London: Academic Press, 319–337.

Buffrénil V de, Canoville A, D'Anastasio R, Domning DP. 2010: Evolution of sirenian pachyosteosclerosis, a model-case for the study of bone structure in aquatic tetrapods. *Journal of Mammalian Evolution* **17:** 101–120.

Carone G, Domning DP. 2007. *Metaxytherium serresii* (Mammalia: Sirenia): new pre-Pliocene record, and implications for Mediterranean paleoecology before and after the Messinian Salinity Crisis. *Bollettino della Società Paleontologica Italiana* **46:** 55–92.

Carus JV. 1868. *Handbuch der Zoologie*. *Erster Band. Wirbelthiere, Mollusken und Molluscoiden.* Leipzig: Wilhelm Engelmann.

Clementz MT, Sorbi S, Domning D.P. 2009. Evidence of Cenozoic environmental and ecological change from stable isotope analysis of sirenian remains from the Tethys-Mediterranean region. *Geology* **4:** 307–310.

Court N. 1990. Periotic anatomy of *Arsinoitherium* (Mammalia, Embrithopoda) and its phylogenetic implications. *Journal of Vertebrate Paleontology* **10:** 170–182.

Court N. 1994a. Limb posture and gait in *Numidotherium koholense*, a primitive proboscidean from the Eocene of Algeria. *Zoological Journal of the Linnean Society* **111:** 297–338.

Court N. 1994b. The periotic of *Moeritherium* (Mammalia, Proboscidea): homology or homoplasy in the ear region of Tethytheria McKenna, 1975? *Zoological Journal of the Linnean Society* **112:** 13–28.

Court N. 1995. A new species of *Numidotherium* (Mammalia: Proboscidea) from the Eocene of Libya and the early phylogeny of the Proboscidea. *Journal of Vertebrate Paleontology* **15:** 650–671.

Cope ED. 1883. On a new extinct genus of Sirenia from South Carolina. *Proceedings of the Academy of Natural Sciences of Philadelphia* **35:** 52–54.

Cope ED. 1889. Synopsis of the families of Vertebrata. *American Naturalist* **23:** 849–877.

Dallanave E, Agnini C, Muttoni G, Rio D. 2009. Magneto-biostratigraphy of the Cicogna section (Italy): Implications for the late Paleocene-early Eocene time scale. *Earth and Planetary Science Letters* **285:** 39–51.

De Blainville HMD. 1844. *Ostéographie ou description iconographique comparée du squelette et du système dentaire des mammifères récent et fossiles pour servir de base à la zoologie et à la géologie*. *Des lamantins (Buffon), (Manatus, Scopoli), ou gravigrades aquatiques.* Volume 3. Paris: J.B. Baillière et Fils.

De Christol J. 1840. Recherches sur divers ossements fossiles attribués par Cuvier à deux phoques, au lamantin, et à deux espèces d'hippopotames, et rapportés au *Metaxytherium,* nouveau genre de cétacé de la famille des dugongs. *L'Institut annaires* **8:** 322–323.

De longh HH, Wenno BJ, Meelis E. 1995. Seagrass distribution and seasonal biomass change in relation to dugong grazing in the Moluccas, East Indonesia. *Aquatic Botany* **50:** 1–19.

Delfortrie E. 1880. Découverte d'un squelette entier de *Rytiodus* dans le falun Aquitanien. *Actes de la Societe Linneenne de Bordeaux* **34:** 131–144.

De Man E, Ivany L, Vandenberghe N. 2004. Stable oxygen isotope record of the Eocene-Oligocene transition in the southern North Sea Basin: positioning the Oi-1 event. *Netherlands Journal of Geosciences / Geologie en Mijnbouw* **83:** 193–197.

Depéret C. 1895. Ueber die Fauna von miocänen Wirbelthieren aus der ersten Mediterranstufe von Eggenburg. *Sitzungsberichte der mathematisch-naturwissenschaftlichen Klasse der Akademie der Wissenschaften* **104:** 395–416.

De Ruig MJ, Hubbard SM. 2006. Seismic facies and reservoir characteristics of a deep-marine channel belt in the Molasse foreland basin, Puchkirchen Formation, Austria. *American Association of Petroleum Geologists Bulletin* **90:** 735–752.

De Zigno A. 1875. Sirenii fossili trovati nel Veneto. *Membro Effettivo del Reale Istituto Veneto di Scienze, Lettre ed Arti* **18:** 1–30.

De Zigno A. 1878. Sopra un nuovo sirenio fossile scoperto nelle colline di Bra in Piemonte. *Reale Accademia dei Lincei Memorie della Classe di scienze fisiche matematiche e naturali* **2:** 3–13.

De Zigno A. 1880. Nuove osservazioni sull'*Halitherium veronense* Z. *Membro Effettivo del Reale Istituto Veneto di Scienze, Lettre ed Arti* **21:** 1–6.

De Zigno A. 1887. Quelques observations sur les siréniens fossiles. *Bulletin de la Société Geologique de France* **15:** 728–732.

Dollo L. 1889. Première note sur les siréniens de Boom (résumé). *Bulletin de la Société belge de géologie, de paléontologie & d'hydrologie* **3:** 415–421.

Domning DP. 1978. Sirenian evolution in the North Pacific Ocean. *University of California Publications in Geological Sciences* **118:** 1–177.

Domning DP. 1980. Feeding position preference in manatees (*Trichechus*). *Journal of Mammology* **61:** 544–547.

Domning DP. 1981. Sea cows and sea grasses. *Paleobiology* **7:** 417–420.

Domning DP. 1982. Evolution of manatees: a speculative history. *Journal of Paleontology* **56:** 599–619.

Domning DP. 1987. *Halianassa studeri* von Meyer, 1838 (Mammalia, Sirenia): proposed designation of a neotype and proposed conservation of *Halitherium* Kaup, 1838 by designation of a type species. *The Bulletin of Zoological Nomenclature* **44:** 122–125.

Domning DP. 1988. Fossil Sirenia of the West Atlantic and Caribbean region I. *Metaxytherium floridanum* Hay, 1922. *Journal of Vertebrate Paleontology* **8:** 395–426.

Domning DP. 1989a. Fossil Sirenia of the West Atlantic and Caribbean region. II. *Dioplotherium manigaulti* Cope, 1883. *Journal of Vertebrate Paleontology* **9:** 415–428.

Domning DP. 1989b. Fossil Sirenia of the West Atlantic and Caribbean region. III. *Xenosiren yucateca*, gen. et sp. nov. *Journal of Vertebrate Paleontology* **9:** 429–437.

Domning DP. 1989c. Kelp evolution: a comment. *Paleobiology* **15:** 53–56.

Domning DP. 1990. Fossil Sirenia of the West Atlantic and Caribbean region. IV. *Corystosiren varguezi*, gen. et sp. nov. *Journal of Vertebrate Paleontology* **10:** 361–371.

Domning DP. 1991a. A new genus for *Halitherium olseni* Reinhart, 1976 (Mammalia: Sirenia). *Journal of Vertebrate Paleontology* **11:** 398.

Domning DP. 1991b: Sexual and ontogenetic variation in the pelvic bones of *Dugong dugon* (Sirenia). *Marine Mammal Science* **7:** 311–316.

Domning DP. 1994. A phylogenetic analysis of the Sirenia. In: Berta A, Deméré T, eds. Contributions in marine mammal paleontology honoring Frank C. Whitmore Jr. *Proceedings of the San Diego Society of Natural History* **29:** 177–189.

Domning DP. 1996. Bibliography and Index of the Sirenia and Desmostylia. *Smithsonian Contributions to Paleobiology* **80:** 1–611.

Domning DP. 1997. Fossil Sirenia of the West Atlantic and Caribean Region. VI. *Crenatosiren olseni* Reinhart, 1976. *Journal of Vertebrate Paleontology* **17:** 397–412.

Domning DP. 2001a. Evolution of the Sirenia and Desmostylia. In: Mazin JM, Buffrénil V de, eds. *Secondary adaptation of tetrapods to life in water. Proceedings of the international meeting Poitiers 1996.* Munich: Verlag Dr. Friedrich Pfeil, 151–168.

Domning DP. 2001b. Sirenians, seagrasses, and Cenozoic ecological change in the Carribbean. *Palaeogeography, Palaeoclimatology, Palaeoecology* **166:** 27–50.

Domning DP. 2001c. The earliest known fully quadrupedal sirenian. *Nature* **413:** 625–627.

Domning DP. 2005. Fossil Sirenia of the West Atlantic and Caribbean region. VII. Pleistocene *Trichechus manatus* Linnaeus, 1758. *Journal of Vertebrate Paleontology* **25:** 685–701.

Domning DP, Aguilera OA. 2008. Fossil Sirenia of the West Atlantic and Caribbean Region. VIII. *Nanosiren garciae*, gen. et sp. nov. and *Nanosiren sanchezi*, sp. nov. *Journal of Vertebrate Paleontology* **28:** 479–500.

Domning DP, Beatty BL. 2007. Use of tusks in feeding by dugongid sirenians: observations and tests of hypotheses. *The Anatomical Record* **290:** 523–538.

Domning DP, Buffrénil V de. 1991. Hydrostasis in the Sirenia: quantitavie data and functional interpretations. *Marine Mammal Science* **7:** 331–368.

Domning DP, Furusawa H. 1994. Summary of taxa and distribution of Sirenia in the North Pacific Ocean. *The Island Arc* **3:** 506–512.

Domning DP, Gingerich PD. 1994. *Protosiren smithae*, new species (Mammalia, Sirenia) from the late middle Eocene of Wadi Hitan, Egypt. *Contributions from the Museum of Paleontology of University of Michigan* **29:** 69–87.

Domning DP, Hayek LA. 1986. Interspecific and intraspecific morphological variation in manatees (Sirenia: *Trichechus*). *Marine Mammal Science* **2:** 87–144.

Domning DP, Pervesler P. 2001. The Osteology and Relationship of *Metaxytherium krahuletzi* Depéret, 1895 (Mammalia: Sirenia). *Abhandlungen der Senckenbergischen Naturforschenden Gesellschaft Frankfurt am Main* **553:** 1–89.

Domning DP, Pyenson ND. 2008. “Snagging” teeth and premolar homologies in Paleoparadoxiidae (Mammalia: Desmostylia). *Journal of Vertebrate Paleontology* **28:** 923–927.

Domning DP, Ray CE. 1986. The earliest sirenian (Mammalia: Dugongidae) from the eastern Pacific Ocean. *Marine Mammal Science* **2:** 263–276.

Domning DP, Thomas H. 1987. *Metaxytherium serresii* (Mammalia: Sirenia) from the early Pliocene of Libya and France: a reevaluation of its morphology, phyletic position, and biostratigraphic and paleoecological significance. In: Boaz N, El-Arnauti A, Gaziry AW, Heinzelin J de, Boaz DD, eds. *Neogene Paleontology and Geology of Sahabi:* New York: John Wiley & Sons Inc, 205–232.

Domning DP, Morgan GS, Ray CE. 1982. North American Eocene sea cows (Mammalia: Sirenia). *Smithsonian Contributions to Paleobiology* **52:** 1–69.

Domning DP, Ray CE, McKenna MC. 1986. Two new Oligocene desmostylians and a discussion of tethytherian systematics. *Smithsonian Contribution to Paleobiology* **59:** 1–56.

Domning DP, Gingerich PD, Simons EL, Ankel-Simons FA. 1994. A new early Oligocene dugongid (Mammalia, Sirenia) from Fayûm Province, Egypt. *Contributions from the Museum of Paleontology, University of Michigan* **29:** 89–108.

Edinger T. 1933. Über Gehirne tertiärer Sirenia Ägyptens und Mitteleuropas sowie der rezenten Seekühe. *Abhandlungen der Bayerischen Akademie der Wissenschaften. Mathematisch-naturwissenschaftliche Abteilung* **20:** 5–36.

Ehrlich C. 1855. Beiträge zur Palaeontologie und Geognosie von Oberösterreich und Salzburg. I. Die fossilen Cetaceen-Reste aus den Tertiär-Ablagerungen bei Linz, mit besonderer Berücksichtigung jener der *Halianassa collinii* H. v. M., und des dazu gehörigen, im August des Jahres 1854 aufgefundenen Rumpfskelettes. *Bericht über das Museum Francisco-Carolinum Linz* **15:** 3–21.

Ernissee JJ, Abbott WH, Huddlestun PF. 1977. Microfossil correlation of the Coosawhatchie Clay (Hawthorn Formation, Miocene) of South Carolina, and its equivalent in Georgia. *Marine Micropaleontology* **2:** 105–119.

Faupl P, Roetzel R. 1990. Die Phosphoritsande und fossilreichen Grobsande: Gezeitenbeeinflußte Ablagerungen der Innviertler Gruppe (Ottnangien) in der oberösterreichischen Molassezone. *Jahrbuch der Geologischen Bundesanstalt Wien* **133:** 157–180.

Felsenstein J. 1985. Confidence limits on phylogenies: an approach using the bootstrap. *Evolution* **39:** 783–791.

Fischer MS. 1990. Un trait unique de l'oreille des éléphants et des siréniens (Mammalia): un paradoxe phylogénetique. *Comptes Rendus de l'Académie des Sciences. Série III.* **311:** 157–162.

Fischer K, Krumbiegel G. 1982. *Halitherium schinzi* Kaup, 1838 (Sirenia, Mammalia) aus dem marinen Mitteloligozän des Weißelsterbeckens (Bezirk Leipzig, DDR). *Hallesches Jahrbuch für Geowissenschaften* **7:** 73–95.

Fitzgerald EMG. 2005. Holocene record of the dugong (*Dugong dugon*) from Victoria, Southeast Australia. *Marine Mammal Science* **21:** 355–361.

Fitzinger LJ. 1842. Bericht über die in den Sandlagern von Linz aufgefundenen fossilen Reste eines urweltlichen Säugers (*Halitherium cristolii*). *Bericht über das Museum Francisco-Carolinum Linz* **6:** 61–72.

Fondi R, Pacini P. 1974. Nuovi resti di sirenide dal Pliocene antico della provincia di Siena. *Palaeontographia Italica* **67(= N.S.37):** 37–53.

Fuchs W, Thiele O. 1987. *Geologische Karte der Republik Österreich 1:50.000. Erläuterungen zu Blatt 34 Perg.* Wien: Geologische Bundesanstalt.

Furusawa H. 2004. A phylogeny of the North Pacific Sirenia (Dugongidae: Hydrodamalinae) based on a comparative study of endocranial casts. *Paleontological Research* **8:** 91–98.

Gheerbrant E. 2009. Paleocene emergence of elephant relatives and the rapid radiation of African ungulates. *Proceedings of the National Academy of Sciences* **106:** 10717–10721.

Gheerbrant E, Tassy P. 2009. L'origine et l'évolution des elephants. *Comptes Rendus Palevol* **8:** 281–294.

Gheerbrant E, Sudre J, Cappetta H. 1996. A Palaeocene proboscidean from Morocco. *Nature* **383:** 68–70.

Gheerbrant E, Domning DP, Tassy P. 2005a. Paenungulata (Sirenia, Proboscidea, Hyracoidea, and relatives). In: Rose KD, Archibald JD, eds. *Origins and relationships and the major clades.* Baltimore: Johns Hopkins University Press, 84–105.

Gheerbrant E, Sudre J, Tassy P, Amaghzaz M, Bouya B, Iarochène M. 2005b. Nouvelles données sur *Phosphatherium escuilliei* (Mammalia, Proboscidea) de l'Éocène inférieur du Maroc, apports à la phylogénie des Proboscidea et des ongulés lophodontes. *Geodiversitas* **27:** 239–333.

Ghibaudo G, Grandesso P, Massari F, Uchman A. 1996. Use of trace fossils in delineating sequence stratigraphic surfaces (Tertiary Venetian Basin, northeastern Italy). *Palaeogeography, Palaeoclimatology, Palaeoecology* **120:** 261–279.

Gill T. 1872. Arrangement of the families of mammals. *Smithonian Miscellaneous Collections* **230:** 1–98.

Gingerich PD. 1992. Marine mammals (Cetacea and Sirenia) from the Eocene of Gebel Mokattam and Fayûm, Egypt: stratigraphy, age, and paleoenvironments. *Papers on Paleontology, University of Michigan* **30:** 1–84.

Gingerich PD, Domning DP, Blane CE, Uhen MD. 1994. Cranial morphology of *Protosiren fraasi* (Mammalia, Sirenia) from the middle Eocene of Egypt: a new study using computed tomography. *Contributions from the Museum of Paleontology, University of Michigan* **29:** 41–67.

Gingerich PD, Arif MM, Bhatti MA, Raza HA, Raza SM. 1995. *Protosiren* and *Babiacetus* (Mammalia, Sirenia and Cetacea) from the Middle Eocene Drazinda Formation, Sulaiman Range, Punjab (Pakistan). *Contributions from the Museum of Paleontology, University of Michigan* **29:** 331–357.

Goloboff PA. 1999. NONA (NO NAME) ver. 2 published by the author, Tucumán, Argentina.

Gradstein FM, Ogg JG, Smith AG, Agterberg FP, Bleeker W, Cooper RA, Davydov V, Gibbard P, Hinnov IA, House MR. 2004. *A Geologic Time Scale 2004*. Cambridge: Cambridge University Press.

Gray JE. 1821. On the natural arrangement of vertebrose animals. *London Medical Repository* **15:** 296–310.

Green RC, Paul DT, Kromhout C, Scott TM. 2008. Text to accompany geologic map of the western portion of the USGS Perry 30 x 60 minute quadrangle, northern Florida. *Florida Geological Survey (Open-File Report)* **92:** 1–29.

Green RC, Williams CP, Paul DT, Kromhout C, Scott TM. 2009. Text to accompany geologic map of the eastern portion of the USGS Ocala 30 x 60 minute quadrangle, North-Central Florida. *Florida Geological Survey (Open-File Report)* **93:** 1–22.

Grill R. 1935. Das Oligocänbecken von Gallneukirchen bei Linz a. D. und seine Nachbargebiete. *Mitteilungen der Geologischen Gesellschaft in Wien* **28:** 37–71.

Grimm KI. 1994. Paläoökologie, Paläogeographie und Stratigraphie im Mainzer Becken, im Oberrheingraben, in der Hessischen Senke und in der Leipziger Bucht während

des Mittleren Rupeltons (Fischschiefer / Rupelium / Unteroligozän). *Mitteilungen der Pollichia* **81:** 7–193.

Grimm KI. 1998. Correlation of Rupelian coastal and basin facies in the Mainz Basin (Oligocene, Germany). *Neues Jahrbuch für Geologie und Paläontologie, Monatshefte* **3:** 146–156.

Grimm KI. 2002. Foraminiferal zonation of early Oligocene deposits (Selztal Group, Latdorfian, Rupelian) in the Mainz Basin, Germany. *Journal of Micropalaeontology* **21:** 67–74.

Grimm KI. 2005. Das Tertiär des Mainzer Beckens in der stratigraphischen Tabelle von Deutschland 2002. *Newsletters on Stratigraphy* **41:** 347–350.

Grimm KI, Grimm MC. 2003. Geologischer Führer durch das Mainzer Tertiärbecken. In: Grimm KI, Grimm MC, Neuffer FO, Lutz H, eds. Die fossilen Wirbellosen des Mainzer Tertiärbeckens. Teil 1-1. *Mainzer Naturwissenschaftliches Archiv, Beiheft* **26:** 1–158.

Grimm KI, Steurbaut E. 2001. Foraminiferal biofacies analysis of the Boom Clay Formation in the Rupel area (Oligocene, Belgium), and correlation with the Mainz Basin (Germany). *Aardkundige Mededelingen* **11:** 9–20.

Grimm KI, Grimm MC, Schindler T. 2000. Lithostratigraphische Gliederung im Rupelium / Chattium des Mainzer Beckens, Deutschland. *Neues Jahrbuch für Geologie und Paläontologie, Abhandlungen* **3:** 343–397.

Grimm KI, Grimm MC, Köthe A, Schindler T. 2002. Der "Rupelton" (Rupelium, Oligozän) der Tongrube Bott-Eder bei Rauenburg (Oberrheingraben, Deutschland). *Courier Forschungsinstitut Senckenberg* **237:** 229–253.

Gürs K, Janssen AW. 2004. Sea-level related molluscan plankton events (Gastropoda, Euthecosomata) during the Rupelian (early Oligocene) of the North Sea Basin. *Netherlands Journal of Geosciences / Geologie en Mijnbouw* **83:** 199–208.

Hartlaub C. 1886. Ueber *Manatherium delheidi*, eine Sirene aus dem Oligocän Belgiens. *Zoologische Jahrbücher* **1:** 369–378.

Hay OP. 1922. Description of a new fossil sea cow from Florida, *Metaxytherium floridanum*. *Proceedings of the United States National Museum* **61:** 1–4.

Heizmann EPJ. 1992. Das Tertiär in Südwestdeutschland. *Stuttgarter Beiträge zur Naturkunde*, *Serie C* **33:** 1–61.

Heuvelmans B. 1941. Notes sur la dentition des Siréniens. III. La dentition du *Dugong*. *Bulletin du Musée Royal d'Histoire Naturelle de Belgique* **17:** 1–14.

Hubbard SM, De Ruig MJ, Graham SA. 2005. Utilizing outcrop analogs to improve subsurface mapping of natural gas-bearing strata in the Puchkirchen Formation, Molasse Basin, Upper Austria. *Austrian Journal of Earth Sciences* **98:** 52–66.

Illiger JKW. 1811. *Prodomus systematis mammalium et avium: additis terminis zoographicis utriusque classis eorumque versione Germanica*. Salfeld: Berolini.

International Commission on Zoological Nomenclature (ICZN). 1989. Opinion 1535. *Halianassa studeri* von Meyer, 1838 (Mammalia, Sirenia): neotype designated; and *Halitherium* Kaup, 1838 (Mammalia, Sirenia): *Pugemeodon schinzii* Kaup, 1838 designated as the type species. *The Bulletin of Zoological Nomenclature* **46:** 83–84.

International Commission on Zoological Nomenclature (ICZN). 2001. *Official lists and indexes of names and works in zoology. Supplement 1986–2000.* The International Trust for Zoological Nomenclature.

Internationale Kommission für Zoologische Nomenklatur (IKZN). 2000. Internationale Regeln für die Zoologische Nomenklatur. *Abhandlungen des Naturwissenschaftlichen Vereins in Hamburg* **(NF) 34:** 1–232.

Jefferies RPS. 1979. The origin of the chordates – a methodological essay. In: House MR, ed. The origin of major invertebrate groups. *Systematics Association, Special Volume* **12:** 443–477.

Kaiser HE. 1975. *Morphology of the Sirenia: a macroscopic and X-Ray atlas of the osteology of recent species*. Basel: S. Karger AG.

Kaup JJ. 1838. *Halytherium* und *Pugmeodon* im Maynzer Becken. *Neues Jahrbuch für Mineralogie, Geognosie, Geologie und Petrefaktenkunde* **1838:** 318–320.

Kaup JJ. 1855. *Beitraege zur naeheren Kenntnis der urweltlichen Saeugethiere*. *Zweites Heft*. Darmstadt: Leske.

Kaup JJ. 1856. Über einen vollständigen *Halitherium*-Gaumen mit Zähnen. *Neues Jahrbuch für Mineralogie, Geognosie, Geologie und Petrefaktenkunde* **1856:** 19–21.

Kaup JJ. 1861. *Beitraege zur naeheren Kenntnis der urweltlichen Saeugethiere*. *Fünftes Heft*. Darmstadt & Leipzig: Eduard Zernin.

Kaup JJ, Scholl JB. 1834. *Verzeichnis der Gypsabgüsse von den ausgezeichnetsten urweltlichen Thierresten des Grossherzoglichen Museum zu Darmstadt.* Darmstadt: Diehl.

Kellogg R. 1966. Fossil marine mammals from the Miocene Calvert Formation of Maryland and Virginia. *United States National Museum Bulletin* **247:** 65–98.

Kilmer FH. 1965. A Miocene dugongid from Baja California, Mexico. *Bulletin of the Southern California Academy of Sciences* **64:** 57-74.

Kleinschmidt A. 1982. Wissenswertes über die Säugerordnung der Seekühe (Sirenia) unter besonderer Berücksichtigung der Stellerschen Riesenseekuh *Rhytina gigas* (Zimmermann, 1780) sowie ihre hochgradige Anpassung an das Wasserleben im Vergleich zu den Walen. *Braunschweiger Naturkundliche Schriften* **1:** 367–418.

Kobayashi S, Horikawa H, Miyazaki S. 1995. A new species of Sirenia (Mammalia: Hydrodamalinae) from the Shiotsubo Formation in Takasato, Aizu, Fukushima Prefecture. *Journal of Vertebrate Paleontology* **15:** 815–829.

Kordos L. 1981. Some complements to the knowledge of a middle Eocene sirenian, *Sirenavus hungaricus*. *Fragmenta Mineralogica et Paleontologica* **10:** 75–78.

Kordos L. 2002. Eocene sea cows (Sirenia, Mammalia) from Hungary. *Fragmenta Palaeontologica Hungarica* **20:** 43–48.

Krauss CFF. 1858. Beiträge zur Kenntnis des Schädel-Baues von *Halitherium*. *Neues Jahrbuch für Mineralogie, Geognosie, Geologie und Petrefaktenkunde* **1858:** 519–531.

Krauss CFF. 1862. Der Schädel des *Halitherium schinzi* Kaup. *Neues Jahrbuch für Mineralogie, Geognosie, Geologie und Petrefaktenkunde* **1862:** 385–415.

Kretzoi M. 1941. *Sirenavus hungaricus* n. g., n. sp. Ein neuer Prorastomide aus dem Mittleozän (Lutetium) von Felsőgalla in Ungarn. *Annales historico-naturales Musei Nationalis Hungarici, Pars mineralogica, geologica et palaeontologica* **34:** 146–156.

Kuhlemann J, Kempf O. 2002. Post-Eocene evolution of the North Alpine Foreland Basin and its response to Alpine tectonics. *Sedimentary Geology* **152:** 45–78.

Kuntner M, May-Collado LJ, Agnarsson I. 2010. Phylogeny and conservation priorities of afrotherian mammals (Afrotheria, Mammalia). *Zoologica Scripta* **40:** 1–15.

Lacépède BGÉ. 1799. *Tableau des divisions, sous-divisions, orders et genres des mammifères.* Paris: Plassan.

Lanyon JM, Sanson GD. 2006. Degenerate dentition of the dugong (*Dugong dugon*) or why a grazer does not need teeth: morphology, occlusion and wear of mouthparts. *Journal of Zoology* **268:** 133–152.

Lartet M. 1866. Note sur deux nouveaux siréniens fossiles des terrains tertiaires de bassin de la Garonne. *Bulletin de la Société Geologique de France* **23:** 673–686.

Laurillard CL. 1846. *Metaxytherium*. *Dictionnaire de l'Université d'Histoire Naturelle* **8:** 171–172.

Lavergne A, Douzery E, Stichler T, Catzeflis M, Springer MS. 1996. Interordinal mammalian relationships: evidence for paenungulate monophyly is provided by complete mitochondrial 12S rRNA sequences. *Molecular Phylogenetics and Evolution* **6:** 245–258.

Lepsius GR. 1882. *Halitherium Schinzi, die fossile Sirene des Mainzer Beckens*. I. Band. Darmstadt: Abhandlungen des Mittelrheinischen geologischen Vereins.

Linnaeus C von. 1758. Systema naturae per regna tria naturae, secundum classes, ordines, genera, species, cum characteribus, differentiis, synonymis, locis. *Holmiae impensis direct. Laurentii Salvii Editio* **10 (reformata):** 6–823.

Lowenstein JM. 1985. Molecular approaches to the identification of species: immunological analysis of proteins from living or fossil organism can be used to identify unrecognizable species and to obtain new information on taxonomic relationships and dates of evolutionary divergences. *American Scientist* **73:** 541–547.

Luckett WP. 1993. An ontogenetic assessment of dental homologies in therian mammals. In: Szalay FS, Novacek MJ, McKenna MC, eds. *Mammal Phylogeny: Mesozoic Differentiation, Multituberculates, Monotremes, Early Therians, and Marsupials*. New York: Springer.

Maddison WP, Donoghue MJ, Maddison DR. 1984. Outgroup analysis and parsimony. *Systematic Zoology* **33:** 83–103.

Madsen O, Scally M, Douady CJ, Kao DJ, DeBry RW, Adkins R, Amrine HM, Stanhope MJ, de Jong WW, Springer MS. 2001. Parallel adaptive radiations in two major clades of placental mammals. *Nature* **409:** 610–614.

Mahboubi M, Ameur R, Crochet JY, Jaeger JJ. 1984. Earliest known proboscidean from early Eocene of North-West Africa. *Nature* **308:** 543–544.

Mahboubi M, Ameur R, Crochet JY, Jaeger JJ. 1986. El Kohol (Saharan Atlas, Algeria). A new Eocene mammal locality in northwestern Africa. *Palaeontographica, Abteilung A* **192:** 15–49.

Marsh H. 1980. Age determination of the dugong (*Dugong dugon* (Müller)) in northern Australia and its biological implications. *Reports of the International Whaling Commission, Special Issue* **3:** 181–201.

Martini E. 1982. Bestandsaufnahme des Nannoplankton im “prä-aquitanen” Tertiär des Mainzer Beckens. *Mainzer geowissenschaftliche Mitteilungen* **10:** 29–36.

Martini E, Müller C. 1971. Das marine Alttertiär in Deutschland und seine Einordnung in die Standard Nannoplankton Zonen. *Erdöl und Kohle* **24:** 381–384.

Matthew WD. 1916. New sirenian from the Tertiary of Porto Rico, West Indies. *Annales of New York Academy of Science* **27:** 23–29.

McKenna MC. 1975. Toward a phylogenetic classification of the Mammalia. In: Luckett WP, Szalay FS, eds. *Phylogeny of the Primates: A Multidisciplinary Approach.* New York and London: Plenum.

McKenna MC, Bell SK. 1997. *Classification of mammals above the species level.* New York: Columbia University Press.

Mellere D, Stefani C, Angevine C. 2000. Polyphase tectonics through subsidence analysis: the Oligo-Miocene Venetian and Friuli Basin, north-east Italy. *Basin Research* **12:** 159–182.

Meulenkamp JE, Sissingh W. 2003. Tertiary palaeogeography and tectonostratigraphic evolution of the northern and southern Peri-Tethys platforms and the intermediate domains of the African-Eurasian convergent plate boundary zone. *Palaeogeography, Palaeoclimatology, Palaeoecology* **196:** 209–228.

Meyer H von. 1847. [Mittheilungen an Prof. Bronn, Frankfurt a. M., 4. Januar 1847]. *Neues Jahrbuch für Mineralogie, Geognosie, Geologie und Petrefaktenkunde* **1847:** 181–196.

Mitchell J. 1973. Determination of relative age in the dugong (*Dugong dugon*, Müller) from a study of skulls and teeth. *Zoological Journal of the Linnean Society* **53:** 1–23.

Monroe WH. 1980. Geology of the middle Tertiary formations of Puerto Rico. *Geological Survey, Professional Paper* **953:** 1–93.

Moussa MT, Seiglie GA. 1970. Revision of mid-Tertiary stratigraphy of southwestern Puerto Rico. *American Association of Petroleum Geologists Bulletin* **54:** 1887–1898.

Murata Y, Nikaido N, Sasaki T, Cao C, Fukumoto Y, Hasegawa M, Okadaa N. 2003. Afrotherian phylogeny as inferred from complete mitochondrial genomes. *Molecular Phylogenetics and Evolution* **28:** 253–260.

Murphy WJ, Eizirik E, Johnson WE, Zhang YP, Ryder OA, O'Brien SJ. 2001a. Molecular phylogenetics and the origins of placental mammals. *Nature* **409:** 614–648.

Murphy WJ, Eizirik E, O'Brien SJ, Madsen O, Scally M, Douady CJ, Teeling E, Ryder OA, Stanhope MJ, de Jong WW, Springer MS. 2001b. Resolution of the early placental mammal radiation using Bayesian phylogenetics. *Science* **294:** 2348–2351.

Neumann D. 1936. Das Handskelett von *Halitherium schinzi* Kaup. *Paläontologische Zeitschrift* **18:** 257–291.

Nixon KC. 1999–2002. WinClada ver. 1.0000 published by the author, Ithaca, NY, USA.

Novacek MJ, Wyss AR. 1986. Higher-level relationships of the recent eutherian orders: morphological evidence. *Cladistics* **2:** 257–287.

Novacek MJ, Wyss AR, McKenna MC. 1988. The major groups of eutherian mammals. In: Benton MJ, ed. The phylogeny and classification of the tetrapods. Vol. 2. Mammals. *The Systematics Association, Special Volume* **35B:** 31–71.

Owen R. 1855. On the fossil skull of a mammal (*Prorastomus sirenoides*, Owen) from the island of Jamaica. *Quarterly Journal of the Geological Society of London* **11:** 541–543.

Owen R. 1875. On fossil evidences of a sirenian mammal (*Eotherium aegyptiacum*, Owen) from the Nummulitic Eocene of the Mokattam Cliffs, near Cairo. *Quarterly Journal of the Geological Society of London* **31:** 100–105.

Palmer TS. 1895. The earliest name for Steller's sea cow and dugong. *Science* **2:** 449–450.

Palmer TS. 1899. [Review of Dr. E. L. Trouessart's *Catalogus Mammalium tam viventium quam fossilium*]. *Science* **10:** 491–495.

Papp A, Grill R, Janoscheck R, Kapounek J, Kollmann K, Turnovsky K. 1968. Zur Nomenklatur des Neogens in Österreich. *Verhandlungen der Geologischen Bundesanstalt* **1968:** 9–18.

Papp A, Kröll A, Fuchs R. 1978. Das Egerien in der Waschbergzone, Niederösterreich. *Verhandlungen der Geologischen Bundesanstalt* **1978:** 63–71.

Pascual R. 1953. Sobre nuevos restos de sirénidos del mesopotamiense. *Revista de la Asociacion Argentina* **8:** 163–181.

Peschel R. 1982. Erläuterungen zur "Geologischen Karte von Linz und Umgebung" (nach J. Schadler, 1964). *Naturkundliches Jahrbuch der Stadt Linz* **28:** 181–236.

Peters KF. 1867. Das Halitheriumskelet von Hainburg: *Halitherium cordieri*, Christol sp. (*Manatus cuvieri* ou fossilis, Blainv.; *Hippopotamus medius cuvieri* var). *Jahrbuch der Kaiserlich-Königlichen Geologischen Reichsanstalt* **17:** 309–341.

Phillips RC, Meñez EG. 1988. Seagrasses. *Contributions to the Marine Sciences* **34:** 1–104.

Pia J, Sickenberg O. 1934. Katalog der in den österreichischen Sammlungen befindlichen Säugetierreste des Jungtertiärs Österreichs und der Randgebiete. *Denkschriften des Naturhistorischen Museums in Wien, Geologisch-Paläontologische Reihe* **4:** 1–544.

Piller WE, Egger H, Erhart CW, Gross M, Harzhauser M, Hubmann B, Van Husen D, Krenmayr H-G, Krystyn L, Lein R, Lukeneder A, Mandl GW, Rögl F, Roetzel R, Rupp C, Schnabel W, Schönlaub HP, Summesberger H, Wagreich M, Wessely G. 2004. Die stratigraphische Tabelle von Österreich 2004 (sedimentäre Schichtfolgen).

Pilleri G. 1985. The Miocene Cetacea of the Belluno sandstones (eastern southern Alps). *Memoire di Scienze Geologiche* **36:** 1–250.

Pilleri G. 1987. *The Sirenia of the Swiss Molasse. With a descriptive catalogue of the fossil Sirenia preserved in Swiss collections*. Ostermundigen (Bern): Brain Anatomy Institute.

Pilleri G. 1988a. A skull of *Metaxytherium serresii (*Mammalia: Sirenia) from the lower Pliocene of Montpellier. In: Pilleri G, ed. *Contributions to the paleontology of some Tethyan Cetacea and Sirenia (Mammalia).* Ostermundigen (Bern): Brain Anatomy Institute, 111–123.

Pilleri G. 1988b. The Pliocene Sirenia of the Po Basin (*Metaxytherium subapenninum* Bruno, 1839). In: Pilleri G, ed. *Contributions to the paleontology of some Tethyan Cetacea and Sirenia (Mammalia).* Ostermundigen (Bern): Brain Anatomy Institute, 45–103.

Pirkenseer C, Spezzaferri S, Berger J-P. 2010. Palaeoecology and biostratigraphy of the Paleogene Foraminifera from the southern Upper Rhine Graben and the influence of reworked planktonic Foraminifera. *Palaeontographica, Abteilung A* **293:** 1–93.

Pocock RI. 1940. Some notes on the dugong. *The Annals and Magazine of Natural History, 11th Series* **5:** 329–345.

Rainey WE, Lowenstein JM, Sarich VM, Magor DM. 1984. Sirenian molecular systematics – including the extinct Steller's sea cow (*Hydrodamalis gigas*). *Naturwissenschaften* **71:** 586–588.

Reinhart RH. 1951. A new genus of sea cow from the Miocene of Colombia. *University of California Publications, Bulletin of the Department of Geological Sciences* **28:** 203–213.

Reinhart RH. 1959. A review of the Sirenia and Desmostylia. *University of California Publications in Geological Sciences* **36:** 1–146.

Reinhart RH. 1976. Fossil sirenians and desmostylids from Florida and elsewhere. *Bulletin of the Florida State Museum, Biological Sciences* **20:** 187–300.

Retzius AJ. 1794. Anmärkningar vid genus Trichechi. *Kongliga Vetenskaps Academiens Nya Handlingar* **15:** 286–300.

Rieppel O. 1999. *Einführung in die computergestützte Kladistik.* München: Verlag Dr. Friedrich Pfeil.

Robineau D. 1969. Morphologie externe du complexe osseux temporal chez les siréniens. *Mémoires du Muséum National d'Histoire Naturelle, Série A, Zoologie* **60:** 1–32.

Rögl F. 1999. Mediterranean and Paratethys. Facts and hypotheses of an Oligocene to Miocene paleogeography (short overview). *Geologica Carpathica* **50:** 339–349.

Rögl F, Steininger F. 1969. *Miogypsina* (*Miogypsinoides*) *formosensis* Yabe & Hanzawa, 1928 (Foraminiferida) aus den Linzer Sanden (Egerien-Oberoligozän) von Plesching bei Linz, Oberösterreich. *Mitteilungen der Geologischen Gesellschaft in Wien* **62:** 46–54.

Roetzel R, Hochuli P, Steininger F. 1983. Die Faziesentwicklung des Oligozäns in der Molassezone zwischen Krems und Wieselburg (Niederösterreich). *Jahrbuch der Geologischen Bundesanstalt* **126:** 129–179.

Rothausen K, Sonne V. 1984. *Sammlung geologischer Führer Band 79: Mainzer Becken.* Berlin, Stuttgart: Gebrüder Bornträger.

Rousse S, Duringer P, Stapf KRG. 2012. An exceptional rocky shore preserved during Oligocene (late Rupelian) transgression in the Upper Rhine Graben (Mainz Basin, Germany). *Geological Journal* **47:** 388–408.

Rupp C. 2008. *Erläuterungen zu Blatt 47 Ried im Innkreis*. Wien: Geologische Bundesanstalt.

Sagne C. 2001a. *Halitherium taulannense*, nouveau sirénien (Sirenia, Mammalia) de l'Éocène supérieur provenant du domaine Nord-Téthysien (Alpes-de-Haute-Provence, France). *Comptes rendus de l'Académie des Sciences de la Terre et des Planètes* **333:** 471–476.

Sagne C. 2001b. La diversification des siréniens á l'Eocène (Sirenia, Mammalia). Etude morphologique et analyse phylogénétique du sirénien de Taulanne, *Halitherium taulannense*. Unpublished D. Phil. Thesis, Muséum National d'Histoire Naturelle Paris.

Samonds KE, Zalmout IS, Irwin MT, Krause DW, Rogers RR, Raharivony LL. 2009. *Eotheroides lambondrano*, new middle Eocene sea cow (Mammalia: Sirenia) from the Mahajanga Basin, northwestern Madagascar. *Journal of Vertebrate Paleontology* **29:** 1233–1243.

Savage RJG. 1976. Review of early Sirenia. *Systematic Zooolgy.* **25:** 344–351.

Savage RJG, Domning DP, Thewissen JGM. 1994. Fossil Sirenia of the West Atlantic and Caribbean region. V. The most primitive known sirenian, *Prorastomus sirenoides* Owen, 1855. *Journal of Vertebrate Paleontology* **14:** 427–449.

Schaarschmidt F. 1982. Bestandsaufnahme der Makroflora im "prä-aquitanen" Tertiär des Mainzer Beckens. *Mainzer geowissenschaftliche Mitteilungen* **10:** 19–28.

Schäfer W. 1962. *Halitherium*: Fossil und Leiche. *Natur und Museum* **92:** 53–56.

Schmidtgen O. 1912. Neue Beiträge zur Kenntnis der hinteren Extremität von *Halitherium schinzi* Kaup. *Zoologisches Jahrbuch* **15** (suppl.)**:** 457–498.

Schöggl H, Micklich N. 2013. Eine Seekuh aus dem Rupelton der Grube Unterfeld. *Kaupia, Darmstätter Beiträge zur Naturgeschichte* **18:** 81–87.

Scott TM. 1988. The lithostratigraphy of the Hawthorn Group (Miocene) of Florida. *Florida Geological Survey Bulletin* **59:** 1–148.

Scott TM. 1990. The lithostratigraphy of the Hawthorn Group of peninsular Florida. In: Burnett W, Riggs SR, eds. Phosphate deposits of the world. *Florida Geological Survey (Open-File Report)* **36:** 325–336.

Shoshani J, McKenna MC. 1998. Higher taxonomic relationships among extant mammals based on morphology, with selected comparisons of results from molecular data. *Molecular Phylogenetics and Evolution* **9:** 572–584.

Sickenberg O. 1934a. Beiträge zur Kenntnis Tertiärer Sirenen. I. Die Eozänen Sirenen des Mittelmeergebietes. II. Die Sirenen des Belgischen Tertiärs. *Mémoires du Musée Royal d'Histoire Naturelle de Belgique* **63:** 1–352.

Sickenberg O. 1934b. Die ersten Reste von Landsäugetieren aus den Linzer Sanden. *Verhandlungen der Geologischen Bundesanstalt* **1934:** 60–63.

Siegfried P. 1965. *Anomotherium langewieschei* n.g.n.sp. (Sirenia) aus dem Ober-Oligozän des Dobergs bei Bünde/Westfalen. *Palaeontographica, Abteilung A* **124:** 116–150.

Simpson GG. 1932a. Fossil Sirenia of Florida and the evolution of the Sirenia. *Bulletin of the American Museum of Natural History* **59:** 419–503.

Simpson GG. 1932b. Mounted skeletons of *Eohippos*, *Merychippus* and *Hesperosiren*. *American Museum Novitates* **587:** 1–7.

Simpson GG. 1945. The principles of classification and a classification of mammals. *Bulletin of the American Museum of Natural History* **85:** 1–350.

Sissingh W. 1998. Comparative Tertiary stratigraphy of the Rhine Graben, Bresse Graben and Molasse Basin: correlation of Alpine foreland events. *Tectonophysics* **300:** 249–284.

Sorbi S. 2007. *The Neogene Euro-North African Sirenia: phylogenetic and systematic study, palaeoecological and palaeobiogeographic considerations*. Unpublished D. Phil. Thesis, Università di Pisa.

Sorbi S, Domning DP, Vaiani SC, Bianucci G. 2012. *Metaxytherium subapenninum* Bruno, 1839 (Mammalia, Dugongidae), the latest sirenian of the Mediterranean Basin. *Journal of Vertebrate Paleontology* **32:** 686–707.

Spain AV, Heinsohn GE. 1974. A biometric analysis of measurement data from a collection of North Queensland dugong skulls, *Dugong dugon* (Müller). *Australian Journal of Zoology* **22:** 249–257.

Spain AV, Heinsohn GE, Marsh H, Correll RL. 1976. Sexual dimorphism and other

sources of variation in a sample of dugong skulls from North Queensland. *Australian Journal of Zoology* **24:** 491–497.

Spiegel C, Kuhlemann J, Frisch W. 2007. Tracing sediment pathways by zircon fission track analysis. Oligocene marine connections in Central Europe. *International Journal of Earth Sciences (Geologische Rundschau)* **96:** 363–374.

Spillmann F. 1959. Die Sirenen aus dem Oligozän des Linzer Beckens (Oberösterreich) mit Ausführungen über "Osteosklerose" und "Pachyostose". *Denkschriften der mathematisch-naturwissenschaftlichen Klasse der Österreichischen Akademie der Wissenschaften* **110:** 1–68.

Spillmann F. 1969. Die fossilen Säugetierfaunen des Linzer Raumes. In: *Sonderdruck aus dem Katalog Geologie und Paläontologie des Linzer Raumes.* Linz: Oberösterreichisches Landesmuseum, 55–69.

Spillmann F. 1973. *Halitherium pergense* (Toula). Eine Polemik um die Taxonomie und Alterseinstufung der Sirenenreste aus dem Sandstein von Perg (OÖ.) und Wallsee (NÖ.). *Jahrbuch des Oberösterreichischen Musealvereines* **118:** 197–210.

Stanhope MJ, Waddell VG, Madsen O, de Jong WW, Hedges SB, Cleven GC, Kao D, Springer MS. 1998. Molecular evidence for multiple origins of the Insectivora and for a new order of endemic African mammals. *Proceedings of the National Academy of Sciences* **95:** 9967–9972.

Steininger FF, Berggren WA, Kent DV, Bernor RL, Sen S, Agusti J. 1996. Circum-Mediterranean Neogene (Miocene and Pliocene) marine-continental chronologic correlations of European mammal units. In: Bernor RL, Fahlbusch V, Mittmann H-W, eds. *The Evolution of Western Eurasian Neogene Mammal Faunas.* New York: Columbia University Press, 7–46.

Takahashi S, Domning DP, Saito T. 1986. *Dusisiren dewana*, n. sp. (Mammalia: Sirenia): a new ancestor of Steller's sea cow from the upper Miocene of Yamagata prefecture northeastern Japan. *Transactions and Proceedings of the Palaeontological Society of Japan* **141:** 296–321.

Tassy P, Shoshani J. 1988. The Tethytheria: elephants and their relatives. In: Benton MJ, ed. The phylogeny and classification of the tetrapods. Vol. 2 Mammals. *The Systematics Association, Special Volume* **35B:** 283–315.

Thenius E. 1960. Wirbeltierfunde aus der paläogenen Molasse Österreichs und ihre stratigraphische Bedeutung. *Verhandlungen der Geologischen Bundesanstalt* **1960:** 82–88.

Thenius E. 1998. *Zähne und Gebiß der Säugetiere. Handbuch der Zoologie. Mammalia.* Berlin: De Gruyter.

Thewissen JGM, Bajpai S. 2009. A new Miocene sirenian from Kutch, India. *Acta Palaeontologica Polonica* **54:** 7–13.

Thewissen JGM, Domning DP. 1992. The role of phenacodontids in the origin of the modern orders of ungulate mammals. *Journal of Vertebrate Paleontology* **12:** 494–504.

Toledo PM de, Domning DP. 1989. Fossil Sirenia (Mammalia: Dugongidae) from the Pirabas Formation (Early Miocene), northern Brazil. *Boletim do Museu Paraense Emilio Goeldi. Série Ciências da Terra* **1:** 119–146.

Toula F. 1899. Zwei Säugetierreste aus dem "kristallisierten Sandstein" von Wallsee in Nieder- und Perg in Oberösterreich. *Neues Jahrbuch für Mineralogie, Geologie und* Palaeontologie, *Beilagen Band* **12:** 447–476.

Vandenberghe N, van Simaeys S, Steurbaut E, Jagt JWM, Felder PJ. 2004. Stratigraphic architecture of the Upper Cretaceous and Cenozoic along the southern border of the North Sea Basin in Belgium. *Netherlands Journal of Geosciences / Geologie en Mijnbouw* **83:** 155–171.

Van Nievelt AFH, Smith KK. 2005. To replace or not to replace: the significance of reduced functional tooth replacement in marsupial and placental mammals. *Paleobiology* **31:** 324–346.

Van Simaeys S, de Man E, Vandenberghe N, Brinkhuis H, Steurbaut E. 2004. Stratigraphic and palaeoenvironmental analysis of the Rupelian–Chattian transition in the type region: evidence from dinoflagellate cysts, foraminifera and calcareous nannofossils. *Palaeogeography, Palaeoclimatology, Palaeoecology* **208:** 31–58.

Velez-Juarbe J, Domning DP, Pyenson ND. 2012. Iterative evolution of sympatric seacow (Dugongidae, Sirenia) assemblages during the past 26 Million years. *PLoS ONE* **7:** 1–8.

Vianna JA, Bonde RK, Caballero S, Giraldo JP, Lima RP, Clark A, Marmontel M, Morales-Vela B, Souza MJ de, Parr L, Rodríguez-Lopez MA, Mignucci-Giannoni AA. Powell JA, Santos FR. 2006. Phylogeography, phylogeny and hybridization in trichechid sirenians: implications for manatee conservation. *Molecular Ecology* **15:** 433–447.

Voss M. 2007. Discoveries of sirenian remains from the early Oligocene of the Rhine-Ruhr area (Germany) and a new look on the genus *Halitherium*. In: Warren A, ed. Conference on Australasian Vertebrate Evolution, Palaeontology and Systematics. *Geological Society of Australia* **85:** 45.

Voss M. 2008. New finds of *Halitherium* (Sirenia, Mammalia) from the lower Oligocene of the Rhine area (Germany). *Neues Jahrbuch für Geologie und Paläontologie, Abhandlungen* **249:** 257–269.

Voss M. 2009a. New aspects on innerspecific variation in the genus *Halitherium* (Mammalia: Sirenia). *Journal of Vertebrate Paleontology* **29(Suppl. 3):** 196.

Voss M. 2009b. Taxonomic and systematic problems within the genus *Halitherium* (Mammalia: Sirenia). *Terra Nostra* **2009(3):** 118.

Voss M. 2010. Character evolution, homoplasy and interrelationships of Sirenia. *Zitteliana B* **29:** 103.

Voss M. 2012. A new sea cow record from the lower Oligocene of western Germany: new indications on the skeletal morphology of *Halitherium schinzii* (Mammalia: Sirenia). *Paläontologische Zeitschrift* **86:** 205–217.

Wiley EO, Siegel-Causey D, Brooks DR, Funk VA. 1991. *The Compleat Cladist: a primer of phylogenetic procedures.* Special Publication No. 19. Kansas: University of Kansas/Museum of Natural History.

Wilhelm W. 1962. Eine versteinerte Seekuh aus dem Alzeyer Meeressand. *Natur und Museum* **92:** 51–53.

Zalmout IS, Gingerich PD. 2012. Late Eocene sea cows (Mammalia, Sirenia) from Wadi Al Hitan in the western dessert, Fayûm, Egypt. *Papers on Paleontology, University of Michigan* **37:** 1–158.

Zalmout IS, Ul-Haq M, Gingerich PD. 2003. New species of *Protosiren* (Mammalia, Sirenia) from the early middle Eocene of Balochistan (Pakistan). *Contributions from the Museum of Paleontology, University of Michigan* **31:** 79–87.

Zampieri D, Grandesso P. 2003. Fracture networks on the Belluno syncline, a fault-propagation fold in the footwall of the Belluno thrust, Venetian Alps, NE Italy. *Geological Society London. Special Publications* **209:** 101–106.

ACKNOWLEDGEMENTS

Above all, I am indebted to my supervisor Oliver Hampe for supporting my project idea of the “Revision of the *Halitherium*-species complex”. Thank you for helping me in bringing forward a proposal for a successful DFG grant! I am also grateful for providing me with the maximum freedom to accomplish all relevant matters of my dissertation under convenient conditions, taking especially into account my employment for “SYNTHESYS”, and having an equal say in planning the project and developing project activities.

This work could not have been realised without the kind assistance of the following colleagues, curators, collection managers and preparators to whom I am much obliged for providing either access to the collections, collection datasets and/or exhibitions.

Germany: Eva Heller-Karneth (Alzey), Irene Mann and Frieder Mayer (Berlin), Martin Walders (Bottrop), Michael Strauss (Bünde), Gabriele Gruber, Norbert Micklich, Eric Milsom and Oliver Sandrock (Darmstadt), Manfred Jäger and Manfred Raisch (Dotternhausen), Rainer Brocke and Mrs. Oelkers-Schaefer (Frankfurt), Dieter Grüll (Gernsheim), Johanna Kontny (Heidelberg), Frank Bach, Reinhardt Baudenbacher and Arnold Müller (Leipzig), Thomas Engel and Michael Wuttke (Mainz), Madelaine Böhme (formerly Munich, now Tübingen), Gertrud Rößner (Munich), Harald Stapf (Nierstein), Elmar Heizmann (Stuttgart), Michael Maisch (Tübingen), Fritz Geller-Grimm (Wiesbaden).

Europe: Burkart Engesser (Basel) and Daniela Schwarz-Wings (formerly Basel, now Berlin), Annelise Folie, Olivier Lambert and Etienne Steurbaut (Brussels), Mihaly Gasparik, László Kordos, Jozsef Palfy and Laszlo Peregovits (Budapest), Fritz Steininger and Johannes M. Tuzar (Eggenburg), Björn Berning (Linz), Jerry Hooker and Richard Sabin (London), Letizia Del Favero and Mariagabriella Fornasiero (Padova), Christine Argot, Christine Lefevre and Claire Sagne (Paris), Ulf Johansson and Thomas Moers (Stockholm).

Overseas: Catherine Kemper and Jim McNamara (Adelaide), Pat Holroyd (Berkeley, CA), Nick Pyenson (formerly Berkeley, CA, now Washington, D.C.), William Amaral and Judy Chupasko (Cambridge, MA), Richard Hulbert and Candace McCaffery (Gainesville, FL.), Erich Fitzgerald, Wayne Longmore, Rory O’Brian and Thomas Rich (Melbourne), Judy Galkin (New York), Barbara Done and Helene Marsh (Townsville, Qld.), David Bohaska, Daryl P. Domning and Charles W. Potter (Washington, D.C.).

This extensive research on fossil and extant sea cows was generously funded by one grant each from the DAAD and DFG, and two SYNTHESYS grants. Many thanks to all these organisations!

Sincere thanks are addressed to Daryl P. Domning for his interest, guidance and helpful suggestions during my stay in Washington D.C. Moreover, I am very grateful for his unselfish support with unpublished data on Eocene Sirenia from Jamaica.

I am deeply thankful to Philip D. Gingerich and Iyad S. Zalmout for giving me the unique opportunity to participate in the Wadi Al Hitan (Egypt) field trip in December 2010, and thereby, to get the chance to have a look at the Eocene sirenians exhibited in the CGM. I learned so much about field work, the Geology of Egypt, and, on a different note, about the wonderful cultural diversity on Earth. Thanks a lot for being so generous!

Michael Ohl (Berlin) is acknowledged for his experience in taxonomy and guidance in elucidating taxonomy related questions.

I have also received help in taxonomical respects from Björn Berning (Linz) to whom I am additionally grateful for his considerable efforts (and also those of his student) discovering sirenian material in the LI collections believed to be lost, for preparing a new and clear inventory list of all sirenian material available in LI (all of this done without losing your humor!), for providing me with helpful photographs and literature, and last but not least, for his kind hospitality during my stay in Linz. Thank you very much my lovely colleague from northern Germany!

I would like to thank Jürgen Kriwet (formerly Berlin and Stuttgart, now Vienna) for his valuable time devoted to fruitful discussions on systematics, helpful comments, and for constructive and humerous treatment of tricky questions.

I was very delighted in receiving the support from Jason Dunlop (Berlin), who kindly checked the spelling and grammar of major parts of this thesis. Warm thanks are dedicated to the adorable Nora Glaubrecht (Berlin) for precisely reviewing the final draft of my thesis. I am also grateful to Matthias Glaubrecht (Berlin) for his interest and attention in my research, and solution-oriented expertise in all areas relating to systematics. Additionally, Carsten Lueter (Berlin) is thanked for his tolerance and confidence giving me the spatial and temporal flexibility for conveniently realising both, my “SYNTHESYS” employment and doctoral studies.

Cordial thanks are given to Jan Müller-Edzards for some of the fabulous illustrations included in this thesis (Figures 21, 22B, 30B, 31A, 34B, 36B, 39B, D, 41B, 44B, 46B, D). Furthermore, I am indebted to Thomas Engel (Mainz) for his additional efforts in helping to clarify the skull morphology of a specimen exposed in MNHM, Claire Sagne (Paris) for kindly providing me with illustrations and photographs especially of specimens I haven’t investigated in person, and Manuela Schellenberger (Munich) for diligently making the photographs of the specimen BSPG 1956 I 540. With respect to the illustrations prepared for this thesis, I sincerely thank Oliver Coleman (Berlin) and my friend Steffen Preetz for giving me their cool drawing boards on loan.

Heike Mewis (Berlin) is acknowledged for her kind help with the software “R” in the course of the preparation of a diagram. I appreciate the courtesy of Kirsten I. Grimm (Mainz)

for mailing essential and hardly available literature on the Geology of the Mainz Basin. My thanks also go to Wighart von Koenigswald (Bonn) for helpful information on mammalian tooth morphology. I thank Ursula Göhlich for checking the history of the potential exchange of collection material between the Oberösterreichisches Landesmuseum Linz and the Naturhistorisches Museum Wien.

My very personal thanks go to Stefanie Klug (formerly Berlin and Stuttgart, now Bristol) for her encouragement, motivation, and company in Berlin, on conferences and even from abroad. That is why I would miss you if I had never made your acquaintance. I thank you for the depth and value of our many scientific conversations (and also for those in other respects), and especially for your sustained and dedicated support in reviewing my thesis and figures and, last but not least, for your essential help in producing the layout of this work. I always can count on you, my honourable friend!

Finally, I would like to express my appreciation and thanks to my bosom friend Mathias for always being there when he is needed (or not☺). Thank you for countless sit-ins and “adventure trips” that amused me a lot, especially since our cherished “Mr. Prange” is around. I extend my thanks to “my girls”: Karina, who has the talent to care for me and build me up despite being so far away, my cousin Katja and my friend Katja for always being my lovely sunshine, and Britta for her friendship and kind hospitality during my research stay in Boston.

Greatest appreciation deserves my much loved family, my parents and my brother, and, of course, our dog. I wouldn’t be where I am without your support!

I conclude by conveying my most important thanks to you, Robert. What can I say other than that your love, patience, gentleness, and humour gave me all I needed in the recent years. I love, love, love you!

APPENDICES

Appendix 1. List of personally investigated specimens (unless otherwise stated) formerly referred to the genus *"Halitherium"* indicating their original species assignment (Orig. spec.), locality and age. * identifies specimens that were excluded from the cladistic analyses *á posteriori.*
Abbreviation: **DE**, Germany; **BE**, Belgium; **CH**, Switzerland; **Fm**., Formation; **FR**, France; **HU**, Hungary.

Gen. nov. 1 *taulannense*

Original species: *Halitherium taulannense* Sagne, 2001a.
Stratigraphic range: Late Eocene (Priabonian).
General remarks: Only known from the locality Taulanne near Castellane (Alpes-de-Haute-Provence, France).

Collection nr.	Locality	Age	Material	Orig. spec.	Remarks
RGHP D040	Alpes-de-Haute-Provence, FR	Priabonian	Skull of adult	*H. taulannense*	**Holotype** of gen. nov. 1 *taulanense*, pers. obs.
D349	Alpes-de-Haute-Provence, FR	Priabonian	Skull of subadult	*H. taulannense*	**Paratype**, Sagne (2001a)
C001	Alpes-de-Haute-Provence, FR	Priabonian	Mandible of subadult and isolated premolars	*H. taulannense*	**Paratype**, pers. obs.
E.7.096a	Alpes-de-Haute-Provence, FR	Priabonian	Mandible of adult	*H. taulannense*	**Paratype**, pers. obs.
D350	Alpes-de-Haute-Provence, FR	Priabonian	Right scapula of adult	*H. taulannense*	**Paratype**, Sagne (2001a)
C035	Alpes-de-Haute-Provence, FR	Priabonian	Right humerus of adult	*H. taulannense*	**Paratype**, Sagne (2001a)
C006	Alpes-de-Haute-Provence, FR	Priabonian	Left radius and ulna of subadult	*H. taulannense*	**Paratype**, Sagne (2001a)
D024	Alpes-de-Haute-Provence, FR	Priabonian	Autopod	*H. taulannense*	**Paratype**, Sagne (2001a)
C050	Alpes-de-Haute-Provence, FR	Priabonian	Left innominate	*H. taulannense*	**Paratype**, Sagne (2001a)
D345	Alpes-de-Haute-Provence, FR	Priabonian	Partial skull of juvenile	*H. taulannense*	Pers. obs.
D057	Alpes-de-Haute-Provence, FR	Priabonian	Braincase of juvenile	*H. taulannense*	Pers. obs.
D349	Alpes-de-Haute-Provence, FR	Priabonian	Skull of adult	*H. taulannense*	Sagne (2001b)
D055	Alpes-de-Haute-Provence, FR	Priabonian	Maxillary fragment of juvenile	*H. taulannense*	Sagne (2001b)
D275	Alpes-de-Haute-Provence, FR	Priabonian	Maxillary fragment of juvenile	*H. taulannense*	Sagne (2001b)
C009	Alpes-de-Haute-Provence, FR	Priabonian	Mandible of subadult	*H. taulannense*	Pers. obs.
E.5.031	Alpes-de-Haute-Provence, FR	Priabonian	Right I1	*H. taulannense*	Sagne (2001b)
C054	Alpes-de-Haute-Provence, FR	Priabonian	Right R1 of adult	*H. taulannense*	Sagne (2001b)
D273	Alpes-de-Haute-Provence, FR	Priabonian	Femur	*H. taulannense*	Sagne (2001b)
E.9.001	Alpes-de-Haute-Provence, FR	Priabonian	Femur	*H. taulannense*	Sagne (2001b)

AGM	13	Alpes-de-Haute-Provence, FR	Priabonian	I1	*H. taulannense*	Sagne (2001b)
	26	Alpes-de-Haute-Provence, FR	Priabonian	Left innominate	*H. taulannense*	Sagne (2001b)

Gen. nov. 2 spec. nov. 1

Original species: *Halitherium schinzii* Kaup, 1838 following the synonymy of Domning (1996).
Stratigraphic range: Early Oligocene (Rupelian).
General remarks: All specimens personally investigated.

Collection nr.	Locality	Age	Material	Orig. spec.	Remarks
ALMD-JBH A92	Ratingen-Lintorf, West Germany	"Transgressionskies"	Parietal-supraoccipital skullcap and fragment of left scapula	*Halitherium* Kaup, 1838	Voss (2008): figs. 9, 10
BSPG 1956 I 540	Eckelsheim, Mainz Basin, DE	Alzey Fm.	Partial skeleton of adult (articulated skull, mandible, vertebrae of all segments, ribs and left innominate)	*H. schinzii*	**Holotype** of gen. nov. 2 spec. nov. 1; in cladistic analyses
1956 I 542	Eckelsheim, Mainz Basin, DE	Alzey Fm.	Supraoccipital	*H. schinzii*	
CDGG S3	Wendelsheim, Mainz Basin, DE	Alzey Fm.	Partial skeleton of adult (partial skull, mandible, vertebrae, ribs, left innominate)	*H. schinzii*	
S5	Wendelsheim, Mainz Basin, DE	Alzey Fm.	Parietal-supraoccipital skullcap	*H. schinzii*	
FIS M2597	Flonheim, Mainz Basin, DE	Alzey Fm.	Partial skull of subadult	*H. schinzii*	In cladistic analyses
M2603	Flonheim, Mainz Basin, DE	Alzey Fm.	Supraoccipital	*H. schinzii*	
M2715	Flonheim, Mainz Basin, DE	Alzey Fm.	Parietal-supraoccipital skullcap	*H. schinzii*	Edinger (1933): fig. 8, pl. 2: fig. 3
M8002	Weinheim, Mainz Basin, DE	Alzey Fm.	Partial skull, ribs and scapular fragment	*H. schinzii*	In cladistic analyses
M8541	Wöllstein, Mainz Basin, DE	Alzey Fm.	Partial skull, ribs and sternal fragment	*H. schinzii*	Schäfer (1962): 53, fig. 1
FMD SRK Eck 124	Eckelsheim, Mainz Basin, DE	Alzey Fm.	Partial skeleton of juvenile (disarticulated skull, (fragmentary) vertebrae, ribs, manubrium, both innominates)	*H. schinzii*	
GPMH unnumbered	Mainz Basin, DE	Alzey Fm.	Parietal-supraoccipital scullcap	*H. schinzii*	
HLMD-WT Az 64	Flonheim, Mainz Basin, DE	Alzey Fm.	Frontoparietal-supraoccipital skullcap of juvenile	*H. kaupi* Krauss, 1858	Kaup (1855): pl. 2: fig. 1; Krauss (1858): 528; **holotype** of *H. kaupi*
Az 84, 85	Flonheim, Mainz Basin, DE	Alzey Fm.	Frontoparietal-supraoccipital skullcap	*H. schinzii*	
Az 101	Flonheim, Mainz Basin, DE	Alzey Fm.	Parietal-supraoccipital skullcap of juvenile	*H. schinzii*	
Az 103	Mainz Basin, DE	Alzey Fm.	Parietal-supraoccipital skullcap of juvenile	*H. schinzii*	
Az 137	Flonheim, Mainz Basin, DE	Alzey Fm.	Parietal-supraoccipital skullcap	*H. schinzii*	
Az 174	Alzey, Mainz Basin, DE	Alzey Fm.	Parietal-supraoccipital skullcap	*H. schinzii*	

Az 102, 177	Mainz Basin, DE	Alzey Fm.	Frontoparietal-supraoccipital skull cap	*H. schinzii*	
Az 185	Mainz Basin, DE	Alzey Fm.	Parietal-supraoccipital skullcap of juvenile	*H. schinzii*	
420	Flörsheim, Mainz Basin, DE	Bodenheim Fm.	Partial skeleton of adult (distorted partial skull, lumbar and caudal vertebrae, chevrons, ribs, fragments of left scapula, elements of right stylopod, zeugopod and autopod, innominates)	*H. schinzii*	Schmidtgen (1912): pl. 29: figs. 4, 5
IRSNB Reg. 4005	Steendorp, BE	Boom Clay Fm.	Skull elements (so, eo, bo, sq), mandibular fragments, vertebrae of all segments, chevrons, ribs, left and right innominate	*H. schinzii* forma *delheidi* Sickenberg, 1934a	Sickenberg (1934a): 210, fig. 2a
M.137	Steendorp, BE	Boom Clay Fm.	Partial skeleton with skull fragments (f, mx), cervical, thoracic and caudal vertebrae, chevrons, ribs, right scapula, humerus and ulna, fragments of left humerus	*H. schinzii* forma *delheidi* Sickenberg, 1934a	Sickenberg (1934a): 209
unnumb.	Mainz Basin, DE	Alzey Fm.	supraoccipial	*H. schinzii*	
LS RLP PW 2005/5042-LS	Wendelsheim, Mainz Basin, DE	Alzey Fm.	Partial skeleton of young adult (disarticulated skull, mandible, vertebrae, ribs, sternum) in find situation		Recently excavated and first considered here; in cladistics analyses
MCZ 8830	Flonheim, Mainz Basin, DE	Alzey Fm.	Parietal-supraoccipital skullcap	*H. schinzii*	
MNHM PW 1949/157	Weinheim, Mainz Basin, DE	Alzey Fm.	Partial skull of adult	*H. schinzii*	
PW 1991/66-LS	Uffhofen near Flonheim, Mainz Basin, DE	Alzey Fm.	Partial skeleton of adult (partial skull, right mandible, cervical, thoracic and caudal vertebrae, ribs, right scapula, left humerus, chevron bones	*H. schinzii*	
unnumbered	Mainz Basin, DE	Alzey Fm.	Parietal-supraoccipital skullcap and right zygomatic process	*H. schinzii*	
MNHN unnumbered cast of MSNVE-3662	Paris Basin, FR	Sables de Fontainebleau	Nearly complete skeleton of subadult (partial skull, mandible, vertebrae, ribs)	*H. schinzii*	Original specimen stored and mounted in MSNVE (Bizzarini, 1995; Bizzarini & Reggiani, 2010)
NHMUK PV M9415	Bodenheim, Mainz Basin, DE	Bodenheim Fm.	Nearly complete skeleton of subadult	*Halitherium* Kaup, 1838	In cladistic analyses
NL PAL 3913	Espenhain, East Germany	Böhlen Fm.	Parietal-supraoccipital skullcap of juvenile	*Halitherium* Kaup, 1838	
NMDU-Geo 0001	Duisburg, West Germany	Upper Ratingen Fm.	Partial skeleton (elements of skull (so, sq), fragment of mandible, thoracic, lumbar and caudal vertebrae, ribs)	*H. schinzii*	Voss (2008): figs. 2–7
NRM M.7844	Fürfeld near Bad Kreuznach, Mainz Basin, DE	Alzey Fm.	Partial skull of young adult, mandible and rib fragments	*H. schinzii*	

PMN SSN12EC55	Eckelsheim, Mainz Basin, DE	Alzey Fm.	Partial skeleton of adult (disarticulated skull, fragment of mandible, tusks, vertebrae of all segments, ribs, fragment of right innominate)	*H. schinzii*	Reconstructed in find situation
SSN12WD14	Wendelsheim Mainz Basin, DE	Alzey Fm.	Partial skeleton of subadult (skull, cervical and thoracic vertebrae, ribs)	*H. schinzii*	Reconstructed in find situation

Gen. nov. 2 *bronni*

Original species: *Halitherium schinzii* Kaup, 1838 following the synonymy of Domning (1996).
Stratigraphic range: Early Oligocene (Rupelian).
General remarks: All specimens personally investigated.

Collection nr.	Locality	Age	Material	Orig. spec.	Remarks
CDGG S1	Weinheim, Mainz Basin, DE	Alzey Fm.	Partial skeleton of adult (nearly complete skull, left mandible, cervical, lumbar and caudal vertebrae, chevrons, ribs, corpus and manubrium of sternum, right scapula, right pelvis)	*H. schinzii*	In cladistic analyses
S2	Weinheim, Mainz Basin, DE	Alzey Fm.	Partial skeleton of adult (partial skull, mandible, vertebrae of all segments, ribs)	*H. schinzii*	Mounted skeleton on display in Museum Alzey
S4	near Alzey, Mainz Basin, DE	Alzey Fm.	Skull elements (so, periotic)	*H. schinzii*	
FIS M8385	Mainz Basin, DE	Bodenheim Fm.	Partial skeleton of adult (skull, mandible, thoracic, lumbar and caudal vertebrae, chevrons)	*Halitherium* Kaup, 1838	In cladistic analyses
FMD SRK Eck-Rat 43	Eckelsheim, Mainz Basin, DE	Alzey Fm.	Disarticulated partial skull and mandible of adult	*H. schinzii*	In cladistic analyses
HLMD-WT Az 100	Mainz Basin, DE	Alzey Fm.	Maxillopremaxillary fragment with left and right M1–3 of young adult	*H. schinzii*	
IRSNB Reg. 4006	Steendorp, BE	Boom Clay Fm.	Skull fragments (pm, p, so, eo, bo, bs, sq, periotics), mandibular fragments, thoracic, lumbar and caudal vertebrae, ribs, metacarpal, femur	*H. schinzii* forma *delheidi* Sickenberg, 1934a	Sickenberg (1934a): 211, fig. 2b
Reg. 4011	Niel, BE	Boom Clay Fm.	Partial skull, vertebral fragments, ribs, fragments of I1, left and right M3 of subadult	*H. schinzii* forma *delheidi* Sickenberg, 1934a	Sickenberg (1934a): 212

MB Ma. 49618	Uffhofen near Flonheim, Mainz Basin, DE	Alzey Fm.	Partial skeleton (elements of skull (f, p, so, sq), mandible; vertebrae, ribs, left scapula, left zeugopod and stylopod, right innominate)	*H. schinzii*	
MCZ 8829	Flonheim, Mainz Basin, DE	Alzey Fm.	Partial skeleton of adult (disarticulated partial skull, partial mandible, tusks, manubrium of sternum, ribs, left scapula)	*H. schinzii*	Bronn (1853–1856): pl. 48: fig. 9
MNHM PW 1945/233	Flonheim, Mainz Basin, DE	Alzey Fm.	Partial skeleton of adult (disarticulated partial skull, mandible, left radius and ulna, vertebrae of all segments, ribs)	*H. schinzii*	
PW 1984/37-1	Bad Kreuznach, Mainz Basin, DE	Alzey Fm.	Partial skeleton of adult (skull, mandible, cervical vertebrae, ribs, left scapula, sternum)	*H. schinzii*	
MWNH-TER-1	Mainz Basin, DE	Alzey Fm.	Partial skull of dentally mature specimen	*H. schinzii*	In cladistic analyses
NHMUK PV M19957	Flonheim, Mainz Basin, DE	Alzey Fm.	Partial skull and mandible of adult	*Halitherium* Kaup, 1838	
PV M44149	Flonheim, Mainz Basin, DE	Alzey Fm.	Parietal-supraoccipital skullcap	*Halitherium* Kaup, 1838	
unnumbered	Flonheim, Mainz Basin, DE	Alzey Fm.	Parietal-supraoccipital skullcap	*H. schinzii*	"M19957" designated on bone is most likely misapplied, because this collection number already identifies another specimen
NMV P 2068/5	Rhine area, West Germany	Most likely from early Oligocene marine sands	Frontoparietal-supraoccipital skullcap	*H. schinzii*	
PMN SSN12FL11	Flonheim, Mainz Basin, DE	Alzey Fm.	Supraoccipital	*H. schinzii*	
QB-4/12.721	Bottrop-Kirchheller Heide, West Germany	Upper Ratingen Fm.	Partial skeleton of adult (disarticulated partial skull, vertebrae of all segments, ribs, sternal element, left innominate)	*Halitherium* Kaup, 1838	Voss (2012): figs. 2–10
SMNS 1539	Flonheim, Mainz Basin, DE	Alzey Fm.	Frontoparietal-supraoccipital skullcap and natural endocast	*H. bronni* Krauss, 1858	**Holotype** of *H. bronni* Krauss, 1858; Krauss (1858): pl. 20; in cladistic analyses
47736	Flonheim, Mainz Basin, DE	Alzey Fm.	Partial adult skeleton (partial skull, mandible, vertebrae of all segments, ribs)	*Halitherium* Kaup, 1838	In cladistic analyses

Gen. nov. 2

Original species: *Halitherium schinzii* Kaup, 1838 following the synonymy of Domning (1996).
Stratigraphic range: Early Oligocene (Rupelian).
General remarks: All specimens personally investigated. Although the specimens listed here can be clearly distinguished from gen. nov. 2. *alleni*, it is not possible to assign these remains unambiguously to gen. nov. 2 spec. nov. 1 or gen. nov. 2. *bronni*.

Collection nr.	Locality	Age	Material	Orig. spec.	Remarks
ALMD-JBH A92	Ratingen-Lintorf, West Germany	“Transgressionskies”	Thoracic vertebra	*Halitherium* Kaup, 1838	Voss (2008): fig. 8
BSPG 1956 I 541	Eckelsheim, Mainz Basin, DE	Alzey Fm.	Humerus of juvenile	*H. schinzii*	
CDGG S6	near Alzey, Mainz Basin, DE	Alzey Fm.	Skull elements (eo, sq)	*H. schinzii*	
FIS M2598a–f	Flonheim, Mainz Basin, DE	Alzey Fm.	Skull and maxillary fragments	*H. schinzii*	
M2599	Flonheim, Mainz Basin, DE	Alzey Fm.	Right frontal	*H. schinzii*	
M2600	Flonheim, Mainz Basin, DE	Alzey Fm.	Skull fragment	*H. schinzii*	
M2605a, b	Flonheim, Mainz Basin, DE	Alzey Fm.	Premaxillary fragments	*H. schinzii*	
M2606	Flonheim, Mainz Basin, DE	Alzey Fm.	Maxillary fragment	*H. schinzii*	
M2607a, b	Flonheim, Mainz Basin, DE	Alzey Fm.	Right and left periotic	*H. schinzii*	
M2610a, b	Flonheim, Mainz Basin, DE	Alzey Fm.	Right maxillary fragment	*H. schinzii*	
M2611	Flonheim, Mainz Basin, DE	Alzey Fm.	Mandibular fragment	*H. schinzii*	
M2612	Flonheim, Mainz Basin, DE	Alzey Fm.	Mandibular fragment	*H. schinzii*	
M2613	Flonheim, Mainz Basin, DE	Alzey Fm.	Mandibular fragment	*H. schinzii*	
M2614–2616	Flonheim, Mainz Basin, DE	Alzey Fm.	Fragments of upper molars	*H. schinzii*	
M2617	Flonheim, Mainz Basin, DE	Alzey Fm.	Right M3	*H. schinzii*	
M2618	Flonheim, Mainz Basin, DE	Alzey Fm.	Left m3	*H. schinzii*	
M2619	Flonheim, Mainz Basin, DE	Alzey Fm.	Right M(?)2	*H. schinzii*	
M2620	Weinheim, Mainz Basin, DE	Alzey Fm.	Frontal	*H. schinzii*	
M2621	Weinheim, Mainz Basin, DE	Alzey Fm.	Frontal	*H. schinzii*	
M2622	Weinheim, Mainz Basin, DE	Alzey Fm.	Left mandibular fragment with m3	*H. schinzii*	
M2626	Weinheim, Mainz Basin, DE	Alzey Fm.	Left mandibular fragment with m1–3	*H. schinzii*	
M2632	Weinheim, Mainz Basin, DE	Alzey Fm.	Right periotic	*H. schinzii*	

M2645a, b	Weinheim, Mainz Basin, DE	Alzey Fm.	Left and right P(?)4	*H. schinzii*	
M2646	Weinheim, Mainz Basin, DE	Alzey Fm.	Left P(?)4	*H. schinzii*	
M2647	Darmstadt, West Germany	Alzey Fm.	Right mandibular fragment with p4 of juvenile	*H. schinzii*	
M2694a, b	Flonheim, Mainz Basin, DE	Alzey Fm.	Fragments of left and right innominate	*H. schinzii*	
M2695a–c	Flonheim, Mainz Basin, DE	Alzey Fm.	Three humerus heads	*H. schinzii*	
M2697	Flonheim, Mainz Basin, DE	Alzey Fm.	Left humerus	*H. schinzii*	
M2698	Flonheim, Mainz Basin, DE	Alzey Fm.	Left humerus	*H. schinzii*	
M2699	Flonheim, Mainz Basin, DE	Alzey Fm.	Right radius and ulna	*H. schinzii*	
M2700	Flonheim, Mainz Basin, DE	Alzey Fm.	Sternal fragment	*H. schinzii*	
M2701	Flonheim, Mainz Basin, DE	Alzey Fm.	(?)sternal fragment	*H. schinzii*	
M2702–2705	Flonheim, Mainz Basin, DE	Alzey Fm.	Left scapula	*H. schinzii*	
M2706	Flonheim, Mainz Basin, DE	Alzey Fm.	Left mandibular fragment	*H. schinzii*	
M2707	Flörsheim, Mainz Basin, DE	Bodenheim Fm.	(?)right femur	*H. schinzii*	Cast
M2708	Flörsheim, Mainz Basin, DE	Bodenheim Fm.	(?)left femur	*H. schinzii*	Schmidtgen (1912): pl. 29: figs. 8, 9
M2709a, b	Flonheim, Mainz Basin, DE	Alzey Fm.	Right and left zygomatic process of squamosal	*H. schinzii*	
M2721a–d	Flonheim, Mainz Basin, DE	Alzey Fm.	Ribs of juvenile	*H. schinzii*	
M2722a–d	Flonheim, Mainz Basin, DE	Alzey Fm.	Ribs of juvenile	*H. schinzii*	
M4054	Flörsheim, Mainz Basin, DE	Bodenheim Fm.	Right humerus, radius and ulna	*H. schinzii*	
M4315	Mainz Basin, DE	Bodenheim Fm.	Left humerus	*H. schinzii*	
M5834a, b	Flonheim, Mainz Basin, DE	Alzey Fm.	Fragments of left exoccipital and right zygomatic process of squamosal	*H. schinzii*	
M5846a	Weinheim, Mainz Basin, DE	Alzey Fm.	Right zygomatic process of squamosal	*H. schinzii*	
M8186	Langenlonsheim, south of Bingen, West Germany	Alzey Fm.	Ribs, rib and vertebral fragments	*H. schinzii*	
M8367	Flörsheim, Mainz Basin, DE	Bodenheim Fm.	Fragments of autopod, corpus of sternum, chevrons	*H. schinzii*	

GPL unnumbered	near Leipzig, East Germany	Böhlen Fm.	Partial skeleton of adult (disarticulated partial skull, partial mandible, vertebrae of all segments, ribs, xiphisternum, innominates)	*Halitherium* Kaup, 1838	
GPMH unnumbered	Mainz Basin, DE	Alzey Fm.	Partial skeleton (vertebrae, ribs, fragments of scapula and innominate)	*H. schinzii*	Mounted skeleton
unnumbered	Mainz Basin, DE	Alzey Fm.	Fragments of right squamosal and left madible	*H. schinzii*	
unnumbered	Mainz Basin, DE	Alzey Fm.	Right zygomatic process of squamosal	*H. schinzii*	
unnumbered	Mainz Basin, DE	Alzey Fm.	Left scapula	*H. schinzii*	
unnumbered	Mainz Basin, DE	Alzey Fm.	Left radius and ulna	*H. schinzii*	
unnumbered	Mainz Basin, DE	Alzey Fm.	Maxillary fragment	*H. schinzii*	
HLMD-WT Az 1	Flonheim, Mainz Basin, DE	Alzey Fm.	Humerus of juvenile	*H. schinzii*	
Az 2–4	Flonheim, Mainz Basin, DE	Alzey Fm.	Metacarpal and phalanges	*H. schinzii*	
Az 5, 6	Flonheim, Mainz Basin, DE	Alzey Fm.	Premolars	*H. schinzii*	
Az 7	Flonheim, Mainz Basin, DE	Alzey Fm.	(?)right femur	*H. schinzii*	
Az 8	Flonheim, Mainz Basin, DE	Alzey Fm.	Proximal humerus fragment of juvenile	*H. schinzii*	
Az 9	Flonheim, Mainz Basin, DE	Alzey Fm.	Right jugal	*H. schinzii*	
Az 10	Flonheim, Mainz Basin, DE	Alzey Fm.	Fragment of I1	*H. schinzii*	
Az 11	Flonheim, Mainz Basin, DE	Alzey Fm.	Rib of juvenile	*H. schinzii*	
Az 12	Flonheim, Mainz Basin, DE	Alzey Fm.	Sternal fragment (manubrium)	*H. schinzii*	
Az 13, 14	Alzey, Mainz Basin, DE	Alzey Fm.	Maxillary fragments	*H. schinzii*	
Az 15	Mainz Basin, DE	Alzey Fm.	Premaxillary fragment	*H. schinzii*	
Az 16	Alzey, Mainz Basin, DE	Alzey Fm.	(?)right femur	*H. schinzii*	
Az 18, 19	Alzey, Mainz Basin, DE	Alzey Fm.	Fragments of R1	*H. schinzii*	
Az 20	Alzey, Mainz Basin, DE	Alzey Fm.	Premolar	*H. schinzii*	
Az 21	Mainz Basin, DE	Alzey Fm.	Left m3	*H. schinzii*	
Az 22	Mainz Basin, DE	Alzey Fm.	Left m(?)2	*H. schinzii*	
Az 23	Mainz Basin, DE	Alzey Fm.	Left m(?)1	*H. schinzii*	
Az 24	Alzey, Mainz Basin, DE	Alzey Fm.	Right maxillary fragment with M1–3	*H. schinzii*	
Az 25, 26	Mainz Basin, DE	Alzey Fm.	Left M3 and right M(?)2	*H. schinzii*	
Az 29–31	Mainz Basin, DE	Alzey Fm.	Premolars	*H. schinzii*	

Az 32, 33	Flonheim, Mainz Basin, DE	Alzey Fm.	Left and right maxillary fragments each with DP5–M3	*H. schinzii*	Kaup (1856): pl. 1; Kaup (1861): pl. 5: figs. 1, 1a
Az 34	Alzey, Mainz Basin, DE	Alzey Fm.	Maxillary fragment with left and right M1–3	*H. schinzii*	
Az 35, 36	Alzey, Mainz Basin, DE	Alzey Fm.	Right and left innominates	*H. schinzii*	
Az 42, 43	Flonheim, Mainz Basin, DE	Alzey Fm.	Maxillary fragments with left M1–2 and right DP5–M1	*H. schinzii*	
Az 45	Mainz Basin, DE	Alzey Fm.	Fragments of squamosal and periotic	*H. schinzii*	
Az 46	Flonheim, Mainz Basin, DE	Alzey Fm.	Bone fragment	*H. schinzii*	
Az 47	Mainz Basin, DE	Alzey Fm.	Right m(?)2	*H. schinzii*	
Az 48	Flonheim, Mainz Basin, DE	Alzey Fm.	Premolar	*H. schinzii*	**Holotype** of *H. schinzii* Kaup, 1838; Kaup (1838): pl. 2: figs. C1, 2
Az 49	Uffhofen near Flonheim, Mainz Basin, DE	Alzey Fm.	Premolar	*H. schinzii*	
Az 50, 51	Flonheim, Mainz Basin, DE	Alzey Fm.	Left radius, ulna, and humerus	*H. schinzii*	
Az 52, 53	Uffhofen near Flonheim, Mainz Basin, DE	Alzey Fm.	Left radius, ulna, and humerus	*H. schinzii*	
Az 54	Flonheim, Mainz Basin, DE	Alzey Fm.	Left innominate	*H. schinzii*	
Az 55	Flonheim, Mainz Basin, DE	Alzey Fm.	Right innominate	*H. schinzii*	
Az 56	Alzey, Mainz Basin, DE	Alzey Fm.	Fragments of left squamosal and periotic	*H. schinzii*	
Az 57	Flonheim, Mainz Basin, DE	Alzey Fm.	Left innominate	*H. schinzii*	
Az 58	Flonheim, Mainz Basin, DE	Alzey Fm.	Frontal	*H. schinzii*	
Az 59	Flonheim, Mainz Basin, DE	Alzey Fm.	Frontal	*H. schinzii*	
Az 60	Alzey, Mainz Basin, DE	Alzey Fm.	Frontal	*H. schinzii*	
Az 61, 62	Mainz Basin, DE	Alzey Fm.	Fragments of left squamosal and periotic	*H. schinzii*	
Az 63	Mainz Basin, DE	Alzey Fm.	Fragments of right squamosal and periotic	*H. schinzii*	
Az 65–67	Flonheim, Mainz Basin, DE	Alzey Fm.	Left and right zygomatic process of squamosal and periotic	*H. schinzii*	
Az 69	Mainz Basin, DE	Alzey Fm.	Tooth fragment	*H. schinzii*	
Az 70	Mainz Basin, DE	Alzey Fm.	Right m(?)2	*H. schinzii*	
Az 71	Mainz Basin, DE	Alzey Fm.	Tooth fragment	*H. schinzii*	

Az 73, 74	Mainz Basin, DE	Alzey Fm.	Tooth fragment and right m(?)2	*H. schinzii*
Az 75, 76	Alzey, Mainz Basin, DE	Alzey Fm.	Right and left maxillary fragment each with M1–3	*H. schinzii*
Az 77	Flonheim, Mainz Basin, DE	Alzey Fm.	Tooth fragment	*H. schinzii*
Az 79	Mainz Basin, DE	Alzey Fm.	Left M(?)2	*H. schinzii*
Az 80	Mainz Basin, DE	Alzey Fm.	Right M(?)1	*H. schinzii*
Az 81	Mainz Basin, DE	Alzey Fm.	Left M(?)1	*H. schinzii*
Az 82	Mainz Basin, DE	Alzey Fm.	Left M(?)3	*H. schinzii*
Az 86	Flonheim, Mainz Basin, DE	Alzey Fm.	Premaxillary fragment	*H. schinzii*
Az 87	Flonheim, Mainz Basin, DE	Alzey Fm.	Fragment of left jugal	*H. schinzii*
Az 90	Weinheim, Mainz Basin, DE	Alzey Fm.	Left mandibular fragment	*H. schinzii*
Az 91	Mainz Basin, DE	Alzey Fm.	Left M(?)2	*H. schinzii*
Az 92	Mainz Basin, DE	Alzey Fm.	Lower molar	*H. schinzii*
Az 93	Mainz Basin, DE	Alzey Fm.	Premolar	*H. schinzii*
Az 94	Mainz Basin, DE	Alzey Fm.	Premolar	*H. schinzii*
Az 95–97	Flonheim, Mainz Basin, DE	Alzey Fm.	Premolars	*H. schinzii*
Az 98	Flonheim, Mainz Basin, DE	Alzey Fm.	Frontal	*H. schinzii*
Az 104a, b	Flonheim, Mainz Basin, DE	Alzey Fm.	Bone fragment	*H. schinzii*
Az 105, 106	Flonheim, Mainz Basin, DE	Alzey Fm.	Metacarpals	*H. schinzii*
Az 109	Mainz Basin, DE	Alzey Fm.	Fragment of left jugal	*H. schinzii*
Az 110, 111	Mainz Basin, DE	Alzey Fm.	Right mandibular fragment	*H. schinzii*
Az 112–116	Alzey, Mainz Basin, DE	Alzey Fm.	Fragments of squamosal and periotic	*H. schinzii*
Az 117, 118	Mainz Basin, DE	Alzey Fm.	Fragments of squamosal and periotic	*H. schinzii*
Az 119	Mainz Basin, DE	Alzey Fm.	Right frontal	*H. schinzii*
Az 124	Mainz Basin, DE	Alzey Fm.	Skull fragments (eo, bo, bs)	*H. schinzii*
Az 125–129	Flonheim, Mainz Basin, DE	Alzey Fm.	Skull fragments (sq, eo, bo, bs)	*H. schinzii*
Az 132–136	Flonheim, Mainz Basin, DE	Alzey Fm.	Vertebral fragments	*H. schinzii*
Az 138	Flonheim, Mainz Basin, DE	Alzey Fm.	Frontal	*H. schinzii*
Az 139, 140	Mainz Basin, DE	Alzey Fm.	Left and right maxillary fragments each with M2–3	*H. schinzii*
Az 142	Flonheim, Mainz Basin, DE	Alzey Fm.	Frontal	*H. schinzii*

Az 143, 144	Alzey, Mainz Basin, DE	Alzey Fm.	Premaxillary fragments	*H. schinzii*
Az 147	Mainz Basin, DE	Alzey Fm.	Tympanic	*H. schinzii*
Az 148	Mainz Basin, DE	Alzey Fm.	Tympanic	*H. schinzii*
Az 149	Mainz Basin, DE	Alzey Fm.	Tympanic	*H. schinzii*
Az 150–152	Mainz Basin, DE	Alzey Fm.	Skull fragments	*H. schinzii*
Az 159	Weinheim, Mainz Basin, DE	Alzey Fm.	Fragment of left mandible with m3 of juvenile	*H. schinzii*
Az 162, 163	Mainz Basin, DE	Alzey Fm.	Fragments of left squamosal	*H. schinzii*
Az 164	Alzey, Mainz Basin, DE	Alzey Fm.	Fragment of left R1	*H. schinzii*
Az 165	Mainz Basin, DE	Alzey Fm.	Left zygomatic process of squamosal	*H. schinzii*
Az 166	Mainz Basin, DE	Alzey Fm.	Right maxillary fragment with M1–2	*H. schinzii*
Az 167	Mainz Basin, DE	Alzey Fm.	Rib of juvenile	*H. schinzii*
Az 168, 169	Alzey, Mainz Basin, DE	Alzey Fm.	Mandibular fragments of juvenile	*H. schinzii*
Az 170	Mainz Basin, DE	Alzey Fm.	Right frontal of juvenile	*H. schinzii*
Az 175	Mainz Basin, DE	Alzey Fm.	Skull fragments (eo, bo, bs)	*H. schinzii*
Az 176	Flonheim, Mainz Basin, DE	Alzey Fm.	Left zygomatic process of squamosal	*H. schinzii*
Az 179	Alzey, Mainz Basin, DE	Alzey Fm.	Left zygomatic process of squamosal	*H. schinzii*
Az 180	Mainz Basin, DE	Alzey Fm.	Left zygomatic process of squamosal	*H. schinzii*
Az 181	Mainz Basin, DE	Alzey Fm.	Skull fragment	*H. schinzii*
Az 182	Mainz Basin, DE	Alzey Fm.	Skull fragments (eo, bo)	*H. schinzii*
Az 183	Mainz Basin, DE	Alzey Fm.	Premaxillary fragments	*H. schinzii*
Az 188	Mainz Basin, DE	Alzey Fm.	Right squamosal	*H. schinzii*
Az 189	Flonheim, Mainz Basin, DE	Alzey Fm.	Left scapula	*H. schinzii*
Az 191, 193,194	Flonheim, Mainz Basin, DE	Alzey Fm.	Left scapula	*H. schinzii*
Az 192	Alzey, Mainz Basin, DE	Alzey Fm.	Scapular fragment	*H. schinzii*
Az 195	Flonheim, Mainz Basin, DE	Alzey Fm.	Left scapula	*H. schinzii*
Az 196	Flonheim, Mainz Basin, DE	Alzey Fm.	Right scapula	*H. schinzii*
Az 198	Alzey, Mainz Basin, DE	Alzey Fm.	Left scapula	*H. schinzii*
Az 199	Flonheim, Mainz Basin, DE	Alzey Fm.	Right scapula	*H. schinzii*
Az 200	Flonheim, Mainz Basin, DE	Alzey Fm.	Fragment of right scapula	*H. schinzii*

Az 205	Flonheim, Mainz Basin, DE	Alzey Fm.	Right scapula	*H. schinzii*
Az 206	Flonheim, Mainz Basin, DE	Alzey Fm.	Left scapula	*H. schinzii*
Az 208	Mainz Basin, DE	Alzey Fm.	Fragment of right scapula	*H. schinzii*
Az 210	Flonheim, Mainz Basin, DE	Alzey Fm.	Left scapula of juvenile	*H. schinzii*
Az 211, 204	Flonheim, Mainz Basin, DE	Alzey Fm.	Left scapula	*H. schinzii*
Az 212	Weinheim, Mainz Basin, DE	Alzey Fm.	Left scapula of juvenile	*H. schinzii*
Az 213, 190	Mainz Basin, DE	Alzey Fm.	Right scapula	*H. schinzii*
Az 219	Flonheim, Mainz Basin, DE	Alzey Fm.	Thoracic vertebra	*H. schinzii*
Az 220	Flonheim, Mainz Basin, DE	Alzey Fm.	Fragments of atlas	*H. schinzii*
Az 221	Mainz Basin, DE	Alzey Fm.	Caudal vertebra	*H. schinzii*
Az 222	Mainz Basin, DE	Alzey Fm.	Caudal vertebra	*H. schinzii*
Az 225–229	Flonheim, Mainz Basin, DE	Alzey Fm.	Fragments of caudal vertebra	*H. schinzii*
Az 230–236	Flonheim, Mainz Basin, DE	Alzey Fm.	Chevron bones and other fragments	*H. schinzii*
Az 237–239	Flonheim, Mainz Basin, DE	Alzey Fm.	Fragments of atlas	*H. schinzii*
Az 240	Flonheim, Mainz Basin, DE	Alzey Fm.	Cervical	*H. schinzii*
Az 241	Alzey, Mainz Basin, DE	Alzey Fm.	Cervical	*H. schinzii*
Az 242	Flonheim, Mainz Basin, DE	Alzey Fm.	Cervical fragments	*H. schinzii*
Az 243–245	Flonheim, Mainz Basin, DE	Alzey Fm.	Skull fragments (bo, eo)	*H. schinzii*
Az 247	Mainz Basin, DE	Alzey Fm.	Skull fragment (eo)	*H. schinzii*
Az 248	Flonheim, Mainz Basin, DE	Alzey Fm.	Axis	*H. schinzii*
Az 249	Alzey, Mainz Basin, DE	Alzey Fm.	Axis	*H. schinzii*
Az 250	Mainz Basin, DE	Alzey Fm.	Skull fragment (bs)	*H. schinzii*
Az 251	Flonheim, Mainz Basin, DE	Alzey Fm.	Fragments of chevrons and tympanics	*H. schinzii*
Az 255	Mainz Basin, DE	Alzey Fm.	Axis fused with C3	*H. schinzii*
Az 256	Mainz Basin, DE	Alzey Fm.	Cervical (C5?)	*H. schinzii*
Az 257	Mainz Basin, DE	Alzey Fm.	Cervical (C6?)	*H. schinzii*
Az 258	Mainz Basin, DE	Alzey Fm.	Cervical (C4?)	*H. schinzii*
Az 259	Flonheim, Mainz Basin, DE	Alzey Fm.	Caudal vertebra	*H. schinzii*
Az 260	Flonheim, Mainz Basin, DE	Alzey Fm.	Lumbar vertebra	*H. schinzii*

Az 261	Flonheim, Mainz Basin, DE	Alzey Fm.	Lumbar vertebra	*H. schinzii*
Az 262	Flonheim, Mainz Basin, DE	Alzey Fm.	Caudal vertebra	*H. schinzii*
Az 263	Flonheim, Mainz Basin, DE	Alzey Fm.	Caudal vertebra	*H. schinzii*
Az 264	Flonheim, Mainz Basin, DE	Alzey Fm.	Lumbar vertebra	*H. schinzii*
Az 265	Flonheim, Mainz Basin, DE	Alzey Fm.	Caudal vertebra	*H. schinzii*
Az 266	Flonheim, Mainz Basin, DE	Alzey Fm.	Caudal vertebra	*H. schinzii*
Az 267	Flonheim, Mainz Basin, DE	Alzey Fm.	Thoracic vertebra	*H. schinzii*
Az 268	Flonheim, Mainz Basin, DE	Alzey Fm.	Thoracic vertebra	*H. schinzii*
Az 269	Flonheim, Mainz Basin, DE	Alzey Fm.	Caudal vertebra	*H. schinzii*
Az 270	Flonheim, Mainz Basin, DE	Alzey Fm.	Thoracic vertebra	*H. schinzii*
Az 271	Flonheim, Mainz Basin, DE	Alzey Fm.	Thoracic vertebra	*H. schinzii*
Az 272	Flonheim, Mainz Basin, DE	Alzey Fm.	Caudal vertebra	*H. schinzii*
Az 273	Flonheim, Mainz Basin, DE	Alzey Fm.	Caudal vertebra	*H. schinzii*
Az 275	Flonheim, Mainz Basin, DE	Alzey Fm.	Caudal vertebra	*H. schinzii*
Az 276	Flonheim, Mainz Basin, DE	Alzey Fm.	Thoracic vertebra	*H. schinzii*
Az 277	Flonheim, Mainz Basin, DE	Alzey Fm.	Lumbar vertebra	*H. schinzii*
Az 278	Flonheim, Mainz Basin, DE	Alzey Fm.	Caudal vertebra	*H. schinzii*
Az 279	Flonheim, Mainz Basin, DE	Alzey Fm.	Thoracic vertebra	*H. schinzii*
Az 280	Flonheim, Mainz Basin, DE	Alzey Fm.	Thoracic vertebra	*H. schinzii*
Az 282	Flonheim, Mainz Basin, DE	Alzey Fm.	Caudal vertebra	*H. schinzii*
Az 283	Flonheim, Mainz Basin, DE	Alzey Fm.	Caudal vertebra	*H. schinzii*
Az 284	Flonheim, Mainz Basin, DE	Alzey Fm.	Caudal vertebra	*H. schinzii*
Az 285	Flonheim, Mainz Basin, DE	Alzey Fm.	Caudal vertebra	*H. schinzii*
Az 286	Flonheim, Mainz Basin, DE	Alzey Fm.	Thoracic vertebra	*H. schinzii*

Az 287	Flonheim, Mainz Basin, DE	Alzey Fm.	Mounted partial skeleton (partial skull, mandible, vertebrae, ribs, innominates, femura) and unmounted thoracic vertebra	*H. schinzii*	Partial skeleton is a composite and on display in HLMD; assignment of individual bones to a certain specimen not clear; diagnostic elements badly preserved; no designation to species level possible
Az 288	Flonheim, Mainz Basin, DE	Alzey Fm.	Thoracic vertebra	*H. schinzii*	
Az 289	Flonheim, Mainz Basin, DE	Alzey Fm.	Caudal vertebra	*H. schinzii*	
Az 290	Flonheim, Mainz Basin, DE	Alzey Fm.	Caudal vertebra	*H. schinzii*	
Az 291	Flonheim, Mainz Basin, DE	Alzey Fm.	Lumbar vertebra	*H. schinzii*	
Az 292	Flonheim, Mainz Basin, DE	Alzey Fm.	Thoracic vertebra	*H. schinzii*	
Az 293	Flonheim, Mainz Basin, DE	Alzey Fm.	Caudal vertebra	*H. schinzii*	
Az 294	Flonheim, Mainz Basin, DE	Alzey Fm.	Thoracic vertebra	*H. schinzii*	
Az 295	Flonheim, Mainz Basin, DE	Alzey Fm.	Caudal vertebra	*H. schinzii*	
Az 296	Flonheim, Mainz Basin, DE	Alzey Fm.	Thoracic vertebra	*H. schinzii*	
Az 297	Flonheim, Mainz Basin, DE	Alzey Fm.	Thoracic vertebra	*H. schinzii*	
Az 298	Flonheim, Mainz Basin, DE	Alzey Fm.	Thoracic vertebra	*H. schinzii*	
Az 299	Flonheim, Mainz Basin, DE	Alzey Fm.	Caudal vertebra	*H. schinzii*	
Az 300	Flonheim, Mainz Basin, DE	Alzey Fm.	Thoracic vertebra	*H. schinzii*	
Az 301	Flonheim, Mainz Basin, DE	Alzey Fm.	Caudal vertebra	*H. schinzii*	
Az 302	Flonheim, Mainz Basin, DE	Alzey Fm.	Caudal vertebra	*H. schinzii*	
Az 303	Flonheim, Mainz Basin, DE	Alzey Fm.	Caudal vertebra	*H. schinzii*	
Az 304	Flonheim, Mainz Basin, DE	Alzey Fm.	Thoracic vertebra	*H. schinzii*	
Az 305	Mainz Basin, DE	Alzey Fm.	Bone fragments	*H. schinzii*	
Az 306	Flonheim, Mainz Basin, DE	Alzey Fm.	Right humerus of juvenile	*H. schinzii*	
Az 307	Flonheim, Mainz Basin, DE	Alzey Fm.	Right humerus	*H. schinzii*	
Az 308	Flonheim, Mainz Basin, DE	Alzey Fm.	Fragments of left humerus	*H. schinzii*	

Az 309	Flonheim, Mainz Basin, DE	Alzey Fm.	Fragments of left humerus	*H. schinzii*
Az 310	Flonheim, Mainz Basin, DE	Alzey Fm.	Fragments of left humerus	*H. schinzii*
Az 311	Flonheim, Mainz Basin, DE	Alzey Fm.	Right humerus	*H. schinzii*
Az 312	Flonheim, Mainz Basin, DE	Alzey Fm.	Right humerus of juvenile	*H. schinzii*
Az 313	Mainz Basin, DE	Alzey Fm.	Right humerus of juvenile	*H. schinzii*
Az 314	Flonheim, Mainz Basin, DE	Alzey Fm.	Right humerus of juvenile	*H. schinzii*
Az 315	Flonheim, Mainz Basin, DE	Alzey Fm.	Left humerus	*H. schinzii*
Az 316	Flonheim, Mainz Basin, DE	Alzey Fm.	Proximal fragment of right humerus	*H. schinzii*
Az 317	Mainz Basin, DE	Alzey Fm.	Humerus of juvenile	*H. schinzii*
Az 318	Mainz Basin, DE	Alzey Fm.	Proximal fragment of right humerus	*H. schinzii*
Az 319	Mainz Basin, DE	Alzey Fm.	Femur fragment	*H. schinzii*
Az 320	Mainz Basin, DE	Alzey Fm.	Innominate of juvenile	*H. schinzii*
Az 321, 321a	Flörsheim, Mainz Basin, DE	Boden-heim Fm.	Rib of juvenile	*H. schinzii*
Az 322	Wonsheim, Mainz Basin, DE	Alzey Fm.	Metacarpal	*H. schinzii*
Az 331–334	Flonheim, Mainz Basin, DE	Alzey Fm.	Rib fragments	*H. schinzii*
Az 339	Flonheim, Mainz Basin, DE	Alzey Fm.	Femur	*H. schinzii*
Az 340	Flonheim, Mainz Basin, DE	Alzey Fm.	Femur	*H. schinzii*
Az 341–343	Mainz Basin, DE	Alzey Fm.	Fragments of femur	*H. schinzii*
Az 342	Flonheim, Mainz Basin, DE	Alzey Fm.	Femur fragment	*H. schinzii*
Az 343	Flonheim, Mainz Basin, DE	Alzey Fm.	Femur fragment	*H. schinzii*
Az 344	Alzey, Mainz Basin, DE	Alzey Fm.	Sternal fragment	*H. schinzii*
Az 345	Flonheim, Mainz Basin, DE	Alzey Fm.	Humerus fragment	*H. schinzii*
Az 347, 348	Flonheim, Mainz Basin, DE	Alzey Fm.	Right R1	*H. schinzii*
Az 349	Flonheim, Mainz Basin, DE	Alzey Fm.	Fragment of left R1	*H. schinzii*
Az 350, 351	Flonheim, Mainz Basin, DE	Alzey Fm.	Fragment of right R1	*H. schinzii*
Az 352	Flonheim, Mainz Basin, DE	Alzey Fm.	Fragment of right R1	*H. schinzii*
Az 353	Rheinhessen, Mainz Basin, DE	Alzey Fm.	Left humerus	*H. schinzii*

Az 354	Flonheim, Mainz Basin, DE	Alzey Fm.	Left humerus	*H. schinzii*
Az 355	Weinnheim, Mainz Basin, DE	Alzey Fm.	Right humerus	*H. schinzii*
Az 356	Weinheim, Mainz Basin, DE	Alzey Fm.	Right humerus of juvenile	*H. schinzii*
Az 357	Flonheim, Mainz Basin, DE	Alzey Fm.	Left humerus	*H. schinzii*
Az 358	Flonheim, Mainz Basin, DE	Alzey Fm.	Left humerus	*H. schinzii*
Az 359	Flonheim, Mainz Basin, DE	Alzey Fm.	Right humerus of juvenile	*H. schinzii*
Az 360	Flonheim, Mainz Basin, DE	Alzey Fm.	Fragments of left humerus	*H. schinzii*
Az 361	Flonheim, Mainz Basin, DE	Alzey Fm.	Right innominate	*H. schinzii*
Az 362	Flonheim, Mainz Basin, DE	Alzey Fm.	Right innominate	*H. schinzii*
Az 363	Mainz Basin, DE	Alzey Fm.	Right innominate	*H. schinzii*
Az 364, 365	Flonheim, Mainz Basin, DE	Alzey Fm.	Fragments of left humerus	*H. schinzii*
Az 366	Flonheim, Mainz Basin, DE	Alzey Fm.	Right innominate	*H. schinzii*
Az 367	Flonheim, Mainz Basin, DE	Alzey Fm.	Fragments of left innominate	*H. schinzii*
Az 368	Flonheim, Mainz Basin, DE	Alzey Fm.	Left innominate	*H. schinzii*
Az 369	Weinheim, Mainz Basin, DE	Alzey Fm.	Left innominate	*H. schinzii*
Az 370	Flonheim, Mainz Basin, DE	Alzey Fm.	Left innominate	*H. schinzii*
Az 371	Flonheim, Mainz Basin, DE	Alzey Fm.	Right innominate	*H. schinzii*
Az 372	Flonheim, Mainz Basin, DE	Alzey Fm.	Left innominate	*H. schinzii*
Az 373	Flonheim, Mainz Basin, DE	Alzey Fm.	Fragments of right innominate	*H. schinzii*
Az 375	Flonheim, Mainz Basin, DE	Alzey Fm.	Rib	*H. schinzii*
Az 376–379	Flonheim, Mainz Basin, DE	Alzey Fm.	Rib	*H. schinzii*
Az 378a, b	Flonheim, Mainz Basin, DE	Alzey Fm.	Fragments of R1	*H. schinzii*
Az 381a	Flonheim, Mainz Basin, DE	Alzey Fm.	Rib fragment	*H. schinzii*
Az 387	Flonheim, Mainz Basin, DE	Alzey Fm.	Rib fragments	*H. schinzii*
Az 388	Flonheim, Mainz Basin, DE	Alzey Fm.	Rib fragment	*H. schinzii*
Az 390	Flonheim, Mainz Basin, DE	Alzey Fm.	Right humerus fragment	*H. schinzii*

Az 391	Flonheim, Mainz Basin, DE	Alzey Fm.	Right humerus	*H. schinzii*	
Az 392	Alzey, Mainz Basin, DE	Alzey Fm.	Right humerus	*H. schinzii*	
Az 393	Flonheim, Mainz Basin, DE	Alzey Fm.	Right radius and ulna	*H. schinzii*	
Az 394	Mainz Basin, DE	Alzey Fm.	Right radius and ulna	*H. schinzii*	
Az 395	Wonsheim, Mainz Basin, DE	Alzey Fm.	Right radius and ulna	*H. schinzii*	
Az 396	Flonheim, Mainz Basin, DE	Alzey Fm.	Left radius and ulna	*H. schinzii*	
Az 397	Flonheim, Mainz Basin, DE	Alzey Fm.	Right radius and ulna	*H. schinzii*	
Az 398	Flonheim, Mainz Basin, DE	Alzey Fm.	Left radius and ulna of juvenile	*H. schinzii*	
Az 399a, b	Flonheim, Mainz Basin, DE	Alzey Fm.	Left radius and ulna	*H. schinzii*	
Az 400	Flonheim, Mainz Basin, DE	Alzey Fm.	Left radius and ulna	*H. schinzii*	
Az 402	Weinheim, Mainz Basin, DE	Alzey Fm.	Right radius and ulna	*H. schinzii*	
Az 403	Mainz Basin, DE	Alzey Fm.	Vertebral fragments	*H. schinzii*	
Az 405	Mainz Basin, DE	Alzey Fm.	Skull fragments	*H. schinzii*	
Az 406	Mainz Basin, DE	Alzey Fm.	28 Ribs	*H. schinzii*	From a single specimen
Az 410	Mainz Basin, DE	Alzey Fm.	Left radius and ulna	*H. schinzii*	
Az 420	Flonheim, Mainz Basin, DE	Alzey Fm.	Left scapula	*H. schinzii*	
Az 421	Flonheim, Mainz Basin, DE	Alzey Fm.	Fragments of right scapula	*H. schinzii*	
Az 422, 423	Alzey, Mainz Basin, DE	Alzey Fm.	I1	*H. schinzii*	
Az-HN-1–14	Mainz Basin, DE	Alzey Fm.	14 Ribs	*H. schinzii*	From a single specimen
Az-HN-15–46	Mainz Basin, DE	Alzey Fm.	Ribs	*H. schinzii*	Not a single specimen
Az 701	Unterfeld near Rauenberg, West Germany	Bodenheim Fm.	Partial skeleton (skull, mandible, vertebrae, ribs, scapulae, humeri)	*H. schinzii*	Recently discovered and prepared (Schöggl & Micklich, 2013); preliminary listed here pending description and determination to species level
unnumbered	Mainz Basin, DE	Alzey Fm.	Three rib fragments	*H. schinzii*	
IRSNB M.151	Antwerp, BE	Boom Clay Fm.	Skull elements (mx, f, bs) of juvenile	*Manatherium delheidi* Hartlaub, 1886	**Holotype** of *M. delheidi* Hartlaub, 1886; Sickenberg (1934a): 213

M.138	Steendorp, BE	Boom Clay Fm.	Thoracic and caudal vertebrae, fragments of sternum and radius	*H. schinzii* forma *delheidi* Sickenberg, 1934a	Sickenberg (1934a): 209
M.139	Steendorp, BE	Boom Clay Fm.	Thoracic vertebrae, sternal element	*H. schinzii* forma *delheidi* Sickenberg, 1934a	Sickenberg (1934a): 209
M.140	Steendorp, BE	Boom Clay Fm.	Fragments of premaxilla with tusks, maxilla and mandible; thoracic, lumbar and caudal vertebrae	*H. schinzii* forma *delheidi* Sickenberg, 1934a	Sickenberg (1934a): 210
M.141	Boom, BE	Boom Clay Fm.	Skull fragments (f, p, so), left m3, fragments of vertebrae, ribs and right scapula; left ulna, manubrium of sternum	*H. schinzii* forma *delheidi* Sickenberg, 1934a	**Holotype** of *H. uytterhoeveni* Abel, 1925; Sickenberg (1934a): 210
M.142	Boom, BE	Boom Clay Fm.	Carpal, left radius and ulna	*H. schinzii* forma *delheidi* Sickenberg, 1934a	Sickenberg (1934a): 211
M.144	Noeveren, BE	Boom Clay Fm.	Left M2–3, thoracic vertebra	*H. schinzii* forma *delheidi* Sickenberg, 1934a	Sickenberg (1934a): 212
M.145	Boom, BE	Boom Clay Fm.	Caudal vertebrae, right humerus, radius and ulna, metacarpals	*H. schinzii* forma *delheidi* Sickenberg, 1934a	Sickenberg (1934a): 211
M.146	Noeveren, BE	Boom Clay Fm.	Thoracic vertebra, fragment of right humerus	*H. schinzii* forma *delheidi* Sickenberg, 1934a	Sickenberg (1934a): 212
M.147	Niel, BE	Boom Clay Fm.	M3 and m3 from left side	*H. schinzii* forma *delheidi* Sickenberg, 1934a	Sickenberg (1934a): 212
M.148	Niel, BE	Boom Clay Fm.	Remains of tusk, premolars, lower molars	*H. schinzii* forma *delheidi* Sickenberg, 1934a	Sickenberg (1934a): 212
M.149	Terhaegen, BE	Boom Clay Fm.	Left M3	*H. schinzii* forma *delheidi* Sickenberg, 1934a	Sickenberg (1934a): 212
M.150	St. Nicolas (Waas), BE	Boom Clay Fm.	Mandibular fragment, thoracic and caudal vertebrae, ribs, fragment of right scapula	*H. schinzii* forma *delheidi* Sickenberg, 1934a	Sickenberg (1934a): 213
M.152	?, BE	Boom Clay Fm.	Premaxillary fragment	*H. schinzii* forma *delheidi* Sickenberg, 1934a	Sickenberg (1934a): 213
M.162	Boom, BE	Boom Clay Fm.	Fragments of skull and mandible	*H. schinzii* forma *delheidi* Sickenberg, 1934a	Sickenberg (1934a): 211

	M.165	Duffel, BE	Boom Clay Fm.	Thoracic vertebra	*H. schinzii* forma *delheidi* Sickenberg, 1934a	Sickenberg (1934a): 212
	M.289	Steendorp, BE	Boom Clay Fm.	Thoracic vertebrae, ribs, right scapula and humerus, left and right zeugopods	*H. schinzii* forma *delheidi* Sickenberg, 1934a	Sickenberg (1934a): 209
	M.290	Steendorp, BE	Boom Clay Fm.	Fragments of vertebrae; ribs, both scapulae	*H. schinzii* forma *delheidi* Sickenberg, 1934a	Sickenberg (1934a): 209
	Reg. 4001	Noeveren, BE	Boom Clay Fm.	Ribs	*H. schinzii* forma *delheidi* Sickenberg, 1934a	Sickenberg (1934a): 212
	Reg. 4003	Steendorp, BE	Boom Clay Fm.	Thoracic and caudal vertebrae, chevrons, ribs, fragment of xiphisternum, both scapulae, left ulna	*H. schinzii* forma *delheidi* Sickenberg, 1934a	Sickenberg (1934a): 209
	Reg. 4004	Steendorp, BE	Boom Clay Fm.	Fragments of skull (p, so, bs, sq) and mandible; thoracic vertebrae, ribs, fragments of both scapulae; right humerus, fragments of left humerus; right ulna, fragment of right radius; carpals, left innominate and fragment of right innominate; femur	*H. schinzii* forma *delheidi* Sickenberg, 1934a	Sickenberg (1934a): 209
	Reg. 4007	Niel, BE	Boom Clay Fm.	Fragments of skull (f, so), vertebrae and ribs	*H. schinzii* forma *delheidi* Sickenberg, 1934a	Sickenberg (1934a): 212
	Reg. 4008	Boom, BE	Boom Clay Fm.	Ribs	*H. schinzii* forma *delheidi* Sickenberg, 1934a	Sickenberg (1934a): 211
	Reg. 4010	Boom, BE	Boom Clay Fm.	Ribs	*H. schinzii* forma *delheidi* Sickenberg, 1934a	Sickenberg (1934a): 211
MCZ 8828		Flonheim, Mainz Basin, DE	Alzey Fm.	Mandibular fragment	*H. schinzii*	
MNHM PW 1910/1		Flörsheim, Mainz Basin, DE	Bodenheim Fm.	Partial skeleton	*H. schinzii*	Schmidtgen (1912): pl. 29: figs. 1, 2
MTTM V.60.642		Újlaki téglagyar, HU	Early Oligocene marine clays	Thoracic vertebrae	cf. *Manatherium delheidi* Hartlaub, 1886	
	V.60.643	Újlaki téglagyar, HU	Early Oligocene marine clays	Ribs	cf. *M. delheidi*	

	V.60.649	Újlaki téglagyar, HU	Early Oligocene marine clays	Mandibular fragment	cf. *M. delheidi*	
	V.60.653	Flonheim, Mainz Basin, DE	Alzey Fm.	Mandibular fragment	*Halitherium* Kaup, 1838	
	V.60.654	Újlaki téglagyar; HU	Early Oligocene marine clays	Right maxillary fragment	cf. *M. delheidi*	
	V.60.655	Újlaki téglagyar, HU	Early Oligocene marine clays	Left maxillary fragment	cf. *M. delheidi*	
	V.60.656	Újlaki téglagyar, HU	Early Oligocene marine clays	Left zygomatic process of squamosal	cf. *M. delheidi*	
	V.60.657	Újlaki téglagyar, HU	Early Oligocene marine clays	Mandibular fragment	cf. *M. delheidi*	
	V.60.659	Újlaki téglagyar, HU	Early Oligocene marine clays	Mandibular fragment	cf. *M. delheidi*	
	V.60.660	Újlaki téglagyar, HU	Early Oligocene marine clays	Frontoparietal-supraoccipital skullcap	cf. *M. delheidi*	Bad state of preservation
	V.60.664	Újlaki téglagyar, HU	Early Oligocene marine clays	Atlas	cf. *M. delheidi*	
	V.60.666	Újlaki téglagyar, HU	Early Oligocene marine clays	Right m3	cf. *M. delheidi*	
	V.60.673	Újlaki téglagyar, HU	Early Oligocene marine clays	Right scapula	cf. *M. delheidi*	
	V.60.676	Újlaki téglagyar, HU	Early Oligocene marine clays	Skull fragment (eo)	cf. *M. delheidi*	
NHMUK	PV M10865	Flohnheim, Mainz Basin, DE	Alzey Fm.	Fragment of right scapula	*Halitherium* Kaup, 1838	
	PV M36766	Flohnheim, Mainz Basin, DE	Alzey Fm.	Partial mandible	*H. schinzii*	
	unnumbered	(?)Darmstadt, West Germany	Alzey Fm.	Isolated elements: frontal, fragment of left zygomatic process of squamosal and right scapula	*Halitherium* Kaup, 1838	Not a single specimen; all elements associated with collection number M19957, which, however, is certainly misapplied

NHMB	78	Alzey, Mainz Basin, DE	Alzey Fm.	Fragment of right innominate	*H. schinzii*	
	Kb. 40	Kleinblauen, CH	Early Oligocene marine sands	Right humerus	*Halitherium* Kaup, 1838	
	Kb. 41	Kleinblauen, CH	Early Oligocene marine sands	Carpal and metacarpal	*H. schinzii*	
	Kb. 377	Kleinblauen, CH	Early Oligocene marine sands	Right zygomatic process of squamosal, ribs and rib fragments	*Halitherium* Kaup, 1838	
	M.G. 2	La Réole (Gironde), FR	Early Oligocene marine sands	Thoracic vertebra	Sirenia *incertae sedis*	
	M.G. 9	La Réole (Gironde), FR	Early Oligocene marine sands	Fragment of right humerus	*H.* cf. *schinzii*	
	M.G. 18	La Réole (Gironde), FR	Early Oligocene marine sands	Fragment of left mandible	Sirenia *incertae sedis*	
	M.G. 19	La Réole (Gironde), FR	Early Oligocene marine sands	Fragments of right mandible	*H. schinzii lareolensis* Pilleri, 1987	**Paratype** of *H. schinzii lareolensis* Pilleri, 1987
	M.G. 20	La Réole (Gironde), FR	Early Oligocene marine sands	Fragments of right jugal	*Halitherium* Kaup, 1838	
	M.G. 47	La Réole (Gironde), FR	Early Oligocene marine sands	Right scapula	*H. schinzii* (ssp. *lareolensis*?)	
	M.G. 48	La Réole (Gironde), FR	Early Oligocene marine sands	Fragment of left maxilla	*H.* cf. *schinzii*	
	M.G. 61	La Réole (Gironde), FR	Early Oligocene marine sands	Fragment of left mandible	*Halitherium* Kaup, 1838	
	M.G. 66	La Réole (Gironde), FR	Early Oligocene marine sands	Three lumbars	*Halitherium* Kaup, 1838	
	O.B. 806	Brislach, CH	early Oligocene marine clays	Partial skeleton with elements of skull (eo, bo), I1, premolars, vertebrae of all segments, ribs, sternum, stylopod, zeugopod, autopod, innominate, femur	*H. schinzii*	

T.D. 134	near Alzey, Mainz Basin, DE	Alzey Fm.	Fragment of left R1	Sirenia *incertae sedis*	
NL PAL 7334	Espenhain, East Germany	Böhlen Fm.	Ribs	*Halitherium* Kaup, 1838	
PAL 2361	Espenhain, East Germany	Böhlen Fm.	Caudal vertebra	*Halitherium* Kaup, 1838	
NMV P 2068/5	Rhine area, West Germany	Most likely from early Oligocene marine sands	Isolated finds: pterygoid, mandibular fragment, right humerus, two caudals, femur	*H. schinzii*	Not a single specimen
PMN SSN12EC50	Eckelsheim, Mainz Basin, DE	Alzey Fm.	Mandible	*H. schinzii*	
SSN12EC52	Eckelsheim, Mainz Basin, DE	Alzey Fm.	Atlas	*H. schinzii*	
SSN12EC54	Eckelsheim, Mainz Basin, DE	Alzey Fm.	Right scapula	*H. schinzii*	
SSN12EC56	Eckelsheim, Mainz Basin, DE	Alzey Fm.	Fragment of right innominate	*H. schinzii*	
SSN12EC57	Eckelsheim, Mainz Basin, DE	Alzey Fm.	Metacarpal	*H. schinzii*	
SSN12FL12	Flonheim, Mainz Basin, DE	Alzey Fm.	Left zygomatic process of squamosal	*H. schinzii*	
SSN12UF1	Uffhofen near Flonheim, Mainz Basin, DE	Alzey Fm.	Partial skeleton composed of vertebrae, ribs and innominates	*H. schinzii*	

Gen. nov. 2 *alleni*

Original species: *Halitherium alleni* Simpson, 1932a.
Stratigraphic range: Late Oligocene or early Miocene.
Locality: Ashley River phosphate deposits near Charleston, South Carolina (USA).
General remarks: All specimens personally investigated unless otherwise stated. Locality and age refers to all material listed here.

Collection nr.	Locality	Age	Material	Orig. spec.	Remarks
MCZ 16484	Charleston, USA	Oligocene / Miocene	Parietal	*H. alleni*	
17142	Charleston, USA	Oligocene / Miocene	Parietal-supraoccipital skullcap	*H. alleni*	**Holotype** of gen. nov. 2 *alleni*
YPM 21335	Charleston, USA	Oligocene / Miocene	Frontoparietal-supraoccipital skullcap	*H. alleni*	Stored in USNM now

Questionably referred material to gen. nov. 2 *alleni*

MCZ 16683	Charleston, USA	Oligocene / Miocene	Humerus	*H. alleni*	
16684	Charleston, USA	Oligocene / Miocene	Humerus	*H. alleni*	
16485	Charleston, USA	Oligocene / Miocene	Caudal vertebra	*H. alleni*	
16496	Charleston, USA	Oligocene / Miocene	Rib	*H. alleni*	

17141	Charleston, USA	Oligocene / Miocene	Humerus	*H. alleni*	
17145	Charleston, USA	Oligocene / Miocene	Zygomatic process of squamosal	*H. alleni*	
USNM 23394	Charleston, USA	Oligocene / Miocene	frontoparietal-supraoccipital skullcap	*H. alleni*	Kellogg (1966): fig. 38
299830	Charleston, USA	Oligocene / Miocene	Parietal fragment	*H. alleni*	
unnumb.	Charleston, USA	Oligocene / Miocene	Right maxillary fragment with M2–3	*H. alleni*	cast

Gen. nov. 3 *cristolii*

Original species: *Halitherium cristolii* Fitzinger, 1842 following the synonymy of Domning (1996).
Stratigraphic range: Upper Oligocene (Chattian).
General remarks: All specimens personally investigated.

Collection nr.	Locality	Age	Material	Orig. spec.	Remarks
LI 1854/327	Linz, Austria	Chattian	Partial skeleton (left scapula, vertebrae, ribs)	*H. cristolii*	
1899/11*	Linz, Austria	Chattian	Parietal-supraoccipital skullcap	*H. pergense*	**Holotype** of *H. pergense* Toula, 1899
1917/7	Linz, Austria	Chattian	Rib fragments	*H. pergense*	
1921/71	Linz, Austria	Chattian	Vertebrae, fragments of vertebrae and ribs	*H. abeli*	
1926/394	Linz, Austria	Chattian	Partial skull	*H. cristolii*	
1926/395	Linz, Austria	Chattian	Rib fragment	*H. cristolii*	
1927/200	Linz, Austria	Chattian	Rib fragment	*H. cristolii*	
1928/82	Linz, Austria	Chattian	Fragments of skull and rib	*H. cristolii*	
1931/21	Linz, Austria	Chattian	Rib fragment	*H. cristolii*	
1931/263	Linz, Austria	Chattian	Vertebral fragment	*H. cristolii*	
1939/257	Linz, Austria	Chattian	Mandible, fragments of basicranium, cervical and other vertebrae	*H. abeli*	**Holotype** of *H. abeli* Spillmann, 1959
1948/33	Linz, Austria	Chattian	Sternal fragment	*H. abeli*	
1992/118	Linz, Austria	Chattian	Rib fragments	*H. cristolii*	
2012/1	Linz, Austria	Chattian	Mandible with left dp5–m2, right m1–3	*H. cristolii*	**Lectotype** of gen. nov. 3 *cristolii*
2012/2	Linz, Austria	Chattian	Maxillary fragment with M1 and DP5 root	*H. cristolii*	**Paralectotype** of gen. nov. 3 *cristolii*
2012/3	Linz, Austria	Chattian	Isolated M3 crown	*H. cristolii*	**Paralectotype** of gen. nov. 3 *cristolii*
2012/4	Linz, Austria	Chattian	Proximal humerus fragment	*H. cristolii*	
2012/5	Linz, Austria	Chattian	Sternal fragment	*H. cristolii*	
2012/6	Linz, Austria	Chattian	Left m3	*H. cristolii*	

2012/7	Linz, Austria	Chattian	Skull fragment	*H. cristolii*	
2013/1	Linz, Austria	Chattian	Partial skeleton with vertebrae, ribs, left scapula and distal humerus fragment	*H. abeli*	Spillmann (1959): fig. 2; vertebrae and ribs of partial skeleton now lost

Gen. nov. 4 *bellunense*

Original species: *Halitherium bellunense* De Zigno, 1875.
Stratigraphic range: Latest Oligocene (upper Chattian).
General remarks: **Holotype** and only known specimen (juvenile). Personally investigated.

Collection nr.	Locality	Age	Material	Orig. spec.	Remarks
MGPD-18Z	Near Belluno, Italy	Upper Chattian	Parietal-supraoccipital skullcap	*H. bellunense*	–
19Z	Near Belluno, Italy	Upper Chattian	Left premaxilla with tusk	*H. bellunense*	–
20/21Z	Near Belluno, Italy	Upper Chattian	Fragment of left maxilla with DP5–M2	*H. bellunense*	–
22Z	Near Belluno, Italy	Upper Chattian	Left zygomatic process of squamosal	*H. bellunense*	–
23Z	Near Belluno, Italy	Upper Chattian	Right zygomatic process of squamosal	*H. bellunense*	–
7358/9Z	Near Belluno, Italy	Upper Chattian	Rib fragments (glued together)	*H. bellunense*	–
7362Z, 7367–9Z, 7374–6Z	Near Belluno, Italy	Upper Chattian	Vertebral fragments	*H. bellunense*	–
7363–4Z, 7366Z, 7381Z	Near Belluno, Italy	Upper Chattian	Rib fragments	*H. bellunense*	–
7383Z	Near Belluno, Italy	Upper Chattian	Fragment of a lower molar	*H. bellunense*	–
7384Z	Near Belluno, Italy	Upper Chattian	Fragment of left jugal	*H. bellunense*	–
7385/6Z	Near Belluno, Italy	Upper Chattian	Fragment of right maxilla with DP5 and M1	*H. bellunense*	–
7387Z	Near Belluno, Italy	Upper Chattian	Fragment of a molar	*H. bellunense*	–

"Halitherium antillense"

Original species: *Halitherium antillense* Matthew, 1916.
Stratigraphic range: Late Oligocene (lower Chattian).
General remarks: *Nomen dubium*.

Collection nr.	Locality	Age	Material	Orig. spec.	Remarks
AMNH 9844*	Near Juana Diaz, Puerto Rico	Lower Chattian	Posterior part of left mandible with m1–3, one cervical and one thoracic vertebra	*H. antillense* Matthew, 1916	Personally investigated

Appendix 2. List of all outgroup (Proboscidea: *Phosphatherium*, *Numidotherium*) and ingroup (sirenian) taxa analysed in this study including references, occurrences, and age. All data concerning the stratigraphical age were adjusted with Domning (1996); in the case of contradictions, the primary data source was considered. Collection numbers are provided for those taxa that were personally investigated. Sirenia *incertae sedis* indicate here taxa that were excluded from the cladistic analyses *á posteriori*.

Taxon	Collection number	Locality	Age	Database
Phosphatherium escuilliei	–	Ouled Abdoun Basin, Morocco	Late Palaeocene – early Eocene (Thanetian – Ypresian)	Gheerbrant *et al.* (1996); Gheerbrant *et al.* (2005b)
Numidotherium koholense	Unnumbered cast of **holotype** skull UO KA 1-18 in SMNS	El Kohol, Saharan Atlas, Algeria	Early Eocene (Cuisian)	Mahboubi *et al.* (1984); Mahboubi *et al.* (1986)
Prorastomus sirenoides	Partial skull and mandible NHMUK PV M44897 (**holotype**)	West-Central Jamaica	Late early Eocene	Owen (1855); Savage *et al.* (1994)
Pezosiren portelli	–	Western Jamaica	Early middle Eocene	Domning (2001c); Domning (in preparation)
Protosiren fraasi	Nearly complete skull of adult CGM 10171 (**holotype**) Cast NHMUK PV M9367 of mandible CGM 42297 that is possibly part of type specimen Partial skulls some with mandibles: BSPG 1905 XIII e7; FIS M3742–3; SMNS 10576 Parietal-supraoccipital skullcaps and/or natural endocranial casts: BSPG 1905 XIII e2–3; SMNS 43963, 43968–9, 43971–2 Skull fragments and teeth: SMNS 43958, 43960–2 Mandibles: MNHN LBE690 Vertebrae: SMNS 43975, unnumbered atlas Scapula: SMNS 43977 Pelvis: SMNS 43976	Cairo, Egypt	Middle Eocene (early – middle Lutetian)	Andrews (1906); Sickenberg (1934a); Gingerich *et al.* (1994)
Protosiren smithae	Partial skull and skeleton of adult CGM 42292 (**holotype**) and cast of it USNM 94810	Wadi Al Hitan, Egypt	Late middle Eocene (Bartonian)	Domning & Gingerich (1994)
Ashokia antiqua	–	Kutch (= Kachchh), India	Early middle Eocene (Lutetian)	Bajpai *et al.* (2009)
Sirenavus hungaricus	Partial skull MTTM V.60.1712 with left mandibular fragment MTTM V.83.42 (**holotype**)	Felsőgalla, Hungary	Middle Eocene (Lutetian)	Kretzoi (1941); Kordos (1981; 2002)
Eotheroides aegyptiacum	Natural endocranial cast NHMUK PV M46722 (**holotype**) Nearly complete and partial skulls: BSPG 1905 XII e1; FIS M4453; NHMUK PV M8152; SMNS 43979, 43990, 44000	Cairo, Egypt	middle Eocene (probably middle Lutetian)	Owen (1875); Abel (1913); Sickenberg (1934a); Gingerich (1992)

	Parietal-supraoccipital skullcap: SMNS 43991 Squamosal: SMNS 44006 Maxillae: SMNS 43993, 44014 Mandible: SMNS 43995 Vertebrae and ribs: FIS M3593a, b Ribs: SMNS 43983a–e, 43989, unnumbered ribs Scapula: SMNS 43984 Humerus: NHMUK PV M9238 Radius and ulna: SMNS 10932			
Eotheroides lambondrano	–	Northwestern Madagascar	Middle Eocene	Samonds *et al.* (2009)
Prototherium veronense	Nearly complete skull MGPD-10Z of adult (**holotype**) Nearly complete or partial skulls: MGPD-9Z, -12Z Premaxilla: MGPD-17Z Squamosal: MGPD-27648 Partial mandible: MGPD-15 Scapulae: MGPD-14Z, -6992	Monte Zuello, Italy	Late Eocene (Auversian)	De Zigno (1875, 1880)
Prototherium intermedium	Partial mandible, skull and skeleton of young adult MGPD-25837–26300 (**holotype**) Partial skulls: MGPD-28997 (including mandible), MGPD-28998	Possagno, Italy	Late Eocene (Priabonian)	Bizzotto (2005)
Eosiren stromeri	Partial skull and postcranial elements of adult SMNS 44007 (**holotype**)	Fayûm, Egypt	Late Eocene (late Priabonian)	Sickenberg (1934a); Gingerich (1992)
Eosiren libyca	Nearly complete skull CGM 10054 (**holotype**) Nearly complete or partial skulls some with mandibles and postcranial elements: BSPG 1902 XI 61; FIS M4056; MNHN LBE689; NHMUK PV M10910; SMNS 2024, 11244–6, 44008 Skull fragments (pm, mx): FIS M7756; NHMUK PV M7854, M8930 Endocranial cast: BSPG 1902 XI 512 Mandibles: NHMUK PV M8926, M10175; YPM 38213; SMNS unnumbered Rib: SMNS 13091 Scapula: SMNS 11247 Humerus: SMNS 11248 Ulna: SMNS 13137 Innominate: SMNS 11249 Vertebrae: BSPG 1902 XI 73	Fayûm, Egypt	Late Eocene (late Priabonian)	Sickenberg (1934a); Gingerich (1992)
Eosiren imenti	Partial skull and four ribs of adult CGM 40210 (**holotype**)	Fayûm, Egypt	Early Oligocene (Rupelian)	Domning *et al.* (1994)
Gen. nov. 1 *taulannense*	Appendix 1	Alpes-de-Haute-Provence, France	Late Eocene (Priabonian)	Sagne (2001a, b)
Gen. nov. 2 spec. nov 1	Appendix 1	Central Europe (Germany, Belgium, France)	Early Oligocene (Rupelian)	Bizzarini (1995); Bizzarini & Reggiani (2010)

Gen. nov. 2 *bronni*	Appendix 1	Central Europe (especially Germany, Belgium)	Early Oligocene (Rupelian)	Bronn (1853–1856); Krauss (1858)
Gen. nov. 2 *alleni*	Appendix 1	Charleston, South Carolina, USA	Probably late Oligocene or early Miocene	Allen (1926)
Gen. nov. 3 *cristolii*	Appendix 1	Linz, Upper Austria	late Oligocene (Egerian)	Fitzinger (1842); Ehrlich (1855); Toula (1899); Abel (1904); Spillmann (1959, 1969, 1973)
Crenatosiren olseni	Skull, partial mandible and skeleton of old adult UF/FGS V6094 (**holotype**) Partial skulls often with mandibles and/or postcranial elements: USNM 425488; SC 89.24.3, 90.104.1	Florida to North Carolina, USA	Latest Oligocene (late early Arikareean; late Chattian equivalent)	Rheinhart (1976); Domning (1997)
Nanosiren garciae	Partial skull of adult UF 201840 (**holotype**) Parietal-supraoccipital skullcaps: USNM 520123, 534359 Premaxillae: USNM 323115, 520106 Jugal: USNM 520117 Squamosal: USNM 531459 Sternum: USNM 534371	Florida, USA	Early Pliocene (latest Hemphillian)	Domning & Aguilera (2008)
Nanosiren sanchezi	Disarticulated partial skull of subadult UNEFM-VF-041 (**holotype**)	Estado Falcón, Venezuela	Late Miocene	Domning & Aguilera (2008)
Dugong dugon	> 300 specimens (skulls often with postcranial skeletons) in the zoological collections of IRSNB, JCU, MCZ, MB, MNHN, NHMB, NHMUK, NMV, SAM	Indo-Pacific tropical and subtropical region from the western Pacific islands to the Red Sea	(?)Pleistocene – recent	Bertram & Bertram (1973)
Bharatisiren indica	–	Kachchh, India	Late Oligocene (Chattian or late Waiorian)	Bajpai *et al.* (2006)
Bharatisiren kachchhensis	–	Kachchh, India	Early Miocene (Aidaian; Aquitanian equivalent)	Bajpai & Domning (1997)
Corystosiren varguezi	Parietal-supraoccipital skullcaps: UF 57291; USNM 181550, 323186	Yucatan, Mexico	Early Pliocene	Domning (1990)
Dioplotherium manigaulti	–	South Carolina and Florida, USA	Early Miocene and presumed early Miocene deposits	Domning (1989a)
Dioplotherium allisoni	Fragment of right mandible UCMP 47250 (**holotype**)	California, USA; Baja California Sur, Mexico	Late early Miocene (Burdigalian) to late middle Miocene (Luisian, Temblorian, Barstovian)	Kilmer (1965); Domning (1978); Toledo & Domning (1989)
Domningia sodhae	–	Kutch (= Kachchh), India	Early Miocene (Aquitanian)	Thewissen & Bajpai (2009)

Kutchisiren cylindrica	–	Kutch (= Kachchh), India	Early Miocene (Aquitanian or Burdigalian)	Bajpai *et al.* (2010)
Rytiodus capgrandi	–	Bournic, Lot-et-Garonne, France	Early Miocene (Aquitanian)	Lartet (1866); Delfortrie (1880); Pilleri (1987)
Xenosiren yucateca	Casts USNM 425735 and unnumbered cast in MNHN of **holotype** IGM 4190 (disarticulated skull elements, tusk, left and right M3)	Yucatan, Mexico	Late Miocene or early Pliocene (Hemphillian)	Domning (1989b)
Gen. nov. 4 *bellunense*	Appendix 1	Belluno area, Italy	Latest Oligocene (upper Chattian)	De Zigno (1875); Abel (1905)
Caribosiren turneri	Partial skull and thoracic vertebrae UCMP 38722 (**holotype**)	Near San Sebastián, Puerto Rico	Middle or late Oligocene	Reinhart (1959)
Metaxytherium krahuletzi	**Type series** comprising six isolated molars: KME GII 21, 22, 25, 26, 29, 34 Large number of uncatalogued specimens in KME and HMH collections comprising mostly fragments of skulls and numerous postcranial elements of a single species. Therefore, only referred specimens with an identification are listed here. Partial skeletons: KÜH 82, 85, 87, 89, 90; SZ: KÜH 88 (on loan for display) Parietal-supraoccipital skullcap: KME GII17 Squamosal: KME G541 Lower cheek teeth: KME GII 28 Sternum: KME G 558 Scapula: cast NHMUK PV M9248 Humeri: KME B516, G535, 538 Radius and/or ulna: KME G539, 551, 552 Metacarpals: KME G554, 555	Central Paratethys and possibly central and western Tethys seaways, Europe (Austria, Switzerland, Slovakia, France)	Early Miocene (upper Eggenburgian to Ottnangian; early to middle Burdigalian-correlative)	Deperet (1895); Domning & Pervesler (2001)
Metaxytherium floridanum	Maxilla USNM 7221 (**holotype**) Nearly complete and partial skulls some with mandibles: MCZ 4432; UF 97337; UF/FGS V5454; USNM 10953, 323193, 356678 (with R1), 377509, 412207, 421520, G-544 Parietal-supraoccipital skullcaps: MCZ 4062; UF 203002; USNM 323136, 323143-5, 323190 (with humerus and rib fragment), 359724, 457212 Frontal: UF/FGS V4250 Maxillae: AMNH 26805; MCZ 4218 Mandible: USNM 356683 Humeri: MCZ 6909, 15752; USNM 23255, 363451, 363454 Rib: UF 160716 Sternum: USNM 359680 Scapulae: USNM 359722, 392249	Florida, USA	Middle and late Miocene (Clarendonian, possibly late Barstovian and early Hemphillian)	Hay (1922); Reinhart (1976); Domning (1988)
Metaxytherium arctodites	–	California, USA; Baja California, Mexico	Middle Miocene (Barstovian)	Aranda-Manteca *et al.* (1994)

Metaxytherium crataegense	Skull of adult: AMNH 26838 (**holotype**) Skull, partial mandible, vertebrae, ribs and scapula of young adult: USNM 16757 Scapula, radius, ulna, pelvis: USNM 23213	Florida and Maryland, USA	Early – middle Miocene (late Hemingfordian or early Barstovian)	Simpson (1932a, b); Kellogg (1966); Aranda-Manteca *et al.* (1994)
Metaxytherium medium	Mandibular element MNHN Fs 2706 (**holotype**) Mounted skeleton "1921-10" in MNHN exhibition representing *M. cuvieri* now synonymous with *M. medium* according to Domning (1996) Partial skull and postcranial elements of adult: MNHN Fs 5001–15 Parietal-supraoccipital skullcaps: MNHN Fs 2880, 3242 Periotic: MNHN Fs 5019 Maxillary element: MNHN Fs 2512	Maine-et-Loire, France	Middle or late Miocene (Serravallian – Tortonian)	Personal investigations
Metaxytherium serresii	Articulated partial skull with tusks and fragment of right mandible with m1–3 of young adult: MNHN unnumbered Fragment of right scapula: MNHN unnumbered Humerus: MNHN 2260 Radius and ulna: MNHN 756 Atlas: MNHN 1868-234	Montpellier, France; Calbria, Italy; Sahabi, Libya	Late Miocene (latest Tortonian) – early Pliocene (early Zanclian)	Domning & Thomas (1987); Pilleri (1988a); Carone & Domning (2007)
Dusisiren reinharti	Disarticulated partial skull and skeleton of juvenile UCMP 39581 (**holotype**)	Baja California Sur, Mexico	Early middle Miocene (Vaquerosian – Temblorian)	Domning (1978)
Dusisiren dewana	–	Yamagata Prefecture, Japan	Late Miocene	Takahashi *et al.* (1986)
Dusisiren jordani	Partial skull and postcranial material of old adult USNM 11051 (**holotype**) Nearly complete skulls and partial skeletons of young adults: UCMP 3794, 77037 Scapula: USNM 23856	California, USA	Late Miocene – earliest Pliocene (Mohnian – early Delmontian)	Reinhart (1959); Domning (1978)
Dusisiren takasatensis	–	Fukushima Prefecture, Japan	Late Miocene	Kobayashi *et al.* (1995)
Hydrodamalis cuestae	Partial skull and skeleton of subadult UCMP 86433 (**holotype**)	California, USA; Baja California, Mexico	Middle – late Pliocene (Hemphillian – Blancan)	Domning (1978)
Hydrodamalis gigas	Complete or partial skulls with mandibles and/or postcranial material: AMNH 14271; MNHN A4764; NHMB 2693; NRM 8385, 608458; UCMP 23050; USNM 22999	Aleutian and Commander Islands; North-Pacific; California, USA	Late Pleistocene – recent	Domning (1978)
Anomotherium langewieschei	Partial skull and skeleton DM 327 (**holotype**)	Doberg near Bünde, Westphalia, Germany	Latest Oligocene (upper Chattian)	Siegfried (1965)
Miosiren kocki	Skull and partial skeleton of adult IRSNB M.136 (**holotype**)	Near Boom, Belgium	Early Miocene (lower Burdigalian)	Sickenberg (1934a)

Potamosiren magdalenensis	Left mandible UCMP 39471 (**holotype**)	Departamento del Huila, Colombia	Middle Miocene (Friasian)	Reinhart (1951); Domning (1982)
Ribodon limbatus	–	Rio Paraná, Entre Rios, Argentinia	Late Miocene – early Pliocene (Huayquerian – Montehermosan)	Ameghino (1883); Pascual (1953); Domning (1982)
Trichechus inunguis	Complete or partial skulls with mandibles and often postcranial material: MB Ma. 34545, 35805–9, 46528; MCZ 1079; MNHN 1945-233, 1945-235, A-2889	Rivers Amazon and Orinoco, South America	Recent	Bertram & Bertram (1973)
Trichechus manatus	> 90 specimens (skulls often with postcranial skeletons) in the zoological collections of MB, MCZ, MNHN and UF	West Indies; southeastern USA; central American coasts and northern South America	Late Pleistocene – recent	Bertram & Bertram (1973); Domning (2005)
Trichechus senegalensis	Complete or partial skulls with mandibles and often postcranial material: MB Ma. 3215, 5188, 8233, 38743, 69317, 69322, 69331–2, 69325–9, 69334–7; MNHN 1885-673	West African Rivers and coastal region from Senegal to Angola	Recent	Bertram & Bertram (1973)
Sirenia *incertae sedis*				
Eotheroides babiae	–	Kachchh, India	Middle Eocene (Lutetian)	Bajpai *et al.* (2006)
"Halitherium antillense"	Fragment of left mandible and vertebrae AMNH 9844 (**holotype**)	Near Juana Diaz, Puerto Rico	Late Oligocene (lower Chattian)	Matthew (1916)
Metaxytherium subapenninum	Cast MGP 26Z and 27Z of adult skull representing the uncatalogued **holotype** of *Felsinotherium gastaldi* now synonymous with *M. subapenninum* according to Domning (1996)	Northwestern coasts of the Mediterranean Basin, Italy, and probably Spain	Pliocene (lower Zanclean – upper Piacenzian)	De Zigno (1878); Fondi & Pacini, (1974); Pilleri (1988a, b); Sorbi *et al.* (2012)

Appendix 3. Cranial, mandibular, dental, and postcranial measurements of the species constituting the former *"Halitherium"*-species complex. Letters in parentheses denote the standard dimensions established by Domning (1978: fig. 7, tabs. 2, 7, 8, 15, 17–19). Measurements in parentheses indicate preserved lengths, "e" estimated dimensions, "l" and "r" measurements from the left and/or right side.

Measurements (in mm if not otherwise stated) of the crania of gen. nov. 1 *taulannense*

	RGHP D040	RGHP D057	RGHP D345
Condylobasal length (AB)	305	–	–
Length of premaxillary symphysis (AH)	106	–	–
Length of premaxilla	157	–	–
Height of jugal below orbit (ab)	44l+r	–	–
Zygomatic width (CC')	159	141	–
Width across exoccipitals (cc')	86	–	–
Top of supraoccipital to ventral sides of occipital condyles (de)	86	–	–
Top of parietals to ventral sides of pterygoid processes	105	–	–
Length of frontals, level of tips of supraorbital processes to frontoparietal suture (F)	111	–	75
Width across supraorbital processes (FF')	119	–	–
Width across occipital condyles (ff')	69	–	–
Width of cranium at frontoparietal suture (GG')	46	(37)	35
Minimum width of parietals	29	25	27
Width of *foramen magnum* (gg')	30	–	–
Length of mesorostral fossa (HI)	71.8	–	–
Width of mesorostral fossa (JJ)	41	–	–
Height of *foramen magnum* (hi)	18	–	–
Maximum height of rostrum (KL)	65	–	–
Posterior width of rostral masticating surface (MM')	46	–	–
Anteroposterior length of zygomatic-orbital bridge of maxilla (no)	68	–	–
Length of zygomatic process of squamosal (OP)	107l; 110r	–	–
Length of parietals, frontoparietal suture to rear of external occipital protuberance (P)	82	66	65
Maximum width of parietals	58	(55)	45
Anteroposterior length of root of zygomatic process of squamosal (QR)	36	–	–
Maximum width between labial edges of left and right alveoli (rr')	79	–	48
Width across sigmoid ridges of squamosal (ss')	118	–	–
Dorsoventral thickness of zygomatic-orbital bridge (T)	(16)l; (18)r	–	–
Anterior width of rostral masticating surface (tt')	27	–	–
Dorsoventral height of zygomatic process of squamosal (WX)	43l+r	35	–
Maximum width between pterygoid processes (yy')	50	–	–
Length of jugal (YZ)	140	–	–
Length of frontals in midline (LFr)	65.5	–	58

Height of supraoccipital (HSo)	44	38	–
Width of supraoccipital (WSo)	73	(51)	–
Height of infraorbital foramen	13l+r	–	–
Width of infraorbital foramen	(15)l; 14.5r	–	–
Length of nasals	(42)	–	25
Width of nasals	53	–	16
Deflection of masticating surface of rostrum from occlusal plane (degrees) (RD)	57°	–	–
Angle between supraoccipital and parietal (degrees)	130°	135°	–

Measurements (in mm if not otherwise stated) of the mandibles of gen. nov. 1 *taulannense*

	RGHP C001	RGHP C009	RGHP E.7.096a
Total length (AB)	216	(213)	235
Anterior tip to front of ascending ramus (AG)	133	150	154
Anterior tip to rear of mental foramen (AP)	–	32	45
Anterior tip to front of mandibular foramen (AQ)	138	–	152
Length of symphysis (AS)	64	60	69
Posterior extremity to front of ascending ramus (BG)	65	(68)	72
Posterior extremity to front of mandibular foramen (BQ)	71	–	73
Height at coronoid process (CD)	162	–	–
Distance between anterior and posterior ventral extremities (DF)	117	95	120
Height at mandibular notch (DK)	(117)	–	112
Height at condyle (DL)	132	–	(122)
Height at deflection point of horizontal ramus (EF)	77	61	81
Deflection point to rear of alveolar row (EU)	90	100	109
Minimum anteroposterior length of ascending ramus (GH)	59	(59)	57
Front of ascending ramus to rear of mental foramen (GP)	–	113	109
Maximum anteroposterior length of dorsal part of ascending ramus (IJ)	73	–	(71)
Top of ventral curvature of horizontal ramus to line connecting ventral extremities (MN)	40	25	31
Minimum dorsoventral height of horizontal ramus (MO)	51	45	52
Maximum width of masticating surface (RR')	55	35	45
Rear of symphysis to front of mandibular foramen (SQ)	89	–	93
Length of the alveolar row (m1–3) (TU)	53	–	53
Maximum width between labial edges of left and right alveoli (VV')	–	–	62
Minimum width between angles (WW')	–	–	(80)
Minimum width between condyles (XX')	–	–	(80)
Retromolar space	0	0	20
Maximum diameter of coronoid foramen	–	–	7
Deflection of symphysal surface from occlusal plane (degrees) (MD)	47°	45°	50°

Dental measurements (in mm) of gen. nov. 1 *taulannense*

Tooth	Specimen	Length	Anterior width (AW)	Posterior width (PW)
DP4	RGHP D345	(13.5)r	(13)r	(12)r
DP5	RGHP D345	(14)	(14)	(13)
M1	RGHP D040	14.8l; 14.5r	17.2l; 16.5r	15.5l; 15r
	RGHP D345	16	16l; 17r	13l; 14r
M2	RGHP D040	17l; 16.5r	18.6l; 18r	15l; 15.5r
M3	RGHP D040	19.9l; 19.7r	19.6l; 19.8r	14.2l; 15.5r
dp5	RGHP C001	(14.8)l; 15.2r	(10)l; 11r	(11)l; 11.5r
m1	RGHP C001	15l; 15.5r	13.4l; 13r	13l; 12.5r
	RGHP C009	17	12.5	13
	RGHP E.7.096a	15.4l; 14r	11l; 12r	11.5l; 12.3r
m2	RGHP C001	18.5l; 18.8r	14l; 15.7r	13.5l; 14.5r
	RGHP C009	20.5l; 20r	14.5	15
	RGHP E.7.096a	17l; 15.9r	13.1l; 13.3r	13l; 13.5r
m3	RGHP C001	20l; 20.5r	15.4	13
	RGHP E.7.096a	22.4l; 21.8r	14.4l; 14.9r	13l; 14r

Dimensions (in mm) of selected postcranial elements of gen. nov. 1 *taulannense* relevant in this study (measurements derived from Sagne, 2001b)

Scapula: RGHP D350 (r)	
Maximum scapular length, vertebral border to border of glenoid fossa (AB)	(215)
Length of scapular spine	118
Maximum width of blade dorsally (CD)	110
Transversal width of infraspinous fossa at about mid-length of scapular spine	18.5
Mediolateral width of glenoid fossa (BI)	31
Anteroposterior length of glenoid fossa (MN)	42
Lateral border of glenoid fossa to inside of concave distal end of spine (BJ)	32
Minimum anteroposterior width of neck (EF)	36
Humerus: RGHP C035 (r)	
Maximum length, greater tubercle to distal end (AB)	162
Length from head to distal end	150
Maximum proximal width	57
Maximum distal width	39
Maximum diameter of mid-shaft	33
Minimum diameter of mid-shaft	22
Radius and Ulna: RGHP C066 (l)	
Total length of ulna (AB)	(148)
Total length of radius (CD)	135
Anteroposterior width of ulna shaft about mid-length	20

Anteroposterior width of radius shaft about mid-length	13
Transversal width of ulna shaft about mid-length	16
Transversal width of radius shaft about mid-length	18

Measurements (in mm if not otherwise stated) of the crania of gen. nov. 2 spec. nov. 1

	BSPG 1956 I 540	FIS M2597	FIS M8002	MNHM PW 1949/157	MNHM PW 1991/66-LS	LS RLP PW 2005/5042-LS	NHMUK PV M9415
Condylobasal length (AB)	310	280e	342e	–	–	330e	(328)
Length of premaxillary symphysis (AH)	(89)	(65)	(64)	–	–	(85)	(51)
Length of premaxilla	(178)	(126)	(164)	–	–	(170)	125e
Height of jugal below orbit (ab)	37l; 38.5r	(19)l	46r	–	–	–	38l+r
Zygomatic width (CC')	155	148	–	–	(168)	–	187
Width across exoccipitals (cc')	96	–	–	–	–	119	–
Top of supraoccipital to ventral sides of occipital condyles (de)	87	–	–	72	–	–	(58)
Top of parietals to ventral sides of pterygoid processes	128	–	–	112	–	–	(68)
Length of frontals, level of tips of supraorbital processes to frontoparietal suture (F)	107	80	103	82	104	104	97
Width across supraorbital processes (FF')	120	(108)	141	(115)	119	109	142
Width across occipital condyles (ff')	69	–	–	77	–	85	86.5
Width of cranium at frontoparietal suture (GG')	49	43	62	57	56	50e	67
Minimum width of parietals	42	39	51	51	45	52	55
Width of *foramen magnum* (gg')	41	–	–	28	–	–	36
Length of mesorostral fossa (HI)	(73)	102	90e	–	–	77.5e	92e
Width of mesorostral fossa (JJ)	42	50	53	–	–	40e	56
Height of *foramen magnum* (hi)	30	–	–	25e	–	–	–
Maximum height of rostrum (KL)	53	(40)	–	–	–	–	(54)
Posterior width of rostral masticating surface (MM')	47	(33)	–	–	–	–	(46)
Anteroposterior length of zygomatic-orbital bridge of maxilla (no)	51l	(54)l+r	52l; 58r	(34)r	–	–	(40)r
Length of zygomatic process of squamosal (OP)	97.5l; 102r	86l; 87r	–	–	107l	–	108l; 111r
Length of parietals, frontoparietal suture to rear of external occipital protuberance (P)	83	90	100	102	104	(87.5)	95
Maximum width of parietals	55	51	57	57	61	62	63
Anteroposterior length of root of zygomatic process of squamosal (QR)	40l; (36)r	38 r	–	–	(38)l	–	(45)l+r

Maximum width between labial edges of left and right alveoli (rr')	67	75	74	72	72	–	86
Width across sigmoid ridges of squamosal (ss')	125	–	–	157	–	–	161
Dorsoventral thickness of zygomatic-orbital bridge (T)	11	14l; (12)r	14l+r	11r	12l; 13r	–	12r
Anterior width of rostral masticating surface (tt')	29	25	–	–	–	–	–
Dorsoventral height of zygomatic process of squamosal (WX)	30l; 31r	(23)l	–	–	30l	–	42l+r
Maximum width between pterygoid processes (yy')	50	56	–	45	–	–	45
Length of jugal (YZ)	(80)l; (75)r	–	(118)r	–	–	(133)l	(160)r
Length of frontals in midline (LFr)	58	60	89	(68)	82	(71)	(65)
Height of supraoccipital (HSo)	(45)	37	(41)	44	45	42e	(47)
Width of supraoccipital (WSo)	68	65	72	68	75	67	77.5
Height of infraorbital foramen	17l	16l; 15r	18r	–	–	–	–
Width of infraorbital foramen	13l	9l+r	12.5r	–	–	–	–
Length of nasals	(40)	40l	(29)	–	(24)	33	–
Width of nasals	51	21l	45	–	43	39	–
Deflection of masticating surface of rostrum from occlusal plane (degrees) (RD)	58°	56°	53°	–	–	60°e	50°e
Angle between supraoccipital and parietal (degrees)	120°	140°	135°	135°	140°	130°e	135°

Measurements (in mm if not otherwise stated) of the mandibles of gen. nov. 2 spec. nov. 1

	BSPG 1956 I 540	MNHM PW 1991/66-LS	LS RLP PW 2005/5042-LS	CDGG S3
Total length (AB)	200	219.5	240	237.5
Anterior tip to front of ascending ramus (AG)	123	(158)	(152)	158
Anterior tip to rear of mental foramen (AP)	43	50	–	(115)
Anterior tip to front of mandibular foramen (AQ)	109	149.5	–	150
Length of symphysis (AS)	64	63.5	–	62
Posterior extremity to front of ascending ramus (BG)	71	(65)	(90)	(80)
Posterior extremity to front of mandibular for amen (BQ)	81	66	–	(83)
Height at coronoid process (CD)	–	–	(152)	140e
Distance between anterior and posterior ventral extremities (DF)	131	135.5	149	135
Height at mandibular notch (DK)	–	–	132	(115)
Height at condyle (DL)	–	–	148	(128)
Height at deflection point of horizontal ramus (EF)	66	(54)	77	63

Deflection point to rear of alveolar row (EU)	75	(103)	111	110
Minimum anteroposterior length of ascending ramus (GH)	67.5	–	71	67
Front of ascending ramus to rear of mental foramen (GP)	77	105	–	103
Maximum anteroposterior length of dorsal part of ascending ramus (IJ)	–	–	78	(70)
Top of ventral curvature of horizontal ramus to line connecting ventral extremities (MN)	25	23	32	23
Minimum dorsoventral height of horizontal ramus (MO)	35	37	40.5	45
Maximum width of masticating surface (RR')	33	–	–	40
Rear of symphysis to front of mandibular foramen (SQ)	61	97	–	90
Length of the alveolar row (m1–3) (TU)	49e	–	–	62.5r
Maximum width between labial edges of left and right alveoli (VV')	76	–	–	62.5
Minimum width between angles (WW')	83e	–	–	(63)
Minimum width between condyles (XX')	–	–	–	146e
Retromolar space	17l; (12)r	14.5r	–	19r
Maximum diameter of coronoid foramen	5.5l; 6.5r	6r	–	7.5r
Deflection of symphysal surface from occlusal plane (degrees) (MD)	45°	47°	50°	45°

Linear dimensions (in mm) of the cheek teeth of gen. nov. 2 spec. nov. 1

Tooth	Specimen	Length	Anterior width (AW)	Posterior width (PW)
DP5	MNHM PW 1991/66-LS	(15.9)l	(16.2)l	(16)l
	MNHM PW 1949/157	(15.6)r	15.7r	15.5r
	NHMUK PV M9415	(16.5)l; 16r	17	16.7l; 16.9r
	BSPG 1956 I 540	14l; 15.7r	14.8l; 15r	15
M1	MNHM PW 1991/66-LS	16.2l; (15.3)r	17.6l; (16.4)r	17l; (16)r
	MNHM PW 1949/157	(15.6)l; (15.7)r	17.3l; 17.9r	16.5l; 17r
	NHMUK PV M9415	18l; 17.5r	18.5l; 18r	18
	BSPG 1956 I 540	15.6l; 16r	18l; 18.7r	16.6l; 17r
M2	FIS M2597	18.6l; 18.2r	18.5l; 19.3r	15.5l; 16r
	MNHM PW 1991/66-LS	20.6l; 21.2r	21.3l; (22)r	20l; 20.5r
	MNHM PW 1949/157	18.7l; 19r	19.7l; 19.3r	18.3
	NHMUK M9415	22.4l; 21.9r	21l; 23r	19.5l; 21r
	BSPG 1956 I 540	18.9	(21.5)l; 21.5r	(19)l; 18.5r
M3	FIS M2597	20.2l; 20r	17.8l; 18.3r	15
	MNHM PW 1991/66-LS	25.2l; 25.8r	23.6	20

	MNHM PW 1949/157	24.7l; 23.7r	20.9l; 20.3r	18l; 17.5r
	NHMUK PV M9415 (not yet fully erupted)	23l; 23.7r	22l; 22.3r	20.5
	BSPG 1956 I 540	22l; 21r	23l; 22.5r	21.5l; 21r
dp5	NHMUK PV M9415	22.2l; 21.4r	(12.9)l; (14.3)r	(16.4)l; (17)r
m1	NHMUK PV M9415	23.6l; 24.3r	19.3l; 18.6r	19.3l; 18.6r
m2	CDGG S3	29.7r	22.4r	22r
	NHMUK PV M9415	28.5	22l; 22.9r	22.9
m3	CDGG S3	32r	21.7r	20.7r

Dimensions (in mm) of the left ribs of gen. nov. 2 spec. nov. 1 (NHMUK PV M9415)

	Capitulum to distal end in straight line	Tip of *capitulum* to lateral edge of *tuberculum*	Maximum diameter at about mid-shaft	Minimum diameter at about mid-shaft
R1	170	50e	30	19
R2	(222)	–	34	23
R3	(243)	–	38	29
R4	268	–	40	31
R5	325	(48)	46	36
R6	337	45	43	32
R7	(357)	–	43	32
R8	(320)	–	45	36
R9	(347)	–	37	32
R10	(354)	–	38	28
R11	(334)	–	43	24
R12	(350)	–	44	24
R13	355	38	41	25
R14	343	23	39	26
R15	315	17.4	41	26
R16	323	14.5	38	24
R17	299	13.4	30	20
R18	(254)	12.2	31	20
R19	125	0	23	16

Dimensions (in mm) of selected postcranial elements of gen. nov. 2 spec. nov. 1 relevant in this study

Scapula	**MNHM PW 1991/66-LS (r)**	**NHMUK PV M9415 (r)**
Maximum scapular length, vertebral border to border of glenoid fossa (AB)	(220)	(259)
Length of scapular spine	108	136
Maximum width of blade dorsally (CD)	(84)	(97)

Transversal width of infraspinous fossa at about mid-length of scapular spine	18	23
Mediolateral width of glenoid fossa (BI)	(37)	(43)
Anteroposterior length of glenoid fossa (MN)	(43)	54
Lateral border of glenoid fossa to inside of concave distal end of spine (BJ)	38	(34)
Minimum anteroposterior width of neck (EF)	32	45
Humerus	**MNHM PW 1991/66-LS (l)**	**NHMUK PV M9415 (r)**
Maximum length, greater tubercle to distal end (AB)	173	186
Length from head to distal end	166	174
Maximum proximal width	66	66
Maximum distal width	50	55
Maximum diameter of mid-shaft	28	32
Minimum diameter of mid-shaft	25	28
Radius and Ulna	**HLMD-WT 420 (r)**	**–**
Total length of ulna (AB)	(167)	–
Total length of radius (CD)	175	–
Anteroposterior width of ulna shaft about mid-length	22	–
Anteroposterior width of radius shaft about mid-length	16	–
Transversal width of ulna shaft about mid-length	23	–
Transversal width of radius shaft about mid-length	21	–

Measurements (in mm if not otherwise stated) of the crania of gen. nov. 2 *bronni*

	CDGG S1	SMNS 47736	SMNS 1539	MWNH-TER-1	MCZ 8829	NHMUK PV M19957	FIS M8385	MNHM PW 1984/ 37-1
Condylobasal length (AB)	342	–	–	(318)	–	–	–	–
Length of premaxillary symphysis (AH)	(97.5)	–	–	(74)	–	–	(83)	–
Length of premaxilla	(190)	–	–	(172.5)	–	–	(143)	–
Height of jugal below orbit (ab)	(44)l; 48r	38r	–	44.5l; 40r	–	–	39l+r	(42)r
Zygomatic width (CC')	219	178e	–	–	190	–	–	(170)
Width across exoccipitals (cc')	118	–	–	–	–	(94)	–	90
Top of supraoccipital to ventral sides of occipital condyles (de)	105	–	–	–	–	103.5	–	65
Top of parietals to ventral sides of pterygoid processes	137.5	–	–	–	–	125	–	83

Length of frontals, level of tips of supraorbital processes to frontoparietal suture (F)	104	104	94	(106)	123	107	101	94
Width across supraorbital processes (FF')	140.5	143e	132	151	157.5	–	144	(125)
Width across occipital condyles (ff')	85.5	–	–	–	–	89	–	73
Width of cranium at frontoparietal suture (GG')	61	62.5	60	71	67	(61)	(61)	44.5
Minimum width of parietals	45	52	48	56e	52e	52	45	41
Width of *foramen magnum* (gg')	43	–	–	–	–	39.5	–	35.5
Length of mesorostral fossa (HI)	(87)	–	–	94e	–	–	(73)	–
Width of mesorostral fossa (JJ)	58	–	–	60	–	–	(51)	–
Height of *foramen magnum* (hi)	31	–	–	–	–	36.5	–	30.5
Maximum height of rostrum (KL)	(65)	–	–	63e	–	–	(64)	–
Posterior width of rostral masticating surface (MM')	46	–	–	43e	–	–	(42)	–
Anteroposterior length of zygomatic-orbital bridge of maxilla (no)	60l+r	–	–	(55)r	(24)l	–	33l	(38)r+l
Length of zygomatic process of squamosal (OP)	122l; 124r	(95)r	–	121l+r	125l+r	–	103l; 101r	109r
Length of parietals, frontoparietal suture to rear of external occipital protuberance (P)	104.5	(93)	88.5	–	92	90	(80)	95
Maximum width of parietals	52	56	56	–	64.5	70	(63)	50
Anteroposterior length of root of zygomatic process of squamosal (QR)	46l; (44)r	33r	–	29l	(38)l; 40r	–	(27)r	64r
Maximum width between labial edges of left and right alveoli, across M1 (rr')	(85)	–	–	(75)	(85)	80	(71)	84
Width across sigmoid ridges of squamosal (ss')	160.5	–	–	–	183	160	–	138
Dorsoventral thickness of zygomatic-orbital bridge (T)	16l+r	–	–	20r	15	(22)	22l	15l; 13r
Anterior width of rostral masticating surface (tt')	38e	–	–	–	–	–	(33)	–
Dorsoventral height of zygomatic process of squamosal (WX)	56l; 54r	46r	–	58l+r	46.5l; 45r	–	37.5l+r	26r
Maximum width between pterygoid processes (yy')	57	55	–	–	–	59	–	53
Length of jugal (YZ)	152l; 150r	–	–	–	–	–	–	–
Length of frontals in midline (LFr)	65	(57)	66	(65)	(65)	(67)	(70)	(50)

Height of supraoccipital (HSo)	50	46.5	49	–	48	(52)	50	48
Width of supraoccipital (WSo)	88	(78)	80	–	80	81	78	75
Height of infraorbital foramen	16l+r	–	–	11.5r	–	–	13l	–
Width of infraorbital foramen	15.5l+r	–	–	10r	–	–	12l	–
Length of nasals	(27)	38e	(37.5)	(40)	(43)	–	(30)	(27)
Width of nasals	47	51e	52	45	(54)	–	(37)	37
Deflection of masticating surface of rostrum from occlusal plane (degrees) (RD)	55°	55°e	–	57°e	55°e	55°e	50°e	–
Angle between supraoccipital and parietal (degrees)	130°	135°e	140°	–	140°	135°	135°e	135°

Measurements (in mm if not otherwise stated) of the mandibles of gen. nov. 2 *bronni*

	CDGG S1	SMNS 47736	FIS M8385	FMD SRK Eck-Rat 43
Total length (AB)	265	235	(233)	161
Anterior tip to front of ascending ramus (AG)	184	146	(150)	(173)
Anterior tip to rear of mental foramen (AP)	58	35	–	(44)
Anterior tip to front of mandibular foramen (AQ)	172	136	(143)	(173)
Length of symphysis (AS)	63	69	(62)	(75)
Posterior extremity to front of ascending ramus (BG)	96	103.5	91	98
Posterior extremity to front of mandibular foramen (BQ)	98	108	93	100
Height at coronoid process (CD)	(157)	–	(170)	–
Distance between anterior and posterior ventral extremities (DF)	151	122	150	166
Height at mandibular notch (DK)	129	148	140	–
Height at condyle (DL)	153	167	157	–
Height at deflection point of horizontal ramus (EF)	89	82	75	92
Deflection point to rear of alveolar row (EU)	107	103.5	–	100
Minimum anteroposterior length of ascending ramus (GH)	76	87	78.5	–
Front of ascending ramus to rear of mental foramen (GP)	111	108	–	126
Maximum anteroposterior length of dorsal part of ascending ramus (IJ)	86l	78l; 76r	75l	–
Top of ventral curvature of horizontal ramus to line connecting ventral extremities (MN)	33	31	36	37
Minimum dorsoventral height of horizontal ramus (MO)	49	55	37	53
Maximum width of masticating surface (RR')	41	51	–	44
Rear of symphysis to front of mandibular foramen (SQ)	99	85	(61.5)	73
Length of the alveolar row (m1–3) (TU)	(55)	59	69	(76)
Maximum width between labial edges of left and right alveoli (VV')	–	64	75	67

Minimum width between angles (WW')	–	84	68	77
Minimum width between condyles (XX')	–	146	176	–
Retromolar space	14	15	18	19r
Maximum diameter of coronoid foramen	(> 5)	8.5r	–	8r
Deflection of symphysal surface from occlusal plane (degrees) (MD)	45°	43°	–	42°

Linear dimensions (in mm) of cheek teeth of gen. nov. 2 *bronni*

		Length	Anterior width (AW)	Posterior width (PW)
DP5	FIS M8385	(13.3)l	(14.7)l	(16)l
M1	FMD SRK Eck-Rat 43	(15.4)	(17)l; (17.7)r	(18)
	MWNH-TER-1	17.5l; 18.7r	21l; 21.2r	19
	FIS M8385	14l; (13.3)r	18l; (16)r	18l; 17.3r
	MNHM PW 1984/37-1	(14)l; 14.5r	16.2l; 16r	(15.6)l; 15.6r
M2	CDGG S1	19	(21.5)l; 22.5r	19
	NHMUK M19957	21.8	23.2l; 24.2r	21l; 21.5r
	FMD SRK Eck-Rat 43	20l; 23r	17.7l; (18)r	(17)l; (17.5)r
	MWNH-TER-1	20l e; 20.2r	24.5l; 23.9r	23.5l; (23)r
	FIS M8385	18	(20)	(18.7)l; 19r
	MNHM PW 1984/37-1	(18)l; 18.5r	(18)l; 18.2r	(16.5)l; 16.9r
M3	CDGG S1	22	23	20l; 19r
	NHMUK M19957	25.2l; 25r e	23.6	21.5l; 22r e
	FMD SRK Eck-Rat 43	(25)l; 23.6r	(19)l; 22r	19l; 20r
	MWNH-TER-1	25.8r	23.6r	21r
	FIS M8385	22.6l; 22.2r	(20)l; 21.3r	16.7l; 16r
	MNHM PW 1984/37-1	(24)r	20r	16.8r
m1	FIS M8385	19l; 18.5r	15.4l; 13.8r	16.2l; 14.6r
	MNHM PW 1984/37-1	(21.5)	17.7l; 16.2r	16.9l; 17.7r
	SMNS 47736	(16)l; (17.2)r	15l e; 15.3r	(16)l; 16r
m2	FIS M8385	23l; 22.3r e	20l; 16.4r	18.5l
	MNHM PW 1984/37-1	(20.8)l; 23.8r	19	(18.5)
	SMNS 47736	(18.9)l; (21.2)r	16l e; 16.9r	16l e; (18.2)r
m3	FIS M8385	32l; 31.5r e	17.7l; 16r e	16.9l; (15.4)r
	MNHM PW 1984/37-1	33.8r	21.5r	19r
	SMNS 47736	22	17	17l; 16r
	FMD SRK Eck-Rat 43	33.3l; (30)r	(17.9)l; (18.5)r	17.8l; (17)r

Dimensions (in mm) of right ribs of gen. nov. 2 *bronni* (MNHM PW 1984/37-1)

	Capitulum to distal end in straight line	Tip of *capitulum* to lateral edge of *tuberculum*	Maximum diameter at about mid-shaft	Minimum diameter at about mid-shaft
R1	177	(38.3)	45	30
R2	247	44.5	48	35
R3	320	50	50	40
R4	334	–	53	41
R5	355	(63)	54	40
R6	383	61.4	54	38
R7	401	56.5	54	36
R8	(390)	60	55	37
R9	405	58.5	55	40
R10	424	(43.8)	56	38
R11	(420)	–	55	38
R12	(395)	–	56	39
R13	(399)	(35.8)	55	37
R14	(395)	44.5	55	39
R15	(410)	–	48	34
R16	307	–	43	32

Dimensions (in mm) of selected postcranial elements of gen. nov. 2 *bronni* relevant in this study

Scapula	**CDGG S1 (r)**	**MNHM PW 1984/37-1 (l)**
Maximum scapular length, vertebral border to border of glenoid fossa (AB)	280	285
Length of scapular spine	160	135e
Maximum width of blade dorsally (CD)	107	(77)
Transversal width of infraspinous fossa at about mid-length of scapular spine	35	–
Mediolateral width of glenoid fossa (BI)	36	38
Anteroposterior length of glenoid fossa (MN)	(52)	(47)
Lateral border of glenoid fossa to inside of concave distal end of spine (BJ)	39	40
Minimum anteroposterior width of neck (EF)	59	45
Humerus	**CDGG S2(l)**	**–**
Maximum length, greater tubercle to distal end (AB)	180e	–
Length from head to distal end	170e	–
Maximum proximal width	65e	–
Maximum distal width	50e	–
Maximum diameter of mid-shaft	30e	–
Minimum diameter of mid-shaft	25e	–

Radius and Ulna	**MNHM PW 1945/233 (l)**	**–**
Total length of ulna (AB)	165	–
Total length of radius (CD)	145	–
Anteroposterior width of ulna shaft about mid-length	16.5	–
Anteroposterior width of radius shaft about mid-length	11	–
Transversal width of ulna shaft about mid-length	20	–
Transversal width of radius shaft about mid-length	18	–

Measurements (in mm if not otherwise stated) of crania of gen. nov. 2 *alleni*

	MCZ 17142	MCZ 16484	YPM 21335
Length of parietals, frontoparietal suture to rear of external occipital protuberance (P)	81	(62)	77
Width of cranium at frontoparietal suture (GG')	(42)	(38)	(47)
Maximum width of parietals	69	54	69
Minimum width of parietals	43	37	45
Height of supraoccipital (HSo)	48	–	(50)
Width of supraoccipital (WSo)	75	–	(75)
Angle between supraoccipital and parietal (degrees)	135°e	130°e	130°e

Measurements (in mm if not otherwise stated) of crania of gen. nov. 3 *cristolii*

	LI 1926/394	LI 1939/257
Zygomatic width (CC')	179	–
Width across occipital condyles (ff')	–	127
Length of zygomatic process of squamosal (OP)	129	(94)
Dorsoventral height of zygomatic process of squamosal (WX)	37	31
Anteroposterior length of root of zygomatic process of squamosal (QR)	(36)	49
Length of frontals in midline (LFr)	76	–
Length of frontals, level of tips of supraorbital processes to frontoparietal suture (F)	130	–
Width across supraorbital processes (FF')	(136)	–
Width of cranium at frontoparietal suture (GG')	62	–
Minimum width of parietals	57	–
Width of *foramen magnum* (gg')	–	50
Length of parietals, frontoparietal suture to rear of external occipital protuberance (P)	89	–
Maximum width of parietals	80	–
Anteroposterior length of zygomatic-orbital bridge of maxilla (no)	–	(47)
Dorsoventral thickness of zygomatic-orbital bridge (T)	–	(17.5)
Maximum width between labial edges of left and right alveoli (rr')	(87)	–
Maximum width between pterygoid processes (yy')	(68)	–
Height of supraoccipital (HSo)	61	–
Width of supraoccipital (WSo)	83	–
Angle between supraoccipital and parietal (degrees)	120°	–

Measurements (in mm if not otherwise stated) of mandibles of gen. nov. 3 *cristolii*

	LI 2012/1	LI 1939/257
Total length (AB)	(307)	305
Anterior tip to front of ascending ramus (AG)	(170)	176
Anterior tip to rear of mental foramen (AP)	–	60
Anterior tip to front of mandibular foramen (AQ)	(174)	164
Length of symphysis (AS)	(82)	90
Posterior extremity to front of ascending ramus (BG)	(150)	(136)
Posterior extremity to front of mandibular foramen (BQ)	(160)	154
Distance between anterior and posterior ventral extremities (DF)	176	176
Height at mandibular notch (DK)	–	206
Height at condyle (DL)	(256)	220
Height at deflection point of horizontal ramus (EF)	(110.5)	120
Deflection point to rear of alveolar row (EU)	122	132
Minimum anteroposterior length of ascending ramus (GH)	126	116
Front of ascending ramus to rear of mental foramen (GP)	(100)	110
Top of ventral curvature of horizontal ramus to line connecting ventral extremities (MN)	48	46
Minimum dorsoventral height of horizontal ramus (MO)	73	74.5l; 74r
Maximum width of masticating surface (RR')	(58.5)	59.5
Rear of symphysis to front of mandibular foramen (SQ)	127	133
Length of the alveolar row (m1–3) (TU)	76	80
Maximum width between labial edges of left and right alveoli (VV')	81	82
Minimum width between angles (WW')	–	190
Minimum width between condyles (XX')	–	220.5e
Retromolar space	17	22
Maximum diameter of coronoid foramen	7.5	9.5l; 7.7r
Deflection of symphysal surface from occlusal plane (degrees) (MD)	60°	60°

Linear dimensions (in mm) of cheek teeth of gen. nov. 3 *cristolii*

Tooth	Specimen	Length	Anterior width (AW)	Posterior width (PW)
M1	LI 1926/394	(15)r	(16)	17.8
M2	LI 1926/394	20r	20.4	17.6
M3	LI 1926/394	23.5l; 24r	19.8	14.5
dp5	LI 1939/257	(17.4)l	15l	15.6l
m1	LI 2012/1	(21)l; 21.5r e	18.4l; 18r e	(17)l; 17r e
	LI 1939/257	21l; 21.5r	16l; 16.5r	15.5
m2	LI 2012/1	24l; 23.8r	19l e; 18.7r	17.5l; 17r
	LI 1939/257	25l; 24.5r	19l; 19.5r	19
m3	LI 2012/1	24.5r	18	17
	LI 1939/257	26l; 25.5r	20l; 20.5r	19l; 19.5r

Dimensions (in mm) of the scapula of gen. nov. 3 *cristolii*

	LI 1854/327 (l)	LI 2013/1 (l)
Maximum scapular length, vertebral border to border of glenoid fossa (AB)	(20)	(290)
Length of scapular spine	95	145
Maximum width of blade dorsally (CD)	(96)	124
Transversal width of infraspinous fossa at about mid-length of scapular spine	21	23
Mediolateral width of glenoid fossa (BI)	25	–
Anteroposterior length of glenoid fossa (MN)	48	–
Lateral border of glenoid fossa to inside of concave distal end of spine (BJ)	50	(46)
Minimum anteroposterior width of neck (EF)	35	45

Measurements (in mm if not otherwise stated) of cranium of gen. nov. 4 *bellunense* (MGPD-18–23Z, 7385/6Z)

Length of premaxillary symphysis (AH)	(94)
Length of premaxilla	(178)
Height of jugal below orbit (ab)	40
Length of mesorostral fossa (HI)	80e
Anteroposterior length of zygomatic-orbital bridge of maxilla (no)	34
Dorsoventral thickness of zygomatic-orbital bridge of maxilla (T)	16
Length of zygomatic process of squamosal (OP)	101l; 99r
Dorsoventral height of zygomatic process of squamosal (WX)	43l+r
Anteroposterior length of root of zygomatic process of squamosal (QR)	(53)
Length of parietals, frontoparietal suture to rear of external occipital protuberance (P)	(77)
Width of cranium at frontoparietal suture (GG')	(65)
Minimum width of parietals	63
Maximum width of parietals	79
Maximum height of rostrum (KL)	(54)
Height of supraoccipital (HSo)	(61)
Width of supraoccipital (WSo)	(83)
Deflection of masticating surface of rostrum from occlusal plane (degrees) (RD)	60°e
Angle between supraoccipital and parietal (degrees)	115°

Linear dimensions (in mm) of cheek teeth of gen. nov. 4 *bellunense* (MGPD-20/21Z)

	Length	Anterior width (AW)	Posterior width (PW)
DP5	(21)	21e	18.5e
M1	21.9	22	19.5
M2	22.5	22.7	20

Appendix 4. Data matrix of all outgroup (Proboscidea: *Phosphatherium*, *Numidotherium*) and in-group (Sirenia) taxa considered in the cladistic analyses of the present study. Subsequent table indicates the percentage of question marks for each species scored. # = multistate character [01].

Outgroup-complex (lumped scoring consisting of *Phosphatherium* and *Numidotherium*)

0000000000 0000000000 0000000000 0000000000 0000000000 ##000#0000 0000000???
??00000000 0000000000 0000000000 0000000000 0000000??? 0000000000 0000000000
00000000## #000000000 000000#000 0000000000 0000000000 0000???00? ??

Phosphatherium escuilliei

0000000000 ?0?0?00000 0000000000 0000000000 0000000000 0000000000 0000000???
??00000000 000000000? ?000000000 0000000000 0000000??? ??????0000 0000000000
0000000000 000000???? ???0?00000 0000000000 00???????? ?????????? ??

Numidotherium koholense

0000000000 0000000000 0000000000 0????000?0 000?000000 1100010??0 0?0???????
??00?00000 0000000000 000000000? 000????000 0??0?????? 000000?000 ?00???0000
0000000011 1000000000 0000001000 0000000000 0000000000 0000???00? ??

Prorastomus sirenoides

1100110101 1000000001 0000000000 0000000000 0000001010 00001?100? 0?00000???
??00010010 00??0000?0 0001001011 0001000001 0?010??00? 0000000?0 0000?00000
0000000?0 000100000? 0000?00000 10000????0 00???????? ?????????? ??

Pezosiren portelli

1100?10111 ?0?1??0001 0000?????? ??????0000 0000001010 000000100? 000?000000
10???????? ????0?0000 ??0100??00 0001110101 01?1000?1 0000000?0 000??10000
0011000000 00?000???0 0000000000 10???????0 0000000?1? ?100011000 01

Protosiren fraasi

1100000011 1011?00001 1000000011 0000000010 0010001010 0001001000 1101000010
10???100?0 0001000000 0010000010 0001000101 0110011001 0100000101 0011011110
0111000??? ????000000 0000000000 1110000000 00000000?? ??????1000 0?

Protosiren smithae

1100000011 1011000001 1000000110 0000000011 0010001010 0001011010 1101000?1?
1000?10010 0001000000 0000000110 0001000101 011001?0?1 ?10000011? 00110?111?
0011001101 1000101?1? 0000?00000 1110011??0 0010000011 010000?000 ??

Ashokia antiqua

110??????? ??0???0001 0001000000 00????0000 0010001010 00?100100? 1100000???
??01110010 0001000010 100001?011 0001110101 ?1100000?? 0010000110 000???????
?????????? ?????????? ??????0000 ?????????0 00???????? ?????????? ??

Sirenavus hungaricus

110??????? ????????01 1?01?????? ?000000000 0000001010 000001000? 111?000???
?????1???0 00010?0010 1010001011 1001110000 ?????????? ????????1?? ?11???????
???????0?0 00101????? ?????????? ?????????0 00???????? ??????0??? ??

Eotheroides aegyptiacum

110??????? ?0????0001 1001000110 0000000000 0010001010 000#011000 1100000000
010001?010 00?10011?0 1001101011 1000110001 1000100000 0010000011 0100011000
0?11000000 00??10???? ???0?00000 1110000000 000000001? ?00?01100? ??

Eotheroides lambondrano

1100011011 1001000001 1001000011 000???00?0 00?0001010 0001011??? 1110?????0
0001110010 0001001110 1?01101??? 100??????? ?0000?0??0 ?????????? ??????????
?????????? ??????000? 0000?00000 0111111000 00???????? ???????1??? ??

Prototherium veronense

1101111011 1001000001 0001110110 0001100000 0010001010 0000011000 1110110???
??0?110010 0001001110 1000001011 1000110001 100001010? 000000011? 001101???0
0?11000000 0010100000 1100000000 0111100000 001001000? 1???01101? ??

Prototherium intermedium

1101111011 1001?00001 0001110110 00????0010 0010001010 0000110000 111?110???
??01110010 00?1001010 1000001011 1000110001 001001100? 0000000010 0011011000
0111001011 1010100000? ???0?00000 0111100000 0010?10??? ????0110?? ??

Eosiren stromeri

1101111011 1001000001 1000?????? ?001100010 0010001010 0001101000 1100110???
?????????? ????0?1110 11?0001011 100????001 0110100000? 0010000011 ?110??????
?????????? ??????000? 0000?0???? 0??0011000 00???????? ??????0??? ??

Eosiren libyca

1101111011 1001000001 1001110011 0001100010 0010001010 00#1101000 1100110000
0100110010 0001001110 1101101011 1000110001 0110010000 001000??11 0110111000
0011001021 1010100000? 0000000000 0111111110 0011010010 0???01100? ??

Eosiren imenti

1011111011 1001000001 1001110110 0001100011 0100001010 0001111010 111011000?
0100?10010 0001001110 1101101111 100??????? ?100010000 ?????????? ??1??1????
?????????? ??????000? 0001?00000 011??????0 00???????? ??????0??? ??

Gen. nov. 1 *taulannense*

1101100011 1101000001 1001000011 0001100000 0100001010 0000110000 1110000111
0101010010 0001001010 1101101011 1000110001 1100000100 0010000011 0110111000
0111001011 1010101100 0001000000 0111100000 0011010011 101001?01? ??

Gen. nov. 2 spec. nov. 1 (lumped scoring consisting of the specimens listed below)

1101111011 1101000001 1001000110 0001100010 0110001010 0000110010 1100000001
0101010011 1001001110 1101101011 1000110001 0110011000 0010000111 0110111000
0111001011 1010101100 0001011000 0111111110 0011010011 0???110010 11

BSPG 1956 I 540

1101111011 1101000001 1001000110 0001100010 0110001010 0000110010 1100000001
0101010011 1001001110 1101101011 1000110001 0110011000 0010000111 0110111000
0111001?11 1010101102 0001?11000 01111????0 00???????? ????11001? ??

LS RLP PW 2005/5042-LS

1101111011 11?1?00001 1001000110 00????0010 0110001010 0000110010 1100000001
0101010011 1001001172 ?????????? ?????????? ?110011000 0010000111 0?????1000
0111001011 10?0101100 0001011000 011??????0 00???????? ?????????0 11

NHMUK PV M9415

110??11011 1101000001 1001?????? 0001100010 0110001010 0000110010 1100000???
?????10011 1001001110 1101101011 1000110001 011001100? 0??0000111 ?110111000
0111001?11 1010101102 0001?1??00 0111111110 0011010011 0???11001? ??

FIS M2597

110??11011 1101000001 1001000110 0001100010 0110001010 0000110010 1100000??1
0101010011 1001001110 1101101??? 100??????? ?1100?1000 ?????????? ?11011????
?????????? ??????110? 0001?11000 0111111110 00???????? ?????????? ??

FIS M8002

110??11011 1101?00001 1001000110 00????0010 0110001010 0000110010 1100000000?
0101010001? ???10011?? ?????????? ?????????? ?110011000 ?????????? ??????????
?????????? ??????110? 0001?11000 011??????0 00???????? ????110??? ??

Gen. nov. 2 *bronni* (lumped scoring consisting of the specimens listed below)

1101111011 1101000001 1001000011 0001100010 0110001010 0000110010 1111000001
0100010011 1001001110 1101101011 1000110001 0110101000 0010000111 0110111000
0111001011 1010101100 0001011100 0111111??0 0011010??? ????110010 11

CDGG S1

1101111011 1101000001 1001000011 0001100010 0110001010 0000110010 1111000???
??00010011 1001001110 1101101011 1000110001 011010100? 0010000111 0110111000
0111001011 1010101100 0001011100 011??????0 0011010??? ??????0010 11

MWNH-TER-1

1101?11011 1101000001 1001000011 000???0010 01?0001010 00001?0010 ??1???????
??00?10011 10010???10 1101101011 1000110??? ?????????? 001000?1?? 0????1????
?????????? ??????110? 0001?11100 0111111??0 00???????? ?????????? ??

FMD SRK Eck-Rat 43

1????11011 11?100???? 1001?????? ?0???????? ?????????? ???01?0??? 11?????001
01???????? ??????11?? ????????11 ????1??001 0110101000 001000011? 0110111000
0111001?11 101010110? 0001?11100 01111????0 00???????? ?????????? ??

SMNS 1539

110??????? ????????01 ?????????? ??????0010 0110001010 0000110010 1111000001
01???????? ????0?11?? ????????11 ?????????? ?110101000 0????????? ??????????
?????????? ?????????? ?????????? ?????????? ?????????? ?????????? ??

SMNS 47736

110??????? ?1??????01 ?????????? ??????00?? 01?0001010 0000110010 1111000000?
01???10??1 1001001110 11011????? 100??????? ?110101000 ????????1?? ?110111000
0111001011 101010???? ????1?11100 01???????0 00???????? ????110??? ??

FIS M8385

1101111011 1101000001 1001000011 000??00010 0110001010 0000110010 1111000001
01???10??? ??01001110 1101101011 100????001 ?110101010 ??????01?? ?110111???
0111001011 101010110? 0001?11?00 011??????0 00???????? ?????????? ??

Gen. nov. 2 *alleni*

?????????? ?????????? ?????????? ?????????? ?????????0 0000110??? 111????001
01???????? ??????11?? ?????????? ?????????? ?110011000 ?????????? ??????????
?????????? ?????????? ?????????? ?????????? ?????????? ?????????? ??

Gen. nov. 3 *cristolii* (lumped scoring of the species *cristolii*, *pergense*, and *abeli*)

101??????? ?1??????01 1?01?????? 0???????11 1000001110 0000010000 1101000000
01???????? ??0?0?1010 1101001011 1?00110001 0000011000 0????????? ?110111107
0110011011 101010???? ????1?11000 0111111000 0011010017 ??????0??0 01

LI 1899/11 (*pergense*)

?????????? ?????????? ?????????? ?????????? ?????????0 0000010??? 11?????000
01???????? ??????10?? ?????????? ?????????? ?000001?0 ?????????? ??????????
?????????? ?????????? ?????????? ?????????? ?????????? ?????????? ??

LI 1939/257 (*abeli*)

?????????? ?1???????? 1001?????? ?????????? ?????????? ?????????? ??????????
?????????? ????????10 1101001011 1000???001 0????????? ?01???00?? 0????11100
0110011011 101010???? ????1?11000 011??????0 00???????? ?????????? ??

Crenatosiren olseni

1011100011 1101?00001 1001110??? 000???1011 1000#01111 0111010000 1101000000
0101111011 1000011110 1101101011 010?110001 000001#000 0010000#11 1110?111?1
?110011010 0010111100 0001011111 01000?1000 0011110011 0010101??0 ??

Nanosiren garciae

1011100011 110100??0? 1101?????? ?00???0111 10????????1 0111110110 1111000110
000??11?11 1000011110 1101101011 0100???001 0101011000 1010001011 0111?11101
??1001?01? ??1?1?000? ????1?11111 010????000 00??0??011 1110?01??1 ??

Nanosiren sanchezi

1011100011 1101000000? 1101?????? ?00???0111 10????????1 0111110110 1100000111
000??11?11 1001011110 1101101011 010011000? ?101010000 1010001?11 0??????????
?????????? ??????0000 0001011111 0101100000 00???????? ???????1??? ??

Dugong dugon

1011111011 0101100001 1101101000 010110##11 1011011001 01#1010110 1101101000
0001111111 0100011110 1101101011 0100110001 0101001100 1010001111 #110111101
1110011011 1010111011 0001111111 0101010100 0011111011 1010101111 00

Bharatisiren indica

1011100011 1001?01101 1001101011 0001010111 1001111??0 0000010??0 1111000???
??00111011 01010?1000 0101101011 100?110001 0?0101???? 001000?11? 111111????
??1001??01 1010111017 0001?11111 0100011000 00???????? ?????????? ??

Bharatisiren kachchhensis

1011111010 0001?01101 10011??000 1001010111 1000111?10 1101110000 1111000???
??01111011 0100011010 1????0?011 ??00110001 ?1??01?00? 001000?110 11101?????
?????????? ??????101? 0001?11111 01000????0 00???????? ?????????? ??

Corystosiren varguezi

1011?1??11 ?0?1?0????1 ?????????? ?????00111 1011?01010 1111010110 111100000?
0101111?11 010?000010 ?1???01111 100????0?1 010101???? 010000??11 ??????????
?????????? ??????101? 1011111111 0100011000 00???????? ?????????? ??

Dioplotherium manigaulti

1011111011 0111?01011 1001101000 1001010111 1001101100 1111010110 111000000?
0001111011 0110011?? ?????????? ?????????1 0001011010 0010000110 1111?1????
?????????? ??????1010 1101111111 010???????0 00???????? ?????????? ??

Dioplotherium allisoni

1011111010 1101?01011 1001101000 1101100111 1000101110 11?101001? 111100000?
0001111011 0111110010 11011010?? 100?110001 0001011000 0010000110 1111?11100
0110011011 1010111011 1101111111 0100000000 00???????? ?????????? ??

Domningia sodhae

1011111011 1001101101 100?1??000 0?0101??1? 10?1101110 1101010??? 1111000???
??0111??11 0101111100 0??1?01011 100?110001 010101001? 0010001111 01101?11?1
0110011O?0 00???1101? 1011?11111 01000????0 00???????? ?????????? ??

Kutchisiren cylindrica

1011100011 0101001101 1001110110 0001011011 1001101000 1100010??0 1110000???
??0?111011 01?00110?0 ????????11 1000110000? ?00101000?? 0????????? ?111111100
011001???? ?????11011 1101?11111 010??????0 00???????? ?????????? ??

Rytiodus capgrandi

10111????? 11???01011 1?0??????? ????????11 10?1101010 11?0110??? 111????00?
?????1?0?1 010?01??10 1101?01011 100????001 ?????????? ?01000?1?? ???0?1????
?????????? ??????1011 1011111111 010??????0 00???????? ??????0??? ??

Xenosiren yucateca

101??????? ??????1011 1110?????? ?10???0111 1001101110 111???0110 ??1???????
??01?11011 101101??00 01000??0?? 100??????? ?????????? ?????????? ??????????
?????????? ??????1011 1???1?1111 0100011??0 00???????? ?????????? ??

Gen. nov. 4 *bellunense*

1??1111011 11???01011 1101?????? ?????????? ?????????0 00010?0??? 11????????
?????1???1 01?1000010 11??????1?? 100??????? ?00001000? ?????????? ??????????
?????????? ??????1100 1101?11111 010????000 00???????? ????0?0??? ??

Caribosiren turneri

1011100011 0101000001 1001110011 0001000011 0111001010 0001100000 1100110000
010111?01? ??0?0?1110 1101101011 1000110001 ??0?0100?0 ?????????? ?11011????
?????????? ??????000? 0001?11111 0100000??0 00???????? ?????????? ??

Metaxytherium krahuletzi

1011?00011 1101000001 1001?????? ?0????0011 01?1001000 0001010010 110?000000
01???10??1 1001001110 1101101011 1001110001 0#00010000 #010000001? 1110?111?#
0110011011 1010110000? 0001?11111 0101111110 0011111011 1110100010 00

Metaxytherium floridanum

1011100011 1101000001 1101110??? 0001100011 0111001000 0001010110 1100101000
0101110011 0101001110 1101101011 1001110001 0100011000 1010000#11 #11011110#
0110011011 1010110000 0001011111 0101111110 00??11?011 1???11011# 00

Metaxytherium arctodites

1011111011 ?101100001 1000110??? 0001010011 1001001000 0001010110 111100011?
0000110111 1001001110 110110?#11 100?110001 00?00100?? 1010000111 1110111101
0110011011 1010110000 0001011111 0101100110 00???????? ?????????0 ??

Metaxytherium crataegense

1011111011 1101?00001 0001101110 00????0011 0101001010 0001010110 1101110000
0101110011 0101001110 1101101111 1001110001 0100011010 1010000011 1110?11101
0110011?11 101011000? 0001?11111 0101100??0 0010111011 1110100011 00

Metaxytherium medium

1011111011 0101000001 0001110011 00????0011 0111001000 0001110010 1111110000
0100110011 0100001110 1101101011 1001110001 0110011000 1010000111 0110111101
0?10011011 10?011110? 0001?11111 0101100110 0010111011 1110?00111 ?0

Metaxytherium serresii

1011111011 0101000001 1001110??? 0011100011 0110001010 0001110010 1101000000
0101110011 0100001110 1101101011 1000110001 0101011000 1100000111 1110?11111
0110011011 1010111100 0001011111 0101100110 0010111011 111011011# 00

Dusisiren reinharti

1011?11011 10?1?0??01 1001?????? ????????11 0111001000 0001111000 1101000000
00???????? ????0?11?? ?????????? ?????????? ?101011010 1100000?11 ?????1110?
0110101011 10???00000 1001011111 010??????0 00???????? ?110??00?? 00

Dusisiren dewana

101??11011 1001?00001 0000110110 00????0111 0111011000 0001111000 11?1??????
??101??1?1 010?001110 1101101010 0010110001 010101100? 110101?111 11101?1101
0110101?11 10?0100000 1001011111 0101100110 0011111110 1110110??0 01

Dusisiren jordani

1011111011 1001000001 0000110110 0001101011 0111011000 0001010000 1101110000
0010110111 0101001110 1101101011 0010110001 0101011000 #101100#11 0110111101
0110101011 1010100000 1001011111 0101100110 0011111110 1110110110 00

Dusisiren takasatensis

1011111011 1001000001 0000110??? 0011001011 ???1001010 00011?1??0 11??000???
??1011?111 0101001?10 1001101?10 001?110001 01??0?100? 1??101?111 111011????
?????????? ??????0000 1001011111 010??????0 0010001 1?? ?110??0??? ??

Hydrodamalis cuestae

1011111011 1010010001 0100110110 0001101011 1011001000 0001011110 1111000000
0011110111 0101001110 1100011010 0010110001 0101011010 110110??11 ?110?1????
0010101011 1010100000 1001011111 0101010100 1011?01110 1111001??1 11

Hydrodamalis gigas

1011111011 1010110001 0101101110 001110##11 10#1000000 000#001110 1101110010
1011110111 0101001110 1000#11110 0011110001 0101101001 1#0101011# 1110111111
1010101010 0000100000 1001011111 0101010100 1011001010 0111101111 11

Anomotherium langewieschei

110??????? ?0??????01 ?????????? ??????0000 00?0001000 1101111001 0101000???
?????????? ??????11?? ??0??11?11 ???0101001 010001000? 0010000111 001??11111
0111001?1? ??1010???? ????1?11110 0111100000 00??????1? ??????0??? ??

Miosiren kocki

1100000011 1010100001 1101000011 0100000000 0001001000 0001111001 0100000000
0000010011 0101001110 1001011111 0000101011 01000?1??0 0010000110 011011????
?????????? ??????1010 0001011100 01110??000 00???????? ?????00110 00

Potamosiren magdalenensis

?????????? ?0???????? ?????????? ?????????? ?????????? ?????????? ??????????
?????????? ?????????? ?????????? ?????????? ?????????? ?????????? ??????1??0
0010100??1 ??1010???? ????1?11111 010??????0 00???????? ?????????? ??

Ribodon limbatus

?????????? ?0???????? ?????????? ?????????? ?????????? ?????????? ??????????
?????????? ?????????? ?????????? ?????????? ?????????? ?????????? ??????1??0
0?10100??1 ???110???? ????1?11111 0101010101 00???????? ?????????? ??

Trichechus inunguis

1010000011 1010100001 1001110011 011110##11 0110001010 0001010010 1111110110
0010110010 0001101001 0001111011 0000101101 0111011000 0101101110 1110111110
1010101111 0111100000 1001011111 0101010101 0101111111 1110001111 00

Trichechus manatus

1010000011 1010100001 1001110011 011110##11 0110001010 0001010010 11#1110110
0010110010 0001101001 0001111011 0000101101 0111011000 0#00001110 1110111110
101##01011 0111100000 1001011111 0101010101 0101111110 1110001111 00

Trichechus senegalensis

1010000011 1010100001 1101110011 011110##11 0110001010 0001010000 1111110110
0010110010 0001101001 0001111011 0000101101 0111011000 0#00001110 1110111110
1010101011 0111100000 1001011111 0101010101 0101111110 1110001111 00

Sirenia *incertae sedis*

Eotheroides babiae

?????????? ?0????????? ?????????? ?????????? ?????????? ?????????? ??????????
?????????? ?????????? ?????????? ?????????? ?????????? ?????????? ??????1000
0011000??? ??1000???? ?????00000 111??????0 00???????? ?????????? ??

"Halitherium antillense"

?????????? ?????????? ?????????? ?????????? ?????????? ?????????? ??????????
?????????? ?????????? ?????????? ?????????? ?????????? ?????????? ??????????
??1???1??1 101010???? ????????00 011??????0 00???????? ?????????? ??

Metaxytherium subapenninum

1011111011 1111000001 0001101110 00?1000011 1011001000 0001010110 110111000?
0?00110111 0100001110 1101101011 1000110001 0001011000 0100000110 111001111#
0110011011 10?0111010 0001011111 0101111??0 001011101? ???0??0??1 00

Phosphatherium escuilliei	23.27
Numidotherium koholense	21.78
Prorastomus sirenoides	21.78
Pezosiren portelli	27.23
Protosiren fraasi	10.40
Protosiren smithae	7.43
Ashokia antiqua	44.06
Sirenavus hungaricus	57.43
Eotheroides aegyptiacum	15.84
Eotheroides lambondrano	42.08
Prototherium veronense	9.41
Prototherium intermedium	14.85
Eosiren stromeri	40.10
Eosiren libyca	4.95
Eosiren imenti	35.15
Gen. nov. 1 *taulannense*	1.98
Gen. nov. 2 spec. nov. 1	1.49
BSPG 1956 I 540-552	10.89
LS RLP PW 2005/5042-LS	28.71
NHMUK PV M9415	15.35
FIS M2597	33.66
FIS M8002	47.52
Gen. nov. 2 *bronni*	3.96
CDGG S1	9.90
MWNH-TER-1	41.58
FMD SRK Eck-Rat 43	51.49
SMNS 1539	72.28
SMNS 47736	46.53
FIS M8385	28.22
Gen. nov. 2 *alleni*	86.63
Gen. nov. 3 *cristolii*	34.16
LI 1899/11 (*pergense*)	87.62
LI 1939/257 (*abeli*)	68.81
Crenatosiren olseni	7.92
Nanosiren garciae	26.24
Nanosiren sanchezi	33.66

Dugong dugon	0.00
Bharatisiren indica	24.26
Bharatisiren kachchhensis	34.16
Corystosiren varguezi	44.55
Dioplotherium manigaulti	34.65
Dioplotherium allisoni	13.86
Domningia sodhae	27.23
Kutchisiren cylindrica	33.66
Rytiodus capgrandi	55.45
Xenosiren yucateca	60.89
Gen. nov. 4 *bellunense*	62.38
Caribosiren turneri	32.18
Metaxytherium krahuletzi	11.88
Metaxytherium floridanum	4.46
Metaxytherium arctodites	14.36
Metaxytherium crataegense	5.45
Metaxytherium medium	4.95
Metaxytherium serresii	1.98
Dusisiren reinharti	41.58
Dusisiren dewana	13.37
Dusisiren jordani	0.00
Dusisiren takasatensis	31.19
Hydrodamalis cuestae	5.45
Hydrodamalis gigas	0.00
Anomotherium langewieschei	46.04
Miosiren kocki	18.81
Potamosiren magdalenensis	86.63
Ribodon limbatus	84.65
Trichechus inunguis	0.00
Trichechus manatus	0.00
Trichechus senegalensis	0.00
Sirenia *incertae sedis*	
Eotheroides babiae	86.63
“Halitherium antillense”	91.58
Metaxytherium subapenninum	6.93

Appendix 5. Distribution of characters and corresponding character states for the phylogenetic hypothesis of Sirenia based on analysis C employing cranial and dental characters (Fig. 71).
* synapomorphy; ** autapomorphy

Node1: 1[1]*, 20[1]*, 76[1]*, 79[1]*, 110[1]*. **Node 2:** 9[1]*, 14[1]*, 108[1], 136[1]*, 143[1]*, 144[1]*. **Node 3:** 43[1], 54[1]*, 61[1]*, 62[1]*, 128[1], 137[1]*, 172[1]*. **Node 4:** 13[1], 39[1], 64[1], 69[1], 116[1], 122[1], 134[1], 138[1], 139[1]. **Node 5:** 24[1], 89[1]*, 91[1]*, 100[1], 123[1]*. **Node 6:** 56[1], 101[1], 108[0], 132[1]*. **Node 7:** 87[1]*, 88[1], 94[1], 104[0]. **Node 8:** 30[1], 116[1], 135[1]*, 147[1], 149[1]*, 171[0], 174[1]*. **Node 9:** 49[0], 60[1]*, 61[0], 96[1], 106[0], 107[1], 164[1], 166[1], 167[1], 168[1]. **Node 10:** 7[1], 63[1], 74[1], 176[1], 177[1]. **Node 11:** 4[1]*, 5[1], 72[1]. **Node 12:** 12[1], 42[1], 54[0], 57[0], 70[1], 157[1], 158[1], 164[1]. **Node 13:** 113[1], 117[1]. **Node 14:** –. **Node 15:** 25[1]*, 26[1], 65[1], 66[1]. **Node 16:** 56[0], 63[0], 113[1]. **Node 17:** 28[1], 30[0]. **Node 18:** 21[0], 54[0], 92[0], 94[0], 95[0], 112[0], 123[0], 132[0], 134[1], 135[0], 176[0], 177[0]. **Node 19:** 2[0], 3[1]*, 40[1], 43[0], 164[1]. **Node 20:** 12[1], 55[0], 57[0], 63[0], 64[1], 65[0], 66[0], 117[1], 166[1], 167[1]. **Node 21:** 131[1]*, 140[1], 168[1], 169[1], 170[1]*, 173[0]. **Node 22:** 50[1]*, 52[1], 53[1]*, 77[1]*, 84[0], 86[1]*, 101[0], 102[1]*. **Node 23:** 38[1], 58[1], 72[0], 114[1], 127[1]. **Node 24:** 55[1], 68[1], 69[1], 131[0]. **Node 25:** 6[1], 7[1], 82[1], 128[1], 159[1], 160[1]*, 165[1]*. **Node 26:** 17[1], 45[1]*, 50[0], 51[1], 63[1], 88[0], 101[1], 102[0], 161[1], 174[0]. **Node 27:** 12[0], 18[1]*, 36[1], 53[0]. **Node 28:** 89[0], 91[0]. **Node 29:** 6[0], 7[0], 29[1], 54[0], 134[1]. **Node 30:** 48[1], 83[1]*, 112[0], 127[0], 130[0], 134[1], 162[1]. **Node 31:** 32[1], 84[1], 87[0]. **Node 32:** 22[1]. **Node 33:** 42[1], 49[0], 104[1], 178[1], 179[1]. **Node 34:** 58[1], 82[1]. **Node 35:** 6[1], 7[1], 176[0], 177[0]. **Node 36:** 128[1]. **Node 37:** 43[1], 55[1]. **Node 38:** 28[0], 30[1], 56[0], 66[1]. **Node 39:** 33[1]*, 114[1], 122[1], 123[0]. **Node 40:** 12[0], 57[1], 72[0], 145[1]*, 146[0], 156[0], 161[1]. **Node 41:** 21[0], 24[0], 124[1]*. **Node 42:** 55[0], 65[1], 66[1]. **Node 43:** 13[1], 14[0], 59[1], 96[1], 139[1], 142[0], 175[0], 176[1], 179[0]. **Node 44:** 16[1]*, 22[1], 41[1], 42[0], 58[1], 74[1], 94[0], 100[0], 181[1]*. **Node 45:** 140[0]. **Node 46:** 154[1], 180[1]*. **Node 47:** 141[1], 182[1]*. **Node 48:** 124[0].

Prorastomus sirenoides*:** 5[1], 55[1], 100[1], 148[1], 154[1]. ***Pezosiren portelli*:** –. ***Protosiren fraasi: 30[1], 93[1]. ***Protosiren smithae*:** 28[1], 40[1], 56[1], 59[1], 98[1], 147[1], 157[1], 159[1], 176[1], 177[1]. ***Ashokia antiqua*:** 74[1], 75[1], 96[1]. ***Sirenavus hungaricus*:** 43[0], 54[0], 57[0], 63[1], 93[1]. ***Eotheroides aegyptiacum*:** 28[1], 72[1], 111[1], 112[0], 115[1]. ***Anomotherium langewieschei*:** 51[1], 52[1], 64[1], 132[0], 169[1]. ***Miosiren kocki*:** 44[1], 109[1]**, 117[1], 130[0]. ***Eotheroides lambondrano*:** 112[0]. **Gen. nov. 1 *taulannense*:** 6[0], 7[0], 43[0], 68[1], 69[1], 88[0], 111[1], 116[0], 118[1], 176[0], 177[0]. **Gen. nov. 2 *alleni*:** –. **Gen. nov. 2 *bronni*:** 64[1], 74[0], 115[1], 116[0], 168[1]. **Gen. nov. 2 spec. nov. 1:** 28[1], 30[0], 63[0]. ***Eosiren stromeri*:** 24[0], 67[1], 94[0], 95[0], 115[1], 116[0], 174[0], 175[0]. ***Eosiren libyca*:** 178[1], 179[1]. ***Prototherium veronense*:** 39[0], 55[0], 111[1], 118[1], 128[1], 147[0], 149[0], 150[0], 151[0]. ***Prototherium intermedium*:** 57[0], 88[0], 113[1], 117[1]. ***Eosiren imenti*:** 42[1], 74[0], 98[1]. **Gen. nov. 3 *cristolii*:** 48[1], 54[0], 88[0], 95[0], 112[0]. ***Crenatosiren olseni*:** 37[1], 48[1], 112[0], 150[0], 151[0], 158[1], 174[0]. ***Nanosiren garciae*:** 63[1]. ***Nanosiren sanchezi*:** 64[0], 70[1], 84[1], 117[0]. ***Dugong dugon*:** 11[0], 32[1], 43[1], 46[1], 49[0], 65[1], 67[1], 78[1], 116[0], 118[1], 141[1], 178[1]. ***Rytiodus capgrandi*:** 54[0], 55[1], 163[1]. ***Corystosiren varguezi*:** 12[0], 43[1], 72[1], 86[0], 87[0], 98[1], 122[1], 123[0], 163[1]. ***Bharatisiren kachchhensis*:** 10[0], 11[0], 44[0], 46[1], 55[1], 130[0], 161[0]. ***Domningia sodhae*:** 48[1], 85[1], 88[1], 131[0], 150[0], 151[0], 163[1]. ***Bharatisiren indica*:** 30[1], 46[1], 51[0], 52[0], 161[0]. ***Kutchisiren cylindrica*:** 11[0], 12[1], 26[1], 27[0], 28[1], 37[1], 38[0], 64[0], 162[1]. ***Dioplotherium manigaulti*:** 13[1], 36[1], 49[0], 64[0], 88[1], 119[1], 160[0]. ***Dioplotherium allisoni*:** 10[0], 44[0], 58[0], 85[1], 176[0], 177[0]. **Gen. nov. 4 *bellunense*:** 51[0], 52[0], 53[0], 86[0], 98[1], 160[0]. ***Xenosiren yucateca*:** 23[1]**, 24[0], 81[1], 82[0],

89[0], 91[0]. ***Metaxytherium krahuletzi*:** 117[0]. ***Metaxytherium floridanum*:** 22[1], 43[1], 64[0], 67[1]. ***Metaxytherium crataegense*:** 21[0], 26[0], 27[1], 49[1], 66[1], 98[1], 119[1]. ***Metaxytherium arctodites*:** 15[1], 36[1], 41[1], 42[0], 63[1], 68[1], 69[1], 72[0], 78[1], 81[1], 82[0], 117[0]. ***Metaxytherium medium*:** 21[0], 63[1], 113[1], 157[1], 158[1]. ***Caribosiren turneri*:** 6[0], 7[0], 49[1], 64[0], 117[0], 174[0], 175[0]. ***Metaxytherium serresii*:** 44[0], 49[1], 139[1], 157[1], 158[1]. ***Dusisiren reinharti*:** 119[1]. ***Dusisiren dewana*:** 38[1], 46[1]. ***Dusisiren takasatensis*:** 49[1], 92[0], 100[0]. ***Dusisiren jordani*:** 33[0], 46[1], 131[0]. ***Hydrodamalis cuestae*:** 33[0], 65[0], 66[0], 119[1]. ***Hydrodamalis gigas*:** 26[0], 27[1], 47[0], 56[0], 71[1], 98[1], 104[1], 115[1], 116[0], 120[1], 126[1], 141[1], 150[0], 153[0]. ***Potamosiren magdalenensis*:** –. ***Ribodon limbatus*:** –. ***Trichechus inunguis*:** 17[1], 148[1]. ***Trichechus manatus*:** – . ***Trichechus senegalensis*:** 22[1], 59[0].

Appendix 6. Distribution of characters and corresponding character states for the phylogenetic hypothesis of Sirenia based on analysis F employing cranial, dental and postcranial characters (Fig. 74). * synapomorphy; ** autapomorphy

Node1: 1[1]*, 20[1]*, 76[1]*, 79[1]*, 110[1]*. **Node 2:** 9[1]*, 14[1]*, 108[1], 136[1]*, 143[1]*, 144[1]. **Node 3:** 43[1], 54[1], 61[1]*, 62[1]*, 128[1], 137[1]*, 172[1]*. **Node 4:** 6[0], 13[1], 39[1], 64[1], 69[1], 116[1], 122[1], 134[1], 138[1], 139[1]. **Node 5:** 24[1], 89[1]*, 91[1]*, 100[1], 123[1]. **Node 6:** 56[1], 101[1], 108[0], 132[1]*. **Node 7:** 87[1]*, 88[1], 94[1], 95[1], 104[0], 128[0]. **Node 8:** 171[0], 174[1]*, 175[1]. **Node 9:** 4[1]*, 5[1], 25[1]*, 24[1]. **Node 10:** 21[0], 28[1], 54[0], 94[0], 95[0], 123[0], 132[0], 134[1]. **Node 11:** 92[1], 112[1], 135[1]*, 184[1]*. **Node 12:** 56[0], 63[0], 113[1]. **Node 13:** 42[1]*, 43[0], 164[1]*. **Node 14:** 12[1], 54[0], 57[0], 65[0], 66[0], 157[1]. **Node 15:** 80[1]*, 81[1], 117[1], 166[1]*, 167[1]*, 195[1]*, 199[1]. **Node 16:** 113[1]. **Node 17:** –. **Node 18:** 2[0], 3[1], 40[1], 55[0], 63[0], 138[1], 144[0], 146[1]*. **Node 19:** 54[1], 131[1]*, 140[1], 168[1], 169[1]*, 170[1]*, 173[0], 185[1]*, 202[0]*. **Node 20:** 50[1]*, 52[1], 53[1]*, 77[1]*, 84[0], 86[1]*, 101[0], 102[1]*. **Node 21:** 38[1], 58[1], 72[0], 114[1], 127[1], 200[1]. **Node 22:** 55[1], 68[1], 69[1], 131[0], 157[0]. **Node 23:** 6[1], 7[1], 81[0], 82[1], 128[1], 159[1], 160[1]*, 165[1]*. **Node 24:** 17[1], 45[1]*, 50[0], 51[1], 63[1], 88[0], 101[1], 102[0], 161[1], 174[0]. **Node 25:** 12[0], 18[1]*, 36[1], 53[0]. **Node 26:** 89[0], 91[0]. **Node 27:** 6[0], 7[0], 29[1], 54[0], 134[1]. **Node 28:** 48[1], 83[1]*, 112[0], 127[0], 130[0], 134[1], 162[1]. **Node 29:** 32[1], 84[1], 87[0]. **Node 30:** 22[1]. **Node 31:** 49[0], 104[1], 157[0], 178[1], 179[1], 192[1]. **Node 32:** 81[0], 82[1]. **Node 33:** 6[1], 7[1], 176[0], 177[0]. **Node 34:** 35[0]. **Node 35:** 65[1], 66[1], 200[1]. **Node 36:** 11[0], 30[1], 55[1], 56[0], 59[0]. **Node 37:** 55[1]*, 104[0], 114[1], 122[1], 123[0]. **Node 38:** 12[0], 59[0], 72[0], 74[0], 101[0], 146[0], 156[0], 188[1]*. **Node 39:** –. **Node 40:** 21[0], 24[0], 124[1]. **Node 41:** 100[0], 185[0], 186[0], 197[1]. **Node 42:** 13[1], 14[0], 16[1]*, 22[1], 55[0], 74[1], 94[0], 96[1], 181[1]*, 194[1]*. **Node 43:** 4[0], 5[0], 6[0], 7[0], 13[1], 14[0], 15[1], 30[1], 32[1], 92[0], 96[1], 106[0], 107[1]*, 121[0], 179[0], 195[0]. **Node 44:** 2[1], 3[0], 39[0], 40[0], 42[0], 60[1]*, 61[0], 114[0], 122[0], 123[1], 131[0], 170[0], 173[1], 178[0]. **Node 45:** 140[0], 142[0]. **Node 46:** 154[1], 180[1]*. **Node 47:** 141[1], 182[1]*. **Node 48:** 59[1].

***Prorastomus sirenoides*:** 5[1], 55[1], 100[1], 148[1], 154[1]. ***Pezosiren portelli*:** –. ***Protosiren fraasi*:** 30[1], 93[1]. ***Protosiren smithae*:** 28[1], 40[1], 56[1], 59[1], 98[1], 147[1], 157[1], 159[1], 176[1], 177[1], 183[1]. ***Ashokia antiqua*:** 96[1]. ***Sirenavus hungaricus*:** 43[0], 54[0], 57[0], 93[1], 197[0]. ***Eotheroides aegyptiacum*:** 28[1], 111[1], 115[1]. ***Eotheroides lambondrano*:** 30[1]. ***Prototherium veronense*:** 111[1], 118[1], 128[1]. ***Prototherium intermedium*:** 57[0], 88[0], 113[1], 117[1]. ***Eosiren stromeri*:** 24[0], 67[1], 94[0], 95[0], 115[1], 116[0], 174[0], 175[0]. ***Eosiren libyca*:** 178[1], 179[1]. ***Eosiren imenti*:** 2[0], 3[1], 28[1], 40[1], 98[1]. **Gen. nov. 1 *taulannense*:** 27[1], 39[0], 68[1], 69[1], 88[0], 111[1], 116[0], 118[1]. **Gen. nov. 2 *alleni*:** –. **Gen. nov. 2 *bronni*:** 30[1], 74[0], 115[1], 116[0], 168[1]. **Gen. nov. 2 spec. nov. 1:** 28[1], 63[0]. **Gen. nov. 3 *cristolii*:** 48[1], 88[0], 95[0], 112[0]. ***Crenatosiren olseni*:** 37[1], 48[1], 112[0], 150[0], 151[0], 174[0], 197[1]. ***Nanosiren garciae*:** 63[1]. ***Nanosiren sanchezi*:** 64[0], 70[1], 84[1], 117[0]. ***Dugong dugon*:** 11[0], 32[1], 43[1], 46[1], 49[0], 65[1], 67[1], 78[1], 116[0], 118[1], 141[1], 178[1]. ***Rytiodus capgrandi*:** 54[0], 55[1], 163[1]. ***Corystosiren varguezi*:** 12[0], 43[1], 72[1], 86[0], 87[0], 98[1], 122[1], 123[0], 163[1]. ***Bharatisiren kachchhensis*:** 10[0], 11[0], 44[0], 46[1], 55[1], 130[0], 161[0]. ***Domningia sodhae*:** 48[1], 85[1], 88[1], 131[0], 150[0], 151[0], 163[1]. ***Bharatisiren indica*:** 30[1], 46[1], 51[0], 52[0], 161[0]. ***Kutchisiren cylindrica*:** 11[0], 12[1], 26[1], 27[0], 28[1], 37[1], 38[0], 64[0], 162[1]. ***Dioplotherium manigaulti*:** 13[1], 36[1], 49[0], 64[0], 88[1], 119[1], 160[0]. ***Dioplotherium allisoni*:** 10[0], 44[0], 58[0], 85[1], 176[0], 177[0]. **Gen. nov. 4 *bellunense*:** 51[0], 52[0], 53[0], 86[0], 98[1], 160[0]. ***Xenosiren yucateca*:** 23[1]**, 24[0], 81[1], 82[0], 89[0], 91[0]. ***Metaxytherium krahuletzi*:** 117[0]. ***Metaxytherium floridanum*:**

22[1], 64[0], 65[1], 67[1]. ***Metaxytherium arctodites*****:** 15[1], 36[1], 41[1], 42[0], 63[1], 68[1], 69[1], 72[0], 74[1], 78[1], 81[1], 82[0], 117[0]. ***Metaxytherium crataegense*****:** 26[0], 27[1], 28[1], 98[1], 119[1], 128[0], 198[0]. ***Metaxytherium medium*****:** 63[1], 74[0], 113[1], 157[1], 158[1]. ***Caribosiren turneri*****:** 6[0], 7[0], 58[0], 64[0], 104[0], 117[0], 174[0], 175[0]. ***Metaxytherium serresii*****:** 11[0], 49[1], 84[0], 157[1], 158[1]. ***Dusisiren reinharti*****:** 119[1], 198[0]. ***Dusisiren jordani*****:** 52[0], 57[0], 65[1], 66[1], 125[1], 131[0]. ***Dusisiren dewana*****:** 38[1]. ***Dusisiren takasatensis*****:** 35[0], 49[1], 184[0]. ***Hydrodamalis cuestae*****:** 63[1], 119[1], 125[1], 195[0]. ***Hydrodamalis gigas*****:** 15[1], 24[1], 26[0], 27[1], 47[0], 56[0], 65[1], 66[1], 69[1], 71[1], 98[1], 104[1], 115[1], 116[0], 120[1], 141[1], 150[0], 151[0], 153[0], 188[0], 191[0]. ***Anomotherium langewieschei*****:** 51[1], 52[1], 117[0], 132[0]. ***Miosiren kocki*****:** 64[0], 109[1]**, 169[0]. ***Potamosiren magdalenensis*****:** –. ***Ribodon limbatus*****:** –. ***Trichechus senegalensis*****:** –. ***Trichechus manatus*****:** –. ***Trichechus inunguis*****:** 17[1], 124[1], 125[1], 148[1].